D9

Workshops Proceedings

DELIVERABLE 9

nano uptake™

cost
EUROPEAN COOPERATION
IN SCIENCE & TECHNOLOGY

Title: Workshops Proceedings

Deliverable 9

© Nanouptake COST Action

Editors: Leonor Hernández López, Oronzio Manca, S. M. Sohel Murshed, Lucía Buj

DOI: http://dx.doi.org/10.6035/CA15119.2020.01

ACKNOWLEDGEMENTS

Contents | **Workshops Proceedings**

Deliverable 9

1. Summary

The idea behind the Workshops Proceedings document is to collect in an eBook the information of all the Nanouptake Working Group (WG) Workshops before April 2019 where the participants have been presenting their last research work in nanofluids.

This has been the case of three Working Group (WG) workshops, with the following dates, locations and participants:
- October 2016, Castellón (Spain), 83 participants
- October 2017, Lisbon (Portugal), 85 participants
- May 2018, Naples (Italy), 76 participants

After this summary, a general index of the research contributions in the field of nanofluids (including title and author/s), followed by the contributions from the four different Working Groups of Nanouptake will be presented

WG1: Heating

WG2: Cooling

WG3: Storage

WG4. Boiling, Solar Application, Modelling and others

To finalize, general conclusions for each of the Working Group close the document.

2. List of contributions

WG1: Heating. Castellón

WG1: Heating. Lisbon

WG1: Heating. Naples

WG2: Cooling. Castellón

WG2: Cooling. Lisbon

WG2: Cooling. Naples

WG3: Storage. Castellón

WG3: Storage. Lisbon

WG3: Storage. Naples

WG4: Boiling, Solar Applications, Modelling and Others.
Castellón

WG4: Boiling, Solar Application, Modelling and Others. Lisbon

WG4: Boiling, Solar Application, Modelling and Others. Naples

WG 1

3. WG 1: Heating

3. Working Group 1: Heating

3.1 Castellón, Spain

Experimental heat transfer coefficients and pressure drop of functionalized graphene nanoplatelets/water nanofluids

Roberto Agromayor[1], Javier P. Vallejo[1,2], David Cabaleiro[2], Ángel A. Pardiñas[1], José Fernandez-Seara[1], Luis Lugo[2,*]

[1] Área de Máquinas y Motores Térmicos, Escola de Enxeñería Industrial, Universidade de Vigo, 36310, Vigo, Spain

[2] Departamento de Física Aplicada, Facultade de Ciencias, Universidade de Vigo, 36310, Vigo, Spain

*Corresponding e-mail: luis.lugo@uvigo.es

Keywords: nanofluid, graphene nanoplatelets, heat transfer coefficient, pressure drop.

INTRODUCTION:

In the last decades, many procedures have been developed with the aim of improving the efficiency of the heat transfer processes. However, the low thermal conductivity of the fluids usually used (water, oils, glycols...) has always been a limiting factor. As it is known, the dispersion of nanometric-sized solid particles with a high thermal conductivity shows good results in improving the performance of heat transfer processes. In this work, an experimental analysis of the heat transfer enhancement of four water-based nanofluids has been carried out. The employed nanomaterials are sulfonic acid-functionalized graphene nanoplatelets at different mass concentrations, 0.25 %, 0.50 %, 0.75 % and 1.0 %. For that purpose, a new experimental facility was performed to evaluate the heat transfer processes determining the heat transfer coefficients and pressure drops. In addition, the needed thermophysical property data for the designed test conditions were obtained.

METHODS:

The preparation of nanofluids was carried out following a two-step method. The corresponding amounts of powder and base fluid were weighed to obtain the necessary mass concentrations. Then, the dispersions were maintained under mechanical stirring for 120 min. and afterwards they were sonicated for 240 min.

To obtain the heat transfer coefficients and pressure losses, it was developed a new experimental facility. The main part of this setup is a tube-in-tube heat exchanger of stainless steel. The tested fluid is pumped through the heat exchanger inner tube and is heated by hot water from the heating circuit. Another heat exchanger in the nanofluid circuit achieves the tested fluid cooling and its returning to the initial conditions.

Different types of tests were performed in order to obtain the convection coefficients and the pressure loss results. The experiments were defined by different pairs of average temperatures of the tested fluid and hot water, and by different flow rates of the tested fluid. The hot water flow rate was kept constant in all cases. The correlations proposed by Gnielinski [1] to concentric annular ducts in turbulent flow conditions were used to obtain the

hot water convection coefficients. More details about the experimental methods and the process of calculation can be found in the reference [2].

Regarding their thermophysical property data, thermal conductivities and dynamic viscosities were experimentally determined using a KD2-Pro Thermal Properties Analyzer (Decagon) and a Physica MCR-101 rotational rheometer (Anton Paar), respectively, whereas densities and heat capacities were obtained from literature values of the base fluid [3] and the nanoadditive [2] by using well-known weighted average equations.

RESULTS AND CONCLUSIONS:

The convection coefficients of the tests in which the average temperatures of the tested fluid/hot water were 303.15 K/323.15 K for different flow rates are shown in Figure 1, as an example. It can be observed the increase of these coefficients with the increasing flow.
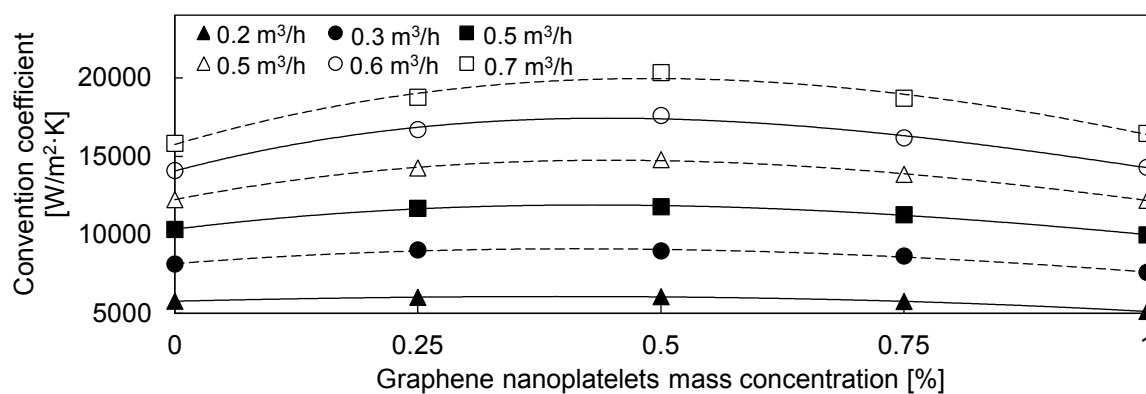
Figure 1. Convention coefficient against graphene nanoplatelets mass concentration for the 293.15 K/313.15 K tests at different flow rates.

Furthermore, nanofluids at 0.25%, 0.50% and 0.75% mass concentrations present an improvement in the convection coefficients with respect to water, while the 1% mass concentration gets worse results. In addition, we observe how the 0.5% reaches the maximum coefficients. The developments observed in the other tests follow the same trends. A comparison between our tests allows concluding that convection coefficients increase with temperature of the tested fluid. On the other hand, the pressure drop results show as this parameter increases with the mass concentration and the flow rate.

ACKNOWLEDGEMENTS:

REFERENCES:

[1] Gnielinski, V., G2 Heat Transfer in Concentric Annular and Parallel Plate Ducts, VDI Heat Atlas, VDI-Gesellschaft Verfahrenstechnik und Chemieingenieurwesen, 2nd Edition, Düsseldorf, 2010.
[2] R. Agromayor, D. Cabaleiro, A. A. Pardinas, J. P. Vallejo, J. Fernandez-Seara y L. Lugo, Materials 9, 455 (2016).
[3] Lemmon, E. W., Huber, M. L., McLinden, M. O., NIST Standard Reference Database 23, Reference Fluid Thermodynamic and Transport Properties, 2010.

Nanofluids characterization for HVACR and heat exchange applications

Simona Barison[1], Laura Fedele[2], Filippo Agresti[1], Valentina Zin[1], Stefano Rossi[2], Sergio Bobbo[2], M. Fabrizio[1]

[1] Istituto di Chimica della Materia Condensata e di Tecnologie per l'Energia, Consiglio Nazionale delle Ricerche, Corso Stati Uniti, 4, 35127 Padova, Italy

[2] Istituto per le Tecnologie della Costruzione, Consiglio Nazionale delle Ricerche, Corso Stati Uniti, 4, 35127 Padova, Italy

Corresponding e-mail: s.barison@ieni.cnr.it , laura.fedele@itc.cnr.it

Keywords: nanofluid, stability, thermal conductivity, dynamic viscosity, heat transfer coefficient, tribology

INTRODUCTION:

Nanofluids can be characterized by interesting thermal and tribological properties, making them a viable alternative to common fluids, when used as heat transfer fluids, lubricants or coolants.

In the last years, our groups have been involved in different financed research projects on nanofluids, considered as potential primary or secondary fluids in heating, ventilating, air conditioning and refrigeration (HVACR), in tribology or solar applications.

Various nanofluids have been investigated in the last years, e.g. water or ethylene glycol based nanofluids with TiO_2, Al_2O_3, ZnO, Cu, Ag, α-FeOOH, carbon nanohorns or carbon black or nanofluids based on oils for engine or for refrigeration containing carbon nanohorns, Cu or TiO_2.[1-7]

In particular, all the activities were on the study of

- synthesis of stable nanofluids;
- stability investigation through DLS (Dynamic Light Scattering) analysis;
- dynamic viscosity, compressed liquid density;
- thermal conductivity, heat transfer coefficient measurements in laminar and turbulent flow regime and, also, solubility measurements of refrigerants in nano-oils;
- tribological behaviour (measure of friction coefficient and wear rate).

METHODS:

In the last years, in CNR-ICMATE and CNR-ITC some laboratories have been set up to perform synthesis and analysis of nanofluids.

At CNR ICMATE, stable nanofluids can be prepared both by single step or two-step methods. As refer to single step methods, various kinds of oxide or metal nanoparticles can be produced by chemical methods, with the possible aid of some facilities e.g. sonication, microwave-assisted processes, autothermal synthesis. When preparing nanofluids with two step methods, various processes have been studied in the last years by CNR ICMATE in cooperation with the CNR ITC, to identify the best method to achieve stable suspensions depending on fluid and nanoparticles [5], among sonication, ball milling and high pressure homogenizer. The morphology of nanoparticles can be investigated by SEM or UV-Vis and the structure by XRD.

At CNR ICMATE the thermal conductivity of fluids can be characterized by a Laser flash thermal diffusivity apparatus (Netzsch LFA 457 Microflash) or by a custom-built apparatus based on photoacoustic effect in the room temperature-70°C range [8]. As to functional characterization of nanofluids based on oils, CNR ICMATE can perform also tribological wear tests by a Bruker UMT-2 tribotester. With this apparatus, coefficient of friction in all tribological regimes can be determined by collecting Stribeck curve, and wear tests can be performed in various configurations and lubrication regimes. Both wear and Stribeck tests can be performed at various temperatures. For each sample, wear track depth, width and mean roughness at the bottom are measured with a stylus profiler.

At CNR-ITC, different experimental apparatus allow a further characterization of nanofluids.

A Zetasizer Nano ZS (Malvern), based on the Dynamic Light Scattering (DLS), can be used to analyse the average dimension of nanoparticles in solution. Usually, 2 samples of the fluid are measured almost every day for thirty days, one without shaking the fluid, to evaluate the changes in size distribution due to natural sedimentation, the other after sonication to evaluate the changes in size distribution after mechanically removing the sedimentation. The Zeta potential of nanoparticles can be also measured.

Thermal conductivity is measured at ambient pressure by means of a TPS 2500 S (Hot Disk). It is based on the hot disk technique and can measure thermal conductivity. The hot disk sensor is a double spiral of thin nickel wire, kapton insulated, and works as a continuous plane heat source. In case of liquids, the sensor is immersed in the fluid and a full contact is provided. The declared instrument accuracy is 5%, even if the tests performed on water showed an uncertainty around 1.5%.

The dynamic viscosity is measured at ambient pressure by means of an AR-G2 rheometer (TA Instruments). It is a rotational rheometer, with a plate-cone geometry. In order to stabilize the measurement temperature, an Upper Heated Plate (UHP) is used. All the measurements are performed at constant temperature and variable shear rate. The declared uncertainty is 5%. However, water dynamic viscosity was measured at each temperature to assess the measurements accuracy (absolute average deviation between data and literature reference correlation below 2%).

A specifically built apparatus can be employed to perform the solubility measurements of refrigerants in lubricants or nano-lubricants [9-10]. The thermodynamic equilibrium between the refrigerant and the lubricant is reached in a stainless steel cell, of about 180 cm^3, provided with glass windows for the mixture visualization and the measurements are performed at isothermal conditions. The overall estimated uncertainty in the liquid composition is 0.003.

Compressed liquid density measurements are performed by means of an apparatus based on a glass vibrating tube densimeter (Anton Paar DMA 602). The measurement principle is based on the relationship between the period of oscillation of the vibrating U-tube densimeter, i.e. a hollow resonating tube, and the density of the sample, determined through calibration by varying temperature and pressure. The experimental uncertainty in density measurements is within 0.05%.

A specifically built experimental apparatus can be used to measure the heat transfer coefficient of nanofluids. A constant heat flux condition is imposed through the wall of a straight copper tube in which the measured fluid flows. The test section is divided in 8 subsections, in each of which a heating electrical resistance is continuously wound around the pipe to achieve a uniform-heat-flux (UHF) boundary condition along the test section. Bulk fluid temperature is measured at the inlet, and outlet of the experimental section by two Pt100 thermometers. Temperature is also measured in the middle point of each subsections by four thermocouples placed in circumferential way. Circumferential wall temperatures at any axial position differs less than 0.2 K, which is closed to thermocouples accuracy. In order to minimize heat losses, the entire experimental section is thermally insulated.

RESULTS AND CONCLUSIONS:

Several nanofluids have been tested by our research groups in the last years, with the aim to find the best secondary fluids (heat vectors or lubricants) in the HCVACR and solar applications. In particular:
- water based nanofluids containing Cu, Ag, FeOOH were prepared by single step chemical methods (with or without surfactants) and tested in terms of stability, viscosity and thermal conductivity

- water based nanofluids containing ZnO, Al$_2$O$_3$, TiO$_2$, carbon nanohorns prepared by various two step methods and tested in terms of stability, viscosity, thermal conductivity and heat transfer coefficient
- glycol and water-glycol based nanofluids containing Ag and carbon nanohorn prepared by single and two step method respectively, tested in terms of stability, viscosity, thermal conductivity
- oils for engine or for compressors containing Cu, TiO$_2$, carbon nanohorns, tested in terms of stability, viscosity, thermal conductivity and tribological performances.

All these activities allowed identifying the best preparation methods and to appreciate which fluids and concentration can have an influence on the properties of the fluids. Furthermore, the Institutes in these years increased competences on these fluids and acquired also skills on the developments of apparatus for the characterization of these fluids such as a custom-built instrument for the measure of thermal conductivity by exploiting of the photoacoustic effect [8] or the apparatus to test the heat transfer coefficient or the efficiency of a refrigeration system.

REFERENCES:

[1] Zin V., Barison S., Agresti F., Colla L., Pagura C., Fabrizio M., "Improved tribological and thermal properties of lubricants by graphene based nano-additives", *RSC Advances*, 2016, 6, 59477-59486.

[2] Zin V., Agresti F., Barison S., Colla L., Fabrizio M., "Influence of Cu, TiO$_2$ nanoparticles and carbon nano-horns on tribological properties of engine oil*", J. Nanosci. Nanotech.*, 2015, 15(5), 3590-3598.

[3] Agresti F., Barison S., Battiston S., Pagura C., Colla L., Fedele L., Fabrizio M., "Tuning the thermal diffusivity of silver based nanofluids by controlling nanoparticle aggregation", Nanotechnology, 2013, 24(36), 365601.

[4] Bobbo S., Fedele L., Benetti A., Colla L., Fabrizio M., Pagura C., Barison S., "Viscosity of water based SWCNH and TiO$_2$ nanofluids", Experimental Thermal Fluid Science, 2012, 36, 65-71.

[5] Fedele L., Colla L., Bobbo S., Barison S., Agresti F., "Experimental stability analysis of different water-based nanofluids" Nanoscale Research Letters, 2011, 6(1), 1-8.

[6] Cabaleiro D., Colla L., Agresti F., Lugo L., Fedele L., "Transport properties and heat transfer coefficients of ZnO/(ethylene glycol + water) nanofluids", Int. J. Heat Mass Transfer, 2015, 89, 433–443.

[7] Fedele L., Colla L., Minetto S., Scattolini M., Bellomare F., Bobbo S., Zin V., "Nanofluids Characterization and Application as Nanolubricants in Heat Pumps Systems", Science and Technology for the Built Environment, Special Issue: Advances in Refrigeration and Heat Transfer Engineering, 2015, 21, 5

[8] Agresti F., Ferrario A., Boldrini S., Miozzo A., Montagner F., Barison S., Pagura C., Fabrizio M., Temperature controlled photoacoustic device for thermal diffusivity measurements of liquids and nanofluids" Thermochimica Acta, 2015, 619, 48-52.

[9] Bobbo S., Scattolini M., Camporese R., Fedele L., Stryjek R., "Solubility of Carbon Dioxide in Pentaerythritol Esters", Proc. IIR International Conference – Thermophysical Properties and Transfer Processes of Refrigerants, Vicenza (Italy), 2005.

[10] Bobbo S., Fedele L., Scattolini M., Camporese R., Stryjek R., "Solubility of carbon dioxide in 2-methylbutiric, 2-methylvaleric and 2-methylhexanoic ester oils", Fluid Phase Equilibria, 2007, 256, 81-85.

Hybrid nanofluids behavior in turbulent flow: numerical techniques applied to studied fluids

Minea Alina Adriana[1], Manca Oronzio[2], Moldoveanu Madalina Georgiana[1], Julia Enrique[3]

[1] Technical University "Gheorghe Asachi" from Iasi, Faculty of Materials Science and Engineering, 700050, Iasi, ROMANIA
[2] Seconda Universita degli Studi di Napoli, 81031 Aversa (CE), ITALY
[3] Universitat Jaume I, 12071 Castellon de la Plana, SPAIN

Corresponding e-mail: aminea@tuiasi.ro

Keywords: hybrid nanofluid, turbulence, numerical

INTRODUCTION

Numerical researches on the nanofluids increased very fast over the last years. In spite of some inconsistency in the reported results due to insufficient understanding of the mechanism of the heat transfer in nanofluids, it has been emerged as a new improved heat transfer fluid [1, 2]. Recently, hybrid nanofluids were defined as a new group of nanofluids and their possible applications can be in almost all the fields of heat transfer, because of the synergistic effect through which they provide promising properties of all of its constituents. It has been found that the augmented thermal conductivity of nanofluids over some basic heat transfer fluids (i.e. water) is one of the driving factors for enhanced performance in heat transfer. Nevertheless, most of the studies are about estimation of thermal conductivity and few on viscosity variation, while other properties are neglected [1].

Nonetheless, the hybrid nanofluids are a very new sort of nanofluids, which can be prepared by mixing two nanofluids or by suspending (i) different types (two or more than two) of nanoparticles in base fluid, and (ii) hybrid (composite) nanoparticles in base fluid [2]. The idea of using hybrid nanofluids is to further improve the heat transfer characteristics of individual suspension and to combine advantageously different properties from oxides, carbon nanotubes, metals, composites etc.

METHODS

As a research proposal, some water based hybrid nanofluids will be compared in terms of main findings. As was depicted earlier, for these new fluids preparation, two methods are widely used: preparation of hybrid nanocomposites and suspending two kinds of nanoparticles in water. Another method, used by Han and Rhi [3], was mixing two already prepared nanofluids.

Table 1. Thermophysical properties of nanofluids at 293 K

Source	Hybrid nanofluid	Thermophysical properties			
		specific heat (J/kg K)	density (kg / m^3)	thermal conductivity(W/mK)	viscosity (Kg/m s)
Suresh et al. [4]	0.1% Al_2O_3-Cu / water	4176.83	1001.3	0.620	9.3×10^{-4}
Sundar et al. [5]	0.1% MWCNT–Fe_3O_4 / water	4182.66	1002.34	0.6734	9.1×10^{-4}
	0.3% MWCNT–Fe_3O_4 / water	4183.99	1010.04	0.6856	10.1×10^{-4}

Esfe et al.[6]	0.5 % Ag–MgO/ water	4163.86	1028.68	0.630	8.38×10^{-4}
	1 % Ag–MgO/ water	4166.64	1058.87	0.659	8.9×10^{-4}
water		4182	998.5	0.602	7.9×10^{-4}

The proposed research is a numerical one for comparing the data available in the literature in regard to hybrid nanofluids. Thus, the numerical domain can be a 3D tube with L = 1.75 m length and D = 0.014 m inner diameter according to Sundar et al. [5] experiment setup. Tube wall boundary condition can be considered as a constant heat flux of 12998.83 W/m^2. At the inlet of the tube, the uniform velocity and temperature field is considered, while at the exit the temperature and velocity gradients are equal to zero. At the channel inlet, profiles of uniform axial velocity, v0, and temperature, T0 = 293 K, are assumed. Moreover, constant intensity turbulence, equal to 1%, is imposed. At the channel exit section, the fully developed conditions are considered, i.e., all axial derivatives are zero. On the channel wall, the non-slip conditions and uniform heat flux are imposed, while both turbulent kinetic energy and dissipation of turbulent kinetic energy are equal to zero.

RESULTS AND CONCLUSIONS

The CFD analysis has led to the following main results and conclusions:

- The convective heat transfer coefficient of nanofluids increased with hybrid nanoparticles concentration and Reynolds number. The effective thermal conductivity of hybrid nanocomposite in the fluid medium paved way for improved heat transfer characteristics of hybrid nanofluid.
- The convective heat transfer coefficient increases with increasing Reynolds number. The numerical results of hybrid nanofluid for turbulent flow showed a maximum enhancement in Nusselt number for 0.3%MWCNT-Fe3O4 nanofluid at Re = 22000.
- All studied hybrids need a relatively reduced increase of pumping power (max. 20 %).

As a general conclusion, the heat transfer performance in a tube is amplified by suspension of hybrid nanoparticles in comparison with that of pure water. However, a considerable increase in specific work is needed in order to shape a consistent theory in regard to these new fluids.

REFERENCES

[1] Sarkar J. A critical review of heat transfer correlations of nanofluids. Renew Sustain Energy Rev 2011; 15: 3271–7.

[2] Sarkar J, Ghosh P, Adil A. A review on hybrid nanofluids: Recent research, development and applications, Ren. and Sustainable Energy Reviews 43 (2015) 164–177.

[3] Han W S, RHI SH, Thermal Characteristics of Grooved Heat Pipe with hybrid nanofluids, Thermal science, 2011, 15(1): 195-206

[4] Suresh S, Venkitaraj KP, Selvakumar P, Chandrasekar M. Synthesis of Al2O3– Cu/ water hybrid nanofluids using two step method and its thermophysical properties. Colloids Surf A: Physicochem Eng Asp 2011; 388: 41–8.

[5] Sundar LS, Singh MK, Sousa, ACM, Enhanced heat transfer and friction factor of MWCNT–Fe3O4/water hybrid nanofluids, International Communications in Heat and Mass Transfer 52 (2014) 73–83

[6] Esfe M.H., Abbasian Arani A.A., Rezaie M., Yan W-M, Karimipour A., Experimental determination of thermal conductivity and dynamic viscosity of Ag–MgO/water hybrid nanofluid, International Communications in Heat and Mass Transfer 66 (2015) 189–195

Mixed convection boundary layer flow past a vertical flat plate embedded in a porous medium saturated by a nanofluid: Darcy-Ergun model

Natalia C. Roşca[1], **Alin V. Roşca[2]**, Teodor Groşan[1], Ioan Pop[1*]

[1]Department of Mathematics, Babeş-Bolyai University, 400084 Cluj-Napoca, Romania
[2]Faculty of Economics and Business Administration, Babeş-Bolyai University,
  400084 Cluj-Napoca, Romania

Corresponding e-mail: alin.rosca@econ.ubbcluj.ro

Keywords: Non-Darcy porous media, nanofluid, mixed convection, stability analysis

INTRODUCTION: During the past few years, the use of nanofluids as a conventional fluid to enhance heat transfer has attracted considerable attentions among scientists. Research showed that dissolving various kinds of nanoparticles such as metal, nonmetal and polymeric in working fluid lead to better thermal properties (Das *et al.* 2007). It seems that Choi (1995) was the first who has used the term nanofluid to define the dilution of nanometer-sized particles (smaller than 100nm) in a fluid such as water, ethylene glycol and oil (Wang and Mujumdar 2008). These nanoparticles, which normally contain metals, oxides, carbides, or carbon nanotubes, have unique chemical and physical properties (Oztop and Abu-Nada 2008), and due to the nanometer-sized, nanoparticles can easily flow smoothly through the microchannels, and as such, nanofluid has better thermal conductivity and convective heat transfer coefficient compared to the base fluid only. There are many researchers that have employed numerical techniques to explore natural convection heat transfer of nanofluids in enclosures. Khanafer *et al.* 2003 developed a model to study heat transfer enhancement of $Cu/water$ nanofluid in a two dimensional enclosure. They employed the finite-volume approach along with the alternating direct implicit procedure to solve the transport equations numerically. It has been found that the heat transfer rate rises significantly as the volume fraction of nanoparticles increases in the base fluid. Buongiorno (2006) found that nanoparticles absolute velocity can be viewed as the sum of the base fluid velocity and a slip velocity, with total of seven slip mechanisms involved: inertia, Brownian diffusion, thermophoresis, diffusiophoresis, Magnus effect, fluid drainage, and gravity settling. The aim of this contribution is to present the steady mixed convection boundary layer flow past a vertical flat plate embedded in a porous medium filled by a nanofluid using the mathematical nanofluid model proposed by Tiwari and Das (2007) and is merely based on the work from paper Rosca *et al.* (2014). Employing appropriate similar variables, the partial differential equations were transformed into ordinary differential equations, which have been solved numerically. The effects of the pertinent parameters such as solid nanofluid volume fraction parameter, non-Darcy parameter and the mixed convection parameter on the flow and heat transfer characteristics have been studied. It is shown that for a regular fluid a very good agreement exists between the present numerical results and those reported in the open literature. We mention that the problem is formulated for three types of nanoparticles, namely, copper (Cu), alumina (Al2O3) and titania (TiO2). However, we present results here only for the (Cu) nanoparticles. We also mention to this end, that the mathematical nanofluid model proposed by Tiwari and Das (2007) has been very successfully used recently by Ahmad and Pop, 2010; Grosan and Pop, 2011a; Grosan and Pop, 2011b; Khan and Pop, 2011; Rosca *et al.* 2012, to study several nanofluid problems.

METHODS: Let us consider the mixed convection flow over a vertical flat plate embedded in a fluid porous medium saturated by a nanofluid. It is assumed that the constant velocity of the ambient fluid

(inviscid flow) is U_∞ and the constant ambient temperature is T_∞, while the constant wall temperature is T_w, where $T_w > T_\infty$ (hot plate) corresponds to the assisting flow and $T_w < T_\infty$ (cooled plate) corresponds to the opposing flow, respectively. Using the non-Darcy equation model along with the Boussinesq approximation and the mathematical nanofluid model proposed by Tiwari and Das (2007), the conservation equations for the problem under consideration can be written after some similarity transformations:

$$f'' + G(1-\phi)^{2.5}(1-\phi+\phi\rho_s/\rho_f)\left[(f')^2\right]'$$

$$- \left[1-\phi+\phi(\rho\beta)_s/(\rho\beta)_f\right](1-\phi)^{2.5}\lambda\theta' = 0 \qquad (1)$$

$$\frac{k_{nf}/k_f}{1-\phi+\phi(\rho C_p)_s/(\rho C_p)_f}\theta'' + f\theta' = 0 \qquad (2)$$

with the corresponding boundary conditions

$$f(0)=0, \quad \theta(0)=1$$
$$f'(\eta)\to 1, \quad \theta(\eta)\to 0 \quad \text{as} \quad \eta\to\infty \qquad (3)$$

The quantity of physical interest in this problem is the skin friction coefficient C_f, which is defined as

$$C_f = \frac{\tau_w}{\rho_f U_\infty^2} \qquad (4)$$

where τ_w is the skin friction or shear stress along the plate and is given by

$$\tau_w = \mu_{nf}\left(\frac{\partial \bar{u}}{\partial \bar{y}}\right)_{\bar{y}=0} \qquad (5)$$

Finally, we obtain

$$(2\,Pe_x)^{1/2}\Pr C_f = f''(0) \qquad (6)$$

where $\Pr = \nu_f/\alpha_f$ is the Prandtl number for the fluid-saturated porous medium.

It is worth mentioning to this end that for $\phi = 0$ (regular fluid) and $G = 0$ (Darcian fluid), Eqs. (1) and (2) reduce to those first established by Merkin (1980). However, for $\phi \neq 0$ (nanofluids) and $G = 0$ (Darcian fluid), Eqs. (1) and (2) reduce to those established by Ahmad and Pop (2010).

The considered problem is formulated in such a way so that we can consider different types of nanoparticles (e.g. Cu, Al_2O_3, TiO_2, etc.) and water as a base fluid. However, in order to save space, we will consider here only the case of Cu nanoparticles. The system of ordinary differential equations (17) and (18) subject to the boundary conditions (19) was solved numerically using the function bvp4c from Matlab. To accomplish this, the first step is to write Eqs. (1) and (2) as a system of first order differential equations by introducing new variables, one for each variable in the original problem plus one for each derivative up to the highest order derivative minus one. The bvp4c function implements a collocation method for the solution of the considered boundary problem. The relative error tolerance was set to 10^{-10}. In this method, we have chosen a suitable finite value of $\eta\to\infty$, namely $\eta = \eta_\infty = 7$. The reduced skin friction coefficient $f''(0)$, the velocity profiles $f'(\eta)$ and the temperature profiles $\theta(\eta)$ have been obtained for the following range of parameters: mixed convection parameter, $0\le\lambda\le 10^2$ (assisting flow) and $\lambda\le 0$ (opposing flow), and non-Darcy parameter, $G = 0, 0.1, 1, 10$ (assisting flow) and $G = 0, 0.1, 0.3, 0.4$ (opposing flow), respectively.

The values of the solid volume fraction ϕ are taken in the range $0 \leq \phi \leq 0.2$ (Oztop and Abu-Nada, 2008). A stability analysis of the steady flow solutions is also performed. This analysis reveals that for $\lambda < 0$ (opposing flow case) the lower solution branch is unstable while the upper solution branch is stable.

RESULTS AND CONCLUSIONS: The effects of volume fraction ϕ, the mixed convection λ and the non-Darcy G parameters on the flow field and heat transfer characteristics have been analyzed and discussed. It was found that the sleep velocity at the plate decreases with ϕ for the buoyancy assisting flow $\lambda > 0$, while dual solutions were found to exist for the opposing flow $\lambda < 0$. A stability analysis has been also performed that shows which solution is physically realizable and which is not. This study would be important for the researchers working in the relatively new area of nanofluids in order to become familiar with the flow behavior and properties of such nanofluids.

REFERENCES:
Ahmad, S. and Pop, I. (2010), "Mixed convection boundary layer flow from a vertical flat plate embedded in a porous medium filled with nanofluids", *Int. Comm. Heat Mass Transf.*, Vol. 37, pp. 987-991.
Buongiorno, J. (2006), "Convective transport in nanofluids", *ASME Journal of Heat Transfer*, Vol. 128 No. 3, pp. 240–250.
Choi, S.U.S. (1995), "Enhancing thermal conductivity of fluids with nanoparticles", in: *Proceedings of the 1995 ASME International Mechanical Engineering Congress and Exposition*, New York, NY, USA. ASME, FED 231/MD, Vol. 231 No. 66, pp. 99-105.
Das, S.K., Choi, S.U.S., Yu, W. and Pradeep, T. (2007), "*Nanofluids: Science and Technology*", Wiley, Hoboken, NJ.
Grosan, T. and Pop, I. (2011a), "Axisymmetric mixed convection boundary layer flow past a vertical cylinder in a nanofluid", *Int. J. Heat Mass Transf.*, Vol. 54, pp. 3139-3145.
Grosan, T. and Pop, I. (2011b), "Forced convection boundary layer flow past a nonisothermal thin needles in nanofluids", *ASME J. Heat Transf.*, Vol. 133, Article ID 054503-1 – 054503-4.
Khan, W.A. and Pop, I. (2011), "Free convection boundary layer flow past a horizontal flat plate embedded in a porous medium filled with a nanofluid", *ASME J.Heat Transf.* Vol. 133, Article ID 094501-1 - 094501-4.
Khanafer, K., Vafai, K. and Lightstone, M. (2003), "Buoyancy-driven heat transfer enhancement in a two-dimensional enclosure utilizing nanofluids", *International Journal of Heat and Mass Transfer*, Vol. 46 No. 19, pp. 3639-3653.
Merkin, J.H. (1980), "Mixed convection boundary layer flow on a vertical surface in a saturated porous medium", *J. Engng. Math.*, Vol. 14, pp. 301-313.
Oztop, H.F. and Abu-Nada, E. (2008), "Numerical study of natural convection in partially heated rectangular enclosures filled with nanofluids", *International Journal of Heat and Fluid Flow*, Vol. 29 No. 5, pp. 1326-1336.
Rosca, N.C., Grosan, T. and Pop, I. (2012), "Stagnation-point flow and mass transfer with chemical reaction past a permeable stretching/shrinking sheet in a nanofluid", *Sains Malaysiana*, Vol. 41, No. 10, pp. 1177-1185.
Rosca N.C., Rosca A.V., Grosan T., Pop I. (2014), **"**Mixed convection boundary layer flow past a vertical flat plate embedded in a non-Darcy porous medium saturated by a nanofluid", *INTERNATIONAL JOURNAL OF NUMERICAL METHODS FOR HEAT & FLUID FLOW*, Vol. 24, No. 5, pp. 970 – 987.
Tiwari, R. K. and Das, M. K. (2007), "Heat transfer augmentation in a two-sided LID-driven differentially heated square cavity utilizing nanofluids", *Int. J.Heat Mass Transf.* Vol. 50, pp.

2002–2018.

Wang, X.-Q. and Mujumdar, A.S. (2008), "A review on nanofluids – Part I: theoretical and numerical investigations", *Brazilian J. Chem. Eng.*, Vol. 25 No. 4, pp. 613–630.

Semi-analytical solution for the flow of a nanofluid over a permeable stretching/shrinking sheet with velocity slip using Buongiorno's mathematical model

Natalia C. Roşca[1*], Ioan Pop[1], Emad H. Aly[2,3]

[1]*Department of Mathematics, Faculty of Mathematics and Computer Science, Babeş–Bolyai University, 400084 Cluj–Napoca, Romania*
[2]*Department of Mathematics, Faculty of Science, University of Jeddah, Jeddah 21589, Saudi Arabia*
[3]*Department of Mathematics, Faculty of Education, Ain Shams University, Roxy 11757, Egypt*

[*]Corresponding e-mail: natalia@math.ubbcluj.ro

Keywords: nanofluid flow, similarity solution, numerical and analytical solutions

INTRODUCTION: The study of fluid flow due to a stretching/shrinking surface has received significant interest among researchers over the past several years, due to its great practical applications. For example, in engineering and industrial processes, these flows have been used in the manufacturing and extraction of polymer and rubber sheets, wire drawing and glass-fiber production, etc. (Sparrow and Abraham [1]). As it is well-known, Crane [2] was the first who has studied the forced convection flow past a stretching sheet in a viscous and incompressible fluid. Also, Miklavčič and Wang [3] investigated the viscous flow over a shrinking surface.

Fluid flow and heat transfer in a base fluid filled by a nanofluid over a stretching/shrinking sheet has become a hot topic and has attracted the interest of many researchers due to its several applications in industrial processes such as in power generation, chemical processes and heating or cooling processes. Choi [4] was the first who utilized the term "nanofluid" to describe the base fluids with suspended nanoparticles. The solid nanoparticles have been suspended into the base fluid which has poor heat transfer properties in order to increase its thermal conductivity.

However, it should be mentioned that Buongiorno [5] noted that the nanoparticle absolute velocity can be viewed as the sum of the base fluid velocity and a relative velocity (that he calls the slip velocity). He considered in turn seven slip mechanisms: inertia, Brownian diffusion, thermophoresis, diffusiophoresis, Magnus effect, fluid drainage, and gravity settling. After examining each of these, he concluded that the Brownian diffusion and the thermophoresis are the most important parameters (see also Nield and Kuznetsov [6]). The boundary-layer flow of nanofluids past stretching/shrinking surfaces using the mathematical nanofluid model proposed by Buongiorno [5] has attracted much attention (Khan and Pop [7], Bachok et al. [8], Aly and Ebaid [9], etc.). As mentioned by Maïga et al. [10], the study of boundary layer flow in nanofluids is important because of the reduction of the thermal boundary layer thickness due to the presence of particles and their random motion within the base fluid. This may have important contributions to such heat transfer improvement as well.

Motivated by the above investigations, the present contribution considers the problem of flow of a nanofluid over a permeable stretching/shrinking sheet with velocity slip using Buongiorno's mathematical model and is based on paper by Roşca et al. [11].

METHODS: We consider a steady, two-dimensional flow of a viscous and incompressible water based nanofluid due to a permeable stretching/shrinking sheet with velocity slip. After some similarity transformations, the following ordinary differential equations are obtained to describe the fluid flow:

$$\Pr f''' + f f'' - f'^2 = 0 \tag{1}$$

$$\theta'' + f\theta' + Nb\phi'\theta' + Nt\theta'^2 = 0 \tag{2}$$

$$\phi'' + Ln\,f\phi' + \frac{Nt}{Nb}\theta'' = 0 \tag{3}$$

subject to the boundary conditions

$$f(0) = S, \quad f'(0) = \lambda + \Lambda\,f''(0), \quad \theta(0) = 1, \quad Nb\phi'(0) + Nt\,\theta'(0) = 0$$
$$f'(\eta) \to 0, \quad \theta(\eta) \to 0, \quad \phi(\eta) \to 0 \quad \text{as} \quad \eta \to \infty \tag{4}$$

where S is the constant mass transfer parameter with $S > 0$ for suction and $S < 0$ for injection, respectively. The dimensionless constants Pr, Ln, Nb, Nt and Λ denote the Prandtl number, nanofluid Lewis number, Brownian motion parameter, thermophoresis parameter and dimensionless slip parameter.

These resulting ordinary differential equations (1–3) along with the boundary conditions (4) are solved both analytically and numerically using a collocation method from MATLAB for different values of the parameters λ, S, Pr, Ln, Nb, Nt and Λ.

RESULTS AND CONCLUSIONS: Multiple (dual: upper and lower branch) solutions are shown to exist in a certain range of the governing parameters. In addition, the reduced skin friction coefficient and the reduced heat transfer from the surface of the sheet as well as the velocity, temperature and concentration profiles are analyzed and discussed subject to several parameters of interest, namely suction parameter, Brownian motion and thermophoresis parameters, Prandtl number, nanofluid Lewis number and dimensionless slip parameter. The results indicate that the skin friction coefficient and the heat transfer from the surface of the sheet increase with suction effect. It is also observed that suction widens the range of the stretching/shrinking parameter for which the solution exists. This contribution is important for the researchers and engineers working in the area of nanofluids in order to become familiar with the flow behavior and important properties of such nanofluids.

REFERENCES:
[1] E.M. Sparrow, J.P. Abraham, Universal solutions for the streamwise variation of the temperature of a moving sheet in the presence of a moving fluid, *Int. J. Heat Mass Transfer* 48 (2005) 3047– 3056.
[2] L.J. Crane, Flow past a stretching plate, *J. Appl. Math. Phys. (ZAMP)* 21 (1970) 645–647.
[3] M. Miklavčič, C.Y. Wang, Viscous flow due to a shrinking sheet, *Quart. Appl. Math.* 64 (2006) 283–290.
[4] S.U.S. Choi, Enhancing thermal conductivity of fluids with nanoparticles, In: *Developments and Applications of Nonnewtonian Flows* (D. A. Singer, H. P. Wang, Eds.), vol. 231, pp. 99–105, 1995. American Society of Mechanical Engineers, New York, NY, USA.
[5] J. Buongiorno, Convective transport in nanofluids, *ASME J. Heat Transfer* 128 (2006) 240–250.
[6] D.A. Nield, A.V. Kuznetsov, The Cheng–Minkowycz problem for natural convective boundary–layer flow in a porous medium saturated by a nanofluid, *Int. J. Heat Mass Transfer* 52 (2009) 5792–5795.
[7] W.A. Khan, I. Pop, Boundary–layer flow of a nanofluid past a stretching sheet, *Int. J. Heat Mass Transfer* 53 (2010) 2477–2483.
[8] N. Bachok, A. Ishak, Pop, Boundary–layer flow of nanofluids over a moving surface

in a flowing fluid, *Int.J. Thermal Sci.* 49 (2010) 1663–1668.

[9] E.H. Aly, A. Ebaid, New exact solutions for boundarylayer flow of a nanofluid past a stretching sheet, *J. Computat. Theoret. Nanoscience* 10 (2013) 2591–2594.

[10] S. E-B. Maïga, S.J. Palm, C.T. Nguyen, G. Roy, N. Galanis, Heat transfer enhancement by using nanofluids in forced convection flows, *Int. J. Heat Fluid Flow* 26 (2005) 530–546.

[11] N.C. Rosca, A.V. Rosca, E.H. Aly and I. Pop, Semi-analytical solution for the flow of a nanofluid over a permeable stretching/shrinking sheet with velocity slip using Buongiorno's mathematical model, *European Journal of Mechanics B/Fluids*, 58 (2016), 39–49.

Modeling and 3ω hot wire measurement of effective thermophysical properties of inhomogeneous media

Mihai Chirtoc*, Jean-Francois Henry, Nicolas Horny

GRESPI Lab., Université de Reims Champagne Ardenne URCA, Moulin de la Housse, BP 1039, 51687, Reims, France

*Corresponding e-mail: mihai.chirtoc@univ-reims.fr

Keywords: 3ω hot wire, effective thermal conductivity, thermal diffusivity, nanofluids, interfacial thermal resistance

INTRODUCTION: The main challenges for accurate measurement of thermal conductivity k are to inhibit the heat transfer by convection and to minimize temperature gradients during the measurement. The transient hot-wire (THW) method has been widely used for obtaining standard reference data for k of fluids and also for gases and solids. A similar method is the 3ω hot-wire (3αHW) which was first applied to solids [1] and subsequently to liquids and gases. As with the THW, the thermal probe plays the role of excitation source and temperature sensor in the same time. The main difference relies in the frequency-domain modulation instead of the time-domain modulation. Due to the available amplitude and phase information, the 3ω signal can be exploited to determine the sample thermal conductivity, simultaneously and independently from the thermal diffusivity, while their time evolution can be monitored continuously.

METHODS: With 3αHW, a sinusoidal current at angular frequency $\omega=2\pi f$ passes through the wire and generates a heat source at 2ω. The corresponding temperature oscillation is retrieved by the voltage component at 3ω, resulting from mixing the current at 1ω with the temperature-dependent electrical resistance at 2ω. The complex temperature of a periodic line heat source immersed in a medium with thermal conductivity k and thermal diffusivity a is proportional to [2]:

$$\theta(f,T) \, \mu \, \frac{1}{k}\left(\ln \frac{\mu}{1.2594\, r} - j\frac{\pi}{4} \right) \tag{1}$$

where $\mu = [a\pi^{-1}(2f)^{-1}]^{1/2}$ is the thermal diffusion length in the medium at thermal frequency 2f and r (=20 μm) is the wire radius. In a relative measurement, the imaginary part of Eq. (1) is used to monitor the temperature-dependent conductivity of a liquid relative to that of a reference fluid: $k(T) = k_r(T)$ [Im(θ_r)/Im(θ)]. The phase of Eq. (1) yields the $a(T)$ value at fixed frequency, which depends only on r without the need for other calibration. By combining the two quantities, the volumetric heat capacity $\rho c_p(T)$ can be derived too. Owing to sensitive lock-in signal processing the thermal excitation amplitude of the wire is kept below 1 K, thus avoiding errors associated with natural convection. The minimum sample quantity

surrounding the wire ($\approx$25 μl) is related to the thermal diffusion length μ ($\approx$ 0.2 mm in water at 1 Hz). These features make the device very attractive for accurate thermophysical investigations of (nano)fluids. We are currently developing a prototype of a commercial instrument based on the 3ωHW method with a patented thermal probe [3].

RESULTS AND CONCLUSIONS: Measurements of water-based Aerosil 200V nanofluids (10-12 %wt, primary SiO_2 particle size $\approx$12 nm) at ambient temperature indicated a 2.5-3.5 % increase in k and 3.8-4.8 % in a relative to distilled water, depending on dispersion method of aggregates [2]. It was concluded that ultrasound treatment is more efficient than high pressure jet dispersion in enhancing their thermal transport properties. Measurement resolution was 0.1 % in k and 0.3 % in a, while long-term reproducibility of absolute values was 0.3 % in k and 0.7 % in a.

Water-based ferrofluids (2 %vol of Fe_3O_4 nanoparticles, 35-90 nm in size) with double-layer steric stabilization by monocarboxylic acids were also investigated. The high resolution of the 3ωHW method (k/k_r = 0.9760 - 0.9965 ± 0.05 %, a/a_r = 0.816-0.874 ± 0.2 %) allowed evidencing the effect of particle size and of the nature of the double molecular stabilization layer on the interfacial thermal resistance (R_{th} = 5.3-31×10^{-8} m^{2}K/W ±10 %) between particles and base liquid. R_{th} was determined using a model which accounts for particle size, shape and orientation distribution [4]. It also predicts lower effective k of the nanofluid than that of water due to the presence of R_{th}, despite the fact that Fe_3O_4 particles have much larger k. The found R_{th} values are significantly larger than the Kapitza boundary resistance and are correlated to the length of the respective fatty acid molecules.

In response to growing need for innovative heat transfer fluids in concentrated solar power plants, the thermal conductivities of different vegetable oils were measured in the temperature range from ambient to 230°C with 2 % uncertainty relative to a reference synthetic oil [5]. The 3ωHW method with single-use wire thermal probes can be applied to solids. Sample - probe assemblies were fabricated by embedding Ni wires in epoxy resin during curing, in view of measuring the effect of roughness of the wire on R_{th}. In another study, Ni wires were immersed in melted polylactic acid (PLA) polymer and its glass transition at $\approx$60°C was revealed in the amplitude and phase of the 3ω signal in the critical region. Similar relaxation studies could be carried out for nanocomposites based on phase change materials (PCM).

REFERENCES:
[1] D.G. Cahill, R.O. Pohl, "Thermal conductivity of amorphous solids above the plateau," *Phys. Rev. B*, **35**, 4067–4073 (1987).
[2] A. Turgut, C. Sauter, M. Chirtoc, J.F. Henry, S. Tavman, I. Tavman, J. Pelzl, "AC hot wire measurement of thermophysical properties of nanofluids with 3ω method", *The Europ. Phys. J. Special Topics* **153**, 349-352 (2008).
[3] M. Chirtoc, J. F. Henry, D. Caron and N. Horny, "Measurement method of thermophysical properties of a medium", *French Patent*, (PR 73627, Submitted 02 /2016).
[4] C.W. Nan, R. Birringer, D.R. Clarke, H. Gleiter, *J. Appl. Phys.* **81**, 6692 (1997).
[5] J.F. Hoffmann, J.F. Henry, G. Vaitilingom, R. Olives, M. Chirtoc, D. Caron, X. Py, "Temperature dependence of thermal conductivity of vegetable oils for use in concentrated solar power plants, measured by 3ω hot wire method", *Int. J. Thermal Sci.* **107**, 105-110 (2016).

Development of a heat exchanger with nanofluids by application of CFD

S. Bikic

Faculty of Technical Sciences, University of Novi Sad, 21000 Novi Sad, Serbia

*Corresponding e-mail: bika@uns.ac.rs

Keywords: CFD simulations, heat exchanger, nanofluid

The subject of this research are nanofluids (nanoparticles dispersed in the water). Different effects (material of nanoparticles, concentration of nanoparticles, size of nanoparticles, geometry of heat exchanger with nanofluids, flow regime of nanofluids and physical models of nanofluids) on heat transfer of heat exchanger were analyzed. In the analysis were as fluids used water and nanofluids (Al_2O_3 and CuO dispersed in the water with the concentration smaller than 2 %). Two different sizes of nanoparticles were considered (with the average particle diameters of the 20 and 50 nm). In terms of the geometry of heat exchanger with the nanofluids the effect of the obstacles inside the exchanger (horizontal pipe without and with obstacle) was analyzed. The number, shape and distance between the obstacles were varied. The analysis was carried out for all three nanofluids flow regimes through the heat exchanger (laminar, transitional and turbulent). For the purpose of research was used computational fluid dynamics (CFD), where the results of numerical simulations were verified with existing experimental data from the literature. In this spirit, the accuracy of three physical models of nanofluids (singlephase flow, multiphase flow and volume of fluid) was analyzed. The results showed that obstacles (number, shape and distance between the obstacles) have influence to heat transfer of heat exchanger with nanofluids (little influence with small values of Reynolds number and great influence with big values of Reynolds number). It was concluded that with increasing of Reynolds number and concentration of nanoparticles heat transfer was increased.

TRANSPORT PROPERTIES OF WATER-BASED NANOFLUIDS WITH DISPERSION OF GRAPHENE-OXIDE NANOPARTICLES

L. Fedele* and S. Bobbo

Istituto per le Tecnologie della Costruzione, Consiglio Nazionale delle Ricerche

Corso Stati Uniti, 4 - Padova, I-35127, Italy

Email: laura.fedele@itc.cnr.it

Keywords: Nanofluids, Graphene-oxide, Thermal conductivity, Viscosity

Introduction

Enhancement of thermal properties of heat transfer fluids is presently the most promising way to increase the performance of heat exchangers and in general of systems where heat transfer is a significant part of the energy flow. Nanofluids, dispersions of solid nanoparticles in a common fluid like water, glycol or oil, are widely studied due to their possibility to increase strongly the thermal properties of the base fluid [1]. However, the results available in the literature are still controversial and several problems (e.g. nanoparticles stability inside the fluid) need to be overcome [2]. Among the possible materials for nanoparticles, carbon nanostructures seem to exhibit the highest potential with respect to other materials, such as metal oxides or metals [3]. In particular, graphene, a graphite carbon allotrope, is one of the most interesting due to its remarkable mechanical, structural, thermal, and electrical properties [4, 5, 6]. Nonetheless, being graphene hydrophobic, it cannot be dispersed in polar solvents directly. Thus, the hydrophilic graphene oxide (GO), even if characterised by lower thermal conductivity, is a good alternative to graphene as additive in nanofluids based on polar fluids, such as water or ethylene-glycol. Only few works are available in the literature on nanofluids based on GO nanoparticles, showing significant thermal conductivity enhancements with respect to the base fluids [7] and thus interesting potentiality to apply these nanofluids as efficient heat transfer fluids. However, significant additional work is necessary to fully understand their thermal properties. Here, commercial nanofluids based on graphene-oxide (GO) nanostructure have been considered as potential substitutes for water as heat transfer fluids in ground source heat pumps (GSHP). Stability along time have been evaluated and transport properties (thermal conductivity and viscosity) have been measured as a function of temperature.

The study has been performed within the research activities of the European Project "Cheap and efficient application of reliable Ground Source Heat exchangers and Pumps" Cheap – GSHPs Grant Agreement Number 657982.

Experimental

Materials: two commercial nanofluids provided by Sigma Aldrich have been used for the experiments. Both fluids are based on water and graphene-oxide platelets, but with two different concentrations of nanoparticles: 1 mg/ml (WG1) and 2 mg/ml (WG2). Nanoparticles are constituted by a structure formed by 15-20 sheets of graphene, edge-oxidized at 4-10%. No information are available about the presence of dispersants.

Nanofluids Stability Characterization: nanoparticles stability in the dispersion has been evaluated applying a method based on the Dynamic Light Scattering (DLS) using a Zetasizer Nano ZS (Malvern) [8]. A sample of fluid is put into a proper cell, which is illuminated by a laser and the particles scatter the light which is measured using a detector. The particles move randomly and their speed is used to determine the particles dimension. The particle size measured in a DLS instrument is the diameter of the ideal sphere that diffuses at the same rate of the considered particle. This instrument can detect particle size from 0.6 nm to 6 μm using the DLS process, with a declared accuracy better than ±2%. All size measurements were made at 25 C° with a scattering angle of 173°. In order to verify the dependency of the diameter size from the concentration of the solution, each nanofluid was sonicated and the nanoparticle size was measured three times.

Thermal Conductivity apparatus: the thermal conductivity measurements were performed using a TPS 2500 S (Hot Disk), an instrument based on the hot disk technique which can measure thermal conductivity and thermal diffusivity of several materials [9]. The main parts of the instrument are the sensor, made of a double spiral of thin nickel wire that works as a continuous plane heat source and as a temperature sensor, a proper box containing the sensor and the fluid and a thermostatic bath to reach the test temperature. The conductivity data were measured at ambient pressure and in a temperature range between 10 and 70°C. The power supplied for each measurement was 30 mW and the time of the power input was 4 s. The declared instrument uncertainty is 5%.

Dynamic Viscosity apparatus: dynamic viscosity data were measured by means of an AR-G2 rheometer (TA Instruments), a rotational rheometer with magnetic bearing which permits ultra-low nanotorque control [10]. A plate-cone geometry with a 1° cone and diameter of 40 mm was employed and a proper device (Upper Heated Plate) was used to stabilize the measurement temperature. A constant quantity of sample, about 0.34 mL, was considered optimal for the analysis. Before the measurements, the rheometer was carefully calibrated at each temperature, as fully described
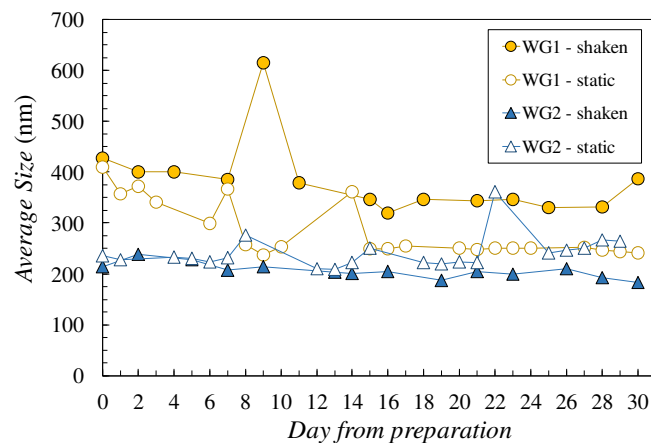
Figure 1. Variation along time of GO nanoparticles mean diameters.

in Bobbo et al. The dynamic viscosity data were measured at ambient pressure and in a temperature range between 10 and 70°C, with steps of 10°C. All the measurements were performed at constant temperature and variable shear rate. The declared instrument uncertainty is 5%.

Discussion and Results

Stability analysis: mean values of the nanoparticles nominal diameters at the starting time were 428 nm and 214 nm for WG1 and WG2, respectively. With the purpose to determine the tendency of the particles in suspension to settle down along time, two samples of the fluid were put in two different measurement cuvettes. The first sample was measured almost every day for thirty days, without shaking the fluid, to evaluate the changes in size distribution due to natural sedimentation. The second sample was measured almost every day for thirty days after sonication of the fluid to evaluate the changes in size distribution after mechanically removing the sedimentation [8]. The variations along time of the GO nanoparticles mean diameters are shown in Figure 1. The shaken WG1 sample average size slowly decrease along time stabilizing after 15 days at around 350 nm, while the static WG1 sample, after a quite fast decrease along the first 15 days, stabilizes at around 250 nm. This probably means that agglomerates with size over 250 nm are not stable and can be partially re-dispersed only after sonication. The starting average diameter of WG2 is below 250 nm and this is probably the reason why both shaken and static samples showed a quite constant size, in the range between 190 and 250 nm for all the thirty days of analysis. In any case, for both WG1 and WG2, no micrometric
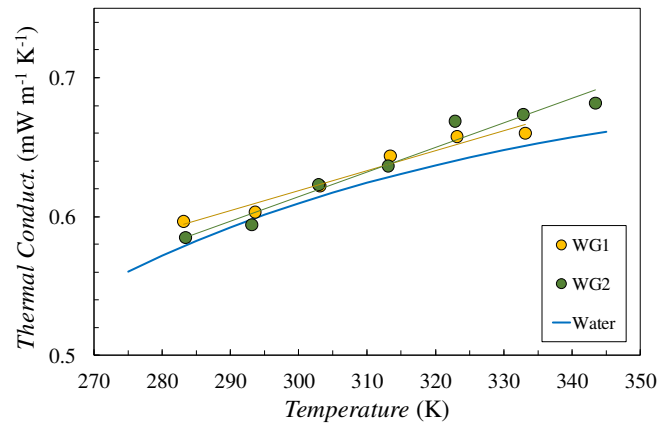
Figure 2: Thermal conductivity of the nanofluids as a function of temperature
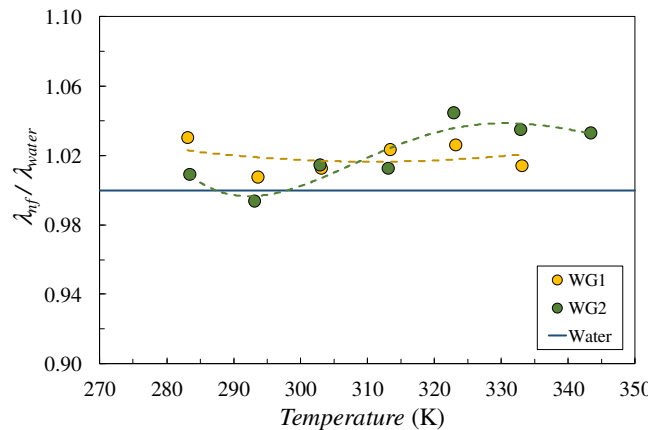
Figure 3: Thermal conductivity ratio between WG1 and WG2 nanofluids and water as a function of temperature

peaks were recorded in the period considered, suggesting there is no tendency of nanoparticles to further agglomerate.

Thermal Conductivity (λ): thermal conductivity data of the two nanofluids, measured from 283 to 333 K and 343 K for WG1 and WG2 respectively, are represented in Figure 2 and compared with the thermal conductivity of water, calculated with the database Refprop 9.1 [10]. For both nanofluids the thermal conductivity increases with temperature, as expected, and is very similar for both nanofluid, thus suggesting a very weak dependence on GO nanoparticles concentration. The fluctuation of λ with temperature are probably due to some instability of the nanofluids and anyway the differences shown by the two nanofluids are within the measurements uncertainties. Moreover, the increments with respect to water, more evident at the highest temperatures, are very moderate and do not suggest any special effect due to the presence of solid nanoparticles inside the base fluid. This is clearly represented in Figure 3, that shows the ratio ($\lambda_{nf}/\lambda_{water}$) between the thermal conductivities of the nanofluids and water. The ratio is practically constant for WG1 and weakly dependent on temperature for WG2, but in any case never exceeds 1.04, *i.e.* the maximum observed increment of thermal conductivity is 4%.

Figure 4: Viscosity of the nanofluids as a function of temperature in comparison with water

Viscosity (μ): the viscosity of the two nanofluids, measured from 283 to 313 K and 323 K for WG1 and WG2 respectively. Viscosity data are represented in Figure 4 and compared with the viscosity of water, calculated with the database Refprop 9.1 [11]. As shown, the viscosity of WG1 was close to that of water up to 303, with a more significant increase at 313 K, while the viscosity of WG2 is generally higher especially at the lowest and the highest temperatures. Figure 5

Figure 5: Viscosity ratio between WG1 and WG2 nanofluids and water as a function of temperature

shows the viscosity ratio (μ_{nf}/μ_{water}) between the viscosities of the nanofluids and water. The ratio for WG1 is almost constant and below 1.04 in the range of temperatures between 283 and 303 K, but suddenly increases to 1.24 at 313 K. For WG2, the ratio tends to increase with temperature from 293 and 323 K, ranging from 1.07 to 1.32, while an unexpected increase to 1.26 is obtained at the lowest temperature (283 K).

Conclusions: Stability, dynamic viscosity and thermal conductivity for two commercial nanofluids (named WG1 and WG2) formed by water and graphite-oxide nanoparticles at two different concentrations (1 mg/ml and 2 mg/ml) were analysed as a function of temperatures. Even if the nanofluids shown to be quite stable at ambient temperature along time, measured thermal conductivity and viscosity behaviour do not suggest any potentiality of the nanofluids to enhance the heat transfer efficiency of the nanofluids with respect to water: thermal conductivity is similar or only slightly higher than that of water in all the temperature range for both nanofluids, despite the very high thermal conductivity of graphene-oxide; at the same time, dynamic viscosity enhancement is negligible for WG1 but suddenly increases by 24% at 313 K, while it is quite significant for WG2, increasing from 7% to 32 % from 283 to 323 K, while is anomalously high (32) at the low temperature of 283 K.

References:

1. S. Choi and J.A. Eastman, Enhancing thermal conductivity of fluids with nanoparticles, *ASME International Mechanical Engineering Congress & Exposition*, San Francisco, CA, November 12-17, 1995.
2. M. Gupta, V., Singh, R. Kumar and Z. Said, A review on thermopysical properties of nanofluids and heat transfer applications, *Renewable and Sustainable Energy Review* 74 (2017) 638-670.
3. E.J. Park, S.D. Park, I.C. Bang, Y.B. Park and H.W., Park, Critical heat flux characteristics of nanofluids based on exfoliated graphite nanoplatelets (xGnPs). *Materials Letters* 81 (2012) 193–197.
4. C. Lee, X. Wei, J.W. Kysar, J. Hone, Measurement of the elastic properties and intrinsic strength of monolayer graphene. *Science* 321 (2008) 385–358.
5. B. Sun, B. Wang, D. Su, L. Xiao, H. Ahn, G. Wang, Graphene nanosheets as cathode catalysts for lithium-air batteries with an enhanced electrochemical performance. *Carbon* 50 (2012) 727–733.
6. A.A. Balandin, S. Ghosh, W. Bao, I. Calizo, D. Teweldebrhan, F. Miao and C.N. Lau, Superior thermal conductivity of single-layer graphene, *Nano Letters* 8 (2008) 902–907.
7. A.K. Rasheed, M. Khalid, W. Rashmi, T.C.S.M. Gupta, A. Chan, Graphene based nanofluids and nanolubricants – Review of recent developments, *Renewable and Sustainable Energy Reviews* 63 (2016) 346–362.
8. L. Fedele, L. Colla, S. Bobbo, S. Barison and F. Agresti, Experimental stability analysis of different water-based nanofluids, *Nanoscale Research Letters* 6 (2011) 300
9. L. Fedele, L. Colla, and S. Bobbo, Viscosity and thermal conductivity measurements of water-based nanofluids containing titanium oxide nanoparticles, *International Journal of Refrigeration* 35 (2012) 1359–1366.
10. S. Bobbo, L. Fedele, A. Benetti, L. Colla, M. Fabrizio, C. Pagura and S. Barison Viscosity

of water based SWCNH and TiO$_2$ nanofluids, *Experimental Thermal and Fluid Science* 36 (2012) 65–71.

11. E.W. Lemmon, M.L. Huber, M.O. McLinden, *NIST Standard Reference Database 23, Reference Fluid Thermodynamic and Transport Properties (REFPROP), version 9.1*, National Institute of Standards and Technology, Gaithersburg, MD, 2010.

RHEOLOGICAL PROPERTIES AND SURFACE TENSION OF STABLE GRAPHENE OXIDE AND REDUCED GRAPHENE OXIDE AQUEOUS NANOFLUIDS

D. Cabaleiro[1], P. Estellé[2],*, H. Navas[3], A. Desforges[3] and B. Vigolo[3]

[1]Dpto. Física Aplicada, Facultade de Ciencias, Universidade de Vigo, 36310 Vigo, Spain

[2]MTRhéo, LGCGM, Université Rennes 1, 35704 Rennes, France

[3]Institut Jean Lamour, CNRS-Université de Lorraine, BP 70239, 54506 Vandœuvre-lès-Nancy, France

*Corresponding author: patrice.estelle@univ-rennes1.fr

Keywords: Graphene, Nanofluid, Surface Tension, Rheological Behavior

Background: The improvements in thermal conductivity reported for nanofluids over the last two decades have evidenced the great potential of these new nanostructured materials to enhance the heat transfer performances of thermal installations. However, an efficient design and subsequent control of heat transfer facilities also require an accurate characterization of thermal or physical properties necessary to define the flow and dynamic wetting behavior of nanofluids, especially for microfluidic systems [1]. Thus, dynamic viscosity does not only influence flow regime but also affects pressure drop and consequent pumping power, while surface tension plays a major role in boiling and two-phase heat transfer flows, and in critical heat flux phenomena or heat pipes, for example [2;3].

Among the different nanomaterials used in the literature to design nanofluids, graphene is receiving increasing attention for its exceptional thermal properties, with ideal thermal conductivities higher than those of carbon nanotubes or diamond [4]. Unfortunately, pristine graphene (G) is hydrophobic and thus it tends to agglomerate in the presence of most of solvents and particularly in water, the most common thermal medium [5]. Alternatively, covalent functionalized graphene oxide (GO) contains hydroxyl and epoxy groups, which makes the material hydrophilic [6]. Nevertheless, the thermal conductivity of GO is considerably lowered compared to that of pristine graphene since the oxidation process destroys the sp^2 conjugated carbon structure of graphene. A controlled reduction of graphene oxide can restore part of graphene structure with a moderate decrease in hydrophilicity. The possibility of reaching a compromise between the advantages of G and GO confers to reduced graphene oxide (rGO) a great potential in the preparation of dispersions with improved thermal properties and long-term stabilities [7].

Tesfai et al. [8] and Kamatchi et al. [7] analyzed the rheological behavior of water-based nanofluids prepared at nanoadditive concentrations between 0.05 and 0.5 g/L of GO and between 0.01 and 0.3 g/L of rGO. Both studies reported non-Newtonian shear thinning behaviors at shear rates lower than 200 s^{-1} in the case of Tesfai et al. [8] and lower than 60 s^{-1} in

the case of Kamatchi et al. [7]; the phenomena being more pronounced as nanoadditive loading increases. Mehrali et al. [9] also carried out flow curve tests for graphene aqueous dispersions prepared using nanoadditives with three different specific surface areas and the authors found a pseudoplastic behavior at low shear rates for some nanofluids. As regards previous works on surface tension, Kamatchi et al. [7] and Zheng [10] studied rGO/water nanofluids and reported increases in this property with rGO concentration up to 3%. In addition, Ahammed et al. [11] experimentally investigated graphene/water nanofluids stabilized with SDBS and observed that surface tension decreases with nanoadditive concentration up to 13.8%.

The present study aims to analyze the effect that nanoparticle loading and graphene functionalization have on rheological behavior and surface tension of graphene aqueous nanofluids. Three different nanofluid sets based on GO and two different rGO at six nanoparticle volume fractions ranging from 0.0005 to 0.1% were studied.

Experimental Method:

The derived Hummers' method was used to prepare GO [12]. Briefly, 2.5 g graphite powder (SFG_6 Primary Synthetic Graphite from Timcal Inc.) and 1.9 g of $NaNO_3$ are added to 85 mL of sulfuric acid and 12.5 g of potassium permanganate at temperature below 20°C. After 2 h at 35°C under stirring, 125 mL of deionized water are slowly added to the above solution and followed by the addition of 10 mL of oxygenated water. GO is then rinsed several times with 10 vol.% hydrochloric acid and water. rGO was prepared by reduction of GO (0.2 vol.%) with various amounts of a 2 vol.% sodium borohydride ($NaBH_4$) solution. Typically, for the nanofluid series studied, concentrations of $NaBH_4$ are 0.2 vol.% (rGO_0.2) and 0.1 vol.% (rGO_0.1). Introduction of oxygen containing groups at the GO surface and also at rGO surface since the chemical reduction is never complete is responsible for a dramatic hydrophobicity reduction. This improved affinity of graphene with water induces a facile dispersion of GO/rGO without any use of surfactant. The GO/rGO solutions were simply homogenized with a low power sonication bath for a few minutes. Flow curve experiments were performed at temperatures of 20 and 30ºC by using a Malvern Kinexus Pro rheometer (Malvern instruments, UK) working with a cone-plate geometry with a diameter of 60 mm, a cone angle of 1º and a gap of 0.03 mm, appropriate for studying low-viscosity colloidal dispersions. Tests were performed in steady-state regime at shear stress logarithmically increasing from 0.01 to 2 Pa with at least 7 points per decimal, necessary to cover the range of shear rates between 10 and 1000 s^{-1}. The estimated uncertainty of this device is less than 4% within the studied shear rate range [13]. Surface tension measurements were carried out at room temperature with a Drop Shape Analyzer DSA-30 (KRÜS, Germany) based on the pendant drop technique. This device records and digitally analyzes the shape of sample drop formed at the end of a vertical syringe just in the moment when the drop snaps from the apex of the needle. Surface tension is obtained from a drop shape analysis through a balance of internal and external forces acting on the drop from Young-Laplace equation with an accuracy better than 0.3 mN/m as given by supplier device. In this study a 15-gauge needle with an outer diameter of 1.83 mm was utilized to produce drops with a volume of around 30 µm. Studies were carried out taking special care to capture the image of the pendant drop as soon as it was formed in order to limit possible perturbations due to air currents and ambient humidity.

Discussion and Results: Stability of the prepared nanofluids was followed by both optical microscopy and visual observation of the solutions over time as shown by Figure 1 which evidences the stability of produced nanofluids. The rheological behaviors of the base fluid and the different nanofluid sets were investigated at temperature of 20 and 30ºC. Results obtained for distilled water exhibit absolute average deviations lower than 1.5% with previous literature [14]. Figure 2 shows the flow curves obtained at 30ºC for different concentrations of the GO and rGO_0.2 nanofluid sets. The result found for the rGO_0.1 are similar to the current presented for rGO_0.2. As it can be observed, nanofluids prepared at volume concentrations lower than or equal to 0.01% follow a Newtonian behavior within the studied shear rate range while a shear-thinning behavior was observed for higher concentrations.
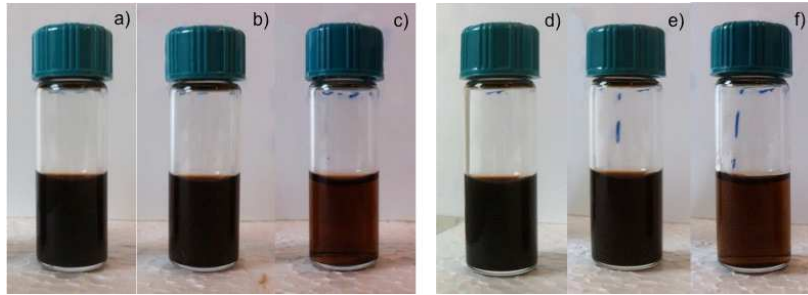
Figure 1. Photographs of rGO_0.1 (a, b and c) and rGO_0.2 (d, e and f) nanofluids one month after their preparation for different nanoparticle volume concentrations: 0.1 (a, d), 0.05 (b, e) and 0.01% (c, f)
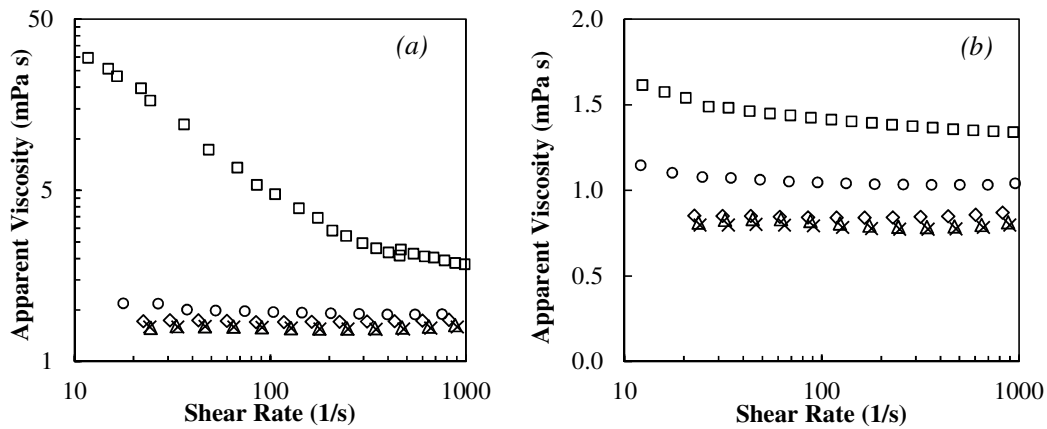
Figure 2. Flow curves of GO (a) and rGO_0.2 (b) nanofluid sets at 30ºC and different nanoparticle volume concentrations: ($\times$) Base Fluid, 0, ($\triangle$) 0.0005,

($\diamondsuit$) 0.01, ($\bigcirc$) 0.05 and ($\square$) 0.1 Vol.%.

Figure 3 presents the relative viscosity values of the three nanofluids sets obtained at a shear rate of about 900 s^{-1} and a temperature of 20ºC. The figure shows that relative viscosity increases with nanoparticle concentration. However, chemical reduction does not have a strong influence on the dynamic and relative viscosity increases, except for the highest nanoparticle concentration for which the rise in this property is considerably higher in the case of GO than for rGO nanofluid sets. Comparing the two studied temperatures, increases in dynamic viscosity at 0.1% volume fraction are higher at 30ºC than at 20ºC, while the variations are within experimental uncertainty for the rest of concentrations. As expected viscosity of nanofluids decrease with the increase in temperature. Also, the evolution of relative viscosity at higher temperature of 30°C is quite similar to 20°C. Finally, relative viscosity appears to be quite independent of tested temperature whatever the nanoparticle content.
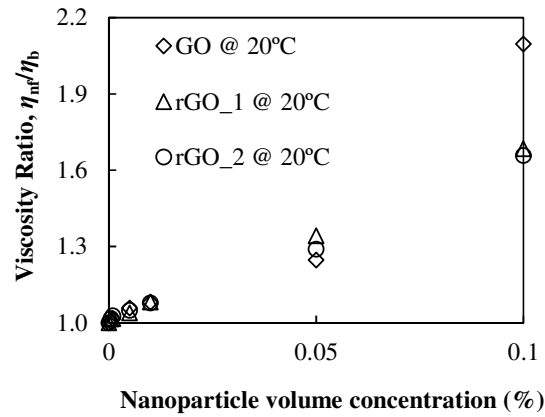
Figure 3. Relative viscosity vs. nanoparticle volume concentration at 20ºC and 900 s^{-1} for:

($\diamond$) GO, ($\triangle$) rGO_0.1 and ($\bigcirc$) rGO_0.2 nanofluid sets.

With the aim of checking the calibration and the followed procedure for measurements, surface tension was first studied for distilled water, ethylene glycol, and toluene at room temperature. A good agreement between literature values and our experimental results was found, with deviations lower than 1.3%. Afterwards, the influence of the nanoadditive concentration on the surface tension of the three sets was analyzed. As an example, captures of the drops obtained for three concentrations of the rGO_0.1 nanofluid set are shown in Figure 3. It was observed that surface tension decreases as graphene loading increases, with a maximum reduction of about 3% for the highest volume fractions, 0.1 vol.%, and without a clear effect of the chemical reduction.
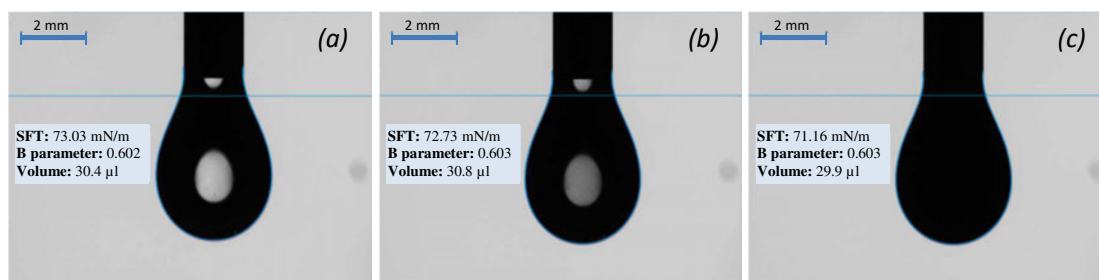
Figure 4. Pendant drop images of rGO_0.1 nanofluids at: (a) 0.0005, (b) 0.005, and (c) 0.1% volume concentrations.

Conclusions: Rheological and surface tension properties of stable reduced graphene nanofluids were experimentally studied. A Newtonian behavior was observed in the analyzed shear rate range for graphene volume fractions lower or equal to 0.01% while nanofluids with higher concentrations exhibit a shear-thinning behavior. Dynamic viscosities for the GO nanofluid are higher that of rGO ones at 0.1 vol.% while differences in this property are similar to experimental uncertainty when comparing the three nanofluid sets at the other concentrations. These results show the influence of chemical treatment on the dispersion state and stability of graphene nanofluids for high concentration considered. Surface tension decreases as graphene loading increases, with maximum reductions of about 3% for the highest volume fractions and without a clear effect of the graphene functionalization process.

References:

1. S.M.S. Murshed, S.H. Tan and N.T. Nguyen, *Journal of Physics D: Applied Physics* 41 (2008) 085502.
2. J. Chinnam, D.K. Das, R.S. Vajjha and J.R. Satti, *International Journal of Thermal Sciences* 98 (2015) 68-80.
3. S.M.S. Murshed and P. Estellé, *Renewable and Sustainable Energy Reviews* 76 (2017) 1134-1152.
4. D. Cabaleiro, L. Colla, S. Barison, L. Lugo, L. Fedele and S. Bobbo, *Nanoscale Research Letters* 12 (2017) 53.

5. E.J. Kim, A. Desforges, L. Speyer, J. Ghanbaja, J. Gleize, P. Estellé and B. Vigolo, *Journal of Nanofluids* 6 (2017) 603-613.

6. P. Bansal, A.S. Panwar and D. Bahadur, *Journal of Physical Chemistry C* 121 (2017) 9847–9859.

7. R. Kamatchi, S. Venkatachalapathy and B. Abhinaya Srinivas, *International Journal of Thermal Sciences* 97 (2015) 17-25.

8. W. Tesfai, P. Singh, Y. Shatilla, M.Z. Iqbal, A.A. Abdala, *Journal of Nanoparticle Research* 15 (2013) 1989.

9. M. Mehrali, E. Sadeghinezhad, S.T. Latibari, S.N. Kazi, M.N.B.M. Zubir and H.S.C. Metselaar, *Nanoscale Research Letters* 9 (2014) 15.

10. Z. Zheng, *Advanced Materials Research* 1082 (2015) 297-301.

11. N. Ahammed, L.G. Asirvatham and S. Wongwises, *Journal of Thermal Analysis and Calorimetry* 123 (2016) 1399-1409.

12 W.S. Hummers Jr., R.E. Offeman, *Journal of the American Chemical Society* 80 (1958) 1339-1339.

13. S. Halelfadl, P. Estellé, B. Aladag, N. Doner and T. Maré, *International Journal of Thermal Sciences* 71 (2013) 111-117.

14. E.W. Lemmon, M.L. Huber, M.O. McLinden, *Reference Fluid Thermodynamic and Transport Properties (REFPROP); NIST Standard Reference Database; National Institute of Standards and Technology,* Gaithersburg, MD, USA, 2010.

NANOFLUIDS ANALYSIS MODEL - BASIS FOR COMPARISON AND PREDICTION

E.W. Marcelino, D. de O. Silva and R.R. Riehl*

National Institute for Space Research, INPE/DMC,
Av dos Astronautas 1758, São José dos Campos, 12227-010 SP Brazil
*Corresponding author: roger.riehl@inpe.br

Keywords: Thermal enhancement, Viscosity, Statistical model, Nanofluids

Abstract: With current increase on the application of nanofluids to enhance the heat transfer capabilities of systems, there is a challenge to accurately compare the available nanofluid results from different authors. Researches show several experimental data using Al_2O_3 (alumina) and CuO (copper oxide) nanofluids, which lead to potentially applying them in several areas, especially industrial and aerospace. However, when comparing the results obtained by different authors, discrepancies are observed even for the same nanoparticle material and size used to form the nanofluid, which directly impact the results related to thermal conductivity, viscosity and density. Therefore, this study has the objective to evaluate some available results in the literature for CuO-water nanofluids comparing the obtained thermal enhancement results with the nanoparticle sizes used, as well as the direct influence on their viscosities. The objective is to provide some statistical trends through the reviewed data by using CuO-water nanofluid based on their particular characteristics.

Introduction:

The study of nanofluids has increased since Choi [1] established the term "nanofluids". Several nanofluid thermophysical properties and their characteristics have been experimentally tested and studied such as viscosity, density and thermal conductivity. Thermal conductivity is the most studied nanofluid property due to the fact that it is related to the increase on the nanofluid thermal enhancement levels obtained when compared to the base fluids. The most used base fluids for preparing the nanofluid are water, ethylene glycol and engine oil, which can be widely applied to several industrial, aerospace and automotive needs. The study of nanoparticle size and its influence on thermal conductivity has been of great interest for several authors [2]. In general, theoretical and experimental studies included the impact of nanoparticles sizes in their models. It is common to find in the literature the average nanoparticle sizes through statistical data over a range of nanoparticle size distribution. However, it is unusual to obtain the same nanoparticle size and shape over the volume concentration (vol.%) of nanoparticles used in any nanofluid.

Thermal conductivity and viscosity models related to nanoparticle sizes:

A review on the literature was performed to evaluate the results obtained for CuO-water nanofluid, related to the thermal conductivity and viscosity models. Tables 1 and 2 summarize

the investigated models and demonstrate how each one consider the nanoparticle size influence on the thermal conductivity or thermal enhancement ratio [3]. The thermal conductivity determination depends on other parameters besides nanoparticle sizes, such as volume fraction, temperature and sonication time. It is clear that even using the same CuO nanoparticle sizes, volume fractions and sonication times different results were obtained by different authors. This is directly related to differences on the nanoparticle purity and preparation from one study to another, as well as differences on nanoparticle shape and average sizes. Following the same trend, Table 3 shows the viscosity models available as well as their considerations on the direct impact on the nanofluid [3]. Since the nanoparticle addition on the base fluid directly changes the nanofluid's dynamic viscosity, the pumping power required to drive the nanofluid throughout the system may present higher levels than those predicted previously.

Table 1. A summary of thermal conductivity models.

Author	Model	Comments
Maxwell [4]	$k_{eff} = k_p + 2k_f + 2\phi_p(k_p - k_f)$ $k_f = k_p + 2k_f - \phi_p(k_p - k_f)$	Based on spherical particles, random suspensions which must be under conduction solution theory through stationary conditions
Hamilton [5]	$k_{eff} = \dfrac{k_p + (n-1)k_f + (n-1)\phi_p(k_p - k_f)}{k_p + (n-1)k_f - \phi_p(k_p - k_f)}$	For high concentrations of spherical particles under conditions of differential effective medium (DEM) theory
Prasher et al. [6]	$k_{eff} = \left(1 + ARe^m Pr^{0.333}\phi_p\right)\left[\dfrac{k_p + 2k_f + 2\phi_p(k_p - k_f)}{k_p + 2k_f - \phi_p(k_p - k_f)}\right]k_f$	Obtained from Maxwell model and included the effects of correction generated by the Brownian motion
Koo and Kleinstreuer [7]	$k_{eff} = k_{static} + k_{Brownian}$ $k_{static} = \dfrac{k_p + 2k_f + 2\phi_p(k_p - k_f)}{k_p + 2k_f - \phi_p(k_p - k_f)}$ $k_{Brownian} = 5x10^4 \beta \phi_p \rho_p c_p \sqrt{\dfrac{k_B T}{\rho_p D}} (T, \phi_p)$	Considers the effects of surrounding liquid motion with random nanoparticles movement. Based on static Maxwell theory and dynamic effect of Brownian motion
Yu and Choi [8]	$k_{eff} = \dfrac{k_p + 2k_f + 2\phi(k_{pe} - k_f)(1+\beta)^3}{k_{pe} + 2k_f - \phi(k_{pe} - k_f)(1+\beta)^3}k_f$ $k_{pe} = \dfrac{2(1-\gamma) + (1+\beta)^3(1+2\gamma)\gamma}{-(1-\gamma) + (1+\beta)^3 + (1+2\gamma)}k_p$	It was based on Maxwell model but addionally taking into account the effects of nanolayer thickness and thermal conductivity parameters

Even with the gain obtained with the increase on the thermal conductivity and on the overall heat transfer capability may not be worth applying the nanofluid, due to the increase on the pumping power and the direct impact on the increase of the energy required to run the cycle. Therefore, the entire system would require to be redesigned increasing its hydraulic diameter to compensate the increase on the pressure drop. However, the tradeoff must be carefully considered and most often, redesigning the system will be well paid off due to the increase on the overall heat transfer compared to the drawback caused by the increase on the pressure drop.

Table 2. Different nanoparticle sizes applied in CuO-water nanofluid and their respective thermal enhancement ratios.

Author	CuO Nanoparticle Size (nm)	Thermal Enhancement Ratio	Volume Fraction (vol.%)	Temperature (°C)	Sonication Time (h)
	8.0	1.020	0.020	20	0.5
	8.0	1.080	0.090	20	0.5
Karthikeyan et al [9]	8.0	1.130	0.100	20	0.5
	8.0	1.190	0.300	20	0.5
	8.0	1.250	0.800	20	0.5
	8.0	1.316	1.000	20	0.5
	33.0	1.197	0.500	55	1
Nemade et el [10]	42.0	1.134	0.500	55	0.75
	46.0	1.124	0.500	55	0.5
	53.5	1.087	0.500	55	0.25
	25.0	1.050	0.010	26	1.5
	25.0	1.120	0.020	26	1.5
Khedkar et al [11]	25.0	1.130	0.030	26	1.5
	25.0	1.160	0.040	26	1.5
	25.0	1.170	0.050	26	1.5
	25.0	1.320	0.075	26	1.5
	42.5	1.080	0.020	25	
Wang et al [12]	42.5	1.100	0.040	25	
	42.5	1.110	0.100	25	not informed
	42.5	1.125	0.150	25	
	42.5	1.160	0.400	25	
	50.0	1.020	0.004	28	6
	50.0	1.060	0.008	28	6
	50.0	1.100	0.012	28	6
	50.0	1.130	0.016	28	6
	50.0	1.050	0.004	50	6
Pryia et al [13]	50.0	1.160	0.008	50	6
	50.0	1.250	0.012	50	6
	50.0	1.320	0.016	50	6
	50.0	0.950	0.004	55	6
	50.0	1.240	0.008	55	6
	50.0	1.330	0.012	55	6
	50.0	1.430	0.016	55	6

Table 3. Viscosity models.

Author	Model	Comments
Einstein [14]	$\mu_{eff} = \left(1 + 2.5\phi_p\right)\mu_f$	Based on phenomenological hydrodynamic equation for infinitely diluted suspensions of spheres with no interaction between spheres. Works well for maximum volume concentration of 2%
Brinkman [15]	$\mu_{eff} = \dfrac{1}{\left(1 + 2.5\phi_p\right)^{2.5}}\mu_f = \left(1 + 2.5\phi_p + 4.375\phi_p^2 + \cdots\right)\mu_f$	Extended Einstein's model by considering the effect of addition of one solute molecule to an existing solution.
Buongiorno [16]	$\mu_{eff} = \left(1 + 39.11\phi_p + 533.9\phi_p^2\right)\mu_f$ $\mu_{eff} = \left(1 + 5.45\phi_p + 108.2\phi_p^2\right)\mu_f$	Curve fitting from experimental data of Al2O3-water nanofluid
Nguyen et al. [17]	$\mu_{eff} = \mu_f 0.904 e^{0.148\phi_p}$ $\mu_{eff} = \left(1 + 0.025\phi_p + 0.015\phi_p^2\right)\mu_f$	Curve fitting from experimental data of Al2O3-water nanofluid
Chen et al. [18]	$\mu_{nf} = \mu_{bf}\left[1 + 10.6\phi_p + \left(10.6\phi_p\right)^2\right]$	Adjusted model for experimental versus theoretical data by considering the rheological effects of shear-rate
Kulkami et al. [19]	$ln\left(\mu_{eff}\right) = A\left(\dfrac{1}{T}\right) - B$ $A = 20587\phi_p^2 + 15857\phi_p + 1078.3$ $B = -107.12\phi_p^2 + 53.54\phi_p + 2.8715$	Curve fiting from experimental CuO-water: $5\% < \Phi_p < 15\%$ dp=29 nm; 278 < T(K) < 323; shear rate = 100 l/s
Namburu et al. [20]	$log\left(\mu_{eff}\right) = A e^{-BT}$ $A = -0.29956\phi_p^3 + 6.738\phi_p^2 - 55.444\phi_p + 236.11$ $B = -6.4745\phi_p^3 + 140.03\phi_p^2 - 1478.5\phi + 20341$	Curve fitting from experimental data of Al2O3-ethylene-glycol nanofluid: $1\% < \Phi_p < 10\%$; dp=53 nm; 278<T (K)<323
Adedian et al. [21]	$\mu_{nf} = \dfrac{\mu_{bf}}{\left(1 - \dfrac{5}{2}\phi_p\right)}$	Extention of Einstein's equation for obtaining good agreement in volume concentration ranges of up to 18-20% in suspension system non-interacting with spherical particles.
Meybodi et al. [22]	$\mu_{nf} = \mu_{bf}\dfrac{A_1 + A_2 exp\left(\frac{\phi_p}{S}\right) + A_3\left[exp\left(\frac{\phi_p}{S}\right)\right]^2 + A_4\left[exp\left(\frac{\phi_p}{S}\right)\right]^3}{A_5 + A_6\frac{ln(S)}{T} + A_7\frac{[ln(S)]^2}{T}}$ $A_1 = 1.3354064976 x 10^2$ $A_2 = -3.4382413843 x 10^2$ $A_3 = 2.9011804759 x 10^2$ $A_4 = -78993120761 x 10^1$ $A_5 = 9.1161630781 x 10^{-1}$ $A_6 = 3.2330142333 x 10^1$ $A_7 = -1.1732514460 x 10^1$	Model obtained from experimental data, which takes into account volume concentration, nanoparticles size and temperature

Conclusions:

The following conclusions can be derived from this study:

- Nanoparticle size can vary according to sonication time;

- As nanoparticle sizes increases, the thermal conductivity decreases;
- Further investigation is necessary for better understanding the impacts over each size percentage of the statistical nanoparticle size distribution versus thermal and pressure drop enhancement ratios;
- The addition of solid nanoparticles in the base fluid directly cause the increase on the nanofluid's viscosity, which impacts on the increase of the overall pressure drop. Proper consideration on the tradeoff related to the enhancement of the overall thermal capability of the system compared to the increase of the pumping power must be done in order to better evaluate the application of nanofluids.

Better evaluation regarding the nanofluid design and application needs to be performed, in order to better predict their thermal behavior, along with the impact on the overall pressure drop. A statistical model that considers the most important aspects of a nanofluid can highly contribute to this purpose.

References

1. S.U.S Choi, Enhancing thermal conductivity of fluids with nanoparticles, *ASME FED* 231 99–105 1995.
2. S.K. Das, S.U.S Choi, W. Yu, T. Pradeep, *Nanofluids Science and Technology,* John Wiley & Sons Inc., New Jersey, 2008.
3. E.W. Marcelino, D. Silva, R.R. Riehl, A review on the influence of nanoparticle size in thermal management of CuO-water nanofluids and their characteristics, *Heat Powered Cycles Conference*, Nottingham, UK, June 27-29, 2016.
4. J.C. Maxwell, *A Treatise on Electricity and Magnetism*, Claredon Press, 2ª Ed., Oxford, UK, 1881.
5. R.L. Hamilton, Thermal conductivity of heterogeneous two-component systems, *Ind Eng Chem Fundam* 1 (1962)182-191.
6. R. Prasher, P. Bhattacharya, P.E. Phelan, Thermal conductivity of nanoscale colloidal solutions (nanofluids), *Phys Rev Lett*. 94 (2005)1-4.
7. J. Koo, C. Kleinstreuer, Laminar nanofluid flow in microheat-sinks, *Int J Heat and Mass Transfer* 48 (2005) 2652-2661.
8. W. Yu, S.U.S. Choi, The role of interfacial layers in the enhanced thermal conductivity of nanofluids: a renovated Maxwell model, *J. Nanoparticle Research* 5 (2003) 167-171.
9. N.R. Karthikeyan, J. Philip, B. Raj, Effect of clustering on the thermal conductivity of nanofluids, *Material Chem. Phys.*, 109 (2008) 50–55.
10. K. Nemade, S. Waghuley, A novel approach for enhancement of thermal conductivity of CuO/H2O based nanofluids, *Applied Thermal Eng*. 95(2016)271-274.
11. R.S. Khedkar, S.S. Sonawane, K.L. Wasewar, Influence of CuO nanoparticles in enhancing the thermal conductivity of water and monoethylene glycol based nanofluids, *Int Comm in Heat and Mass Transfer* 39(2012)665-669.
12. X.J. Wang, X.F. Li, Influence of pH on nanofluids' viscosity and thermal conductivity, *Chin Phys Lett* 26(2009)056-061.

13. K.R. Priya, K.S. Suganthi, K.S. Rajan, Transport properties of ultra-low concentration CuO–water nanofluids containing non-spherical nanoparticles, *Int J of Heat and Mass Transfer* 55(2012)4734-4743.
14. A. Einstein, Eine neue bestimmung der moleküldimensionen, *Ann Phys* 324(1906)289–306.
15. H. Brinkman, The viscosity of concentrated suspensions and solutions, *J Chem Phys* 20 (1952) 571–571.
16. J. Buongiorno, Convective transport in nanofluids, *Journal of Heat Transfer* 128(2006)240-250.
17. C.T. Nguyen, F. Desgranges, G. Roy, N. Galanis, T. Mafe, S. Boucher, H.A. Mintsa, Temperature and particle-size dependent viscosity data for water-based nanofluids - hysteresis phenomenon, *Int J Heat Fluid Flow* 28(2007)1492-156.
18. H. Chen, Y. Ding, C. Tan. Rheological behaviour of nanofluids, *New Journal of Physics* 9 (2007) 367.
19. D.P. Kulkarni, D.K. Das, S.L. Patil, Effect of temperature on rheological properties of copper oxide nanoparticles dispersed in propylene glycol and water mixture, *J Nanoscience Nanotechnology*, 7(2007)2318-2322.
20. P.K. Namburu, D.K. Das, K.M. Tanguturi, R.S. Vajjha, Numerical study of turbulent flow and heat transfer characteristics of nanofluids considering variable properties, *Int J Therm Science* 48(2009)290-302.
21. B. Abedian, M. Kachanov, On the effective viscosity of suspensions, *Int J Eng Sci* 48(2010)962–5.
22. M.K. Meybodi, A. Daryasafara, M.M. Koochia, J. Moghadasia, R.B. Meybodib, A.K. Ghahfarokhia, A novel correlation approach for viscosity prediction of water based nanofluids of Al_2O_3, TiO_2, SiO_2 and CuO, *Journal of Taiwan Institute of Chemical Engineers* 58(2015)19-27.

A NEW ANALYTICAL MODEL FOR THE EFFECTIVE THERMAL CONDUCTIVITY OF NANOFLUIDS

T.M. Koller[*,] **K.N. Shukla, M.H. Rausch and A.P. Fröba**

Erlangen Graduate School in Advanced Optical Technologies (SAOT) ,

Friedrich-Alexander-University Erlangen-Nürnberg (FAU) ,

Paul-Gordan-Straße 6, D-91052 Erlangen, Germany

[*]Corresponding author: thomas.m.koller@fau.de

Keywords: Effective thermal conductivity, Modeling, Nanofluids, Nanoparticles

Introduction: Dispersions of nanometer-sized particles in liquids, usually called nanofluids, have been reported to possess substantially higher thermal conductivities than anticipated from Maxwell's classical theory [1]. A large number of experimental results have claimed an anomalous increase in the thermal conductivity of nanoparticle suspensions [2], which would make them very attractive as potential heat transfer fluids for many applications. However, results from other experiments have not shown any anomalous increase in thermal conductivity [2,3]. This has triggered controversy regarding the actual value of the thermal conductivity of nanofluids and the reliability of the experimental methods.

The aim of the present study is to develop a new analytical model for the effective thermal conductivity of macroscopically static nanofluids taking into account the heat transfer mechanisms caused by convection as well as thermal conduction of the particles and the base fluid. It should enable the prediction of the temperature-dependent effective thermal conductivity of nanofluids as a function of volume fraction, diameter, and shape of the nanoparticles. The main information on our developed model [4] is given below.

Description of the model: In the presented analytical model, the thermal resistances of the base fluid and the nanoparticles as well as of convection induced in the fluid due to Brownian motion of the nanoparticles are determined. It is assumed that N nanoparticles of spherical shape with diameter d_p are uniformly suspended in a volume V of the nanofluid. By this, a corresponding volume fraction of the nanoparticles φ is given. The volume V is divided into N equal parts such that each nanoparticle is located in a cube with a side of length L. Fig. 1a depicts a three-dimensional sketch of such a nanoparticle-cube system.
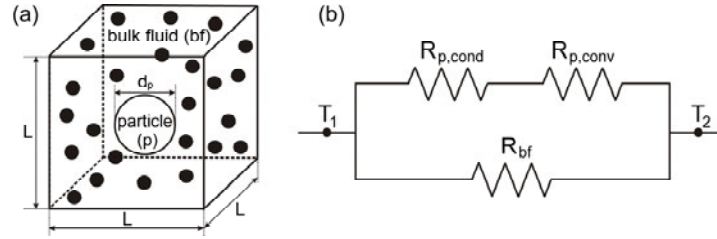
Fig. 1: (a) Conceptual three-dimensional sketch of a cube with length L containing a spherical nanoparticle of diameter d_p and bulk fluid molecules. (b) Circuit diagram for the thermal resistances of the bulk fluid due to conduction and of the nanoparticle due to conduction and convection associated with Brownian motion.

The basic idea of the present modeling approach is to treat the heat transfer problem in connection with nanofluids by the analysis of the thermal resistances present in such systems. In Fig. 1b, the corresponding circuit diagram for the total thermal resistance of the nanofluid R_{eff} subjected to a temperature difference between the hot temperature T_1 and cold temperature T_2 is illustrated based on the cube shown in Fig. 1a. The thermal resistance of the base fluid, R_{bf}, is considered to be parallel to the thermal resistance of the nanoparticle, R_p. Thus, R_{eff} can be expressed by

$$\frac{1}{R_{eff}} = \frac{1-\varphi}{R_{bf}} + \frac{\varphi}{R_p} \ . \tag{1}$$

Arranging the resistances of the bulk fluid and the particles in parallel is reasonable because a heat flux can be either conducted through the base fluid or through the particle along a one-dimensional temperature gradient. The key for a realistic description of the thermal resistance of the nanofluid is that the base fluid as a continuum fluid phase is analogously treated as a continuum resistance. To account for the volumes in which the resistances of the two phases are present, the inverse values of the thermal resistances R_{bf} and R_p are weighted in Eq. (1) by the corresponding volume fractions $(1-\varphi)$ and φ.

R_{eff} and R_{bf} are related to the thermal conductivities k_{eff} and k_{bf}, respectively, and the cube geometry. The thermal resistance caused by heat transfer between the nanoparticles and the boundary layer is modeled by the resistance of the sphere due to thermal conduction, $R_{p,cond}$, and by that due to convection at its surface, $R_{p,conv}$, in series. The term $R_{p,conv}$ depends on the surface area of the particle A_p and the convective heat transfer coefficient h. The latter can be expressed by a corresponding correlation for the Nußelt number Nu for creep flow around nanoparticles. In connection with A_p, the sphericity of a particle can be used which is the ratio of the surface area of a sphere, $A_{p,sph}$, having the same volume as the particle, V_p, to the surface area of the particle, A_p. Decreasing sphericity of the particles ($\psi < 1$) results in an increasing surface area and a decreasing value for $R_{p,conv}$.

The final simple expression for the dimensionless effective thermal conductivity k_{eff}/k_{bf} of nanofluids containing spherical or non-spherical particles

$$\frac{k_{\mathrm{eff}}}{k_{\mathrm{bf}}} = (1-\varphi) + \pi\left(\frac{6}{\pi}\right)^{1/3}\varphi^{4/3}\left[\frac{1+0.5\left(\frac{6\varphi}{\pi}\right)^{1/3}}{2}\left(\frac{k_{\mathrm{bf}}}{k_{\mathrm{p}}}\right) + \frac{\psi}{Nu}\right]^{-1} \tag{2}$$

contains three contributions. The first term $(1-\varphi)$ considers the influence of the bulk fluid while the second term is related to the nanoparticles. In the latter term, the brackets include the contributions from conduction through the particles (associated with the thermal conductivity of the particle k_{p}) and from convective heat transfer between the particles and the bulk fluid (given by ψ/Nu).

Discussion and Results: To analyze the quality of our model for the effective thermal conductivity of nanofluid systems by Eq. (2), we selected the four simple systems Al_2O_3/H_2O, TiO_2/H_2O, Al_2O_3/EG, and TiO_2/EG, containing the liquids water (H_2O) and ethylene glycol (EG) as well as the particles aluminum oxide (Al_2O_3) and titanium dioxide (TiO_2). Data for the thermophysical properties of the nanoparticles and base fluids at atmospheric pressure were employed from literature.

In Fig. 2a, the percentage enhancement factor ($k_{\mathrm{eff}}/k_{\mathrm{bf}} - 1$) calculated according to Eq. (2) is shown as a function of the volume fraction φ of spherical particles for the two systems Al_2O_3/EG and TiO_2/H_2O at a temperature of $T = 300$ K. Regarding the influence of convection, the enhancement found on basis of our model, which includes the effect of convection due to Brownian motion, is compared with a "theoretical" enhancement which does not account for this effect. The system related to the latter enhancement would consist of static particles suspended in the liquid, neglecting any thermal resistance in the boundary layer where heat is transferred from the liquid to the solid particle. In this case, $R_{\mathrm{p,conv}} = 0$ which is equivalent to omitting the term ψ/Nu in Eq. (2). Neglecting the thermal resistance contribution from the convective heat transfer between particles and base fluid results in much larger enhancement factors because the thermal resistance of the nanoparticle is significantly reduced to only the resistance of conduction through the particle $R_{\mathrm{p,cond.}}$. Of course, an enhancement of the convective heat transfer with, e.g., increasing Nu numbers decreases the corresponding resistance, but this effect is rather small with respect to k_{eff}. This is caused by the almost stagnant flow behavior of nanoparticles in the fluid. These findings valid for nanofluids with spherical particles are in contradiction to the widely spread opinion in the literature [5,6] that convection associated with Brownian motion of the particles is mainly responsible for the enhancement of the effective thermal conductivity of nanofluids.
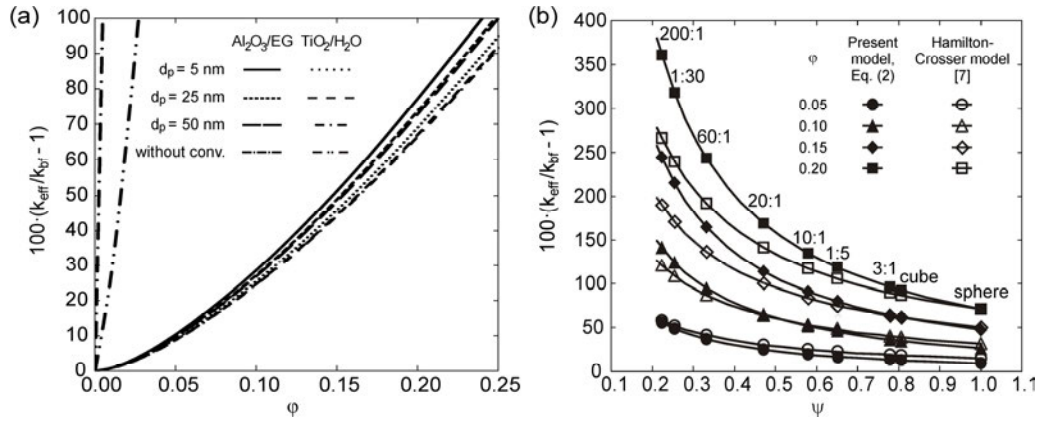
Fig. 2: (a) Percentage enhancement factor ($k_{eff}/k_{bf} - 1$) on the basis of Eq. (2) as a function of the volume fraction φ for different diameters d_p of spherical particles at $T = 300$ K for the nanofluids Al_2O_3/EG and TiO_2/H_2O. (b) Percentage enhancement factor as a function of the sphericity of the particle ψ at $T = 300$ K for the nanofluid Al_2O_3/H_2O containing volume-equivalent (diameter 30 nm) nanoparticles of different shape calculated by the present model (Eq. (2)) and the Hamilton-Crosser model [7] for various φ values.

Fig. 2a also shows that the effective thermal conductivity increases with increasing φ. Mainly due to the about eight times larger k_p/k_{bf} ratio for Al_2O_3/EG than for TiO_2/H_2O, enhancement in the effective thermal conductivity is stronger for Al_2O_3/EG for a given particle size. For $\varphi = 0.25$ and $d_p = 5$ nm, a difference in the enhancement of about 11% is found for the two nanofluids. For all the systems studied, k_{eff}/k_{bf} decreases with increasing particle size. The influence of temperature on the effective thermal conductivity enhancement of nanofluids is even less pronounced for various φ and d_p values.

Due to the obscure situation of experimental data in the literature [2], we preferred to check our model by comparing with other common models in the literature. Here, the effective medium model of Hamilton and Crosser [7] is considered to be one of the most reliable ones. For all the nanofluid systems tested, very good agreement between our model and the continuum model of Hamilton and Crosser [7] for various particle volume fractions is found. Regarding the enhancement factors, the relative deviations between the continuum model and ours are less than 8% for volume fractions between 0 and 0.25 for the studied conditions. Also for varied temperatures and particle diameters, this deviation is not exceeded. The very good agreement of the Hamilton-Crosser model [7] with our model indicates that the convective heat transfer associated with the Brownian motion of the nanoparticles needs to be considered for the heat transfer in nanofluids.

In Fig. 2b, the enhancement of the thermal conductivity ($k_{eff}/k_{bf} - 1$) modeled according to our prediction from Eq. (2) is exemplarily shown as a function of the sphericity of the particle ψ for the nanofluid Al_2O_3/H_2O containing particles with $d_p = d_{p,eq} = 30$ nm at $T = 300$ K and different volume fractions φ. Spherical particles are compared with cubic particles as well as seven cylindrical particles with varying aspect ratios, i.e., the ratio of length to diameter, which are specified in Fig. 2. While prolate cylindrical particles have aspect ratios larger than 1, they are smaller for oblate particles.

Also for systems with non-spherical nanoparticles, our modeled data and those predicted by Hamilton and Crosser [7] agree well for the various particle geometries. Both models show that decreasing sphericity of the nanoparticles goes along with a distinct increase in the effective thermal conductivity. For example, our model predicts that the enhancement for cylinders with an aspect ratio of 10:1 ($\psi = 0.58$) is already twice as large as that for spherical particles ($\psi = 1$). The reduced convective heat transfer resistance caused by the larger specific surface area of non-spherical particles compared to spherical particles seems to reasonably account for the increased enhancement factors in our developed model. Furthermore, the trends regarding the distinct influence of the volume fraction and the negligible influences of temperature as well as particle diameter on the enhancement of the thermal conductivity found for systems containing spherical particles can also be observed for the corresponding systems containing non-spherical particles.

Conclusions: A new analytical model for the effective thermal conductivity in fluids containing well-dispersed spherical and non-spherical nanoparticles is presented. It reveals the significant role of the convective heat transfer resistance in reducing the effective thermal conductivity of a nanofluid compared with a theoretical nanofluid showing no thermal contact resistance between particle and base fluid. The convective heat transfer resistance turned out to control the achievable thermal conductivity enhancement. For four typical nanofluid systems, very good agreement was found between our calculation results and the commonly recommended model from Hamilton and Crosser [7]. In accordance with this continuum model, our model does also not show any anomalous enhancement of the effective thermal conductivity of nanofluids for low volume fractions of spherical nanoparticles as it is often reported in the literature. The present model also suggests that a stronger enhancement in the effective thermal conductivity of nanofluids is found using non-spherical particles due to their larger volume-specific surface areas. A further reduction of the convective heat transfer restrictions can be expected by the formation of rows of nanotubes having a large surface to volume ratio.

References:

1. J.C. Maxwell, *A Treatise on Electricity and Magnetism*, Clarendon, Oxford, 1892.

2. G. Tertsinidou, M.J. Assael, and W.A. Wakeham, The apparent thermal conductivity of liquids containing solid particles of nanometer dimensions: A critique, *Int. J. Thermophys.* 36 (2015) 1367-1395.

3. P. Keblinski, J.A. Eastman, and D.G. Cahill, Nanofluids for thermal transport, *Mater. Today* 8 (2005) 36-44.

4. K.N. Shukla, T.M. Koller, M.H. Rausch, and A.P. Fröba, Effective thermal conductivity of nanofluids – A new model taking into consideration Brownian motion, *Int. J. Heat Mass Transf.* 99 (2016) 532-540.

5. S.P. Jang and S.U.S. Choi, Role of Brownian motion in the enhanced thermal conductivity of nanofluids, *Appl. Phys. Lett.* 84 (2004) 4316-4318.

6. J. Koo and C. Kleinstreuer, A new thermal conductivity model for nanofluids, *J. Nanopart. Res.* 6 (2004) 577-588.

7. R.L. Hamilton and O.K. Crosser, Thermal conductivity of heterogeneous two-component systems, *Ind. Eng. Chem. Fundam.* 1 (1962) 187-191.

METAL OXIDE NANOFLUIDS FOR ENHANCING THERMAL PROPERTIES THROUGH AN EXPERIMENTAL AND THEORETICAL PERSPECTIVE

A. Sánchez-Coronilla[1]*, J. Navas[2]*, E.I. Martín[3], T. Aguilar[2], R. Gómez-Villarejo[2], J.J. Gallardo[2], P. Martínez-Merino[2], R. Alcántara[2] and C. Fernández-Lorenzo[2]

[1]Departamento de Química Física, Universidad de Sevilla, Spain

[2]Departamento de Química Física, Universidad de Cádiz, Spain

[3]Departamento de Ingeniería Química, Universidad de Sevilla, Spain

*Corresponding authors: antsancor@us.es; javier.navas@uca.es

Keywords: Nanofluid, Concentrating Solar Power, Heat Transfer Fluid, Thermal Conductivity

Introduction: Concentrating Solar Power (CSP) is one of the most interesting option as renewable energy today. In plants based on parabolic mirrors, a thermal fluid flowing through a tube covered with a coating capable of absorbing radiation is used. The absorbed radiation heats the thermal fluid. One option in order to improve the efficiency of the plants is to enhance the thermal properties of the heat transfer fluid (HTF) by using nanofluids. Suspending nanoparticles in an HTF has been shown to improve properties such as the thermal conductivity, the heat transfer coefficient or the isobaric specific heat [1-4]. A typical HTF used in CSPs is a eutectic mixture of biphenyl ($C_{12}H_{10}$) and diphenyl oxide ($C_{12}H_{10}O$). In the present work we have used this eutectic mixture as base fluid in the preparation of NiO nanofluids with benzalkonium chloride (BAC) and 1-octadecanethiol (ODT) as surfactants. The stability of the nanofluid was analysed using techniques as UV-vis spectroscopy, particle size measurements using the dynamic light scattering technique and ζ potential measurements. Properties as density, viscosity, heat capacity, and thermal conductivity were characterized. The NiO nanofluids improved the thermal properties and the heat transfer coefficient compared with the HTF. In addition, we also report a molecular dynamics study of the NiO nanofluids described before. The structural properties of these systems were determined by analysing their radial distribution function (RDF) and spatial distribution function (SDF). The significant thermal properties such as the isobaric specific heat and thermal conductivity were obtained theoretically and were shown to follow the same tendency as values obtained experimentally, which validates the theoretical study method proposed. From the theoretical results the interactions between the NiO nanoparticles and the oxygen from the diphenyl oxide of the base fluid were shown to play a key role in the structural disposition of the fluid around the metal. That structural disposition can explain the improvement of the thermal properties and the heat transfer coefficient of the NiO-nanofluids compared with the HTF.

Discussion and Results: Our results show that a high proportion of BAC is necessary for improving the stability of nanofluids as compared with the presence of ODT. The presence of

phenyl groups from BAC may be stabilised with the base fluid molecules. In this sense, the theoretical analysis agree with those results. As an example, Figure 1 shows the SDF for the nanofluid. In this Figure, the red lobes are the oxygen atoms and the blue sky ones, the C atoms from the diphenyl oxide molecules that are distributed around the NiO (yellow colour). There are 7 diphenyl oxide molecules around the metal oxide. The BAC molecules are depicted in green (C atoms) and violet colour (N atoms). An increase in the values of both isobaric specific heat and thermal conductivity as compared with the base fluid are observed experimentally for the experimental proportions that are also theoretically assessed.
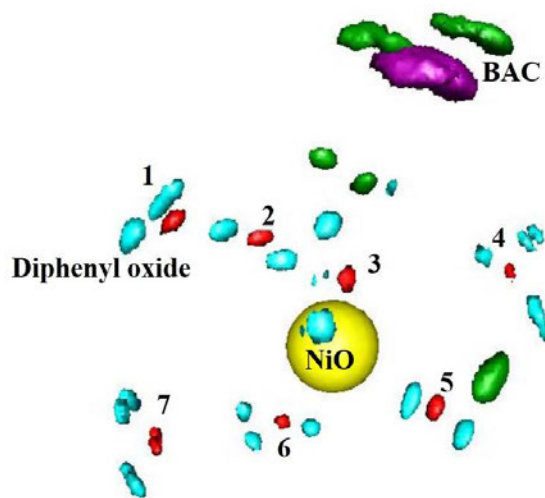
Figure 1. SDF from the NiO nanofluid.

Conclusions: The addition of NiO nanoparticles in the HTF fluid increases thermal properties of the nanofluid considerably. Thus, an enhancement of the conductivity is observed experimentally for this metal oxide nanofluid as compared with the values from the base fluid. The theoretical results agree with the experimental tendency for isobaric specific heat and thermal conductivity values. Our results indicate the interactions between the metal oxide and the oxygen from the base fluid play a key role in the structural disposition of the fluid around the metal oxide. This disposition may be involved in the increase of the thermal properties of the NiO-nanofluid compared with the base fluid.

References:

1. D.H. Yoo, K.S. Hong and H.S. Yang, Study of thermal conductivity of nanofluids for the application of heat transfer fluids, *Thermochimica Acta* 455 (2007) 66-69.

2. S.M.S. Murshed and C.A. Nieto de Castro, *Nanofluids: Synthesis, Properties and Applications*, Nova Science Publishers Inc., New York, 2014.

3. S. Lee, S. Choi, S. Li and J.A. Eastman, Measuring thermal conductivity of fluids containing oxide nanoparticles, *Journal of Heat Transfer-T. Asme* 11 (1999) 280-289.

4. W.H. Yu, D.M. France, J.L. Routbort and S. Choi, Review and comparison of nanofluid thermal conductivity and heat transfer enhancements, *Heat Transfer Engineering* 29 (2008) 432-460.

MEASUREMENT OF ELECTROKINETIC MOBILITY OF COLLOIDAL PARTICLES CLOSE TO SOLID-LIQUID INTERFACE USING EVANESCENT WAVES

K. Shirai[1]*, S. Kaji[2], T. Kawanami[3] and S. Hirasawa[2]

[1]Shibaura Institute of Technology, 3-7-5, Toyosu, Koto, 135-8548, Tokyo, Japan

[2]Kobe University, Kobe 657-8501, Japan

[3]Meiji University, Kanagawa 214-8571, Japan

*Corresponding author: kshirai@shibaura-it.ac.jp

Introduction: Thermal transporting colloids receive higher attentions in thermal engineering. Colloidal solutions containing nanometer-sized solid particles are called as nanofluids. They are widely investigated to clarify the possibilities of heat transfer enhancement since they have been reported to exhibit higher thermal conductivities compared to the mixture ratios. Another thermal transport colloid is emulsion made of phase-change materials [2] for thermal storage. The latent heat at the solid-liquid phase change can effectively store thermal energy compared to its volume.

In the solvent of colloidal solution, solute particles are dispersed by repulsive forces originating from electrical charges of their surface. When an electric field is induced to colloid, solute particles move according to the surface charge state and the induced field. The particles of thermal transporting colloid exhibit complex motion under heat transfer at a solid-liquid interface because of additional electrokinetic forces also coming from the charged surface of the solid wall. Hence, it is important to know the movement of the colloidal particles in the vicinity of a solid wall under heat transfer.

We developed a measurement system for investigating the complex mobility of colloidal particles near a solid wall. The principle is based on laser Doppler technique, which provides the mobility of colloidal particles in a direction parallel to the interfacial plane. We use
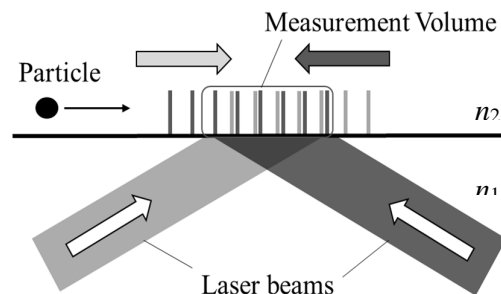
Fig. 1 Schematic of the laser-Doppler velocimetry using evanescent waves. The measurement volume is created by interference of two evanescent waves generated by total internal reflection of laser beams.

evanescent waves to realize the laser Doppler measurement. The measurement volume automatically restricted to the vicinity of a solid wall, because an evanescent wave has a very short penetration depth in the range of a few hundred nanometers at a solid-liquid interface. The measurement method had not been applied for electrokinetic studies of colloids since it was first proposed by Yamada [3]. Evanescent waves are also used in imaging techniques such as totally-internally reflected fluorescent microscopy, but they suffer from deteriorated image quality from nanometer-sized particles.
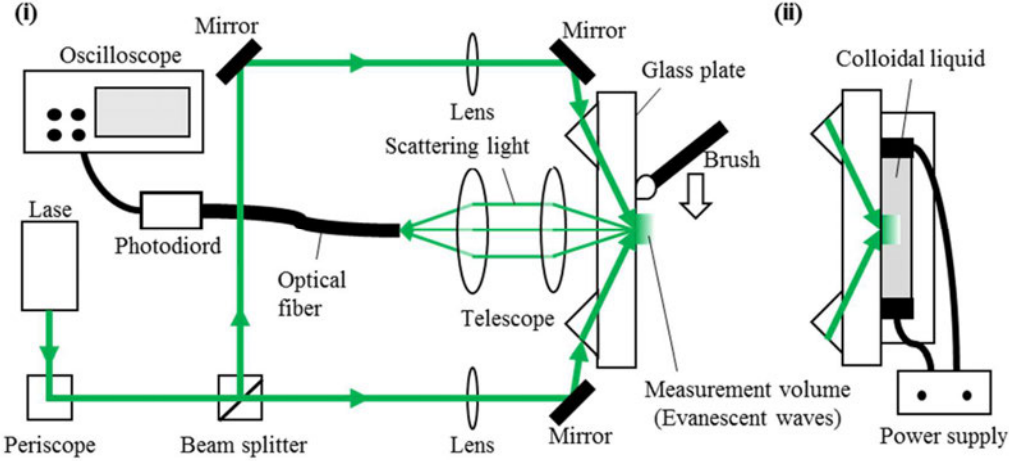
Fig. 2. Schematic overview of the measurement system: (i) scratching experiment on the glass surface with the Al_2O_3 particles and (ii) electrophoresis experiment of the Al_2O_3 particles. The optical setup was identical for both cases until the glass plate.

In the following, we report on the measurement system and its applications. We present the measurement principle and experimental results of submicrometer-sized particles.

Principle: We use evanescent waves created at the interface between colloidal liquid and a solid glass. An evanescent wave is generated at a total internal reflection of light incident at an angle beyond the critical value. The penetration depth of the evanescent wave is within a few hundred nanometers from the glass surface [4]. In the measurement, a pair of evanescent waves originated from a single-mode coherent laser source. The evanescent waves are intentionally created at a single point on the test surface so that they create an optical interfere at the surface as Fig. 1. The interference pattern forms a fringe pattern perpendicular to the surface within the penetration depths of the evanescent waves. Colloidal particles passing through the measurement volume scatter the light and the resulting signals have modulation frequencies depending on the velocities of the colloidal particles in the direction perpendicular to the fringes. The velocity is measured through

$$u = f \cdot d, \tag{1}$$

with v, d, and f being the velocity, fringe spacing, and Doppler frequency. The fringe spacing d is derived as

$$d=\lambda/(2n_1 \sin \theta_i), \qquad\qquad (2)$$

where λ, n_1, θ_i are the wavelength, refractive index of the colloid, and the incident angle of the laser at the interface of the solid and liquid. Hence, the mobility of the colloidal particles is obtained by measuring the Doppler frequencies of the scattering light.

Experimental Setup: We developed a measurement system. Fig 2 (i) schematically shows the overview of the system and (ii) the experiment with colloidal test liquid at the test section. A continuous-wave laser (wavelength: 532 nm, single longitudinal mode) was employed as the light source. The measurement volume was formed on a BK7 (refractive index 1.519 for 532 nm light) glass surface by a pair of coherent evanescent light waves. The scattering light from the measurement volume was detected by receiving optics in the backward direction. The angle of total internal reflection was set to 64.1°, and the fringe spacing derived from Eq. (2) was d =195 nm. The penetration depth of the evanescent waves was estimated to be 290 nm, based on the distance defined as the location where the intensity becomes $1/e$ of the initial amplitude at the interface [4]. The details of the system should be referred to another publication from our group [5].

Experiments: We carried out the following two experiments:

(i) The measurement volume was scratched with Al_2O_3 particles (average diameter: 300 nm) put on the tip of a paint brush. The brush was moved by a hand and the velocity was maintained in the range of $O(10^{-2})$ m/s in the direction parallel to the glass surface. The scattering signals were obtained in a digital oscilloscope and the resulting power spectrum densities were obtained.

(ii) Then, we attached the removable test section and filled with Al_2O_3 aqueous solution. A DC electric field with 4000 V/m was induced to the test colloid through the electrode. The particles move in the cell according to the combined effects of electrophoresis and electro-osmosis. The scattering signals were observed and the power spectrum densities were calculated from the time signals.

Result and Discussion: Fig. 3 exhibits typical time signal and the resulting power spectrum density of the signal in the experiment (i). The time signal forms a low frequency component with an arch shape corresponding to the Gaussian distribution of the optical intensity in the measurement volume. The signal also contains a high frequency component, which corresponds to the Doppler frequency. The sharp frequency peak around 260 kHz leads to the velocity 5.1×10^{-2} m/s based on Eq. (1). The velocity value agrees well with the expected moving velocity of the particles with the brush.

(a)

(b)

Frequency peak ~ 260 kHz
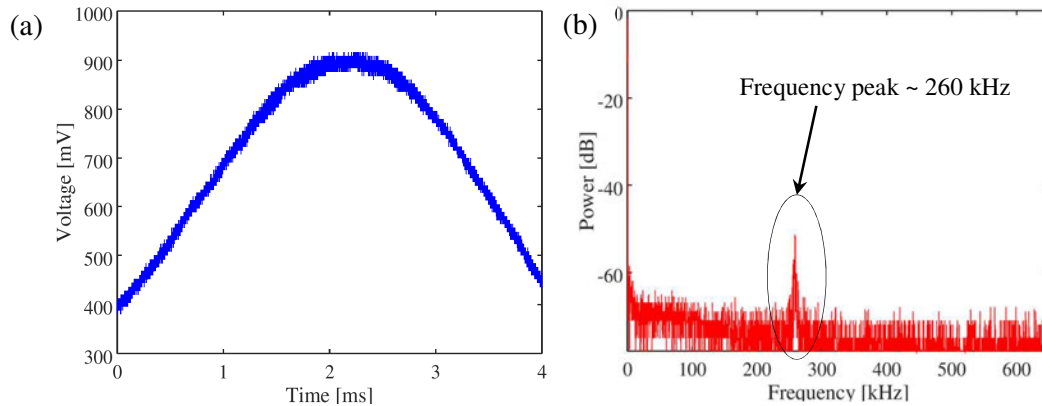
Fig. 3 Typical measurement result in the scratching experiment (i) using 300 nm Al_2O_3 particles, (a) time signal and (b) the resulting power spectrum density.

Fig. 4 shows the typical time signal and the resulting power spectrum density at the experiment (ii). The time signal oscillates with the amplitude of 1 mV and exhibits a frequency peak approximately at 130 Hz. The velocity derived from Eq. (1) becomes 2.5×10^{-5} m/s, which leads to a zeta potential of 8.8 mV through Helmholtz-Smoluchowski relation, provided that the Debye length is small compared to the flow dimension [6]. Indeed, the interpretation of the zeta potential value is not straightforward. The mobility was obtained in the vicinity of the solid wall, which should have been also electrically charged. Besides, the local flow in the cell was influenced by the combination of the electrophoresis and electro-osmosis. However, the magnitude of the zeta potential is considered to be reasonable, since the Al_2O_3 particles tended to aggregate shortly after they were mixed. Moreover, the power spectrum density in this case exhibits a peak broadened compared to the experiment (i). This is realistic because the signals are likely from multiple particles, which had slightly different velocities due to Brownian motion in the measurement volume. This feature is different from the single-particle realization of conventional laser Doppler velocimetry widely used in fluid mechanics measurements.

The above results indicate that the measurement of the particle mobility was feasible. The measured velocities obtained in the experiments were within the expected values in the same orders of magnitude. The next step is to measure the mobility of nanofluid particles. The measurement system has to be improved before the application. The photo detector has to be sufficiently sensitive to the Rayleigh scattering signals by nanometer-sized particles. The modulation depth of the scattering signals should also be improved as it affects the measurement uncertainty through the signal quality.

Summary: We developed a measurement system for investigating the complex relation between the electrokinetic mobility and heat transfer characteristics of colloids used for thermal transport applications. The system is based on laser Doppler method using a pair of evanescent waves formed at an interface between colloid and solid. The short penetration depth of the waves enables to restrict the measurements of electrokinetic mobility of colloids within a few hundred nanometers from a liquid-solid interface. We carried out two experiments and confirm the

feasibility of the measurement. In the next step, we apply the measurement system to Au nanofluids, which is undertaken at the laboratory.
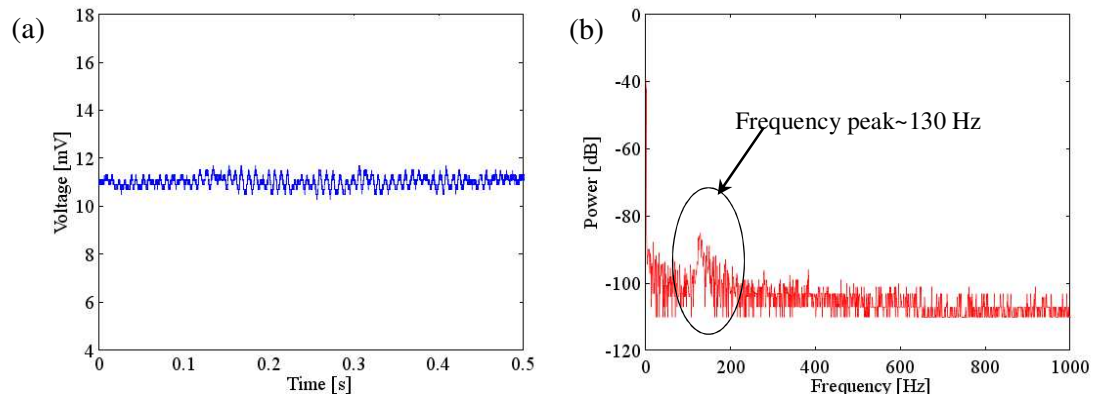
Fig. 4. Typical measurement result in the electrophoresis experiment (ii) using 300 nm Al_2O_3 particles, (a) time signal and (b) the resulting power spectrum density.

References:

1. S.U.S. Choi and J.A. Eastman, Enhancing thermal conductivity of fluids with nanoparticles, *in: Development and Applications of Non-Newtonian Flows, ASME New York,* 231 (1995) 99–105.
2. T. Kawanami, K. Togashi, K, Fujimoto, S. Hirano, P. Zhang, K. Shirai, and S. Hirasawa, Thermophysical properties and thermal characteristics of phase change emulsion for thermal energy storage media, *Energy* 117 (2016) 562–568.
3. J. Yamada, Evanescent wave Doppler velocimetry for a wall's near field, *Applied Physics Letters,* 75 (1999) 1805–1806.
4. E. Hecht, *Optics*, 4th edition Pearson, Harlow, 2001.
5. K. Shirai, S. Kaji, T. Kawanami, S. Hirasawa, Development of measurement system using evanescent waves for characterizing colloidal liquids in heat transfer applications, *Int J of Comp Methods and Exp Measurements*, 5 (2017) 34–43.
6. R.F. Probstein, Physicochemical Hydrodynamics, 2nd editon John Wiley & Sons, Hoboken, 2003.

Effect of SiO$_2$ nanoparticles on the internal structure of molten Solar Salt.

Argyrios Anagnostopoulos[1], Anabel Palacios[1], Nuria Navarrete[2], Helena Navarro[1], Yulong Ding[1]

[1] Centre for Thermal Energy Storage, School of Chemical Engineering, University of Birmingham, B15, Birmingham, United Kingdom

[2] Departamento de Ingeniería Mecánica y Construcción, Universitat Jaume I, Campus de Riu Sec. 12071, Castellón de la Plana, Spain

*Corresponding e-mail: axa1217@student.bham.ac.uk

Keywords: Solar Salt, Contact Angle, SiO$_2$, DLS, Structure

INTRODUCTION:

In this work the internal structure of Solar Salt (SS) – SiO$_2$ nanofluids is investigated. A series of contact angle (CA) measurements were conducted to investigate the effect of nanoparticles on the wettability of the SS and hence the surface energy of the material. In order to explain the results of the CA measurements, Dynamic Laser Scattering (DLS) equipment was used to study the agglomeration rate with respect to temperature and time.

METHODS:

The Solar Salt (60% NaNO3 – 40% KNO3) was mixed and sonicated with 1% amorphous SiO$_2$ particles. After drying, the material was scrapped and milled.

All samples were ensured to be of the same weight and were compressed at same rates. In this way drop dimension and heterogeneity related effects were minimized. The samples were tested on an Al$_2$O$_3$ {0 0 0 1} substrate (30mmx30mmx10mm), with a roughness of S=0.364μm.

RESULTS AND CONCLUSIONS:

Experiments where performed on the CA of SS with concentration of 0%, 0.5%, 1.0%, 1.5% and 2.5% SiO$_2$.

In the case of the base salt the CA is linearly reduced with an increase in temperature, which is what commonly occurs. However, with the presence of silica the CA appears to remain stable up until the temperature of 310°C. At that point there is a large drop in the CA, followed by a second drop at 330-340°C. After that the CA of the nanofluid retain similar values to the base case. 310°C is the melting point of sodium nitrate (NaNO$_3$).Therefore, the fact that there is a rapid CA drop, indicates some internal skeleton collapse. Probably, the nanoparticles formulate a certain internal matrix that is affected by the melting of the NaNO$_3$. Similarly 334°C is the melting point of potassium nitrate (KNO$_3$), which has a similar effect on the CA.
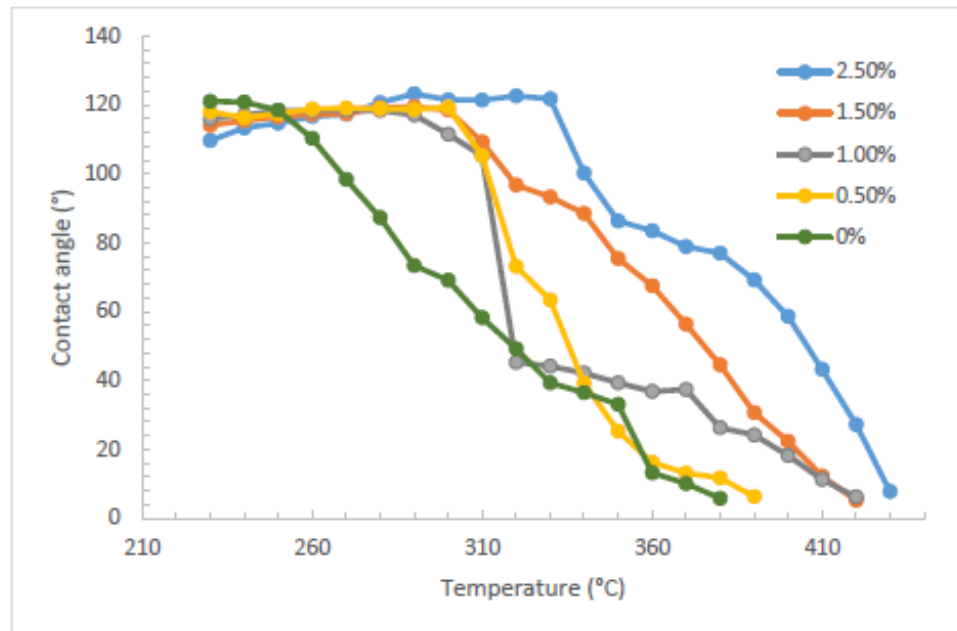
Figure 1: CA measurements of SS-SiO$_2$ on Al$_2$O$_3$

To further validate this effect DLS measurements were conducted with respect to time and temperature. To better evaluate the effect of time and temperature the sample was first heated up at 250°C where measurements were taken every 30min until the mean nanoparticle diameter was stable for 2 consequent values. These measurements were conducted 3 times and led to an average nanoparticle diameter of 205 nm at the start of the experiment, 485nm after 30min, 863nm after 1h, 1065nm at 1:30h and 1082nm at 2h. After 2 hours the sample was heated up to 350°C in order to evaluate the effect of temperature on the agglomeration. The resulting measurements showed that the average mean diameter was above 3000nm. Certain measurements provided no results as the diameter was <10000nm. To identify if this effect was gradual, measurements were taken after waiting at 290°C, 310°C 330°C and 340°C. The resulting diameters were 1103nm, 1169nm, 853nm and 3329nm respectively. It was deduced that agglomeration is largely increased between 330°C to 340°C confirming CA observations. To further strengthen this observation experiments were started at 270°C, 290C and 310°C. Results provided patterns almost identical to the experiments started at 250°C.

In conclusion, there is an internal structure change in the SS-SiO$_2$, nanofluid between 310C and 340C, which leads to high agglomeration of SiO$_2$ nanoparticles past this point. This effect is independent of time and is related to the temperature. It is hypothesized, since 310C is the melting point of NaNO$_3$ and 334C the melting point of KNO$_3$, that nanoparticle agglomeration affects the formulation of eutectic mixtures.

Wetting of $NaNO_3$ on MgO, $NaNO_3$- SiO_2 nanofluid. Thermal Energy storage through Molecular Dynamic Simulations.

Argyrios Anagnostopoulos[1], Alessio Alexiadis[1], Yulong Ding[1]

[1] Centre for Thermal Energy Storage, School of Chemical Engineering, University of Birmingham, B15, Birmingham, United Kingdom

Corresponding e-mail: axa1217@student.bham.ac.uk

Keywords: $NaNO_3$, MgO, SiO_2, molecular, simulations

INTRODUCTION:

Molecular dynamic (MD) simulations is a trending tool used to effectively calculate and validate properties in the nanoscale and subsequently interpret macroscopical phenomena. Wetting behavior plays an important role in the formulation of composite materials. The contact angle (CA), is the most frequently quoted property, used to describe the wetting between materials. Molten salt based nanofluids are of special interest, due to the increments reported in both thermal conductivity and heat capacity as well as for its practical application in Thermal Energy Storage systems. The physical phenomena involved in the thermal properties increment is still a source of controversy. In this work interactions of thermal energy storage materials is investigated through MD simulations.

METHODS:

The Large-scale Atomic/Molecular Massively Parallel Simulator (LAMMPS) software was used to perform a series of MD simulations on the CA and surface tension of $NaNO_3$ on MgO, as well as on the thermal conductivity of the $NaNO_3$- SiO_2 nanofluid. The Lennard-Jones interatomic potential was used to calculate the interactions between atoms. A set of parameters was specifically formulated for the purpose of this work.

To validate the formulated interatomic potential, thermal conductivity, viscosity, specific heat capacity, density and surface tension were all calculated and compared with experiments.

A quenching procedure was applied to obtain the structure of molten $NaNO_3$. The crystalline cell structure of $NaNO_3$ was replicated, leading to a periodic dimension boundary box containing 5040atoms. The salt was heated up to 1200K in the NVT ensemble, followed by a rapid cooling process in the NPT ensemble from 1200K to 593.15K and ending with an equilibration process in the NVT ensemble at 593.15K.

For the formulation of the silica nanoparticle a similar process was followed. Upon obtaining the structure of amorphous silica, a 1nm particle was extracted from the bulk and placed in the center of the box containing molten salt atoms.

RESULTS AND CONCLUSIONS:

The CA of $NaNO_3$ on MgO has been calculated at temperature intervals of 10K. The agreement with experimental data is excellent. The model predicts accurately the wetting process of molten $NaNO_3$ on MgO. Since, both surface tension and CA data were calculated throughout these simulations the work of adhesion was also computed from the Young-Durpe equation. It was found that the work of adhesion is over appreciated, due to a base deviation of the surface tension values for molten $NaNO_3$ from experimental results. However, since the trend of the values is guided by the change in the CA the results had a similar trend with the experimental ones, proving that the force in the contact line can be computed from the Young-Durpe equation, also in the nanoscale for the case of ionic liquids. Validity of this equation has been observed also for the case of water.
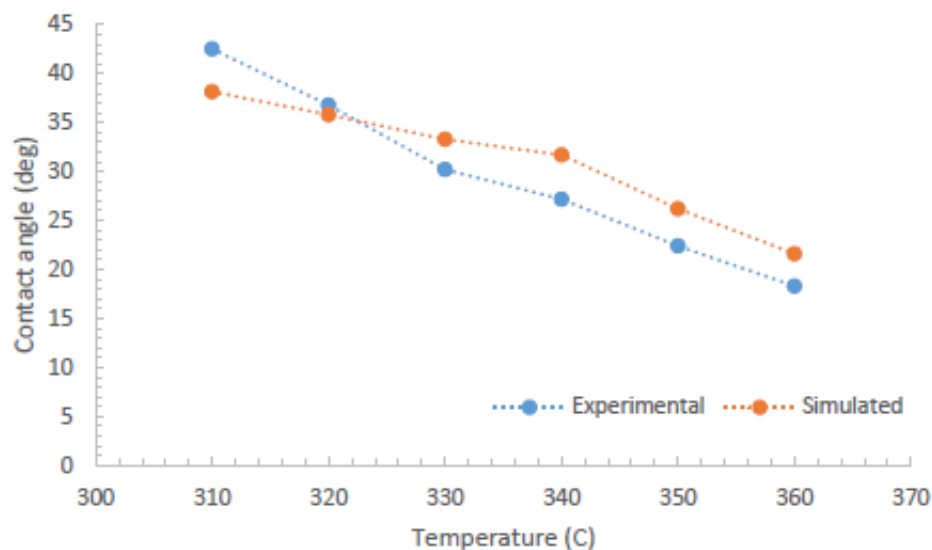
Figure 1: Contact angle of NaNO3 on MgO, comparison with experimental data

In terms of the molten salt nanofluid simulation, the thermal conductivity was calculated for the case of the 0.5% and 1.0% SiO_2 and was found to be 0.97 (W/mK) and 1.13 (W/mK compared to 0.78 (W/mK) and 0.832 (W/mK) obtained from experimental values. This amount of deviation is considered satisfactionary for MD simulations. Furthermore, the trajectory of the atoms at the nanoparticle-salt interface was visualized. It was observed that in the initial steps of the simulations the salt atoms attach themselves to the surface of the nanoparticle and create a solid-like structure. As the nanoparticle moves throughout the simulation these particles remain attached to the surface creating a layer of a thickness of 0.5nm for a 1nm simulated nanoparticle. The formulation of this layer was linked to the van der Waals forces between salt and silica atoms being stronger than those between the salt atoms.

Further studies are necessary, to evaluate the effect of the nanoparticle diameter on the thermal properties, and the identification of the reasons behind the plateau in enhancement.

HNO₃ oxidation of Single Wall Carbon Nanohorns for the production of surfactant free black nanofluids

Filippo Agresti[1,*], Simona Barison[1], Alessia Famengo[1], Cesare Pagura[1], Laura Fedele[2], Stefano Rossi[2], Sergio Bobbo[2], Marzio Rancan[3]

[1] Institute of Condensed Matter Chemistry and Technologies for Energy (ICMATE), National Research Council of Italy (CNR), Corso Stati Uniti 4, 35127 Padova, Italy
[2] Institute of Construction Technologies (ITC), National Research Council of Italy (CNR), Corso Stati Uniti 4, 35127 Padova, Italy
[3] Institute of Condensed Matter Chemistry and Technologies for Energy (ICMATE), National Research Council of Italy (CNR), c/o Dept. Chemical Science, University of Padua, Via Marzolo 1, 35131 Padova, Italy

*Corresponding e-mail: filippo.agresti@cnr.it

INTRODUCTION: Single wall Carbon Nanohorns (SWCNHs), tiny graphene sheets wrapped to form horn-shaped cones with a half-fullerene cap, having 30–50 nm length and 2–5 nm diameter, are not easily dispersible in water due to the hydrophobic nature of their surface, as other graphene-based materials [1]. Thus, surfactants are generally used to achieve a sufficient nanofluid stability [2]. Despite the abundant use of surfactants for nanofluid stabilization, they have some drawbacks like formation of foam, chemical interaction in covalent functionalization, degradation in extreme conditions, easy desorption from the surface to cite some [3-4], with consequent destabilization of the suspension.

In this work, we exploited the partial surface oxidation of SWCNHs as a clean and strategical tool to achieve stable suspensions in water without the need of surfactants.

METHODS: In order to get stable suspensions in water of SWCNHs without surfactants, a surface oxidation by using concentrated HNO₃ was performed. 0.05 g SWCNH were poured into 25 mL HNO₃. Four samples were prepared by stirring the suspension at different temperatures (50 – 80 °C) and for different times (1 – 4 h) in order to investigate different degrees of surface oxidation. The processed powders were then separated from HNO₃ by paper filtering and thoroughly washed with deionized water until the filtrate reached a neutral pH. Finally, the powders were washed with 100 mL ethanol and dried in air at 120 °C for 2 h.

Suspensions of oxidized SWCNHs were prepared at the concentration of 0.05 g/L by pouring 0.0125 g of each powder in 250 mL deionized water in two steps: (a) sonication for 10 min using a Sonics VCX130 (Sonics & Materials, Inc.) operating at 20 kHz and 65 W, equipped with a 12 mm tip, in order to get a pre-disaggregation of nanopowders; (b) processing the sonicated suspensions for 15 min with a high-pressure homogenizer (Panda, GEA Niro Soavi), operated at 1000 bar. For comparison, a reference nanofluid was prepared by using the non-oxidized pristine powder of SWCNHs. Since no stable colloid can be obtained using the pristine powder "as it is", a surfactant solution of Sodium Dodecyl Sulfate (SDS) at the concentration of 0.005 g/L was used as a dispersing media. The surface damage and oxidation degree of SWCNHs were evaluated by SEM microscopy, Thermogravimetric Analysis, Residual Gas Analysis, XPS and UV–visible spectroscopy. Moreover, the carboxylation influence on suspension stability was evaluated by Dynamic Light Scattering and ζ-potential measurements.

RESULTS AND CONCLUSIONS: TGA and RGA measurements showed that increasing time and temperature of treatment leads to the formation of functional groups, like carbonyl or carboxyl, which decompose by the release of water and CO_2. SEM micrographs confirmed that the oxidation process partially damages the peculiar structure and morphology of SWCNH aggregates, which is also confirmed by UV–Vis measurements showing the reduction of the interband π plasmon peak (π-π* transition) at about 260 nm, related to the graphene-like structure. Anyway, we demonstrated that the oxidation route can be optimized in order to maximize the carboxylic presence, as detected by XPS, and the nanofluid stability, at the same time reducing the material damage, so minimizing the influence of a mild oxidation on functional features, like optical and spectral properties. This method leaded to stable nanofluids of these important carbon nanostructures by avoiding the use of surfactants, thus opening to new potential applications of water-based colloids.

REFERENCES:

[1]   N. Karousis, I. Suarez-Martinez, C.P. Ewels, N. Tagmatarchis, *Structure, properties, functionalization, and applications of carbon nanohorns,* Chem. Rev., 116 (2016), pp. 4850-4883.

[2]   L. Fedele, L. Colla, S. Bobbo, S. Barison, F. Agresti, *Experimental stability analysis of different water-based nanofluids,* Nanoscale Res. Lett., 6 (2011), p. 300.

[3]   E.R. Bandala, M.A. Peláez, M.J. Salgado, L. Torres, *Degradation of sodium dodecyl sulphate in water using solar driven Fenton-like advanced oxidation processes,* J. Hazard. Mater., 151 (2008).

[4]   H. Hidaka, S. Yamada, S. Suenaga, H. Kubota, N. Serpone, E. Pelizzetti, M. Grätzel, Photodegradation of surfactants. V. *Photocatalytic degradation of surfactants in the presence of semiconductor particles by solar exposure, J. Photochem. Photobiol. A,* 47 (1989), pp. 103-112.

Thermal conductivity of aqueous iron oxides nanofluids

Mihail Iacob[1,*], Maria Cazacu[1], Leonor Hernandez[2]

[1] "Petru Poni" Institute of Macromolecular Chemistry, Aleea Gr. Ghica Voda 41A, 700487 Iasi, Romania

[2] Universitat Jaume I. Departamento de Ingenieria Mecanica y Construccion, Castellon de la Plana, 12071, Spain

*Corresponding e-mail: Iacob.mihai@icmpp.ro

Keywords: *nanofluids, thermal conductivity, magnetite, maghemite, goethite, ferrihydrite*

INTRODUCTION:

There are more than 20 iron oxides, oxo-hydroxide and hydroxide, which differ in structure, chemical and physical properties. For example, magnetite, maghemite, hematite and feroxyhyte are ferromagnetic; lepidocrocite and akaganeite are paramagnetic while goethite is antiferromagnetic at room temperature. The magnetic properties of iron oxides also depend on particle size. The most common example is magnetite which became superparamagnetic at sizes bellow 15 nm [1]. Under optimum conditions (medium, pH, pressure, temperature), most of the them can be converted to anther iron oxide [1]. Hematite and goethite are the most stable iron oxides, representing often the end products of the polymorphs transformation. Iron oxide nanoparticles find applications in targeted drug delivery, biosensors, magnetic hyperthermia, contrast agents in magnetic resonance imaging (MRI), magnetic storage media, magnetic ink and many other [2]. Using of iron oxides in nanofluids for heat exchange system are usually limited to magnetite and maghemite. In this study, the thermal conductivity of four aqueous iron oxides (magnetite, maghemite, goethite and ferrihydrite) nanofluids were determined.

METHODS:

Iron(III) chloride hexahydrate ($FeCl_3·6H_2O$), iron(II) chloride tetrahydrate ($FeCl_2·4H_2O$), Iron(III) nitrate nonahydrate ($Fe(NO_3)_3·9H_2O$) and sodium hydroxide (NaOH) were purchased from Sigma-Aldrich and used as received.

Thermal conductivity study was performed at room temperature and 50 °C on KD2Pro (Decagon Devices) using the transient hot wire technique. The hydrodynamic size of nanoparticles was determined using the dynamic light scattering (DLS) technique using a Zetasizer Nano ZS (Malvern Instruments Ltd.).

RESULTS AND CONCLUSIONS:

Iron oxide nanoparticles can be prepared using various methods such as thermal decomposition, sol-gel, microwave irradiation, calcination, hydrothermal method and others [3]. In the present work, precipitation in strong alkaline medium was chosen as preparation method for magnetite, maghemite, goethite and ferrihydrite nanoparticles due to its reproducibility, scalability and the quality of prepared nanoparticles. The structure of iron oxides was confirmed using Raman spectroscopy and wide-angle X-ray diffraction, while the morphology was studied using transmission electron microscopy. Thus, magnetite and maghemite nanoparticles are spherical with some irregularities and the size of about 7 and respectively 8 nm, ferrihydrite have irregular shape and the goethite was found to be rod-like particles of about 85 nm in width. In the next step, the iron oxide nanoparticles were used to prepare aqueous nanofluids. In order to obtain stable nanofluids, the aqueous dispersions of iron oxides were ultrasonicated. The hydrodynamic size of nanoparticles was studied using dynamic light scattering. It was found that initially the aqueous maghemite nanofluids consist of aggregates of 141 and 1181 nm. After three minutes of ultrasonication, the aggregate size decreased to 107 and 1063 nm, while after five minutes these became even smaller, dropping at 37 nm and 157 nm. By ultrasonication for longer time, the hydrodynamic size of nanoparticles didn't change significantly. Therefore, before analysing, all the samples were ultrasonicated for five minutes. The aqueous nanofluids were prepared using 10 g/L of magnetite, maghemite or ferrihydrite nanoparticles. Because at this concentration the goethite fluid was unstable, lower concentration, 1 g/L, was used for this iron oxide species.

The thermal conductivity of the prepared aqueous iron oxide nanofluids was measured at room temperature and 50 °C. At room temperature the thermal conductivity was 0.610 W/mk for pure water increasing to 0.642, 0.649, 0.649 and 0.658 W/mk in the case of ferrihydrite nanofluids (10 g/l), magnetite (10 g/l), maghemite (10 g/l) and goethite (1 g/l), respectively. At 50 °C, the difference between thermal conductivity of pure water (0.644 W/mk) and those of nanofluids was lower: 0.651, 0.659, 0.659 and 0.662 W/mk for ferrihydrite, magnetite, maghemite and goethite nanofluids, respectively. Also, the thermal conductivity dependence on the magnesium concentration of aqueous nanofluids was studied. As expected, increasing the concentration of nanoparticles in nanofluids leads to an increase in thermal conductivity from 0.643 at 1 g/l to 0.649 at 10 g/l. Thus, aqueous goethite nanofluids, even at the lowest concentration, have the highest thermal conductivity of the four studied oxides nanofluids.

REFERENCES:

[1]   R.M. Cornell, U. Schwertmann, The Iron Oxides: Structure, Properties, Reactions, Occurences and Uses, Second Edition, Wiley-VCH, Wiley-VCH, Weinheim, 2004.
[2]   S. Laurent, D. Forge, M. Port, A. Roch, C. Robic, L. Vander Elst, R.N. Muller, Chem. Rev. 108 (2008) 2064–110.
[3]   M. Iacob, C. Racles, C. Tugui, G. Stiubianu, A. Bele, L. Sacarescu, D. Timpu, M. Cazacu, Beilstein J. Nanotechnol. 7 (2016).

Thermal Conductivity of Ionic Melts and Nanofluids - Where we are.

Carlos A. Nieto de Castro, Maria José V. Lourenço

Centro de Química Estrutural, Faculdade de Ciências, Universidade de Lisboa, Campo Grande, 1749-016 Lisboa, Portugal

*Corresponding e-mail: cacastro@ciencias.ulisboa.pt

Keywords: ionic melts, nanofluids, thermal conductivity

INTRODUCTION: Thermal conductivity has been proved to be one of the most difficult properties of materials to be measured with high accuracy. This fact is due to the different molecular mechanisms of heat transfer in solids, liquids and gases, with neutral of ionic media, and to the difficulties in isolation of pure conduction from other mechanisms of heat transfer, like convection and radiation, a fact that arises from the contradictory requirement of imposing a temperature gradient on the fluid while preventing its motion. Its accurate measurement in fluids has been a very successful task since the late 70's, due to the efforts of several schools in Europe, Japan and United States. However, the application of the most accurate techniques to several systems with technological importance, like ionic liquids, nanofluids and molten salts, has not been made in the last ten years in a correct fashion, generating highly inaccurate data, which do not reflect the real physical situation. It is the purpose of this paper to review critically the best available techniques for the measurement of thermal conductivity of fluids, with special emphasis in transient methods and their application to ionic liquids, nanofluids and molten salts.

GENERAL EQUATIONS: For isotropic fluids, the thermal conductivity is defined by the Fourier's law, and depends on the thermodynamic state of the fluid prior to the perturbation, and must be related with a reference state, not necessarily equal to the initial one [1]:

$$q = -\lambda \nabla T \tag{1}$$

where q is the instantaneous flux of heat, the response of the medium to the instantaneous temperature gradient ∇T, and λ the thermal conductivity of the medium. As it is impossible to measure local fluxes and local gradients Fourier equation cannot be used directly, and the energy equation has to be adapted to a given geometry. The equation of energy conservation in the system is the basis for the formulation of the working equation of any method of measurement. The equation of change for non-isothermal systems can be found on the excellent book by Bird, Stuart and Lightfoot [2], which written for unit mass is:

$$\rho \frac{DU}{Dt} = -(\nabla \cdot q) - P(\nabla \cdot v) - (\tau : \nabla v) \tag{2}$$

where ρ is the fluid density, U is the internal energy, t the time, P the hydrostatic pressure, v the hydrodynamic velocity of the fluid and τ the stress tensor. This equation does not include nuclear, radiative, electromagnetical or chemical terms for energy. In addition it is applicable to Newtonian fluids. The notation D/Dt represents the substantial derivative, meaning that the time rate of change is reported as one move with the fluid. If the sample is not moving (solid of stationary fluid, no convection), the properties of the sample do not vary with temperature (small temperature gradients) and using Fourier law (Equation (1)), this last equation cane be transformed to:

$$\rho C_P \frac{\partial T}{\partial t} = \lambda \nabla^2 T \qquad (3)$$

where ∇^2 is the symbol for the Laplacian. It is important to recognize that transport of energy by radiation is always present, and must be corrected for each measuring technique, especially if measurements are performed at high temperatures. Equation (3) is the basis of all experimental methods for the measurement of thermal conductivity.

A variety of experimental methods have been developed, for gaseous, liquid, supercritical or solid phases, over wide range of thermodynamic states. These methods are based on the simplified energy equation (1) and can be classified in two main categories [1, 3-4]:
-   Unsteady state or transient methods, in which the full equation (4) is used and the principal measurement is the temporal history of the fluid temperature (transient hot-wire, transient hot-strip, the interferometric technique adapted to states near the critical point etc.);
-   Steady state methods, for which $\partial T/\partial t=0$ and the equation reduces to $\nabla^2 T=0$, which can be integrated for a given geometry (parallel plates, concentric cylinders, etc.).

CONCLUSIONS: The use of methods of measurement today, uses and abuses of the previous equations. Examples will be given on the problems that arise to measure accurately the thermal conductivity of ionic melts, its nanosalts, and nanofluids in general, and how NANOUPTAKE can contribute to the production of accurate data, necessary for the design of industrial applications.

REFERENCES:
[1] Nieto de Castro, C. A., "Absolute measurements of the viscosity and thermal conductivity of fluids", JSME Int. J., Series II, 31, 387- 401 (1988)
[2] Bird, R. B., Stewart, W. E. and Lightfoot, E. N., "Transport Phenomena", 2nd Edition (John Wiley Sons, Inc., New York, 2002)
[3] Wakeham, W. A. Nagashima A. and Sengers, J. V. (eds), Measurement of the transport properties of fluids, Experimental Thermodynamics, Vol. III (Blackwell Scientific Pubs, Oxford, UK, 1991), namely chapters 6, 7 and 8.
[4] Assael, M. J., Goodwin, A. R. H., Vesovic, V., Wakeham, W. A. (eds), Experimental Thermodynamics Volume IX: Advances in Transport Properties of Fluids (Royal Society of Chemistry, London, UK, 2014), especially chapter 5.

Heat transfer enhancement by impinging slot jets with nanofluids in channels with and without metal foams

Bernardo Buonomo[1], Anna di Pasqua[1], Davide Ercole[1],
Oronzio Manca[1*], Sergio Nardini[1]

[1] Dipartimento di Ingegneria, Università degli Studi della Campania "Luigi Vanvitelli", Real Casa dell'Annunziata, Via Roma 29, Aversa, Italy

*Corresponding e-mail: oronzio.manca@unicampania.it

Keywords: *Heat Transfer Enhancement, Impinging Slot Jet, Channels, Metal foam, Numerical simulation.*

INTRODUCTION: The analysis of impinging jets is fundamental due to its strong impact in heat enhancement and its combination with other heat enhancement methods can determine very efficient systems in heat transfer removal and control [1]. Moreover, the simultaneous application of nanofluids and porous media allows to realize the heat transfer enhancement in thermal systems [2]. Configurations with slot jets have recently attracted more attention because of their cooling effectiveness, uniformity and controllability, as demanded by modern electronic equipment, featured by increasing heat flux and decreasing dimensions [3]. Different fluids could be selected in order to work with impinging jets. Additives in the working fluids can be considered in order to improve the thermal properties, like nanoparticles added to pure liquids. Such fluids are called nanofluids and they are made by a base fluid with dispersed nanosize structures. In this work a configuration, representing a confined and submerged slot jet impinging in a channel with or without metal foam on a moving or stationary target surface, heated at constant uniform temperature. The aim consists into the evaluation of the differences among four configurations of impinging slot jet with water/Al_2O_3 nanofluids in a channel with: stationary target surface (1) without or (2) with foam and moving target surface (3) without and (4) with foam. Moreover, the jet can also be inclined with an angle equal to 30°.

METHODS: A two-dimensional confined slot-jet impinging normally in an aluminum foam on a stationary or moving target surface at uniform assigned temperature, and working with water/Al2O3 nanofluids is studied numerically. The impinging jet is featured by a width, W, and a distance between the nozzle, H, while L denoted the target surface length. H/W is equal to 4 (H=24.8 mm and W=6.2 mm) as reported in Fig. 1. The target velocity is 0.2 times the uniform velocity of the fluid at the inlet section (the slot jet). The single phase model is used to describe the nanofluid behavior and the metal foam is assumed in local thermal equilibrium. The governing equations of continuity, momentum and energy are solved in rectangular coordinates for a steady state, turbulent and incompressible flow with thermophysical
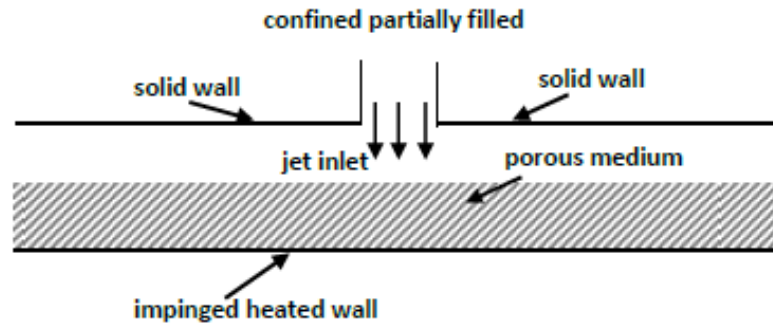
Figure 1: Sketch of the confined impinging slot jet.

properties considered temperature independent. The k-ε model is employed to close the turbulent flow problem. A uniform velocity profile, with Reynolds number equal to 5000, and a uniform temperature profile are applied at the inlet section as boundary condition while on the outlet sections, the static pressure was defined. The governing equations with the assumed boundary conditions are solved by means of Ansys Fluent code.

RESULTS AND CONCLUSIONS: Simulations are performed for the four different configurations for vertical jet and inclined jet with an angle of 30°. The velocity of the target is 0 and 0.2 the inlet jet velocity and the assigned temperature is 303 K. The jet inlet temperature is 293 K and the velocity is correspondent to a Reynolds number equal to 5000. The thermophysical properties are evaluated with the correlations given in [4]. The aluminium foam has a porosity of 0.92 and 10 pore per inches. The nanoparticles volumetric concentration is 0% and 4%, in water. The results are given in terms of local Nusselt number profiles along the target surface and are given in Figure 2 and 3 for the configurations without metal foam and with metal foam, respectively.
The increase due to the nanofluid is lower than the one due to the metal foam at this assigned Reynolds number. It could be very interesting to evaluate the behaviors for laminar flow (Re<2000) and extend the investigation in a larger range of Reynolds number.

REFERENCES
[1] B. Buonomo, O. Manca, S. Nardini, D. Ricci, Nanofluid Impinging Jets in Porous Media, Chapter 6, in J.M.P.Q. Delgado, ed., Diffusion Foundations, vol. 7, pp. 84-113, 2016, doi:10.4028/www.scientific.net/DF.7.84.

[2] A. Kasaeian, R.D. Azarian, O. Mahian, L. Kolsi, A.J. Chamkha, S. Wongwises, I. Pop. (2017) Nanofluid flow and heat transfer in porous media: A review of the latest developments, International Journal of Heat and Mass Transfer, 107, pp. 778-791.

[3] A.K. Shukla, A. Dewan, (2017) Flow and thermal characteristics of jet impingement: Comprehensive review, International Journal of Heat and Technology, 35(1), pp. 153-166.

[4]   S.J. Palm, G. Roy, C.T. Nguyen, Heat Transfer Enhancement with the Use of Nanofluids in Radial Flow Cooling Systems considering Temperature Dependent Properties, Appl. Therm. Eng., vol. 26, pp. 2209-2218, 2006.
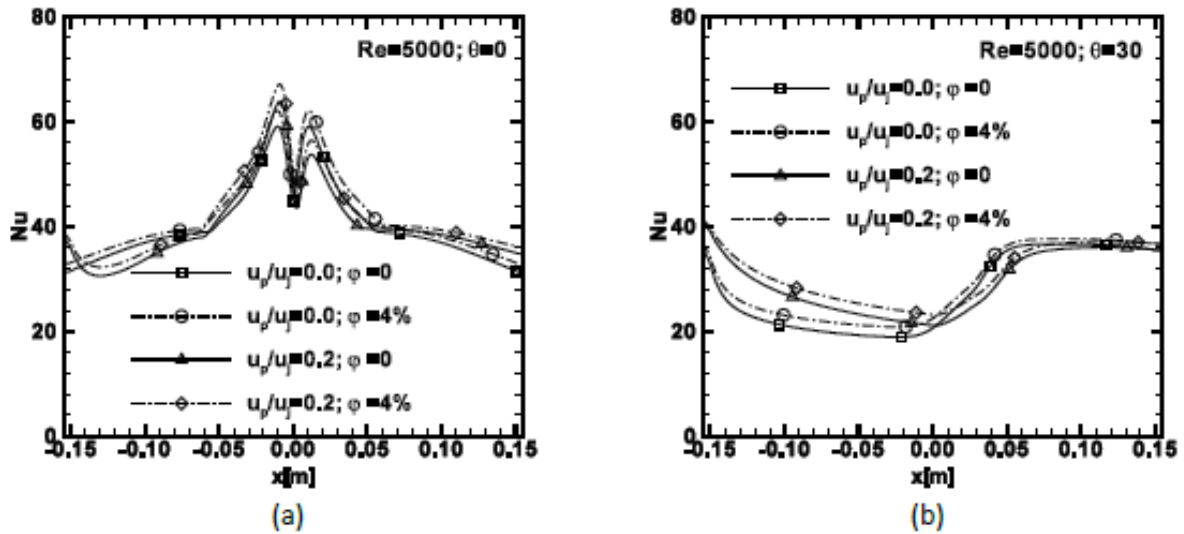
Figure 2: Local Nusselt number profile at Re=5000 for impinging jet with nanofluid without metal foam: (a) vertical jet and (b) inclined jet, 30°
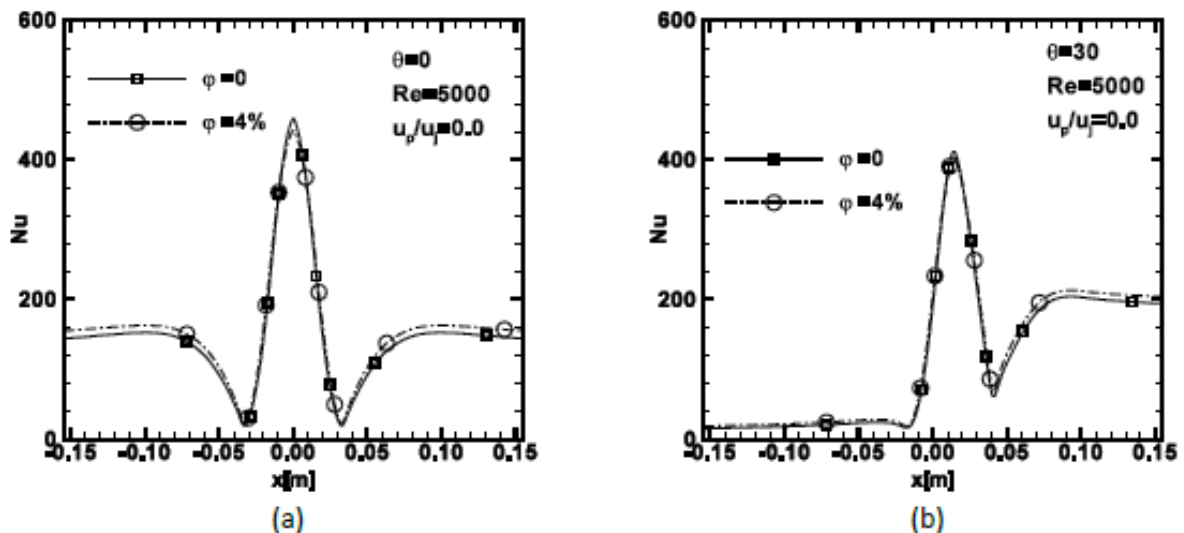
Figure 3: Local Nusselt number profile at Re=5000 for impinging jet with nanofluid with metal foam: (a) vertical jet and (b) inclined jet

WG 2

4. WG 2: Cooling

Application of Nanofluids in Heat Exchangers: Performance and Challenges

Bengt Sunden

Department of Energy Sciences, Lund University, SE-22100, Lund, SWEDEN
*Corresponding e-mail: Bengt Sunden, bengt.sunden@energy.lth.se

Keywords: Nanofluids; helical heat exchanger; plate heat exchanger; hybrid nanofluid; thermophysical property

INTRODUCTION: Our work focuses on performance and challenges of nanofluids in heat exchanger applications. Heat exchangers are equipment being used for transfer of heat between two or more fluids at different temperatures [1]. Due to advancement in manufacturing processes, various passive heat transfer enhancement techniques have been routinely used in heat exchangers to improve their thermal efficiency. Convective heat transfer performance of nanofluids in straight smooth tubes has been extensively investigated. However, there are few studies on heat transfer characteristics of nanofluids in heat exchangers with enhanced geometries. Therefore, it might be interesting to study the coupled effects of nanoparticles and enhanced geometries on the hydraulic and thermal performances of heat exchangers.

METHODS: The hydraulic and thermal performances of various nanofluids of different nanoparticle concentrations in a helically coiled heat exchanger and two chevron plate heat exchangers have been experimentally investigated [2-6]. The test rig is shown as below in Fig. 1. Ten nanofluids listed in Table 1 were tested in heat exchangers. The nanofluids were obtained by diluting the concentrated Al_2O_3/water nanofluids without surfactants (from Nano-phase Technologies Corporation, US) and the concentrated MWCNT/water nanofluids with 2.0 wt% surfactant SDBS (from Nanocyl, Belgium).
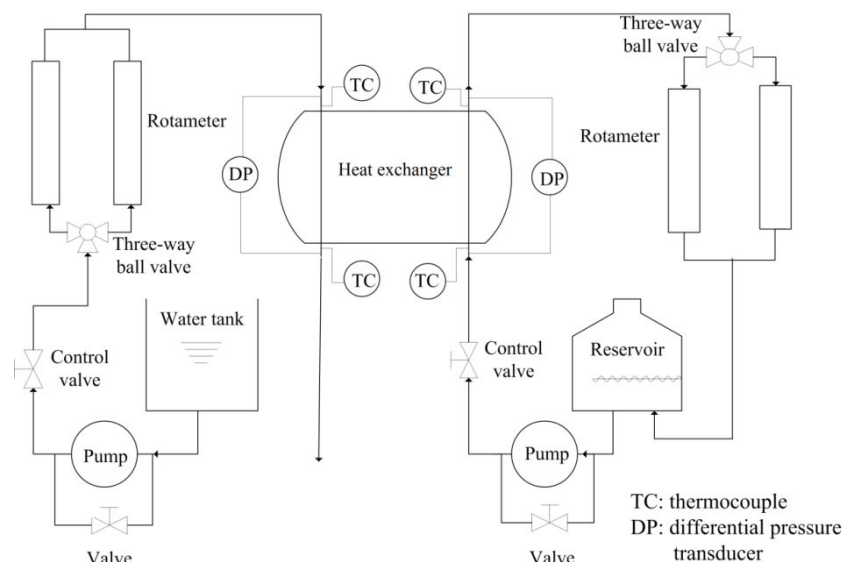
Fig. 1 Schematic of the test rig

Table 1 The ten tested nanofluids

Nanofluids	Volume concentration (weight concentration)
γ-Al$_2$O$_3$/water nanofluid	0.2 vol% (0.78 wt%)
	0.56 vol% (2.18 wt%)
	1.02 vol% (3.89 wt%)
	1.5 vol% (5.68 wt%)
	1.88 vol% (7.04 wt%)
	2.84 vol% (10.56 wt%)
MWCNT/water nanofluid	0.0111 vol% (0.02 wt%)
	0.0278 vol% (0.05 wt%)
	0.0555 vol% (0.1 wt%)
Hybrid Al$_2$O$_3$+MWCNT/water nanofluid	1.89 vol% Al$_2$O$_3$/water + 0.0111 vol% MWCNT/water at a volume ratio of 1:2.5

RESULTS AND CONCLUSIONS: The nanofluids and base fluid show very similar heat transfer performances in heat exchangers, which indicates that the net effect of nanoparticles on the thermal performance in heat exchangers is probably insignificant, especially for single-component nanofluids such as the tested alumina-water nanofluids and MWCNT-water nanofluids. When the measured nanofluid properties were used for calculation, especially the viscosity and thermal conductivity, conventional heat transfer correlations can reproduce the thermal behaviors of the tested nanofluids for laminar flow and turbulent flow very well. Heat transfer comparison with the base fluid at a constant Reynolds number can be misleading and should not be used to evaluate heat transfer enhancement. Based on the fixed flow velocity and the fixed pumping power, no heat transfer enhancement can be achieved by nanoparticle additions for single-component nanofluids because the increase in viscosity is generally much larger than the increase in thermal conductivity. For hybrid alumina and MWCNT nanofluid mixtures, the heat transfer coefficient is slightly larger than those of the alumina-water nanofluid and water, when comparison is based on the same power consumption. However, the increase in heat transfer is still within the error range. More advanced nanofluid synthesis methods are needed to explore the potential of hybrid nanofluids for heat transfer augmentation.

REFERENCES:

[1] B. Sundén, Introduction to Heat Transfer, WIT Press, Southampton, 2012.

[2] Z. Wu, L. Wang, B. Sundén, Pressure drop and convective heat transfer of water and nanofluids in a double-pipe helically coiled heat exchanger, Appl. Therm. Eng. 60 (2013) 266-274.

[3] Z. Wu, L. Wang, B. Sundén, L. Wadsö, Aqueous carbon nanotube nanofluids and their thermal performance in a helical heat exchanger, Appl. Therm. Eng. 96 (2016) 364-371.

[4] D. Huang, Z. Wu, B. Sundén, Pressure drop and convective heat transfer of Al2O3/water and MWCNT/water nanofluids in a chevron plate heat exchanger, Int. J. Heat Mass Transfer 89 (2015) 620-626.

[5] D. Huang, Z. Wu, B. Sundén, Effect of hybrid nanofluid mixture in late heat exchangers, Exp. Therm. Fluid Sci. 72 (2016) 190-196.

[6] B. Sundén, Z. Wu, Performance of Heat Exchangers using Nanofluids, in V. Bianco, O. Manca, S. Nardini, & K. Vafai (Eds.) Heat Transfer Enhancement with Nanofluids, pp. 207-236, 2015, CRC Press, Florida.

Numerical study of the heat transfer characteristics in double tube helical heat exchangers using hybrid nanofluids

HUMINIC Gabriela [1], HUMINIC Angel [1], DUMITRACHE Florian [2], FLEACA Claudiu [2], MORJAN Ion [2]

[1] Mechanical Engineering Department, Transilvania University of Brasov, 500036, brasov, Romania
[2] National Institute for Laser, Plasma and Radiation Physics, PO Box MG-36, 077125, Magurele, Bucharest, Romania

[*]*Corresponding e-mail: gabi.p@unitbv.ro*

Keywords: hybrid nanofluids, double tube helical heat exchanger, turbulent flow.

INTRODUCTION:

The hybrid nanofluids are very new kind of nanofluids, which can be prepared by suspending two or more nanoparticles in base fluid. These nanofluids combine physical and chemical properties of different materials simultaneously and provide these properties in a homogeneous phase [1]. The study of the hybrid nanofluids (synthesis, characterization, preparation, thermo-physical properties and heat transfer characteristics) became a interesting topic in last year's. Only few studies regarding the thermo-physical properties of the hybrid nanofluids and their heat transfer characteristics are available in literature. Thus, Madhesh et al. [2] investigated the heat transfer and rheological characteristics of Cu-TiO2 hybrid nanofluids in a tube-in-tube counter flow heat echangers. The results showed that the surface functionalized and highly crystalline nature of the hybrid nanofluids improved thermal conductivity and heat transfer characteristics of nanofluids. The heat transfer and friction factor characteristics of multi-walled carbon nanotubes (MWCNT)–Fe_3O_4/ water nanocomposite nanofluids flow in a tube with longitudinal strip inserts were studied experimentally by Sundar et al. [3]. The MWCNT–Fe_3O_4 nanocomposite was synthesized by in-situ growth and chemical co-precipitation method and characterized by various techniques. The results showed that the Nusselt number enhancement for 0.3% nanofluid flow in a tube without inserts was 32.72% and with inserts of aspect ratio 1 was 50.99% at a Reynolds number of 22,000. The thermo-physical properties, heat transfer performance and friction factor for fully developed turbulent flow of graphene nanoplatelets (GNP)–Ag/water nanofluids flowing through a circular tube at a constant heat flux were investigated by Yarmand et al. [4]. The authors founded that the maximum enhancement of Nusselt number was 32.7% with a penalty of 1.08 times increase in the friction factor for the weight concentration of 0.1% at a Reynolds number of 17,500 compared to distilled water. Madhesh

et al. [5] studied the heat transfer potential and rheological characteristics of copper–titania hybrid nanofluids (HyNF) using a tube in the tube type counter flow heat exchanger. The nanofluids were prepared by dispersing the surface functionalized and crystalline copper–titania hybrid nanocomposite (HyNC) in the base fluid. The results showed that the convective heat transfer coefficient, Nusselt number and overall heat transfer coefficient were increased by 52%, 49% and 68% respectively, up to 1.0% volume concentration of HyNC.

Studies concerning the application of the hybrid nanofluids in double tube helical heat exchangers are not reported in literature. Thus, the scope of the present study is to investigate on the heat transfer characteristics, such hybrid nanofluids and water temperatures, heat transfer rates and heat transfer coefficients along inner and outer tubes for turbulent flow in double tube helical heat exchangers.

METHODS:

In the present analysis, the hybrid nanofluid flows through the inner tube with the inlet temperature of 353 K and water flows through annulus with the inlet temperature of 288 K. The mass flow rate of the nanofluid is kept constant and mass flow rate of the water from the annulus was set at either half from the value of the mass flow rate from inner tube, full, or double the value. The properties of the inner and outer tube were set to copper, with a thermal conductivity of 401 W/m K, density of 8930 kg/m^3 and a specific heat of 385 J/kg K.

RESULTS AND CONCLUSIONS:

A numerical study has been carried out on the heat transfer behavior of hybrid nanofluids flowing through a counter-flow double tube helical heat exchanger under a turbulent flow condition. The effect of particle concentration volume and the Dean number on the heat transfer characteristics of hybrid nanofluids and water were investigated. From the results of the present study, it was found out that the use of hybrid nanoparticles as the dispersed in water can significantly enhance the convective heat transfer in the turbulent flow regime, and the enhancement increases with Dean number, as well as particle concentration volume under the conditions of this work. Also, outlet water temperature increases with increasing particle concentration volume from the inner tube. The results obtained from the numerical study are validated by comparing with the empirical equations.

REFERENCES:

[1] Jahar Sarkar, Pradyumna Ghosh,Arjumand Adil, A review on hybrid nanofluids: Recent research,development and applications, Renewable and Sustainable Energy Reviews 43 (2015) 164–177.

[2] D. Madhesh, R. Parameshwaran, S. Kalaiselvam, Experimental investigation on convective heat transfer and rheological characteristics of Cu–TiO$_2$ hybrid nanofluids, E*xperimental Thermal and Fluid Science*, *Volume 52*, *January 2014*, *Pages 104-115*

[3] L. Syam Sundar, G. Otero-Irurueta, Manoj K. Singh, Antonio C.M. Sousa, Heat transfer and friction factor of multi-walled carbon nanotubes-Fe3O4 nanocomposite nanofluids flow in a tube with/without longitudinal strip inserts, International Journal of Heat and Mass Transfer, Volume 100, September 2016, Pages 691-703.

[4] H. Yarmand, S. Gharehkhani, G. Ahmadi, S. F. S. Shirazi, S. Baradaran, E. Montazer, M. N. M. Zubir, M. S. Alehashem, S.N. Kazi, M. Dahari, Graphene nanoplatelets–silver hybrid nanofluids for enhanced heat transfer, Energy Conversion and Management 100 (2015) 419–428.

[5] D. Madhesh, R. Parameshwaran, S. Kalaiselvam, Experimental investigation on convective heat transfer and rheological characteristics of Cu–TiO2 hybrid nanofluids, Experimental Thermal and Fluid Science 52 (2014) 104–115.

Characterization of the wettability of complex nanofluids using 3D Laser Scanning Confocal Fluorescence Microscopy

Vânia Silvério[1], Ana S. Moita[1], António L. N. Moreira[1,*], Rui Lima[2], Nuno Pereira[1]

[1] Instituto Superior Técnico, University of Lisbon, Center on Innovation, Technology and Policy Research, 1049 – 001 Lisboa, Portugal

[2] University of Minho, Department of Mechanical Engineering, 4804 – 533 Guimarães, Portugal

Corresponding e-mail: Corresponding author e-mail address

Keywords: Microchannel heat sink, Electronici Cooling, Micro heat transfer

INTRODUCTION:

Microchannel heat sinks have long been viewed as efficient cooling devices for high-powered integrated circuits. By relying on mostly latent heat transfer, two-phase flows give better performance than single-phase devices, as they require smaller flow rates at the same time that allow maintain the sink at a uniform temperature [1]. But, conversely, due to the reduced dimensions of the confinement, bubble inception and growth and subsequent bubble/bubble and bubble/channel wall interactions induce vigorous mixing and disruption of the confined channel flow, thus potentiating pressure fluctuations, reverse flow and temperature fluctuations, characteristic of instabilities in the flow, which are further complicated for multiple channel configurations [2]

One way of increasing the efficiency of single-phase microchannel flow but still avoiding the drawbacks of boiling instabilities is to make use of suspensions of nano-sized particles (1–100 nm) in a base fluid, known as nanonfluids, to improve the heat transfer characteristics of the original fluid [3, 4]. Although, nanofluids are a relatively new class of fluids several recent reviews can already be found in the literature concerning their synthesis [5, 6], heat transfer [6, 7, 8] and applications [9, 10]. Overall, several experiments have shown relevant common findings such as nanofluid thermal conductivity increases with the nanoparticle volume concentration and tends to increase as the nanoparticle size decreases. However, still several features need further clarification such as the effect of the temperature on the fluid viscosity and Brownian motion of the nanoparticles, the effect of the surface wettability of the nanofluids, the effect of additives and surfactants in the long term stability of nanoparticles dispersion. A major study is planned to focus on the clarification and improvement of all the mentioned features. The final objective is to promote the development of nanofluids as a new class of heat transfer fluids. In this context, experiments will be conducted making use of different kinds of nanofluids, such as iron oxide nanoparticles [11] and alumina [12], in an integrated microchannel heat sink device to evaluate the cooling performance of this promising combination. Here, the emphasis is put on the characterization of the wettability, as it is the key parameter governing heat, mass and momentum transport at liquid- solid-vapor interfaces determining the performance of any cooling system, particularly at micro scales.

METHODS:

A first task is directed towards the production of MONs, searching optimized conditions to obtain nanostructured composites with low particle size having high thermal properties and dispersion stability. To achieve the proposed objectives, a thorough screening of synthesis conditions are envisaged using the co-precipitation [16] and solvothermal [11] methods. The morphology is analysed by scanning and transmission electron microscopies, which also give information about the phase structures and chemical composition, complemented by Fourier transform infrared spectroscopy, X-ray diffraction, Raman and X-ray photoelectron spectroscopy.

Wettability is usually quantified by the apparent contact angle θ_e, which is obtained at the equilibrium between the interfacial tensions acting as a droplet is gently deposited over the surface. As quasi-static angles do not accurately characterize dynamic wetting situations and very small dynamic angles are very difficult to obtain, the work will also make use of Laser Scanning Confocal Microscopy with fluorescent droplets and 3D reconstruction to characterize the wettability within extreme wetting regimes [14]. In this context, the work explores the influence that surface patterning may have on the wetting properties of different nanofluids, depending of the relation between the micro patterning and the size, concentration and thermo-physical properties of the nanoparticles.

PRELIMINARY RESULTS:

The Laser Scanning Confocal Fluoresce Microscopy - LSCFM has been assessed as an accurate tool to characterize the wettability of nanofluids on complex surfaces. The technique is firstly validated by measuring the equilibrium contact angles of liquids on smooth glass slides, for a wide range of droplet sizes, from tens of microns to 2.6mm. Under these conditions, the contact angles measured by the LSCFM are consistently similar to those measured by the tensiometer, although generally lower (Fig. 1a). A different scenario is nevertheless observed when characterizing micro-patterned surfaces. The LSCFM technique can provide a detailed reconstruction of the surface topology at the liquid-solid interface region, thus allowing identifying stable Wenzel wetting regimes, in geometries for which the apparent contact angles measured from the tensiometer can be up to 40º higher than those obtained with this non-intrusive technique LSCFM Fig 1b-c). Following these results, a few usual approaches to predict the wetting regimes, based on geometric relations are revisited.

a)   b)   c)
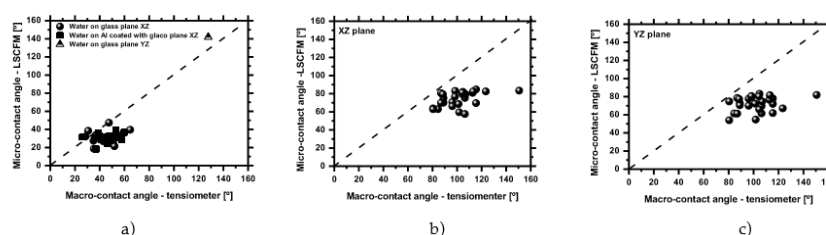
REFERENCES

[1] Kandlikar, S. G., Colin, S., Peles, Y., Garimella, S., Pease, R. F., Brandner, J. J. and Tuckerman, D. B., «Heat transfer in microchannels - 2012 status and research needs,J. Heat Transfer 135 (2013) 091001-1, http://dx.doi.org/10.1115/1.4024354.

[2] Silvério, V., Cardoso, S., Gaspar, J., Freitas, P.P., Moreira, A.L.N., Design, fabrication and testo f na integrated multi-microchannel heat sink for electonics cooling, Sensors and Actuators A: Physical, vol. 235, pp. 14-27, November, 2015

[3] Choi, S.U.S., In: Singer, D.A., Wang, H.P., editors, Development and application of non-Newtonian flows, New York: ASME, pp. 99–105, 1995

[4] Hwang, Y.J., Ahn, Y.C., Shin, H.S., Lee, C.G., Kim, G.T., Park, H.S., Lee, J.K., Investigation on characteristics of thermal conductivity enhancement of nanofluids, Current Applied Physics, vol. 6. Issue 6, pp. 1068–71, October, 2006

[5] Pang, C., Lee, J.W., Tae, Y.T., Review on combined heat and mass transfer characteristics in Nanofluids, International Journal of Thermal Sciences, vol. 87, pp. 49-67, January, 2015

[6] Keblinski, P., Eastman, J.A., Cahill, D.G., Nanofluids for thermal transport, Materials Today, vol. 8, issue 6, pp. 36–44, June, 2005

[7] Lomascolo, M., Colangelo G., Milanese M., Risi A., Review of heat transfer in nanofluids: Conductive, convective and radiative experimental results, Renewable and Sustainable Energy Reviews, vol. 43, pp. 1182–1198, March, 2015

[8] Godson, L., Raja, B., Lal, M. D., Wongwises, S., Enhancement of heat transfer using nanofluids — An overview, Renewable and Sustainable Energy Reviews, vol. 14, issue 2, pp. 629–641, February, 2010

[9] Wang, X.Q., Mujumdar, A.S., A review on nanofluids - part ii: experiments and applications, Brazilian Journal of Chemical Engineering, vol. 25, No. 04, pp. 631 – 648, 2008.

[10] Saidur, R., Leong, K.Y., Mohammad, H.A., A review on applications and challenges of nanofluids, Renewable and Sustainable Energy Reviews, vol. 15, issue 3, pp. 1646–1668, April, 2011

[11] Pastrana-Martínez, L.M., Pereira, N., Lima, R., Faria, J.L., Gomes, H.T., Silva, A.M.T., Degradation of diphenhydramine by photo-Fenton using magnetically recoverable iron oxide nanoparticles as catalyst, Chemical Engineering Journal, vol. 261, pp. 45-52, 2015

[12] Sridhara V. and Satapathy L. N., Al2O3-based nanofluids: a review, Nanoscale Research Letters, 6:456, 2011.

[13] Rodrigues, O.R., Bañobre-López, M., Gallo, J., Tavares, P.B., Silva, A.M.T., Lima, R., Gomes, H.T., Hemocompatibility of Iron Oxide Nanoparticles synthetized for Theranostic Applications: a Novel Microfluidic Study, Journal of Nanoparticle Research, 2016 (in press), DOI: 10.1007/s11051-016-3498-7

[14] Vieira, D., Moita, A. S. M. and Moreira, A. L. N. "Non-intrusive wettability characterization on complex surfaces using 3D Laser Scanning Confocal Fluorescence Microscopy", 18th International Symposium on the Application of Laser and Imaging Techniques to Fluid Mechanics, Lisbon, Portugal, July 4 – 7, 2016.

Transformer oil based magnetic fluid for effective cooling medium in power transformers

Milan Timko[1], Peter Kopcansk[1], M. Rajnak[1], Matus Molcan[1], Bystrik Dolnik[2], Juraj Kurimsky[2]

[1]Institute of Experimental Physics, Slovak Academy of Sciences, 040 01 Kosice, Slovakia
[2]Faculty of Electrical Engineering and Informatics, TU in Košice, Letna 9, 040 01 Kosice, Slovakia
Corresponding e-mail: timko@saske.sk

Keywords: transformer oil, magnetic fluid, power transformer, cooling effect

INTRODUCTION:
Transformer oils (TO) act mainly as the electrical insulation system in many types of electrical equipment. Besides the electrical insulation, they provide effective heat transfer, acting as a coolant. To increase the lifetime and reliability of electrical equipment it is necessary to decrease their operation temperature. For that purpose, researchers look for additives enhancing the TO's thermal properties and retaining their excellent insulating characteristics. One of the promising additives are superparamagnetic nanoparticles (MNP).

METHODS:
The stable dispersion of MNP (spherical magnetite nanoparticles) in TO constitutes magnetic liquids or ferrofluids with volume concentration of MNP up to 1.02%. The magnetic and dielectric properties, dielectric breakdown and size distribution were measured on prepared sample. According to dielectric properties of ferrofluids there is a potential application in electrical engineering as sealing and grinding technologies, heat transfer and hydrodynamic flow. One from the application is the cooling and isolative medium in power transformer where the magnetoconvection effect is present.

RESULTS AND CONCLUSIONS:
From dielectric point of view, the presence of MNP in TO increases their electric permittivity, and can even increase their dielectric breakdown field strength [1]. This paradoxical finding is still not fully understood. A theoretical modeling has indicated that MNP in TO can act as free charge scavengers which slow down the streamer velocity leading to dielectric breakdown [2]. It is therefore intuitive that knowledge about interactions and structural behavior of MNP in electric fields are of fundamental importance in the comprehension of the peculiar breakdown mechanism. Recently, MNP aggregation in electric fields was deduced from dielectric measurements [3] and formation of anisotropic structures was proved by small angle neutron scattering [4]. Now, an open question is focused on a relation between the electric field induced structural changes and magnetic properties of ferrofluids based on TO. Such investigation can provide understanding of the breakdown mechanism and open a new avenue of ferrofluid research.

The cooling effect of magnetic fluid in magnetic field was analyzed by finite element method. The real experimental results in 10 kW industrially produced power transformer filled by TO based magnetic fluid. will be reported too. It was shown that the existence of disperse magnetic field increases of magnetic fluid magnetoconvection circulation and so the improvement of transformer cooling. The effect of cooling can be more effectively by using of expansion container too.

REFERENCES:

[1] J.-C. Lee, H.-S. Seo, Y.-J. Kim, Int. J. Therm. Sci., 62, pp. 29–33 (2012).

[2] J. G. Hwang, M. Zahn, F. M. O'Sullivan, L. A. A. Pettersson, O. Hjortstam, R. Liu, J. Appl. Phys. 107, 1, pp. 014310–014310–17 (2010).

[3] M. Rajnak, J. Kurimsky, B. Dolnik, P. Kopcansky, N. Tomasovicova, E. A. Taculescu-Moaca, M. Timko, Phys. Rev. E 90, 032310 (2014).

[4] M. Rajnak, V. I. Petrenko, M. V. Avdeev, O. I. Ivankov, A. Feoktystov, B. Dolnik, J. Kurimsky, P. Kopcansky, and M. Timko, Appl. Phys. Lett., 107, 7, p. 073108, (2015).

Thermophysical properties of ethylene glycol based yttrium aluminum garnet (Y$_3$Al$_5$O$_{12}$–EG) nanofluids

Gaweł Żyła [1*]

[1] Department of Physics and Medical Engineering, Rzeszow University of Technology, Rzeszow, 35-905, Poland

Corresponding e-mail: gzyla@prz.edu.pl

Keywords: nanofluids, viscosity, thermal conductivity

INTRODUCTION: The paper presents results of measurements of basic thermophysical properties of ethylene glycol based yttrium aluminum garnet (Y$_3$Al$_5$O$_{12}$–EG) nanofluids. Nanofluids used in presented measurements were prepared with two-step method based on commercial nanoparticles manufactured by Baikowski (Annecy, France), ID LOT: 18513.

METHODS: Basic rheological properties were investigated on HAAKE MARS 2 rheometer (Thermo Electron Corporation, Karlsruhe, Germany). Dynamic viscosity curves in the range of shear rates from 10 to 1000 s^{-1} at a constant temperature of 298.15 K were determined. To determinate thermal conductivity of nanofluids a KD2 Pro Thermal Properties Analyzer (Decagon Devices Inc., Pullman, Washington, USA) was used. The dependence of thermal conductivity of Y$_3$Al$_5$O$_{12}$–EG nanofluids on the concentration of nanoparticles was measured at constant temperature of 298.15 K.

RESULTS AND CONCLUSIONS: Viscosity curves are presented in Fig. 1, and it shows the experimental results and the Newton model fit. Studies have shown that nanofluids viscosity is not dependent on shear rate, so that material definitely can be classified as Newtonian.
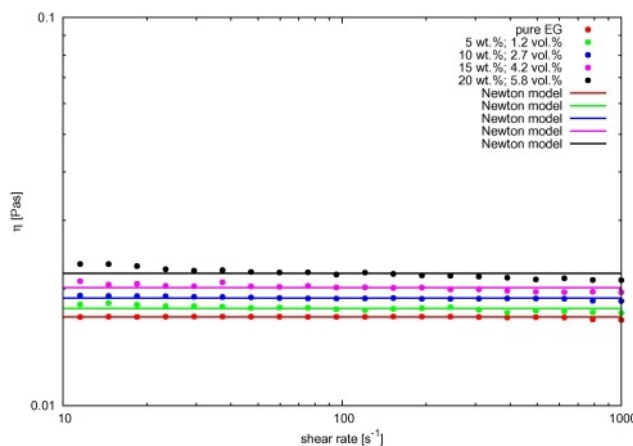
1. Dynamic viscosity curves of Y$_3$Al$_5$O$_{12}$–EG at 298.15 K. Dots represent measuring points, lines – the theoretical model fit. [1]

As expected, viscosity of the nanofluids increases with increasing concentration of nanoparticles in suspension. Chow proposed variable degree volume fraction polynomial to model the η_{nf}/η_0 ratio, and as presented in Fig. 2 it works correctly in this case.
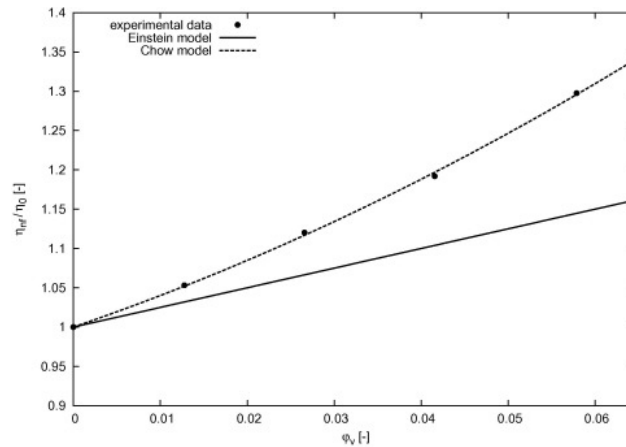
2. Viscosity enhancement in $Y_3Al_5O_{12}$–EG nanofluid vs. volume fraction at 298.15 K. Dots represent measuring points, lines – the theoretical models fits. [1]

A studies on the thermal conductivity of various fraction of particles in $Y_3Al_5O_{12}$–EG nanofluids at constant temperature 298.15 K was conducted. The results presented in Fig. 3 indicate that the thermal conductivity increases non-linearly with increasing concentration of nanoparticles, and this enhancement could not be described by classical theoretical models.
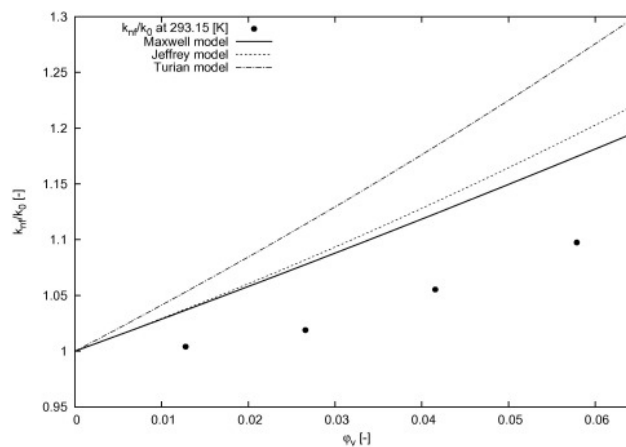
3. Thermal conductivity enhancement of $Y_3Al_5O_{12}$–EG nanofluid vs. volume fraction at 298.15 K. Dots represent measuring points, lines – the theoretical models fits. [1]

REFERENCES: [1] G. Żyła, *Thermophysical properties of ethylene glycol based yttrium aluminum garnet ($Y_3Al_5O_{12}$–EG) nanofluids*, **International Journal of Heat and Mass Transfer**, 92, 751–756 (2016), http://dx.doi.org/10.1016/j.ijheatmasstransfer.2015.09.045

Carbon nanotubes nanofluids:
Thermophysical properties and applications to heat exchange

Patrice Estellé [1]

[1] Laboratoire de Génie Civil et Génie Mécanique, Matériaux et Thermo-Rhéologie, Université Rennes 1, 35704 Rennes, France

*Corresponding e-mail: patrice.estelle@univ-rennes1.fr

Keywords: CNT nanofluids, thermal conductivity, influence of composition, thermophysical properties, heat exchange efficiency

INTRODUCTION: It is now well established that nanofluids are challenging materials with promising use in heat exchangers, energy and convective systems, solar collectors, electronic devices... They also appear as a worldwide research topic due to their potential applications. Nanofluids exhibit higher thermal conductivity than base fluids which is significantly increased with increasing concentration of nanoparticles. The nature of nanoparticle also plays a role in these benefits over conventional fluids. Also, carbon-based nanomaterials such as carbon nanotubes and graphene are of main interest because of their excellent intrinsic thermal properties.

As a main characteristic of potential application, thermal conductivity measurement of water-based multi-walled carbon nanotubes is here reported, considering the effect of surfactant, volume fraction and temperature. An attempt is also made to correlate experimental data to theoretical model taking into consideration different findings and possibly explain the thermal conductivity enhancement of nanofluids [1].

Then, other thermophysical properties such as rheological behaviour [2], density, heat capacity [3] are also studied and discussed. This allows to investigate and demonstrate the efficiency of these nanofluids in energy systems. Finally, some applications in different configurations of heat exchange are also presented [3-6].

METHODS: Nanofluids consists of MWCNT (purity of 90%) dispersed in a mixture of deionized water and ionic surfactant and obtained by the two step method. An initial starting suspension with 1% in weight fraction of nanotubes and 2% in weight fraction of surfactant was prepared by Nanocyl ffrom their commercial nanotubes. Then, nanofluids with lower volume fraction were obtained from serial dilution of the starting suspension, as in [2], conserving constant surfactant/carbon nanotubes weight ratio of 2. Consequently, it is assumed that preparation of nanofluids does not affect the TC measurement performed in the following. Finally, the whole volume fraction range investigated varies between 0.005% and 0.55% at ambient temperature.

Thermaf conductivity measurements of nanofluids and base fluids were performed with a KD2 Pro thermal property analyzer (Decagon Devices Inc.), which is based on the transient hot wire method. The experimental set-up for thermal conductivity measurement was previously used

and described in [1]. In short, each sample is placed in a vessel, itself located in a temperature control bath. The sensor probe and a platinum probe (with an accuracy of 0.1°C) are inserted within the sample. Before starting TC measurement, both the sample and the probes were first maintained 30 min at the required temperature. Each reported value was an average of ten measurements. Thermal conductivity values were measured at 20, 30 and 40°C respectively for each tested volume fraction of nanofluids and base fluids. Temperature was limited to 40°C as surfactant may fail for higher temperature.

RESULTS AND CONCLUSIONS: It was observed that TC enhancement of CNT nanofluids increase with volume fraction and temperature. The thermal conductivity enhancement is really significant at very low volume fraction, in particular at 30 and 40°C. The effect of the used surfactants on TC enhancement of nanofluids is weak, TC is also weakly affected by the influence of CNT aspect ratio considered here.

The comparison between experiments and models show that theoretical predictions presented above cannot clearly capture the TC enhancement of CNT water based nanofluids presently investigated within the entire range of volume fraction considered and temperature. This evidences a need both to develop appropriate model for TC enhancement prediction of CNT nanofluids and measure TC of this kind of nanofluids before performing numerical studies in heat exchangers and cavities.

Finally, based on the comprehensive characterization of thermophysical properties, efficiency of some of these nanofluids following temperature and volume fraction is demonstrated for laminar and turbulent flow conditions [3] and different configurations of heat exchangers [3-6].

REFERENCES:

[1] P. Estellé, S. Halelfadl, T. Maré, Thermal conductivity of CNT water based nanofluids: Experimental trends and models overview, *Journal of Thermal Engineering* 1(2) (2015) 381-390.

[2] S. Halelfadl, P. Estellé, et al., Viscosity of carbon nanotubes water-based nanofluids: Influence of concentration and temperature, *International Journal of Thermal Science*, 71 (2013) 111-117

[3] S. Halelfadl, T. Maré, P. Estellé, Efficiency of carbon nanotubes water based nanofluids as coolants, Experimental Thermal and Fluid Science 53 (2014) 104-110

[4] P. Estellé et al., Heat transfer properties of aqueous carbon nanotubes nanofluids in coaxial heat exchanger under laminar regime, *Experimental Thermal and Fluid Science* 55 (2014) 174-180

[5] P. Estellé et al., Optimization of thermal performance and pressure drop of a rectangular microchannel heat sink using aqueous carbon nanotubes based nanofluid, *Applied Thermal Engineering* 62/2 (2014) 492-499

[6] P. Estellé et al., Natural Convection of CNT Water Based Nanofluids in a Differentially Heated Square Cavity, submitted to *International Communications in Heat and Mass Transfer* (2016)

ASSESSING THE FLOW CHARACTERISTICS OF NANOFLUIDS DURING TURBULENT NATURAL CONVECTION

K. Kouloulias[1]*, A. Sergis and Y. Hardalupas

Imperial College London, Mechanical Engineering Department, London SW7 2AZ, UK

Corresponding author: k.kouloulias13@imperial.ac.uk

Keywords: Turbulent natural convection, Rayleigh-Benard, Nanofluids, Particle Image Velocimetry, Cooling

Introduction: Nanofluids have attracted significant attention due to their intriguing heat transfer properties under different heat transfer modes. According to an extended statistical analysis of data available in the literature, the heat transfer enhancement when nanofluids are involved is 5-9% for the conductive heat transfer, 10-14% for the mixed conductive-convective, 40-44% for pool boiling and up to 200% increase for the value of the critical heat flux [1]. Despite the reported promising heat transfer characteristics of nanofluids, the physical understanding of the underlying processes is missing and a controversy remains regarding their capability and applicability in engineering applications. This controversy arises from inconsistency in the observations of reported studies, accompanied by insufficient understanding of the physical mechanisms involved in nanofluids. For example, while heat transfer enhancement is reported for forced convection [2-5], opposing results are observed for natural convection with additional puzzling discrepancy between numerical [6-10] and experimental [11-14] natural convection studies. Two types of natural convection are distinguished based on the resulting flow conditions: laminar and turbulent. Out of those, turbulent natural convection has drawn greater attention due to the complex features associated with turbulence. In turbulent convection two discrete states have been identified according to the Rayleigh number, Ra, of the flow and the aspect ratio, Γ, of the employed cell. In cells with aspect ratios close to unity, a soft turbulent state has been observed for $Ra < 10^7$ and hard turbulence for Ra between 4×10^7 to 10^{12} [15-17], with the difference lying on the way in which the thermals and plumes are developed and traverse inside. It has been widely reported that, at the hard turbulent state, a large-scale coherent flow exists [18-20], which is self-organised by the hot rising and cold falling plumes. This flow mode is known as mean wind or large scale circulation (LSC). Up to date, the LSC remains an attractive feature to study and further analyse, as the heat transport in turbulent natural convection takes place primarily along the periphery of the cell, in the direction of the LSC [21, 22]. Therefore, the study of nanofluids under natural convection is an attractive way to assess the heat transfer properties of these new coolants and establish the underlying physical mechanisms.

Methodology: Experimental set-up: A classical Rayleigh-Benard (RB) configuration with optical access is operated in the current study. Fig. 1(a) shows a schematic drawing of the RB cell, including all the major components. A detailed description of this configuration can be found in Ref. [12], whilst a brief overview of its components is included herein. The cell consists of a

heating plate, A, at the bottom, a cooling plate, B, at the top and lateral walls, C. It incorporates four quartz windows, 2 square (40 mm x 40 mm) and 2 rectangular (10 mm x 40 mm), D, to allow laser-based visualization studies. Teflon plates, E, are inserted among all the conductive components to prevent their thermal connection. Finally, insulating pans, F and a Plexiglas cover, G are placed outside the core of the cell to eliminate the heat losses from the sides. At the same direction, a second set of heating elements, H is placed below the heating plate to prevent any heat losses downwards. The operation of the RB cell is monitored and controlled through LabVIEW software, coupled with National Instruments (NI) hardware and an in-house electrical device that is connected to the heating plates (A, H) and thermocouples placed in the cell.

Particle Image Velocimetry (PIV): A high spatial resolution (0.49 mm) flow velocimetry method, PIV, is employed for the test fluids inside the RB cell, through the available optical access. A double-pulsed Nd-Yag laser (Nano T 135-15 PIV) is used to illuminate micron-sized tracer particles (hollow glass spheres (HGS) with nominal diameter of 10 μm) dispersed in the flow. The particles are illuminated twice by the pulsed laser with fixed time interval (20 ms) on planes defined by a thin laser sheet. A charge coupled device camera (LaVision Imager Intense) is utilized to record the displacement via the change of the pattern of the intensity of the scattered light from the HGS particles during the time delay between the two laser pulses. Due to the small size of the tracers, no drift velocities are present between the liquid flow and the HGS for the timescales of the experiments. Commercial software (DaVis 8.2.2) is used to control the laser and process the recorded images. Each laser pulse pair is emitted at a rate of 0.25 Hz, while 2000 independent pairs of images of the instantaneous flow are recorded at steady state conditions. Each 2D velocity vector is calculated from an interrogation window of 32 x 32 pixels with a 75% overlap. The field of view for the PIV measurements is slightly smaller than the square windows, as the data close to the edges of the window, where light reflections could affect the reliability of the results, are neglected. In Fig. 1(b), the field of view (pink-coloured square) and the Cartesian coordinates for the analysis of the PIV results are depicted.
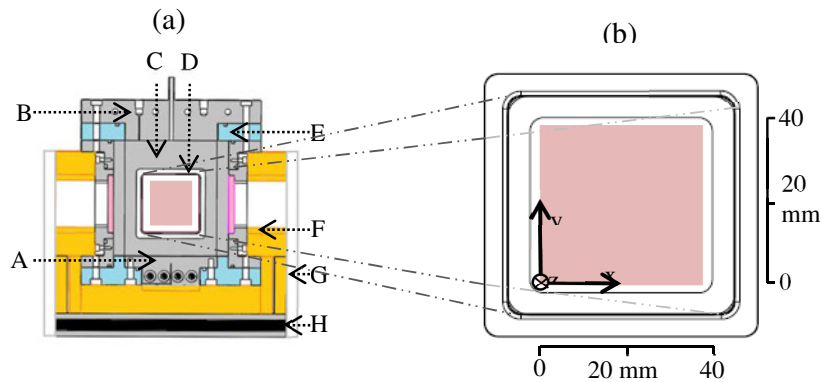
Fig. 1. Schematic drawing of the (a) Rayleigh-Benard cell [22] and (b) field of view. The marked components are explained in the text.

Experimental Procedure: Dilute Al_2O_3-deionised (DI) H_2O nanofluids with a mean concentration of 0.00026 vol.% were synthesized, tested and compared with DI H_2O under turbulent natural convection. The employed nanoparticles were supplied by Alfa Aesar with an average particle size of 45 nm and a particle density of 3965 kg/m^3. A constant temperature gradient between the heating and cooling plates of DT = 63.2 °C and a constant temperature of T_c = 26.4 °C at the cooling plate were the imposed conditions. In this way, our system had two control parameters: Rayleigh, Ra = 4.1 x 10^9, and Prandtl, Pr = 3.1, and two response parameters: Nusselt, Nu, and temporally averaged velocities, V_{avg}. The PIV measurements were obtained at three different planes in the z direction of the coordinate system of Fig. 1(b) inside the cell, to record the impact of nanoparticles on the three dimensional flow structure and properties of the base fluid. The first plane was at the centre of the cell, z = 0, (central plane), the second was at an absolute distance z of 3 ±1 mm behind the centre (back plane) and the third one was at an absolute distance z of 4 ±1 mm in front (front plane) of the centre. The measurements on each plane were based on 2000 images to reduce the statistical uncertainties. In addition, the measurements on each plane were repeated at least four times to ensure that random uncertainties are minimised and. Therefore, in this work mean values are presented and compared for each plane. The fractional uncertainty in mean for the temporally and spatially averaged velocity $\overline{|V|}_{avg} \leq 2.6\%$ and for the Nu is $\leq 1.0\%$. Thus, the results presented herein are repeatable, reliable and precise. Finally, for the operating conditions in this study and the characteristics of the RB cell (shape and aspect ratio), the LSC is observed to develop along a diagonal of the cell. Therefore, the reported planar PIV flow measurements are projections of the diagonal flow field on the measurement plane, as seen through the square window depicted in Fig. 1.

Discussion and Results: In Table 1, the heat transfer performance, the calculated temporally and spatially averaged velocity characteristics, $\overline{|V|}_{avg}$, *Stdev*, $\delta \overline{|V|}_{avg}$ and *TI* for water and dilute nanofluid are presented. It is noted that the spatially averaged velocity is calculated over the applicable field of view in Fig. 1(b).At first, by comparing the general heat transport, as expressed with the Nu, for both test fluids, no clear trend can be observed. This is due to the very small concentration of nanoparticles in the base fluid, the operating conditions in this study and the associated experimental uncertainty.

Table 1. Heat transfer performance and velocity characteristics for water and dilute nanofluids at three different planes inside the RB cell.

	Water				Nanofluids			
Plane	$\overline{\lvert V \rvert}_{avg}$	Stdev	TI	Nu	$\overline{\lvert V \rvert}_{avg}$	Stdev	TI	Nu
	(cm/s)	(cm/s)	(%)		(cm/s)	(cm/s)	(%)	
back	0.3311	0.2604	79	76.4	0.3551	0.2651	75	76.2
central	0.3444	0.2635	77	76.1	0.3537	0.2673	76	76.2
front	0.3115	0.2578	83	76.5	0.3449	0.2662	77	77.4

The spatial distribution of the flow velocity field demonstrates differences between water and nanofluids, despite the small concentration of the nanoparticles. For instance, the temporally and spatially averaged velocity $\overline{\lvert V \rvert}_{avg}$ of the base fluid increases by 6.9% (on average in the planes) in the field of view when nanoparticles are employed. This trend is emphasised by examining the contours of the time-averaged mean velocity for water and nanofluids for the front plane, depicted in Fig. 2. It can be seen that the area close to the heating surface, where maximum velocities in the field of view are recorded, is notably larger for the nanofluid than for pure water. In the same figure, the direction of the velocity vectors (their length is proportional to the pixel displacement) indicates the existence of the LSC and the preferential clockwise direction. Except for $\overline{\lvert V \rvert}_{avg}$ the temporally and spatially averaged turbulent intensity of the velocity fluctuations, *TI*, in the field of view is consistently modified with the presence of nanoparticles in the base fluid. More specifically, *TI* for nanofluids is 4.3% (on average in the planes) smaller compared to water in the field of view. *TI* is defined as the ratio of the temporally and spatially averaged standard deviation of the turbulent velocity fluctuations to the temporally and spatially averaged velocity in the field of view.

Conclusions: This study examines the heat and mass transfer characteristics of a dilute Al_2O_3 – DI H_2O nanofluid inside a Rayleigh-Benard cell under turbulent natural convection. In this work, the behavior of nanofluids in applications where the thermal management results are only due to the density gradients in the working fluid is evaluated. Thermal studies along with a high spatial resolution velocimetry method (PIV) were conducted to assess the contribution of the addition of nanoparticles in traditional heat transfer fluids. We report that the addition of a small amount of Al_2O_3 nanoparticles, concentration of 0.00026 vol.%, to DI water alters the mass transfer behavior of the base fluid significantly. More specifically, the temporally and spatially averaged velocity

$\overline{|V|}_{avg}$ for nanofluids is higher than for water in the field of view for all three planes inside the RB cell. In addition, the temporally-averaged and spatially-averaged turbulent intensity of the velocity fluctuations, *TI*, in the field of view is decreased when nanoparticles are added. Finally, concerning the heat transfer performance of nanofluids, no consistent trend is observed, mainly due to the small nanoparticle concentration.
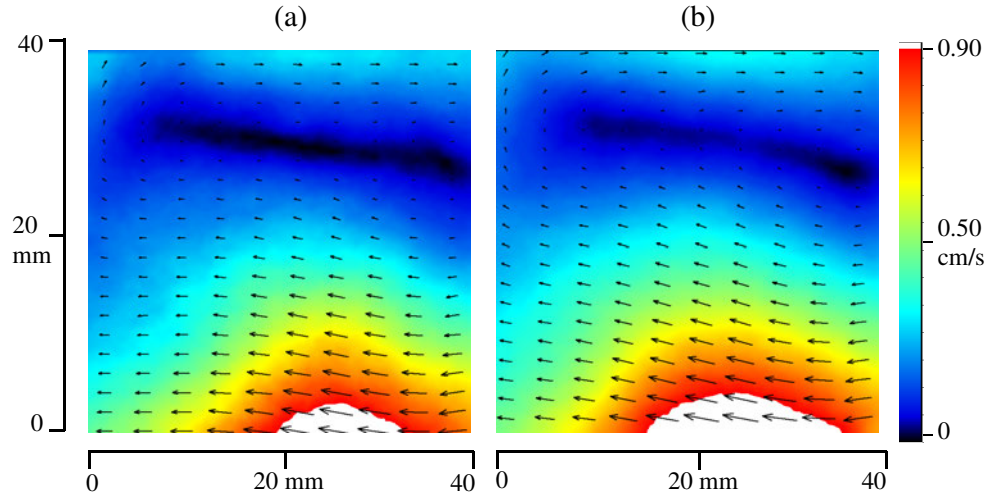
Fig. 2. Contours of the temporally averaged velocity $|V|_{avg}$ at the front plane for (a) water and (b) dilute nanofluid under $Ra = 4.1 \times 10^9$.

References:

1. A. Sergis, Y. Hardalupas, Anomalous heat transfer modes of nanofluids: a review based on statistical analysis, Nanoscale research letters, 6(1) (2011) 391.
2. Y. Xuan, Q. Li, Investigation on Convective Heat Transfer and Flow Features of Nanofluids, Journal of Heat Transfer, 125(1) (2003) 151.
3. S. Kakaç, A. Pramuanjaroenkij, Review of convective heat transfer enhancement with nanofluids, International Journal of Heat and Mass Transfer, 52(13-14) (2009) 3187-3196.
4. A.K. Nayak, M.R. Gartia, P.K. Vijayan, An experimental investigation of single-phase natural circulation behavior in a rectangular loop with Al2O3 nanofluids, Experimental Thermal and Fluid Science, 33(1) (2008) 184-189.
5. S.E.B. Maïga, S.J. Palm, C.T. Nguyen, G. Roy, N. Galanis, Heat transfer enhancement by using nanofluids in forced convection flows, International Journal of Heat and Fluid Flow, 26(4) (2005) 530-546.

6. S. Savithiri, A. Pattamatta, S.K. Das, A single-component nonhomogeneous lattice boltzmann model for natural convection in Al2O3/water nanofluid, Numerical Heat Transfer, Part A: Applications, 68(10) (2015) 1106-1124.

7. M. Eslamian, M. Ahmed, M.F. El-Dosoky, M.Z. Saghir, Effect of thermophoresis on natural convection in a Rayleigh–Benard cell filled with a nanofluid, International Journal of Heat and Mass Transfer, 81 (2015) 142-156.

8. H. Oztop, E. Abu-Nada, Numerical study of natural convection in partially heated rectangular enclosures filled with nanofluids, International Journal of Heat and Fluid Flow, 29(5) (2008) 1326-1336.

9. C.J. Ho, M.W. Chen, Z.W. Li, Numerical simulation of natural convection of nanofluid in a square enclosure: Effects due to uncertainties of viscosity and thermal conductivity, International Journal of Heat and Mass Transfer, 51(17-18) (2008) 4506-4516.

10. F.S. Oueslati, R. Bennacer, Heterogeneous nanofluids: natural convection heat transfer enhancement, Nanoscale research letters, 6(1) (2011) 222.

11. C.H. Li, G.P. Peterson, Experimental studies of natural convection heat transfer of Al2O3/DI water nanoparticle suspensions (Nanofluids), Advances in Mechanical Engineering, 2010 (2010).

12. K. Kouloulias, A. Sergis, Y. Hardalupas, Sedimentation in nanofluids during a natural convection experiment, International Journal of Heat and Mass Transfer, 101 (2016) 1193-1203.

13. D. Wen, Y. Ding, Natural convective heat transfer of suspensions of titanium dioxide nanoparticles (nanofluids), IEEE Transactions on Nanotechnology, 5(3) (2006) 220-227.

14. R. Ni, S.-Q. Zhou, K.-Q. Xia, An experimental investigation of turbulent thermal convection in water-based alumina nanofluid, Physics of Fluids, 23(2) (2011) 022005.

15. F. Heslot, B. Castaing, A. Libchaber, Transitions to turbulence in helium gas, Physical Review A, 36(12) (1987) 5870-5873.

16. G. Zocchi, E. Moses, A. Libchaber, Coherent structures in turbulent convection, an experimental study, Physica A, 166(3) (1990) 387-407.

17. B. Castaing, G. Gunaratne, F. Heslot, L. Kadanoff, A. Libchaber, S. Thomae, X.-Z. Wu, S. Zaleski, G. Zanetti, Scaling of hard thermal turbulence in Rayleigh-Bénard convection, Journal of Fluid Mechanics, 204 (2006) 1-30.

18. R. Krishnamurti, L.N. Howard, Large-scale flow generation in turbulent convection, Proceedings of the National Academy of Sciences of the United States of America, 78(4) (1981) 1981-1985.

19. M. Sano, X.Z. Wu, A. Libchaber, Turbulence in helium-gas free convection, Physical Review A, 40(11) (1989) 6421-6430.

20. X.L. Qiu, P. Tong, Large-scale velocity structures in turbulent thermal convection, Physical Review E, 64 (2001) 036304.

21. X.D. Shang, X.L. Qiu, P. Tong, K.Q. Xia, Measured local heat transport in turbulent Rayleigh-Benard convection, Phys Rev Lett, 90(7) (2003) 074501.

22. K. Kouloulias, A. Sergis, Y. Hardalupas, T.R. Barrett, Measurement of flow velocity during turbulent natural convection in nanofluids, Fusion Engineering and Design, (2017).

AN EXPERIMENTAL SETUP FOR FLOW HEAT TRANSFER INVESTIGATION OF NANOFLUIDS

A. Nikulin* and A.L.N. Moreira

Instituto Superior Técnico, Universidade de Lisboa, IN+,
Av. Rovisco Pais 1, Lisboa, Portugal
*Corresponding author: artem.nikulin@tecnico.ulisboa.pt

Keywords: Nanofluids, heat transfer enhancement, Nanoparticles, Convective Heat Transfer

Introduction: Efficient cooling is one of the major technical challenges currently faced by energy sector. In this context, the use of nanoparticles to enhance heat exchange characteristics of working bodies and heat-carrying agents has recently attracted the close attention of researchers [1].

Many experimental studies have been reported in the literature, which suggest that the addition of nanoparticles enhance the heat transfer coefficient in the laminar and turbulent flow regime as well as during pool and flow boiling. However, the effect on heat transfer is not clear as many of these studies have also shown that nanoparticles have no effect or deteriorate heat transfer coefficient [2]. Though, in our opinion, despite the abundance of published works devoted to the study of nanofluids, the reported results on heat transfer performance still need a correct physical interpretation. Thus, it is premature to use the obtained physical data for the modeling of heat exchange processes and additional systematic experimental data on heat transfer characteristics of nanofluids is required. With this in mind, an experimental set-up is designed as a multifunction installation with the ability to study heat transfer in the laminar and turbulent regimes as well as during flow boiling in a cylindrical minichannel. The present paper is part of a major work aimed at providing careful and systematic data on the heat transfer features of nanofluids, which can contribute to the development of more rigorous physical models for convective heat transfer.

The experimental methodology: The experimental setup is shown in Fig. 1. The working fluid is pumped using the magnetically coupled vane pump 7 through a closed loop. The pump is connected to frequency converter in order to control the flow rate of the working fluid and the Coriolis mass flow meter (mini CORI-FLOW M15) 8 was used to measure mass flow rate. The flow meter allows to carry out measurements from 0.2 to 300 kg/h with the accuracy of 0.2%. Moreover, the application of this type of mass flow meter provide data on density of working fluid with the accuracy of ± 5 kg/m^3.

The test section 3 is a stainless steel (AISI 321) tube 4 mm in diameter, 2.3 m long with wall thickness of 0.2 mm. A part of the tube of 0.4 m before the heating section is serve as calming

length. In order to obtain the straight and horizontal position of the test section the stretching device 10 was employed. The weight of 20 kg produce the stretching force. The stabilized power supply (HY5050EX) with the power stabilization accuracy of 0.3% was used to produce and control the heat flux supplied to the test section. This technique allows obtaining a constant wall heat flux boundary conditions. In addition, the heated area of the tube is divided into seven parts and can vary by power switch 4. Sections 2 and 11 are used for electrical insulation of the test section from the other parts of the experimental setup. To prevent heat loss to the ambient, the test section is placed in the vacuum chamber 12, where a dynamic vacuum on the order of less than 100 Pa is created by a vacuum system. All the connecting pipes are insulated by rubber insulation with the thermal conductivity less than 0.04 W/m·K.
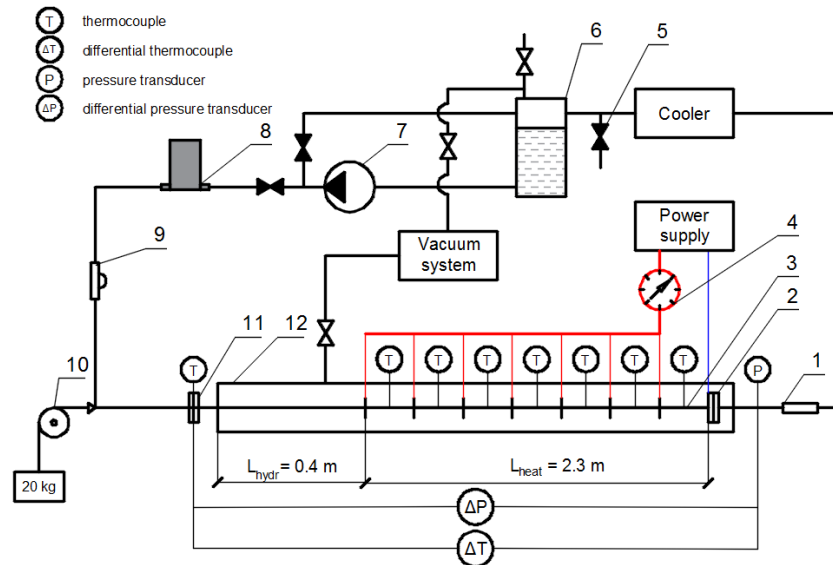
Figure 1. Schematic diagram of the experimental setup

Seven copper-constantan thermocouples fixed on the tube wall to measure the local temperature of the tube. As known [3], the heat transfer coefficient in a pipe flow greatly depends on the inlet temperature. In this context, the thermocouple is installed at the inlet of test section and the cooler serve to maintain the inlet temperature in the range of 0.2 K. Also, the differential thermocouple and differential pressure transducer (PX2300) used to control the temperature change and pressure drop along the test section. Special mixing chambers were mounted before the thermocouples at the inlet and outlet of test section, in order to obtain the mean temperature of the flow. All the thermocouples were calibrated "in situ" in turbulent flow regime using the platinum resistance thermometer installed in flow meter 8.

In addition, for carrying out the flow boiling experiments, the outlet of test section is equipped with the absolute pressure transducer (OMEGA MMA050C1B3MC0T3A6CE). The sight glasses 1 and 9 allows to study the flow boiling regimes and to control the absence of bubbles entering the test section respectively.

The filling of the experimental setup was performed through the receiver 6 and the whole loop was preliminarily evacuated by vacuum system. During the experiment on nanofluids flow heat transfer a certain amount of liquid can be sampled for further analysis by the valve 5. All electrical measurements are performed with the data acquisition system (RIGOL M300).

Preliminary tests of experimental setup using water have shown that disagreement of electric power with the heat capacity transferred to liquid is no more than 2%. Moreover, the difference of Nusselt number obtained in experiment with the calculated value by known empirical correlation $Nu = 0.021 \cdot Re^{0.8} \cdot Pr^{0.43}$ for the turbulent flow regime in the range of Reynolds number 4000 - 20000 do not exceed 4%. The reproducibility of Nusselt number in the set of three experiments agrees within 1%.

The Nusselt number was calculated as follow

$$Nu = \alpha \cdot d / \lambda \tag{1}$$

where $\alpha = G\, C_p\, (T_{out} - T_{in})\, S^{-1}(T_w - \overline{T})^{-1}$ is the mean heat transfer coefficient (W/(m$^2 \cdot$K)); G is the mass flow rate (kg/s); C_p is the specific heat of the liquid (J/(kg$\cdot$K)); S is the surface area of channel (m^2); T_{in} and T_{out} is the inlet and outlet temperatures of the fluid (K); $\overline{T}$ is the mean temperature of the fluid (K); T_w is the arithmetic mean temperature of the channel wall obtained by data averaging from seven thermocouples (K); d is the diameter of the channel (m); λ is the thermal conductivity of liquid (W/(m$\cdot$K)).

Preliminary results: Sigma-Aldrich isopropanol/Al_2O_3 nanofluid (Product Number 702129) with a nanoparticle concentration of 20±1 mass.% is used in this study. This nanofluid was chosen because isopropanol forms stable solutions with Al_2O_3 nanoparticles over a wide range of concentrations and temperatures. According to the manufacturer, the size of the Al_2O_3 nanoparticles is not greater than 50 nm (DLS). The test samples are prepared by diluting isopropanol/Al_2O_3 nanofluid with pure isopropyl alcohol.

Preliminary data, aimed at analyzing the influence of Al_2O_3 nanoparticles on Nusselt number for different Reynolds numbers, are shown in figure 2. The experimental data on thermal conductivity and viscosity was used [4] to calculate the Nusselt number of pure isopropanol and isopropanol/Al_2O_3 nanofluid.
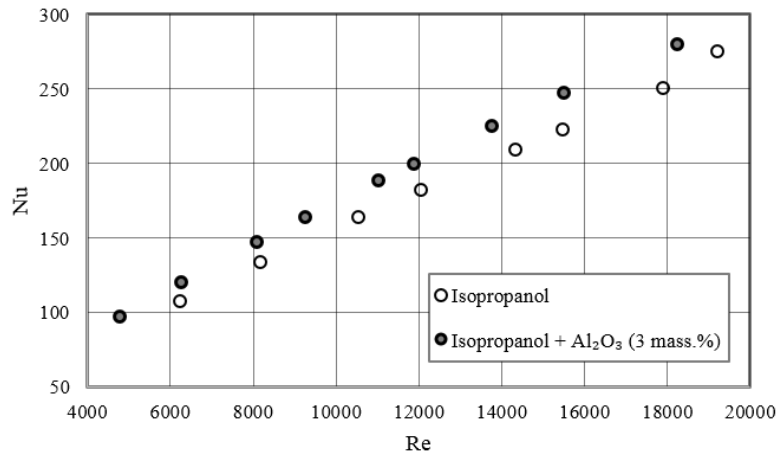
Figure 2. Nusselt number versus Reynolds number for isopropanol and isopropanol/Al_2O_3 nanofluid (3 mass.%)

The conducted test experiments indicate that the created experimental setup allows to obtain consistent and reproducible characteristics on turbulent flow heat transfer.

The preliminary results obtained shows that Al_2O_3 nanoparticles added to isopropanol lead to a significant change in heat transfer process. The average enhancement of Nusselt number depending on Reynolds number was around 10% in the range of Re number from 4000 to 20000. However, as was demonstrated in [3], the heat transfer process of nanofluids depend nonlinearly on particles concentration and size, viscosity and temperature and have to be investigated in more details.

References:

1. S.M.S. Murshed and C.A. Nieto de Castro, Nanofluids: Synthesis, Properties and Applications, *Nova Science Publishers Inc*., New York, 2014.
2. W.Yu, D.M. France, S.U.S. Choi, J.L. Routbort, Review and assessment of nanofluid technology for transportation and other applications, *Argonne National Laboratory*, 2007.
3. A. V. Minakov, D. V. Guzei, M. I. Pryazhnikov, V. A. Zhigarev, V. Y. Rudyak, Study of turbulent heat transfer of the nanofluids in a cylindrical channel. *International Journal of Heat and Mass Transfer*, 102 (2016), 745-755.
4. V.Z. Geller, N.A. Shimchuk, S.N. Gubanov, Transport properties of nanofluids (experiment and calculationmethods). Refrigeration Engineering and Technology, 51 (6) (2015) (72-77) (in Russian).

NATURAL CONVECTION FROM A PAIR OF DIFFERENTIALLY-HEATED HORIZONTAL CYLINDERS ALIGNED SIDE BY SIDE IN A NANOFLUID-FILLED INCLINED SQUARE ENCLOSURE

A. Quintino, E. Ricci*, E. Habib, and M. Corcione

DIAEE Sezione Fisica Tecnica - Sapienza Università di Roma, via Eudossiana 18, 00184 Rome, Italy

*Corresponding author: elisa.ricci@uniroma1.it

Keywords: Nanofluid; Natural convection; Differentially-heated horizontal cylinders; Two-phase modeling; Enhanced heat transfer; Optimal particle loading and tilting angle

Introduction: Buoyancy-induced convection of nanofluids inside adiabatic enclosures containing heated and cooled cylinders has recently gained a lot of interest. Studies on this topic were carried out numerically by Garoosi and colleagues [1,2], and Khalili et al. [3], yet a number of points have to be raised regarding these works. In fact, both studies executed by Garoosi and colleagues are based on the single-phase approach, thus neglecting the effects of the slip motion that actually occurs between the suspended nanoparticles and the base liquid. On the other hand, in the two-phase investigation performed by Khalili and co-workers, the thermophoretic velocity of the suspended nanoparticles is calculated by the way of the McNab-Meisen empirical relationship [4], whose applicability to water-based nanofluids with suspended metal oxide nanoparticles implies an underestimation of the thermophoretic velocities, as displayed by Aminfar and Haghoo [5], and thoroughly discussed by Corcione et al. [6]. Framed in this general background, a comprehensive numerical study on natural convection from a pair of differentially-heated horizontal cylinders set side by side in a nanofluid-filled adiabatic square enclosure, inclined with respect to gravity so that the heated cylinder is located below the cooled one, is performed using a two-phase model based on the double-diffusive approach. It is assumed that Brownian diffusion and thermophoresis are the only slip mechanisms by which the solid phase can develop a significant relative velocity with respect to the liquid phase. The system of the governing equations of continuity, momentum and energy for the nanofluid, and continuity for the nanoparticles, is solved through a control-volume formulation of the finite-difference method. Pressure-velocity coupling is handled using the SIMPLE-C algorithm. Convective terms are approximated by the QUICK discretization scheme, wheras a second-order backward scheme is applied for time integration. Full details on the computational code, and its validation, can be found in a recent study conducted by Quintino et al. [7].

Discussion and Results: Numerical simulations are performed using alumina-water nanofluids, for different values of (a) the average volume fraction of the solid phase, φ_{av}, in the range between 0 and 0.04, (b) the tilting angle of the enclosure, γ, in the range between 0° and 60°, and (c) the average temperature of the nanofluid, T_{av}, in the range between 300 K and 330 K. The cavity

width, W, is set as 0.04 m, the nanoparticle diameter, dp, is set as 25 nm, the temperature difference between the cylinders, ΔT, is set as 10 K, the ratio between the cylinders diameters and the cavity width, δ, is set as 0.2, and the ratio between the center-to-center distance an the cavity width, λ, is set as 0.4. Typical local results are reported in Fig. 1, in which steady-state streamline, isotherm and isoconcentration contours relative to different tilting angles in the range $0°-60°$ are plotted for $\varphi_{av} = 0.02$ and $T_{av} = 315$ K. It is apparent that, for all the tilting angles considered, the flow field consists of a primary circulation occurring between the cylinders, due to the rise of the hot nanofluid adjacent to the heated cylinder and its descent past the opposite cooled cylinder, and of a secondary cell, driven by the same imposed temperature difference, that embraces both cylinders. Moreover, the combined effects of the nanofluid circulation due to the imposed
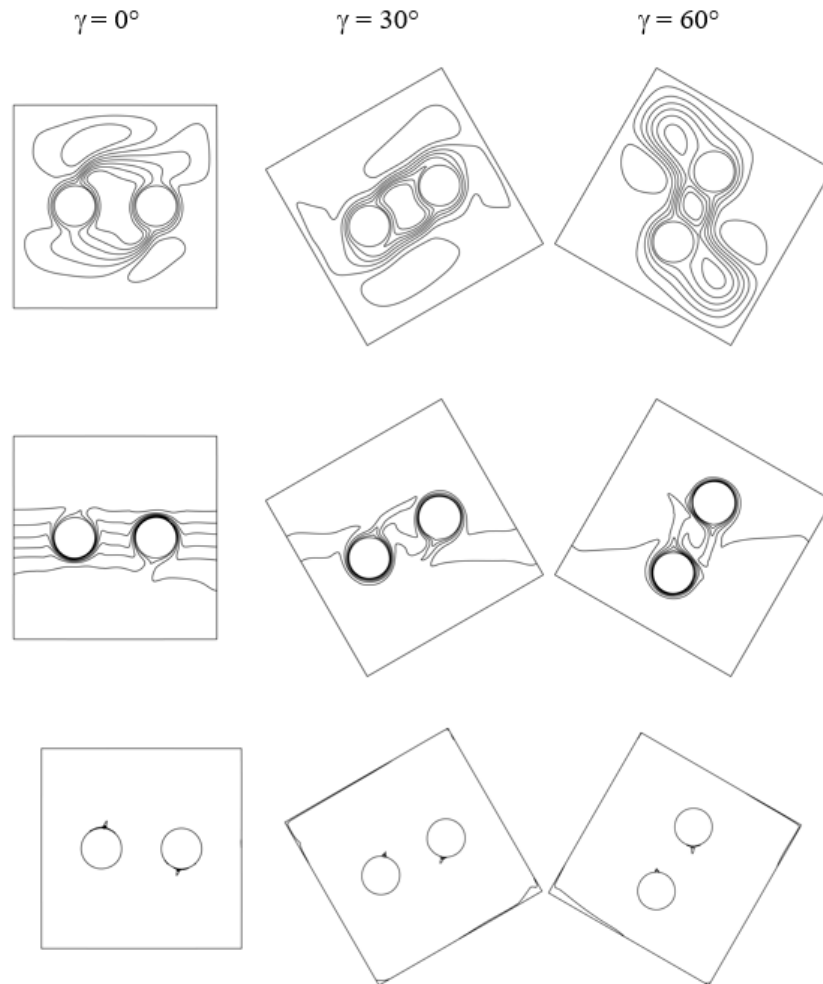
Fig. 1. Streamline, isotherm and isoconcentration contours for $Al_2O_3 + H_2O$, $\varphi_{av} = 0.02$, $T_{av} = 315$ K, at different tilting angles γ in the range $0°-60°$.

differential heating, and the diffusion of the suspended nanoparticles in the direction from hot to cold, give rise to the formation of a low-concentration boundary layer adjacent to the heated cylinder surface, and a high-concentration boundary layer adjacent to the cooled cylinder surface, which means the establishment of a concentration gradient across the enclosure, whose role in determining the heat transfer performance of the nanofluid needs being discussed.
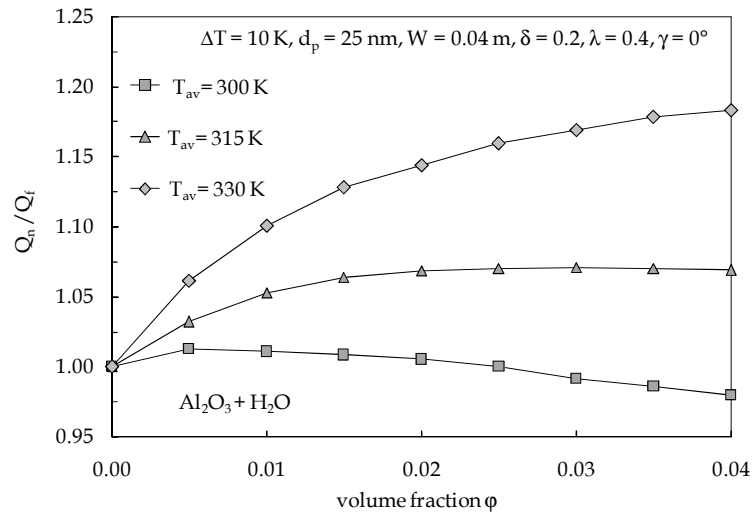
Fig. 2. Distribution of Q_n/Q_f vs. φ_{av} for $Al_2O_3 + H_2O$, W = 40 mm, d_p = 25 nm, λ = 0.4, δ = 0.2, γ = 0°, and ΔT = 10 K, using T_{av} as a parameter.
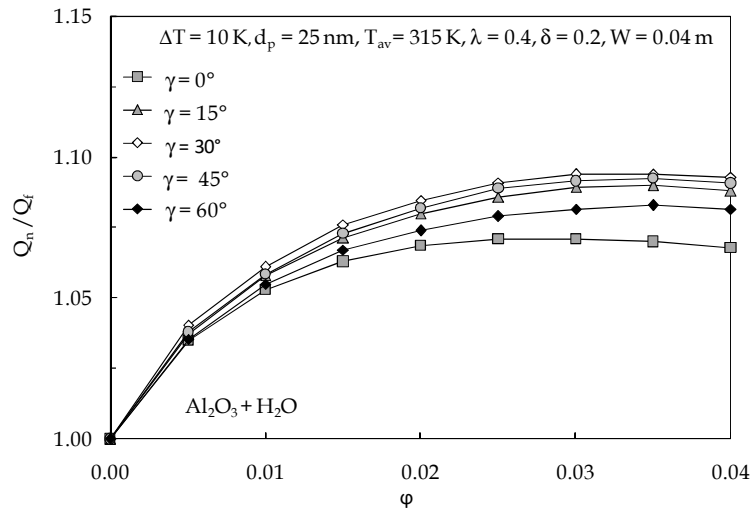
Fig. 3. Distribution of Q_n/Q_f vs. φ_{av} for $Al_2O_3 + H_2O$, W = 40 mm, d_p = 25 nm, λ = 0.4, δ = 0.2, T_{av} = 315 K, and ΔT = 10 K, using γ as a parameter.

In fact, the nanofluid behavior is primarily affected by the two opposite effects arising from the increase of both the thermal conductivity and the dynamic viscosity produced by the dispersion of the nanoparticles into the base liquid: the first effect, which tends to enhance the nanofluid heat transfer performance, prevails at small volume fractions of the suspended solid phase, whereas the second effect, which tends to degrade the nanofluid heat transfer performance, prevails at higher volume fractions. On the other hand, due to the mentioned concentration gradient, a cooperating solutal driving force arises. The situation is such that, as a rule, this extra-buoyancy tends to compensate the increased friction consequent to the viscosity growth, thus implying that the beneficial effect of the increased thermal conductivity plays the major role in determining the heat transfer performance of the nanofluid. Hence, owing to the strong dependence of the effective thermal conductivity on temperature, a pronounced heat transfer enhancement has to be expected at high average temperatures, as shown in Fig. 2, where a number of distributions of the ratio between the heat transfer rates across the nanofluid and the pure base fluid, Q_n / Q_f, are plotted versus φ_{av} for the horizontal alignment, i.e. $\gamma = 0°$, using T_{av} as a parameter, in which the existence of an optimal particle loading, φ_{opt}, is clearly pointed out. As the tilting angle γ is increased, the increase of the cooperating solutal driving force, as well as the increase of the vertical path available for the acceleration of the nanofluid, result in a growth of the motion intensity, which enhances the heat transfer performance, on the other hand, as γ is further increased, the interactions occurring between the hot and the cold plumes result in a significant decrease of the heat transfer rate. A set of distributions of Q_n/Q_f plotted versus φ_{av} using γ as a parameter is reported in Fig. 3, confirming the existence of an optimal tilting angle for maximum heat transfer.

Conclusions: The main results obtained in the present study may be summarized as follows: (a) the inclination of the cavity and the dispersion of the nanoparticles into the base liquid have their maximum effect on the nanofluid heat transfer performance at an optimal tilting angle of the cavity and an optimal particle loading; (b) the impact of the nanoparticle dispersion into the base liquid increases remarkably with increasing the average temperature, which, without any doubt, is the key parameter that determines the heat transfer performance of the nanofluid.

References

1. F. Garoosi, F. Hoseininejad and M.M. Rashidi, Numerical study of natural convection heat transfer in a heat exchanger filled with nanofluids, *Energy* 109 (2016) 664-678.
2. F. Garoosi and F. Hoseininejad, Numerical study of natural and mixed convection heat transfer between differentially heated cylinders in an adiabatic enclosure filled with nanofluid, *Journal of Molecular Liquids* 215 (2016) 1-17.
3. E. Khalili, A. Saboonchi and M. Saghafian, Natural convection of Al2O3 nanofluid between two horizontal cylinders inside a circular enclosure, *Heat Transfer Engineering* 38 (2017) 177-189.
4. G.S. McNab and A. Meisen, Thermophoresis in liquids, *Journal of Colloid Interface Science* 44 (1973) 339–346.

5. H. Aminfar and M.R. Haghgoo, Brownian motion and thermophoresis effects on natural convection of alumina-water nanofluid, *Journal of Mechanical Engineering Science* 227 (2012) 100-110.
6. M. Corcione, M. Cianfrini and A. Quintino, Temperature effects on the enhanced or deteriorated buoyancy-driven heat transfer in differentially heated enclosures filled with nanofluids, *Numerical Heat Transfer, Part A* 70 (2016), 223-241.
7. A. Quintino, E. Ricci and M. Corcione, Thermophoresis-induced oscillatory natural convection flows of water-based nanofluids in tilted cavities, *Numerical Heat Transfer, Part A* 71 (2017), 270-289.

NANOENGINEERED WETTABILITY FOR HEAT TRANSFER ENHANCEMENT IN SPRAY COOLING

A.S Moita*, M. Maly and A.L.N. Moreira

IN+, Instituto Superior Técnico, Universidade de Lisboa,

Av. Rovisco Pais 1, Lisboa, Portugal

*Corresponding author: anamoita@tecnico.ulisboa.pt

Keywords: Spray cooling, Nanofluids, Wettability

Introduction: Spray impingement is a popular cooling strategy used in different industrial applications, from metallurgy to electronics cooling [1-2]. In the latter, despite offering high heat transfer coefficients of the order of 10^4-10^5 W/m^{2}K or higher [3] the efficient implementation of this strategy must cope with the increasingly demanding heat loads that are dissipated. In this context, several authors addressed surface modification to enhance the heat transfer processes, *e.g.* [2-3]. Alternatively, several authors have explored the use of nanofluids to reach the same goal [4]. However, while many of these researchers dealt with nanofluids as being a single-fluid with novel thermo-physical properties (e.g. surface-tension and viscosity), the mechanisms of liquid atomization, droplet-wall interaction and droplet/droplet interactions, which strongly affect the heat transfer mechanisms depend on the intermolecular forces as described by wettability. In this context, a microscopic approach needs to be introduced by considering the external and internal forces on the nanoparticles and the mechanical and thermal interactions between nanoparticles, fluid and surface molecules. Though most applications aim to phase-change heat transfer devices, the mechanisms by which a surface is wetted by a liquid loaded with nanoparticles is not yet completely understood, as studies have yielded contradictory results: while some experiments show inhibition of wetting by nanoparticle addition [5], others show an improvement of wetting with the increase in the nanoparticle concentration [6]. It has been suggested that the spreading of a nanofluid droplet depends on the relation between time-scales associated with wetting and with diffusion of nanoparticles near the confined three-phase contact region, respectively. Moreover, since wettability depends on the micro structure of the nanofluid, it is expected to change with the synthesis process. This is an important issue, since preparation techniques are required to produce uniform and stable suspensions, with negligible agglomeration of particles and no chemical changes of the base fluid. Hence, wettability of a surface by a nanofluid and, therefore, spray-wall interactions, cannot be disregarded from the process of fluid synthesis, particularly in the presence of heat transfer. In line with this, the present study addresses the effect of nanofluid synthesis on the local physical properties of the resulting fluid and their consequent effect on the atomization characteristics (droplet size and velocity distribution and spray angle, among others) and on spray impingement using nanfluids. The nature and the concentration of the nanoparticles of the based fluid are taken as influencing parameters, giving

particular emphasis on their effect on the interfacial mechanisms present in atomization and then in droplet/spray impingement.

Sample Results and Discussion: Different nanofluids, obtained from alumina, zinc, copper and iron oxide and alumina in water, are synthesised using the co-precipitation and solvothermal methods [7]. Different surfactants are used (e.g. citric acid, oleic acid, CTAB - Cetyl trimethylammonium bromide) to infer on their effect in the stability of the nanofluid The morphology is analysed by scanning and transmission electron microscopies, which also give information about the phase structures and chemical composition, complemented by Fourier transform infrared spectroscopy, X-ray diffraction, Raman and X-ray photoelectron spectroscopy. Surface wetting is then quantified with a goniometer, by the apparent macro-contact angle obtained at the equilibrium between the interfacial tensions acting as a droplet is gently deposited over the surface. In addition, a Laser Scanning Confocal Microscopy – LSCFM - and 3D reconstruction allows to visualize the micro-layer in the very vicinity of the triple contact line and characterize wettability within extreme wetting regimes [8]. High-speed visualization using a Phantom v4.2 and image post-processing is combined with Phase Doppler measurements (a 2 component system from Dantec) to fully describe the atomization characteristics and the spray/droplet wall interactions. The results show that despite surface tension of the bulk fluid does not change with nanoparticles (Table 1), local particle interactions seem to affect the atomization processes, at relatively low particle concentrations, thus affecting the mean size (quantified by the Sauter Mean Diameter) and axial velocity of the spray droplets (Figure 1a and 1b, respectively). These preliminary results suggest that similar interactions may affect droplet/wall interactions at spray impingement.

Table 1. Composition and surface tension of the prepared nanofluids taken at 20±3ºC.

Fluid	Base fluid	Nanoparticle		Surfactant		Surface tension (mN/m)
		Composition Concentration wt (%)		Composition	Concentration wt (%)	
1	Water	-	-	-	-	73.5
2	Water	-	-	Citric acid	0.15	73.4
2	Water	Al_2O_3	2	Citric acid	0.15	72.8
3	Water	Al_2O_3	0.5	Citric acid	0.15	73.4
4	Water	ZnO	0.5	Citric acid	0.15	74.3
5	Water	ZnO	0.01	Citric acid	0.15	73

6	Water	C_4H_6CuO	0.1	Citric acid	0.15	72
7	Water	$Cl_2Fe_4H_2O$	0.1	Citric acid	0.15	71.6

a)   b)
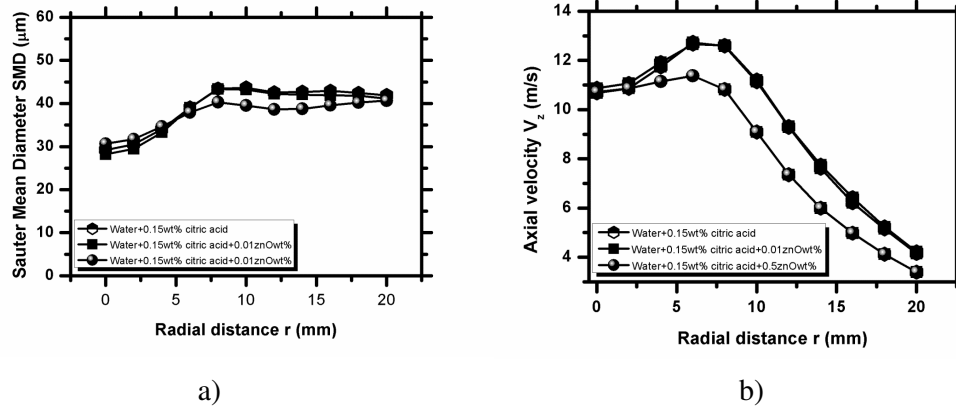
Figure 1. Effect of the nature and concentration of the nanoparticles on: a) the Sauter Mean Diameter and b) the axial velocity of the droplets resulting from the atomization of the nanofluids.

Conclusions: This manuscript addresses the effect of the nature and concentration of nanoparticles on the atomization processes of nanofluid sprays. Emphasis is also given to the potential effect of local wetting modifications caused by the interactions between the nanoparticles and the impinging surfaces on the wettability and consequently on spray/wall interactions. Preliminary results solely performed at ambient temperature show that despite surface tension of the bulk fluid does not change with nanoparticles, local particle interactions seem to affect the atomization processes, at relatively low particle concentrations.

References:

1. Kim, J., Spray cooling heat transfer: The state of the art., *Int. J. Heat Fluid Flow*, 28(4) (2007), 753-767.
2. Moreira, A. L. N., Moita, A. S. and Panão, M. R., Advances and challenges in explaining fuel spray impingement: how much of single droplet impact research is useful? *Progress Energy and Combustion Sci*. 36 (2010), 554-580.
3. Bostanci, H., Daniel, R., John, K. and Louis, C., Spray cooling with ammonia on microstructured surfaces: performance enhancement and hysteresis effect, *J. Heat Transfer,* 131 (2009).
4. Duursma, G., Sefiane, K. and Kennedy, A., Experimental studies of nanofluid droplets in spray cooling, *Heat Transfer Engineering*, 30(13) (2017), 1108-1120.

5. Vafaei, S., Borca-Tasciuc, T., Podowski, M. Z., Purkayastha, A., Ramanath, G. and Ajayan, P. M., Effect of nanoparticles on sessile droplet contact angle, *Nanotechnology*, 17 (2006) 2523–2527.
6. Wasan, D. T. and Nikolov A D., Spreading of nanofluids on solids, *Nature*, 423 (2003), 156.
7. Pastrana-Martínez, L.M., Pereira, N., Lima, R., Faria, J.L., Gomes, H.T. and Silva, A.M.T., Degradation of diphenhydramine by photo-Fenton using magnetically recoverable iron oxide nanoparticles as catalyst, *Chemical Engineering J.*, 261 (2015), 45-52.
8. Vieira, D., Moita, A. S. M. and Moreira, A. L. N., Non-intrusive wettability characterization on complex surfaces using 3D Laser Scanning Confocal Fluorescence Microscopy, *18th International Symposium on the Application of Laser and Imaging Techniques to Fluid Mechanics*, Lisbon, Portugal, July 4 – 7, 2016.

POSSIBLE APPLICATION OF NANOFLUIDS TO IMPROVE PERFORMANCE OF WET COOLING TOWERS

V. Mijakovski*, T. Geramitcioski and V. Mitrevski

University "St. Kliment Ohridski", Faculty of Technical Sciences, str. Makedonska Falanga 33, 7000 Bitola, Macedonia

*Corresponding author: vladimir.mijakovski@tfb.uklo.edu.mk

Keywords: Nanofluids, Heat transfer, Cooling tower, Power plant, Reduced water usage

Introduction: Nano meter-sized particles suspended in fluids forming colloidal solutions are called nanofluids [1]. Nanofluids are typically made of metals, oxides, carbides or carbon nanotubes in a base fluid like water, oil and ethylene glycol and have an advantage, in terms of heat exchange (heat transfer) over pure cooling fluids. Their great potential in heat removal improvement was first discovered in 2001, [2]. It was discovered that less than 1% volume fraction of copper nanoparticles or carbon nanotubes dispersed in ethylene glycol or oil can increase their thermal conductivity by 40% and 150% respectively. The ongoing research after that extended to a utilization of nanofluids in many processes and industries, especially where intensive heat transfer/exchange occurs.

Thermal power plants are large consumers of water. This especially refers to the so called cold end of the power plant. It is comprised of condenser, cooling tower, circulating pumps, connecting pipelines and air removal system.

Lignite fired thermal power plants have the highest share in electricity production in the Republic of Macedonia. Thermal power plant Bitola is the biggest producer of electricity in the country. It consists of three units having total installed capacity of 699 MW. Since this power plant does not have access to abundant water, it uses wet cooling towers for cooling of the condenser.

Two circulational pump stations are in operation at TPP "Bitola". One is for units 1 and 2, while the other one is for unit 3 with the possibility of enlargement for another unit. Pumps are of axis type, vertical with variable geometry of the working blades, [3, 4]. Unit is comprised of steam generator, turbine, electric generator, condenser and cooling tower. Two pumps, working in parallel, are used on each unit, while the third one is engaged during extreme weather conditions as an auxilary pump according to needs. Cold water from the cooling tower basin, through open channel that later transforms into two underground pipes (with diameter DN2400 each) is transported into pump station's open basin (chamber). From the open basin water is transported by pumps into main distributive pipeline DN2400. From this pipeline, water flow is divided on two pipes (DN1600) leading to both condenser halves, [5]. Cold end of the Unit-3 is shown on Fig. 1. Nominal flow rate of cooling water through this system is 30000 m^3/h per

unit. Nominal cooling range (difference between the cooling tower water inlet and outlet temperature) of the tower is 9,2 K. Evaporation losses are calculated to be approximately 1% of the nominal flow of water through the system, [6].
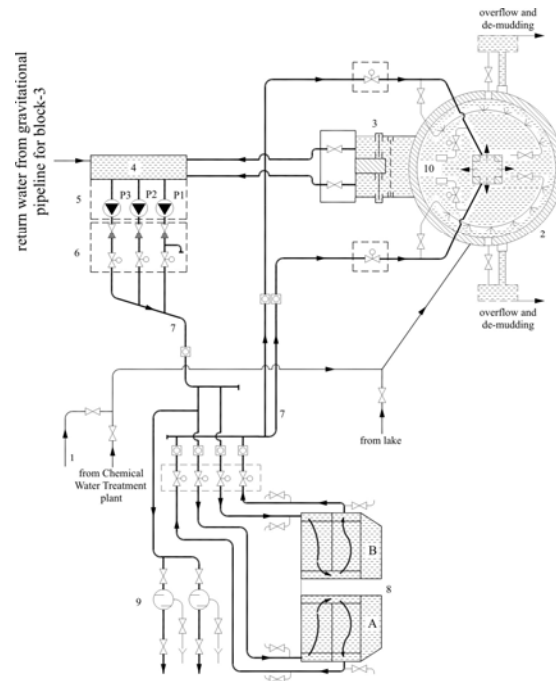
Fig. 1. Schematics of the circulation cooling water system for Unit-3; 1 – water treatment station; 2 – natural draught cooling tower; 3 – valves with colander; 4 – entering water chamber; 5 – pump station; 6 – pit with valves; 7 – circulation pipelines; 8 – condenser; 9 – mechanical water filters; 10 – unit for winter operation of the cooling tower.

Discussion and Results: A review of scientific and technical literature with reference to research conducted in this field has been made in order to determine feasible utilization of nanofluids for enhancing the heat transfer at the cooling tower in the above described power plant.

Improved efficiency of the whole system due to enhanced thermophysical properties (i.e. thermal conductivity) of nanofluids compared to the base fluid (in this case water) is the main motive of its application. Nanoparticle materials include chemically stable metals (i.e. gold, copper), metal oxides (i.e. alumina, silica, zirconia, titania), oxide ceramics (SiC), metal nitrides (diamond, graphite, carbon nanotubes, fullerene) and functionalised nanoparticles, [7]. Typical nanofluid is characterised with uniform dispersion of nanoparticles.

There are few ways to optimize operating parameters of the cooling tower, such as water flow rate, water temperature, thermal characteristics of tower's fill, geometry of the tower etc. While some of these parameters are not controllable or cost-effective to change, some are not applicable for already operational cooling towers.

The use of nanofluids as coolants in intensive heat transfer processes has been extensively studied, mostly for nuclear reactor applications, [8, 9]. The use of nanofluids in cooling tower is an excellent option to improve its performance. Nanofluids can improve the heat performance of the cooling tower by increasing the sensible and evaporating heat transfer leading to significant reduction in water use of the tower and power plant in general. This is very important because around 60% of the total annual water consumption of the above described thermal power plant is attributed to evaporation from the cooling towers, [6].

Recent researches showed that the use of nanofluid improves the performance of both condenser and cooling tower leading to reduction of sizes of both. Application of nanofluids incorporating nanoparticles with phase-change material cores that melt to absorb heat from steam turbine condensate and solidify as cooling proceeds could reduce overall water consumption by as much as 20%. The improved thermal properties offered by these multifunctional nanoparticles also are expected to decrease coolant flow rates by about 15%, helping lower the associated pumping loads and thus own needs' energy losses, [10], Fig. 2. Internal reports regarding own needs' electricity consumption at the TPP Bitola, [11], show that the electricity consumption of pumps used at power plant's cold end amount to 10% of the total annual own needs' electricity consumption.
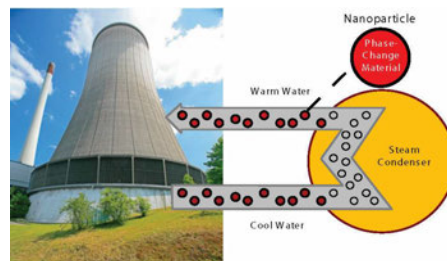
Fig. 2. Heat – absorption nanoparticles are expected to significantly improve the thermophysical performance of steam-condensing coolants, reducing freshwater consumption at power plants with wet cooling towers, Source: [10].

Evaporation rate of cooling water at wet cooling tower with natural draught highly depend on external air conditions (mainly air temperature and humidity). According to [12] and by assuming linear correlation between heat transfer coefficient increase by using nanofluids and decrease in evaporation rate of cooling water, dependence between evaporation rate and external air temperature for nominal cooling range of 9,2 K are shown on Fig. 3. Assumption is made for 4 different rates of heat transfer coefficient increase (5%, 10%, 15% and 20% respectively). Other reference parameters for cooling tower of TPP Bitola: relative air humidity 50%, nominal flow of cooling water 30000 m^3/h.

Conclusions: In this paper, a review on potential applications of nanofluids in heat removal from wet cooling tower is addressed. Current level of research in this potentially promising field of thermal engineering is also briefly described. Lignite fired thermal power plant Bitola in Macedonia, as largest electricity producer in the country has been used as a model for comparison of possible benefits from utilization of nanofluids in steam-condensing process.

There are many advantages of using nanofluids in cooling towers, such as: increase in heat transfer performance of the cold end (cooling tower and condenser) leading to overall increase in efficiency; reduction of water loss through evaporation leading to reduction of water consumption in the cooling tower and in the power plant in general; reduction of sizes of cooling tower and condenser and reduction of electricity consumption of pumps used in this system.
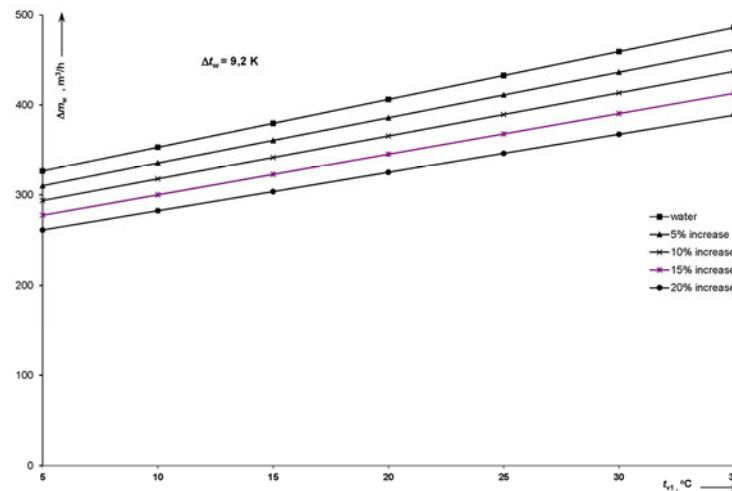
Fig. 3. Dependence of evaporation rate of cooling water vs external air temperature relative to increase in heat transfer coefficient by using nanofluids; Δm_w – evaporation rate of cooling water, t_{v1} – external air temperature.

Applied on the model power plant these improvements can significantly reduce consumption of fresh water in the plant. At the moment, the plant uses around 12 million m^3 of fresh water every year, out of which approximately 7,15 million m^3 are consumed by the cold-end itself. Electricity consumption of pumps is estimated at the level of 35 – 40 GWh/year which is more than 1% of the total electricity produced from the power plant in 2014 (3317 GWh), [13]. Thus, possible improvements applied to the referent power plant have great potential.

Still, despite many possible advantages in utilization of nanofluids in the cooling tower application, there are a lot of challenges that need to be addressed and solved prior to wide-scale usage, [7]. These include: high cost of nanofluids and difficulties in production process, stability of nanoparticles in the base fluid, development of practical methods for adding

nanoparticles to cooling system to replace losses through drift, evaporation and blowdown. Also, full-scale field demonstrations will be required.

References:

1. R. Kumar and V. Kumar Goud, Nanofluids: a promising future, *Journal of Chemical and Pharmaceutical Sciences,* special issue 2014, ISSN: 0974-2115.
2. Eastman JA, Choi SUS, Li S., Yu W., Thompson LJ., Anomalously increased effective thermal conductivities of ethylene glycol based nanofluids containing copper nanoparticles, *Applied Physics Letters,* Volume 78, issue 6, 718 (2001).
3. Mijakovski I., Mijakovski V., Extreme values from the climatic curve and their influence on thermal power plant's Bitola cold-end, *14th international symposium on thermal science and engineering*, Sokobanja, Serbia, October 13-16, 2009.
4. Mijakovski V., Optimal operating regime of the cooling water pump station in TPP "Bitola", *Symposium power plants 2006*, Society of thermal engineers of Serbia and Montenegro, Vrnjačka Banja, Serbia, September 19-22, 2006.
5. Pecakov S., Petreski T., Hristov T., *Local instruction for exploitation of circulation pump stations and technical water systems*, Public Enterprise "Macedonian power plants", Skopje, Macedonia, 1999 (in Macedonian).
6. Mijakovski V., *Influence of the climate conditions on the performance of the cooling tower*, PhD thesis, Faculty of Mechanical Engineering Skopje, Macedonia, 2009 (in Macedonian).
7. Sarkar J., Improving Performance of Cooling Tower, *Cooling India,* (august 2016) 30-32.
8. Buongiorno J., Hu L-W., Nanofluid Heat Transfer Enhancement for Nuclear Reactor Applications, *Proceeding of the ASME 2009 2nd Micro/Nanoscale Heat&Mass Transfer International Conference,* Shanghai, China, December 18-21, 2009.
9. Fahnmy A.A., A Comparative Thermal – hydraulic Study on Nano-fluids as a Coolant in Research Nuclear Reactors, *International Journal of Scientific&Engineering Research,* Volume 4, Issue 9, September 2013, ISSN 2229-5518.
10. Heat-absorption nanoparticle additives for reducing cooling tower water consumption, *Report from Electric Power Research Institute (EPRI) published in July 2013*, Palo Alto, California, USA.
11. Internal annual report on the own needs' electricity consumption of the TPP Bitola, JSC "Macedonian Power Plants", Skopje, Macedonia, 2013 (in Macedonian).
12. DIN EN 14705:2005-10, Heat exchanger – Method of measurement and evaluation of thermal performances of wet cooling towers.
13. Annual report on realized results from the operation of JSC "Macedonian power plants" in 2014, Skopje, Macedonia, 2015.

THERMOPHYSICAL PROFILE AND HEAT TRANSFER PERFORMANCE OF DISPERSIONS OF FUNCTIONALIZED GRAPHENE NANOPLATELETS IN AN INDUSTRIAL COOLANT

J. P. Vallejo[1,2], E. Álvarez-Regueiro[1,2], D. Cabaleiro[1], J. Fernández-Seara[2], J. Fernández[3] and L. Lugo[1*]

[1]Departamento de Física Aplicada, Facultade de Ciencias, Universidade de Vigo, 36310, Vigo, Spain

[2]Área de Máquinas e Motores Térmicos, Escola de Enxeñería Industrial, Universidade de Vigo, 36310, Vigo, Spain

[3]Laboratorio de Propiedades Termofísicas, Grupo NaFoMat, Departamento de Física Aplicada, Universidade de Santiago de Compostela, 15782, Santiago de Compostela, Spain

*Corresponding author: luis.lugo@uvigo.es

Keywords: Functionalized graphene nanoplatelets; Ethylene glycol; Heat transfer; Thermophysical properties

Introduction: The moderate thermal conductivity of current working fluids is a continuous restriction in the process of enhancing heat transfer performance. Hence, during the last decades the attention has been focused on its improving. Nanofluids have been suggested as a promising solution because of the high thermal conductivity of the potential dispersed solids. Thus, numerous studies have been carried out determining their heat transfer performance using metals [1], nitrides [2], oxides [3] and carbon allotropes [4] as nanoadditives. Since the graphene isolation discovery, graphene nanoplatelets have proved their efficiency in this field due to their enhancement of thermal conductivity in base fluids like water [5], ethylene glycol [6] and different oils [7]. Nevertheless, scarce studies have been carried out using commercial coolants as base fluids.

Thermophysical characterization based on the determination of density, heat capacity, thermal conductivity and viscosity, is essential to assess a fluid heat transfer performance. In this study, the thermophysical profile of functionalized graphene nanoplatelet dispersions in an industrial heat transfer fluid ensuring a good stability have been determined. In addition, heat transfer coefficients were experimentally determined together with the associated pressure drops at different flow conditions by using a sensorized experimental facility.

Discussion and Results: Following a two-step method, four different mass concentrations (0.25, 0.50, 0.75 and 1.0) % of polycarboxylate chemically modified graphene nanoplatelets, fGnP, commercially available as graphenit-HYDRO (NanoInnova Technologies S.L., Madrid, Spain), were dispersed in Havoline XCL Premixed 50/50 (Chevron, London, United Kingdom). This commercial working fluid is a long-life coolant based on an ethylene glycol–water mixture and used in many applications providing corrosion protection at high temperatures for the majority of

engine metals and frost protection down to 233.15 K. Furthermore, as part of the base fluid it was added an optimized mass fraction of sodium dodecyl benzene sulphonate dispersant, SDBS (Sigma-Aldrich, Louis, Missouri, USA). The corresponding amounts of each component were weighted in a CPA225 electronic balance (Sartorius AG, Goettingen, Germany) and the dispersions were sonicated by an ultrasonic bath (Ultrasounds, JP Selecta S.A., Barcelona, Spain) at 200 W sonication power and 20 kHz frequency for 240 min.

The thermophysical characterization of the commercial coolant, without and with SBDS, and the different nanofluids was performed in the temperature range from (293.15 to 323.15) K. Densities were experimentally measured using a borosilicate glass Gay-Lussac pycnometer for liquids of 25 ml (Hermanos Alamo, Spain). Specific heat capacities were experimentally determined for the nanopowder and base fluid through a heat-flux differential scanning calorimeter, DSC Q2000 (TA Instruments, New Castel, USA) and then determined for the nanofluids [8]. Effective thermal conductivities, k, were experimentally measured by a KD2 Pro thermal analyzer (Decagon Devices, Inc., Pullman, USA) with a KS-1 probe [9]. Dynamic viscosities, η, under different flow conditions were experimentally determined by a rotational rheometer Physica MCR 101 (Anton Paar, Graz, Austria) with a cone-plate geometry of 25 mm diameter and 1° cone angle [10], observing Newtonian behaviour for all the analysed samples.

Experimental properties of Havoline XCL Premixed 50/50, defined by the supplier as a mixture of 50 vol.% Havoline (93 wt.% ethylene glycol) and 50 vol.% water, were compared to thus published by Melinder [11] for a mixture of 50 vol.% ethylene glycol and 50 vol.% water. Absolute average deviations (AADs) of 0.29 %, 0.45 %, 0.35 % and 2.1 % were found for density, heat capacity, thermal conductivity and viscosity, respectively.

Measured properties of Havoline XCL Premixed 50/50 do not undergo significant changes with the addition of SBDS. The maximum AAD is reached for the viscosity, with a 0.83 %.

Regarding to the nanofluids, densities increase with the nanoadditive loading up to 0.44 % and decrease with the temperature rise up to 1.5 %. With respect specific heat capacities, the dispersion of fGnP leads to decreases of 7.1-7.4 % for the 1 wt.% nanofluid and the increasing temperature causes rises of up to 5.4 % in the analysed temperature range. Figure 1 plots the enhancement in the thermal conductivity and dynamic viscosity increases for the four designed nanofluids in relation to the base fluid at the analysed temperatures.
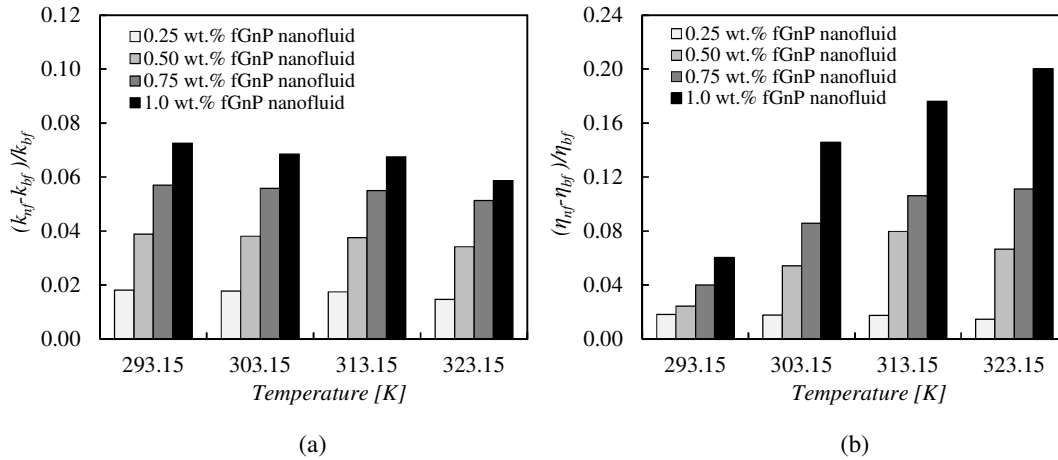
Figure 1: Thermal conductivity (a) and dynamic viscosity (b) increases of fGnP nanofluids regarding the base fluid at different temperatures.

Thermal conductivity enhancements with the fGnP addition achieve 7.3 % for the 1 wt.% nanofluid at 293.15 K, as it can be seen in Figure 1 (a). The observed enhancements are quite similar for each nanofluid concentration overall temperature range whereas the effective thermal conductivity increases with the increasing temperature reach up to 8.9 %, for 1 wt.% nanofluid.

Dynamic viscosity shows an increasing trend with the nanoadditive mass fraction rises, as expected. Percentage increase values range between 1.1 % and 20% as it can be seen in Figure 1 (b). There were also found viscosity decreases with the rising temperature of up to 38 % for the 0.25 wt.% nanofluid.

The experimental facility used to determine the heat transfer coefficients and pressure drops consists of three different circuits: the tested fluid circuit, the heating circuit and the cooling circuit. The main part of this setup is a tube-in-tube heat exchanger of stainless steel. The tested fluid is pumped through the inner tube of the heat exchanger and is heated by the hot water from the heating circuit. The cooling circuit allows the tested fluid to return to its initial conditions and three electric resistances heat the water of the heating circuit again. Various temperature sensors and a differential pressure sensor allow collecting all the test information [5].

Different tests were performed to obtain the convection coefficients and the pressure drops at varied conditions. The tests were defined by the tested fluid flow rate and the average temperatures of tested fluid and hot water. The hot water flow rate was kept constant at 700 $L \cdot h^{-1}$ in all tests. The well-known Gnielinski correlations for concentric annular ducts in turbulent flow conditions were used to obtain the hot water convection coefficients [12].

In Figure 2, we can see the convection coefficients, h, for those tests in which average temperature pairs of tested fluid/hot water were 308.15/323.15 K and 318.15/333.15 K.
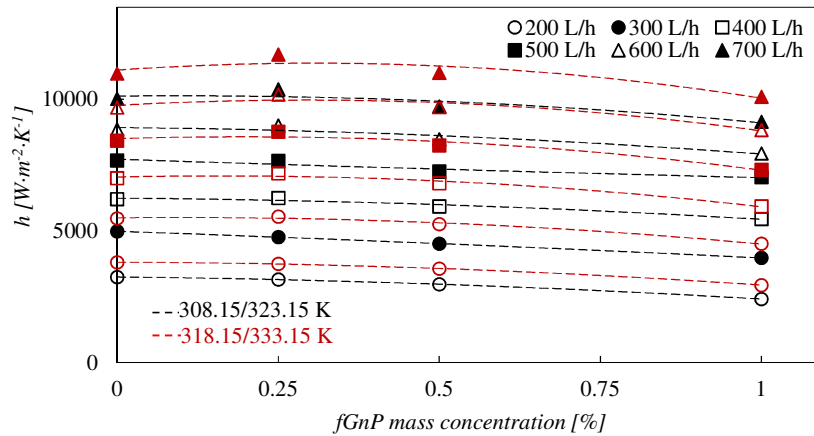
Figure 2: Convection coefficients against functionalized graphene nanoplatelet mass concentration for the 308.15/323.15 K and 318.15/333.15 K tests at different flow rates.

Despite the increases observed in thermal conductivity for all the analysed fGnP mass concentrations, in Figure 2 it can be seen as the only concentration that enhances the convection coefficients of the base fluid at the majority of the flow rates, especially at the highest ones, is 0.25 wt.%. A maximum enhancement of 6.5 % was reached. Furthermore, it can be seen as the increasing flow rate leads to higher convection coefficients and as the increasing tested fluid temperature produces the same effect. With respect to the pressure drop tests, it was detected a slight increasing trend with the increasing fGnP concentration, which does not exceed 1.5 % for the 0.25 % nanofluid for the tested conditions.

Conclusions:

In this work, it was determined the thermophysical profile of four nanofluids consisting of different functionalized graphene nanoplatelet dispersions in a commercial coolant with SDBS for ensure stability, in the temperature range between (293.15 and 323.15) K. Thermal conductivity enhancements up to 7.3 % were reached with the fGnP dispersion, with dynamic viscosity increases between 1.1 % and 20 %.

Furthermore, the heat transfer performance of these new fluids was tested in an experimental facility, determining the heat transfer coefficients and the pressure drops at different flow conditions. Despite the increases observed in thermal conductivity for all the analysed mass concentrations, it was detected that only the 0.25 wt.% nanofluid gets better convection coefficients that the base fluid for most of the tested conditions, achieving enhancements up to 6.5 % for high flow rates. The pressure drop increase with respect base fluid for this concentration is lower than 1.5 % for the analysed test conditions.

References:

1. J.A. Eastman, S. Choi, S. Li, W. Yu, L. Thompson, Anomalously increased effective thermal conductivities of ethylene glycol-based nanofluids containing copper nanoparticles, *Applied physics letters* 78 (2001) 718-720.
2. C. Zhi, Y. Xu, Y. Bando, D. Golberg, Highly thermo-conductive fluid with boron nitride nanofillers, *ACS nano* 5 (2011) 6571-6577.
3. D. Cabaleiro, M. Pastoriza-Gallego, M. Piñeiro, L. Lugo, Characterization and measurements of thermal conductivity, density and rheological properties of zinc oxide nanoparticles dispersed in (ethane-1, 2-diol+ water) mixture, *The Journal of Chemical Thermodynamics* 58 (2013) 405-415.
4. J. Wang, H. Xie, Z. Xin, Y. Li, Increasing the thermal conductivity of palmitic acid by the addition of carbon nanotubes, *Carbon* 48 (2010) 3979-3986.
5. R. Agromayor, D. Cabaleiro, A.A. Pardinas, J.P. Vallejo, J. Fernandez-Seara, L. Lugo, Heat Transfer Performance of Functionalized Graphene Nanoplatelet Aqueous Nanofluids, *Materials* 9 (2016) 455.
6. W. Yu, H. Xie, D. Bao, Enhanced thermal conductivities of nanofluids containing graphene oxide nanosheets, *Nanotechnology*, 21 (2009) 055705.
7. S.S.N. Azman, N.W.M. Zulkifli, H. Masjuki, M. Gulzar, R. Zahid, Study of tribological properties of lubricating oil blend added with graphene nanoplatelets, *Journal of Materials Research* 31 (2016) 1932-1938.
8. D. Cabaleiro, C. Gracia-Fernández, J. Legido, L. Lugo, Specific heat of metal oxide nanofluids at high concentrations for heat transfer, *International Journal of Heat and Mass Transfer* 88 (2015) 872-879.
9. D. Cabaleiro, J. Nimo, M. Pastoriza-Gallego, M. Piñeiro, J. Legido, L. Lugo, Thermal conductivity of dry anatase and rutile nano-powders and ethylene and propylene glycol-based TiO$_2$ nanofluids, *The Journal of Chemical Thermodynamics* 83 (2015) 67-76.
10. D. Cabaleiro, M.J. Pastoriza-Gallego, C. Gracia-Fernández, M.M. Piñeiro, L. Lugo, Rheological and volumetric properties of TiO$_2$-ethylene glycol nanofluids, *Nanoscale Research Letters* 8 (2013).
11. Å. Melinder, Properties of Secondary Work Fluids for Indirect Systems: Secondary Refrigerants Or Coolants, Heat Transfer Fluids, International institute of refrigeration, 2010.
12. V. Gnielinski, G2 Heat Transfer in Concentric Annular and Parallel Plate Ducts,in *VDI Heat Atlas*, Ed. VDI-Gesellschaft Verfahrenstechnik und Chemieingenieurwesen, Chapter G2, pp. 701-708, Düsseldorf, Springer, 2010.

PERFORMANCE INVESTIGATION OF A MINIATURE PLATE HEAT EXCHANGER WITH GRAPHENE NANOPLATELET BASED EG/WATER NANOFLUIDS

Z. Wang, Z. Wu and B. Sundén*

Department of Energy Sciences, Faculty of Engineering, Lund University

Lund SE 22100, Sweden

*Corresponding author: bengt.sunden@energy.lth.se

Keywords: Graphene nanoplatelet nanofluids, Miniature plate heat exchanger, Ethylene glycol, Performance

Introduction:

With the advancement in miniaturization, more efficient miniature heat transfer equipments are needed. As a lot of research [1-2], especially in the design of heat transfer enhancement, focused on extending the heat transfer area, creating turbulence to destroy the boundary layer and adding vortex generators, etc. However, these measures often bring unnecessary pump work to increase flow resistance. For constant surface temperature, the Nusselt number is constant in the laminar flow fully-developed region, which indicates that the smaller the hydraulic diameter, the larger the convective heat-transfer coefficient [3]. The conventional direct technology such as those mentioned above cannot be applied to the miniature equipment with higher heat flux. Another approach to improve the heat transfer is using a fluid medium with better thermophysical properties [4-5]. Because water, ethylene glycol (EG) and engine oil have relatively poor thermophysical properties, some nanoparticles (metal, oxides, carbides, or carbon nanotubes) were added to the above base fluids, forming a colloidal suspension of nanoparticles [6]. These nanofluids usually have higher heat transfer performance than the base fluids and tend to cause little friction penalty. This potential makes them widely usable in microelectronics, fuel cells, heat exchangers, vehicle thermal management, domestic refrigerators, etc. Pantzali et al. [7], Huminic et al. [8] and Solangi et al. [9] presented reviews of nanofluids for heat transfer applications. These reviews implied that nanofluids could have greater potential for usage in different types of heat exchangers. Previous experimental work mainly focused on simple flow geometries, such as a horizontal tube, square heated pipe, and circular tube, etc. The investigations on nanofluids in complex geometries of the heat exchangers are limited. Recent investigations [10] show that the graphene nanoplatelet nanofluids (GNP) could provide higher thermal conductivity enhancement (up to 5000W/m·K) in comparison to that of other examined nanofluids. Because of the special 2D structure with a thickness from 5 to 10 nm, GNP has a high specific surface area (up to 750 m^2/g), also has characteristics such as high crystal quality and ballistic electronic transport at room temperature. Some studies found that using the GNP improved heat transfer performance [11]. However, the literature described above focused on the constant heat flux/wall temperature

boundary condition [12]. The heat transfer and flow characteristics of GNP in a miniature plate heat exchanger (MPHE) have not been studied deeply.

The present work investigates the performance of a miniature plate heat exchanger with graphene nanoplatelet-based EG/water nanofluids. The main reasons for choosing this are: no previous research has been performed regarding effect of GNP nanofluids on MPHEs, and the significant improvement in convective heat-transfer coefficient may be obtained in MPHE based on the high thermal conductivity of GNP. For this reason, some relevant experiments and analyses on heat transfer performance and pressure drop are required to apply GNP in the MPHE system.

Results and Discussion:

In this study, commercial nanofluids of EG/water (50:50) graphene nanoplatelet (GNP R-7, 5 wt.%) that present satisfying stability was provided by XG Sciences, Inc., Lansing, MI, USA. The primary thickness of the GNP is about 2 nm, their diameter is about 2 μm, and the average specific surface area is 750 m^2/g. The tested weight concentrations (0.01 to 2 wt.%) were obtained by diluting the 5 wt.% nanofluid. The diluted GNP nanofluid was mechanically mixed for 1 hour, followed by using a high-power ultrasonication to oscillate four hours. The effective thermal conductivity under different concentrations were measured by a thermal constants analyzer (Hot Disk TPS 2500S, Sweden). The uncertainty deviations of thermal conductivity were verified by several standard specimens, which is lower than 3.0%. A DV2TLV viscometer with UL adapter accessory (Brookfield AMETEK, US) was used to measure viscosity of different concentrations. The range of accuracy with test data is ±1.0% and the repeatability is ±0.2%.
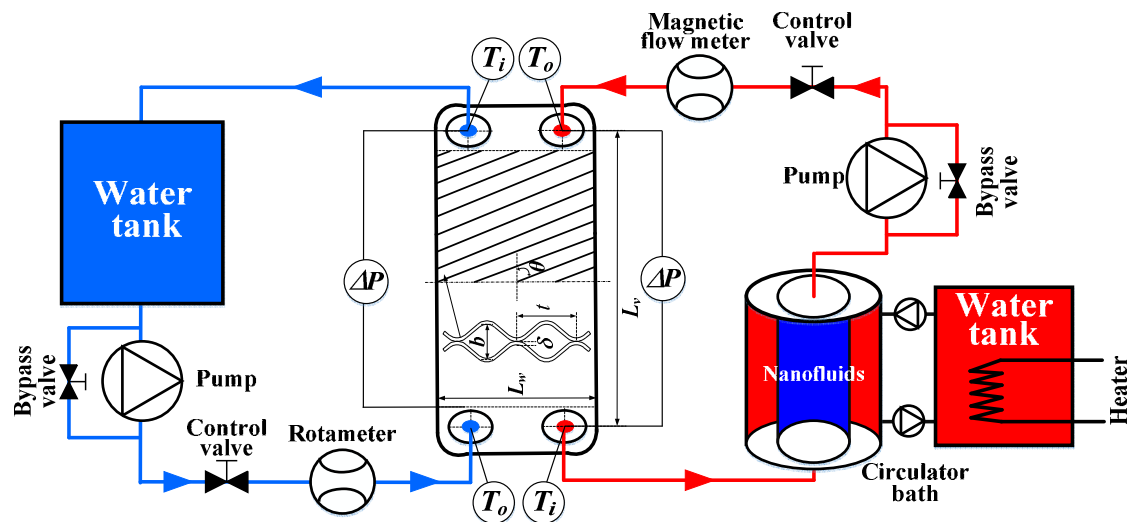
Figure 1. Schematic diagram of the experimental setup and MPHE

Table 1. Error analysis of relevant parameters

Measurement items	Unit	Value
Temperature	K	±0.1
Pressure drop	kPa	±1.5%
Thermal conductivity	W/m·K	±3.0%
Viscosity	cp	±1.0%
Flow rate	L/h	±2.0%
Heat flux	W/m^2	±3.7%
LMTD	K	±1.5%
Heat transfer coefficient	W/m^2·K	±4.1%

The MPHE, provided by Alfa Laval, comprises several stainless steel chevron-type plates that form two spaced fluid passages for the hot and cold fluids. The experimental setup for heat transfer in MPHE is shown in Figure 1. It mainly consists of a hot fluid closed loop, a cold fluid open loop and the corresponding temperature, mass flow rate and pressure measuring instruments. The GNP nanofluid was the hot fluid and heated to the required inlet fluid temperature in a heating tank. Then it was fed into the MPHE by a pump, passing through a rotameter, and returned to the heating tank. The water was stored in a cold tank and circulated by a pump. It passed a control valve, a rotameter and then entered the PHE in a counter flow. After absorbed the heat from the nanofluid, the cold water was drained. The measurement parameters of test bed consist of rotameters, K-type thermocouples and a differential pressure transducer, etc. The error of relevant parameters of this experiment system was shown in Table 1.

Experiments using water-to-water were carried out first to obtain heat transfer and pressure drop correlations for pure fluids flowing in the MPHE. The experimental measurements were temperature at inlet and outlet of the MPHE, pressure and flow rates for hot and cold water. These data were used to calculate the related heat transfer and pressure drop parameters. The comparisons of the heat transfer performance between the GNP nanofluids and water are shown based on a constant flow velocity, which avoids the effect of nanofluid physical properties on a constant Reynolds number basis. Figure 2 shows the heat transfer coefficient (HTC) versus flow velocity. The flow velocity is defined as $u=V/L_w b_c N$, where V is the volumetric flow rate, and N is the number of flow channels. With increasing flow velocity, the heat transfer coefficient increases in the MPHE. The relationship between the pressure drop ΔP and the volumetric flow rate V for water is displayed in Figure 3. The fluid properties, flow velocity and geometry of heat exchanger determine the pressure drop.
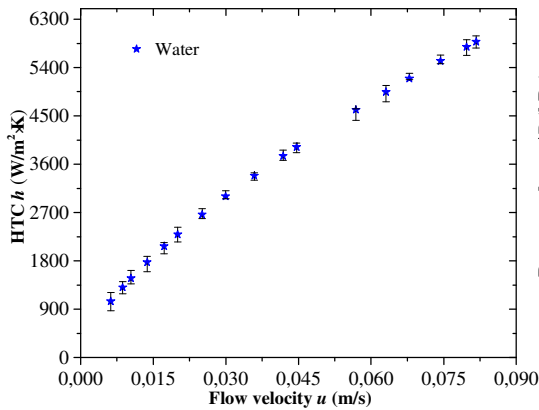
Figure 2. HTC versus *u*
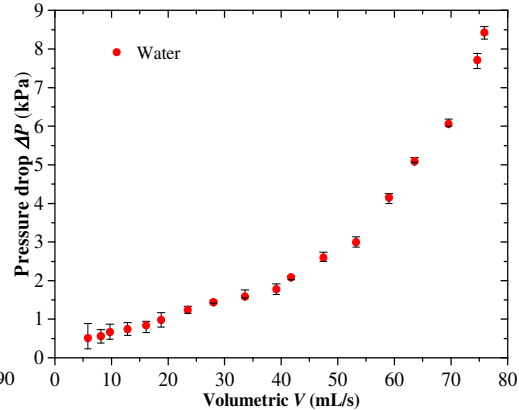
Figure 3. *ΔP* versus *V*

Next, the effect of concentrations (0.01-2 wt.%) and temperature (20-55℃) of GNP nanofluids on convective heat transfer coefficient and pressure drop in the MPHE will be investigated and compared with water.

Summary: As a general conclusion, it is evident in most cases that nanofluids provide a plausible solution to high heat flux and small size limit situation. Motivated by these challenges, the thermal conductivity and viscosity along with convective heat transfer and pressure drop of graphene nanoplatelet-based EG/water nanofluids at various concentrations and temperatures in MPHE have been studied experimentally. The preliminary results show that the heat transfer performance improves with an increase in flow velocity and with a decrease in nanofluid concentration. The GNP nanofluid has brought an acceptable pressure drop penalty but has a higher heat transfer performance compared with water in the MPHE. The enhancement of pumping power is moderate under this experimental condition which favors GNP nanofluid to be used in the MPHE for thermal systems. The results from the latest experiment of GNP nanofluid are now being analyzed, and further improvement work is ongoing.

References:

1. Wang Z, Li Y, Layer pattern thermal design and optimization for multistream plate-fin heat exchangers-A review, *Renewable and Sustainable Energy Reviews* 53 (2016) 500-514.
2. Wang Z, Li Y, A combined method for surface selection and layer pattern optimization of a multistream plate-fin heat exchanger, *Applied Energy* 165 (2016) 815-827.
3. Mohammed, H. A., Bhaskaran, G., Shuaib, N. H., & Saidur, R., Heat transfer and fluid flow characteristics in microchannels heat exchanger using nanofluids: a review, *Renewable and Sustainable Energy Reviews* 15 (2011) 1502-1512.
4. Murshed S M S, de Castro C A N. Conduction and convection heat transfer characteristics of ethylene glycol based nanofluids-A review, *Applied Energy* 184 (2016) 681-695.
5. Solangi, K. H., Kazi, S. N., Luhur, M. R., Badarudin, A., Amiri, A., Sadri, R., Teng, K. H., A comprehensive review of thermo-physical properties and convective heat transfer to nanofluids, *Energy* 89 (2015) 1065-1086.

6. Hussien A A, Abdullah M Z, Moh'd A A N, Single-phase heat transfer enhancement in micro/minichannels using nanofluids: Theory and applications, *Applied Energy* 164 (2016) 733-755.
7. Pantzali M N, Mouza A A, Paras S V, Investigating the efficacy of nanofluids as coolants in plate heat exchangers (PHE), *Chemical Engineering Science* 64 (2009) 3290-3300.
8. Huminic G, Huminic A, Application of nanofluids in heat exchangers: a review, *Renewable and Sustainable Energy Reviews* 16 (2012) 5625-5638.
9. Sajedi R, Taheri M, Taghilou M., On the multi-objective optimization of finned air-cooling heat exchanger: Nano-fluid effects. *Journal of the Taiwan Institute of Chemical Engineers* 68 (2016) 360-371.
10. Sadeghinezhad, E., Mehrali, M., Saidur, R., Mehrali, M., Latibari, S. T., Akhiani, A. R., Metselaar, H. S. C., A comprehensive review on graphene nanofluids: recent research, development and applications. *Energy Conversion and Management* 111 (2016) 466-487.
11. Amiri, A., Arzani, H. K., Kazi, S. N., Chew, B. T., Badarudin, A., Backward-facing step heat transfer of the turbulent regime for functionalized graphene nanoplatelets based water–ethylene glycol nanofluids, *International Journal of Heat and Mass Transfer* 97 (2016) 538-546.
12. Akhavan-Zanjani, H., Saffar-Avval, M., Mansourkiaei, M., Sharif, F., Ahadi, M., Experimental investigation of laminar forced convective heat transfer of Graphene–water nanofluid inside a circular tube, *International Journal of Thermal Sciences* 100 (2016) 316-323.

LAMINAR FORCED CONVECTION IN FLAT TUBES WITH Al$_2$O$_3$-WATER MIXTURE FOR AUTOMOTIVE APPLICATIONS

B. Buonomo[1], D. Ercole[1], O. Manca[1]*, A. Minea[2] and S. Nardini[1]

[1]Dipartimento di Ingegneria Industriale e dell'Informazione, Università degli Studi della Campania, Via Roma 29, Aversa (CE) , 81031, Italy

[2]Faculty of Materials Science and Engineering, Technical University "Gh. Asachi" from Iasi Bd. D. Mangeron 60, Iasi, 700050, Romania

*Corresponding author: oronzio.manca@unicampania.it

Keywords: Nanofluids, Numerical models, Mixture, Flat tubes, Automotive

Introduction: In recent years, the fast development of vehicle engine performance has determined a strong request of high cooling efficiency of a vehicle radiator and it is a vital equipment to remove the engine waste heat for keeping normal operating of automotive system as underlined in [1]. Convective heat transfer can be enhanced passively by changing flow geometry, boundary conditions or by enhancing the thermal conductivity of the working fluid [2]. For an assigned heat exchanger system, conventional fluids, such as pure water and ethylene glycol, present low thermal conductivity and, consequently, a low heat transfer performance. Therefore, it is highly desired to have innovative and effective heat transfer fluids to enhance vehicle radiator cooling rate [3]. Engine cooling system using nanofluids provides a new foundation for technological integration and innovation. Nowadays, an increased attention is focused on the using nanofluids for vehicle radiator in order to improve the heat transfer performance of engine cooling systems, as reviewed in [1, 4-11]. Moreover, a technique which is employed for heat transfer augmentation is the use of flattened tubes and a recent study which combines both nanofluids and flattened tubes was proposed in [10-12].

The use of nanofluids instead of the conventional fluids in car radiators was studied for the first time in [13]. In this study was reported a project to target fuel savings for the automotive industries through the development of energy efficient nanofluids and smaller and lighter radiators. Later, several numerical and experimental investigations have been accomplished on the use of nanofluids in automotive car radiators.

A short review on numerical studies is accomplished, mainly on laminar flow. Laminar flow in the flat tubes of an automobile radiator with two mixtures of Al$_2$O$_3$ and CuO nanoparticles in an ethylene glycol and water was presented in [14]. The cooling performances of an automotive radiator using ethylene glycol based CuO nanofluids as coolants was studied in [15]. A three-dimensional analysis was used to study the heat transfer performance of nanofluid flows through a flattened tube in a laminar flow regime and constant heat flux boundary condition.

More recent numerical studies in laminar flow are reported in [10,11,16-18]. Steady state laminar convection in a flat tube with nanofluids, Al2O3 in water or in water-ethylene glycol mixture, was numerically investigated in [16]. The friction factor and forced convection heat transfer of SiO_2 nanoparticle dispersed in water as a base fluid were evaluated in a car radiator experimentally and numerically in [17]. A numerical investigation on laminar forced convection flow of Al2O3 nanoparticles in water or water and glycol in a flat tube was accomplished in [18]. A three-dimensional numerical study to evaluate the laminar heat transfer and flow behaviors of Al2O3–water nanofluids through a flat tube at constant heat flux boundary condition is reported in [10]. A flat tube of an engine radiator was numerically studied in [11] to enhance the cooling process or heat recovery of the engine using nanofluids.

Some issues in laminar convective flow in flat tubes geometry with nanofluids presents a lack of information such as the effect of tube/duct thickness on heat transfer inside the duct and the effective convenience to employ the nanofluids in practical applications such as car cooling systems and radiators. Moreover, the comparison between single phase and mixture models allows to evaluate the possible errors related to the use of a simpler model. In the present study both single phase model and mixture model are employed to simulate laminar convective flow in Al_2O_3-water nanofluid mixtures in a flat duct with assigned wall heat flux on the external surface of a duct with an assigned thickness.

Discussion and Results: The geometrical configuration under consideration consists in a duct with two parallel flat plates and the lateral sides with a circular shape as shown in Fig. 1. The length of the duct, the edge one and the channel height is 0.5 m, 0.0081 m and 0.00254 m, respectively. In this way, the hydraulic diameter is set equal to 4.58×10^{-3} m. The thickness of the duct is 0.23×10^{-3} m. A steady laminar flow and different nanoparticle volume fractions have been considered. The analysis has been performed for nanofluids with water as base fluid and spherical nanoparticles of alumina (Al2O3) with a diameter equal to 38 nm. Thermophysical properties are considered constant with temperature. The CFD commercial code Ansys-Fluent [19] was employed in order to solve the 3-D numerical model. A grid independence analysis has been accomplished to evaluate the optimal node number in terms of computational time and accuracy. Moreover, a validation procedure was performed in the case of pure water and fully developed laminar flow, with data reported in [20].
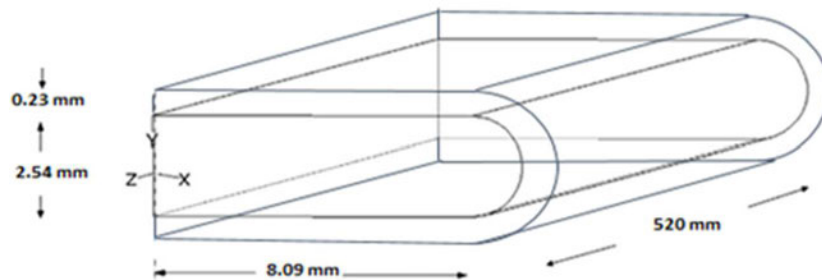
Figure 1. Sketch of the geometrical model.

Results are presented in terms of internal wall and bulk temperatures, local and average convective heat transfer coefficient, pressure drops, required pumping power profiles and two energy performance ratios, as a function of Re, ranging from 100 to 1000, and particle concentrations, in the range 0%-5% in pure water mixture. A constant and uniform heat flux of 2 kW/m^2 is applied on all the channel walls.

In Fig. 2, the internal wall and bulk temperatures, Fig. 2a, and the heat transfer coefficient, Fig. 2b, are given, along the axis, for a volumetric concentration equal to 5%. The temperature profiles are evaluated for three Re values and it is noted, as expected, that the greater the Re the temperature values. In Fig. 2b, the h profiles are evaluated for the single phase and mixture models. At the entrance the h values evaluated with mixture model are higher than that the ones evaluated with the single phase model. The differences decreases with the increase of z coordinate and are smaller in fully developed conditions. It is interesting to observe that the h values along z, for different volumetric concentrations and not reported, are greater as greater the volumetric concentration with the higher differences at the entrance zone. In Fig. 3, pressure losses and C_f coefficient are reported for single phase and mixture models for different volumetric concentrations. It is noted, in Fig. 3a, that the pressure losses are slightly higher in the mixture model whereas the friction factor, C_f values, does not depend on the model and volumetric concentrations. In order to evaluate the performance of the heat transfer by means of nanofluids and its advantage the evaluation performance ratio, EPR, is considered. In Fig. 4, two different EPRs are reported:

$$ EPR = \frac{Q_{nf} - Q_{bf}}{W_{nf} - W_{bf}} \quad \text{and} \quad EPR' = \frac{Nu_{nf}/Nu_{bf}}{\left(C_{f,nf}/C_{f,bf}\right)^{1/3}} \tag{1} $$
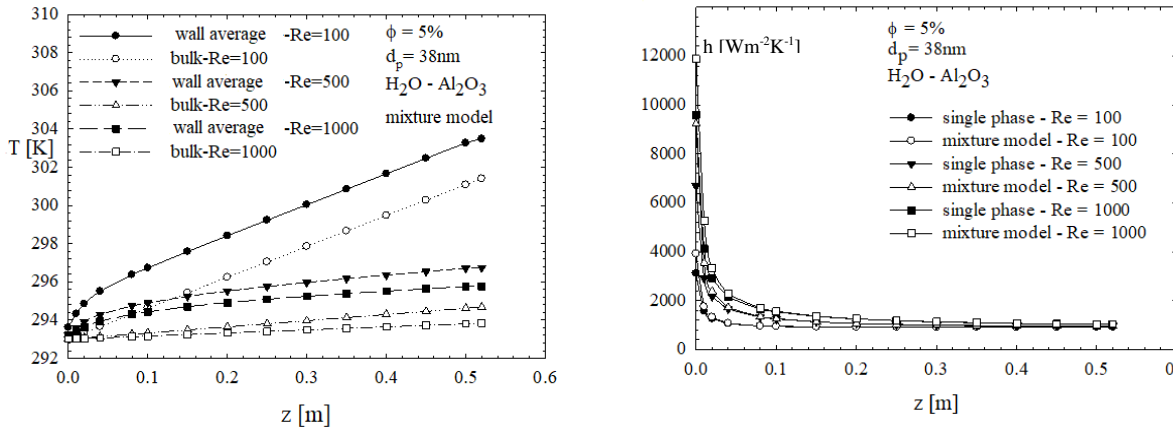
Figure 2. Profiles of local variables along the tube axis: a) wall and bulk temperatures
b) convective heat transfer coefficient.
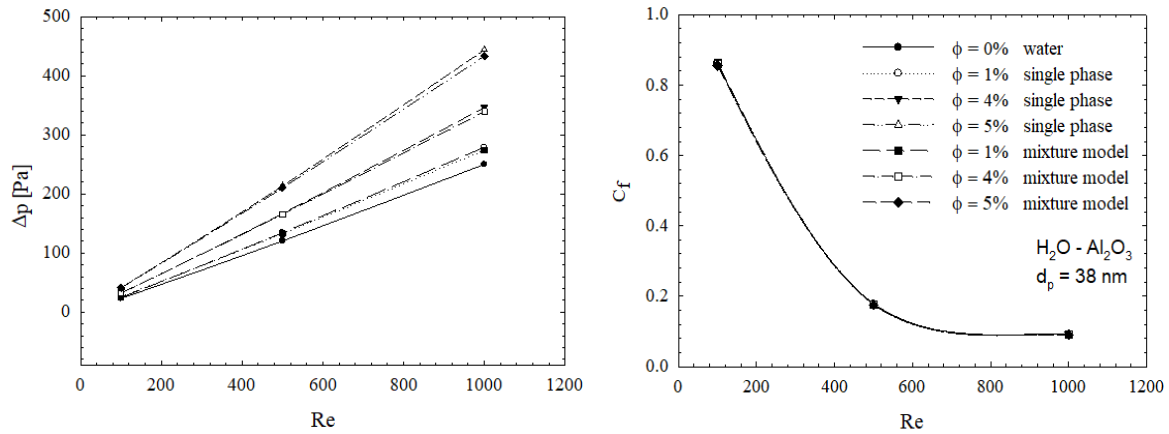
Figure 3. Fluid dynamics variables as a function of Reynolds number: a) pressure losses

b) friction factor.

with Q and W the heat transfer rate moved to the fluid and the mechanical power given to move the fluid, nf and bf are related to the nanofluid and base fluid, respectively. The first ratio indicates that the pure fluid has the best performances but the differences decrease as the Reynolds number increases whereas the second ratio, EPR', provides an opposite information, i.e., the use of nanofluids determines a better performance of the heat transfer.
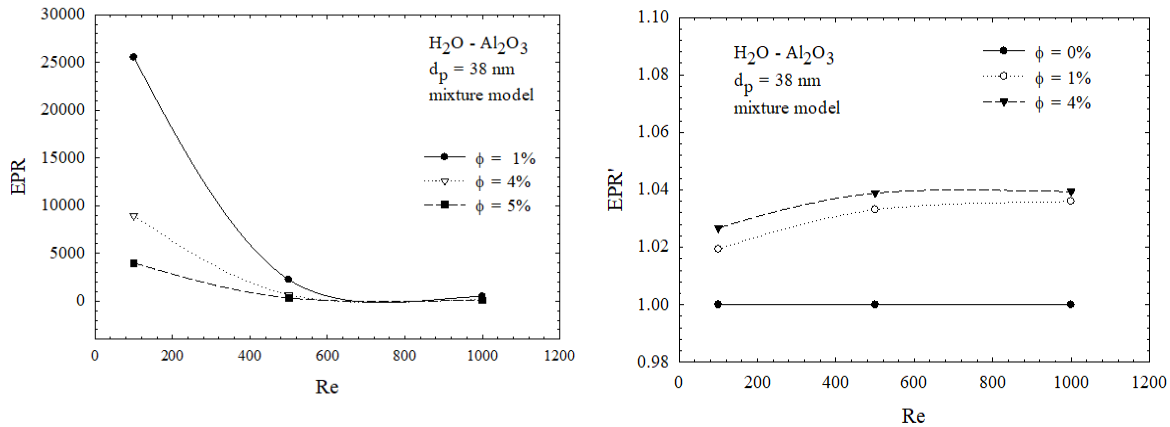
Figure 4. Evaluation performance ratio as in eq. (1).

Conclusions: A numerical investigation on laminar convective heat transfer in flattened ducts with nanofluids was performed to compare single phase and mixture models and evaluate the performance of the system by means of two different ratios. Some differences in terms of heat transfer coefficients and pressure drops were detected between the two models. As expected, the heat transfer coefficients increase as the volumetric concentration increases and for local heat

transfer coefficients the most significant increases were detected in the entrance zone. It was showed that the definition of evaluation performance ratio determined if the nanofluid presents a better performance with respect to the base fluid. In fact, in terms of energy ratio the base fluid is more convenient whereas in terms of Nusselt ratio related to the friction factor ratio the nanofluid provides a better performance.

References:

1. N.A. Che Sidik, M.N.A. Witri Mohd Yazid and R. Mamat, Recent advancement of nanofluids in engine cooling system, *Renewable and Sustainable Energy Reviews* 75 (2017) 137-144.
2. R.L. Webb and N.H. Kim, *Principles of Enhanced Heat Transfer*, 2nd ed., Taylor&Francis Group, New York, 2005.
3. P. Kulkarni Devdatta, S. Vajjha Ravikanth, K. Das Debendra and D. Oliva, Application of aluminum oxide nanofluids in diesel electric generator as jacket water coolant, *Applied Thermal Engineering* 28 (2008) 1774-1781.
4. N.A.C. Sidik, M.N.A.W.M. Yazid and R. Mamat, A review on the application of nanofluids in vehicle engine cooling system, *International Communications in Heat and Mass Transfer* 68 (2015) 85-90.
5. N. Zhao, S. Li and J. Yang, A review on nanofluids, Data-driven modeling of thermalphysical properties and the application in automotive radiator, *Renewable and Sustainable Energy Reviews* 66 (2016) 596-616.
6. S.S. Murshed, K. Leong and C. Yang, A combined model for the effective thermal conductivity of nanofluids, *Applied Thermal Engineering* 29 (2009) 2477–2483.
7. S.S. Murshed and C.N. de Castro, Conduction and convection heat transfer characteristics of ethylene glycol based nanofluids–a review, *Applied Energy* 184 (2016) 681–695.
8. S.S. Murshed and P. Estellé, A state of the art review on viscosity of nanofluids, *Renewable and Sustainable Energy Reviews* 76 (2017) 1134–1152.
9. G. Zyła, J. Fal and P. Estellé, Thermophysical and dielectric profiles of ethylene glycol based titanium nitride (TiN–EG) nanofluids with various size of particles, *International Journal of Heat and Mass Transfer* 113 (2017) 1189–1199.
10. N. Zhao, J. Yang, H. Li, Z. Zhang and S. Li, Numerical investigations of laminar heat transfer and flow performance of Al2O3-water nanofluids in a flat tube*, International Journal of Heat and Mass Transfer* 92 (2016) 268-282.
11. M. Hatami, M. Jafaryar, J. Zhou and D. Jing, Investigation of engines radiator heat recovery using different shapes of nanoparticles in H2O/(CH2OH)2 based nanofluids, *International Journal of Hydrogen Energy* 42 (2017) 10891-10900.
12. A.M. Hussein, H.K. Dawood, R.A. Bakara and K. Kadirgamaa, Numerical study on turbulent forced convective heat transfer using nanofluids TiO2 in an automotive cooling system, *Case Studies in Thermal Engineering*, 9 (2017) 72–78
13. S. Choi, Nanofluids for improved efficiency in cooling systems, *Heavy Vehicle Systems Review*, Argonne National Laboratory, April 18-20, 2006.

14. R.S. Vajjha, D.K. Das and P.K. Namburu, Numerical study of fluid dynamic and heat transfer performance of Al2O3 and CuO nanofluids in the flat tubes of a radiator, *International Journal of Heat and Fluid Flow* 31 (2010) 613–621.
15. G. Huminic and A. Huminic, Numerical analysis of laminar flow heat transfer of nanofluids in a flattened tube, *International Communication in Heat and Mass Transfer* 44 (2013) 52–57.
16. B. Buonomo, O. Manca, L. Marinelli, S. Nardini, Laminar Forced Convection in Flat Tubes with Nanofluids for Automotive Applications, *Proceedings of Third International Conference on Computational Methods for Thermal Problems THERMACOMP2014*, pp. 125-128, Lake Bled, Slovenia, June 2-4, 2014.
17. Hussein AM, Bakar RA, Kadirgama K. Study of forced convection nanofluid heat transfer in the automotive cooling system. Case Stud Therm Eng 2014; 2:50–61.
18. B. Buonomo, D. Ercole, O. Manca and A.A. Minea, A numerical investigation on laminar forced convection with nanofluid in heated flat tubes, paper n. 88, *Proceedings of 26th International Symposium on Transport Phenomena (ISTP-26)*, Leoben, Austria, 27 September - 01 October, 2015.
19. Ansys Incorporated, *Fluent 16.0 User Manual*, 2016.
20. R.K. Shah and A.L. London, *Laminar Flow Forced Convection in Ducts*, Academic Press, New York, 1978.

THERMAL PERFORMANCE OF SUSPENSIONS OF GRAPHANE NANOPLATELETS IN PLATE HEAT EXCHANGER

F.E.B. Bioucas, M.L. Matos Lopes*, S.M.S. Murshed and C.A. Nieto de Castro

Centro de Química Estrutural, Faculdade de Ciências, Universidade de Lisboa,

1749-016 Lisboa, Portugal

*Corresponding author: matoslopes@ciencias.ulisboa.pt

Keywords: Nanofluids, Convective heat transfer, Overall heat transfer coefficient, Pressure drop, Graphene

Introduction:

Many experimental studies have been reported in the literature, which suggest that the addition of nanoparticles enhance the heat transfer coefficient (HTC) in the laminar and turbulent flow regime as well as during pool and flow boiling. However, the effect on heat transfer is not clear as many of these studies have also shown that nanoparticles have no effect or deteriorate HTC [1].

In the present work, the effect of the use of a nanofluid consisting of a mixture of nanoplatelets of graphene (with a concentration between 0.027 to 0.10 w/w %) in a miniature plate heat exchanger (PHE) with corrugated surface has been experimentally studied. The PHE performance was compared to that of a conventional thermal fluid, water and ethylene-glycol mixture.

Experimental:

The heat exchanging experiments were performed with the setup shown in Figure 1. A miniature plate heat exchanger (PHE) was used, using a relative small quantity of cooling liquid (~0.3L) for its operation. This PHE is part of a Technical Teaching Equipment (EDIBON), and is connected to a tubing base unit comprising flow pump, valves and, flowmeters. The ensemble is operated through a computer controlled system that also measures the inlet and outlet temperatures and fluxes of both hot and cold fluids. The cold fluid is demineralized tap water and the hot fluid under study, is heated/refrigerated thermostatic bath, kept in closed circuit with approximately 4L total volume. For each experiment different inlet temperatures of the hot fluid are obtained by setting the thermostatic bath temperatures and the flow rates of the two streams. After steady state is established the data is recorded, allowing to obtain the heat

flux in both hot and cold streams and the average heat transfer rate $\bar{Q}$ in the PHE.
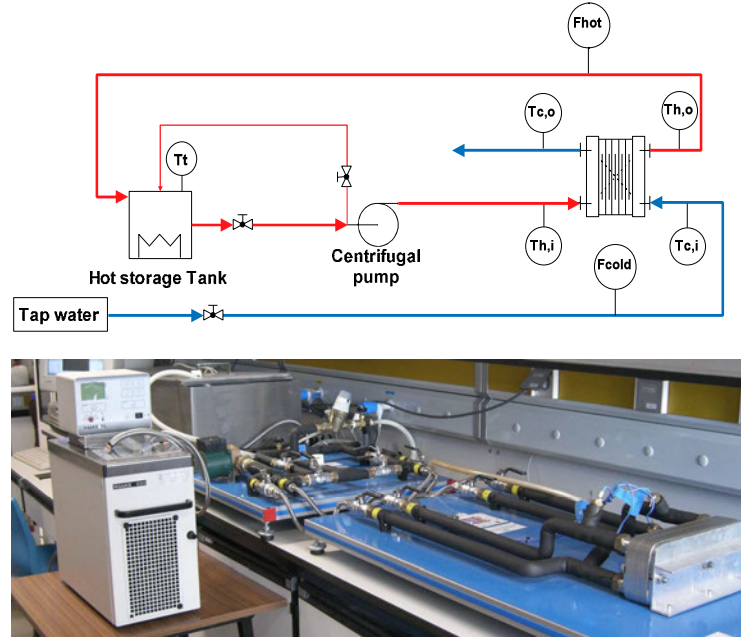
Figure 1. Schematic diagram (top) and picture (bottom) of the heat exchanger experimental setup

Correlation Development Methodology:

The correlation was developed based on the experimental results for water in both hot and cold streams following the algorithm schematically presented in Figure 2.

$$U = \frac{\bar{Q}}{A.LMTD} \quad \text{(i)} \qquad Nu_c = 1.615[f.Re.Pr.(D/L)]^{1/3}$$

$$Nu_c = \frac{h_c.D}{k} \Leftrightarrow h_c = \frac{Nu_c.k}{D} \quad \text{(ii)}$$

$$Nu_c = a.Re^b.Pr^{0.4}$$

$$\frac{1}{U} = \frac{1}{h_c} + \frac{\delta}{k_{plate}} + \frac{1}{h_h}$$

$$Nu_h = \frac{h_h.D}{k}$$

$$Nu_h = a.Re^b.Pr^{0.3} \Leftrightarrow \log(\frac{Nu_h}{Pr^{0.3}}) = \log(a) + \log(Re)b$$

$$\text{where in Eq. (i), } LMTD = \frac{(T_{ho} - T_{ci}) - (T_{hi} - T_{ci})}{\ln(\frac{T_{ho} - T_{ci}}{T_{hi} - T_{co}})}$$
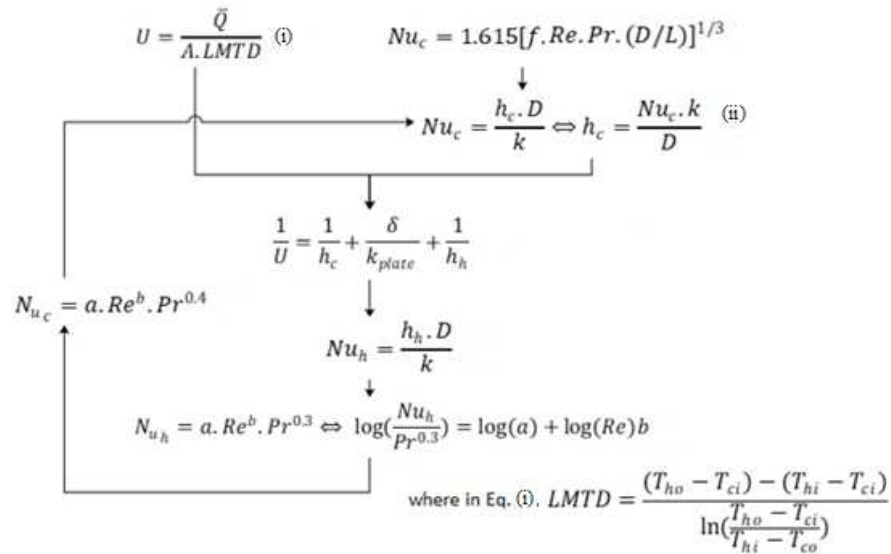
Figure 2. Schematic of the concept of development of correlations for hot and cold fluids.

This uses well known equations and definitions for, (i) the overall heat transfer coefficient, U, related to the hot and cold heat transfer coefficients, h_h, h_c, and the wall resistance, δ/k_{plate}, and calculated from the heat transfer rate, $\bar{Q}$, the heat transfer area, A and the logarithmic mean temperature difference, $LMTD$ and (ii) for the Nusselt number related to the heat transfer coefficient, h, the thermal conductivity, k, of each stream and the equivalent diameter, D of the PHE ducts. General correlations of the Nusselt number with the Reynolds and Prandtl numbers were used in the form $Nu = a.Re^b.Pr^c$, where the parameter c is taken as 0.3 and 0.4 for cold and hot streams, respectively and parameters a and b, are adjusted in the iteration process until no change is obtained for their values. For the starting value of h_c, any common correlation based on a Lévêque type equation with a suitable form for the friction factor, f, can be used [2]. This same procedure has been used by other authors [3-6] and allows to take into account, with the parameters a and b, the geometry and flow patterns of different types of heat exchangers. From different operating conditions (temperature and flow rates) we obtained for our PHE the values shown Table 1, where they are also compared with values reported by other authors for similar plate heat exchangers. The differences observed correspond in reality to different observed heat transfer coefficients because each of these correlations is applied to slightly different geometries for the same kind of chevron-type corrugation pattern plate heat exchangers.

Table 1. Parameters in the correlation obtained for similar PHE.

a	b	Ref.
0.456	0.548	This work
0.247	0.66	Pantzali et al. (2009)
0.455	0.66	Maré et al. (2011)
0.2302	0.745	Huang et al. (2015)
0.3762	0.6681	Huang et al. (2016)

This results in different flux patterns that of course influence the value of the heat transfer coefficient.

Results and Discussion:

The correlation was used for water as cold stream and hot streams of water and water, ethylene glycol mixtures. The expected effect was observed (Figure 3). That is, the ethylene glycol as known decreases the HTC. Nevertheless, its use mixed with water in heat exchangers is quite spread since it works as anti-freezing agent.

From the measurements performed no apparent effect is observed when adding graphene nanoplatelets of characteristic dimensions length 15 µm width 6-8 nm. In the representation we use a simple linear fit to the experimental data which is very dispersed. There seems to be a tendency for lower HTC relating to the base fluids but, within the experimental uncertainty there is no effect.
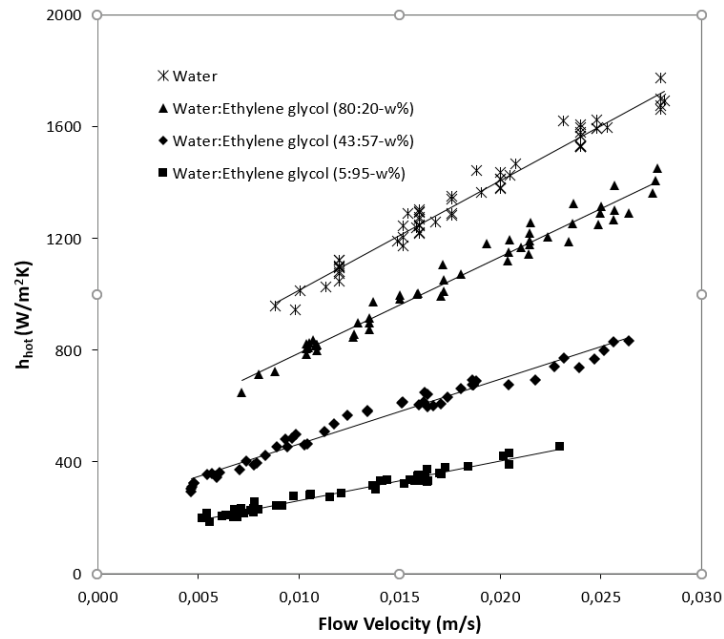
Figure 3. Heat transfer coefficients for water and water, ethylene glycol mixtures with different weight fractions
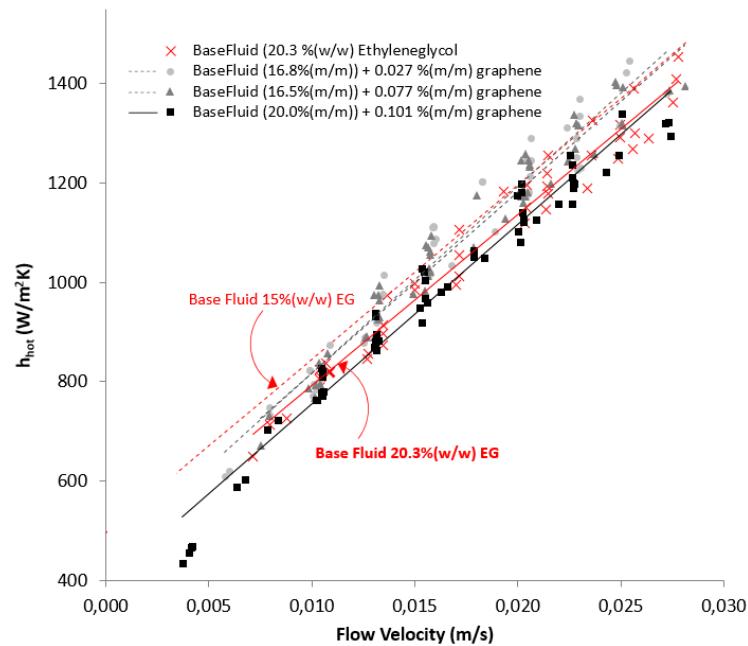
Figure 4. Heat transfer coefficients for graphene nanoplatelets nanofluids with different concentrations, in relation with the base fluids.

However, we have reasons to believe that there is deposition of the nanoparticles on the surfaces of the heat exchanger plates that would alter the geometry and flow patterns of the PHE making the correlation determined not valid to obtain reliable results for the heat transfer coefficients. We are currently investigating this possibility and a thorough study of the suspension stability, particle size control, occurring agglomeration and sedimentation, will follow before being able to take any conclusions regarding the existence of any enhancement of the HTC related to the presence of the graphene nanoplatelets.

Summary/Conclusions:

At its present stage, the study shows inconclusive results for the use of this kind of nanofluids as a solution towards designing efficient heat exchanging systems and points out the concern to the well-known instability of the nanoparticle suspensions. In cases like this where flow is involved, suspension stability, particle size control and sedimentation and agglomeration of nanoparticles is critical in the development and application of these heat transfer fluids.

References:

1. S.M.S. Murshed and C.A. Nieto de Castro, Nanofluids: Synthesis, Properties and Applications, *Nova Science Publishers Inc.*, New York, 2014.
2. H. Martin, A theoretical approach to predict the performance of chevron-type plate heat exchangers. *Chemical Engineering and Processing* 35 (1996) 301-310.
3. M.N. Pantzali, A.G. Kanaris, K.D. Antoniadis, A.A. Mouza, S.V. Paras, Effect of nanofluids on the performance of a miniature plate heat exchanger with modulated surface. *International Journal of Heat and Fluid Flow* 30 (2009) 691–699.
4. T. Maré, S. Halelfadl, O. Sow, P. Estellé, S. Duret, F. Bazantay, Comparison of the thermal performances of two nanofluids at low temperature in a plate heat exchanger. *Experimental Thermal and Fluid Science* 35 (2011) 1535–1543
5. D. Huang, Z. Wub, B Sunden, Pressure drop and convective heat transfer of Al2O3/water and MWCNT/water nanofluids in a chevron plate heat exchanger. *International Journal of Heat and Mass Transfer* 89 (2015) 620–626.
6. D. Huang, Z. Wub, B Sunden, Effects of hybrid nanofluid mixture in plate heat exchangers. *Experimental Thermal and Fluid Science* 72 (2016) 190–196.
7. V. Kumar, A. K. Tiwari, S. K. Ghosh, Application of nanofluids in plate heat exchanger: A review. *Energy Conversion and Management* 105 (2015) 1017–1036.

ASPECT RATIO EFFECT ON THE EFFECTIVENESS OF A SINGLE PHASE NATURAL CIRCULATION MINI LOOP

S. Doğanay[1], M. Alaboud[2], Z.H. Karadeniz[3]* and A. Turgut[4]

1Department of Mechatronics Engineering, The Graduate School of Natural and Applied Sciences, Dokuz Eylül University, Buca, İzmir, Turkey

2Department of Mechanical Engineering, The Graduate School of Natural and Applied Sciences, İzmir Kâtip Çelebi University, Çiğli, İzmir, Turkey

3Department of Mechanical Engineering, İzmir Kâtip Çelebi University, Çiğli, İzmir, Turkey

4Department of Mechanical Engineering, Dokuz Eylül University, Buca, İzmir, Turkey

*Corresponding author: zhaktan.karadeniz@ikc.edu.tr

Keywords: Aspect ratio, nanofluid, natural circulation loop, numerical study

Introduction: Technological developments have led to miniaturization of electronic devices which cause high heat flux rates from considerably small areas for past few decades. Liquid cooling systems satisfy higher heat flux rates than air cooled heat sinks [1]. Natural circulation loops (NCLs) are known as passive, reliable and safe systems, owing to its simple working principle without any moving or rotating mechanical components. The first attempts on single-phase NCL (SPNCL) appeared in the literature five decades ago [2]. Wang et al. [3] made a transient numerical study by considering the experimental setup of Misale et al. [4] and the results were compared with the experimental results. Their predicted results show a good agreement with the experimental results. The fluid type is the one of the most essential parameter for a mini SPNCL (SPNCmL). For a decade, a new generation heat transfer fluid called as nanofluid has drawn researchers' attention. Turgut et al. [5] made an experimental effort with a SPNCmL at a constant heat sink temperature (20°C) and input power between 10-50 W. Doganay et al. [6] conducted their experiments by varying input power, heat sink temperature and inclination angle. Turgut et al. [5] and Doganay et al. [6] concluded that the thermal performance of the SPNCmL enhanced with the increase of the particle concentration of nanofluid, input power and inclination angle. Koca et al. [7] performed an experimental study similar to Turgut et al. [5] by using Ag-water nanofluid. They observed that effectiveness of the SPNCmL enhanced by using nanofluid rather than DIW. Although nanofluid based SPNCmL studies are available in the literature, the number of numerical studies still under the expectations. Karadeniz et al. [8] investigate the effect of using nanofluid on the thermal performance of a SPNCmL in inclined conditions by using a three dimensional steady numerical model. They use the experimental setup of Turgut et al. [5] as base for the numerical study. Their results indicated a good agreement with the experimental results. Among geometrical parameters, aspect ratio is the one of the most essential geometrical parameter to be

taken into account while designing a miniaturized loop. Chen [9] carried out a pioneering analytical and numerical study for different aspect ratios. It is found that flow is least stable when the aspect ratio of the water based rectangular loop approaches unity.

In perusing the available literature, it seems that there is a gap in numerical nanofluid based SPNCmL studies focused on the aspect ratio. This three dimensional steady numerical study aims to investigate the influence of aspect ratio on Al_2O_3-DIW nanofluid based SPNCmL. During the study, the loop length kept constant and the aspect ratio altered between 0.4 and 1.38. The analyses were conducted with DIW and Al_2O_3-DIW nanofluids with 1, 2, 3 % volumetric particle concentrations. The input power was varied among 10-50 W.

Discussion and Results: 3D numerical model was adopted from the experimental study of Turgut et al. [5] (Figure 1). An aspect ratio (A) has been defined as the ratio of loop height to the loop width. The aspect ratio of the experimental setup calculated as 1.38.

Parameter	Dimension (mm)
D_{tube}	4.75
$D_{expansiontank}$	19
D_{ventil}	10
H	304
L	220
L_c	110
L_h	140
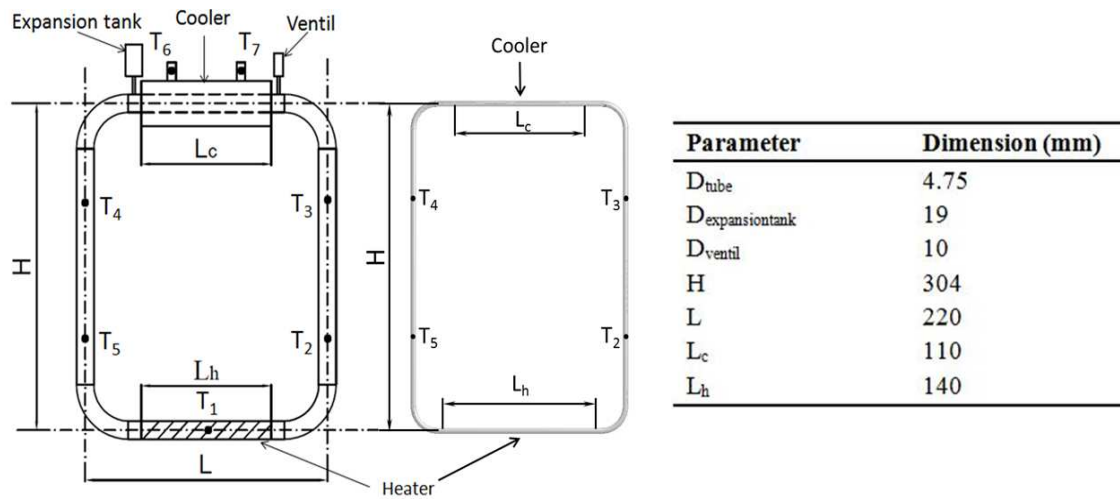
Figure 1 Schematic view of experimental setup [5], corresponding numerical model and dimensions.

In order to keep comparable numerical results with the results of Turgut et al. [5], the dimensions of elbows have been taken as constant. Hence, the minimum possible aspect ratio was observed as 0.18. As a result, the aspect ratio range was determined as 0.4 and 1.38 by keeping the total loop length constant (Figure 2).
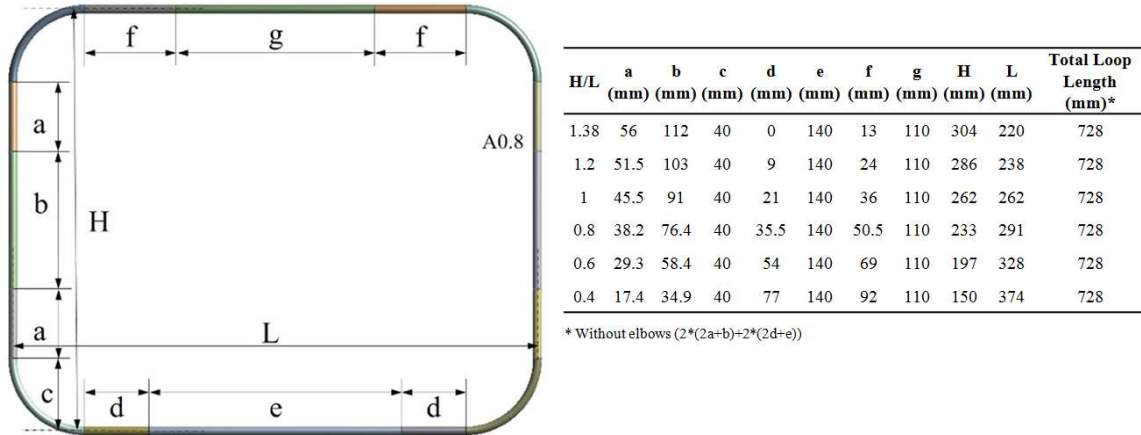
Figure 2 Geometrical parameters of the numerical study.

H/L	a (mm)	b (mm)	c (mm)	d (mm)	e (mm)	f (mm)	g (mm)	H (mm)	L (mm)	Total Loop Length (mm)*
1.38	56	112	40	0	140	13	110	304	220	728
1.2	51.5	103	40	9	140	24	110	286	238	728
1	45.5	91	40	21	140	36	110	262	262	728
0.8	38.2	76.4	40	35.5	140	50.5	110	233	291	728
0.6	29.3	58.4	40	54	140	69	110	197	328	728
0.4	17.4	34.9	40	77	140	92	110	150	374	728

* Without elbows (2*(2a+b)+2*(2d+e))

In order to build the model and solve the model with the corresponding boundary conditions, a commercial software (ANSYS CFX) was used. Heater and cooler parts were modelled as boundary conditions. Cooler part was assumed to be at constant temperature (20°C) which is the cooling fluid temperature for the experimental study. Constant wall heat flux (10, 30, 50 W) was applied to the heater part. All other boundaries of the numerical model were defined as adiabatic walls. A full buoyancy model was used for modelling the laminar natural convection flow. Viscosity, thermal expansivity and thermal conductivity were taken as functions of temperature in the numerical calculations. The effective specific heat (C_e) values have been calculated by Eq. (1) and taken as constant at the average loop temperature for each sample. Table values were used to define the dependency of properties on temperature when water is the working fluid. However, for Al_2O_3-DIW nanofluid, models adopted from the literature for determining the effective density (ρ_e) and effective thermal expansivity (β_e) for different volumetric concentrations as given in Eq. (2) and Eq. (3), respectively.

$$C_e = \frac{\phi_p(\rho C)_p + (1 - \phi_p)(\rho C)_f}{\phi_p \rho_p + (1 - \phi_p)\rho_f},\qquad(1)$$

$$\rho_e = (1 - \phi_p)\rho_f + \phi_p \rho_p,\qquad(2)$$

$$(\rho\beta)_e = (1 - \phi_p)(\rho\beta)_f + \phi_p(\rho\beta)_p,\qquad(3)$$

Further information on the numerical study details, mesh dependency, validation study and some other results were presented by Karadeniz et al. [8].

144
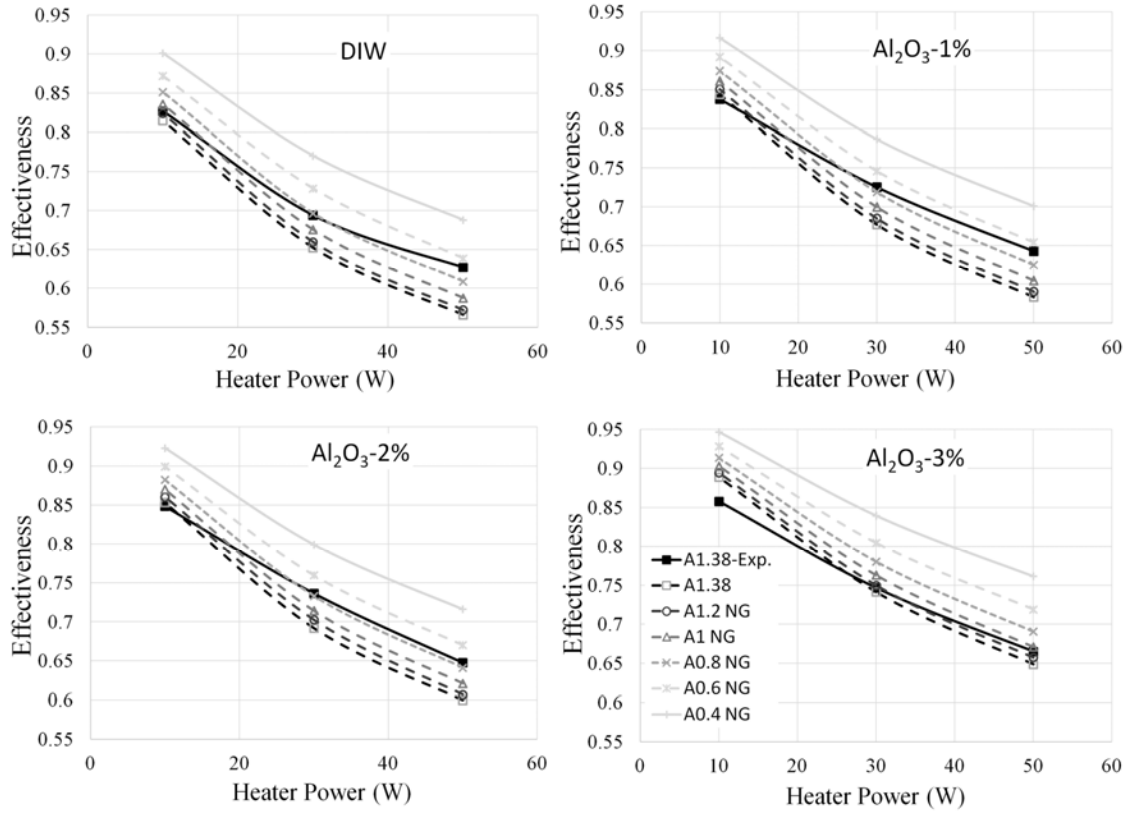
Figure 3 Effectiveness factor with respect to heater power for all aspect ratios and samples.

$$\varepsilon = \frac{T_2 - T_5}{T_2 - T_6}$$
(4)

As the thermal performance criteria effectiveness factor (ε) were employed (Eq. 4). It represents the ratio of the actual heat transfer to the maximum possible heat transfer [5]. Figure 3 depicts the variation of effectiveness factor with respect to applied power and aspect ratio for all nanofluid samples. It seems that numerical results in a good agreement with experimental results for 10 W applied power for all cases. When heater power increases, a difference occurs between numerical and experimental results. This is probably caused by not modelled heat losses from the numerical model. Moreover, the highest difference between numerical and experimental study happens for 3% vol. concentration and this can be related to the measured thermophysical properties in the experimental study. Figure 3 indicates that the system has higher effectiveness values when nanofluid samples are used rather than using DIW. Besides, the effectiveness factor increases with the increment of volumetric concentration and decrement of applied power. In terms of aspect ratio, it is clearly seen from Figure 3 that effectiveness factor increases with decreasing aspect ratio. Although, the loop length is constant for all aspect ratio values which mean the amount of

nanofluid in the system is same, the aspect ratio influences the effectiveness of the SPNCmL. This reveals the importance of the geometry when the SPNCmL are designed.

Conclusions: In this study the thermal performance of a SPNCmL has been investigated numerically. The conclusions can be drawn have been presented as follows:

- The effectiveness factor of nanofluid based SPNCmL increases with the increasing vol. concentration and decreasing aspect ratio and applied power.
- Decreasing the aspect ratio provides an enhancement up to 20% in effectiveness.
- Numerical model is powerful to estimate the loop performance with small errors.
- The designed numerical model can be useful to save time, where comparative results are necessary for different geometries and different nanofluid types and concentrations.

References:

1. X.C. Tong, *Advanced materials for thermal management of electronic packaging,* Springer Science & Business Media, New York, 2011.
2. J.B. Keller, Periodic oscillations in a model of thermal convection, *Journal of Fluid Mechanics* 26 (1966) 599-606.
3. J.Y. Wang, T.J. Chuang and Y.M. Ferng, CFD investigating flow and heat transfer characteristics in a natural circulation loop, *Annals of Nuclear Energy* 58 (2013) 65-71.
4. M. Misale, P. Garibaldi, J.C. Passos and G. G. Bitencourt, Experiments in a single-phase natural circulation mini-loop, *Experimental Thermal Fluid Science* 31 (2007) 1111–1120.
5. A. Turgut and S. Doganay, Thermal performance of a single phase natural circulation mini loop working with nanofluid, *High Temperatures-High Pressures* 46 (2014) 311-320.
6. S. Doganay and A. Turgut, Enhanced effectiveness of nanofluid based natural circulation mini loop, *Applied Thermal Engineering* 75 (2015) 669-676.
7. H.D. Koca, S. Doganay and A. Turgut, Thermal characteristics and performance of Ag-water nanofluid: Application to natural circulation loops, *Energy Conversion and Management* 135 (2017) 9-20.
8. Z.H. Karadeniz, S. Doganay and A. Turgut, Numerical study on nanofluid based single phase natural circulation mini loops: A steady 3D approach, *High Temperatures--High Pressures*, 45 (2016) 321-335.
9. K. Chen, On the oscillatory instability of closed-loop thermosyphons, *Journal of Heat Transfer*, 107 (1985) 826-832.

THERMAL ENHANCEMENT USING NANOFLUIDS ON HIGH HEAT DISSIPATION ELECTRONIC COMPONENTS

R.R. Riehl

National Institute for Space Research, INPE – DMC
Av dos Astronautas 1758, São José dos Campos, 12227-010 SP Brazil

Email: roger.riehl@inpe.br

Keywords: thermal enhancement, electronics cooling, thermal control, pressure drop, nanofluids

Abstract: Following today's needs for improvement on heat transfer, new technologies and innovative solutions must be found in order to meet current requirements for both active and passive thermal control. There has been substantial growth on the heat fluxes that need to be dissipated, which require different approaches from designers, especially those designed for defense purposes. With the increase of heat dissipation needs, conventional designs are not suitable due to several factors such as operation in hostile environments, high thermal density of electronics that need their temperature to be controlled, which require innovative designs. In such cases, the application of nanofluids can greatly contribute to give designers more degrees of freedom to face the project's requirements. The subject of this article is related to a surveillance system designed for defense purposes, which needs to dissipate high levels of heat loads. For this present investigation, a single-phase forced circulation loop has been designed to promote the thermal management of up to 50 kW of heat, being dissipated to the environment by a fan cooling system. Results show that with an addition of 20% by mass of copper oxide nanoparticles to the base fluid (water), enhancements of 12% on the heat transfer coefficients were achieved but the increase on the pressure drop was around 32%.

Introduction

The need for thermal management has increased dramatically over the last decade and the prediction is that a steeper increase is yet to come for the next years. Such an increase is directly related to more powerful electronics used for data processing in high-tech equipments used for satellites and defense/military purposes. Several investigations related to nanofluids applications have been conducted with important contributions to many areas (Ebrahimnia-Bajestan et al., 2011; Ghadimi et al., 2011).Considering previous experiences, current and future thermal management needs, the use of nanofluids is becoming inevitable. The use of nanofluids present to be an important approach to enhance the heat transfer capability of heat pipes and loop heat pipes systems, which has already been proven (Riehl and Santos, 2012). Similar investigation has also been performed by Alizad et al (2012) where it showed that smaller sizes heat pipes can be used when operating with nanofluids. Other applications are related to the use of nanofluids in regular heat exchanger devices already installed in industries

in order to enhance their performance in face of the increase of heat dissipation needs (Leong et al., 2012). Evaluation of nanofluids have been performed by many researchers in order to better understand the effects of the nanoparticles on transport properties, which are important for the prediction of the pumping requirements (Murshed et al., 2011; Murshed and Estellé, 2017). Applications related to PCB thermal management using nanofluids have also been reported (Colla et al. 2016). However, important issues still require attention, especially when considering the verification of a nanofluid regarding its own design, since many authors have reported different results for the same combination of base fluid and nanoparticles (Marcelino and Riehl, 2016). An important application for today's needs for heat dissipation is related to surveillance systems designed for defense/military purposes. As more compact and powerful defense equipments are necessary, higher heat fluxes need to be properly addressed. Considering the need for designing a reliable and effective thermal management system that need to operate in hostile environments, with potential use of nanofluid, this article presents an investigation on this subject.

Nanofluid's Properties Consideration

The base fluid's transport properties is influenced by the addition of the solid nanoparticles, which in one hand enhances the fluid's thermal conductivity but also directly contribute to enhance its liquid density and viscosity. Proper consideration must be made regarding the addition of the solid nanoparticles as those properties might directly influence the overall thermal management and pumping analysis. Some models have been developed to better describe the influence of the addition of nanoparticles in pure substances and the gain on the liquid thermal conductivity that might represent (Koo and Kleinstreuer, 2004) as usually the Maxwell model is applied on this case as

$$k_n = \frac{k_p + 2\ k_l + 2(k_p - k_l)\ f}{k_p + 2\ k_l - (k_p - k_l)\ f} k_l . \qquad \text{W/m°C} \qquad [1]$$

Equation [1] represents the effective thermal conductivity of a homogeneous nanofluid (k_n), while k_p, k_l and f are the particle and base fluid thermal conductivities and f is the nanoparticle mass fraction, respectively. Since the liquid thermal conductivity is affected by the addition of a nanoparticle in the substance, proper consideration and evaluation of the solid particles in a liquid must be taken according to the two-phase theory (Carey, 2008). Thus, the nanofluid density (ρ_n) is then calculated as

$$\frac{1}{\rho_n} = \left(\frac{f}{\rho_p} + \frac{1-f}{\rho_l} \right), \qquad \text{kg/m}^3 \qquad [2]$$

where $\square_p$ and $\square_l$ are the nanoparticle and the base fluid densities, respectively. The nanofluid dynamic viscosity ($\square_n$) can then calculated as (Xuan and Roetzel, 2000)

$$\mu_n = \mu_l \frac{1}{(1-f)^{2.5}}, \qquad \text{Pa.s} \qquad [3]$$

where $\square_l$ is the base fluid dynamic viscosity. The modification of the transport properties indicated in Eqs. [1] to [3] should be included in any analysis to correctly address their influence on the system's thermal performance. In the present analysis, Eqs. (1)-(3) were implemented in a design model to predict the nanofluid influence on the overall thermal and hydraulic performance of the surveillance thermal management system.

Equipment Design and Operation

A specific design for a surveillance system has been conceived to operate in hostile environments where the ambient temperatures can range from +5 to +50 °C and humidity levels up to 95%. In this case, a single-phase thermal control loop has been designed to use a nanofluid, presenting a forced circulation using a pump to move the working fluid throughout the circuit to remove heat from the electronic components, rejecting this heat to the environment by a fan cooling system. For this thermal management system, a hybrid design has been applied where the heat generated by all PCBs are removed by open loop pulsating heat pipes, delivering the heat to the heat sinks allocated thorough the surveillance equipment (cold plates). The heat sinks are then connected to the single-phase thermal control loop that collects all the heat and dissipate it to the environment. The schematics of such arrangement is presented by Fig. 1a and the surveillance equipment where it is installed is shown by Fig. 1b, whilst Fig. 1c presents the hybrid setup where the pulsating heat pipe and the heat sink are connected.

(a) (b) (c)
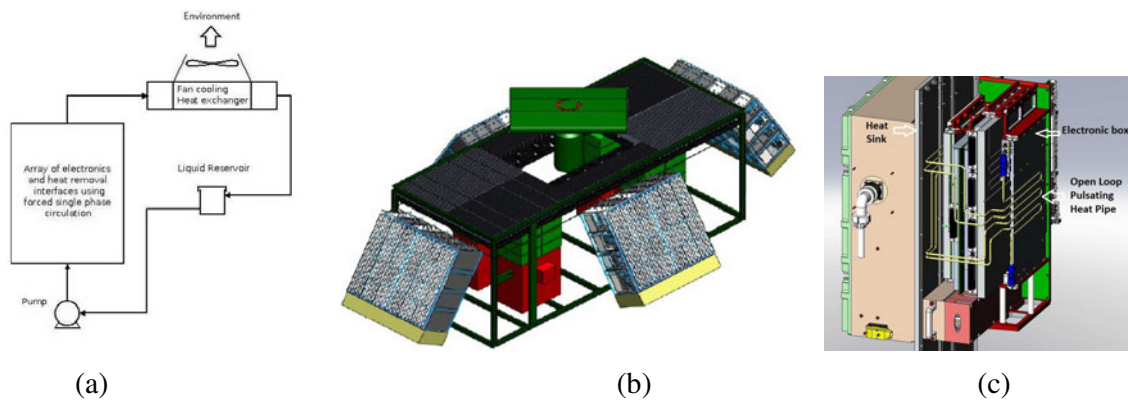
Figure 1: Schematics of the thermal control system arrangement.

As the base fluid, water has been selected for this approach. The CuO nanoparticles present an average diameter of 29 nm and purity of 99.8%. The nanoparticles concentration (*f*) shall vary from 3.5% to 20% (by mass of the base fluid) to verify their effect on the overall thermal performance of the system.

Results and Discussion

The presented results were well correlated to the thermal tests applied to this equipment, and further analysis will be disclosed in future reports. For the sake of presenting the most important results obtained so far, the following data were selected among several hours of operation and follow the NDA (non-disclosure agreement) set between all parts.

Figures 2a and 2b present some results for the pressure drop and heat transfer coefficients, respectively, on a comparison between the use of pure water and the addition of copper nanoparticles at different concentrations (*f*), by mass percentage of the working fluid in the system. The results are related to each individual electronics module (composed of 3 PCBs), which dissipate a maximum of 50 W of heat, thus, based on the module's footprint and heat dissipation, the calculation for the heat transfer coefficient was performed. As shown by Fig. 2c, less volumetric flow rate is necessary to promote the heat dissipation when using the nanofluid, as the heat transfer coefficient increases. It is clear that as the nanoparticle concentration increases, the pressure drop also increases up to 32% for *f*=20% as more solid nanoparticles are present in the system (Fig. 2d). The pump needs to overcome the extra resistance as the transport properties are changed with the addition of the nanoparticles. However, the increase on the heat transfer coefficients is also clear and can represent a gain around 12% for the same *f*=20% which cannot be neglected.
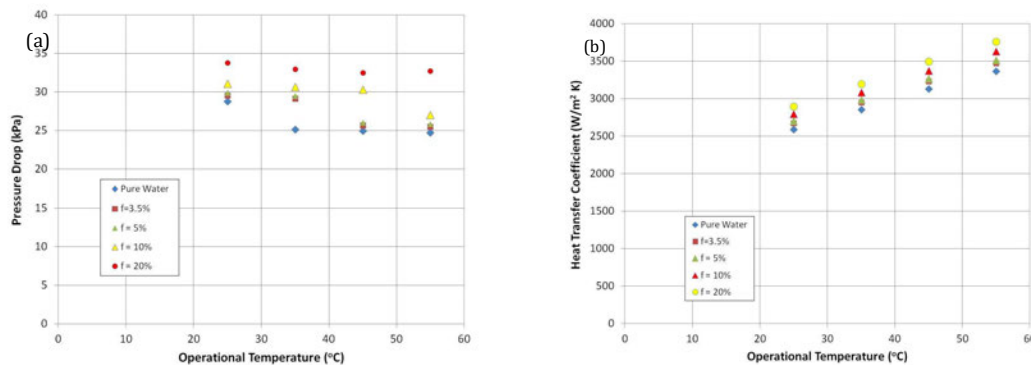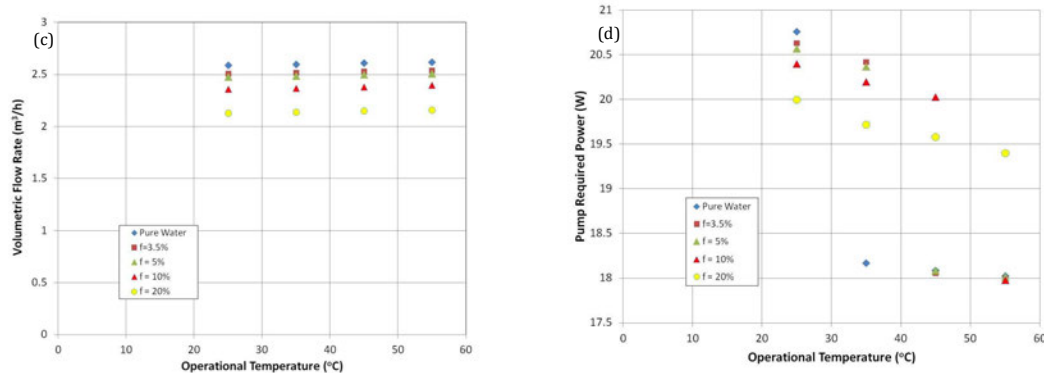
Figure 2: Results for (a) pressure drop and (b) heat transfer coefficient (c) volumetric flow rate and (d) pump required power.

Conclusions

In general, the main conclusions that can be derived from this investigation are:

1. Higher heat transfer coefficients can be reached with the increase of the solid nanoparticles concentration, representing an enhancement of up to 12% for f=20% at 55 °C when compared with the operation with water;
2. The pressure drop also increases as the concentration of nanoparticles increases, which could compromise the pump operation;
3. Lower volumetric flow rates are observed for higher concentration of nanoparticles, as this factor contributes to increase the working fluid's viscosity and density;
4. Even with the use of solid nanoparticles, the required pumping power does not represent to be the major issue on this specific project, as this requirement can be easily addressed as the calculated values are rather low;
5. The overall analysis indicates that the application of the nanofluid with higher concentrations can be used, as the major parameter for this analysis is the heat transfer coefficient, which is reducing the size of the thermal management system applied to control the temperature of the electronics components.

When considering that the thermal management system is operating at higher capacities, while keeping the working fluid's temperature differences between the fan cooling inlet and outlet within certain required parameters, the use of a nanofluid presents to be an important innovative approach for this project. This is directly resulting in more gains than loses for the overall thermal system analysis and should remain as the most indicated solution for this application.

References

1. Alizad, K., Vafai, K., Shafahi, M., "Thermal performance and operational attributes of the startup characteristics of flat-shaped heat pipes using nanofluids", *International Journal of Heat and Mass Transfer* 55 (2012) 140-155.

2. Leong, K. Y., Saidur, R., Mahlia, T. M. I., Yau, Y. H., "Modeling of shell and tube heat recovery exchanger operated with nanofluid based coolants", *International Journal of Heat and Mass Transfer* 55 (2012) 808-816.

3. Murshed, S. M. S., Estellé, P., "A state of the art review on viscosity of nanofluids", *Renewable and Sustainable Energy Reviews* 76 (2017) 1134-1152.

4. Murshed, S. M. S., Nietro de Castro, C. A., Lourenço, M. J. V, Lopes, M. L. M., Santos, F. J. V, "A review of boiling and convective heat transfer with nanofluids", *Renewable and Sustainable Energy Reviews* 15 (2011) 2342-2354.

5. Colla, L., Fedele, L., Mancin, S., Bobbo, S., Ercole, D., Manca, O., "Nano-PCMs for electronics cooling applications", *Proceedings of the 5th International Conference on Micro/Nanoscale Heat and Mass transfer, Jan 4-6, 2016, Biopolis, Singapore*.

6. Marcelino, E., Riehl, R. R., "A review on thermal performance of CuO-water nanofluids applied to heat pipes and their characteristics", *Proceedings of the 15th IEEE Intersociety Conference on Thermal and Thermomechanical Phenomena in Electronic Systems (ITherm)*, May 31 - June 3, 2016, Las Vegas NV, USA.

7. Ebrahimnia-Bajestan, E., Niazmand, H., Dungthondsuk. W., Wongwises, S., "Numerical investigation of effective parameters in convective heat transfer of nanofluids flowing under a laminar flow regime", *International Journal of Heat and Mass Transfer* 54 (2011) 4376-4388.

8. Ghadimi, A., Saidur, R., Metselaar, H. S. C., "A review of nanofluid stability properties and characterization in stationary conditions", *International Journal of Heat and Mass Transfer* 54 (2011) 4051-4068.

9. Riehl, R. R., Santos, N., "Water-copper nanofluid application in an open loop pulsating heat pipe", *Applied Thermal Engineering* 42 (2012) 6-10.

Heat transfer enhancement in automotive cooling circuits by nanofluids

Bernardo Buonomo[1], Luca Cirillo, Anna di Pasqua[1], Davide Ercole, Oronzio Manca[1*]

[1] Dipartimento di Ingegneria, Università degli Studi della Campania "Luigi Vanvitelli", Real Casa dell'Annunziata, Via Roma 29, Aversa, Italy

*Corresponding e-mail: oronzio.manca@unicampania.it

Keywords: Automotive cooling circuit, Nanofluids, Heat Transfer Enhancement, Power Consumption, Transient simulation.

INTRODUCTION: Continuous technological development in automotive industries has increased the demand for high efficiency engines. Optimizing design and size of a radiator in order to reduce a vehicle weight is a requirement for making the world green. Using of fins is one of the technique to increase the cooling rate of the radiator. However, traditional approach of enhancing the cooling rate by using fins and microchannels has already showed to their limit [1]. Furthermore, heat transfer fluids such as water and ethylene glycol have very low thermal conductivity. As result there is an urgency for new and innovative heat transfer fluids for increasing heat transfer rate in an automotive cooling circuit. Nanofluids represent potential substitute of conventional coolants in engine cooling system. Recently different studies have demonstrated superior heat transfer performances of nanofluids [1-3]. Bozorgan et al. [4] carried out a numerical analysis on an application of CuO-water nanofluid in automotive diesel engine radiator. The results showed that for the nanofluid at 2% volume concentration circulating through the flat tubes while the automotive speed is 70 km/hr, the overall heat transfer coefficient and pumping power are approximately 10% and 23.8% more than that of base fluid for given conditions, respectively. An experimental study was accomplished by Hwa Ming Nieh [5]. An alumina (Al_2O_3) and titania (TiO_2) nano-coolant (NC) were used to enhance the heat dissipation performance of an air-cooled radiator. The experimental results showed that the heat dissipation capacity and the efficiency factor of the nanofluid are higher than ethylene glycol, and that the nanofluid with TiO_2 is more efficient than one with Al_2O_3 according to most of the experimental data. Gulhane and Chincholkar [6] carried out an experimental study on the application of water-based Al_2O_3 nanofluid at lower concentrations in a car radiator. The results showed that the heat transfer coefficient enhances with an increase in particle concentration, flow rate, and inlet temperature of coolant and the maximum increase in heat transfer coefficient is 45.87 % compared to pure water.

METHODS: A heating system, a hydraulic pump and a heat exchanger are considered for the simulation of the cooling circuit. The heat exchanger represents the car radiator in the circuit.

The nanofluid consisted of water containing 0 - 2 - 4 - 6 vol% Al_2O_3 nanoparticles. flows into the circuit. The studies are conducted for three different engine operating conditions (Low, Medium and High). Physical properties of the Al_2O_3 nanoparticles and water such as thermal conductivity, specific heat capacity, density and dynamic viscosity are evaluated by means [7-9]. The described automotive cooling system is fully modelled in TRNSYS (version 17).

RESULTS AND CONCLUSIONS: Simulations are performed for four different volume concentration values of nanoparticles, from 0% to 6%, in water. The investigation is carried out in order to evaluate the energy consumption by the pump and the temperatures at the radiator outlet (Figure 1).
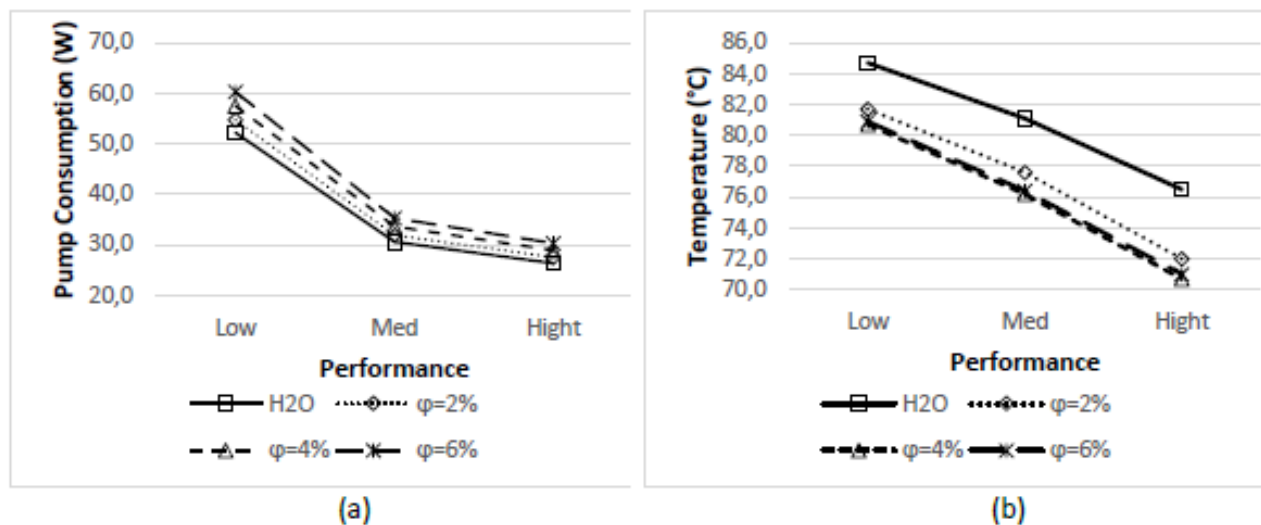
Figure 1. Pumping consumption (a) and outlet radiator temperature (b) for different nanoparticles concentrations

The increase of the volumetric concentration of nanoparticles φ in the working fluid leads to an increase in its density with respect to the pure water, which implies an increase in energy consumption. Furthermore, a reduction of pumping consumption occurs as the operating conditions increase, due to the reduction of the mass flow of the refrigerant, necessary for the cooling of the engine. The temperatures at the outlet of the radiator show a decreasing trend with the increase in the volumetric concentration of the nanoparticles in the base fluid. Furthermore, it shows that the outlet temperature is a function of the refrigerant velocity.

The heat transfer rate is also evaluated for the three different engine operating conditions and it can be seen, in the Figure 2, as the nanofluids with a higher volumetric concentration of nanoparticles have a higher heat transfer rate. This increase is not significant for volumetric concentrations above 2%.
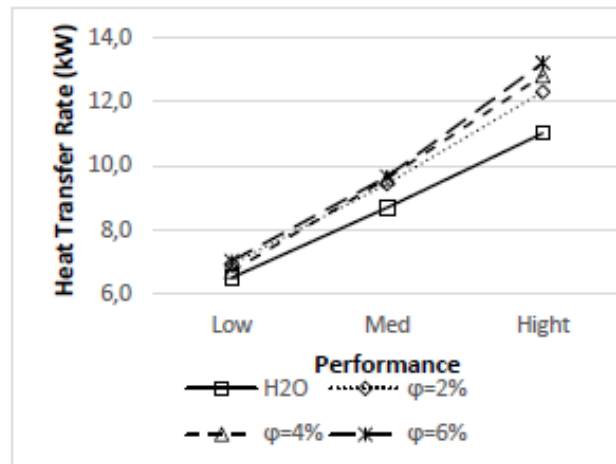
Figure 2. Heat transfer rate for different nanoparticles concentrations

REFERENCES

[1] K.Y. Leong, R. Saidur, S.N. Kazi, A.H. Mamun. (2010). Performance investigation of an automotive car radiator operated with nanofluid-based coolants (nanofluid as a coolant in a radiator). Applied Thermal Engineering. 30(17-18), pp. 2685-92.

[2] A.M. Hussein, R.A. Bakar, K. Kadirgama, K. V. Sharma. (2014). Heat transfer enhancement using nanofluids in an automotive cooling system. International Communications in Heat and Mass Transfer. 53, pp. 195-202.

[3] D.G. Subhedar, B.M. Ramani, A. Gupta. (2017). Experimental Investigation of Overall Heat Transfer Coefficient of Al2O3/Water–Mono Ethylene Glycol Nanofluids in an Automotive Radiator. Heat Transfer – Asian Research. 46(7), pp. 863-877.

[4] N. Bozorgan, K. Krishnakumar, N. Bozorgan. (2012). Numerical Study on Application of CuO- Water Nanofluid in Automotive Diesel Engine Radiator. Modern Mechanical Engineering. 2, pp. 130-136.

[5] Hwa-Ming Nieh, Tun-Ping Teng, Chao-Chieh Yu. (2014). Enhanced heat dissipation of a radiator using oxide nano-coolant. International Journal of Thermal Sciences, vol. 77, pp. 252-261, 2014.

[6] A. Gulhane, S.P. Chincholkar. (2017). Experimental investigation of convective heat transfer coefficient of Al2O3/water nanofluidi at lower concentrations in a car radiator. Heat Transfer – Asian Research. 46, pp. 1119-1129.

[7] A. Kasaeian, R. Daneshazarian, F. Pourfayaz. (2017). Comparative study of different nanofluids applied in a through collector with glass-glass absorber tube. Journal of Molecular Liquids. 234, pp. 315-23.

[8] S.U.S. Choi, Z.G. Zhang, W.Yu, F.E. Lockwood, E.A. Grulke. (2001). Anomalous thermal conductivity enhancement in nanotube suspensions. Applied Physics Letters. 79, pp. 2252-54.

[9] Y. Xuan and W. Roetzel. (2000). Conceptions for heat transfer correlation of nanofluids. International Journal of Heat and Mass Transf. 43, pp. 3701-7.

Heat transfer efficiency in a double pipe heat exchanger of functionalized graphene nanoplatelets/glycolated water nanofluids

Javier P. Vallejo[1,2], Julián Pérez-Tavernier[1,2], David Cabaleiro[1,3], José Fernández-Seara[2], Luis Lugo[1*]

[1] Departamento de Física Aplicada, Facultade de Ciencias, Universidade de Vigo, 36310 Vigo, Spain

[2] Área de Máquinas e Motores Térmicos, Escola de Enxeñería Industrial, Universidade de Vigo, 36310, Vigo, Spain

[3] Istituto per le Tecnologie della Costruzione, Consiglio Nazionale delle Ricerche, 35127, Padova, Italy

*Corresponding e-mail: luis.lugo@uvigo.es

Keywords: graphene nanoplatelets, propylene glycol, heat transfer, pressure drop, nanofluid

INTRODUCTION: Thermal energy is one of the most employed energy forms in industrial and domestic applications. The poor thermal conductivity of the classical thermal fluids is currently the most limiting feature for their performance enhancement. Over the last two decades, nanofluids have progressively received more attention as improved heat transfer fluids. Nevertheless, despite the evidence on their improved thermophysical profiles, there exists discrepancy about their potential improvement in real heat exchange processes. Glycolated waters like propylene glycol + water mixtures are heat transfer fluids commonly employed due to their protection against low freezing temperatures. The forced-convection heat transfer performances in a double pipe heat exchanger of four different loaded graphene nanoplatelet dispersions in propylene glycol:water 30:70 wt.% solution have been analysed in this work. Convection heat transfer coefficients and pressure drops were firstly determined. Then, a dimensionless analysis was carried out through Nusselt, *Nu*, and Reynolds, *Re*, numbers.

METHODS: Graphene nanoplatelets were supplied by Ionic Liquids Technologies GmbH (Heilbronn, Germany), propylene glycol was purchased from Sigma-Aldrich (Missouri, USA) while water was obtained by a Milli-Q 185 Plus system from Millipore Ltd (Watford, UK).
The preparation of the analysed nanofluids was carried out by a two-step method. The amount of each component of the base fluid and the amount of nanoadditive corresponding to each designed mass concentration (0.25, 0.50, 0.75 and 1.0 wt.%) were firstly weighed and then, after mixing, maintained under an ultrasonication process for 240 min. The thermophysical properties necessary to the analyses were experimentally determined in a previous work [1]. An experimental facility consisting of a double pipe heat exchanger as main component was used to obtain heat transfer coefficients and pressure drops. In this device, the cold tested fluid (base fluid or nanofluid) is pumped through the inner tube and the hot water through the outer

tube. Both tested fluid and water return to the desired initial conditions through the different facility circuits [2]. The data acquisition system allows directly measuring the temperatures in the inlet and outlet of the double pipe heat exchanger for both fluids, their flow rates, as well as the tested fluid pressure drop. For each tested fluid, the flow rates were varied from 0.2 to 0.7 $m^3 \cdot h^{-1}$ for the temperatures of 298.15, 308.15 and 318.15 K. The values of the water convection coefficients were obtained by the corresponding Gnielinski correlations [3].

RESULTS AND CONCLUSIONS: Obtained convection heat transfer coefficients for analysed nanofluids show an improvement with respect to base fluid for most conditions. The highest enhancements were achieved for the 0.50 wt.% or 0.75 wt.% concentration, reaching a maximum increase of 15.3 % for the 0.50 wt.% nanofluid at 298.15 K. Figure 1 shows as Nu increases with the increasing loading of nanoadditive for the same level of turbulence.
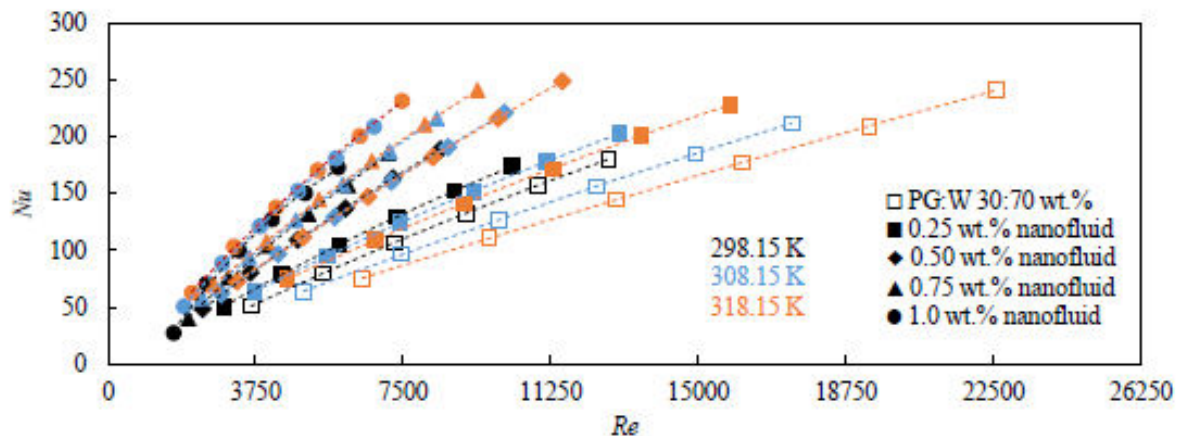
Figure 1. Nusselt number, Nu, as a function of Reynolds number, Re, for the base fluid and several concentrations at different tested fluid temperatures.

As an example, Nu increase achieves 167 % at 318.15 K with Re = 7500 for the 1.0 wt.% nanofluid. Figure 1 also shows as Nu enhancements are different between the lowest concentration and the three highest, between which the values are closer. Regarding pressure drop results, slightly increases with the rising nanoparticle loading were found, with a maximum increase of 12.4 % for the 1.0 wt.% concentration.

REFERENCES:
[1] J.P. Vallejo, J. Pérez-Tavernier, D. Cabaleiro, J. Fernández-Seara, L. Lugo, J. Chem. Thermodyn. 123,174-184 (2018).
[2] R. Agromayor, D. Cabaleiro, A.A. Pardiñas, J.P. Vallejo, J. Fernández-Seara, L. Lugo, Materials 9, 455 (2016).
[3] Gnielinski, V., G2 Heat Transfer in Concentric Annular and Parallel Plate Ducts, VDI Heat Atlas, VDI-Gesellschaft Verfahrenstechnik und Chemieingenieurwesen, 2nd Edition, Düsseldorf, 2010.

Isothermal analysis of Nanofluid Flow inside HyperVapotrons using Particle Image Velocimetry

Antonis Sergis [1*], Yannis Hardalupas[1], Thomas Barrett [2]

[1]The Department of Mechanical Engineering, Imperial College London, London SW7 2AZ, UK
[2]EURATOM/CCFE, Culham Science Centre, Abingdon, Oxfordshire, OX14 3DB, UK

*Corresponding e-mail: a.sergis09@ic.ac.uk

Keywords: Nanofluids, HV, HHF, Viscosity, PIV, Cooling

INTRODUCTION: The focus of this work is to understand if and how the geometry of heat exchangers might be potentially affecting the nanofluid coolant flow boundary conditions established and how this might be hence further affecting their thermal characteristics.

This work contains a cold isothermal high spatial resolution particle image velocimetry (PIV) study of the instantaneous and mean flow structures of a nanofluid flowing inside two HyperVapotron (HV) models and compares them to those present when using water [1]. HVs are two phase High Heat Flux exchangers popular with the nuclear fusion industry. The properties of nanofluids alone might have the potential of improving the overall HV device performance. However; the operation of the device is strongly linked to the flow field of the coolant. The study attempts to quantify possible changes in the flow and hence examines whether the replacement of the traditional coolant with a nanofluid in a HV might disrupt the designed flow field of the device during operation in single phase heat transfer mode.

METHODS: Two variations of the HV models from the Joint European Torus (JET) and Mega Amp Spherical Tokamak (MAST) experiments were used. The basic difference between the two models is the free stream channel height which is expected to affect the size of the momentum boundary layers formed inside the devices when operated with the same free stream velocities (this is a boundary condition). The models are shortened to include five grooves and are manufactured from high optical quality transparent Perspex. The choice of the number of grooves used was based at this stage on a qualitative computational fluid dynamics (CFD) investigation performed on the models at the design process that reproduced the irregular signature vortices expected in HV for the mean flow. A closed circuit isothermal coolant flow was established through these models.

A laser-based Particle Image Velocimetry (PIV) technique [2] was used to measure with high spatial resolution (30µm) the flow velocity field inside the models. An Nd-Yag pulsed laser (a Litron Nano T PIV) was used at a beam wavelength of 532nm [1]. The pulse width of the laser was 7-9ns, while the delay between the two pulses was adjusted from 5-40ms, according to the expected velocities. A non-intensified LaVision Imager Intense CCD camera with a resolution of 1376x1040 pixels was used to capture the images. The camera was coupled to a Nikkor 50mm F/2.8 lens with manual focus. A band pass optical filter with 10nm bandwidth around the 532nm wavelength was used to reduce optical noise on the recordings. The beam was steered and manipulated into an almost 2D laser sheet before entering and illuminating tracing particles dispersed in the flow. Cross correlation algorithms and an image recognition vortex detection algorithms were used to process the tracked flow fields. A total of 1000 image

pairs were collected which led to maximum statistical uncertainties of the order of ±3.8% and ±3.5% for the mean of JET and MAST respectively within a 95% confidence level. The maximum uncertainty of the measurements considering the PIV and flow meter uncertainty is hence estimated to be around 6% of the given quantities. The uncertainty of the image recognition analysis for the characterisation of the vortex location was below ±500μm.

Water based 50nm diameter Al_2O_3 nanoparticles were prepared using the two step preparation method from a dry powder. The final nanofluid used had a volumetric particle loading of 0.0001%.

RESULTS AND CONCLUSIONS: It is apparent from this work that small nanoparticle volumetric concentration nanofluids can significantly modify the hydrodynamic flow fields inside HVs. The changes were geometry dependent and cannot be explained using classical relationships (e.g. Einstein viscosity equation). The changes can be traced down to the momentum boundary layers of the flow. It is speculated that shear thinning occurs inside the momentum boundary layers due to dynamic nanoparticle migration effects when Nanofluids are used [2] . The flow changes are expected in their turn to be affecting significantly the temperature boundary layers in the presence of a heat flux either favourably or adversely.

It is clear from this work that more studies of the hydrodynamic effects of nanofluids inside given geometries is required – this is a novel finding with severe implications when nanofluids are used as a retrofitted solution to already existing heat exchangers. Caution also must be followed upon using shear inducing viscometers as these are expected to suffer from particle migration effects as well. An overall rethinking of the viscosity definition for nanofluids should be carried out to better describe and model them analytically.

The effects of heat flux on the performance of devices operated with nanofluids is under way that will be able to provide more answers regarding the complex physical phenomena observed.

This abstract is part of a larger study on HV devices published by the authors [3]–[7] with ongoing investigations under the EUROfusion fellowship of the lead author.

REFERENCES: [1] A. Sergis, Y. Hardalupas, and T. R. Barrett, "Isothermal velocity measurements in two HyperVapotron geometries using Particle Image Velocimetry (PIV)," *Exp. Therm. Fluid Sci.*, vol. 61, pp. 48–58, Feb. 2015. [2] M. Raffel, C. Willert, and J. Kompenhans, *Particle Image Velocimetry, a Practical Guide*, vol. 2nd. Springer, 2000. [3] A. Sergis, Y. Hardalupas, and T. R. Barrett, "Isothermal analysis of nanofluid flow inside HyperVapotrons using particle image velocimetry," *Exp. Therm. Fluid Sci.*, vol. 93, 2018. [4] A. Sergis, Y. Hardalupas, and T. R. Barrett, "Flow characteristics in HyperVapotron elements operating with nanofluids," *Fusion Eng. Des.*, vol. 128, 2018. [5] A. Sergis, K. Resvanis, Y. Hardalupas, and T. Barrett, "Comparison of measurements and computations of isothermal flow velocity inside HyperVapotrons," *Fusion Eng. Des.*, vol. 96–97, 2015. [6] T. R. Barrett, S. Robinson, K. Flinders, A. Sergis, and Y. Hardalupas, "Investigating the use of nanofluids to improve high heat flux cooling systems," *Fusion Eng. Des.*, pp. 3–6, Apr. 2013. [7] A. Sergis, Y. Hardalupas, and T. R. Barrett, "Potential for improvement in high heat flux HyperVapotron element performance using nanofluids," *Nucl. Fusion*, vol. 53, no. 11, p. 113019, Nov. 2013.

Analysis of the Thermal Signature of Wind-turbine Generators: implications for their main Operative Parameters and future application of nanofluids

Fran García[1,2], Federico Argenio[1], Jorge Asensio[1], Luis M. Varela[2], Luis Lugo[3]. Josefa Fernández[2]

[1]Enel Green Power, Wind Competence Center 00198 Rome, Italy

[2]NaFoMat Group, Departments of Applied Physics and of Particle Physics, University of Santiago de Compostela, 15782, Santiago de Compostela, Spain

[3]Applied Physics Department, Sciences Faculty, University of Vigo, 36310, Vigo, Spain

*Corresponding e-mail: Fran García, francisco.garcia@enel.com

Keywords: Thermal Signature, Failure Modes, Energy Availability, Cooler improvements, Derating

INTRODUCTION: The replacement of heat transfer fluids employed in the wind turbine cooling systems by nanofluids is one of the main objectives of a coordinated project of the universities of Santiago de Compostela and Vigo for which Enel Green Power is collaborating [1]. Wind Energy is a relevant vector in the Energy mix at a global level. Due to its entrance in the electric system operators, and due to the high percentage of wind share in the energy mix, the Levelized Profit of Energy has suffered a big discount during the last 5 years in all the major countries. Due to this fact, it is very important to control the operative expenses, by reducing the average time to return after a failure, increase the average time between failures, and the energy availability. The majority of Wind Turbines have a lot of sensors, to control the operative parameters, especially the temperature. With these sensors it is possible to develop the thermal signature per wind turbine model, age, site conditions etc. The information provided by these sensors allows protecting the component's integrity and in the majority of the cases are the responsible of the deratings due to high temperature conditions. Moreover, this information has a high value that may be later treated to perform correlations, regressions, and to analyse the thermal signature as a function of variables that can predict future behaviours due to aging effect, increase power, or prevent failures.

METHODS: Enel Green Power has a Control and Diagnostic Centre located in Rome. This Centre receives all the signals from all the installed turbines and storage these signals in a Database, including the events (error messages) from each turbine. Statistical analysis of any kind is possible to using any conventional statistical software. The cost of interventions

to solve the errors, outages, maintenance, operations etc. is tracked with a specific software The Case study, the Root Cause Analysis and all the documents that show the history and the know-how is tracking with a Case-Method software. For this study, we have chosen a type of MW-Rate turbine for which we have data of 1000 units.

RESULTS AND CONCLUSIONS: The events are classified in external and internal, which are always related to stoppage of the wind turbine. The external events are due to atmospheric conditions or force majeure and in our study correspond to the 22.7% of the total events. The internal events (87.8 %) can be due to possible or real failures in the electronic (35.3 %), hydraulic (8%), electrical (10.8 %) and mechanical (23.2 %) components. In this MW-Rate turbine type, we have an incidence of 10% of the outages related temperature alarms. These events may cause either a downgrade of cooling capability, or a stoppage to recover as soon as the temperature goes down, and they decrease the global electrical energy availability. Similar effects appear in other turbine models. The main heat sources contributing to these events were the Converter, Generator, Transformer and Gearbox. We have calculated the correlation coefficients, r, among the temperatures of these components as well with the active and reactive power. The configuration of the turbine (Double Fed Induction Generator) entails a high temperature correlation between Converter temperature and Generator temperature (r=0.72). We did not extract the cooling effect, meaning that each of these last components has their own cooling system that affects the correlation. But a large part of the correlation of both temperatures is based in the super synchronous stage, in which the generator and the converter are working at a full capacity. In general terms, the electrical components have an important correlation coefficients with the reactive power or super synchronous situation, and the gearbox temperature correlates with the active power (r=0.62), and not necessary in the same range as the electrical components. Therefore, we may act in two aspects reducing either the gearbox temperature or that of the electrical component. We conclude that a significant fraction of the total time the turbine is not working with the active nominal power. This is due to the temperature trigger, telling us that we have at least 10% of entitlement if we are able to reduce the temperature of the cooling vector, in this case glycol mixed with water, as well as in the transformer and in the converter. These studies are necessary for example to know how nanofluids or nanolubricants might increase the competitiveness of the wind energy. For this purpose, in situ test with nanofluids will be performed soon.

[1] J.P. Vallejo, E. Alvarez-Regueiro, D. Cabaleiro, J. Fernandez-Seara, J. Fernandez, L. Lugo Thermophysical properties of functionalized graphene nanoplatelet dispersions for improving efficiency in a wind turbine cooling system. HEFAT, 13th International Conference on Heat Transfer, Fluid Mechanics and Thermodynamics, Slovenia: 17-19 July 2017

Gr-Al$_2$O$_3$ Hybrid Nanoparticles based Multi-Functional Drilling Fluid

Mortatha Al-Yasiri [1*], and Dongsheng Wen[1, 2]

[1] School of Chemical and Process Engineering, University of Leeds, Leeds, UK

[2] School of Aeronautic Science and Engineering, Beihang University, Beijing, China

INTRODUCTION:

The global demand of energy is expected to increase as much as 50% in the next 20 years and the demand for oil and gas will also increase [1]. The area of finding "easy oil" is coming to an end, and future supply will become more reliant on hydrocarbons produced from unconventional hydrocarbon sources and enhanced oil recovery (EOR) processes. The performance of a drilling fluid is important for smooth and stable production of hydrocarbons. Drilling fluid is an essential element in the well-construction process that remains in direct contact with the wellbore throughout the entire drilling operation. A well-constructed and reliable wellbore can significantly reduce the nonproductive time. The design of a drilling-fluid system is central to achieve this objective [2]. Drilling fluids should be formulated to work appropriately under expected wellbore conditions, possessing good rheological and thermos-physical properties. Quite recently, considerable attention has been paid to using nanoparticles to improve drilling fluid performance [3]. A considerable effort has been recently devoted to employing nanoparticles in drilling fluids to control the mud filtrate volume [4-6], minimizing differential pipe sticking [7], improving drilling and production at high pressure and high temperature (HPHT) conditions [8-10], enhancing shale stability [11-13] and improving rheological properties [14-16]. Nanoparticles were used by some researchers to develop thermal, electrical and HPHT rheology of water-based mud [10, 17]. It is detected that the increase of nanoparticle concentration promotes thermal and electrical features of drilling fluids. The results of recent studies showed that nanoparticles enhanced thermal and electrical characteristics by approximately 35% compared to water based mud (WBM)

These studies have shown that the addition of nanoparticles could improve some properties of the drilling fluid, which shows some promise for future applications. However current state-of-art studies have a number of limitations, as commented here. Firstly, the understanding of the properties of nanoparticle- based drilling fluids is insufficient. Most of the studies have

been focused on one property, such as rheological property or filtration property [ref]. As a drilling fluid provide multi-functions during the drilling operation, such as cooling, lubrication and cutting transport. Addition of nanoparticles would clearly affect these functions, and it is essential to understand the variations of related properties for have a complete assessment of the nanoparticle effects. Secondly, the effect of nanoparticles is multi-facets and their influence on different properties are different. The addition of one nanoparticle may improve one property but may not improve the other. It is unlikely that the addition of one type of particle could improve all related properties. The search for right nanoparticle or hybrid particles is still ongoing. Thirdly, prior studies have been largely focused on the steady state operation, which may not reflect the real conditions. A drilling fluid cycle is often unsteady, varied between a movement and a steady state, and it is essential to investigate the performance of Nano-mud based on both static and dynamic conditions. t. Finally the drilling fluids behave as viscoelastic materials, exhibiting both viscous and elastic behavior, but the study of the viscoelasticity behavior of Nano-drilling fluid is very limited in the literature [ref xx]. Identifying the differences in viscoelastic response could lead to better design of a drilling fluid recipe.

Aiming to address these limitations, this work develops a novel hybrid nanoparticle system, Gr-Al2O3, dispersed in a WBM, and examines their properties under both dynamic and static conditions. The rheological, electrical and thermal properties of the newly formed drilling fluids are examined to reveal their potential functions.

.

2.1 Preparation of Nano Drilling Fluids

The drilling fluids were prepared in the laboratory according to the table (2-1). The formulation of the fluid was conducted by scaling the water to 335ml. Bentonite is the first component added to water; this was mixed until the fluid was observed to be smooth. The nanoparticles were always the last additive to the mud. The weight percentage of the nanoparticles was based on a calculation of the entire weight of the fluid. The fluid was set to mix by a Hamilton beach mixer for 20 minutes. The laboratory analysis was initially performed on base mud to apply them as a reference to evaluate the development of nanoparticles additives.

Table 1 Components of prepared Water-based mud

Component	Quantity
Water	335 ml
Bentonite	20 gm

At this stage of experimental work, different types of the nanoparticle are used. In Table 2.2, nanoparticles additives and their properties are mentioned: The Morphology of the particles was characterised by a transmission Electron microscope (TEM) and is shown in figure 1.
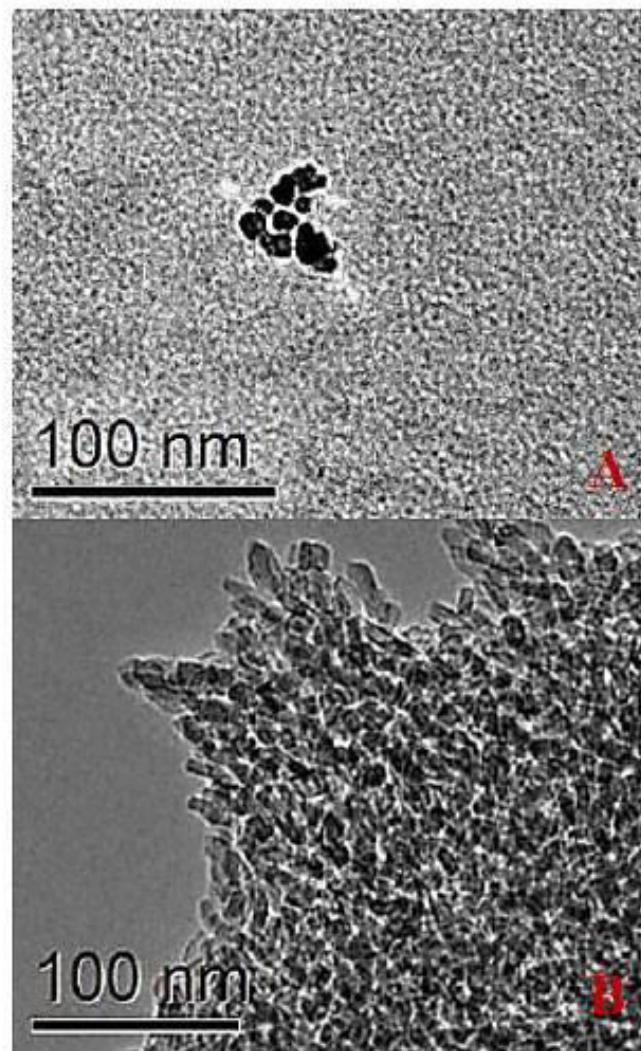
Figure 1 Transmission Electron Microscope (TEM) images of Graphite nanoparticles (A) and Aluminum oxide nanoparticles (B)

Table 2 Properties of nanoparticles

Nanoparticles	Average size	Supplier
Graphite nanopowder	1-2 nm	Nanoshel
Aluminium oxide	45 nm	Nanophase

2.2 Experimental apparatus

In general, Fann 35 Viscometer is used to measure the rheology of the drilling fluid in most oil fields across the world. However, in this research, viscosity measurements are done by the Anton Paar MCR301

Rheometer (Fig. 2). This Rheometer is more precise and more advanced: it can measure viscosity and related attributes. The MCR301 was used to do more analysis of fluids while Fann 35 failed [17-19]. The flow behaviour of drilling fluids was investigated by using a rotational system. The oscillation amplitude sweep test was employed to find the linear portion of the viscoelasticity and to observe the structural characteristics of fluids, While the combination oscillation-rotation-oscillation was utilised to study the thixotropy.
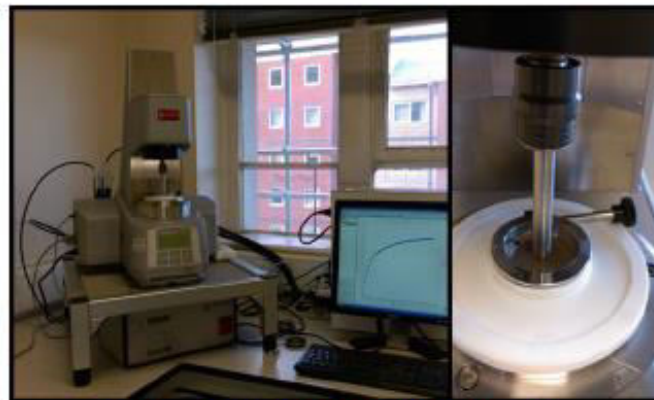
Figure 2 Anton Paar MCR301 Rheometer

The KD2 Pro Thermal Properties Analyzer made by Decagon Devices, Inc. has been employed to conduct the thermal conductivity of the prepared Nano-drilling fluids with the accuracy of 5%. The KD2 Pro is a handheld device, battery-operated, menu-driven device which works based on the transient heated needle to conduct thermal properties of solid and fluid media. The KD2 pro KS-1 a sensor with 60 mm in length and 1.3 mm in diameter, is designed explicitly for use in fluids.

The Zetaprobe manufactured by Colloidal Dynamics, LLC has been used to measure the zeta potential of various Nano-drilling fluids without dilution. The Colloidal Dynamics Zetaprobe worked based on the electroacoustic method which offers straight measurement (without dilution) for colloidal dispersions with moderate and high particle concentrations while the other techniques necessitate sample dilution and sample preparation which are both time-consuming and error-prone. The Zetaprobe builds from a compact design with built-in titration, a versatile dip probe sensor, and software wizards as in figure (3).

Figure 3 The Zeta probe used to measure Zeta potential of drilling fluids

3. Results and Discussion
3.1 Rheology

Rheology is a crucial parameter of drilling-fluid performance. Modification, the rheology of drilling fluid, can be a convenient solution to most drilling difficulties like pipe sticking, loss circulation and formation damage. The drilling fluid behaves as viscoelastic materials. This confirms that drilling fluids display both viscous and elastic behaviour. Therefore, it's essential to investigate the viscoelasticity behaviour of drilling fluids to understand how additives can develop the structure of drilling fluids. Identifying the differences in viscoelastic response could lead to better design of a drilling fluid recipe. The speed of the structural recovery (thixotropy) is also essential. To evaluate flow and viscoelastic properties of drilling muds and it is regularly suitable to deal with them separately, some rheometric assessments that can be conducted on a rheometer. Flow curves usually use the graphical description of flow behaviour. It exhibits the flow behaviour at low shear rates as well as high shear rates. The viscosity of drilling fluid decreases with increasing shear rate. This flow behaviour is called shear-thinning as in figure 4
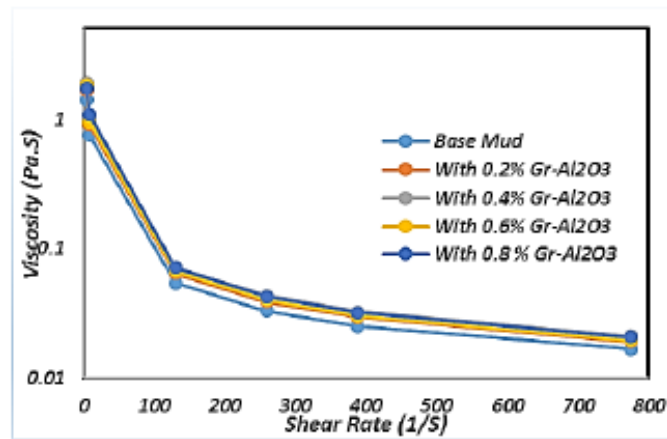
Figure 4 Measure viscosity of the prepared drilling fluids as a function of shear rate

. Therefore, it is not sufficient to indicate only the viscosity. It is consistently necessary to designate also the shear rate that was utilised for the mensuration. The viscosity of drilling fluid is slightly increased with hybrid nanoparticle addition. The reason behind that could be because there is more than one type of nanoparticles settled into the pore structure on the surface of clay particle. These nanoparticles don't have the same structure, size, conformation and properties that contribute to gain a stronger connection between bentonite particles, which might promote gelation of the bentonite.

The concentration of nanoparticles in drilling fluid also plays a role in general flow behaviour. As nanoparticles concentration increase, the viscosity of the drilling fluid increase as clear for Gr-Al2O3 addition.
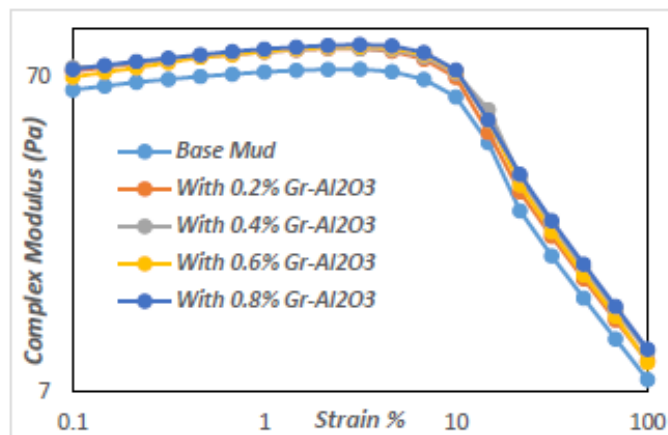
Figure 5 Measured Complex modulus of the prepared drilling fluids as a function of deformation percentage

Characteristics such as loss and storage modulus, complex modulus, dynamic yield point, structural

stability, and phase angle describe the viscoelastic behaviour of drilling fluids. The inter-particle interaction plus the particle networks in the drilling fluids can be measured by noting the passage from a solid-like condition to a liquid-like status. Presentation of variation complex modulus (overall resistance to deformation) as a function of strain obtained through oscillatory amplitude test is used as a suitable tool for investigation of the strength of the particle connection in the fluid (the stiffness of material; the higher the modulus, the more stringent the material).

As clear from figure 5, the complex modulus increase with increasing nanoparticles concentration. This means that nanoparticles give more elastic properties to the fluid before flow point and this what we need since this state helps retain cuttings and weighting materials suspended in the drilling fluid instead of allowing for settling into the wellbore.

The results also indicate that nanoparticles can develop the structure of drilling fluid. Moreover, even nanoparticles give the more elastic property to drilling fluid; the yield stress is still same. This means that Nano drilling fluids display sufficient abilities both at rest and in the movement since they have better gel structure and this gel can break with same shear stress. When drilling fluid pumps are shut off or running at very low speed, the drilling fluid will take on a gel-like state. This state of the drilling fluid helps retain cuttings and weighting materials suspended in the drilling fluid instead of allowing for settling into the wellbore. It is appropriate that the drilling fluid quickly develops high gel strength to resist the settling of massive particles out of suspension.
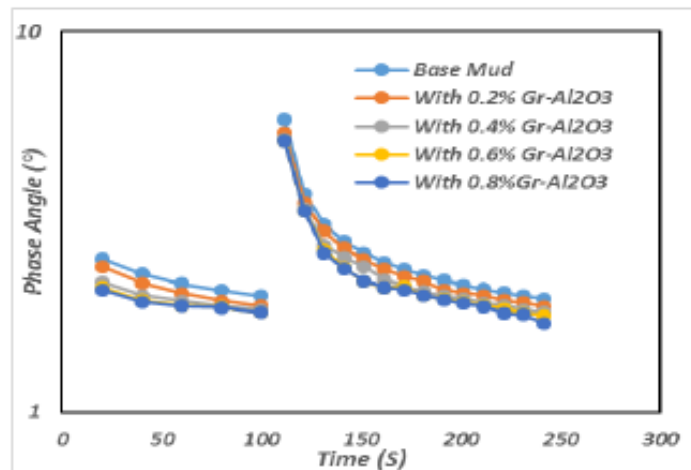
Figure 6 Measured Thixotropy of the prepared drilling fluids as a function of time and shear rate

The laboratory results proved that the addition of hybrid nanoparticles could develop the thixotropic properties of drilling fluids. As clear from the figure (5), the increase of nanoparticles concentration secures more elastic behaviour to the drilling fluid and increase the degree and the speed of the

structural recovery through reducing the time required for rebuilding. It is preferable to minimise the reconstruction time to prevent the sedimentation of the weighting materials and drilled cuttings.

3.2 Thermal conductivity

The thermal conductivities of the prepared drilling fluids have been measured by using KD2 pro apparatus. This device has been standardized by using distilled water before the measurements. The thermal conductivity measurements were done at constant temperature. The thermal Conductivities of the prepared drilling fluids as a function of nanoparticle concentration are investigated. Table 3 and Figure 7 show the thermal conductivity improvement as a function of nanoparticles concentration for base water-based fluid at room temperature. Results indicate that an increase in the nanoparticle Concentration enhances the thermal conductivity.

The laboratory results illustrate that the water-based drilling fluid thermal conductivity is improved by around 10% in the presence of 0.8 wt% Gr-Al2O3 at room temperature. An improved drilling fluid thermal conductivity is an indication of the ability of the fluid to cool faster as it moves up to the surface. On the other hand, with enhancement the heat transfer between the drill bit and drilling fluid, the bit remains cooler and this possibly helpful for innovative design of drilling muds for high temperature and high pressure (HTHP).
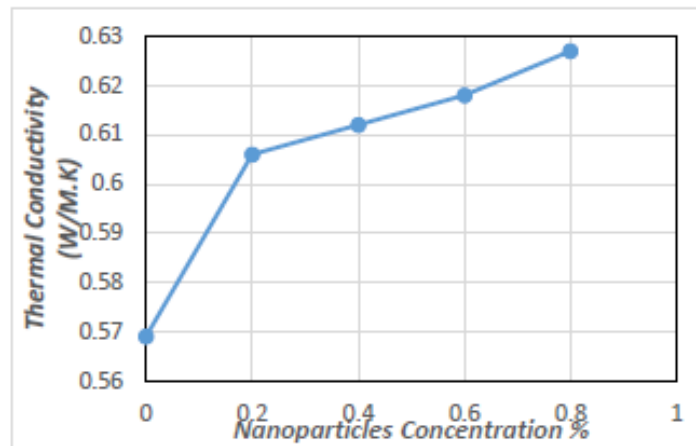
Figure 7 Thermal conductivity of prepared drilling fluids as a function of nanoparticles concentration

Table 3 Thermal conductivity measurements of drilling fluids at 20 °C (w/m.k)

Fluid Samples	Thermal Conductivity	Improvement %
WBM	0.569	0
0.2 wt% Gr-Al2O3	0.606	6.5
0.4 wt% Gr-Al2O3	0.612	7.55
0.6 wt% Gr-Al2O3	0.618	8.61
0.8 wt% Gr-Al2O3	0.627	10

3.3 Electrical conductivity

Table 5 records, the electrical conductivity values of water-based muds measured at each nanoparticles concentration. It is noticed that the addition of Nano-particles to base mud enhances the electrical conductivity. These tabulated results are used to generate a graph of thermal conductivity improvement against nanoparticle concentration as illustrated in the figure. The laboratory outcomes indicate that the water-based drilling fluid electrical conductivity is improved by around 4% in the presence of 0.2 wt% Gr-Al2O3. The enhancement of the electrical conductivity is observed to be from about 4 to 8.4% when the concentration of Gr-Al2O3 increased from 0.2 to 0.8 wt%. The electrical conductivity has a significant influence of the nature of the drilling fluid upon electric logs (resistivity imaging) as the drilling fluid must be the medium through which the electric logging device is made to traverse the formations. Electrical logs have been used to distinguish the differences between shales, sandstones, limestones, and other rock forms readily. Besides electric logs have been found, in some instances, to be useful in estimating the nature of fluid contained within the pores of a rock. The electrical conductivity of a drilling mud, its filtrate, and filter cake are three of its more important qualities, as far as electric logging is concerned.

Table 4 Electrical conductivity measurements of drilling fluids at 20 °C (mS/cm)

Fluid Samples	Electrical Conductivity	Improvement
WBM	2.84	0
0.2 wt% Gr-Al2O3	2.93	3.2
0.4 wt% Gr-Al2O3	2.97	4.6
0.6 wt% Gr-Al2O3	3.01	6
0.8 wt% Gr-Al2O3	3.08	8.4

3.4 Zeta potential

The nanoparticles charge and zeta potential play a significant role in the performance of the rheological behaviour. The nanoparticles with a positive charge displace the dissociated cations from

the surface of bentonite which result in a different clay platelet structure, yielding higher yield stress values [5, 20]. While the nanoparticles with a negative surface charge increase the repulsion forces between the clay platelets, which leads to deflocculating of the platelets and, thus, higher viscosities and weaker yield structure. Sodium montmorillonite, the main component of the standard bentonite, has a lot of permanent negative charge on the basal surface [21]. They are between 90–95% of the total charge [22]. As a result, the zeta potential of Bentonite drilling fluids is negative over the entire pH range [23, 24].

Figure (8) displays the enhancement of zeta potential as a function of nanoparticles concentration for base water-based mud at room temperature. Results indicate that an increase in the nanoparticle Concentration enhances the zeta potential. The laboratory results display that the zeta potential of the water-based drilling fluid is improved by around 13% in the presence of 0.8 wt% Gr-Al2O3 at room temperature. The drilling fluid suspensions with high charge are appropriate during drilling operations to retain the suspension components discretely. The resultant drilling mud particles can penetrate to the porous wall of the wellbore and clog the pores. Also, a thin and impermeable cake is formed which minimise drilling fluid losses
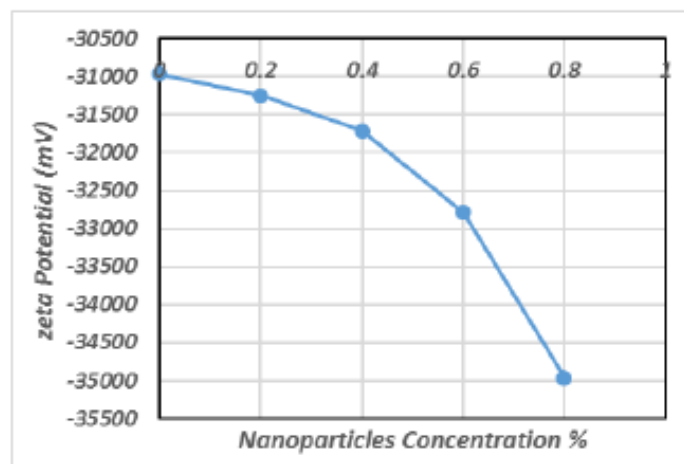
Figure 8 Zeta potential of prepared drilling fluids as a function of nanoparticles concentration

Conclusions

During recent decades, researchers and scientists discovered nanoparticles, and currently, there are efforts to use this technology in the drilling operation. In this research, we explore the possibility of using hybrid nanoparticles to develop water-based drilling fluids properties. Based on experiential research that has been undertaken, it is possible to conclude that hybrid nanoparticles could be employed as multi-functional additive for drilling muds. In the present work, Gr-Al2O3 nanoparticles were applied as additives to water-based drilling fluids and below outcomes could be identified:

- Based on rheological investigations, the Nanoparticles addition has the power to form a drilling mud that displays sufficient features both at relaxation and in movement.
- The experimental outcomes demonstrate that the water-based drilling mud thermal conductivity is improved by around 10% in the presence of 0.8 wt% Gr-Al2O3 at room temperature.
- The laboratory results indicate that the water-based drilling mud electrical conductivity is improved by around 8.4% when the concentration of Gr-Al2O3 was 0.8 wt%.
- The laboratory outcomes identify that the water-based drilling fluid zeta potential is enhanced by around 13% in the presence of 0.8 wt% Gr-Al2O3.

In our future research, we intend to concentrate on the possibility to use different hybrid nanoparticles to enhance lubrication, filtration and other drilling fluid properties.

Acknowledgments

References

1. Mitchell, R.F., *Petroleum engineering handbook, volume II: drilling engineering.* Society of Petroleum Engineers ISBN, 2007: p. 978-1.
2. Al-Yasiri, M.S. and W.T. Al-Sallami, *How the Drilling Fluids Can be Made More Efficient by Using Nanomaterials.* American Journal of Nano Research and Applications, 2015. 33: p. 41-45.
3. Contreras, O., et al. *Application of in-house prepared nanoparticles as filtration control additive to reduce formation damage.* in *SPE International Symposium and Exhibition on Formation Damage Control.* 2014. Society of Petroleum Engineers.
4. Srivatsa, J.T. and M.B. Ziaja. *An experimental investigation on use of nanoparticles as fluid loss additives in a surfactant-polymer based drilling fluids.* in *International Petroleum Technology Conference.* 2011. International Petroleum Technology Conference.
5. Barry, M.M., et al., *Fluid filtration and rheological properties of nanoparticle additive and intercalated clay hybrid bentonite drilling fluids.* Journal of Petroleum Science and Engineering, 2015. **127**: p. 338-346.
6. Javeri, S.M., Z.M.W. Haindade, and C.B. Jere. *Mitigating loss circulation and differential sticking problems using silicon nanoparticles.* in *SPE/IADC Middle East Drilling Technology Conference and Exhibition.* 2011. Society of Petroleum Engineers.
7. Singh, S.K., R.M. Ahmed, and F. Growcock. *Vital role of nanopolymers in drilling and stimulations fluid applications.* in *SPE Annual Technical Conference and Exhibition.* 2010. Society of Petroleum Engineers.
8. Nguyen, P.-T., et al. *Evaluation on the EOR potential capacity of the synthesized composite silica-core/polymer-shell nanoparticles blended with surfactant systems for the HPHT offshore reservoir conditions.* in *SPE International Oilfield Nanotechnology Conference and Exhibition.* 2012. Society of Petroleum Engineers.
9. William, J.K.M., et al., *Effect of CuO and ZnO nanofluids in xanthan gum on thermal, electrical and high pressure rheology of water-based drilling fluids.* Journal of Petroleum Science and Engineering, 2014. **117**: p. 15-27.

10. Hoelscher, K.P., et al. *Application of nanotechnology in drilling fluids*. in *SPE International Oilfield Nanotechnology Conference and Exhibition*. 2012. Society of Petroleum Engineers.

11. Li, G., J. Zhang, and Y. Hou. *Nanotechnology to improve sealing ability of drilling fluids for shale with micro-cracks during drilling*. in *SPE International Oilfield Nanotechnology Conference and Exhibition*. 2012. Society of Petroleum Engineers.

12. Riley, M., et al. *Wellbore Stability in Unconventional Shales-The Design of a Nano-Particle Fluid*. in *SPE Oil and Gas India Conference and Exhibition*. 2012. Society of Petroleum Engineers.

13. Jain, R., V. Mahto, and V. Sharma, *Evaluation of polyacrylamide-grafted-polyethylene glycol/silica nanocomposite as potential additive in water based drilling mud for reactive shale formation*. Journal of Natural Gas Science and Engineering, 2015. **26**: p. 526-537.

14. Mao, H., et al., *Hydrophobic associated polymer based silica nanoparticles composite with core–shell structure as a filtrate reducer for drilling fluid at utra-high temperature*. Journal of Petroleum Science and Engineering, 2015. **129**: p. 1-14.

15. Sadeghalvaad, M. and S. Sabbaghi, *The effect of the TiO 2/polyacrylamide nanocomposite on water-based drilling fluid properties*. Powder Technology, 2015. **272**: p. 113-119.

16. Hassani, S.S., et al., *The effect of nanoparticles on the heat transfer properties of drilling fluids*. Journal of Petroleum Science and Engineering, 2016. **146**: p. 183-190.

17. Jahns, C., *Friction Reduction by using Nano-Fluids in Drilling*. 2014.

18. Jabrayilov, E., *Friction reduction by using nanoparticles in oil-based mud*. 2014.

19. Riveland, F.A., *Investigation of Nanoparticles for Enhanced Filtration Properties of Drilling Fluid*. 2013.

20. Ramos-Tejada, M., et al., *Scaling behavior of the rheological properties of montmorillonite suspensions: Correlation between interparticle interaction and degree of flocculation*. Journal of colloid and interface science, 2001. **235**(2): p. 251-259.

21. Avadiar, L., Y.-K. Leong, and A. Fourie, *Physicochemical behaviors of kaolin slurries with and without cations—Contributions of alumina and silica sheets*. Colloids and Surfaces A: Physicochemical and Engineering Aspects, 2015. **468**: p. 103-113.

22. Duc, M., F. Gaboriaud, and F. Thomas, *Sensitivity of the acid–base properties of clays to the methods of preparation and measurement: 1. Literature review*. Journal of Colloid and Interface Science, 2005. **289**(1): p. 139-147.

23. Missana, T. and A. Adell, *On the applicability of DLVO theory to the prediction of clay colloids stability*. Journal of Colloid and Interface Science, 2000. **230**(1): p. 150-156.

24. Yalçın, T., et al., *The viscosity and zeta potential of bentonite dispersions in presence of anionic surfactants*. Materials Letters, 2002. **57**(2): p. 420-424.

A Benchmark Study on Heat Capacity of Nanofluids and Nanosalts

S M Sohel Murshed[1,2]

[1] Centro de Química Estrutural, Faculdade de Ciências, Universidade de Lisboa 1749-016 Lisboa, Portugal

[2] Centre for Innovation, Technology and Policy Research, Instituto Superior Técnico, Universidade de Lisboa, 1049-001 Lisboa, Portugal
e-mail: smmurshed@ciencias.ulisboa.pt; smurshed@tecnico.ulisboa.pt

INTRODUCTION: It is well-known that literature data on various thermophysical properties of nanofluids are very scattered and anomalous which hinder not only to reach unanimous conclusions on these properties but also to fully identify and understand the underlying mechanisms [1-4]. Although intensive research works on nanofluids have been continued and scattered data keep piling up in the literature, no co-ordinated joint research efforts have been devoted on the heat capacity of nanofluids as well as of nanosalts. It is therefore of great importance to conduct a benchmark study on this key property of these new nanosystems. For the first time a Europe-based benchmark study on this property (C_p) of these emerging nanoparticles dispersed systems (nanofluids and nanosalts) has recently been launched under the auspices of Nanouptake COST action. The main objective of this co-ordinated work is to reach unanimous conclusions on heat capacity of nano fluids and nanosalts by conducting research in different laboratories under a set of defined protocols for different types of sample nanofluids and nanosalts.

METHODS: A set of standard protocols will be made and will be followed by the participating researchers/groups to conduct this benchmark study. Different types of sample nanofluids as well as nanosalts will be prepared following under same preparation and stability protocols in different laboratories and heat capacity of those samples will be measured in all participating laboratories using various types of available measurement methods and devices (calorimetry).

RESULTS AND CONCLUSIONS: The results of this benchmark study will be presented, compared and analysed thoroughly. It is anticipated that the findings of this study not only help to reach conclusions on the status (e.g., enhancement/no change/deterioration) of heat capacity of these two new nano-media, but also to explore the actual factors behind the results. Most importantly, this extensive multi-lab study will certainly be a step-forward to explore and assess the application potential of these emerging nanofluids and nanosalts in heat storage and energy harvesting areas.

REFERENCES:

[1] S.M.S. Murshed and C.A. Nieto de Castro, Nanofluids: Synthesis, Properties and Applications, New York: Nova Science Publishers. 2014.

[2] S.M.S. Murshed, K.C. Leong and C. Yang, Thermophysical and electrokinetic properties of nanofluids- A critical review, Applied Thermal Engineering 28 (2008) 2109-2125.

[3] S.M.S. Murshed, Determination of effective specific heat of nanofluids, Journal of Experimental Nanoscience 6(2011)539-546.

[4] I.M. Shahrul, I.M. Mahbubul, S.S. Khaleduzzaman, R. Saidur and M.F.M. Sabri, A comparative review on the specific heat of nanofluids for energy perspective, Renewable and Sustainable Energy Reviews 38(2014)88-98.

Thermomagnetic properties of magnetic nanofluids and hybrid nanofluids

M. Timko[1], M. Rajnak[1,2], T. Tobias[1], K. Paulovicová[1], Z. Mitroova[1],   Z. Wu[3], B. Sundén[3], P. Kopcansky[1]

[1]Institute of Experimental Physics, Slovak Academy of Sciences, Watsonova 47, Košice, Slovakia
[2]Faculty of Electrical Engineering and Informatics, Technical University of Košice, Letná 9, Košice, Slovakia
[3]Department of Energy Sciences, Lund University, 22100 Lund, Sweden

*Corresponding e-mail: timko@saske.sk

Keywords: thermal conducrtivity, transformer oil, magnetic nanoparticles, carbon nanotubes

Within two Nanouptake STSMs, the measurements of thermal conductivity of a magnetic nanofluid and a hybrid nanofluid containing magnetic nanoparticles and carbon nanotubes (CNT) in dependence on particle volume fraction and magnetic field were performed at the Department of Energy Sciences, Faculty of Engineering at the Lund University, Sweden. For this purpose, the nanofluids based on a novel type of transformer oil MOL TO 40 were prepared at Institute of Experimental Physics. From the concentrated magnetic nanofluids, another samples with various particle volume fractions were prepared by dilution procedure.

In order to measure the thermal conductivity of the studied nanofluids, a thermal constants analyzer (TPS 2500S from Hot Disk AB, Sweden) was employed. A special attention was paid to the fixation of the commercial thermal conductivity double spiral Hot Disk sensor with Kapton insulation (Fig. 1a). The sensor was fixed in a Teflon frame in order to ensure its stable position in stronger magnetic fields. In order reduce the amount of the measured sample volume; a homemade Teflon container was prepared too (Fig. 1b). The sensor was inserted vertically into the container with liquid samples to avoid the risk for bubbles. To apply an external magnetic field on the investigated samples, an ensemble of permanent magnets were attached to the Teflon container as depicted in Fig. 1c. In this way, the nanofluid was exposed to a quasi-homogenous magnetic field. The intensity of the field was measured in the empty container by means of a Hall probe. The thermal conductivity as well as the thermal diffusivity was measured on all the prepared samples at various magnetic field values (0, 45 mT, 90 mT and 210 mT). The experiments were performed at ambient temperature set to 21 °C. The heating applied to the sample was 30 mW, the measurement time was set to 3 s. Finally, the statistical values were determined as an average of 5 measured values.

(a) (b) (c)
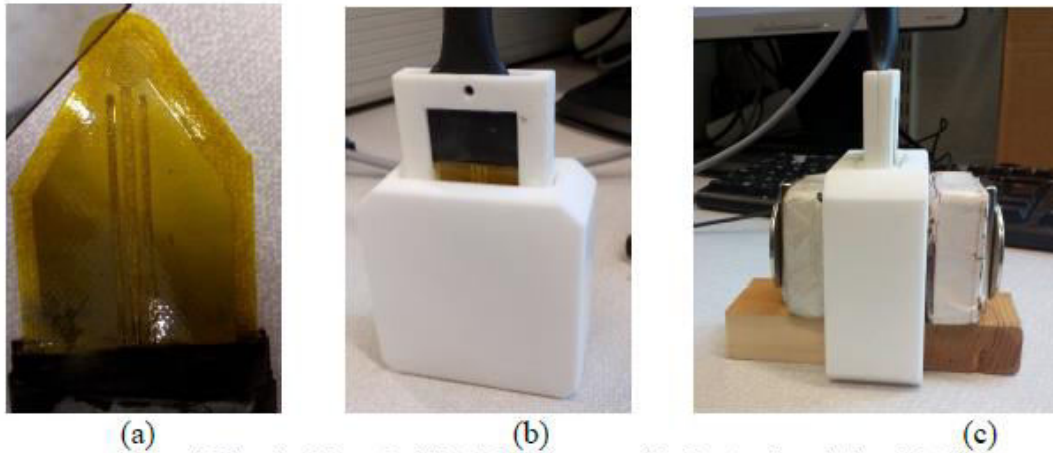
Fig. 1 The double spiral Hot Disk sensor with Kapton insulation (a). The sensor fixed in a teflon frame inserted in the experimental container (b). The ensemble of permanent magnets attached to the Teflon vessel walls (c).
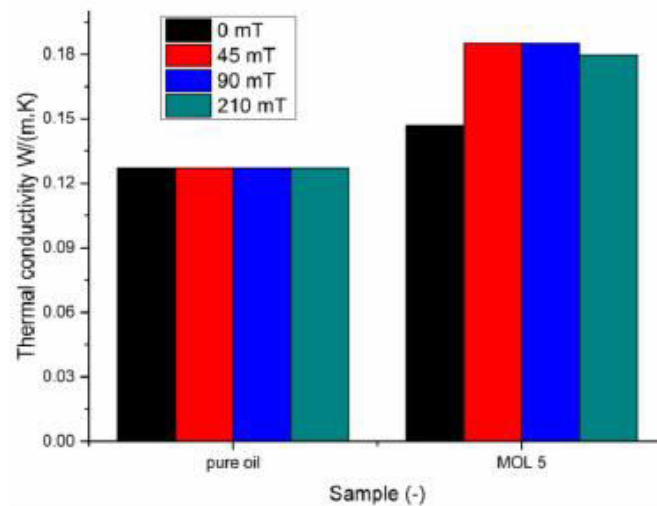
Fig. 2 Thermal conductivity of the pure oil and the most concentrated magnetic nanofluid (3.5 %) measured a various magnetic fields.

The thermal conductivity measured on the transformer oil and the most concentrated magnetic nanofluid at various magnetic fields is presented in Fig. 2
It is clear that the oil thermal conductivity is independent on the applied magnetic field. Then, the presence of the magnetic nanoparticles increases the thermal conductivity by about of 15.7 %. Moreover, with increasing magnetic field, this thermal conductivity increases too, as 45,8 % enhancement has been achieved at the value of 90 mT. At higher magnetic field (210 mT) the thermal conductivity starts to decrease. This decrease can be caused by the inhomogeneous particle distribution in the strong magnetic field, where the majority of the particles is accumulating near the magnets, leaving so the sensor area surrounded by a lower particle concentration.

WG 3

5. WG 3: Storage

5. Working Group 3: Storage

5.1 Castellón, Spain

Innovative solutions for geothermal heat exchangers with nanofluids

Luciu Razvan Silviu[1,2,*], Mateescu Teodor Dorin[1], Popovici George Catalin[1,3], Cazacu Ionela[1], Baran Andreea Irina[1]

[1] Department of Building Services Engineering, Faculty of Civil Engineering and Building Services, "Gheorghe Asachi" Technical University of Iasi, 700050, Iasi, ROMANIA

[2] Department of Research, SC AIR-PROJECTS SRL IASI, 700697, Iasi, ROMANIA [3] Department of Research, SC CLIMA THERM CENTER SRL IASI, 700545, Iasi, ROMANIA

*Corresponding e-mail: airprojects@yahoo.com,

Keywords: nanofluids, heat exchangers, variable geometry

INTRODUCTION:
Common types of geothermal exchange, the surface and the depth is characterized by demanding uneven ground. Uniformity thermal load of the massive and efficiency may be a solution in the sense of optimizing energy storage capacity and therefore reduced surface / volume of land used.

A solution atypical geothermal heat exchanger, shallow, variable spatial geometry using cylindrical or tapered channels, which compared with geothermal drilling or pilots, presents significant recovery in terms of thermal capacity of the soil.

From a functional perspective and energy, the solution is obvious superior to any surface or deep usual, the heat transfer in the heat exchanger is variable.

The novelty of the suggested solutions, is favorable argument optimizing surface geothermal exchangers, used in hybrid realization of heating / cooling using renewable energy and nanofluids.

Those new geothermal heat exchangers were studied with water as heat transfer fluid, using a CFD (Computational Fluid Dynamics) approach for validation of analytical calculations. In order to compare water with nanofluids, a numerical study was made in same conditions.

The results indicate a increase of the thermal performances with 20% of nanofluids compared to pure water. The nanofluid is composed of aluminum oxide (γAl_2O_3) particles dispersed in water for various concentrations ranging (1, 2, 3 and 4%).

METHODS:
The study presents the results of numerical simulation of a new types of sol-water heat exchangers using nanofluids and geothermal resources.

The heat exchangers, which is subject to **File Patent - OSIM A201600061** is made of modules in series with variable geometry (Fig. 1).

Modular transfer distribution and sizing of the surface there of in inverse ratio to the difference in temperature, ensures uniform heat flux along the device and consequently the heat load stock balanced.

From the point of view of construction, geo modular heat exchanger with variable geometry, can be done in following ways:

- Cylindrical modules - rectangular ring section and flow baffle

- Modules cylindrical with constant diameter (D) and variable height (Hi) made of bundles of pipes whose side surface is the surface heat transfer.
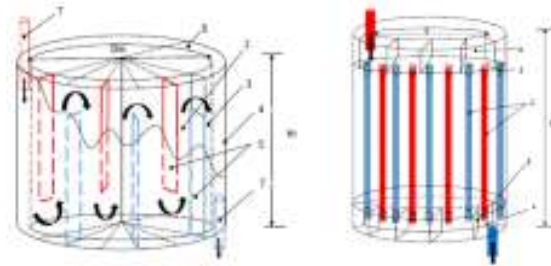
Figure 1. – Geothermal heat exchangers with variable geometry

All variants are embedded in devices made with sand of the stock heat with thermos-controlled grain size and characteristics, the large diameter drilling (pilot) or holes, isolated environment. The analytical calculation is performed with properly heat exchangers heat accumulation.

To analyze the efficiency of a geothermal exchanger with variable geometry was carried out numerical modeling of the thermal behavior of some modules in series diameter D_m = 0,425m and 1,00m lengths imposed, 1,25m and 1,50m in different operating regimes with flow and temperature.

The numerical study was made, in CFD – Ansys Fluent, in the same conditions.

RESULTS AND CONCLUSIONS:

The results obtained by numerical simulation for water validates analytical calculation model proposed.

Comparing the numerical results obtained for nanofluid and water, increase when using nanofluids as a heat transfer agent is 20%, under the same conditions.

Depending on the characteristics and parameters of objective function served cold source exchanger can be equipped with modular variable geometry and dimensions adopted accordingly.

Depending on the assumptions accepted, the proposed model allows the modules to be determining the length of a temperature difference required either to determine the geometrical dimensions outlet temperature data modules.

Compared with usual solutions require land areas for significantly less planning and operational flexibility by offsetting seasonal.

The next challenge is the experimental validation of this model, so our team has made on a small scale these heat exchangers and these will be tested in the near future.

REFERENCES:

[1] Minea, A. A., Luciu Razvan Silviu, MANCA Oronzio, Influence Of Microtube Heating Geometry On Behavior Of An Alumina Nanofluid At Low Reynolds Numbers, Applied Mechanics and Materials Vol. 371 (2013) pp 596-600

[2] Minea, A. A., Luciu Razvan Silviu, Investigations on electrical conductivity of stabilized water based Al2O3nanofluids, Microfluidics and Nanofluidics, Springer-Verlag 2012, ISSN 1613-4982

[3] BFE - Geothermie, Praktische Nutzung Von Erdwärne, Swiss Federal Office for Energy, BERN, 1998, 23 P.; Geothermal Heat Pumps, Ubeg.

[4] Ph.Ackerer; M.A.Bues, Simulation numerique du transfert de chaleur dans un milieu poreux sature Et Non-Sature

Nano-PCMs characterization and modelling

Paolo Bison[1], Sergio Bobbo[1], Laura Fedele[1,*], Stefano Rossi[1], Simone Mancin[2], Davide Ercole[3], Oronzio Manca[3]

[1] Istituto per le Tecnologie della Costruzione, Consiglio Nazionale delle Ricerche, Corso Stati Uniti, 4, 35127 Padova, Italy

[2] Dept. of Management and Engineering, University of Padova, Str.lla S. Nicola, 3, 36100, Vicenza, Italy.

[3] Dipartimento di Ingegneria Industriale e dell'Informazione, Seconda Università degli Studi di Napoli, via Roma 29, 81031 Aversa, Italy

*Corresponding e-mail: laura.fedele@itc.cnr.it

Keywords: Phase Change Materials (PCMs), thermal conductivity, latent heat, storage, model

INTRODUCTION:

Phase Change Materials (PCMs) are commonly used to adsorb and release heat loads, exploiting phase change process and the related latent heat. The latent heat absorption phenomenon can be useful to delay and control the temperature rise of a system subjected to high and intermittent heat fluxes or to storage heat loads.

Several complete reviews are available in the literature on PCMs [amongst others 1-3], where their use for thermal storage is deeply considered. PCMs can be organic, inorganic or eutectic materials, and can be chosen on the base of the required melting temperature and application. An ideal PCM should exhibit a suitable phase-transition temperature, high latent heat of fusion, and high thermal conductivity; it should be characterized by high density associated with a small volume change during the melting process and low vapour pressure in the melt; moreover, it should be chemically stable, non-toxic and non-hazardous, and compatible with the constructional materials. Finally, it should be abundant, available, and cost effective.

Paraffin waxes are largely used as PCMs, showing many of the requested characteristics such as high latent heat, low vapour pressure in the melt, chemical stability. However, they are characterized by very low thermal conductivity, which limits its heat transfer capabilities during the melting and solidification, delaying the loading and unloading processes.

Several techniques have been proposed to enhance thermal properties of PCMs. Amongst others, the addition of nanoparticles seems to be an interesting solution. For example, Khodadadi and Hosseinizadeh [4] seeded nanoparticles to improve thermal energy storage by increasing heat conductivity. Shin and Banerjee [5] and Chieruzzi et al. [6] showed that nanoparticles enhance the heat capacity of the molten salt PCM. Zhichao et al. [7] measured 8% total heat storage capacity enhancement, dispersing TiO_2 nanoparticles at 0.2 vol% in erythritol. Jiang et al. [8] studied PCM paraffin microcapsules modified with different percentages of nano-Al_2O_3, obtaining enhanced thermal transfer and phase change properties. Karkri et al. [9] used a PCM based on high-density polyethylene (HDPE) mixed with micro-encapsulated paraffin wax. He et al. [10] studied thermophysical properties of nano-PCM, based on $BaCl_2–H_2O$, in low temperature cool storage, using TiO_2 nanoparticles. Thermal

conductivity increased up to 16.7%, indicating the use of this PCM for low temperature energy storage, as refrigeration and air conditioning systems, solar energy systems and heating and cooling of buildings. Recently, our research groups have started a research project on the characterization and modelling of nanostructured PCMs [11-15], in order to investigate the potentiality of nanoparticles in improving thermal properties of PCMs.

With this aim, the expertise of the different groups is involved in the analyses of the possible solutions for the employment of PCMs in thermal storage and temperature insulation.

METHODS:

Several experimental facilities are available to perform this study.

First of all, thermal conductivity and latent heat must be measured, to evaluate the differences between the base PCM and the nano-PCM.

Thermal conductivity measurements can be performed using a ThermTest TPS2500S, based on the Hot Disk technique, working with the transient plane source mode. The plane source is a disk sensor, Kapton-insulated to be thermally neutral. It is made from a double spiral of electrically-conducting Nickel metal that works both as transient heater, to increase the temperature of the sample, and temperature reader, to record the time-dependent temperature increase. The declared instrument uncertainty is 5%; however, it has been calibrated with a standard stainless steel sample showing a deviation lower than 1.1%.

The measurements of latent heat are performed using a Differential Scanning Calorimeter (DSC), Setaram Instrumentation. The DSC measures specific heat capacity by heating a sample and by measuring the temperature difference between the sample and a reference sample. Three measurements are repeated with an identical programmed variation of temperature, between an initial and a final value, and with a predefined velocity. The instrument experimental uncertainty is 2%.

Furthermore, dedicated setup for the experimental characterization of the phase change process of nano-PCMs, under constant and intermittent heat loads, is available at the laboratories of Nano Heat Transfer (NHT-Lab) of the University of Padova. The experimental measurements permit to highlight the potential benefits achievable by the addition of nanoparticles to pure paraffin waxes, in terms of maximum junction temperature and melting time.

Numerical investigations can be also accomplished on Nano-PCMs, solving the governing equations that are involved in the physical and geometrical system. The equations are written assuming the single phase model, which consider the mixture as a single solid or a single fluid with thermophysical properties evaluated by the described measurements. The melting of paraffin wax is modeled with enthalpy-porosity method [16], given that the paraffin wax does not melt in a determined value of temperature, but in a temperature range. While the melting is developing, there is a mixed solid-liquid zone where a new parameter is defined to indicate the amount of the liquid fraction in a cell. The numerical model is accomplished to simulate the heat transfer inside a cavity with PCM and nano-PCM. Numerical simulations are carried out using the Ansys-Fluent 15.0 code. Preliminary verification and validation can be examined. The results can be presented in terms of loading and unloading time, and total amount of stored energy.

RESULTS AND CONCLUSIONS:

This research project is recent and new data are under measurements.

At the moment, paraffins added with alumina (Al_2O_3) and Carbon black (CB) nanoparticles have been considered, giving promising results in terms of thermal conductivity, but showing a high instability un the phase change process, since nanoparticles tend to settle in the liquid phase.

A great effort is now put on the synthesis of stable nano-PCMs, in order to avoid sedimentation and instability.

Moreover, preliminary experimental tests on the phase change process of nano-PCMs under constant and intermittent heat loads are on-going at the NHT-Lab of the University of Padova

REFERENCES:

[1] Zalba B, Marìn JM, Cabeza LF and Mehling H 2003 *Appl. Therm. Eng*. **23** 251–283.

[2] Sharma A, Tyagi VV, Chen CR and Buddhi D 2009 *Ren. Sust. Energy Reviews* **13** 318–345.

[3] Agyenim F, Hewitt N, Eames P and Smyth M 2010 *Ren. Sust. Energy Reviews* **14** 615–628.

[4] Khodadadi JM and Hosseinizadeh SF 2007 *Int. Commun. Heat Mass Transfer* **34** (5) 534–543.

[5] Shin D and Banerjee D 2011 J*. Heat Transfer* **133** (2) 024501.

[6] Chieruzzi M, Cerritelli GF, Miliozzi A and Kenny JM 2013 *Nanoscale Res. Lett*. **8** (1) 448.

[7] Zhichao L, Qiang Z and Gaohui W 2015, *Int. J. Heat Mass Transfer* **80** 653–659.

[8] Jiang X, Luo R, Peng F, Fang Y, Akiyama T and Wang S 2015 *Appl. Energy* **137** 731–737.

[9] Karkri M, Lachheb M, Nógellovác Z, Boh B, Sumiga B, AlMaadeed MA, Fethi A and Krupa I 2015 *Energy and Build*. **88** 144–152.

[10] He Q, Wang S, Tong M and Liu Y, 2012 *Energ. Convers. Manage.* **64** 199–205.

[11] L. Colla, L. Fedele, S. Mancin, L. Danza, O. Manca, "Nano-PCMs for enhanced energy storage and passive cooling applications", accepted by Applied Thermal Engineering - Special Issue. Available online 11 April 2016.

[12] L. Colla, L. Fedele, S. Mancin, S. Bobbo, D. Ercole, O. Manca, "Nano-PCM for electronics cooling applications", Proc. "5th Micro/Nanoscale Heat and Mass Transfer Conference", 4-6 gennaio 2016, Biopolis, Singapore.

[13] O. Manca, L. Colla, L. Fedele, S. Mancin, S. Bobbo, D. Ercole, "Nano-PCMs for enhanced energy storage applications", Proc. "5th Micro/Nanoscale Heat and Mass Transfer Conference", 4-6 gennaio 2016, Biopolis, Singapore.

[14] L. Colla, L. Fedele, S. Mancin, B. Buonomo, D. Ercole, O. Manca, "Nano-PCMs for passive electronic cooling applications", Proc. "33rd UIT Heat Transfer Conference", 22-24 giugno 2015, L'Aquila, Italy. IOP Journal of Physics: Conference Series, 655 (2015) 012030.

[15] Barizza, P. Bison, L. Colla, L. Fedele, G. Ferrarini, A. Taffurelli, D- Tinazzi, "Highly Efficient Phase Change Materials (PCMs) for Building Applications", presented at "Nineteenth Symposium on Thermophysical Properties", 21 – 26 giugno 2015, Boulder, CO (USA).

[16] Voller, V. R., Prakash, C., 1987, "A fixed grid numerical modelling methodology for convection-diffusion mushy region phase-change problems", International Journal of Heat and Mass Transfer, Vol. 30, pp.1709-1719.

Graphene/PEG400 Nanostructured Materials for Thermal Energy Storage and Lubrication. Thermal Analysis and Thermophysical Profile

David Cabaleiro[1*], Marco A. Marcos[1], María Jesús G. Guimarey[2], María J.P. Comuñas[2], Josefa Fernández[2], Luis Lugo[1]

[1] Departamento de Física Aplicada, Universidade de Vigo, E-36310, Vigo, Spain

[2] Laboratorio de Propiedades Termofísicas, Departamento de Física Aplicada, Universidade de Santiago de Compostela, E-15782, Santiago de Compostela, Spain

*Corresponding e-mail: dacabaleiro@uvigo.es

Keywords: Nano-PCM, Nanolubricant, Polyethylene glycol 400, Graphene nanoplatelets

INTRODUCTION: It is undoubtedly the case that our society in general and industry in particular require of more efficient machines and thermal facilities. Thus, the improvement of the thermal and antifriction capabilities of heat transfer fluids and lubricants plays a major role in enhancing the reliability and performance of thermal installations. In recent years layered nanomaterials such as graphene have been proven as effective solid nanoadditives to develop new nanostructured materials with enhanced properties [1-2]. However, this process needs of a thorough optimization of parameters such as the nanoadditive concentration or the preparation conditions in order to actually improve the properties of the base fluid. This work aims to develop new nano-Phase Change Materials (PCMs) and nanolubricants designed as dispersions of graphene nanoplatelets in a poly(ethylene glycol) with an average molecular weight of 400 g/mol, PEG400. The influences of nanoadditive loading on the thermophysical properties of density, dynamic viscosity, thermal conductivity and heat capacity were experimentally studied in a wide temperature range. In addition, the temperatures and enthalpy changes associated with (solid-liquid) phase change transitions were also investigated for the designed dispersions.

METHODS: Nanofluids were prepared following a two-step method by dispersing different mass concentrations, wt.%, of graphene nanoplatelets, GnPs, (with a mass purity of 99.5%) in a PEG 400 (pharmaceutical grade) supplied by IoLitec and Panreac, respectively. The nanopowder was characterized using scanning electron (SEM) and atomic force microscopies (AFM) while the purity of the base fluid was analysed through electrospray ionisation mass spectrometry (ESI-MS). Subsequently, the temporal stability of the dispersions was assessed by dynamic light scattering (DLS) and the thermal stability of nanoadditive, base fluid, and nanostructured fluids was studied by thermogravimetric analysis (TGA).

Viscosity and density of dispersions were experimentally obtained in the temperature range from (283 to 373) K with a Stabinger SVM 3000 (Anton Paar) rotational viscometer which also incorporates a vibrating U-tube cell to density measurements [3]. Thermal conductivity was studied at temperatures from (283 to 333) K using a KD2-Pro (Decagon) based on the

transient hot wire technique, while heat capacity was obtained in the range between (233 and 373) K using a differential scanning calorimeter, DSC, Q2000 (TA Instruments) equipped with a RSC90 cooling system and operating in quasi-isothermal method (TMDSC) [4-5]. In addition, the characteristics of (solid-liquid) phase transitions were analysed at temperatures between (188 and 313) K using the DSC Q2000.

RESULTS AND CONCLUSIONS: Thermal conductivity noticeably improves with nanoplatelets addition, enhancements reaching up to 20% for the 0.5% mass concentration. Density, dynamic viscosity and isobaric heat capacity exhibit the characteristic behavior of nanofluids. The temperature and concentration dependences of dynamic viscosity are presented in Figure 1.
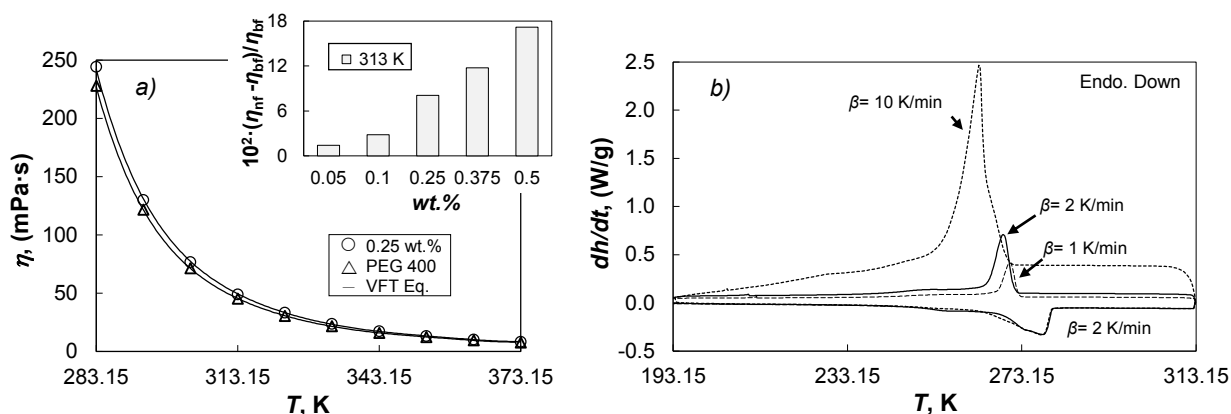
Figure 1. a) Temperature and nanoadditive concentration dependences on dynamic viscosity and b) thermograms obtained by DSC at different cooling rates and a heating rate of 2 K/min for the 0.25 wt.% graphene mass concentration.

Dynamic viscosity rises with nanoadditive concentration up to 18%, without an obvious temperature influence on this property. The thermograms obtained for the GnPs/PEG400 dispersion at 0.25 wt.% using cooling rates between 1 and 10 K/min and a heating rate of 2 K/min are presented in Figure 1. The addition of graphene nanoplatelets eases the nucleation during solidification and reduces the temperature range in which melting takes place.

REFERENCES:
[1] M. Mehrali, E. Sadeghinezhad, S.T. Latibari, S.N. Kazi, M.N.B.M. Zubir, H.S.C. Metselaar, Nanoscale Res. Lett. 9, 15 (2014).
[2] B. Gupta, N. Kumar, K. Panda, S. Dash, A.K. Tyagi, Sci. Rep. 6, 18372 (2016).
[3] F.M. Gaciño, T. Regueira, L. Lugo, M.J.P. Comuñas, J. Fernández, J. Chem. Eng. Data 56, 4984-4999 (2011).
[4] D. Cabaleiro, J. Nimo, M.J. Pastoriza-Gallego, M.M. Piñeiro, J.L. Legido, L. Lugo, J. Chem. Thermodyn. 83, 67-76 (2015).
[5] D. Cabaleiro, C. Gracia-Fernández, J.L. Legido, L. Lugo, Int. J. Heat Mass Transf. 88, 872-879 (2015).

Specific Heat increment of nitrate salts

M. E. Navarro [1,*], G. Qiao[2], Yulong Ding[1]

[1] Birmingham Centre of Energy Storage (BCES), School of Chemical Engineering, University of Birmingham, B152TT, Birmingham UK

[2] Global Energy Interconnection Research Institute (GEIRI), 10117, Berlin, Germany

[*]*Corresponding e-mail: h.navarro@bham.ac.uk*
Keywords: Nanofluids, viscosity, nanoparticles

INTRODUCTION:

Nanofluids are solid–liquid mixtures in which the solid particles have usually a size comprised between 1 nm and 100 nm [1]. Nowadays, nanofluids open a new and promising gateway for different applications due to their desirable properties Nanofluids as heat transfer fluids (HTF), are stable suspensions of colloidal nanoparticles that present enhanced thermal properties, better stability and considerably higher thermal conductivities comparing to conventional HTF and microsized HTF. They can be improve the performance of devices and systems in different applications such as: cooling electronic components, industrial cooling, heating buildings, energy storage, solar absorption [2]. It is a relatively new field, which is less than two decades old that in recently years it has been demonstrated that the addition of nanoparticles to a based material (solid composites, aqueous and oil based nanofluids, and molten salts) can be used to improve some thermal properties such as thermal conductivity and specific heat. Moreover, experimental and numerical studies showed an improvement in the efficiency of solar energy applications by using nanofluids. Yousefi et al. [3] suggested that the nanofluids in different volume fractions should be tested to find the optimum volume fraction, for example in solar collector applications efficiency increases up to 10% when using nanofluids [4]. However, various experiments have shown that the improvement on the thermal performance might be offset by an increase of viscosity and pressure drop [5]. The viscosity of nanofluids is as important as thermal conductivity due to the internal resistance of a fluid to flow, explained by the viscosity. Therefore, as a result of dispersion of nanoparticles in base fluids, the viscosity increases requiring a higher energy for pumping them through the system .

The aim of this work is to formulate nanofluids for Thermal Energy storage for high temperature applications. In this case, three nitrate based nanofluids have been formulated ($NaNO_3$, KNO_3 and $LiNO_3$) and characterized to study the optimal formulation for this purpose, taking into account the viscosity as it is an important parameter when the nanofluid is used as a HTF.

METHODS:

Sodium nitrate, potassium nitrate, and lithium nitrate (Sigma Aldrich) were used as a base material for the nanofluids. Silica nanoparticles in the size of 15–20 nm from US Research Nanomaterials) were selected as nanoparticles. The percentage of SiO_2 nanoparticles added into the nitrates based materials was comprised between 0.5 to 4%.

There are two fundamental methods for the fabrication of nanofluids: one- step method (chemical synthesis technique or direct evaporation method) in which particles are formed directly in the base liquid or two-step method in which the nanoparticles are synthesized by different methods and then are dispersed into the base liquid. In this work a two-step method is used to prepare molten salt based nanofluids to obtain stable suspensions with improved thermal properties in order to be used in Thermal Energy Storage applications.

The formulation procedure was a two step method shown in Figure 1. Salt and nanoparticles were measured on an analytical balance with ±0.1 µg precision (Mettler Toledo, type XP6U). The nanoparticles were dispersed in f distilled water and mixed by an ultra-sonicator (Fisher scientific, CL-334) for two minutes. The salt was added to the aqueous nanofluid, and the mixture was subjected to sonication for another 2 min. Then, the solutions were placed on an oven to evaporate the water to obtain finally the salt-based nanomaterial. A Zetasizer (Malvern Instruments) was used to measure the particle size in salt-water solution during the sonication process and the average size remain around 200 nm after 2 or more min sonication.
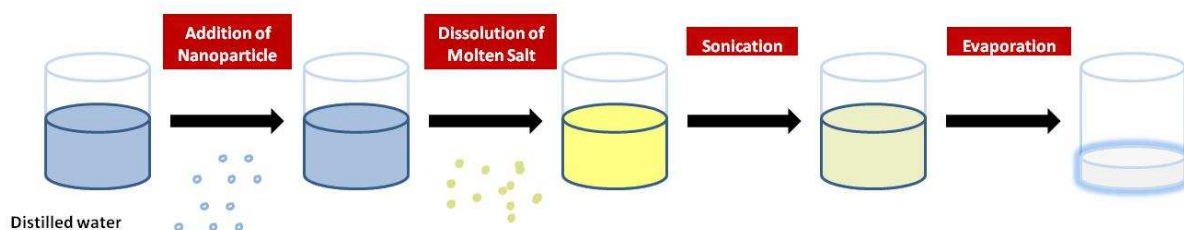
Figure 1Two-step method nanofluid formulation

RESULTS AND CONCLUSIONS:

The specific heat capacity of the samples was measured using a differential scanning calorimeter (DSC-2, Mettler Toledo). A platinum crucible was used to place the sample in the DSC. The sample mass was around 10 mg. Three different samples were measured three times each one in order to obtain a representative result of the thermal properties of the nanofluids. A sapphire standard material was used as a reference to perform the specific heat capacity measurements. The sample was heated under nitrogen atmosphere at a constant heating rate of 10°Cmin -1 from room temperature up to the starting decomposition temperature. First measurements were addressed to characterize the specific heat capacity

of the pure salts, (Figure 2). The results obtained show an average results dispersion of ±0.05 in sodium and potassium salts, and ±0.1 in Lithium salt. $LiNO_3$ salt present the highest specific heat capacity, which is followed by $NaNO_3$ salt and KNO_3.
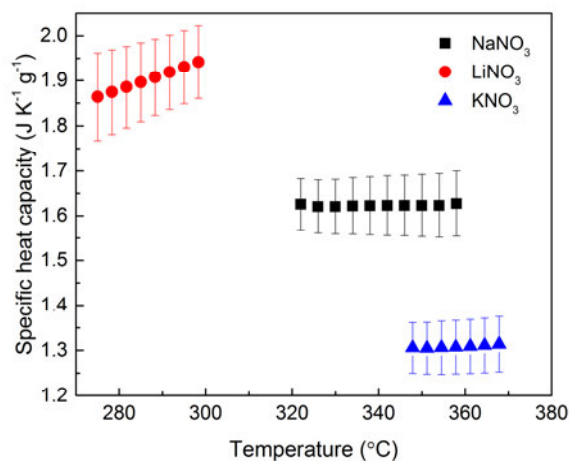
Figure 2 Specific heat capacity of the pure salts

After the pure salts were tested, the different formulations with nanoparticles additive were tested to characterize their specific heat capacity following the described process above. As it can be seen in Figure 3, the addition of nanoparticles into nitrates molten salts increase the specific heat capacity depending on the mass ratio added, despite of the lower SiO_2 specific heat capacity value. In the three cases the specific heat capacity reaches a maximum enhancement. However, when the nanoparticle fraction increases more, the specific heat capacity decreases, due to agglomeration processes [6].
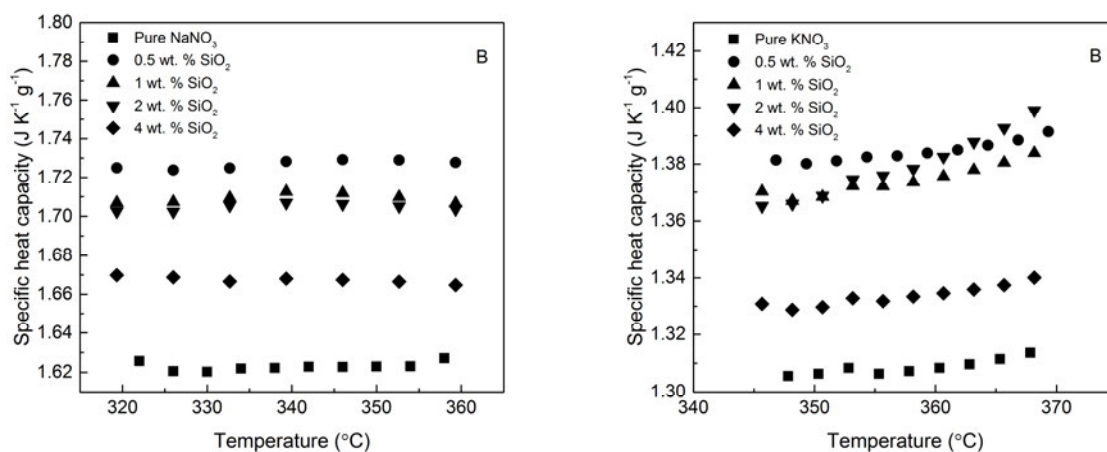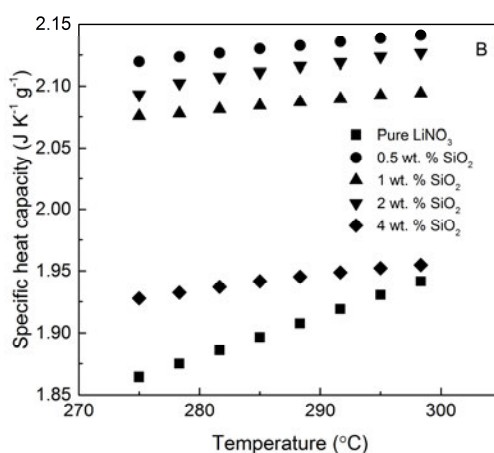
Figure 3 Specific heat capacity of nitrate salts with different amounts of SiO₂ nanoparticles

Determining the rheological behaviour of nanofluids is essential to establishing adequate pumping power as well as the convective heat transfer coefficient, as the Prandtl and Reynolds numbers (functions of viscosity) will be influenced. Among the methods which can be used for high temperature viscosity measurement: capillary, falling body, rotational and oscillation methods, only capillary and oscillation are suitable for molten salt due to their low viscosity. In Figure 4 it can be seen the viscosity of nitrate based molten salts according to the literature [7]. Lithium nitrate is the most viscous molten salt followed by potassium nitrate and sodium nitrate. As expected the viscosity decreases with the temperature. This viscosity reduction behaviour can be explained by the increases the Brownian motion due to the increase of temperature, thermal movement of molecules and their average speed, resulting in weakened intermolecular interaction and adhesion forces between molecules [8], see Figure 4.
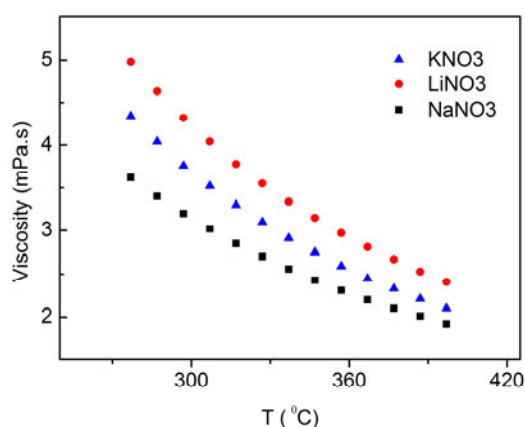
Figure 4 Viscosity versus T of nitrate salts.

A Rheometer (MC502, Anton Paar) was used in order to study the increment on the viscosity when nanoparticles are added. The viscosity was measured through the parallel plate model, a stainless steel 35mm diameter plate was used for this purpose. The rheometer has a furnace to control the temperature in order to perform the test and characterized the nanoluids. The nanofluids with different mass concentration (0.5%, 1%, 2% and 4%) were loaded at room temperature at solid state and then viscosity measurements were performed at different temperatures and up to 250 s -1 shear rate. The relative viscosity of the formulated nanoparticles, in comparison with the base fluid, is presented in Figure 5. It can be seen that at higher nanoparticle concentrations the viscosity increases in a non-linear way. It is clear that the particles have a huge tendency to agglomerate and this might be one reason for the enormous enhancement of viscosity while nanopaticles load exceeds 2%.
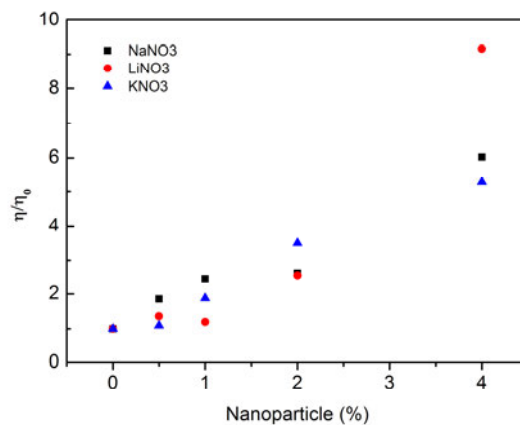
Figure 5 Relative viscosity of molten salt versus nanoparticles content

CONCLUSIONS:

Several nanofluids with different amounts of nanoparticles have been formulated to be used as HTF in thermal energy storage applications. A two step method has been used to prepare the different mixtures. The formulations present higher specific heat capacity comparing to the base fluid. However, according to the rheological results, viscosity increases with the nanoparticle contents as well. This work has a significant impact on the utilization of nanofluids as HTF or thermal energy storage media because any further energy storage technology that considers employing nanofluids has to balance the influence on thermal conductivity, specific heat capacity and viscosity.

REFERENCES:

[1] O. Mahian, A. Kianifar, A.Z. Sahin, S. Wongwises, Performance analysis of a minichannel-based solar collector using different nanofluids, Energy Convers. Manag. 88 (2014) 129–138. doi:10.1016/j.enconman.2014.08.021.

[2]   R. Saidur, K.Y. Leong, H.A. Mohammad, A review on applications and challenges of nanofluids, Renew. Sustain. Energy Rev. 15 (2011) 1646–1668. doi:10.1016/j.rser.2010.11.035.

[3]   T. Yousefi, F. Veysi, E. Shojaeizadeh, S. Zinadini, An experimental investigation on the effect of Al2O3–H2O nanofluid on the efficiency of flat-plate solar collectors, Renew. Energy. 39 (2012) 293–298. doi:10.1016/j.renene.2011.08.056.

[4]   R.A. Taylor, P.E. Phelan, T.P. Otanicar, C.A. Walker, M. Nguyen, S. Trimble, et al., Applicability of nanofluids in high flux solar collectors, J. Renew. Sustain. Energy. 3 (2011) 023104. doi:10.1063/1.3571565.

[5]   D.K. Das Ravikanth S. Vajjha, A review and analysis on influence of temperature and concentration of nanofluids on thermophysical properties, heat transfer and pumping power, (n.d.).

[6]   G. Qiao, M. Lasfargues, A. Alexiadis, Y. Ding, Simulation and experimental study of the specific heat capacity of molten salt based nanofluids, Appl. Therm. Eng. (2016). doi:10.1016/j.applthermaleng.2016.07.159.

[7]   G.J. Janz, U. Krebs, H.F. Siegenthaler, R.P.T. Tomkins, Molten Salts: Volume 3 Nitrates, Nitrites, and Mixtures: Electrical Conductance, Density, Viscosity, and Surface Tension Data, J. Phys. Chem. Ref. Data. 1 (1972) 581. doi:10.1063/1.3253103.

[8]   M. Nabeel Rashin, J. Hemalatha, Viscosity studies on novel copper oxide–coconut oil nanofluid, Exp. Therm. Fluid Sci. 48 (2013) 67–72. doi:10.1016/j.expthermflusci.2013.02.009.

Investigation of specific heat capacity of solar salt-based nanofluids

Yanwei Hu [1, 2], Yurong He [2], Dongsheng Wen[1,*]

[1] School of Chemical and Process Engineering, University of Leeds, LS2 9JT, Leeds, United Kingdom

[2] School of Energy Science and Engineering, Harbin Institute of Technology, 150001, Harbin, China

*Corresponding e-mail: D.Wen@leeds.ac.uk

Keywords: solar salt-based nanofluids, specific heat capacity, material characterization

INTRODUCTION: With thermal stability at high temperature, comparable viscosity and low vapor pressure [1], molten salts are widely used in modern concentrating solar power systems. However, there are some disadvantages that sets a limitation on the application of molten salt in solar plants, such as relatively low specific heat capacity and low thermal conductivity [2]. Since nanofluids, firstly proposed by Choi [3], have shown the excellent capability to improve the effective thermal properties of solutions, doping nanoparticles into molten salt may be a prospective way to modify the thermal properties of molten salt based nanofluids. Several investigations have shown great successful in enhancing specific heat capacity of molten salt based nanofluids, using carbonate mixed salts [4-6], Hitec [7], solar salt [8-9] as solvents. However, the experimental data for the effect of doping nanoparticles into molten salt on specific heat capacity is insufficient and the mechanism is still unclear. Hence, in present work, specific heat capacity of different mass concentrations of solar salt based SiO_2 nanofluids was investigated and material characterization analyses were carried out.

METHODS: Liquid solution method proposed by Shin [10] was used to formulate molten salt based nanofluids. Sodium nitrate ($NaNO_3$) and potassium nitrate (KNO_3) were used as base salt with a ratio of 60:40 by mass. Silica nanoparticles with an average diameter of 10 nm were used in the experiment. Firstly, nanoparticles were dispersed into deionized water and sonicated to form uniform suspensions. Then base salt was solved into the suspensions and sonicated for another time. In the end, the suspensions were heated in a vacuum drying oven to get the solid phase nanocomposites without moisture. The specific heat capacity of nanocomposites was measured by a differential scanning calorimetry (DSC) and material characterization analyses were performed using a scanning electron microscopy (SEM).

RESULTS AND CONCLUSIONS: Results show that specific heat capacity of solar salt based nanofluids increases with adding SiO_2 nanoparticles at a relative low concentration. Further adding nanoparticles will result in a weakened enhancement or even deteriorated on specific heat capacity. The optimal mass concentration of 10 nm SiO_2 nanoparticles was 1.0%. From the material characterization analyses, it was observed that special

microstructures were formed when doping nanoparticles into molten salt. With the amount of microstructures increases, specific heat capacity of nanocomposites increases. The enhancement of specific heat capacity is related to the formulation of microstructures.

REFERENCES:

[1] Vignarooban K, Xu X, Arvay A, et al. Heat transfer fluids for concentrating solar power systems–A review[J]. Applied Energy, 2015, 146: 383-396.

[2] Ye F, Ge Z, Ding Y, et al., Multi-walled carbon nanotubes added to Na_2CO_3/MgO composites for thermal energy storage[J]. Particuology, 2014, 15: 56-60.

[3] Choi S U S. Enhancing thermal conductivity of fluids with nanoparticles[J]. ASME-Publications-Fed, 1995, 231: 99-106.

[4] Jo B, Banerjee D. Enhanced specific heat capacity of molten salt-based nanomaterials: Effects of nanoparticle dispersion and solvent material[J]. Acta Materialia, 2014, 75: 80-91.

[5] Shin D, Banerjee D. Enhanced thermal properties of SiO_2 nanocomposite for solar thermal energy storage applications[J]. International Journal of Heat and Mass Transfer, 2015, 84: 898-902.

[6] Tiznobaik H, Shin D. Enhanced specific heat capacity of high-temperature molten salt-based nanofluids[J]. International Journal of Heat and Mass Transfer, 2013, 57(2): 542-548.

[7] Ho M X, Pan C. Optimal concentration of alumina nanoparticles in molten Hitec salt to maximize its specific heat capacity[J]. International Journal of Heat and Mass Transfer, 2014, 70: 174-184.

[8] Lasfargues M, Geng Q, Cao H, et al. Mechanical dispersion of nanoparticles and its effect on the specific heat capacity of impure binary nitrate salt mixtures[J]. Nanomaterials, 2015, 5(3): 1136-1146.

[9] Schuller M, Shao Q, Lalk T. Experimental investigation of the specific heat of a nitrate–alumina nanofluid for solar thermal energy storage systems[J]. International Journal of Thermal Sciences, 2015, 91: 142-145.

[10] Shin D, Banerjee D. Enhanced specific heat of silica nanofluid[J]. Journal of heat transfer, 2011, 133(2): 024501.

Effect of silica nanoparticles in the specific heat of Solar Salt

Rosa Mondragon1, N. Navarrete1, Leonor Hernandez1, Luis Cabedo2, Raul Martinez-Cuenca1, Salvador Torro1, J. Enrique Julia1

1 Departamento de Ingenieria Mecanica y Construccion, Universitat Jaume I, 12071-Castellon de la Plana, Spain

2 Dept. Ingenieria de Sistemas Industriales y Diseño. Universitat Jaume I. Campus de Riu Sec. Castellon de la Plana, Spain

Corresponding e-mail: enrique.julia@uji.es

Keywords: molten salts, nanoparticles, specific heat

INTRODUCTION: Molten salts are used in Concentrated Solar Power plants as Thermal Energy Storage material because of its high operational temperature and stability up to 500ºC. Its main drawbacks are its relative poor thermal properties (energy storage density and heat transfer coefficient) and its high melting temperature (220ºC). A simple cost-effective way to improve thermal properties of fluids is to dope them with nanoparticles (defined as salt-based nanofluids).

Nanofluids, defined as fluids containing nanometer-sized particles, have been extensively studied in past years and have shown better thermal conductivity than its corresponding base fluid [3]. However the influence of adding nanoparticles on the specific heat of the heat transfer and/or thermal storage fluid is still under research. According to the mixture rule, the addition of nanoparticles presenting a lower value of cp than the base fluid, results in a decrease in the specific heat of the nanofluid. Nevertheless, recent works have shown that the specific heat of molten salts is increased when adding nanoparticles [9, 10, 11, 12, NUESTRA]. Nevertheless, the mechanism of enhancement of specific heat is still under controversy, although the most accepted proposal is related with the semi-solid layering of the salt ions. The nanoparticles introduced in the salt act as a nucleation point for the crystallization of a new phase around them having higher thermo-physical properties than the bulk molten salts. Therefore, a deeper understanding of the relevant physical-chemical mechanisms involved in the thermal enhancement is needed to be able to optimize the results. In addition, essential parameters such as nanofluid stability at high temperature, sedimentation and thermal cycling tolerance have not been addressed yet.

In this work the dependence of the specific heat enhancement in Solar Salt with the nanoparticle concentration (from 0.1% to 3%) was analyzed for silica nanoparticles.

METHODS: Solar Salt commonly used in CSP plants is composed of a mixture of 60% NaNO3 - 40% KNO3. This nitrate mixture was used as a based fluid and crystalline silica nanoparticles (Sigma Aldrich) with primary particle size of 12 nm and density of 2600 kg/m3 were used. Salt-based nanofluids were prepared by means of the dissolution method [5-11]. In this method,

salts (60% NaNO3 - 40% KNO3) are first dissolved in water. The concentration of salt mixture in water was kept at 0.1 g/ml and nanoparticles were dispersed into the dissolution by means of ultrasonic treatment using an ultrasound probe Sonopuls HD2200 (Bandelin). Finally, the dissolution containing nanoparticles was dried in order to remove the water and to obtain the nanoparticles homogeneously distributed within the salt recrystallized. The drying process was performed in a hot plate at 100ºC during 1 hour.

Specific heat of salt-based nanofluids was measured by Differential Scanning Calorimetry (DSC) using a differential calorimeter DSC2 (Mettler-Toledo, Inc.). For each sample 20 mg of doped-salt was introduced in the aluminum hermetic pan. Samples were first dried in a hot plate for 30 min to remove any moisture content and then the pan was sealed. The DSC tests were carried out according to the following heating/cooling cycle. First the sample was heated up to 150ºC and held at this temperature for 5 min to obtain a stable heat flux. Then the sample was heated from 150ºC to 500ºC at a fixed heating rate of 20 ºC/min. After that, the sample was held at 500º for 5 min to reach a steady state heat flow condition. Finally, the sample was cooled from 500ºC to 150ºC at a fixed cooling rate of 20 ºC/min. Each sample was submitted to two consecutive heating and cooling cycles.

RESULTS AND CONCLUSIONS: Specific heat of pure nitrate mixture and salt-based nanofluids was measured at different nanoparticle concentrations: 0.1%, 0.5%, 1.5% and 3%. Figure 1 shows the specific heat increments Mean values for the specific heat in the 350ºC-450ºC temperature range were used in order to do the calculations.

It can be observed that the specific heat enhancement depends on the nanoparticle content and the available interfacial area [12].

REFERENCES:

1. [1]   Tamme, R., Laing, D., Steinmann, W.D., Zunft, S. 2002. Innovative thermal energy storage technology for parabolic trough concentration solar power plants. Proceedings EuroSun 2002.
2. [2]   Tiznobaik, H., Shin, D., 2013. Enhanced specific heat capacity of high-temperature molten salt-based nanofluids. International Journal of Heat and Mass Transfer 57, 542.
3. [3]   Mondragon, R., Segarra, C., Martínez-Cuenca, R., Julia, J. E., Jarque, J. C., 2013. Experimental characterization and modelling of thermophysical properties of nanofluids at high temperature conditions for heat transfer applications. Powder Technology 249, 516-529.
4. [4]   Nieto de Castro, C.A., Murshed, S.M.S., Lourenço, M.J.V., Santos, F.J.V., Lopes, M.L.M., França, J.M.P., 2012. Enhanced thermal conductivity and specific heat capacity of carbon nanotubes ionanofluids. International Journal of Thermal Sciences 62, 34-39.
5. [5]   Shin, D., Banerjee, D., 2011. Experimental investigation of molten salt nanofluid for solar thermal energy application. 8th Thermal Engineering Joint Conference AJTEC.

6. [6]   Shin, D., Banerjee, D., 2013. Enhanced specific heat capacity of nanomaterials synthesized by dispersing silica nanoparticles in eutectic mixtures. Journal of Heat Transfer 135, 32801.

7. [7]   Tiznobaik, H., Shin, D., 2013. Experimental validation of enhanced heat capacity of ionic liquid-based nanomaterial. Applied Physic Letters 102, 173906.

8. [8]   Shin, D., Banerjee, D., 2011.Enhancement of specific heat capacity of high-temperature silica-nanofluids synthesized in alkali chloride salt eutectics for solar thermal-energy storage applications. International Journal of Heat and Mass Transfer 54, 1064-1070.

9. [9]   Dudda, B.,Shin, D., 2013. Effect of nanoparticle dispersion on specific heat capacity of a binary nitrate salt eutectic for concentrated solar power applications. International Journal of Thermal Sciences 69, 37-42.

10. [10]   Chieruzzi, M., Cerritelli, G.F., Miliozzi, A., Kenny, J.M., 2013. Effect of nanoparticles on heat capacity of nanofluids based on molten salts as PCM for thermal energy storage. Nanoscale Research Letters 8, 448.

11. [11]   Lu, M-C., Huang, C-H., 2013. Specific heat capacity of molten salt-based alumina nanofluid. Nanoscale Research Letters 8, 292.

12. [12]   Ho, M-X., Pan, C., 2014. Optimal concentration of alumina nanoparticles in molten Hitec salt to maximize its specific heat capacity. International Journal of Heat and Mass Trasnfer 70, 174-184.

Development of novel nanofluids based on solar salt and ceramic nanoparticles for sensible thermal storage applications

B. Muñoz-Sánchez[1,2], J. Nieto-Maestre[1,*], A. García-Romero[2]

[1] Tecnalia Research and Innovation, Mikeletegi Pasealekua, 2. 20009 - San Sebastián (Gipúzcoa). Spain. +34 671 729 012

[2] Department of Mining Engineering, Metallurgy and Materials Science, University of the Basque Country (UPV/EHU), Rafael Moreno "Pitxitxi", 2. 48013 - Bilbao (Vizcaya). Spain.

[*]*Corresponding e-mail:* javier.nieto@tecnalia.com

Keywords: nanoparticles, silica, alumina, thermal energy storage, specific heat, solar energy

INTRODUCTION: In recent years, the use of thermal energy storage (TES) systems is widely used in concentrating solar power (CSP) Plants. The possibility to store part of the energy produced during sunny days, and dispatch it during the night and cloudy periods is an important advantage of solar thermal energy (STE) in relation to photovoltaic (PV) and other renewable energies. The current industrial TES system consists of two molten salt tanks (hot and cold) filled with solar salt (SS), a non-eutectic mixture made of sodium and potassium nitrate (60:40% wt.). These tanks are of great capacity (14000 T. each) in order to comply with the energy storage requirements of modern CSP Plants. Due to this fact, the investment cost on the storage material is very elevated. Higher specific heats (c_p) of the base salt would lead to lower quantities of storage material required for the same energy stored and therefore, important savings on the investment costs. Moreover, an increase in the thermal conductivity (k) would allow a better performance of the TES systems. A significant research effort is being dedicated to develop novel materials with enhanced heat transfer properties.

Nanofluids (NFs) based on molten salts and ceramic nanoparticles (NPs) are attracting great interest in recent years. Different authors [1–5] reported enhancements on the c_p when adding tiny amounts of SiO_2 or Al_2O_3 nanoparticles. Shin and Barnejee [1] reported a 25% enhancement on the c_p of a molten salt mixture (KCO_3-$NaCO_3$) when adding 1% wt. of SiO_2 NPs. The same authors [2] reported 20% enhanced c_p on a mixture ($BaCl_2$-$CaCl_2$-$LiCl$-$NaCl$) with SiO_2 nanoparticles at a mass fraction of 1%. A maximum increase of 25% on specific heat of SS was found by Andreu-Cabedo et al. [4] when a 1% of SiO_2 NPs were added. Betts reported increments of 20% and 19% on the specific heat when adding 1% wt. of Al_2O_3 and SiO_2 NPs respectively to an eutectic mixture of $NaNO_3$ (55% mol) and KNO_3 (45% mol). This author measured the c_p during 3 cycles and found a considerable decrease in the specific heat of the SiO_2-doped NF at 450 ºC after 3 cycles. The c_p of the Al_2O_3-doped NF was stable after 3 cycles.

The mechanism of enhancement is still not well known. A mechanism proposed by Shin and Barnejee was the formation of an interfacial layer between the surface of NPs and the molten salt [2]. However, Shin et al. proposed in a recent paper [3] the formation of a fractal-like nanostructure as the responsible of these enhancements. Thoms [6] discussed in depth the adsorption of the molten salts molecules on the NP surface. He showed that there is a strong influence of the NP size on the c_p enhancements. There is still a great discrepancy about the reasons why these anomalous increments occur.

In this work, SS-based nanofluids doped with SiO_2 and Al_2O_3 nanoparticles were synthetized. The distribution of sizes for the final nanofluids was measured and the NPs were shown to be adequately dispersed on the SS matrix. The c_p of the NFs was measured at 396 ºC showing important enhancements with respect to the base salt.

The stability of the NPs within the NF is also of great concern for their final application. In these sense, stability tests were performed where the concentration of SiO_2 and Al_2O_3 NPs was measured at different times (0.5, 1 and 5 h) in the molten state. The results of these tests are still pending of publication.

METHODS: Commercial water-based NFs of alumina (Alumisol 10A, Kawaken Fine Chemicals) and silica (Ludox SM-30, Sigma-Aldrich) were used as a source of NPs. Their primary size and shape was analysed by Transmission Electronic Microscopy (TEM, JEOL 2100). Their size distribution were measured by Dynamic Light Scattering (DLS ZetaSizer nano ZS, Malvern Instruments).

The NFs were synthesized by the well-known hot plate method [4-5] Solar Salt was prepared by mixing 60% wt. of $NaNO_3$ (SQM, Industrial grade) and 40% wt. of KNO_3 (HAIFA, Multi-KGG). Water dispersions of NPs were added over an aqueous solution of the salt. The mixture was dried at 100 ºC, milled and melted at 396 ºC for 30 minutes. The specific heat of the SS and these two NFs was measured at 396 ºC (liquid state) with a Differential Scanning Calorimeter (DSC Q100, TA Instruments) using an isothermal procedure with MDSC method (amplitude 0.6ºC, period 110 s). The NP size distribution was obtained by DLS. The dispersion of NPs into the molten salt and their sizes was evaluated by Scanning Electronic Microscopy (SEM LEO 440i, Leica-Zeiss).

RESULTS AND CONCLUSIONS: NFs based on SS and SiO_2 and Al_2O_3 NPs were successfully synthetized. The final sizes of NPs were lower than 100 nm, as measured by DLS technique (Figure 1). The NPs were uniformly distributed within the molten salt matrix, as shown in SEM pictures (Figure 2). The shape of SiO_2 NPs was spherical, while Al_2O_3 were flat-shaped. The shape of the NPs was also shown in Figure 2.

Enhancements of 30% and 34% on the c_p were found for SiO_2 and Al_2O_3 doped NFs respectively with respect to the base salt. These improvements were achieved with a concentration of 1% wt. of NPs. The results are shown in Figure 3. The enhancements were higher than those expected by the mixing rule, taking into account the individual c_p of the SS and SiO_2 and Al_2O_3 NPs.

(a)   (b)

Fig. 1: Nanoparticle size distribution of the raw NPs dispersions SiO_2 NPs (a) and Al_2O_3 NPs (b) and the samples SS1Si (a) and SS1A (b).
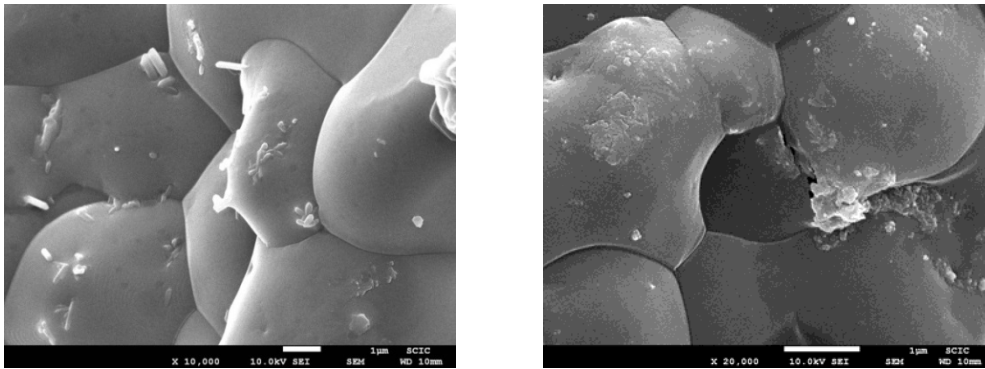
Fig. 2: SEM images of alumina (left) and silica nanofluids (right).
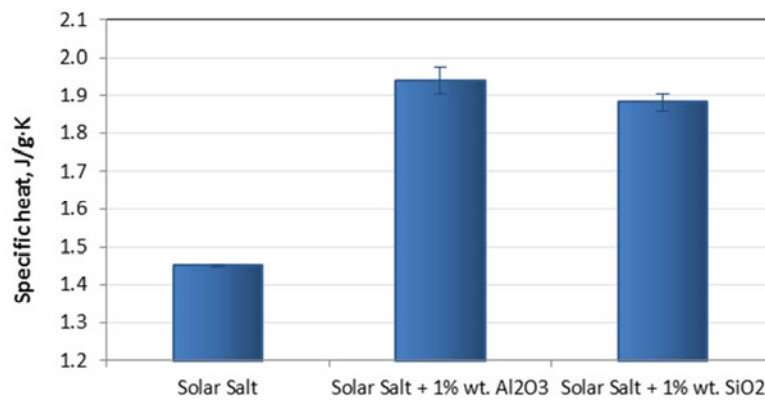
Fig 3 : Specific heat of the pure SS and the SS-based NF in the liquid state (396 ⁰C). The bars on each column represent the standard deviation of each measurement.

It is worth mentioning that this work will be presented in the next SolarPACES 2016 Conference as an oral communication titled "Silica and alumina nano-enhanced molten salts for thermal energy storage: a comparison"

REFERENCES:

[1]   D. Shin and D. Banerjee, "Enhanced Specific Heat of Silica Nanofluid," *J. Heat Transfer*, vol. 133, p. 024501, 2011.

[2]   D. Shin and D. Banerjee, "Enhancement of specific heat capacity of high-temperature silica-nanofluids synthesized in alkali chloride salt eutectics for solar thermal-energy storage applications," *Int. J. Heat Mass Transf.*, vol. 54, pp. 1064–1070, 2011.

[3]   D. Shin, H. Tiznobaik, and D. Banerjee, "Specific heat mechanism of molten salt nanofluids," *Appl. Phys. Lett.*, vol. 104, no. 12, 2014.

[4]   P. Andreu-Cabedo, R. Mondragon, L. Hernandez, R. Martinez-Cuenca, L. Cabedo, and J. E. Julia, "Increment of specific heat capacity of solar salt with SiO2 nanoparticles," *Nanoscale Res. Lett.*, vol. 9, no. 1, pp. 1–11, 2014.

[5]   M. Betts, "The Effects of Nanoparticle Augmentation of Nitrate Thermal Storage Materials for Use in Concentrating Solar Power Applications," Texas A&M University, 2011.

[6]   M. W. Thoms, "Adsorption at the Nanoparticle Interface for Increased Thermal Capacity in Solar Thermal Systems," Massachusetts Institute of Technology, 2012.

ON THE USE OF NANO-ENCAPSULATED PHASE CHANGE MATERIALS FOR THERMAL-OIL AND MOLTEN SALT-BASED NANOFLUIDS

N. Navarrete[1], A. Gimeno-Furio[1], R. Mondragon[1], L. Hernandez[1], L. Cabedo[2], E. Cordoncillo[3] and J.E. Julia[1]*

[1]Departamento de Ingeniería Mecánica y Construcción. Universitat Jaume I.

12071-Castellón de la Plana, Spain

[2]Polymers and Advanced Materials Group (PIMA) . Universitat Jaume I.

12071-Castellón de la Plana, Spain

[3]Departamento de Química Inorgánica y Orgánica. Universitat Jaume I.

12071-Castellón de la Plana, Spain

[*]Corresponding author: enrique.julia@uji.es

Keywords: Thermal oil, Molten salt, Heat capacity, Thermal conductivity, Nanoencapsulated Phase Change Materials

Introduction: The thermal properties of Heat Transfer Fluids (HTF) play an important role in the efficiency of Concentrated Solar Power (CSP) plants. Thermal oils and molten salts are used as HTF in medium and high temperature applications since they present high stability at high temperature conditions. However, the thermal properties of these HTFs are quite poor, with thermal conductivity (k) and specific heat capacity (cp) values lower than 0.4 W/m K and 2.5 J/g K, respectively. Nanofluids are defined as engineered colloidal suspensions of nanoparticles in a base fluid. They allow to introduce a solid inside a liquid, transferring, to some extent, the solid properties to the liquid and keeping, also to some extent, its liquid transport properties. Therefore, nanofluids present an effective route to improve the thermal properties of HTFs.

Earliest nanofluid works were related to the thermal conductivity enhancement using water as base fluid [1, 2]. After that, nanofluid related research topics were expanded and nanofluid viscosity and specific heat were involved. From 2010, new nanofluid approaches using additional solid particle properties have been researched. One of them is the use of nano-encapsulated Phase Change Materials (nePCM) as solid phase. In this approach, the nanoparticles have a PCM core and a high melting temperature shell that keeps the PCM confined when it is in liquid phase. The use of nePCM allows to increment the thermal conductivity as well as the thermal capacity of the base fluid by the latent heat contribution of the cores of the nePCM. Metal and metal alloy nanoparticles can be used as cores of nePCMs suitable for mid and high temperature applications. In most cases, the encapsulation is obtained growing a silica shell [3-8] or trioctyl phosphine oxide TOPO [9] around them. Different metal cores have been investigated. Lower crystallization temperature values, defined as

supercooling, are always found due to the absence of nucleation spots inside the nuclei. The nePCM supercooling depends on the nucleus material and size. One important parameter in shell-type nePCMs is the encapsulation ratio defined as the ratio between the phase change enthalpy per unit of mass of the nePCM and the PCM bulk material. Encapsulation ratios below 1 are found due to the mass contribution of the nePCM shell (which is not melted in the temperature working range of the nePCM) and the enthalpy decrement due to size effects (only for nePCM with nuclei smaller than 50 nm). In order to maximize the nePCM latent heat contribution, the encapsulation ratio should be as high as possible, assuring the shell mechanical integrity.

Silica or TOPO-shell type nePCMs can be dispersed into fluids to develop nePCM-based nanofluids. In this regard, a wide range of base fluids, such as methanol [3], molten salt [6, 9], poly-alpha-olefin (PAO) [4], and commercial thermal oil (Therminol 66) [7], have been used.

NePCM present important advantages over conventional nanoparticles such as heat capacity increment. However, complex chemical synthesis process are needed to obtain shell-type nePCMs, involving, at least, four chemical processes: the first one to produce the metal nanoparticles, a second one to grow a polymeric template around them, the third one to grow the silica or TOPO shell on the template and the last one to eliminate the polymeric template.

In this work, a new approach to simplify the nePCMs production is proposed and experimentally checked. This way, it is proved that the metal oxide shell that is produced during the metal nanoparticle fabrication process using standard commercial methods can be used as self-encapsulation in static and dynamic conditions. However, potential chemical reactions between the metal oxide shell and the solar salt components should be taken into account.

Discussion and Results: Two types of nePCMs nanofluids have been tested. The first one consists of commercial Sn nanoparticles of nominal size <80 nm purchased from US Research Nanomaterials, Inc. added to a synthetic thermal oil used frequently as a HTF, Therminol 66 (Solutia, Inc.) in a weight concentration of 30% and sonicating the mixture.

The second nanofluid was prepared adding commercial Zn nanoparticles of nominal size 35-45nm (US Research Nanomaterials, Inc.) in a weight concentration of 30% to solar salt (60% wt. NaNO3, 40% wt. KNO3, Sigma-Aldrich), following the preparation procedure described in [4].

Both commercial metal NPs have a metal oxide shell that can be used as self-encapsulation (Figure 1a). NePCM morphology, shell thickness and diameters have been measured using a Transmission Electronic Microscope (TEM, JEOL 2100).

NFs heat capacity and NePCM strength inside the base fluid have been measured using a Differential Scanning Calorimeter (DSC, DSC2 Mettler Toledo) using different thermal heating and cooling rates as well as several thermal cycles.

Figure 1 shows some example of the results. Figure 1a) shows a TEM image of a NePCM (SnOx shell/Sn core) after thermal cycling (200 cycles between 70ºC and 250ºC). It is possible to observe the shell integrity after thermal cycling. Figure 1b) shows the phase change enthalpy of the SnOx shell/Sn core NePCMs inside the thermal oil after thermal cycling in the DSC. Thermal cycles have been performed at 40K/min and the enthalpy measurement at 5K/min. It is

possible to observe that both enthalpies, melting and crystallization, are almost constant after 200 thermal cycles.

Figure 1. a) TEM image of a Sn/SnOx nePCM after thermal cycling, and b) Evolution of the enthalpies of nePCM/Thermal oil nanofluid with thermal cycling.

Figure 1 shows some example of the results. Figure 1a) shows a TEM image of a NePCM (SnOx shell/Sn core) after thermal cycling (200 cycles between 70°C and 250°C). It is possible to observe the shell integrity after thermal cycling. Figure 1b) shows the phase change enthalpy of the SnOx shell/Sn core NePCMs inside the thermal oil after thermal cycling in the DSC. Thermal cycles have been performed at 40K/min and the enthalpy measurement at 5K/min. It is possible to observe that both enthalpies, melting and crystallization, are almost constant after 200 thermal cycles.

Conclusions: In this work it has been proven that the metal oxide shell that is present in Sn and Zn nanoparticles can be used as encapsulation for thermal engineering applications. This shell is present in several metal nanoparticles produced by different methods and it is formed during the nanoparticle fabrication process. This new encapsulation proposal simplifies the production of nePCMs, showing that commercial metal nanoparticles are self-encapsulated by its own metal oxide shell. However, potential interactions between the metal oxide shell and the base fluid components should be taken into account in order to select the nePCM.

References:

1. S. Choi, Enhancing thermal conductivity of fluids with nanoparticles, *ASME Fluids Engineering Division* 231 (1995) 99.
2. H. Masuda, A. Ebata, K. Teramae and N. Hishinuma, Alteration of thermal conductivity and viscosity of liquid by dispersing ultrafine particles (dispersion of gamma-al2o3, sio2 and tio2 ultrafine particles) *Netsu Bussei* 4 (1993) 227–233.
3. M. Zhang, Y. Hong, S. Ding, J. Hu, Y. Fan, A.A. Voevodin, M. Su, Encapsulated nano-heat-sinks for thermal management of heterogeneous chemical reactions, *Nanoscale* 2 (2010) 2790–2797.

4. Y. Hong, S. Ding, W. Wu, J. Hu, A.A. Voevodin, L. Gschwender, E. Snyder, L. Chow, M. Su, Enhancing heat capacity of colloidal suspension using nanoscale encapsulated phase-change materials for heat transfer, *ACS Applied Materials & Interfaces*. 2 (2010) 1685–1691.

5. Y. Hong, W. Wu, J. Hu, M. Zhang, A.A. Voevodin, L. Chow, M. Su, Controlling supercooling of encapsulated phase change nanoparticles for enhanced heat transfer *Chemical Physics Letters* 504 (2011) 180–184.

6. C.-C. Lai, W.-C. Chang, W.-L. Hu, Z.M. Wang, M.-C. Lu, Y.-L. Chueh, A solar-thermal energy harvesting scheme: enhanced heat capacity of molten HITEC salt mixed with Sn/SiO(x) core-shell nanoparticles *Nanoscale* 6 (2014) 4555–9.

7. M. Wang, B. Duong, H. Fenniri, M. Su, Nanomaterial-based barcodes *Nanoscale* (2015) 11240–11247.

8. S. Cingarapu, D. Singh, E.V. Timofeeva and M.R. Moravek, Nanofluids with encapsulated tin nanoparticles for advanced heat transfer and thermal energy storage *International Journal of Energy Research* 38 (2014) 51–59.

9. S. Cingarapu, D. Singh, E. V. Timofeeva, M.R. Moravek, Use of encapsulated zinc particles in a eutectic chloride salt to enhance thermal energy storage capacity for concentrated solar power *Renewable Energy* 80 (2015) 508–516.

THE INFLUENCE OF Al$_2$O$_3$ NANOPARTICLES ON THE HEAT CAPACITY OF ISOPROPANOL

I. Motovoy[*], V. Zhelezny and T. Lozovsky

Department of Thermal Physics and Applied Ecology, Odessa National Academy of Food Technologies, Kanatna str., 112, Odessa, Ukraine

[*]Corresponding author: motovoj@gmail.com

Keywords: Nanofluid, Isopropanol, Al$_2$O$_3$ nanoparticles, Heat capacity

Introduction: Nanofluids are colloidal solutions that are formed by means of dispersing solid nanoparticles in base fluids. Despite a large number of publications dedicated to investigation of the thermophysical properties of nanofluids, the amount of experimental data describing the nanofluid thermal capacity in a wide range of temperatures is negligible. This aspect hinders the potential for developing the model to predict the nanofluids' heat capacity.

Nanofluid solutions of the nanofluid isopropyl alcohol (IPA) / nanoparticles Al$_2$O$_3$ (702129 Aldrich 20 wt.% of Al$_2$O$_3$ nanoparticles) with isopropyl alcohol (CAS # 67-63-0) were chosen as study subjects.

Discussion and Results: The two-phase heat capacity was measured on a variable-temperature adiabatic calorimeter by means of monotonic heating within the temperature range of 190-330 *K*, at mass concentrations of nanoparticles of 2.01%, 5.11% and 9.96% (1.2, 3.1 and 6.1 mole%, respectively). The results of the study of the heat capacity of nanofluids are shown in Fig. 1. Experimental uncertainty for the heat capacity values does not exceed 0.7%.

The obtained data show that nanoparticle additives provide for the decrease of the heat capacity in the liquid phase.

The performed analysis shows that the correlations for predicting isobaric heat capacity published by Pak and Cho [1], and Xuan and Roetzel [2] do not reflect the structural transformations in the nanofluid.

Nanofluid heat capacity values calculated using Pak and Cho, Xuan and Roetzel correlations are always higher than the values obtained in the experiment (see Fig. 2).

It is our opinion that that these results were to be expected, since the published correlations[1, 2] do not take into considerations that any time-stable nanofluid is a colloidal system. When considering a colloid solution, some of the molecules of the base liquid (i.e. isopropyl alcohol) are absorbed on the surface of the nanoparticles. This effect will provide the excess heat capacity that should be taken into consideration when predicting nanofluid heat capacity.
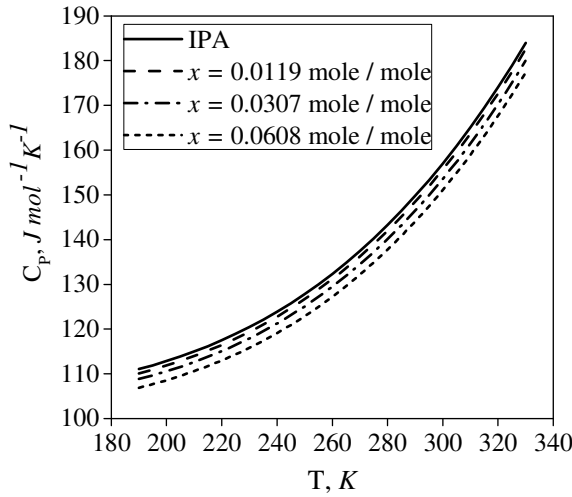
Fig. 1. Heat capacity dependence of temperature.
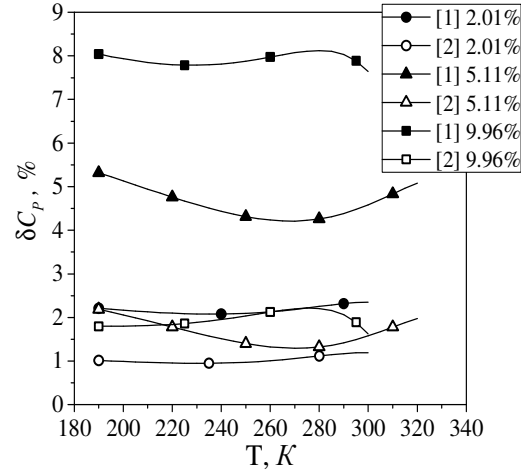
Fig. 2. The relative deviations of the values of the isopropyl alcohol / Al_2O_3 nanoparticles heat capacity calculated using the models [1] and [2] from the experimental data acquired

Therefore, prediction model for the nanofluid heat capacity can be represented as:

$$C_P^{nf} = C_P^{np} x_{np} + C_P^{bf} \left(1 - x_{np}\right) + \Delta C_P^{ex}, \tag{1}$$

where C_P^{nf} is nanofluid heat capacity, $J\ mole^{-1}K^{-1}$; C_P^{np} is the heat capacity of nanoparticles material (Al_2O_3), $J\ mole^{-1}K^{-1}$; x_{np} is the mole fraction of the nanoparticle material in the nanofluid, mole/mole; C_P^{bf} is the heat capacity of the dispersion medium (base fluid - isopropyl alcohol) in the nanofluid, $J\ mole^{-1}K^{-1}$; ΔC_P^{ex} is the excess heat capacity of the nanofluid, $J\ mole^{-1}K^{-1}$.

Hence, we suggest to consider the nanofluid as a thermodynamic system that includes: 1 - nanoparticles, 2 - surface adsorption phase, 3 - diffuse layer, 4 - base liquid. Figure 4 shows the effective values of diameters, thicknesses, and volumes of the phases formed with certain effective thermophysical properties.

The proposed model assumes that nanoparticles are spherical. This assumption is justified in condition of the multilayer adsorption of the base material molecules on the surface of the nanoparticle, as well as the presence of nanoparticles of different sizes and temporal cluster-type [3].

To predict the excess heat capacity, we suggest to consider the excess heat capacity as follows:

$$\Delta C_P^{ex} = C_P^{al} x_{al} + C_P^{dl} x_{dl} - C_P^{dl} \left(x_{al} + x_{dl}\right), \tag{2}$$

where C_P^{al} is the heat capacity of the dispersion medium within the absorption layer, *J mole^{-1}K^{-1}*; x_{al} is the mole fraction of the dispersion medium within the absorption layer, *mole/mole*; C_P^{dl} is the heat capacity of the dispersion medium within the diffuse layer, *J mole^{-1}K^{-1}*; x_{dl} is the mole fraction of the dispersion medium within the diffuse layer, *mole/mole*.
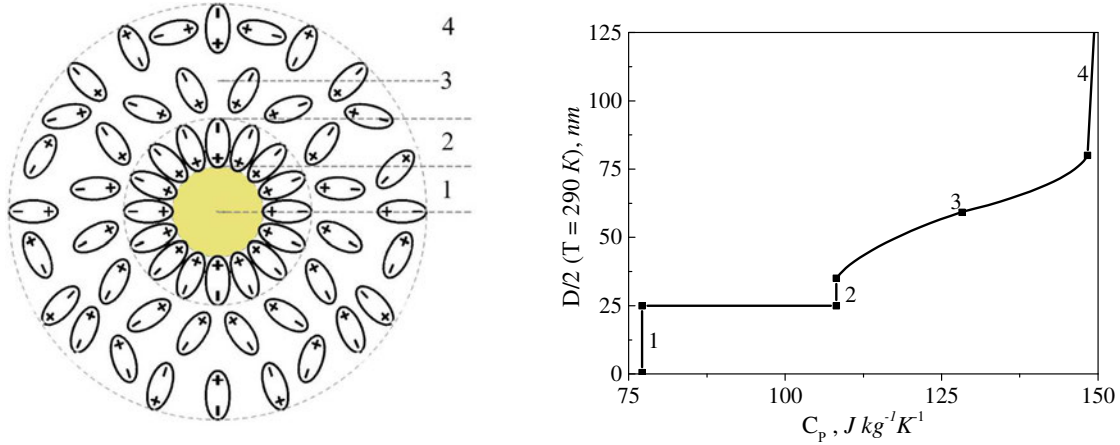
Fig. 3. "Four-phase" prediction model for nanofluid heat capacity

Figure 5 demonstrates comparison of the experimental data on the heat capacity of the nanofluids (at 3 concentrations) and calculating values of the heat capacity by (Eqs. (1) and (2)) at 293 *K*.
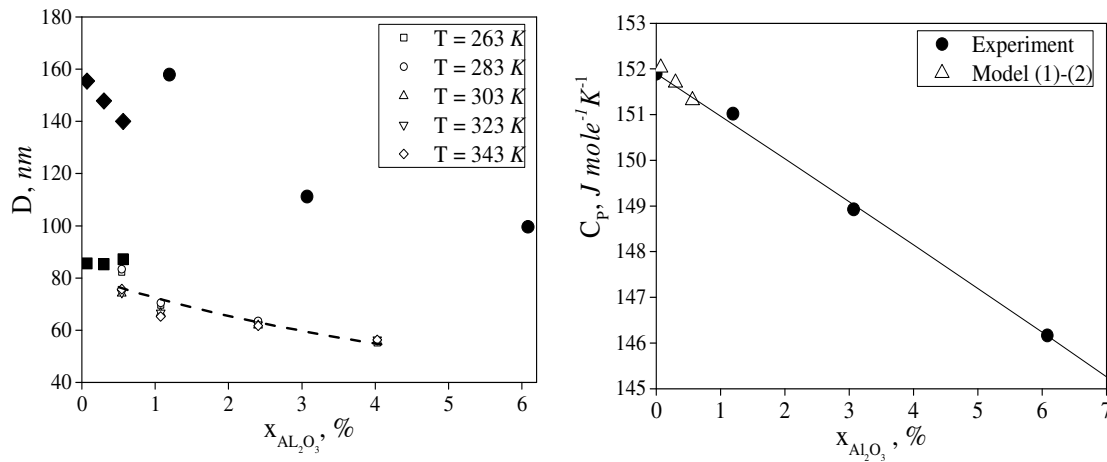
Fig. 4. Concentration dependence of diameters of the adsorbed D_{al} layer and diffuse layer D_{dl} of isopropyl alcohol molecules on the surface of Al$_2$O$_3$ nanoparticles

Fig. 5. Concentration dependence of nanofluid heat capacity at 293 K

Figure 5 shows: ♦ – spectroturbidimetry method at 293 K; ■ – dynamic light scattering at 293 K; ━ ━ – the diameter of the adsorption phase obtained from the data on the density of nanofluids [3]; ● – data on the diameter of the diffuse layer obtained from data on the heat capacity at 293 K.

The performed study shows that the diameter values of adsorption phase, and the diffuse layer of micelles can be determined from the nanofluids density data [3]; these values could also be obtained by using the dynamic light scattering [3] , and spectrophotometric methods. The results of calculating the adsorption layer D_{al}, and diffuse layer D_{dl} for the molecules of isopropyl alcohol on the surface of Al_2O_3 nanoparticles are shown in Fig. 4.
The information in Fig. 5 shows that the values of the isobaric molar heat capacity calculated using the typical sizes of nanoparticles in the base fluid are consistent with the experimental data on the heat capacity of the isopropyl alcohol / Al_2O_3 nanoparticle at a temperature of 293 K.

To predict the heat capacity of nanofluids over a wide temperature range, we suggest to use the extended scaling model, which was proposed in [4]:

$$C_P = C_{P0}t^{(-\gamma\psi)} \tag{3}$$

where C_{P0} is an amplitude depended on the properties of the substance; γ is a critical index, which has a universal value of $\gamma = 1.24$ [5] for various substances; Ψ (t) is the crossover function which is universal for the studied nanofluids and depended from $t = 1 - \dfrac{T}{T_c}$; T_c is the critical temperature of isopropyl alcohol.

This correlation contains only one unknown amplitude C_{P0}. The value of C_{P0} can be calculated using model (1), and (2) at the temperature used to perform optical measurements of diameters D_{al} and D_{dl}. The deviations of the heat capacity values calculated by Eqs. (1) - (3) from experimental data in the temperature range of 190-330 K do not exceed 0.75%.

Conclusions: The experiments show that Al_2O_3 nanoparticle additives lead to a decrease of the isopropyl alcohol heat capacity in the liquid phase throughout the whole temperature range of the experimental study.
It was also found that calculating the heat capacity using Pak and Cho, Xuan and Roetzel models leads to obtaining slightly higher values of the heat capacity for nanofluids.
In our paper, we introduce a new "four-phase" model to predict the nanofluid heat capacity that includes the excess molar heat capacity of nanofluid. This value is determined by the heat capacity of structurally oriented layers of base fluid molecules near the surface of nanoparticles. The deviations of nanofluid heat capacity values for isopropyl alcohol / Al_2O_3 nanoparticles calculated using the proposed model are commensurate with the experimental uncertainty.

References:

1. B.C. Pak and Y.I. Cho, *Hydrodynamic and heat transfer study of dispersed fluids with*

submicron metallic oxide particles, Exp. Heat Transf., 1998.

2. Y. Xuan and W. Roetzel, *Conceptions for heat transfer correlation of nanofluids*, Int. J. Heat Mass Transf., 2000.

3. V.P. Zhelezny, T.L. Lozovsky, V. Gotsulskiy, N. Lukianov, I.V. Motovoy, *Research into the influence of Al_2O_3 nanoparticle admixtures on the magnitude of isopropanol molar volume*, Eastern-European J. Enterp. Technol. pp.33–38, 2017.

4. S.N. Ancherbak, YU.V. Semenyuk, T.L. Lozovsky and D.A. Ivchenko, *Methods for predicting the caloric properties of substances on characteristic curves (in Russian),* Holodilnaya tehnika i tehnologiya, № 4,- p.32-40, 2009.

5. M.A. Anisimov, *Critical phenomena in liquids and liquid crystals,* CRC Press, p.272, 1991.

AN INFLUENCE OF AL$_2$O$_3$ NANOPARTICLES ON THE HEAT CAPACITY OF ISOPROPYL ALCOHOL IN METASTABLE AND SOLID PHASE

I. Motovoy*, V. Zhelezny and T. Lozovsky

Department of Thermal Physics and Applied Ecology, Odessa National Academy of Food Technologies, Kanatna str., 112, Odessa, Ukraine

*Corresponding author: motovoj@gmail.com

Keywords: Heat capacity, Metastable state, Solid phase, Nanoparticles

Introduction: Effects of the influence of nanoparticles on the caloric properties and parameters of basic substances' phase transitions in condensed state remain understudied. When exposed to low temperatures (below the melting point of the base liquid), the nanofluid sample can be in various aggregate states, such as metastable liquid, crystalline phase or glassy state. Crystalline solids have a high degree of orderliness, i.e. have a long-range order of the molecules of the base material and nanoparticles. Molecules of the base material and nanoparticles in amorphous solid state are more chaotic, and can be distinguished by short-range order. Therefore, the properties of nanofluids in condensed state are determined by their structure and the interaction between molecules and nanoparticles. The mechanism of this interaction remains understudied so far. Available publications currently provide no data regarding the effect of nanoparticles on the caloric properties of thermodynamic systems or the solid phase of the basic substance / nanoparticle. There is also no reliable observed data regarding the influence of nanoparticles on the parameters of phase transitions for the investigated samples in condensed state.

Nanofluid solutions of the isopropyl alcohol (IPA) / Al$_2$O$_3$ nanoparticles (702129 Aldrich 20 wt.% of Al$_2$O$_3$ nanoparticles) with isopropyl alcohol (CAS67-63-0) were chosen for experimental investigation.

Discussion and Results: The two-phase heat capacity was measured on a variable-temperature adiabatic calorimeter by means of monotonic heating within the temperature range of 85-180 K, at mass concentrations of nanoparticles of 2.01%, 5.11% and 9.96% (1.2, 3.1 and 6.1 mole%, respectively). Experimental uncertainty of the heat capacity measurements does not exceed 0.7%.

The obtained results show that nanoparticle additives caused the decrease of the heat capacity in the solid phase. The conducted experiments show that the cooling rate of the test sample is of great importance. At a cooling rate of 0.1 to $4.8 \cdot 10^{-2}$ *K/s*, the test sample turned into a solid amorphous state, showing no apparent crystal lattice (glassy state of the substance). The validity of this statement is confirmed by the information given in the thermogram (see Fig.1). As is seen from Fig. 1, the several phase transitions take place at the heating of the samples of isopropanol / Al$_2$O$_3$ that cooled down (thermogram section 1-2) till 85 *K* at a rate ranging from 0.1 to $4.8 \cdot 10^{-2}$ *K/s*.

The characteristics of the reference points on the thermogram refer to the sample that has a composition of isopropanol 94.89 wt.% / nanoparticle 5.11 wt.%. Section 2-3 of the thermogram describes heating of the glassy sample (the rate of temperature change from 0.009 to 0.007 *K/s*). At point 3, the samples begin to turn into the state of the supercooled liquid. Section 3-4 of the thermogram describes continuous transition from glassy state to supercooled liquid. This process is followed by a partial destruction of intermolecular bonds. Therefore, the temperature variation rate for the samples in the temperature range of $112 \leq T \leq 135$ is decreased from 0.007 *K/s* to 0.005 *K/s*. The effective heat capacity of the supercooled liquid is increased from about 1027.5 *J kg⁻¹K⁻¹* to about 1640 *J kg⁻¹K⁻¹* (see Fig.2).
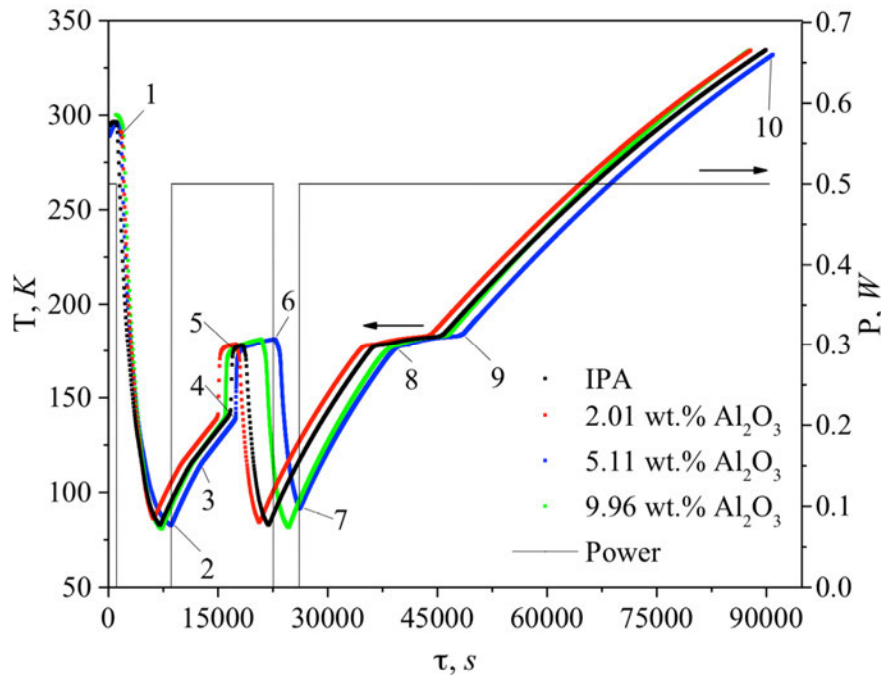
Figure 1. Thermogram of heating nanofluid samples.

It should be noted that increase of the concentration of Al_2O_3 nanoparticles in the sample, leads to decrease the effective heat capacity. This result is quite expected, since the heat capacity of Al_2O_3 nanoparticles is less than the heat capacity of the base liquid. Thermogram section 4-5 (Fig. 1) describes the phase transition from the supercooled liquid to solid phase. This phase transition is followed by a large release of heat, since the temperature of the sample increases from 136 K to the temperature of the solid state - liquid phase transition. Performed experiments show that in order to turn the investigated samples to the crystalline phase, it is necessary to re-cool the sample (thermogram section 6-7). These thermogram sections describe the following: process of increasing temperature of the sample in the crystalline phase (7-8),

melting (8-9), and increase the temperature of the sample in the liquid phase (9-10). At the reheating of the sample (7-8), which was in the crystalline phase, the structural phase transitions up to the melting point were not observed.
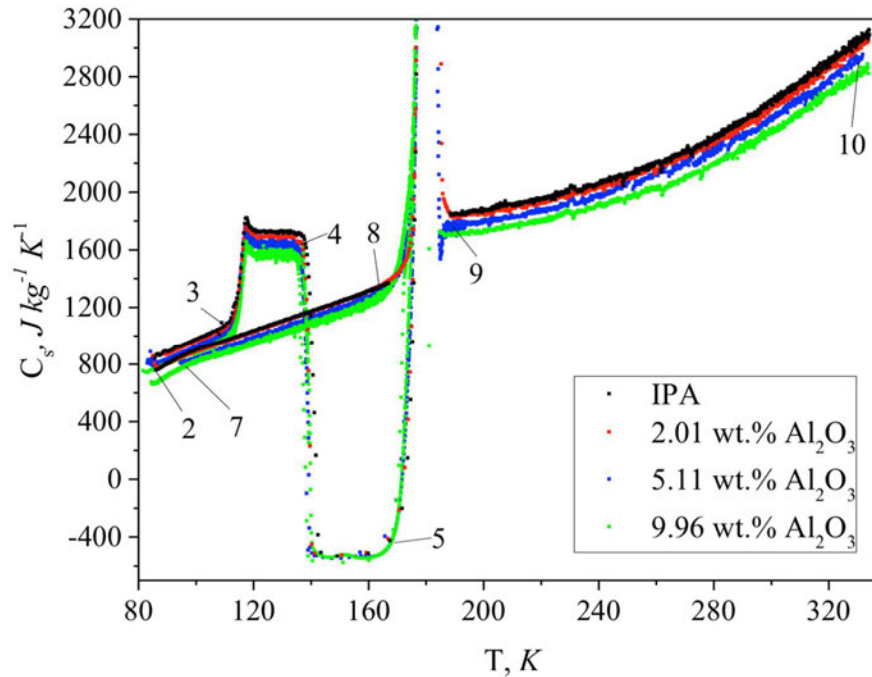
Figure 2. Temperature dependence of the effective heat capacity for heating nanofluid samples.

The presented above model of structural transformations can be confirmed by temperature dependence of the effective heat capacity (Fig.2). The effective heat capacity describes the amount of heat necessary to raise the temperature of the investigated by a degree under the conditions of experiment (including the thermal effects of phase transitions during crystallization and melting).

As follows from the information given in the figures, the presence of nanoparticles in isopropyl alcohol contributes to reducing the heat capacity in both the solid and liquid phases.

The performed study shows that the decrease of the heat capacity is not proportional to the concentration of the nanoparticle. The heat capacity of the samples in the glassy state is higher than the heat capacity of the samples of the same concentration in the crystalline phase. The heat capacity of a substance in a metastable state is higher than its heat capacity in a glassy state. Figs. 3-5 demonstrate more detailed information on the specific heat capacity values of the samples in various aggregate states.

The conducted calorimetric experiments made it possible to determine the quantitative effects of the nanoparticle influence on the characteristics of phase transitions (see Table 1). It was demonstrated that the nanoparticle additives in isopropyl alcohol cause an insignificant change in the temperature of the phase transitions - $T_{pt.}$ The effect of the nanoparticle influence on the heat of phase transitions λ depends on the concentration of nanoparticles, and is very significant.
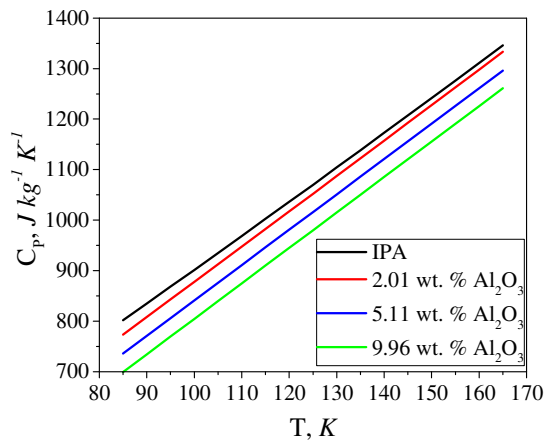
Figure 3 Temperature dependence of heat capacity of nanofluid in the solid phase
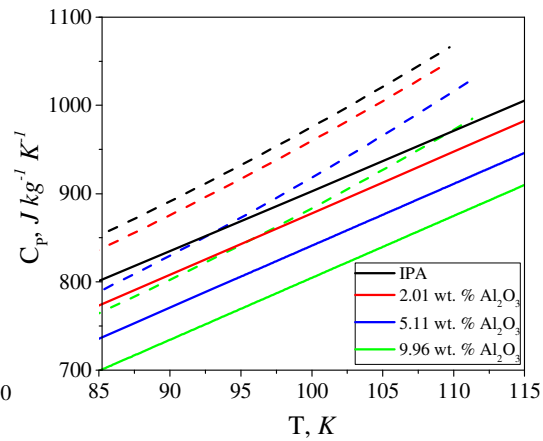
Figure 4 Temperature dependence of the heat capacity of nanofluid in the crystalline phase (solid lines) and the glassy state (dashed lines)
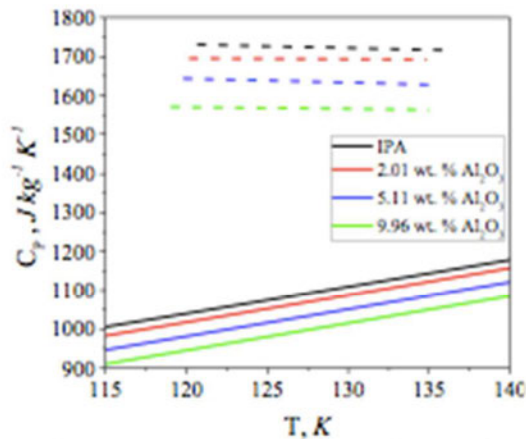
Figure 5 Temperature dependence of heat capacity of nanofluid in the solid phase (solid lines) and metastable state (dashed lines)

Table 1 Parameters of phase transitions in nanofluids

$\omega_{np.}$ wt.%	T_{pt} K	Δc_P $J\ kg^{-1}K^{-1}$	λ $J\ kg^{-1}$
Crystalline - liquid			
0	184.7	271.8	88647.2
2.01	184.9	290.0	86473.0
5.11	185.1	313.5	83855.6
9.96	185.1	253.5	78427.0
Glassy state- metastable state			
0	117.1	602	1202.4
2.01	117.1	576.3	1150.4
5.11	117.0	570.9	1131.8
9.96	117.2	531.6	1109.9

Summary: The conducted calorimetric experiments prove that nanoparticle additives decrease the heat capacity and values of the heat of phase transitions for the isopropyl alcohol in the solid phase. This effect is caused by the complex structure of the nanofluids in the liquid phase. The dispersion phase (base liquid) in the vicinity of nanoparticle has an absorption phase structure that is similar to the glassy state. Therefore, a smaller amount of the dispersion phase changes its aggregate state during phase transitions. The thickness of the absorbed layer of isopropyl alcohol molecules near the nanoparticles depends on their concentration, size and temperature.

References:

1. V.P. Zhelezny, T.L. Lozovsky, M.A. Shimchuk, An experimental investigation and modelling of the heat capacity for nanofluids isopropanol/ Al_2O_3 on the saturation line, *7th International Conference Physics of liquid matter: modern problems (PLMMP7),* May 27-30, pp.5-9, 2016.

SOLAR SALT WITH SIO$_2$ NANOPARTICLES FOR THERMAL ENERGY STORAGE HIGH TEMPERATURE APPLICATIONS: SCALE UP OF THE SYNTHESIS PROCEDURE

A. Solé[1], M. Liu[2], F. Bruno[2], J.E. Julià[1] and L.F. Cabeza[3],*

[1]Department of Mechanical Engineering and Construction, Universitat Jaume I, Campus del Riu Sec s/n, 12071 Castelló de la Plana, Spain

[2]Barbara Hardy Institute, School of Engineering, University of South Australia, Mawson Lakes Boulevard, Mawson Lakes, SA5095 Australia

[3]GREA Innovació concurrent, INSPIRES Research Centre, University of Lleida, Pere de Cabrera s/n, 25001, Lleida, Spain

*Corresponding author: lcabeza@diei.udl.cat

Keywords: Nanoparticles, Solar salt, Concentrated solar power (CSP) plants, Thermal energy storage

Introduction: The solar salt (60 wt.% NaNO$_3$ and 40 wt.% KNO$_3$) is being used for thermal energy storage in high temperature applications (i.e. concentrated solar power (CSP) plants). Since 2013, in different laboratories around the world, nanofluids based on the solar salt have been synthetized doped with alumina (Al$_2$O$_3$), silica (SiO$_2$) and titanium dioxide (TiO$_2$) nanoparticles to enhance its specific heat capacity (Cp). Figure 1 shows that depending on the concentration of the nanoparticle in the salt, the enhancement differs. This leads to think that there is an optimum concentration of the nanoparticle in the salt, which is 1 % in the case of solar salt (blue bars in Figure 1).
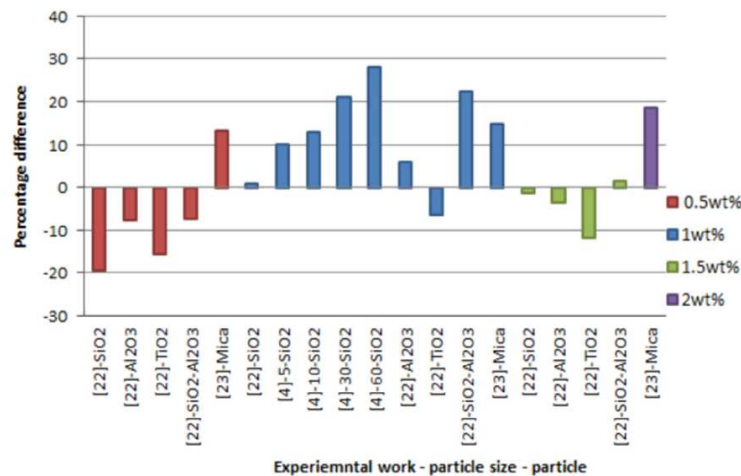
Figure 1. Specific heat enhancement of the solar salt with different nanoparticles and concentrations [1].

The three published studies concerning solar salt and nanoparticles addition agreed that there is around a 25 % of Cp enhancement in liquid state for 1 wt.% of nanoparticles concentration [2-4]. Furthermore, in spite of presenting some differences in ultrasonic bath time and evaporation temperature, the methodology that is being followed to produce molten salt nanofluids is widespread and all the studies [2-4] refer to Shin and Banerjee's methodology [5]. Until now, all the manufacturing process of the nanofluid at the different labs is being done up to 200 mg samples scale.

Therefore, to ensure to the industry that this process is scalable and reproducible maintaining the expected properties (mainly Cp and degradation temperature), the objective of the present study is to synthetize the nanofluid in larger scale, specifically 250 times larger than ever done.

Materials and methodology: Two types of silica (SiO_2) nanoparticles were used: own synthetized and commercial ones. The followed procedure to synthetize the nanoparticles is detailed in [6], where different SiO_2 particle sizes can be derived depending on the reactants concentration. As a starting point, 80 nm was chosen. There is only one study comparing how the nanoparticle size affects the Cp and the best results are given by 60 nm of SiO_2 particle size (being the higher particle size that the authors tested) [3]. Commercial SiO_2 nanoparticles, 250 nm particle size, used for this study were manufactured by Fiber Optic center in New Bedford, Massachusetts. $NaNO_3$ and KNO_3 are technical grade purchased from the company ACE Chemical from Australia.

Two batches of the nanofluid, each one of 50 g, with both types of nanoparticle, own synthetized and commercial, were done to ensure repeatability of the results. After the synthesis procedure of the nanofluid, based on Shin and Banerjee methodology [5], the samples were placed in an oven for a certain period of time (200 and 400 h) at 450 ℃ to simulate the behavior in a CSP plant. The nanofluid starts to decompose at 750 ℃ under nitrogen atmosphere [4]. Under oxygen atmosphere, degradation is expected somewhere around 500 ℃.

The developed nanofluid at medium scale (50 g each batch) has been characterized, before and after the oven test, seeking for the Cp enhancement, morphology and composition, degradation temperature, and particle size distribution. The used techniques along with the obtained information are:

Differential scanning calorimeter (DSC) allows measuring the specific heat of the nanofluid in solid and liquid state. From each nanofluid batch 3 samples and 3 runs of each sample will be analyzed to obtain the Cp. The solar salt is also analyzed to have a reference. The DSC is a Mettler-Toledo 822e.

Scanning electron microscopy (SEM) shows how the morphology of the nanofluid is and it allows knowing how the nanoparticles are dispersed in the salt, if they are clustering or not and have a rough number of the nanoparticles size. The samples were mounted on SEM stub with double-sided carbon adhesive. The SEM is Merlin with the GEMINI II column and made by Carl Zeiss Microscopy.

Energy dispersive spectrometry (EDS) gives the composition and the percentage of each chemical element of a given sample. This technique is coupled to SEM. This information will

support SEM one, by showing if SiO_2 is found in the nanofluid (mainly for the own synthetized samples). The EDS is Silicon Drift Detector (SDD) – X-MaxN (20 mm^2) and made by Oxford Instruments.

TEM shows the morphology and gives a rough value of particle size. This technique is used only for the own synthetized silica nanoparticles. The TEM is a JEM-2100F-HR by JEOL.

With thermogravimetric analysis (TGA) TG-STDA Mettler Toledo model TGA/SDTA851e/LF/1600, the maximum working/operating temperature will be known. This technique will allow knowing whether the addition of the nanoparticles can positively or negatively change the maximum operating temperature.

Dynamic light scattering (DLS) technique, Zetasizer nano ZS (Malvern Instruments Ltd., UK), provides useful information about the particle size distribution.

Discussion and results: The experimental testing is on-going, but the first results which show the material synthesis and morphology are promising.

In Figure 2 left, a sample of the own synthetized silica nanoparticles can be observed. Figure 2 left shows that the nanoparticles were successfully synthetized and, although they were expected to be 80 nm of particle size, they seem to be around 200 nm. The morphology of the commercial nanoparticles can be seen in Figure 2 right, from where it can be deduced that nanoparticles are pretty similar in diameter size, uniformity and they seem to be around 200 nm.
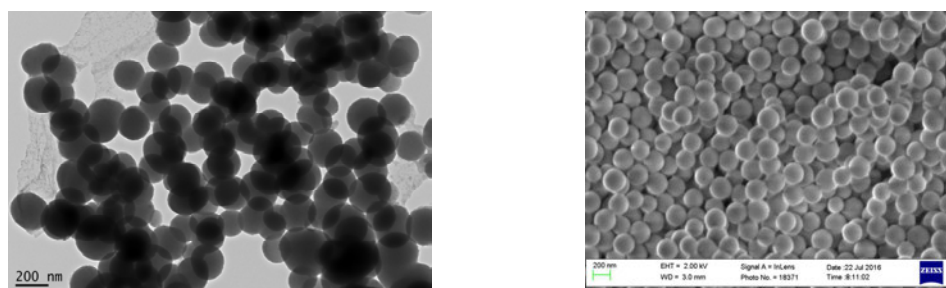
Figure 2. Left: TEM image of own synthetized SiO_2, right: SEM image of commercial SiO_2.

SEM images of the solar salt with of own synthetized nanoparticles clearly show that the nanoparticles have been successfully dispersed in the solar salt and show some clusters formation (Figure 3).

EDS spectrum confirms that Si and O are present, coming from the SiO_2 nanoparticles, also oxygen is present in the solar salt and Na, K, and N account for the salt. In addition, C, Cl and even S are found which the last two could be due to impurities in the salts.
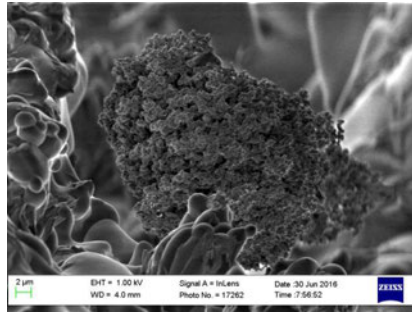
Figure 3. SEM image of batch 1 of the solar salt with own synthetized SiO_2.

Conclusions: Two nanofluids based on the solar salt and silica nanoparticles, with own synthetized nanoparticles and with the commercial nanoparticles, were produced at medium scale in the lab. The feasibility that molten salt based nanofluid with promising Cp can be manufactured at larger scale will be proven depending on the experimental results. The results of the present study provide a step forward for the industrial processing of this potential material for real high temperature applications.

References:

1. O. Arthur and M.A. Karim. An investigation into the thermophysical and rheological properties of nanofluids for solar thermal applications, *Renewable and Sustainable Energy Reviews* 55 (2016) 739-755.
2. M. Chieruzzi, G. F. Cerritelli, A. Miliozzi and J. M. Kenny. Effect of nanoparticles on heat capacity of nanofluids based on molten salts as PCM for thermal energy storage, *Nanoscale research letters* (2013) 8:448.
3. B. Dudda and D. Shin. Effect of nanoparticle dispersion on specific heat capacity of a binary nitrate salt eutectic for concentrated solar power applications, *International journal of thermal sciences* 69 (2013) 37-42.

4. P. Andreu-Cabedo, R. Mondragon, L. Hernandez, R. Martinez-Cuenca, L. Cabedo and J. E. Julia. Increment of specific heat capacity of solar salt with SiO2 nanoparticles, *Nanoscale Research Letters* (2014) 9:582.

5. D. Shin and D. Banerjee. Enhancement of specific heat capacity of high-temperature silica-nanofluids synthesized in alkali chloride salt eutectics for solar thermal-energy storage applications, *International Journal of Heat and Mass Transfer* 54 (2011) 1064-1070.

6. K.S. Rao, K. El-Hami, T. Kodaki, K. Matsushige and K. Makino. A novel method for synthesis of silica nanoparticles, *Journal of colloid and interface science* 289 (2005) 125-131.

Characterization Of Nano-Encapsulated Metal Alloy Phase Change Materials For A Molten Salt-Based Nanofluid

Nuria Navarrete[1,*], Rosa Mondragón[1], Dongsheng Wen[2], Maria E. Navarro[3], Yulong Ding[3], J. Enrique Julia[1]

[1] Dpto. de Ingeniería Mecánica y Construcción, Universitat Jaume I, 12071 Castellón, Spain.

[2] Institute of Particle Science and Engineering, University of Leeds, LS3 PJT, Leeds, UK.

[3] Birmingham Centre of Energy Storage, University of Birmingham, B15 2TT, Birmingham, UK.

*nnavarre@uji.es

Keywords: Thermal storage, Solar energy, Nanofluids, Molten salts, Phase-change materials

INTRODUCTION: A nanofluid is a Heat Transfer Fluid (HTF) or Thermal Energy Storage (TES) material with enhanced heat transfer properties by the addition of nanoparticles [1]. Their use usually implies an increment in the thermal conductivity of the fluid, but additional enhancements in the heat capacity of molten salts and ionic liquids have been registered [2].

Heat capacity of fluids can also be increased by using nanoencapsulated Phase Change Materials (nePCM). These nanoparticles are composed of a PCM core and a covering shell with high melting temperature. Thus, an increase in the heat capacity of the nanofluid compared to the base fluid can be obtained due to the latent heat of the cores [3]. The main drawbacks of nePCM are the complexity in the synthetization process of the shell and the high supercooling they sometimes present (the difference between the core melting and crystallization temperatures, due to homogeneous crystallization)[4].

The present work proposes a nanofluid composed of a mixture of molten nitrates widely used in Concentrated Solar Power plants, and nePCM consisting of an Al/Cu nucleus encapsulated by the metallic oxide formed when exposed to oxygen. NePCM and nanofluids with different concentrations have been characterized regarding their physical and thermal properties, and the suitability of the encapsulation has been proven for high temperature working conditions.

METHODS: Nanoparticles of an Aluminium-Copper alloy in an 80%Al-20%Cu percentage were obtained from Advanced Powder Technologies LLC. The base fluid used was the mixture of sodium and potassium nitrates known as solar salt (60% and 40% wt. respectively. Labkem, analytical grade ACS). Nanofluids consisting of solar salt and Al/Cu nanoparticles with mass concentrations of 0.5%, 1%, 1.5%, 5% and 10% were synthesized adding the nanoparticles to the previously mixed nitrates and mechanically blending.

The nePCMs were observed by TEM (JEOL-JEM 2100) and SEM (JEOL-JSM 6510) to analyse their morphology, size, shell thickness and distribution in the base fluid.

Differential Scanning Calorimetry (DSC2, Mettler Toledo) was used to study the melting and crystallization processes regarding temperatures, phase-change enthalpies and their evolution through thermal cycling. Besides, specific heat was measured at 300, 350 and 400°C.

RESULTS AND CONCLUSIONS: The suitability of Al/Cu nePCM in nanofluids for their use in thermal engineering applications has been tested. Figure 1 shows some example of the results. Figure 1a) depicts the DSC analysis of Al/Cu nePCM where the melting and crystallization peaks are shown. It can be observed that there is very little supercooling in this nePCM. Figures 1b) and 1c) show the resistance of the nePCM to thermal cycling, both alone and in the nanofluid proving the oxide encapsulation is resistant to working conditions.
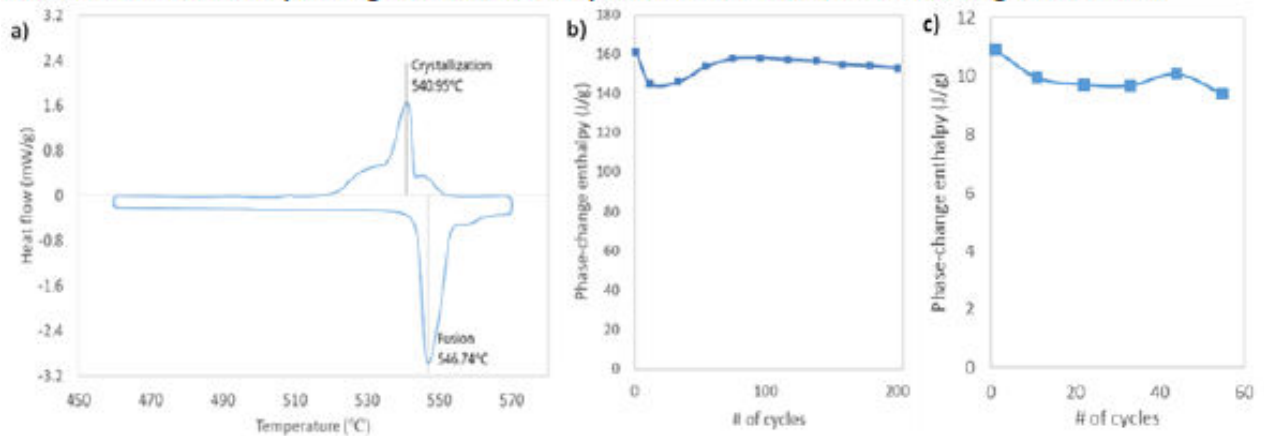
Fig 1. a) DSC of Al/Cu nePCM with fusion and crystallisation peaks marked. b) Evolution of phase-change enthalpies through thermal cycling (nePCM). c) Evolution of the enthalpies when immersed in the nanofluid.

Taking into account changes in specific heat and the contribution of the latent heat from the nePCM, increases in heat capacity from 0.2% up to 7.8% have been registered for the higher concentration nanofluids (5% and 10% mass loadings) with respect to the base fluid alone.

REFERENCES:

[1] Taylor, R. et al. "Small particles, big impacts: A review of the diverse applications of nanofluids", J. Appl. Phys., 113, 011301 (2013)

[2] Shin, D., Tiznobaik, H., Banerjee, D., "Specific heat mechanism of molten salt nanofluids", Appl. Phys. Lett., 104, 121914 (2014)

[3] Cingarapu, S. et al. "Use of encapsulated zinc particles in a eutectic chloride salt to enhance thermal energy storage capacity for concentrated solar power" Renew. Ener. 80, 508-516 (2015)

[4] Navarrete, N. et al. "Nanofluid based on self-nanoencapsulated metal/metal alloys phase change materials with tuneable crystallisation temperature", Sci. Rep., 7, 17580 (2017)

Corrosion properties of nanofluids based on molten nitrate salts for thermal energy storage applications

Nithiyanantham Udayashankar[1], Yaroslav Grosu[2], Luis González[3], Abdessamad Faik[4]

[1]M.Sc, Ph.D-Student; [2]PhD, Associate researcher; [3]PhD, Postdoctoral researcher; [4]PhD, Group Leader.
Address: CIC Energigune, Albert Einstein 48, 01510 Miñano (Álava), Spain.
Phone: +34 945297108. E-mail: afaik@cicenergigune.com.

Keywords: Corrosion, Nanofluid, Molten salt, Thermal energy storage, Carbon steel (CS)

Introduction

Nowadays, rapid increase of renewables with simultaneous decrease of fusil fuels share in the overall energy consumption is considered mandatory worldwide. Concentrated solar power (CSP) is considered as one of the most efficient technologies taking advantage of its relatively simple method for energy storage in the form of heat - thermal energy storage (TES). The use of TES for electricity production has provided several important benefits, like lower environmental impact and higher dispatchability compared to other methods [1]. Different combinations of alkaline salt mixture were used to store the thermal energy for CSP. The salt combinations were $NaNO_3$–KNO_3 (60:40 wt%), $NaNO_3$–KNO_3-$NaNO_2$ (7:53:40 wt%) and $NaNO_3$–KNO_3- $Ca(NaNO_3)_2$ (15:43:42 wt%) etc. [2]. Currently binary $NaNO_3$-KNO_3 molten salt is used in most of the commercial plants due to the acceptable operating temperature and compatibility [1]. Many investigations were focused on the enhancement of thermophysical properties of molten salts (heat capacity, thermal conductivity) by the addition of minor percentage of the nanoparticle - molten salt based nanofluids. The results already had shown the enhancement of the specific heat capacity, thermal conductivity and enthalpy when SiO_2, Al_2O_3, TiO_2 nanoparticles were used [3-5]. Although, the enhancement of thermophysical properties was achieved, the corrosion aspects of molten salt nanofluids need to be investigated. There is a very few works on corrosion properties of such nanofluids. Recently, it was demonstrated the corrosion rates increase for HitecXL (($NaNO_3$–KNO_3- $Ca(NaNO_3)_2$ (15:43:42 wt%)) based nanofluids at 310 °C as compared to the pure HitecXL [6].

The present work mainly focused on the corrosion properties of binary nitrate eutectic salt nanofluid formed by $NaNO_3$-KNO_3 nitrates and Al_2O_3 and SiO_2 nanoparticles. Such properties were demonstrated for common construction material - carbon steel A516.Gr70 at 390 °C for the exposure time periods of 250, 500, 1000 and 1500 hours. The corrosion rates were found and were demonstrated to be considerably affected by the presence of nanoparticles in the molten nanofluid. Particularly, the presence of nanoparticles decreases the corrosion layer thickness more than twice. From SEM-EDX and XRD analysis the mechanisms as well as the reasons for observed results were revealed. It was demonstrated that incorporation of nanoparticles into corrosion-oxide layer may be responsible for its stabilization and lowering corrosion rates. Obtained results were compared to the previous study on the corrosivity of HitecXL based nanofluid in order to formulate some general anticorrosion guidelines for molten salt based nanofluids [6].

Experimental

The immersion corrosion tests were conducted under atmospheric conditions for carbon steel A516.Gr70 in contact with eutectic $NaNO_3$-KNO_3 salt, eutectic salt + 1 wt% of Al_2O_3 NPs and eutectic salt + 1 wt% of SiO_2 NPs. The eutectic salt was prepared by melting of 51wt% $NaNO_3$ and 49 wt% KNO_3. The nanofluids were prepared by an innovative dry method by using 1 wt% Al_2O_3 and SiO_2 nanoparticles. Experiments at 390 °C of 250, 500, 1000, 1500 hours were conducted. The samples before and after the corrosion tests were analysed by means of SEM-EDX (surface and cross section), XRD and mass variation. In addition, differential scanning calorimetry (DSC) and thermal gravimetric analysis (TGA) were applied in order to verify the absence of fluid degradation after 1500 hours corrosion test. As an example, figure 1 shows the SEM images of the cross section of carbon steel after 1500 corrosion tests with pure molten salt, Al_2O_3 based nanofluid and SiO_2 based nanofluid.

Eutectic salt   Eutectic salt + 1% Al_2O_3 NPs   Eutectic salt + 1% SiO_2 NPs
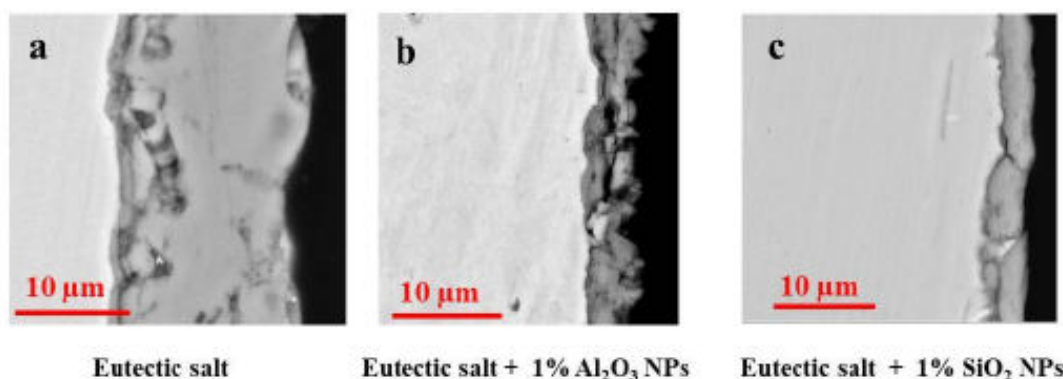
Figure 1. SEM images of the cross section of carbon steel after 1500 hours corrosion tests at 390 °C with a) pure molten salt, b) molten salt + Al_2O_3 NPs, c) molten salt + SiO_2 NPs.

Conclusion

From the performed analyses, oxidation was determined as the main mechanism of carbon steel degradation upon high-temperature corrosion tests with molten nitrate salt. It was found that adding 1%wt of Al_2O_3 and SiO_2 nanoparticles in this salt decreases more than twice the corrosion layer thickness compared to the pure salt. That was explained by observed incorporation of Al_2O_3 and SiO_2 nanoparticle into the corrosion layer. By comparing the obtained results with previous study, it was concluded that adding nanoparticles can have both positive and negative effect on the corrosivity of nanofluid depending on the conditions of the test (temperature for example). It was shown that it is particularly important to control the conditions of microbubbles formation in nanofluid, which enhances the oxidation process.

References

1. E. González-Roubaud, D. Pérez-Osorio, C. Prieto, Renewable and Sustainable Energy Reviews 80 (2017) 133–148.
2. Y.Y. Chen, C.Y. Zhao, Solar Energy 146 (2017) 172–179.
3. Shin D, Banerjee D. Int J Heat Mass Transf 84 (2015) 898–902.
4. B. Ma, D. Banerjee, AIP Adv. 7 (2017) 115124. doi:10.1063/1.5007885.
5. M. Chieruzzi, G. F. Cerritelli, A. Miliozzi, J. M. Kenny, Nanoscale Res.Lett.8 (2013) 448.
6. Y. Grosu, N. Udayashankar, O. Bondarchuk, L. González-Fernández, A. Faik, Solar Energy Materials and Solar Cells 178 (2018) 91–97.

Design and Characterization of Phase Change Material Nanoemulsions as Thermal Energy Storage and Transport Media

Filippo Agresti [1], David Cabaleiro [2], Simona Barison [1,*], Laura Fedele [3], Stefano Rossi [3], M. A. Marcos [2], Louis Lugo [2], Sergio Bobbo [3]

[1] CNR ICMATE, Corso Stati Uniti 4, 35127 Padova, Italy

[2] Departamento de Física Aplicada, Facultade de Ciencias, Universidade de Vigo, Vigo, Spain

[3] CNR ITC, Corso Stati Uniti 4, 35127 Padova, Italy

[*]Corresponding e-mail: simona.barison@cnr.it

INTRODUCTION: Phase change materials, PCMs, have been presented as promising solutions to bridge the gap between energy request and its availability. Phase change material emulsions (PCMEs) or phase change slurries (PCS) have been largely investigated in the last years as potential working fluids which could be used to reduce energy consumption in HVAC systems.[1] They basically contain water and PCMs and as such do possess much larger energy storage capacity than currently used chilled water based systems and higher thermal conductivity of PCMs. Phase change material emulsions (PCMEs), consisting of PCM-droplets stabilized with appropriate surfactants in carrier fluids, are receiving increasing attention to face these limitations [1-2]. Nanometric-sized drops are desirable to ensure long-term stability and ease pumping during phase transition. Nevertheless, sub-cooling issues are typically observed in nanometric sized PCMEs [3]. Thus, a nucleating agent must be incorporated to the dispersed phase in order to reduce the temperature difference between melting and crystallization, a phenomenon that undesirably broadens the operating temperature range. This study presents the preparation and characterization of three different types of paraffin-in-water emulsions as potential thermal energy storage and transport media, covering the temperature range from 20 to 70 °C.

METHODS: PCM-in-water nanoemulsions were prepared by solvent-assisted emulsification and high-energy ultrasonication. Commercial RT55 and RT70HC paraffin waxes (Rubitherm GmbH) and pure n-heptadecane (Alfaesar, 99%) were used as disperse phases, sodium dodecyl sulphate (Alfa Aesar) was utilized as surfactant, while commercial RT55 and n-octacosane (Alfaesar, 99%) were considered as nucleating agents.

Drop size distributions in both solid and liquid states of PCMs were determined by Dynamic Light Scattering (DLS) using a Malvern Zetasizer Nano ZS apparatus. In order to evaluate stability in the long-term and after cycling, DLS measurements at room temperature were conducted for at least 30 days and repeated for 25 freeze-thaw cycles.

Latent heats and phase change temperatures were determined using two Differential Scanning Calorimeters (Setaram Instrumentation and Q2000 from TA Instruments). Thermal diffusivity was studied by a photoacoustic device and by a ThermTest TPS2500S Hot Disk Thermal Analyzer® (Hot Disk AB), while dynamic viscosity measurements were performed by an AR-G2 rheometer (TA Instruments), with a plate-cone geometry.

RESULTS AND CONCLUSIONS:

A peculiar solvent-assisted procedure has been developed to prepare PCM-in-water emulsions. With this procedure, stable PCMEs with PCM concentrations of 2, 4 and 10 wt% in water were prepared. All emulsions showed very high negative ζ-potentials, meaning a high colloidal stability that decreased in absolute value by increasing paraffin concentration. The reduction of ζ-potential reflected on the particle size that increased with paraffin concentration starting to a minimum of around 60 nm to a maximum of around 220 nm depending on paraffin. The stability was also verified during 25 repeated freeze-thaw cycles, as demonstrated in Figure 1.
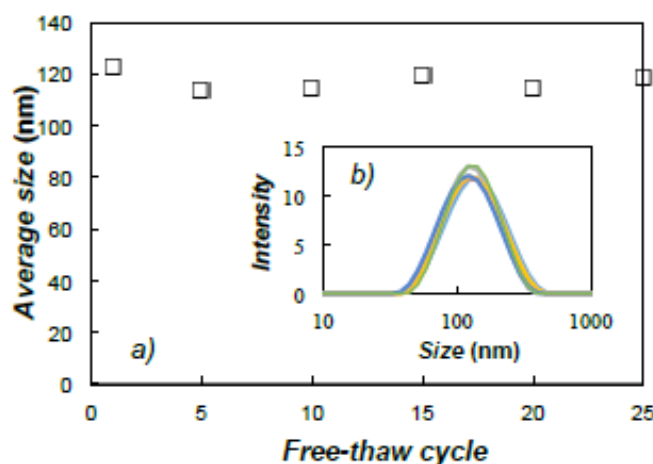
Figure 1. (a) Average size and (b) size distribution of 4wt.% heptadecane-in-water emulsion after repeated freeze-thaw cycles.

Thermal diffusivity measurements showed a moderate reduction of these values with respect to pure water, which increased with paraffin concentration due to the lower thermal diffusivity of paraffin. All samples showed a small increase in paraffin melting temperature, but particularly a sub-cooling effect, that can reach also 15-20°C below the solidification temperature. Therefore, various nucleating agents were tested and will be presented.

Considering the paraffin concentration and the reported heat of melting of bulk materials, the estimated heat of melting of paraffin into the emulsions was sensibly lower with respect to the expected values and this fact is under investigation. Moreover, the PCM particles size influence on PCMEs was investigated.

REFERENCES:
[1] J. Shao, J. Darkwa, G. Kokogiannakis, *Energ. Buildings*, 94 (2015) 200-217.
[2] S. Puupponen, A. Seppälä, O. Vartia, K. Saari, T. Ala-Nissilä, *Thermochim. Acta*, 601 (2015) 33-38.
[3] L. Huanga, E. Güntherb, C. Doetscha, H. Mehlingc, *Thermochim. Acta*, 509 (2010) 93-99.

Gold-silica core-shell nanoparticle dispersions in PEG400 as stable phase change materials for thermal energy storage

Marco A. Marcos[1], Martín Testa-Anta[1], David Cabaleiro[1,2], Verónica Salgueiriño[1],

Luis Lugo[1]

[1] Departamento de Física Aplicada, Universidade de Vigo, 36310, Vigo, Spain

[2] Istituto per le Tecnologie della Costruzione, Consiglio Nazionale delle Ricerche, 35127, Padova, Italy

*Corresponding author: david.cabaleiro@uvigo.es

INTRODUCTION: Energy has been and still is one of the fundamental bases for the progress of humanity and contributes directly to the well-being of societies. It is evident though that energy consumption has a negative impact on the environment and thus enhancing the performance of most thermal facilities has become mandatory. Energy storage allows improving the flexibility of thermal installations by correcting unforeseen imbalances between supply and demand, but also enhances their efficiency and maximize their use [1]. Among different energy storage technologies, phase change materials (PCMs) are particularly attractive due to their large densities of energy storage with reduced temperature differences. In order to face the two main problems preventing practical implementation of PCMs, namely subcooling and low heat transfer rates, the dispersion of additives with high thermal conductivities, also known as Nano-enhanced Phase Change Materials (NePCMs), has been proposed as a promising solution. In this study, new NePCMs were designed as dispersions of synthetized gold-silica core-shell nanoparticles, Au@SiO$_2$, in a poly(ethylene glycol) PEG400. The influence of Au@SiO$_2$ concentration on (solid-liquid) phase change characteristics and isobaric heat capacity were analysed in order to provide an insight about the potential of these materials to be used as thermal energy storage media.

METHODS: ~12 nm oleylamine-coated gold nanoparticles were synthesized by quickly injecting a solution of HAuCl$_4$ and oleylamine in toluene onto a boiling mixture containing toluene and oleylamine. After refluxing for two hours, the resultant gold nanoparticles were precipitated with ethanol, washed several times and redispersed in cyclohexane. In order to enhance their stability in poly(ethylene glycol), the as-prepared nanoparticles were coated with a silica shell by means of a water-cyclohexane reverse microemulsion, using Igepal CO-520 as surfactant, tetraethyl orthosilicate as silica precursor and ammonia as basic catalyst.

A pharmaceutical-grade poly(ethylene glycol) PEG400 supplied by Panreac AppliChem was used as base PCM. Molecular weight and purity of pure polymer were determined by electrospray ionisation mass spectrometry, while thermal stability was evaluated through

thermogravimetric analysis. NePCMs were prepared following a two-step method by dispersing Au@SiO$_2$ nanoparticles in the PEG400 with an ultrasonic bath (Ultrasounds, JP Selecta S.A.) working at 20 kHz and with a maximum power of 200 W. The long-term stability of dispersions was evaluated using a Zetasizer Nano ZS (Malvern Instruments) based on dynamic light scattering technique.

The (solid-liquid) phase transitions of the NePCMs were characterized in the temperature range from (193 to 315) K with a Q2000 (TA Instruments) differential scanning calorimeter, DSC, equipped with a RSC90 cooling system. This same device operating with the quasi-isothermal method (TMDSC) was also utilized to obtain isobaric heat capacities in both solid and liquid phases.

RESULTS AND CONCLUSIONS: Dispersed nanoparticles exhibit in NePCMs an average hydrodynamic diameter relatively close to those sizes observed by using Transmission Electron Microscopy, which indicates that no significant agglomeration occur. The addition of Au@SiO$_2$ does not show any remarkable penalty in isobaric heat capacity, within the studied nanoparticle concentration range. Figure 1 shows the thermograms obtained for base poly(ethylene glycol) and for the NePCM at 0.5% mass concentration, using a heating rate of 2 K·min^{-1} and cooling rates of 1, 5 and 10 K·min^{-1}.
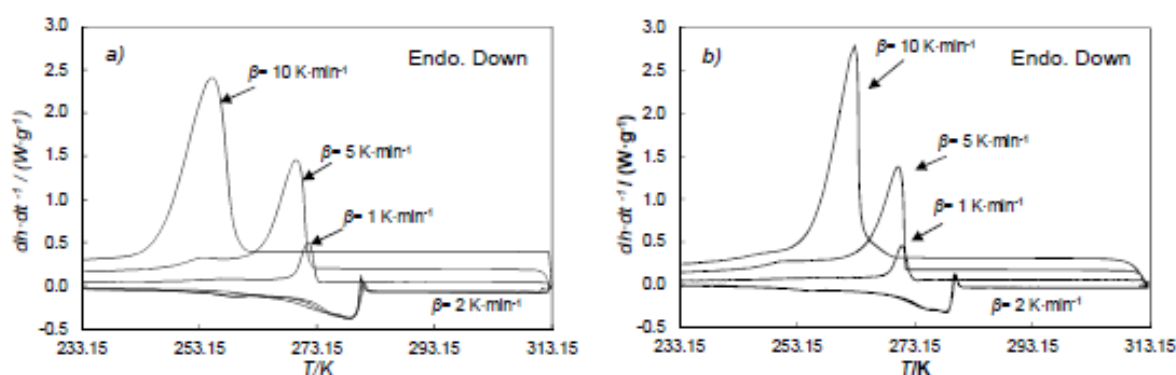
Figure 1. Thermograms obtained at 2 K·min^{-1} heating rate and different cooling rates for: a) PEG 400, b) 0.5 wt.% Au@SiO$_2$/PEG400 NePCM.

The addition of Au@SiO$_2$ nanoparticles eases the heat transfer and reduces subcooling by facilitating heterogeneous nucleation.

REFERENCES:
[1] A. Sharma, V.V. Tyagi, C.R. Chen, D. Buddhi, *Renew. Sust. Energy Rev.* 13 (2009) 318-345.
[2] M.A. Kibria, M.R. Anisur, M.H. Mahfuz, R. Saidur, I.H.S.C. Metselaar, *Energy Convers. Manage.* 95 (2015) 69-89.
[3] M.A. Marcos, D. Cabaleiro, M.J.G. Guimarey, M.J.P. Comuñas, L. Fedele, J. Fernández, L. Lugo, *Nanomaterials, 8* (2018)16.

Heat transfer study of nanosalt for solar energy storage

Afrah Awad [1,*], Dongsheng Wen [1,2]

[1] School of chemical and process engineering, University of Leeds, LS2 9JT, Leeds, UK.

[2] School of Aeronautic Science and Engineering, Beihang University, Beihang, China.

*Corresponding e-mail: mnata@leeds.ac.uk

Keywords: nano-nitrate salt (nanosalt), solar energy storage, thermal conductivity, experimental work, CFX of PCM/nano-PCM.

Abstract

My PhD project is about the solar energy storage system using the nitrate salt without and with nanoparticles as a storage medium. Nanoparticles could improve thermophysical properties of the nanosalt material. The specific heat capacity, latent heat and thermal conductivity of nanosalt were increased in comparison to the base nitrate salt without any additives [1]. We tested different types of nitrate salt such as the single salt (potassium nitrate, KNO_3) or the binary solar salt (sodium nitrate ($NaNO_3$): potassium nitrate (KNO_3) with 60:40 molar ratio). Furthermore, different types and concentrations of nanoparticles were studied such as iron oxide nanoparticle, copper oxide nanoparticles and titanium dioxide nanoparticles [1]. In addition, we studied the effect of the preparation method of nanosalt, as shown in Figures (1 and 2). The in-situ method was compared with the well-known two step method using same concentration and type of nanoparticles and the same base material [2]. In the one step method, the copper oxide nanoparticle was directly prepared inside the binary solar salt under different condition for the preparation procedure [2]. An improvement in the storage energy observed [2]. The other aspect of the PhD project is the large scale experimental setup [3]. In this experimental rig, the heat transfer is studied for nitrate salt and compared with nanosalt. In the experimental rig, temperatures were measured in different radial, axial and theta directions. The effect of nanoparticles types and concentrations were considered and an improvement in the charging process and the cooling process were obtained. The nanosalt showed faster charging and cooling processes than the nitrate salt without any additives. Additionally, a CFX code is built to study the heat transfer using the same dimensions of the experimental set up. The average value of the measured thermophysical properties (such as thermal conductivity and latent heat) were inserted in the CFX code. In addition, the cp of solid

phase and cp of liquid phase were function of temperature and measured using differential scanning calorimeter device. The density in the CFX code was function of temperature. The CFX code is validated with the experimental data and good matching is resulted as shown in Figure (3).
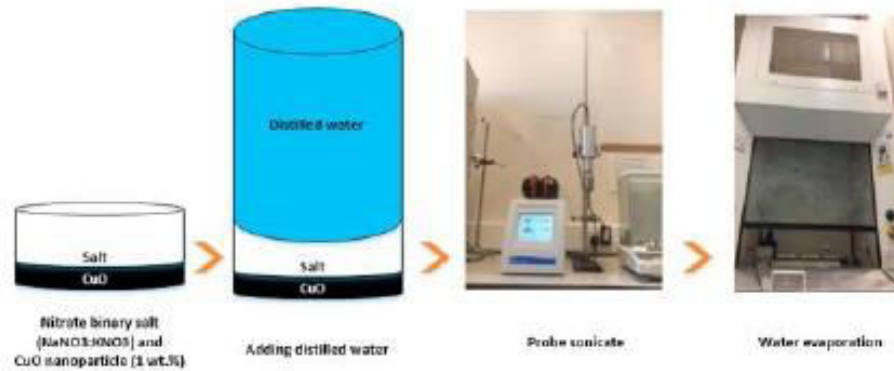
Figure (1) Shows the two-step method of nanosalt preparation.
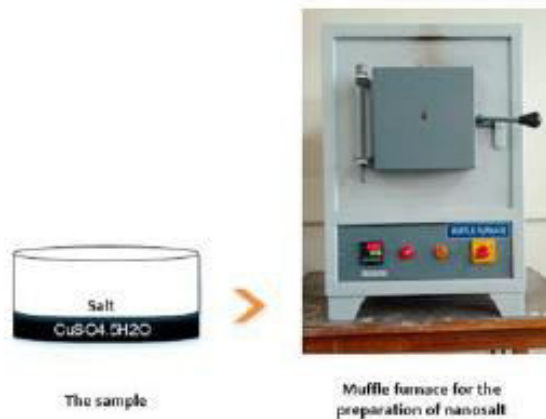
Figure (2) Shows the one-step method of nanosalt preparation.
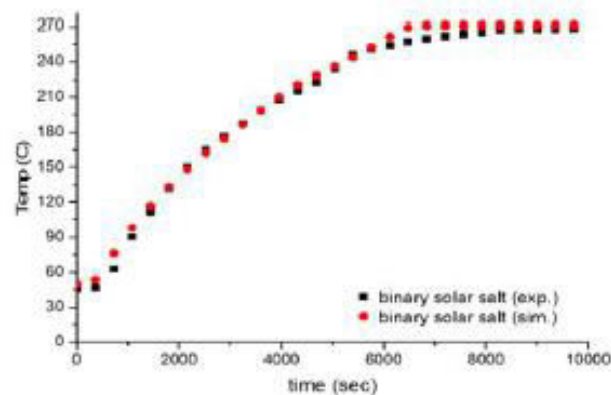
Figure (3) Show the transient temperatures distributions of solar salt (experimental vs simulation data)

REFERENCES:

[1] AWAD, A., NAVARRO, H., DING, Y. & WEN, D. 2018. Thermal-physical properties of nanoparticle-seeded nitrate molten salts. Renewable Energy, 120, 275-288.

[2] AWAD, A., BURNS, A., WALEED, M., AL-YASIRI, M. & WEN, D. 2018. Latent and sensible energy storage enhancement of nano-nitrate molten salt. Solar Energy.

[3] AWAD, A., Wen, D S. HEAT TRANSFER STUDY OF NITRATE SALT AND NANO-SALT AS ENERGY STORAGE MEDIA. The 16th International Heat Transfer Conference. Beijing: 2018, IHTC16-1234.

Progress Report about Two-phase CFD Simulations of a Heat Storage Device with Nanofluid

Peter Farber [1*], Christian Maraun[1.*], Peer Ueberholz[1]

[1] IMH - Institute of Modelling and High-Performance Computing, Hochschule Niederrhein, Reinarzstr. 49, 47798 Krefeld, Germany

*Corresponding e-mail: peter.farber@hsnr.de

Keywords: *Computational Fluid Dynamics, CFD, Nanofluid, Heat Storage*

INTRODUCTION: Thermal energy storage systems can be used if there is a difference between demand and supply of energy. There are several application areas, one of which is the storage of solar power [1].

Nanofluids can be beneficial for heat storage processes with phase change materials due to the increased thermal conductivity because this could lead to higher heat flux through the boundaries. On the other hand the higher dynamic viscosity of nanofluids compared to the base fluid may deteriorate the flow at the boundaries and therefore lower the heat flux. A literature research was conducted about nanofluids, heat storage devices and Computational Fluid Dynamics (CFD) simulations [2]. CFD is the numerical simulation of fluid flow together with heat and mass transfer [3]. CFD enhances the insight in the physical processes under investigation and reduces time-to-market and development cost of engineering systems. To our knowledge no publications about experiments of nanofluid heat storage devices in the sense of an engineering heat storage device with nanofluids investigated experimentally was found as well as no publication about CFD simulations of an engineering heat storage device with nanofluids is available. The CFD simulations with nanofluids focussed on forced convection heat transfer in tubes [e.g. 4] or on natural convection in enclosed cavities [e.g. 5].

To close this lack of knowledge a publication with experiment and CFD simulations of an engineering heat storage device with a phase change material without nanofluids presented in [6] was taken to set up a math. model of it and to validate it. The model was then enhanced with an Eulerian-Lagrangian model for the two-phase modelling of the nanoparticles and first simulations of the heat flux through the boundaries were conducted.

METHODS: For mesh generation Ansys ICEM CFD 17.1 and as the solver Ansys Fluent 17.1 was utilized. The equations solved were for the fluid the continuity equation, the momentum balance equation (to model the change between liquid and solid of the phase change material a porous domain is incorporated) and the energy balance equation with an enthalpy-porosity technique to model the transition domain between solid and liquid [7, 8]. For the nanoparticles Newtons second law was used to model the movement and the energy balance equation for every solid particle was utilised to calculate the temperature [7, 8]. A two-way coupling between particles and fluid was set to calculate the interaction between the

phases with respect to momentum and thermal energy. The working fluid was an eutectic mixture of potassium nitrate (KNO_3) and sodium nitrate ($NaNO_3$) with 54:46 wt. %. For the nanoparticles copper was used with a diameter of 100 nm and a concentration of 1.0 vol%.

RESULTS AND CONCLUSIONS: As the design or assessment parameter, i.e. the parameter of interest, the heat flux through the boundary was taken. Comparison of the experimental results without nanoparticles with the simulation outcomes (also without nanoparticles) show acceptable to good agreement.

The simulations with nanoparticles were applied to the charging and discharging process of the heat storage device. For modelling the particles not every single particle was calculated but instead so called parcels were used, were a specific number of particles is put together in a heap. Using the nanoparticles in the simulations for the discharging process converged solutions in time could be obtained, while for the charging process no converged solution in time could be achieved, due so far to unknown reasons. For the discharging process a strong influence of parcel size (i.e. number of particles in a parcel) on the heat flux was noticed. A solution converged with respect to the parcel size could be accomplished for the discharging. Another influence is the numerical mesh size. Meshes up to 16 million cells were investigated for the discharging. So far no mesh converged solution has been achieved. These preliminary results indicate that the heat flux through the boundary is higher for the simulations with nanoparticles. This research will be continued in the second half of 2018 using a 128 core compute cluster in order to achieve mesh converged solutions.

REFERENCES:

[1] Cingarapu S, Singh D, Timofeeva EV, Moravek MR (2015) Use of encapsulated zinc particles in a eutectic chloride salt to enhance thermal energy storage capacity for concentrated solar power. Renewable Energy (80): 508-516.
[2] Karacan A, Maraun K (2017) Modelling and simulation of heat storage with nanofluids using Computational Fluid Dynamics. Internal report (master project report), IMH - Institute of Modelling and High-Performance Computing, Hochschule Niederrhein, Krefeld, Germany, March 2017.
[3] Ferziger JH, Peri ́c M (1996) Computational methods for fluid dynamics. Springer, Berlin.
[4] Azari A, Kalbasi M, Rahimi M (2014) CFD and experimental investigation on heat transfer characteristics of alumina nanofluids under the laminar flow regime. Brazilian Journal of Chemical Engineering (31): 469-481
[5] Jang SP, Choi SUS (2004) Free convection in a rectangular cavity (Benard convection) with nanofluids. Proceedings of IMECE, Anaheim, California, USA, 13–19.
[6] Vogel J, Johnson M, Eck M, Laing D (2014) Numerical analysis of natural convection in a latent heat thermal energy storage system containing rectangular enclosures. Eurotherm Seminar #99, EUROTHERM99-01-074.
[7] Ansys Fluent Theory Guide 17.1, April 206
[8] Ansys Fluent Users Guide 17.1, April 2016

Thermal performance of organic phase change material in the presence of graphene nanoplatelets

Jose I. Prado[1,2], M. Tomás Alonso[1], José Fernández-Seara[2], Luis Lugo[1,*]

[1] Departamento de Física Aplicada, Facultade de Ciencias, Universidade de Vigo, 36310 Vigo, Spain

[2] Área de Máquinas e Motores Térmicos, Escola de Enxeñería Industrial, Universidade de Vigo, 36310, Vigo, Spain

*Corresponding e-mail: luis.lugo@uvigo.es

INTRODUCTION: Thermal Energy Storage, TES, with Phase Change Materials, PCMs, has been consolidating as a growing area of research. This can be illustrated by means of the increasing number of publications in the literature in the last two decades [1]. TES has a great number of applications such as space heating and cooling, domestic hot water production or solar energy storage [1].

Commonly used PCMs must have a phase change temperature in a desirable range, a high latent heat and a congruent and reproducible transition [2]. Most of these PCMs have low thermal conductivities, hindering heat transfer processes and so, restricting their field of use [1, 2]. Different possibilities to increase the thermal conductivity appeared in the last years, such us utilization of composites, addition of fins or use of nanoparticles [3]. Dispersions of nanoparticles into PCMs, named as Nano-enhanced Phase Change Materials, NePCMs, improves heat transfer but also the phase change transition, acting as nucleating agent [4].

In this work, graphene nanoplatelets dispersions in PureTemp® 8 for cold storage at mass concentrations of 0.5% and 1% were designed. Thermal performance of these dispersions has been characterized by measuring heat capacities, thermal conductivities, and densities.

METHODS: Graphene nanoplatelets, GnP, with a mass purity of 99.5% and a declared size of 11-15 nm were provided by IoLiTec (Heilbrom, Germany), while PureTemp® 8, PT8, was purchased from Entropy Solutions (Plymouth, USA). PT8 is characterized, according with manufacturer specifications, by a melting point of 281 K and a latent heat of 178 J·g^{-1}. Acetic acid was purchased from Sigma-Aldrich (St. Louis, USA) with a mass purity of 99.7% and a declared density of 1.049 kg·m^{-3}. Each component of the designed NePCMs was weighted in an analytical balance Sartorius CPA225 (Göttingen, Germany) with an uncertainty of 10^{-5} g.

The dry nanoplatelets were characterized by means of Transmission Electron Microscopy, TEM, analyses. The used microscope is a JEOL JEM-1010 TEM (JEOL, Tokyo, Japan) operating at an acceleration voltage of 100 kV. Nanoparticles exhibit a plate-like shape of up to some micrometers, as can be seen in Fig. 1.

Dispersions of nanoplatelets in PureTemp® 8, GnP/PT8, were performed following a two-step method. GnP were dispersed at 0.5 wt% and 1 wt% by means of an ultrasonic homogenizer Bandelin Sonopuls HD 2200 (Berlin, Germany) during 30 min.

0.5 μm
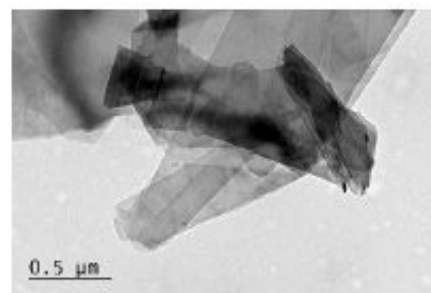
Figure 1. TEM image of dry GnP at x10,000 magnification.

Densities were experimentally obtained with a DMA 500 (Anton Paar, Graz, Austria) vibrating U-tube densimeter, with an estimated relative uncertainty of 0.1%. Thermal conductivities were determined by using a KD2 Pro Thermal Properties Analyser (Decagon Devices, Inc., Pullman, USA) coupled with a KS-1 probe of 1.3 mm diameter and 60 mm long. The estimated standard uncertainty is better than 0.01 $W \cdot m^{-1} \cdot K^{-1}$ for the 0.02-0.2 $W \cdot m^{-1} \cdot K^{-1}$ range. Heat capacities were measured by a Differential Scanning Calorimeter, DSC, Q2000 (TA Instruments, New Castle) with an estimated standard uncertainty better than 3% overall the entire temperature.

RESULTS AND CONCLUSIONS: Thermal conductivity and heat capacity of the base PCM and the designed NePCMs were measured in the temperature range from (283.15 to 333.15) K. Instead, density was measured in the temperature range from (288.15 to 313.15) K.

PT8 and GnP/PT8 dispersions exhibit low thermal conductivity values and a decreasing behaviour with the temperature as an organic material. Thermal conductivity enhancements of 12.6% and 23.5% were found for GnP/PT8 dispersions at 0.5 wt% and 1.0 wt% mass concentration, respectively. These enhancements have not temperature dependence.

REFERENCES:
[1] Pielichowska, K., Pielichowski, K., "Phase change materials for thermal energy storage", *Prog. Mater. Sci*, 65 (2014) 67-123.
[2] Sharma, A., Tyagi, V.V., Chen, C.R., Buddhi, D., "Review on thermal energy storage with phase change materials and applications", *Renew. Sust. Energ. Rev.*, 13 (2009) 318-345.
[3] Liu, L., Su, D., Tang, Y., Fang, G., "Thermal conductivity enhancement of phase change materials for thermal energy storage: A review", *Renew. Sust. Energ. Rev.*, 62 (2016) 305-317.
[4] Khodadadi, J.M., Fan, L., Babaei, H., "Thermal conductivity enhancement of nanostructure-based colloidal suspensions utilized as phase change materials for thermal energy storage: A review", *Renew. Sust. Energ. Rev.*, 24 (2013) 418-444.

Morphologies and thermal characterization on nanoparticle-seeded salt enhanced by metal foam

Xin Xiao[1,*], Dongsheng Wen[1, 2]

[1] School of Chemical and Process Engineering, University of Leeds, LS2 9JT, Leeds, United Kingdom

[2] School of Aeronautic Science and Engineering, Beihang University, 100191, Beijing, China

*Corresponding e-mail: x.xiao@leeds.ac.uk

INTRODUCTION: Energy crisis accelerate the development of utilization of renewable energy. Molten salts as a phase change material (PCM) can be a potential media for the storage of solar energy as one of renewable energy. HITEC salt (40 wt. % $NaNO_2$, 7 wt. % $NaNO_3$, 53 wt. % KNO_3) as a typical molten salt has been extensively studied. However, it normally exhibits low thermal conductivity, and effectively improving its thermal conductivity is of great interest. Impregnating PCMs into metal foam appears to be an effective way to compensate the low thermal conductivity, where it might decrese the latent heat and specific heat capacity of the composite to some extent. Dispersing nanoparticles into PCMs can keep and increase the specific heat capacity of the nanocomposite slightly. Thus the integration of metal foam and nanoparticles should be attractive to enhance the thermo-physical properties of pure salt. In this study, alumnium oxide (Al_2O_3) nanopowder seeded HITEC salt/copper foam composite were prepared and characterized.

METHODS: Sodium nitrite, sodium nitrate, and potassium nitrate were mixed with the mass ratios of 40:7:53, and Aluminium oxide nanopowder (Al_2O_3) and nickel with the porosity of 95% were used to enhance the thermo-physical properties of pure salt. Firstly, HITEC salt/Al_2O_3 nanocomposite was made with dissolution methods, as shown in Fig. 1(a). Pure salt was dissolved into deionized water, and Al_2O_3 with the mass fraction of 1%, 2% and 3% was dissolved in the suspension and the suspension was sonicated for good dispersion, respectively. Then copper foam with the porosity of 95% was physically immersed in the solution. Finally the solution with sonication was reheated in a oven at 250 °C to evaporate the water and make good impregnation. Then the porous copper foam impregnated with salt/Al_2O_3 nanocomposite was taken out (Fig. 1a). Subsequently scanning electron microscope (SEM) and X-Ray Micro Tomography were used to analyse the material morphologies and inner structure, and both X-ray diffraction (XRD) and Fourier Transform Infrared Spectrometer (FT-IS) were used as the suppliment of the component analysis. The effective thermal conductivities of the salt/copper foam composite seeded with Al_2O_3 nanopowder were theoretically predicted with the models, while differential scanning calorimeter (DSC) was used to characterize the phase change change behaviour of the composites.

RESULTS AND CONCLUSIONS: SEM image in Fig. 1b indicates that Al_2O_3 nanopowder and copper foam are compatible with salt, as no significant changes of wavelength peaks and intensities were found between pure salt and salt/Al_2O_3 nanocomposite (Fig. 1c). It was estimated that the effective thermal conductivity of the salt/3

wt. % Al_2O_3 nanocomposite is 0.818 W/(m K) with modified Maxwell-Garnett model, while that of the salt/copper foam composite seeded with Al_2O_3 is 8.32 W/(m K) using the Calmidi and Mahajan model [1-2], comparing with pure salt of about 0.7 W/(m K), as shown in Fig. 1d and 1e. In addition, slight variation of the extrapolated onset melting temperatures was found between pure salt and the composite. The composite PCMs with good physical and thermal characteristics can be the effective medium in the solar energy storage application.
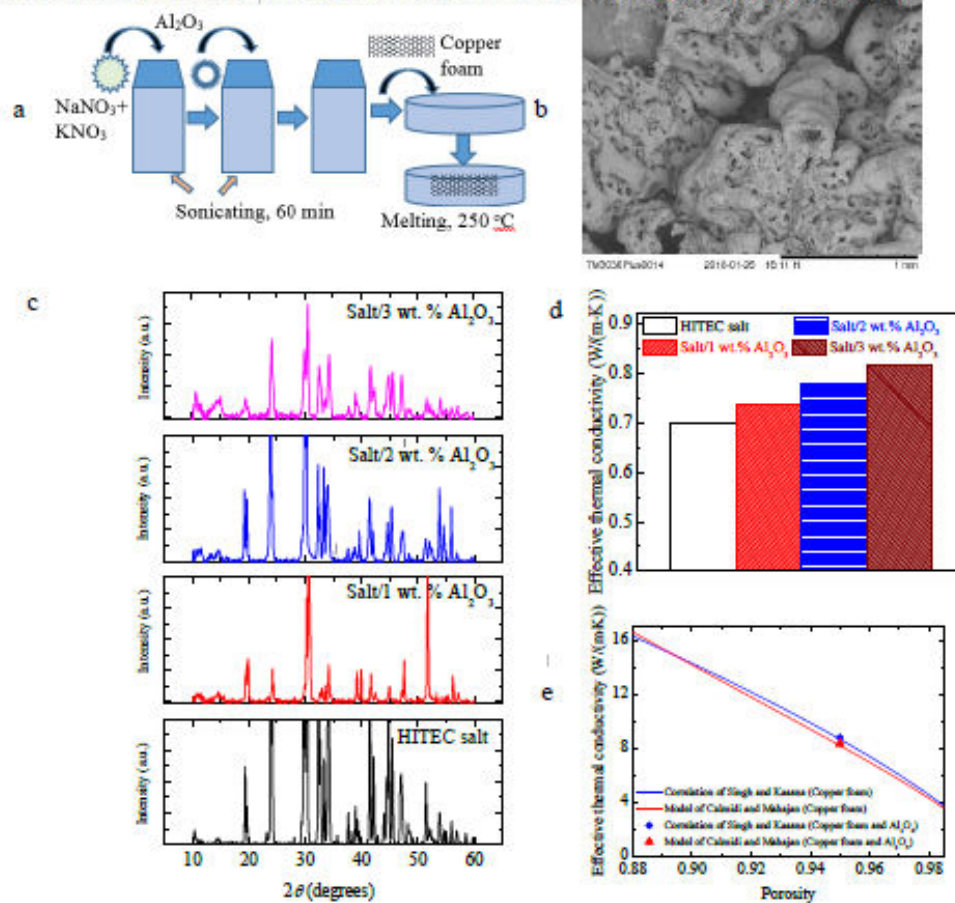
Figure 1: Preparation and thermal characterization of salt/copper foam composite seeded by Al_2O_3: synthesis process (a), SEM picture (b), XRD (c), effective thermal conductivities of salt/Al_2O_3 nanocomposites (d) and effective thermal conductivity (e).

REFERENCES:
[1] Siegel, N.P., Bradshaw, R.W., Cordaro, J.B., Kruizenga, A.M., "Thermophysical property measurement of nitrate salt heat transfer fluids," *Proc. of the ASME 2011 5th Int. Conf. on Energy Sustainability,* ES2011-54058, pp. 1-8, (2011).
[2] Xiao, X., Zhang, P., Li, M., "Effective thermal conductivity of open-cell metal foams impregnated with pure paraffin for latent heat storage," *Int. J Therm. Sci.,* 81, pp. 94-105, (2014).

Tailoring the properties of Nanoparticles by ALD Nanocoatings

D. Valdesueiro[*], A. Goulas and B. van Limpt

[1] Delft IMP B.V., Molengraaffsingel 10, 2629 JD, Delft, The Netherlands

[*]Corresponding author: d.valdesueiro@delft-imp.nl

In this paper we present a gas-phase coating technology, atomic layer deposition (ALD) that allows the deposition of nanometer-thin conformal coatings on a wide variety of particles (Figure 1). The versatility of ALD covers both the nature and size of the particles, as well as to the chemistry of the coating [1]. For example, particles ranging from nanoparticles to particles of several hundreds of micrometers can be coated with this technique. Additionally, the nature of the substrate can be ceramic (e.g. Al_2O_3, TiO_2, SiO_2), metallic (Ti), and polymeric (powder coating paints), amongst many others. The nature of the coating can be also selected from metal oxides (Al_2O_3) or nitrides (e.g. AlN), pure metals (e.g. Pt), organic coatings and even inorganic-organic hybrid coatings [2]. These thin films can be also used for nanofluid applications, achieving an encapsulation of the nanoparticles comprising the nanofluids without interfering with their intrinsic heat properties.

Figure 1. (left) Reaction mechanism of one cycle of atomic layer deposition. (right) Titanium oxide nanoparticles coated with aluminium oxide using ALD [3].

In recent years, atomic layer deposition (ALD) has become a standard tool to apply ultrathin and conformal coatings on substrates of complex geometries, mostly driven by an interest from semiconductor industry applications. The intrinsic advantages of controlling the structure growth at the (sub)nanometer level, while coating complex surfaces – either for providing protection to the substrate or boosting its activity – are also relevant for other industrial applications related to particle technology, such as nanofluids.

In this presentation we will also show one example of the influence of nanometer-thin aluminium oxide films used to encapsulate a polymer-based powder, which confined the softened core material without altering the thermal properties. That can be of use with nanofluids based on phase change materials.

This example aimed at tuning the surface finish of a standard polyester-based powder coating paint, from gloss to matt (Figure 2, left), by depositing ultrathin films of Al_2O_3 on the powder coating particles [4]. The coating experiments were performed in a fluidized bed reactor at 1 bar and 27 °C, using an alternating exposure of the particles to the two precursors (trimethylaluminium and water). By varying the number of coating cycles from 1 to 9, we deposited alumina films ranging from 1 to 30 nm. When the average alumina

shell was thicker than 6 nm, the shell prevented the flow of the core particles, even though the powder particles did soften above their glass transition temperature. With the particles morphology intact, this resulted in a rough and matte surface finish of the coating after curing. Additionally, the alumina coating acted as a barrier able to encapsulate the softened powder coating above the glass transition temperature, without altering other thermal properties as such as the glass transition temperature (Figure 2, right). This type of application can be extended to the encapsulation of phase change materials with thin alumina films, that would contain a molten core without modifying the thermal properties, which is of crucial importance in the development of efficient nanofluids.

Figure 2. (left) Tuning of the surface finish of the paint from gloss to matte depending on the thickness of the deposited aluminium oxide film. (right) Differential scanning calorimetry profiles of the uncoated and coated powder coating samples.

In this presentation we will show the process of depositing ultrathin films on particles with the coating technique atomic layer deposition, and will present an example on how the performance of a material can be tuned without altering other physical properties such as density, heat capacity, shape or size. Additionally, we will explain how the coating process works, and what can be further done with this versatile technique, aiming at a scaled up process able to produce coated particles at industrially relevant volumes. Finally, we will discuss how this technique could contribute to the development of new nanofluids. This technique can be interesting for this emerging application, since from other fields is has been proven that ultrathin films can enhanced the performance of other materials, perhaps applications for nanofluids being the next one.

References.

1. George, S.M., *Atomic layer deposition: An overview.* Chemical Reviews, 2010. **110**(1): p. 111-131.
2. Miikkulainen, V., et al., *Crystallinity of inorganic films grown by atomic layer deposition: Overview and general trends.* Journal of Applied Physics, 2013. **113**(2): p. 1-101.
3. Valdesueiro, D., et al., *Gas-Phase Deposition of Ultrathin Aluminium Oxide Films on Nanoparticles at Ambient Conditions.* Materials, 2015. **8**(3): p. 1249-1263.
4. Valdesueiro, D.H., H, et al., *Tuning roughness and gloss of powder coating paint by encapsulating the coating particles with thin Al2O3 films.* Submitted for publication, 2017.

WG 4

6. WG 4: Boiling, Solar Application, Modelling and Others

6. Working Group 4: Boiling, Solar Application, Modelling and Others

6.1. Castellón, Spain

Experimental Analysis of Nanofluid Pool Boiling in Plain and Nanostructured Surfaces

Simone Mancin[1,*], Luca Doretti[2]

[1] Dept. of Management and Engineering, University of Padova, Str.lla S. Nicola, 3, 36100, Vicenza, Italy.

[2] Dipartimento Ingegneria Civile Edile ed Ambientale, Università degli Studi di Padova, Via Venezia, 1, 35131,Padova, Italy.

*Corresponding e-mail: simone.mancin@unipd.it

Keywords: Nanofluid, Pool boiling, Deposition, Wettability

INTRODUCTION:

Pool boiling is widely used in many different engineering systems: chemical and nuclear reactors, refrigerating and air conditioning equipment, and electronic thermal management devices. Most of these applications have a common limitation: the maximum heat flux that can be rejected by the cooling systems under safe, reliable, and efficient operation.

The study of the pool boiling has been a topic of the worldwide research since 1934 when Nukiyama [1] conducted his experiments and developed the boiling curve in stagnant liquid. Nowadays, it is well known that surface treatments may provide effective boiling heat transfer enhancement, and many variants of treated surfaces have been developed. Several authors, among them [2-3], experimentally demonstrated the interesting enhancement capabilities of microparticle coatings on the Critical Heat Flux (CHF).

The recent work on nanoscale domain has led to new concepts for surface modification. In the last decade, nano-structured materials (i.e. nanowires coatings, nanoporous layers, Carbon Nano Tube arrays, ect.) have been proved to enhance the Nucleate Boiling (NB) by several authors. A comprehensive review can be found in [4] and among the cited works, we could highlight [5-7].

Another way to improve the boiling heat transfer is using fluid additives, for instance by seeding with a small concentration of nanoscale particles to produce a nanofluid. The heat transfer behaviour of nanofluids has been intensively studied by many researchers since the late 1990s. For nanofluids applications under pool boiling conditions, some significant, even though quite scattered, boiling enhancement has been reported [8-12] (from 10% to 400% on the CHF), which however contrasts significantly to others where large deterioration was reported [13-16]. As highlighted by Wen [17], the results were very inconsistent even for the same nanoparticle under similar experimental conditions. There are a few possible parameters affecting boiling heat transfer with nanofluids, which includes morphological and thermophysical properties of nanoparticles and nanofluids, the stability of nanofluids, the

content of nanofluids such as the presence of surfactants and ions, and the deposition and interactions of nanoparticles with the heating surface. As boiling heat transfer is very sensitive to surface characteristics especially the number and shape of potential nucleate sites, any change in the surface would probably result in different boiling behaviours. There is a general scientific agreement on the fact that the enhancement or the deterioration recorded during nanofluids NB are due to the modification of the surface through nanoparticles deposition.

The present research activity aims at rigorously investigating the nanofluids pool boiling in order to clearly asses the real potential improvement of this technique in obtaining either higher CHF values or new coated surfaces which can promote the NB performance.

METHODS:

The tests are run in a new experimental setup designed and built to study water and nanofluids pool boiling on flat, smooth and nanostructured, surfaces. The heater assembly consists of two copper heater blocks: the first one is the test sample while the second one contains 9 electrical cartridge heaters (200 W/240 V). The sample blocks were designed to have the main size equal to the Rayleigh-Taylor wavelength, being 27.2 mm in the case of water. Each copper block is glued in a Peek plate and presents a smooth or nanostructured (27.2 x 27.2 mm) top surface exposed to the working fluid. Two different boiling chambers were designed to analyze the confined and unconfined pool boiling; both chambers are constructed from two glass and two Peek 200 mm high walls, the sealing is accomplished by means of a set of Silicon o-ring cords.
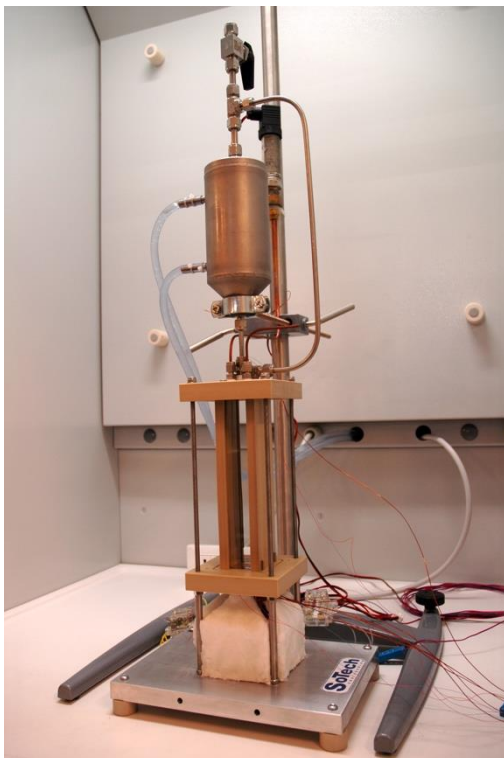
Photo of the experimental setup.

One chamber has exactly the same size of the heating block to study the confined pool boiling while the other presents a larger section (54.2 x 54.2 mm) to study the unconfined pool boiling. The sample is equipped with four calibrated T-type thermocouples located in as many 13.6 mm deep holes drilled every 5 mm from 1 mm below the top surface. The imposed heat flux and wall superheat can be estimated from the evaluation of the temperature gradient along the four thermocouples. Three additional calibrated T-type thermocouples were similarly located in the main heating copper block to verify the estimated heat flux. Finally, a high speed camera is used to visualize the boiling phenomenon and a SEM microscope with XPS detector are used to fully characterized the tested surfaces.

Furthermore, the Nano Heat Transfer lab is equipped with: a 25 MHz Sonicator Hielscher UP200S, a mechanical stirrer Heidolph RZR 2021, a ASEM EN RAK class "0" fume cabinet, and a Malver Zetasizer Nano ZS.

RESULTS AND CONCLUSIONS:

This research project is new and the experimental campaigns are undergoing.

[1] Nukiyama, J. of the Japan Society of Mech. Eng., 37(206) (1934) 367-374

[2] Hwang and Kaviany, Int. J. Heat Mass Transf. 49 (2006) 844-849

[3] Kim et al., J. Heat Transf. 124 (2002) 500-506

[4] Lu and Kandlikar, Heat Transf. Eng. 32 (10) (2011) 827-842

[5] Ujereh et al., Int. J. Heat Mass Transf. 50 (2007) 4023-4038

[6] Li et al., Adv. Funct. Mater. 18 (2008) 2215-2220

[7] El-Genk and Ali, Int. J. Multiphase Flow 36 (2010) 780-792

[8] Kedzierski, J. Heat Transf. 131 (2009) 043205

[9] Park and Jung, Int. J. Heat Mass Transf. 50 (2007) 4499-4502

[10] Liu et al., Int. J. Multiphase Flow 33 (2007) 1284-1295

[11] Park et al., Int. J. Multiphase Flow 35 (2009) 525-534

[12] Kathiravan et al., J. Heat Transf. 131 (2009) 081902

[13] Trisaksri and Wongwises, Int. J. Heat Mass Transf. 52 (2009) 1582-1588

[14] Kim and Kim, App. Phys. Lett. 91 (2007) 014104

[15] Bang and Chan, Int. J. Heat Mass Transf. 48 (2005) 2407-2419

[16] Das et al., Int. J. Heat Mass Transf. 46 (2003) 851-862

[17] Wen, Applied Therm. Eng. 41 (2012) 2-9

Pool Boiling Heat Transfer and Critical Heat Flux of Nanofluids

Zan Wu, Bengt Sunden

Department of Energy Sciences, Lund University, SE-22100, Lund, SWEDEN
*Corresponding e-mail: Zan Wu, zan.wu@energy.lth.se

Keywords: Nanofluids; pool boiling; heat transfer; critical heat flux; hybrid nanofluid

INTRODUCTION: Many industrial applications such as high-power electronic devices, nuclear and conventional power plants, refrigeration and air conditioning systems, manufacturing plants, automotive industry, to mention a few, rely on boiling to transfer large heat fluxes across system boundaries. Boiling heat transfer enhancement is an extremely important topic with huge relevance in existing, future and renewable energy systems as well as for energy conservation. The effectiveness of boiling heat transfer phenomenon can be greatly enhanced through careful control of the chemico-physical characteristics of the heat transfer surface [1-2]. A method to modify the heat-transfer surface is to deposit nanoparticles onto the surface to change the surface properties like wettability and porosity. The nucleation sites might also be affected by nanoparticles as some nanoparticles may fill the nucleation sites on the original surface or form new nucleation sites. Pool boiling of nanofluids is such a simple method as nanoparticles tend to deposit on the surface during the boiling process. Such nanoparticle depositions have a large potential to enhance the boiling critical heat flux (CHF), beyond which the nucleate boiling regime will transit to the film boiling regime – a very poor heat transfer mechanism covered by a vapor film. However, the pool boiling heat transfer coefficient (HTC) might increase or decrease depending on parameters like the thickness of the nanoparticle deposition layer. For thick layers, the HTC might be deteriorated as the thick porous deposition layer presents an additional and relatively large resistance to heat transfer.

METHODS: We have established a pool boiling test rig to experimentally investigate the effects of nanofluids on HTC and CHF. Different types of single-component nanofluids and hybrid nanofluid mixtures of different concentrations will be tested. It is important to note that only nanofluids without surfactant additions will be used for pool boiling in our experiments as a small amount of surfactant will also affect the boiling phenomenon and therefore complicate the analysis or confuse the effect of nanofluids on HTC and CHF. Specifically, we plan to do two series of experiments:

1. To monitor pool boiling of nanofluids with time at different heat flux levels. We can know the HTC trends with boiling time.
2. Pool boiling performance of pure fluids on surfaces with nanoparticle depositions. We know certain boiling times with decent heat transfer enhancements from step 1. We first boil the nanofluids at such boiling times at corresponding heat flux levels. Then we investigate the pool boiling performance of pure base fluids on such modified surfaces.

The surface morphologies of the heating surfaces before and after pool boiling of nanofluids will be characterized by SEM and TEM. These information are important to explain the HTC and CHF trends. More series of experiments might be planned based on the results of the above two series of experiments.

RESULTS AND CONCLUSIONS: Results are not ready yet as these tasks are ongoing.

REFERENCES:
[1] Attinger, D., Frankiewicz, C., Beta, A.R., Schutzius, T.M., Ganguly, R., Das, A.,. Kim, C.J, Megaridis, C.M. (2014). *MRS Energ. Sustain.*, 1, E4.
[2] Wu, Z., Sundén, B. (2014). *Renew. Sust. Energ. Rev.*, 40(1), 11-27.

Nanofluids Influence on the Thermal Behaviour of Loop Heat Pipes and Pulsating Heat Pipes

Roger R. Riehl

National Institute for Space Research, Space Mechanics and Control Division (INPE/DMC), 12227-010, Av dos Astronautas 1750, São José dos Campos, SP BRAZIL

*Corresponding e-mail: roger.riehl@inpe.br

Keywords: thermal control, heat pipes, loop heat pipes, nanofluids

INTRODUCTION: The increasing need for thermal management enhancement has guided researchers to look for new technologies and methodologies to improve the capabilities of active and passive thermal control systems. Due to physical limitations of regular heat transfer equipments, special attention has been given to the working fluid responsible to transport the heat absorbed on the source and dissipated on the sink. In this case, nanofluids have been seriously considered the next technological step for improving the heat transfer capabilities on both active and passive equipment. Since the nanofluid is formed by a base fluid with the addition of metallic nanoparticles. Depending on the material applied, the nanofluid can present important enhancements of its thermal characteristics when compared to the base fluid itself, specially related to its thermal conductivity improvement. With nanoparticles sizes below 40 nm, when added to the base fluid and properly mixed, they remain in suspension and act on the benefit of improving the thermal management system capability on the heat transfer process. However, the addition of metallic nanoparticles may directly influence on the increase of the working fluid's density and viscosity, which impact on the pumping requirements.

One of the great potentials upon applying nanofluids is the one related to passive thermal control systems, such as loop heat pipes and pulsating heat pipes, commonly used in aerospace and military applications. Improvements have been achieved upon using nanofluids on those passive thermal control systems [1-2], but since they operate by means of capillary pressure driving the working fluid, concerns related to the increase of the overall pressure drop can limit their use. Proper consideration regarding the nanoparticle and the base fluid must be taken to avoid the undesirable generation of non-condensable gases (NCGs) that could potentially limit the device's operating along time. It is important to continuously investigating the nanofluid influence on passive thermal control systems in order to better understand the direct effect on their thermal behaviour and also to contribute on the achievement of reliable designing tools for such an application.

METHODS: For the related application, different types of nanofluids were used depending on the thermal control device under analysis. Numerical and experimental methodologies were applied to better understand the direct effects of the nanofluid application on passive thermal

control devices, with the objective to develop reliable designing tool and analysis methodologies for future applications. Since the information currently available on nanofluids application are rather scattered [3], an adequate data reduction and analysis are required to effectively describe the effects of nanofluids on the overall transport behaviour of passive thermal control devices. For the loop heat pipes, a nanofluid made with water as base fluid and nickel nanoparticles was used, once this device presented a primary wick made from sintered nickel. Thus, minimizing the effect of NCG generation was the main goal on this research, even though water and nickel are not fully compatible. This selection was made due to the fact that the nickel nanoparticles presented a better suspension characteristics when compared to other base fluids. For the pulsating heat pipes, the nanofluid was made using water as the base fluid and copper nanoparticles, since their chemical compatibility and stability would allow this application due to the fact that the pulsating heat pipe was made from copper tubing. On both nanofluids, the mixing technique applied was with ultra-sonic bath with mixing time of 2 hours for the water-copper nanofluid and up to 4 hours for the water-nickel nanofluid. On both cases, a homogeneous solution was achieved with no sedimentation after at least 2 hours of the solution staying steady prior to its charging to the thermal control device.

RESULTS AND CONCLUSIONS: Upon operating the loop heat pipe, a comparison made for its thermal performance with the water-copper nanofluid was compared directly with its performance with water. For low heat loads, the loop heat pipe presented a sensible improvement on its operation as the evaporator's temperature was lower when using the nanofluid, with an enhancement around 25% on the heat transfer coefficient. However, at higher heat loads the loop heat pipe presents better thermal performance when operating with water, which can be as much as 45% better, as the nanofluid imposes a higher pressure drop to the working fluid to flow across the primary wick structure. Since the nanofluid's viscosity and density are higher than the base fluid alone, a direct impact was on the evaporator's temperature, which was higher for all heat loads tested. This indicates that the nanofluid, on the presence of a porous structure responsible for generating the capillary pressure that drives the working fluid throughout the loop faces a decrease on its transport properties capabilities.

For the operation with the pulsating heat pipe, substantial improvement on its thermal behaviour was observed when operating with the water-copper nanofluid when compared to its operation with water. The evaporator section temperatures were lower when operating with the nanofluid for all orientations tested, which could be 25% lower with the nanofluid compared to water. This is an important thermal characteristics for the pulsating heat pipe, since it is a wickless device and the dynamics of slug/plug generation is enhanced on the presence of nanoparticles. Since the nanoparticles were acting as nucleation sites, pulsations were more evident when the pulsating heat pipe was operating with the nanofluid, indicating that this device can be highly benefitted with the application of this technology.

Despite the lower thermal performance of the loop heat pipe operating with its related nanofluid, some applications that require its operation at reduced heat loads applied to the evaporator have been implemented in some projects. Also, due to its reliable operation, pulsating heat pipes using nanofluids have been applied to some applications, mainly related

to ground systems that present high heat transfer density. Results have demonstrated the potential on using nanofluids on the thermal management of highly sensitive equipment and surveillance systems, which opens a new frontier for the use of nanofluids.

REFERENCES:

[1] Riehl, R. R., Santos, N., "Water-Copper Nanofluid Application in an Open Loop Pulsating Heat Pipe", Applied Thermal Engineering 42, 2012, pp. 6-10.

[2] Riehl, R. R., Performance evaluation when using nanofluids in loop heat pipe and pulsating heat pipe, in: Proceedings of the 37th International Conference on Environmental Systems (ICES), July 10-15 (2007), Chicago, IL USA, paper 2007-01-3193.

[3] Marcelino, E., Oliveira, D., Riehl, R. R., "A Review on Thermal Performance of CuO-water Nanofluids Applied to Heat Pipes and Their Characteristics", ITherm - The Intersociety Conference on Thermal and Thermomechanical Phenomena in Electronic Systems, May 31 - June 3, Las Vegas, NV USA, 2016.

Carbon nanohorn-based nanofluids for solar thermal harvesting applications

Simona Barison[1,*], Laura Fedele[2], Filippo Agresti[1], Stefano Rossi[2], Sergio Bobbo[2], Cesare Pagura[1]

[1] Istituto di Chimica della Materia Condensata e di Tecnologie per l'Energia, Consiglio Nazionale delle Ricerche, Corso Stati Uniti, 4, 35127 Padova, Italy

[2] Istituto per le Tecnologie della Costruzione, Consiglio Nazionale delle Ricerche, Corso Stati Uniti, 4, 35127 Padova, Italy

[*]*Corresponding e-mail: simona.barison@cnr.it*

Keywords: nanofluid, stability, thermal conductivity, viscosity, volumetric solar absorption

INTRODUCTION:

In the last years, our groups started to research on nanofluids, considered as potential primary or secondary fluids in heating, air conditioning and refrigeration (HVACR) or solar applications.

As to solar applications, many absorber fluids have been characterized in literature as volumetric solar absorbers [1]. The addition of suspended particles is the key to optimize radiation collection and dimensions of absorbers units, thus improving efficiency and minimizing losses [2]. Among the carbon-based nanostructured materials, the carbon nanohorns (CNHs), that are graphene sheets wrapped to form structures like nanostars, have shown very promising characteristics of extinction coefficient and solar absorption in various fluids [3,4] particularly thanks to their peculiar morphology.

In particular, all the activities, supported by financed projects, focused on the synthesis of stable nanofluids, the stability investigation through DLS (Dynamic Light Scattering) analysis and dynamic viscosity and thermal conductivity characterization, followed by the optical absorption characterization performed in cooperation with CNR INO.

METHODS:

In the CNR-ICMATE and CNR-ITC laboratories, different facilities are available to perform synthesis and deep analysis of nanofluids.

At CNR ICMATE, various facilities allow the preparation of stable nanofluids both by single step or two-step methods. As to single step methods, there are the skills to produce various kinds of oxide or metal nanoparticles by chemical methods, with the possible aid of some facilities e.g. sonication, microwave-assisted processes, autothermal synthesis. As refer to two step methods, various processes have been studied in the last years to identify the best method to achieve stable suspensions depending on fluid and nanoparticles [5], among sonication, ball milling and high pressure homogenizer. The morphology of nanoparticles can be investigated by SEM or UV-Vis and the structure by XRD. The synthetic process can also be investigated by the aid of simultaneous thermogravimetric and differential scanning calorimetry analysis.

At CNR ICMATE the thermal conductivity of fluids can be characterized by a Laser flash thermal diffusivity apparatus or by a custom-built apparatus based on photoacoustic effect [6].

At CNR-ITC, nanofluids can be further characterized. A Zetasizer Nano ZS (Malvern), based on the Dynamic Light Scattering (DLS), can be used to analyse the average dimension of nanoparticles in solution. To determine the tendency of the particles in suspension to settle down along time, two samples of the selected fluid are measured almost every day for thirty days, one without shaking the fluid to evaluate the changes in size distribution due to natural sedimentation and the other after sonication to evaluate the changes in size distribution after mechanically removing the sedimentation. The Zeta potential of nanoparticles can be also measured. In general, the higher the Zeta potential, the higher the stability of the particles in suspension.

Thermal conductivity data are measured at ambient pressure by means of a TPS 2500 S (Hot Disk). The hot disk sensor is made of a double spiral of thin nickel wire, kapton insulated, and works as a continuous plane heat source. In case of liquids, the sensor is immersed in the fluid and a full contact is provided.

The dynamic viscosity is measured at ambient pressure by means of an AR-G2 rheometer (TA Instruments). It is a rotational rheometer, with a plate-cone geometry. A 1° cone, with a diameter of 40 mm, is employed. In order to stabilize the measurement temperature, an Upper Heated Plate (UHP) is used. All measurements are performed at constant temperature and variable shear rate. The declared dynamic viscosity measurement uncertainty is 5%. However, dynamic viscosity of water was measured at each temperature to assess the measurements accuracy (absolute average deviation between data and literature reference correlation below 2%).

RESULTS AND CONCLUSIONS:

Carbon nanohorns are tiny graphene sheets, wrapped to form horn-shaped cones with a half-fullerene cap, having 30–50 nm length and 2–5 nm diameter. They generally group together and form aggregates (spherical clusters or bundles), like nanostars [7]. These nanostructures were provided by Carbonium S.r.l. and were produced by a process based on rapid condensation of carbon atoms, without any catalyst and with highly reduced costs of production [8]. Fig. 1b shows a SEM picture of their morphology. The aggregation is due to the drying process in preparing the specimen for SEM observation. The mean size was evaluated through image analysis carried out on SEM micrographs by using ImageJ 1.46r software. The estimated mean diameter was (80 ± 6) nm.

The CNH dispersions with concentrations varying from 0.002 to 0.1 g/l in water and ethylene glycol were prepared by the following procedure: the CNHs were mechanically dispersed in a water solution containing sodium dodecyl sulphate (SDS) as surfactant (in various ratios) or in ethylene glycol without surfactants. With the procedure developed, long term stability was assured to the dispersions (no settling has been detected after a month) and was verified by a constant mean size of nanoparticles measured by DLS also 6 months after the preparation.

The scattering and spectrally resolved absorption properties were investigated at CNR INO, finding these nanofluids very interesting for increasing the overall efficiency of a thermal sunlight-exploiting device.[3,4]

REFERENCES:

[1]   T. P. Otanicar, P. E. Phelan, J. S. Golden, "Optical properties of liquids for direct absorption solar thermal energy systems," Solar Energy 83, 969–977 (2009).
[2]   R. Bertocchi, A. Kribus, J. Karni "Experimentally determined optical properties of a polydisperse carbon black cloud for a solar particle receiver", J. Sol. En. Eng. 126, 833-841 (2004).

[3]   E. Sani, S. Barison, C. Pagura, L. Mercatelli, P. Sansoni, D. Fontani, D. Jafrancesco, and F. Francini, "Carbon nanohorns-based nanofluids as direct sunlight absorbers", Optics Express, 18, 5179-5187 (2010).

[4]   E. Sani, L. Mercatelli, S. Barison, C. Pagura, F. Agresti, L. Colla, P. Sansoni, "Potential of carbon nanohorn-based suspensions for solar thermal collectors", Solar Energy Materials & Solar Cells, 95, 2994-3000 (2011).

[5]   L. Fedele, L. Colla, S. Barison, F. Agresti, "Experimental stability analysis of different water-based nanofluids", Nanoscale Res. Lett., 6, X1-8 (2011).

[6]   F. Agresti, A. Ferrario, S. Boldrini, A. Miozzo, F. Montagner, S. Barison, C. Pagura, M. Fabrizio, "Temperature controlled photoacoustic device for thermal diffusivity measurements of liquids and nanofluids" Thermochimica Acta, 619, 48-52 (2015).

[7]   S. Iijima, M. Yudasaka, R. Yamada, S. Bandow, K. Suenaga, F. Kokai and K. Takahashi, Chem. Phys. Lett., 309(3–4), 165 (1999).

[8]   C. Pagura, S. Barison, C. Mortalò, N. Comisso. M. Schiavon, Large scale and low cost production of pristine and oxidized Single Wall Carbon Nanohorns as material for hydrogen storage, Nanosci. Nanotech. Lett., 4, 160-164 (2012).

Optical properties of nanofluids for direct solar thermal harvesting

Elisa Sani*, Luca Mercatelli, Marco Meucci

Istituto Nazionale di Ottica, Consiglio Nazionale delle Ricerche, Largo Fermi 6, 50125 Firenze, Italy
*Corresponding author e-mail: elisa.sani@ino.it

Keywords: nanofluid, volumetric solar absorption, solar absorber, solar thermal

INTRODUCTION:

The assessment of optical properties of materials is needed for all applications requiring the interaction of the material itself with electromagnetic radiation. The INO-CNR group in Florence, Italy, is working from many years in the field of optical properties of materials, in particular for solar energy applications. Since 2009 we are working on nanofluids. We have investigated carbon-nanoparticle based nanofluids (carbon nanohorns [1-3]), nanofluids with metal nanoparticles [4] and mixed systems [5]. In addition, as in real sunlight exploitation systems the architecture needs to be optimized by optical ray tracing calculations, the real refractive index of the base fluid must be known. Thus, exploiting the extremely wide light wavelength range available for analysis in our laboratory, we have obtained optical constants (real and imaginary part of the complex refractive index) of ethylene glycol [6] with a method which can be applied also to other liquids.

METHODS:

The optical transmittance at room temperature in the range 190-3000 nm is measured using a double-beam spectrophotometer (PerkinElmer Lambda900). For diagnostic purposes and for the calculation of refractive index, the transmittance can be measured also in mid-infrared from $\sim$1.8 to $\sim$25 µm (wavenumber range 5500–400 cm^{-1}) using a Fourier transform "Excalibur" Bio-Rad spectrometer with KBr optics and in far-infrared from $\sim$24 to $\sim$55 (420–181 cm^{-1}) using a Fourier transform "Scimitar" Bio-Rad spectrometer with polyethylene windows and mylar beam splitter.

RESULTS AND CONCLUSIONS:

Carbon nanohorns (CNHs) consist of graphene sheets, wrapped to form tubules with an end closed by a half-fullerene cap. Typical lengths are 30–50 nm and diameters 2–5 nm. They assemble to form roughly spherical aggregates with different typical morphologies and diameters of about 100–120 nm [7].
We investigated light scattering and spectrally resolved light absorption properties of CNH suspensions dispersed both in water and in ethylene glycol in view of their use in a solar collector, at the same time as volumetric absorbers of sunlight and thermal transfer fluids. This scheme is able to overcome drawbacks of conventional solar receivers made by a black surface deposed on a metallic tube and transferring thermal energy to an exchange fluid flowing within the tube. Figure 1(a) shows the transmittance spectra of CNHs in water for

different nanoparticle concentration (10 mm path length), while Figure 1(b) compares the

absorbed sunlight fraction $F(x) = 1 - \dfrac{\int_{\lambda_{min}}^{\lambda_{MAX}} I(\lambda) \cdot e^{-\mu_a(\lambda)x} d\lambda}{\int_{\lambda_{min}}^{\lambda_{MAX}} I(\lambda) d\lambda}$ for water and glycol-based suspensions.
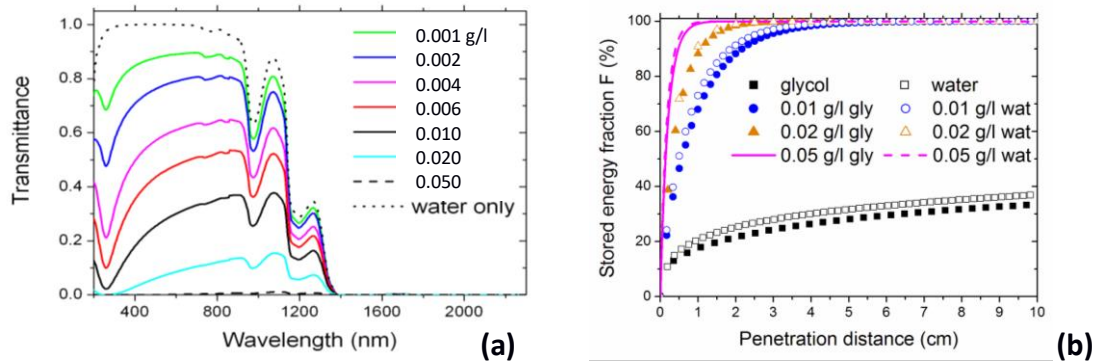
Figure 1. a) Transmittance spectra for CNHs in water for different nanoparticle concentrations; b) Comparison of sunlight absorption for glycol- and water-CNH nanofluids.

We can appreciate how CNHs considerably reduce the absorber transmittance with respect to the pure fluid even at very low concentrations and boost the amount of absorbed light. The volumetric absorption of sunlight should lead to reduced thermal emission losses with respect to conventional surface absorption [8], where the maximum temperature is always reached on the black surface itself.

REFERENCES:

[1] E. Sani, S. Barison, C. Pagura, L. Mercatelli, P. Sansoni, D. Fontani, D. Jafrancesco, and F. Francini, "Carbon nanohorns-based nanofluids as direct sunlight absorbers", Optics Express, 18, 5179 (2010).
[2] E. Sani, L. Mercatelli, S. Barison, C. Pagura, F. Agresti, L. Colla, P. Sansoni, "Potential of carbon nanohorn-based suspensions for solar thermal collectors", Solar Energy Materials & Solar Cells, 95, 2994 (2011).
[3] L. Mercatelli, E. Sani, A. Giannini, P. Di Ninni, F. Martelli, G. Zaccanti "Carbon nanohorn-based nanofluids: characterization of the spectral scattering albedo", Nanoscale Research Letters, 7, 96 (2012)
[4] R. Mondragon, R.O. Torres-Mendieta, M. Meucci, G. Mínguez-Vega, J.E. Julia, E. Sani, "Synthesis and characterization of gold/water nanofluids suitable for thermal applications produced by femtosecond laser radiation", J. Ph. Energy, in press (2016)
[5] E. Sani, P. Di Ninni, L. Colla, S. Barison, F. Agresti, Optical properties of mixed nanofluids containing carbon nanohorns and silver nanoparticles for solar energy applications, J. Nanosc. Nanotechn. 15, 3568 (2015)
[6] E. Sani, A. Dell'Oro "Optical constants of ethylene glycol over an extremely wide spectral range", Optical Materials, 37, 36 (2014)
[7] S. Iijima, M. Yudasaka, R. Yamada, S. Bandow, K. Suenaga, F. Kokai and K. Takahashi, Chem. Phys. Lett., 309, 165 (1999).
[8] A. Moradi, E. Sani, M. Simonetti, F. Francini, E. Chiavazzo, P. Asinari "Carbon-nanohorn based nanofluids for a direct absorption solar collector for civil application" J. Nanosc. Nanotechn. 15, 3488 (2015)

High stable nanofluids produced by Pulsed Laser Ablation in Liquids

O. Torres-Mendieta[1], R. Mondragón[2], E. Juliá[2*], O. Mendoza-Yero[1], J. Lancis[1], and G. Mínguez-Vega[1], E. Sani[3]

[1] GROC, UJI, Institut de Noves Tecnologies de la Imatge (INIT), Universitat Jaume I., 12080, Castelló, Spain.

[2] Departmento de Ingeniería Mecánica y Construcción, Universitat Jaume I., 12071, Castelló, Spain.

[3] Istituto Nazionale di Ottica, Consiglio Nazionale delle Ricerche, Largo Fermi 6, 50125 Firenze, Italy

*Corresponding e-mail: enrique.julia@uji.es

Keywords: nanofluid, stability, volumetric receiver

INTRODUCTION: A nanofluid is an engineered colloidal suspension composed of a heat transfer fluid and nanoparticles (NPs). The small size and weight of nanoparticles allows its Brownian motion inside the fluid avoiding sedimentation (if agglomeration is avoided). Solar nanofluids constitute an innovative type of nanofluids that are able to direct harvest solar radiation, they were proposed as a potential replacement of the classical heat transfer fluids in renewable solar thermal power applications [1]. The basic idea of a solar nanofluid is to improve the performance of heat transfer fluids by exploiting optical properties of NPs. The NPs inside the liquid will absorb directly solar radiation and they will transfer the heat to the fluid. The high specific area of NPs allows very fast and efficient heat transfer processes. In this way, a volumetric absorption within the solar fluid itself is promoted, which increases the photo-thermal efficiency of the heat transfer fluids by at least 10% [2].

The synthesis method of the NPs have a crucial impact on their physicochemical properties as well as the nanofluid stability [3]. Pulsed laser ablation in liquids (PLAL) technique has gained a lot of attention since 1987 when, for the first time, Patil et al. reported the laser ablation of a solid iron target in water [4]. The PLAL technique produces nanofluids using a single step procedure with high stability without the use of surfactants.

In this work gold NPs dispersed in water were produced by PLAL-PF and characterized. Thermal and optical properties of the nanofluids were measured and compared to those of available commercial nanofluids containing additives.

METHODS: Size and shape of primary nanoparticles as well as the formation of clusters of nanoparticles were observed by means of Transmission Electron Microscopy using a JEOL 2100 TEM. The elemental composition of the NPs was analysed by means of Energy Dispersive X-ray Spectroscopy using an EDX system (Oxford Instruments INCA Penta FETX3) attached to TEM.

The size distributions of nanoparticles in suspension were measured by dynamic light scattering (DLS) using a Zetasizer nano ZS (Malvern Instruments Ltd., UK). Optical transmittance spectra at room temperature have been measured using a double-beam UV-VIS spectrophotometer (PerkinElmer Lambda900). The thermal conductivity of all nanofluids was measured using a KD2 Pro conductimeter (Decagon Devices Inc.). The KD2 Pro is the commercial device that measures the thermal conductivity with the help of the transient hot wire technique.

Nanofluids produced by the PLAL-PF technique were compared to commercial nanofluids (Sigma Aldrich) containing gold nanoparticles with 20 nm nominal primary diameter dispersed in water and either stabilized in 1) 0.1 mM of phosphate buffered saline (PBS) solution or 2) stabilized in citrate buffer solution.

All samples were subjected to heating-cooling cycles in order to study the influence of the thermal treatment on the properties of nanoparticles and on nanofluid stability. To do this, samples were introduced in a sealed container and heated from room temperature to 100ºC in a hot bath. After 1 hour heating, nanofluids were cooled down to reach room temperature. A total number of 6 cycles were run for each sample. Table I lists the investigated samples.

RESULTS AND CONCLUSIONS:

a)   b)   c)
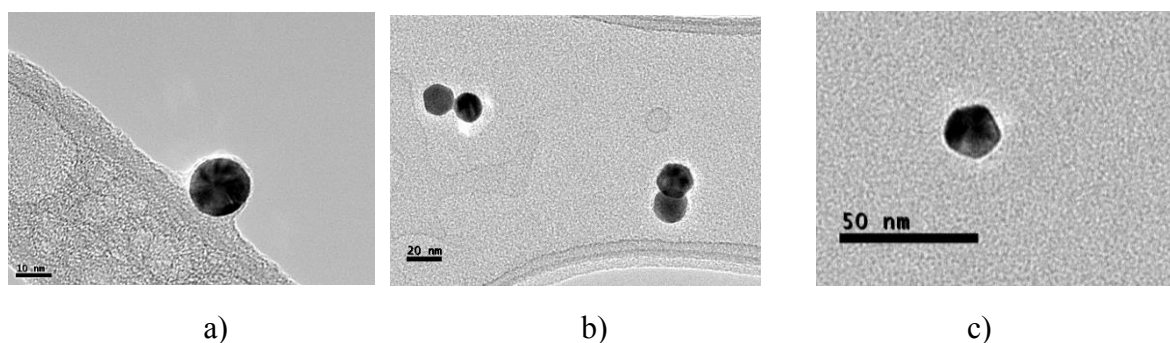
Figure 1. TEM micrographs of a) NPs produced by PLAL (S1), b) commercial NPs in PBS (S3) and c) commercial NPs in citrate buffer before cycling (S5).

In this work we have reported on the production, by means of the PLAL-NF technique without the use of chemical additives, of gold nanoparticles-based aqueous nanofluids. The laser-produced samples have been compared with PBS and citrate chemically-stabilized commercial suspensions as for composition, nanoparticle shape and size distribution, optical properties, thermal transfer coefficient and stability under thermal cycling. While offering the great advantage of a higher purity with no need of additional chemicals, PLAL-PF samples show physical properties comparable to commercial chemically-stabilized samples and in some cases even better, e.g. a higher sphericity of suspended particles. In all cases, nanofluids have been shown to be able to work in thermal cycling. PLAL-PF samples stability under cycling appears better than that of citrate samples and comparable to that of PBS stabilized-nanofluids. From the measured extinction coefficient and the calculated spectral scattering albedo, sunlight absorption characteristics have been assessed in the perspective to use gold-nanoparticles nanofluids as direct absorbers in solar collectors. It should be noticed that optical

absorption can be tuned by changing nanoparticle concentration and size. Moreover, it is known that thermal conductivity of nanofluids increases with the nanoparticle volume load. Thus, the advantage of using PLAL-PF technique, which produces stable nanofluids without chemical surfactants can be even larger when high nanoparticle concentrations are required.

REFERENCES: Please, include the references used in the extended abstract. References should be included in the text with brackets

1. T. P. Otanicar and P. E. Phelan, J. S. Golden, Sol. Energy 83, 969 (2009).

2. A. Lenert and E. N. Wang, Sol. Energy 86, 253 (2012).

3. T. Asahi, F. Mafuné, C. Rehbock and S. Barcikowski, Appl. Surf. Sci. 348, 1 (2015).

4. P. P. Patil, D. M. Phase, S. a. Kulkarni, S. V. Ghaisas, S. K. Kulkarni, S. M. Kanetkar, S. B. Ogale, and V. G. Bhide, Phys. Rev. Lett. 58, 238 (1987).

IoNanofluids for Thermal Applications

Carlos Nieto de Castro, S. M. Sohel Murshed, Maria José Lourenço, Fernando J. V. Santos, Manuel Matos Lopes, João M. P. França, Salomé I. C. Vieira, Francisco Bioucas

Centro de Química Estrutural, Faculdade de Ciências, Universidade de Lisboa, Campo Grande, 1749-016 Lisboa, Portugal

Keywords: Ionanofluids, nanoparticles, ionic liquids, Stability, Thermal systems

An IoNanofluid is defined as a stable dispersion of the nanomaterial in an ionic liquid (IL). Since we first reported the enhanced thermal conductivity of this new class of fluids with respect to the pure ionic liquid [1], many experimental and theoretical studies have been performed, using several nanomaterials like carbon nanotubes and graphene in various ILs. There are several reasons to study these emerging nanomaterials-ILs complex systems that can be summarized in the following points:

- Enhanced thermal properties for heat transfer and heat storage
- Complex interactions create nano-regions that enhance reactivity and selectivity of chemical reactions (nanocatalysis)
- IoNanofluids are designable and fine-tunable through base ILs to meet any specific application or task requirement
- Non-flammability and non-volatility at ambient conditions, environmentally friendly solvents, and reaction fluids

However, the success of its use in scientific or industrial applications depends how we analyze and characterize the emulsion prepared and its stability, as particle aggregation can destroy our purpose. Aggregation of nanoparticles (NPs) in ionic liquids is caused by a competition between Van der Waals (VDW) or polar forces and double layer (DL) forces screening caused by ions (DL), at the particle/IL interface. VDW forces are attractive and DL forces are repulsive. Balance between these forces control aggregation of NPs in ILs, and therefore the stability of a dispersion in the IoNanofluid. In the end, aggregation can originate phase separation, as explained in Fig. 1. Although achieving proper and long-term stability of such complex fluids is challenging, it is crucial for their application particularly in thermal systems.
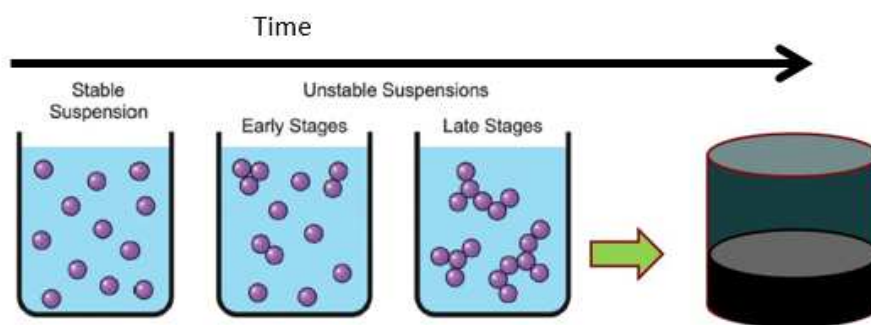
Fig. 1. Illustration of nanoparticle aggregation (partially adapted from [2]).

It is the purpose of this paper to give an overall view of the actual situation in the field, with special emphasis in the applications of IoNanofluids to thermal systems as new heat transfer fluids.

References:

[1] C.A. Nieto de Castro, M.J.V. Lourenço, A.P.C. Ribeiro, E. Langa, S. C. Vieira, P. Goodrich, C. Hardacre, J. Chem. Eng. Data 55 (2) (2010) 653–661
[2] Szilagyi et al., Phys. Chem. Chem. Phys. 16 (2014) 9515-9524

The rheological properties of silver nanofluids for enhancing thermal behaviour

T. Parametthanuwat[1]*, N. Bhuwakietkumjohn[1], S. Rittidech[2], and Y. Ding[3]

[1]Heat Pipe and Nanofluid Technology Research Unit

King Mongkut's University of Technology North Bangkok, Thailand

[2]Heat Pipe and Thermal Tool Design Research Unit (HTDR)

Division of Mechanical Engineering, Faculty of Engineering, Mahasarakham University, Thailand

[3]Birmingham Centre for Thermal Energy Storage School of Chemical Engineering

University of Birmingham: UK

*Corresponding e-mail: Thanya.p@fitm.kmutnb.ac.th

Keywords: Rheological properties, Rectangular thermosyphon, Potassium oleate surfactant, Aspect ratio and Relative thermal efficiency

INTRODUCTION: This research reports on the rheological properties of silver nanoparticle-based nanofluids (NF) containing potassium oleate surfactant (NFOAK$^+$) [1] for enhancing thermal behaviour applied as a working fluid in a two phase closed thermosyphon (TPCT) and a two phase closed rectangular cross sectional thermosyphon (RTPTC) [2]. It highlights theories for investigating NF properties such as the particles size, thermal conductivity, rheological behaviour and wet ability [1, 3]. Points of importance will be emphasized, with significance given to the thermal behaviour characteristics of TPCT and RTPCT and their use in this experiment [2].

METHODS: The study of integrated instruments for characterizing RTPTC was presented. The most important thermal behaviour characteristic to be examined in this experiment is the relative thermal efficiency. Five working fluids are: deionized water, 0.5 wt% silver nanoparticles-based nanofluids potassium oleate surfactant (OAK$^+$) with concentrations of 0.5, 1, and 1.5 wt% respectively. The TPCT and RTPCT were made from stainless tube (AISI-304). The length and circumference of TPCT and RTPCT were of equal size with the 3 aspect ratios of 5, 10 and 20. The heat supplied 20%, 40%, 60%, 80% and 100% from heater 2,000 Watts. The filling ratio was 30%, 50% and 80% in respect to the evaporator section volume [2].

RESULTS AND CONCLUSIONS: The NF containing OAK$^+$ showed a higher thermal behaviour characteristic than deionized water in all of the experimental conditions in this study. Expectedly, the thermal behaviour characteristic of RTPCT is superior in heat performance over all other experimental conditions studied when using NF containing OAK$^+$ at 1 wt% with relative thermal efficiency value of 1. Moreover, it was further found that the thermal behaviour had higher than the base fluid/nanofluids by approximately 80%.

REFERENCES:

1. Parametthanuwat, T., et al., *Experimental investigation on thermal properties of silver nanofluids.* International Journal of Heat and Fluid Flow, 2015. **56**: p. 80-90.
2. Bhuwakietkumjohn, N. and T. Parametthanuwat, *Heat transfer behaviour of silver particles containing oleic acid surfactant: application in a two phase closed rectangular cross sectional thermosyphon (RTPTC).* Heat and Mass Transfer, 2016: p. 1-12.
3. Parametthanuwat, T. and N. Bhuwakietkumjohn, *Application of Nanofluid in Thermosyphon (TPCT) - A review*, in *Nanotechnology fundamentals and applications*, J.N. Govil, Editor. 2013, Studium Press LLC.: U.S.A. p. 293-310.

Development of numerical methods for simulations of flow and heat transfer by nanofluids

J. Ravnik[*], J. Tibaut, L. Škerget

Faculty of Mechanical Engineering, University of Maribor, Smetanova 17, SI-2000 Maribor, Slovenia

Abstract

This document presents an abstract of the work to be presented at the working group *NFs in boiling and solar applications* meeting at Castellon de la Plana, Spain, $25^{th} - 26^{th}$ October 2016.

Keywords: boundary element method, fluid flow, heat transfer, velocity-vorticity, variable nanofluid properties

1. Introduction

Cooling is one of the major challenges in development of efficient devices. Choice of a working fluid is very important, as its thermal properties determine heat transfer characteristics. As thermal conductivity of water, oil and other working fluids are low, Choi [2] introduced nanofluids. Nanofluid is a suspension consisting of uniformly dispersed and suspended nanometre-sized (10–50 nm) particles in base fluid. Nanofluids have a very high thermal conductivity at a very low nanoparticle concentrations and exhibit considerable enhancement of convection. A wide variety of experimental and theoretical investigations have been performed, as well as several nanofluid preparation techniques have been proposed.

Several numerical methods have been proposed for the simulation of nanofluids. Garoosi [4] carried out a numerical study of natural and mixed convection heat transfer of nanofluid in a two-dimensional square cavity with several pairs of heat source-sinks using the finite volume method. Control

---

[*]Corresponding author.
Email address: `jure.ravnik@um.si` (J. Ravnik)

volume based finite element method was used by Seyyedi et al. [9] to simulate the natural convection heat transfer of Cu-water nanofluid in an annulus enclosure. El Abdallaoui et al. [1] used the lattice Boltzmann method for numerical simulation of natural convection between a decentered triangular heating cylinder and a square outer cylinder filled with a pure fluid or a nanofluid. Elshehabey et al. [3] developed a finite difference method for natural convection in an inclined L-shaped enclosure filled with Cu-water nanofluid that operates under differentially heated walls in the presence of an inclined magnetic field. Kefayati [5] used a finite difference lattice Boltzmann method heat transfer and entropy generation due to laminar natural convection in a square cavity.

2. Numerical method

At the working group meeting we will present a boundary element method based algorithm for simulation of flow and heat transfer of nanofluids. We formulate the Navier-Stokes equations in velocity-vorticity form and couple them with the energy conservation equation.

We consider three types of simulations. The simplest simulation considers the nanoparticles to be uniformly dispersed in the base fluid and thus the nanofluid suspension can be treated as a new fluid with constant effective material properties. This type of simulation can be performed using standards CFD codes without any modification. We used our in-house code to study nanofluid natural convection [7, 6].

Secondly, we developed an Euler-Lagrange type simulation, where nanoparticles are tracked in a Lagrangian manner. As the particles are nano-metre sized, their Stokes number is vary low and we may assume that they follow the fluid with the addition of Brownian motion and thermophretic effects. Based on particle locations at a specific time instant, the particle volume fraction is calculated and from there the nanofluid material properties. In this case, due to tracking of movement of particles, the material properties vary with location and time and depend on the velocity and temperature field in the fluid. We performed a heat enhancement study using 10^5 nanoparticles [8].

Currently we are developing the velocity-vorticity formulation of Navier-Stokes equations with temperature, location and time dependent nanofluid material properties, which are based on experimentally obtained correlations.

3. Results

Since we developed new numerical algorithms we have been testing and validating the algorithms against experimental and numerical data of other researchers. Grid sensitivity and time step sensitivity analyses have also been made.
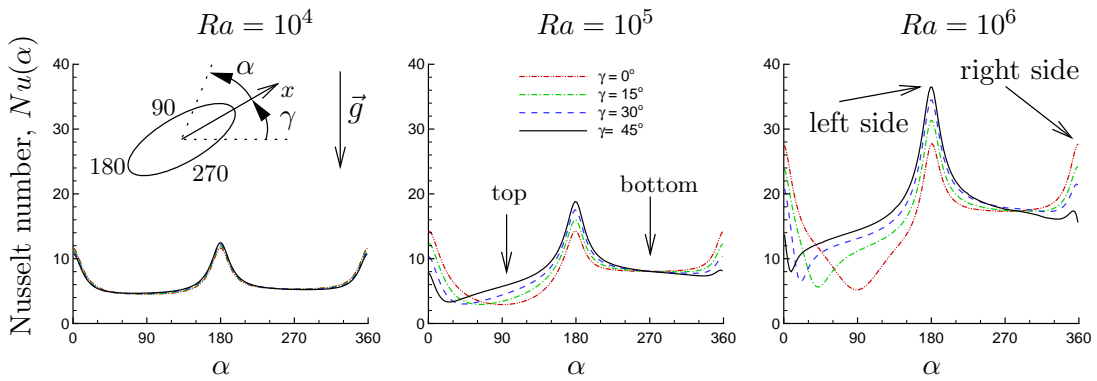
Figure 1: A hot ellipsoidal cylinder is placed in a nanofluid, around which natural convection develops. The charts show heat flux around the circumference of the ellipsoidal cylinder expressed as Nusselt number. Results of simulations of $\varphi = 0.1$ Al_2O_3 nanofluid are shown for three different cylidner temperatures. Results for different cylinder tilts γ against gravity are also presented, [6].

Several problems have been considered, among which nanofluid heat transfer enhancement for the case of a hot cylinder in a cold enclosure. Circular and elliptical cylinders were considered for various Rayleigh number values and inclinations against gravity. The main conclusions of the analysis are: (1) Use of nanofluid enhances heat transfer the most in the case, where the majority of the heat is transferred by conduction. In cases, where convection is the dominant heat transfer mechanism, the heat transfer enhancement due to the use of a nanofluid is lower. (2) Tilting the elliptical cylinder against gravity increases the heat transfer rate and changes the flow structure. The increase is small in flows, where conduction dominates, while it is larger in convection dominated flows. Furthermore it changes the locations on the cylinder, where lowest heat transfer is observed. (3) Comparison of 2D and 3D simulations shows, that 3D simulations yield slightly lower heat transfer rates. The difference is very small for conduction dominated flows, while in convection dominated flows it is larger.

References

[1] M El Abdallaoui, M Hasnaoui, and A Amahmid. Numerical simulation of natural convection between a decentered triangular heating cylinder and a square outer cylinder filled with a pure fluid or a nanofluid using the lattice Boltzmann method. *Powder Technology*, 277:193–205, 2015.

[2] S U S Choi. Enhancing thermal conductivity of fluids with nanoparticles. *Develop. Appl. Non Newtonian Flows*, 66:99–106, 1995.

[3] Hillal M Elshehabey, F M Hady, Sameh E Ahmed, and R A Mohamed. Numerical investigation for natural convection of a nanofluid in an inclined L-shaped cavity in the presence of an inclined magnetic field. *International Communications in Heat and Mass Transfer*, 57:228–238, 2014.

[4] Faroogh Garoosi, Gholamhossein Bagheri, and Mohammad Mehdi Rashidi. Two phase simulation of natural convection and mixed convection of the nanofluid in a square cavity. *Powder Technology*, 275:239–256, 2015.

[5] G H R Kefayati. FDLBM simulation of entropy generation due to natural convection in an enclosure filled with non-Newtonian nanofluid. *Powder Technology*, 273:176–190, 2015.

[6] J Ravnik and L Škerget. A numerical study of nanofluid natural convection in a cubic enclosure with a circular and an ellipsoidal cylinder. *International Journal of Heat and Mass Transfer*, 89:596–605, 2015.

[7] J. Ravnik, L. Škerget, and M. Hriberšek. Analysis of three-dimensional natural convection of nanofluids by BEM. *Engineering Analysis with Boundary Elements*, 34:1018–1030, 2010.

[8] J Ravnik, L Skerget, J Tibaut, and B W Yeigh. Solution of energy transport equation with variable material properties by BEM. In C A Brebbia, editor, *BEM/MRM 39*, Sienna, 2016. WIT Press.

[9] S M Seyyedi, M Dayyan, Soheil Soleimani, and E Ghasemi. Natural convection heat transfer under constant heat flux wall in a nanofluid filled annulus enclosure. *Ain Shams Engineering Journal*, 6(1):267–280, 2015.

Laser pyrolysis synthesis of Fe-Si-C nanoparticles and their evaluation for water-based nanofluids

MORJAN Ion[1], DUMITRACHE Florian[1,*], FLEACA Claudiu[1],
HUMINIC Gabeiela[2], HUMINIC Angel[2]

[1]Lasers Department, National Institute for Laser, Plasma and Radiation Physics (NILPRP) , PO Box MG-36, 077125, Magurele, Bucharest, Romania\
[2] Mechanical Engineering Department, Transilvania University of Brasov, 500036, Brasov, Romania

*Corresponding e-mail: dumitracheflorian@yahoo.com

Keywords: laser pyrolysis, nanoparticles, silicides, water-based nanofluid

INTRODUCTION:

The nanofluids can be defined as systems containing very small particles with sizes under 100 nm (nanoparticles) suspended in conventional liquids: water, oils or glycols [1] Due to their ultrasmall size and to the electrostatic and/or steric repulsions, the Brownian motion will prevail against the gravitationally-induced deposition of the suspended nanoparticles, contributing thus to the stability of nanofluids when compared with micron-size particles suspended in the same liquids. Generally, the introduction of nanoparticles in the base fluid enhances the thermal properties of the system, such as thermal conductivity and heat transfer coefficient. The composiotional diversity of the nanoparticles tested in nanofluids for thermal applications is very wide, from metals (such as Ag, Au, Al, Cu, Ni) or metal oxides (Al_2O3, CuO,MgO,TiO_2) to non-metalls such as carbon in various forms (nanotubes, nanoparticles, graphenes) or silicon and their compounds (SiO_2, SiC) [2]. Fe-containing nanoparticles also were studied for water-based nanofluids with enhanced thermal properties such as those reported by us based on iron oxide [3] or metallic-carbidic iron coarted with carbon [4] . In this work we report the synthesis of new ternary nanoparticles containing Fe-Si phases embedded in carbon shells.

METHODS: For the synthesis of Fe-Si-C nanoparticles we employed the one-step laser pyrolysis technique based by the intense absorption of Iinfrared CO_2 laser photons by some of the precursors, the silane which plays also the role of sensitizer together with the ethylene which also act as carbon source . The iron precursor is the volatile $Fe(CO)_5$ introduced as vapors together with C_2H_4, the CO from this precursor can be aloso a carbon source for thr resultedc particles. A visible soothing flame (surrounded byan inertAr flow) marks the reaction zone which generate the flow of nanoparticles, collected upstream on a porous filter. The powders were then dispersed in water with the aid of a powerful ultrasonication horn in the presence of polyelectrolyte sodium carboxymethylcellulose (CMCNa)

RESULTS AND CONCLUSIONS:

As synthesized powders were analyzed by EDS, XRD, Raman, TEM and FT-IR. The experimental studies revealed conditions to synthesis nanomaterials having a mixed crystalline structure containing nanocrystals of Si, FeSi and $FeSi_2$. When a reactive mixture with high silane percent (95%) were used nanoparticles having crystalline structure predominantly based on Si (19 nm mean size) with a minor contribution from $FeSi_2$ phase (with 11 nm mean size) are obtained. If the synthesis were performed from approximately flows of Si and Fe precursors and high laser power densities (more than 2500 W/cm^2) only nanoparticles with FeSi crystalline phase is evidenced. The experiment performed at low laser density generate nanoparticles containing also iron oxide: $Fe_3O_4/\gamma Fe_2O_3$ generated post-synthesis with oxygen from air. The average crystallite size and the ratio Si / Fe nanoparticles synthesized in equal ratio between silane and $Fe(CO)_5$ laser power density decreases. Preliminary studies involving the dispersion of these nanoparticles in aqueous media were performed. Even if the dispersions without stabilizers are generally unstable, some of the powders synthesized at low laser densities disperse better than the others. Some of the dispersions prepared from these nanopowdwer in the presence of CMCNa are more stable, others show a partial settlement, the unsettled separated fraction being very stable. Also, these nanofluids show an thermal conductivity enhancement compared with pure water.

REFERENCES:

[1] R. Taylor, S. Coulombe, T. Otanicar, P. Phelan, A. Gunawan, W. Lu, G. Rosengarten, R.Prasher, H.Tyagi, Small particles, big impacts: A review of the diverse applications of nanofluids, J. Appl. Phys. 113, 011301 (2013);

[2] J.P. Meyer, S.A. Adio, M. Sharifpur, P.N. Nwosu. The viscosity of nanofluids: a review of thetheoretical, empirical and numerical models, 37, 387-421, 2016

[3] F.Dumitrache, I. Morjan, C. Fleaca, A. Badoi, G. Manda, S. Pop, D. Marta, G. Huminic, A. Huminic, L. Vekas, C. Daia, O. Marinica, C. Luculescu, A.-M. Niculescu "Highly magnetic Fe_2O_3 nanoparticles synthesized by laser pyrolysis used for biological and heat transfer applications" Appl. Surf. Sci. 336 (2015) 297-303

[4] A. Huminic, G. Huminic, C. Fleaca, F. Dumitrache, I. Morjan "Thermal conductivity, viscosity and surface tension of nanofluids based on FeC nanoparticles" Powder Technol. 284 (2015) 78-84

AN EXPERIMENTAL STUDY OF HEAT TRANSFER COEFFICIENT AND INTERNAL CHARACTERISTICS OF NUCLEATE POOL BOILING OF NANAOFLUID R141B/TiO₂

O. Khliyeva[1]*, A. Nikulin [2], T. Gordeychuk [1], N. Lukianov [1] and Y. Semenyuk[1]

[1]Odessa National Academy of Food Technologies, Odessa, Kanatnaya str. 112, Ukraine

[2]Instituto Superior Técnico, Universidade de Lisboa, IN+, Lisbon, Portugal

*Corresponding author: khliyev@ukr.net

Keywords: Nanofluids, Pool boiling, Heat transfer coefficient, Internal characteristics of boiling process

Introduction: The main purpose of this study was to evaluate the effect of surfactant and TiO_2 nanoparticles additives into the refrigerant R141b on the heat transfer coefficient (HTC) and internal characteristics of the nucleate pool boiling process.

The experiments were carried out with the following substances: refrigerant R141b; solution R141b / surfactant Span-80 (0.1 % mass.) (CAS No. 1338-43-8, Sigma-Aldrich); nanofluid R141b / surfactant Span-80 (0.1 % mass.) / TiO_2 nanoparticles (0.1 % mass.). The size of TiO_2 nanoparticles (nanopowder) did not exceed 25 nm (CAS No. 1317-70-0, Sigma-Aldrich).

Discussion and Results: The two-step method was used to prepare the nanofluid. The nanofluid R141b / TiO_2 without surfactant was unstable and nanoparticles aggregation was observed. Although, as reported in paper [1] the stable nanofluid R141b / TiO_2 can be prepared without surfactants. The measurements of the mean size of nanoparticles (by spectro-turbidimetry method) in the R141b / surfactant / TiO_2 were carried out both during the experimental study of HTC and during storage within three months. It was found that nanofluid has a good aggregative stability with mean nanoparticle radius of 125 ± 7 nm.

The study of HTC during nucleate pool boiling was carried out using the original experimental setup [2] under the pressure of 0.2, 0.3 and 0.4 MPa and in the range of heat fluxes from 5 to 70 kW·m⁻². A stainless steel (AISI 321) capillary with 2 mm in diameter was used as a heating surface. The experimental results of HTC depending on heat flux are shown in the Fig. 1.a – 1.c.

The internal boiling characteristics (bubble departure diameter, bubble departure frequency and mean velocity of bubble growth) were studied experimentally under atmospheric pressure and in the range of heat fluxes from 29 to 57 kW·m⁻². The snapshots of boiling process were taken using the camera and the stroboscope. The exposure time was 50 μs and the intervals between flashes were 3 ms. During the obtained images processing (see Fig. 2) the number of bubbles was 80-140 to determine the mean bubble departure diameter $\bar{d}_0$ and 50-110 to determine the mean bubble departure frequency $\bar{f}$. The mean velocity of bubble growth $\bar{w}'' = \bar{d}_0 \times \bar{f}$ defined

by mean values of $\bar{d}_0$ and $\bar{f}$ is shown in the Fig. 3.
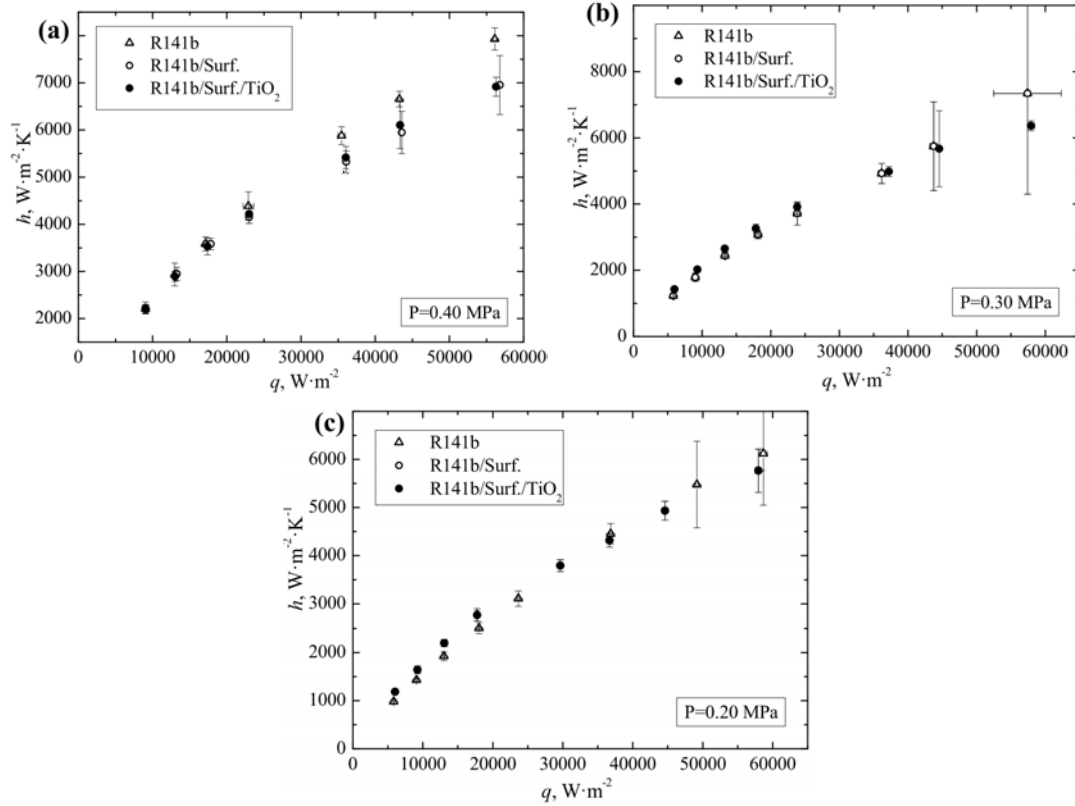
Figure 1. HTC and expanded uncertainty of experimental data for R141b / surfactant and R141b / surfactant / TiO$_2$ solutions in contrast with pure R141b: (a) 0.4·MPa, (b) 0.3·MPa, (c) 0.2·MPa

A comparison of the experimental values of HTC with calculated ones using the proposed by V.I. Tolubinsky [3] equation (1) has been carried out.

$$\frac{h}{k} = \sqrt{\frac{\sigma}{g(\rho'-\rho'')}} = 75\left(\frac{q}{h_{vap}\rho''\,\overline{w}''}\right)^{0.7}\left(\frac{\alpha}{\nu}\right)^{0.2} \tag{1}$$

where h is the heat transfer coefficient, W·m^{-2}·K^{-1}; k is the thermal conductivity, W·m^{-1}·K^{-1}; σ is the surface tension, N·m^{-1}; ρ' and ρ'' are the density of liquid and vapor respectively, kg·m^{-3}; q is the heat flux, W·m^{-2}; h_{vap} is the latent heat of vaporization, J·kg^{-1}; α is the thermal diffusivity, m^2·s^{-1}; ν is the kinematic viscosity, m^2·s^{-1}.

The experimental data on mean velocity of bubble growth $\overline{w}''$ were used in order to predict HTC by equation (1). To estimate the mean velocity of bubble growth at the pressures under which the experiments were performed the empirical equation (2) [3] was used.

$$\overline{w}''\big/\overline{w}''_{0.1} = \left(\rho''_{0.1}\big/\rho''\right)^{2.3+0.5lg\,\pi} \qquad (2)$$

where $\overline{w}''_{0.1}$ and $\rho_{0.1}$ are the mean velocity of bubble growth and vapor density at $P=0.1013\cdot$MPa respectively; $\pi = P\big/P_C$ is the reduced pressure.
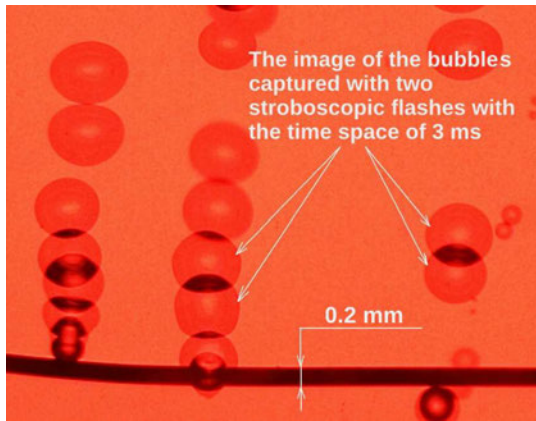
Figure 2. The snapshots of boiling process for R141b / surfactant at heat flux 29.6 kW·m^{-2} (150 pixel per 1 mm)
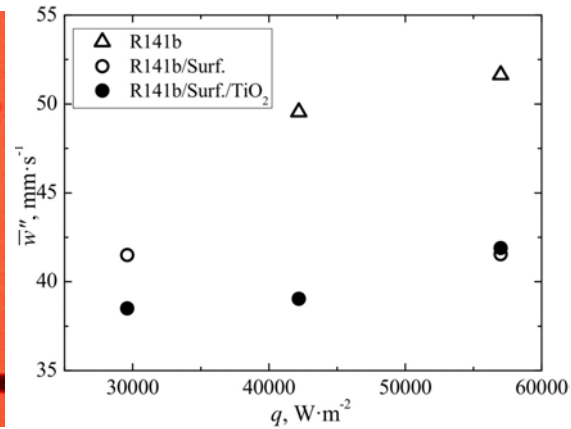
Figure 3. Mean velocity of bubble growth $\overline{w}''$ for R141b / surfactant and R141b / surfactant / TiO$_2$ solutions in contrast with pure R141b

The properties of pure R141b were used for HTC calculation using the eq. (1). However, it is known that the nanoparticles additives lead to increase in thermal conductivity and viscosity of base fluids. The information on nanofluids surface tension is rather scant in the published works. Nevertheless, it was shown in the paper [4] that the additives of 0.5 % mass. TiO$_2$ nanoparticles with oleic acid (as surfactant) into the solution of R600a / compressor oil leads to a slight decrease in surface tension.

Experimental and calculated HTC values depending on heat flux at P = 0.3 MPa are shown in Fig. 4.

Conclusions: As follow from the obtained data, the pool boiling heat transfer coefficient of R141b / surfactant / TiO$_2$ nanofluid is higher in contrast with R141b at low heat fluxes and lower at high heat fluxes. The most significant effect of nanoparticles additives on heat transfer coefficient enhancement was observed at low heat fluxes and pressure. The results of pool boiling HTC calculation by Eq.1 using the experimental values of mean velocity of bubble growth had shown a good agreement with the experimental HTC data for pure refrigerant.

At the same time, the calculated HTC data for the R141b / surfactant solution and R141b / surfactant / TiO$_2$ nanofluid is higher than experimental HTC. There are several explanations of such results. Firstly, the effect of nanoparticles and surfactant additives on the thermophysical properties was not taken into account. Secondly, the alteration in nucleation sites density during boiling caused by nanoparticles and surfactant additives to R141b also can effect HTC. Thus, the further studies of thermophysical properties and the nucleation sites density change on nanofluids pool boiling HTC are of high interest.
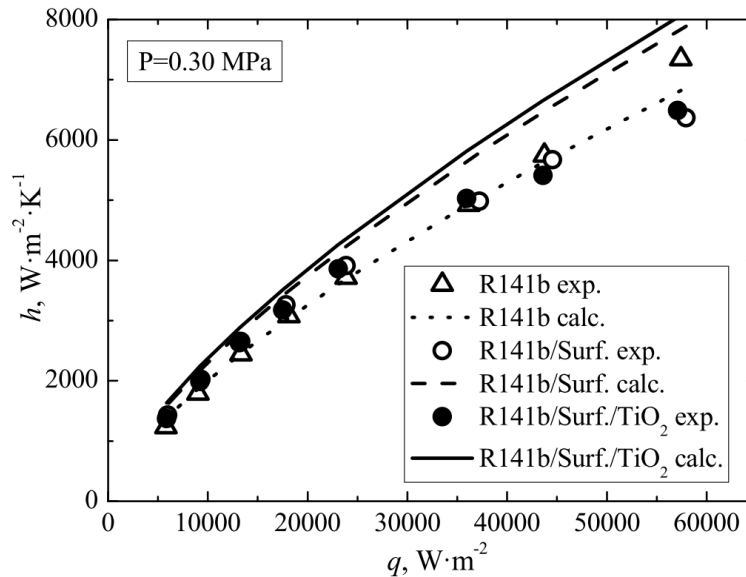
Figure 4. Experimental and calculated HTC for R141b / surfactant and R141b / surfactant / TiO₂ solutions in contrast with R141b.

References:

1. V. Trisaksri, S. Wongwises Nucleate pool boiling heat transfer of TiO₂–R141b nanofluids, *International Journal of Heat and Mass Transfer*, 52/5 (2009) 1582-1588.
2. A. Nikulin, A. Melnyk, Y Semenyuk, M. Lukianov, V. Zhelezny, Effect Of Nanoparticles On Pool Boiling Characteristics, *International Symposium on Convective Heat and Mass Transfer (CONV-14 ICHMT)*, Kusadasi, Turkey, 2014.
3. V.I. Tolubinskiy, Heat Transfer under Boiling (in Russian), Naukova Dumka, Kiev, 1980 (Chapters 4 and 5).
4. V. P. Zhelezny, N. N. Lukianov, O. Y. Khliyeva, A. S. Nikulina, A. V. Melnyk A complex investigation of the nanofluids R600a-mineral oil - AL2O3 and R600a-mineral oil - TiO2. Thermophysical properties, *International Journal of Refrigeration* 74 (2017) 486-502.

EXPERIMENTAL STUDY OF POOL BOILING HEAT TRANSFER ON NANOPARTICLE-DEPOSITED SURFACES

Z. Cao, Z. Wu, S. Abood and B. Sunden[*]

[1]Department of Energy Sciences, Lund University, Lund Sweden

*Corresponding author: bengt.sunden@energy.lth.se

Keywords: Pool boiling, Nanofluid, Al_2O_3, Graphene

Introduction: Heat transfer dissipation has been a major issue in many industries, such as power plants, electronic chip cooling, refrigeration systems and heat-exchanger systems [1]. Usually, the single-phase heat transfer cannot satisfy the requirements of heat removal in the aforementioned cases. Therefore, phase-change heat transfer, like pool boiling, is highly requested to facilitate transport of high heat flux at low superheat. Many factors can affect the performance of pool boiling heat transfer, like subcooling, the surface materials and morphology, properties of the liquid and nucleation sites density. Nanofluid, first reported by Choi [2] in 1995, is a new type of fluid by dispersing nanoparticles (1-100 nm) in the base fluids and has more preferable thermal properties. Compared with other technologies to enhance pool boiling heat transfer, nanofluid technology is an easier way to implement. Nanofluid boiling studies began to increase from 2003 and has become an important research branch until now [3].

Up to now, different type of nanoparticles, e.g., Al_2O_3, CuO, TiO_2 with different base liquids, e.g., water, ethylene glycol, have been tested. However, here only water-based nanofluids arereviewed. Neto et al. [4] studied the pool boiling heat transfer of Al_2O_3, Fe_2O_3 and CNTs nanofluids. The results showed that CHFs were increased by 26-37%, but heat transfer coefficients were the same or lower compared with distilled water. They explained that the increase in wettability and the thickness of the deposition layer resulted in the outcomes. A reduction in the static contact angle required more power to activate boiling. Karimzadehkhouei et al. [5] compared the performance of TiO_2 and CuO nanofluids. It was found that heat transfer was enhanced and deteriorated by the nanofluid with low (0.001 wt.%) and high mass fraction (0.2 wt.%) of TiO_2, respectively, while CuO nanofluids with different concentrations always enhanced the heat transfer. It was conceived that the deposition of nanoparticles on the surface might cause deterioration or enhancement of heat transfer coefficient, depending on the type of nanoparticles and other factors. Similarly, very high fraction of TiO_2 (12 wt.% and 15 wt.%) were tested by Ali et al. [6] and enhanced heat transfer was achieved. Cheedarala et al. [7] prepared a type of nano composites with CuO and Chitoan, namely CuO-chitosan nanofluid. The new type of nanofluid gavehigher CHF than CuO nanofluid. This is probably because that

the nanoparticle is hydrophilic which provides better liquid supply. Shoghl and Bahrami [8] carried out experiments to study pool boiling heat transfer of ZnO and CuO nanofluid. Deterioration of heat transfer was observed in both types of nanofluid with mass fractions of 0.01% and 0.02%, which resulted from the roughness changes by the nanofluid, as stated by the authors. Quan et al. [9] investigated the wettability effect of Si nanoparticles in pool boiling of a nanofluid. It was concluded that nanofluids containing moderately hydrophilic nanoparticles are most effective in enhancing boiling heat transfer, because moderately hydrophilic nanoparticles could decrease the size of departing bubbles and the deposited moderately hydrophilic nanoparticles promote roughness of the heater surface, providing more active nucleation cavities. Though several kinds of water-based nanofluids were described as aforementioned, Al_2O_3 nanofluid is still the most commonly studied [9]. Therefore, attentions are concentrated on Al_2O_3/ water nanofluid next. Table 1 provides a brief review on Al_2O_3/ water nanofluid. It shows conflicting results on HTC and CHF in different studies. However, some conclusion could be extracted. In most cases, heat transfer of nanofluid is deteriorated or unchanged, but CHF is increased compared to water. The concentration of nanofluid has a significant effect on HTC and CHF. It is expected that the low concentration benefits boiling heat transfer performance in comparison to high concentration. In addition, the roughness of heating surfaces is strongly coupled with the performance. Usually, a nanofluid performs better on the smooth surface. Several possible mechanisms were also proposed to explain the results of nanofluid in pool boiling. Normally the explanations derived from the coating on the surface due to nanoparticle deposition which could change the wettability, the number of active nucleation sites, the roughness, thermal resistance and even bubble behaviors.

In summary, Al_2O_3/ water nanofluid has been investigated a lot on pool boiling heat transfer, but hybrid nanofluid has not been tested to the best knowledge of the authors. In the present study, the pool boiling of Al_2O_3/ water nanofluid with low concentrations will be tested and grapheme nanoplatelets will be added to the nanofluid to study the pool boiling of mixed nanofluids.

Discussion and Results: The pool boiling experiments were first conducted on a bare copper plate. The results regarding superheat and heat flux were compared with the commonly used Rohsenow correlation to validate the accuracy and reliability of the setup. Fig. 1 compares the present experimental results and the correlation with n = 1 for water and C_{sf} = 0.009. It is indicated that the results of experiments agree well with those of the correlation. In addition, the critical heat flux (CHF) on the bare copper surface was also tested. At present, CHF was measured to 101.7 W/cm^2 which is smaller than the prediction of the well-known CHF model proposed by Zuber ~110 W/cm2. The deviation is about 8% which might be acceptable . The experiments on nanofluids are still onging. No results are shown at the moment, but will be available soon.
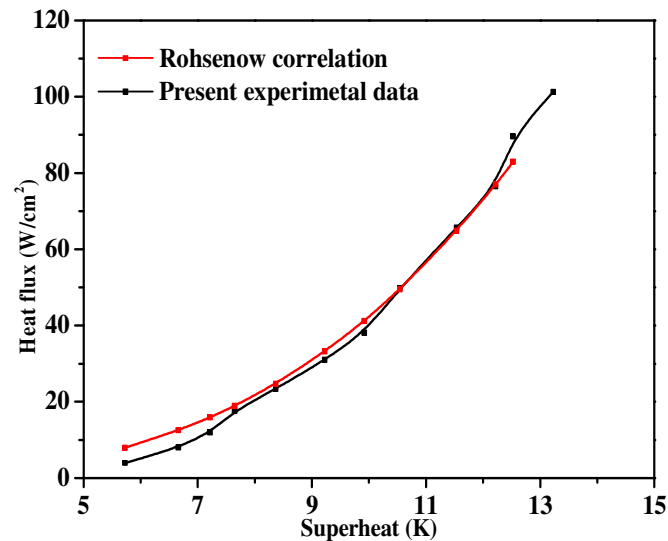
Fig. 1 The comparison between the present results and Rohsenow correlation on bare copper surface.

Table 1 Literature review of Al_2O_3/ water nanofluid on pool boiling

Ref.	Concentration	Surface	Results, explanations and remarks
9	0.0007 vol.% 0.007 vol.%	Copper	HTC increases and max. 75% and 15% are achieved at low concentration and below400 W/cm^2 on smooth surface Ra=0.05 µm and on rough surface Ra=0.23 µm, respectively; The behaviour is caused by the deposition of nanoparticles, which increase active nucleation sites, but increase the thermal resistance of nanolayer from a certain heat flux threshold
10	0.001, 0.005, 0.01, 0.025, 0.05 g/L	Copper 3 kPa	HTCs are almost not affected. Maximum CHF 300% is achieved at 0.025g/L beyond which CHF almost does not change. The average size of departing bubbles increases and the bubble frequency decreases significantly in nanofluids compared to those in the pure water.
11	0.026, 0.05, 0.1, 0.25, 0.525, 1.02 g/L	Copper	CHF degrades or is unchanged at the concentration under 0.1 g/L, and increases from 0.25 g/L and maximum CHF is achieved at a concentration of 0.525

			g/L
			HTC degrades or is unchanged.
			The CHF improvement is contributed to the wetting improvement
12	0.001, 0.005, 0.01, 0.025, 0.1, 0.5, 1 g/L	Copper	HTC of nanofluid is almost the same as for pure water and CHF increases with increasing concentration and becomes stable at the concentration of 0.025 g/L (80% enhancement, optimal)
			HTC on the coating surfaces is almost the same as that of nanofluid
			The coating due to microlayer evaporation changes the surface wettability
13	0.01, 0.1, 0.5 vol.%	Copper	HTC is enhanced, almost the same and deteriorated at concentration of 0.01, 0.1 and 0.5 vol.%, respectively
			HTC on the coating surfaces is deteriorated
			The enhancement is due to the dominant effect of thermal conductivity of nanofluid but less due to nanoparticle deposition
			The deterioration is due to the deposition which decreases the number of active nucleation sites and increases thermal resistance.
14	0.001, 0.01, 0.05, 0.1 vol.%	Copper 3 kPa	On the surface Ra=177.5 nm, HTC is almost the same as for pure water.
			On the surface Ra=292.8 nm, HTC deteriorates.
			On both surfaces, CHF is increased and highest at 0.05 vol.%
			The results are due to the contribution by the nanoparticle deposition and wettability changes

Table 2 The tests in the present study

Runs	Concentration of Al_2O_3	Concentration of graphene
1	0.0001 vol.%	0
2	0.001 vol.%	0
3	0.01 vol.%	0
4	0.0001 vol.%	0.001 vol.%
5	0.001 vol.%	0.0001 vol.%

References:
1. D. Ciloglu, A. Bolukbasi, A comprehensive review on pool boiling of nanofluids, *Applied Thermal Engineering.*84 (2015) 45–63.
2. Please correct and write as for other refs. , Enhanceing thermal conductivity of fluids with nanoparticles, *Fluids Engineering Division, FED 231. ASME Publication*. (1995) 99-105
3. X.D. Fang, Y.F. Chen, H.L. Zhang, W.W. Chen, A.Q. Dong, R. Wang, Heat transfer and critical heat flux of nanofluid boiling: A comprehensive review, *Renewable and Sustainable Energy Reviews*. 62 (2016) 924-940.
4. Neto, A. R., Oliveira, J. L. G., & Passos, J. C., Heat transfer coefficient and critical heat flux during nucleate pool boiling of water in the presence of nanoparticles of alumina, maghemite and CNTs. *Applied Thermal Engineering*, 111 (2017)1493-1506.
5. Karimzadehkhouei, M., Shojaeian, M., Şendur, K., Mengüç, M. P., & Koşar, A., The effect of nanoparticle type and nanoparticle mass fraction on heat transfer enhancement in pool boiling. *International Journal of Heat and Mass Transfer*, 109 (2017) 157-166.
6. Ali, H. M., Generous, M. M., Ahmad, F., & Irfan, M., Experimental investigation of nucleate pool boiling heat transfer enhancement of TiO 2-water based nanofluids. *Applied Thermal Engineering*, 113 (2017) 1146-1151.
7. Cheedarala, R. K., Park, E., Kong, K., Park, Y. B., & Park, H. W., Experimental study on critical heat flux of highly efficient soft hydrophilic CuO–chitosan nanofluid templates. *International Journal of Heat and Mass Transfer*, 100 (2016) 396-406.
8. Shoghl, S. N., Experimental investigation on pool boiling heat transfer of ZnO, and CuO water-based nanofluids and effect of surfactant on heat transfer coefficient. *International Communications in Heat and Mass Transfer*, 45 (2013) 122-129.
9. Manetti, L. L., Stephen, M. T., Beck, P. A., & Cardoso, E. M., Evaluation of the heat transfer enhancement during pool boiling using low concentrations of Al_2O_3-water based nanofluid. *Experimental Thermal and Fluid Science*. (2017)
10. You, S. M., Kim, J. H., & Kim, K. H., Effect of nanoparticles on critical heat flux of water in pool boiling heat transfer. *Applied Physics Letters*, 83 (2003) 3374-3376.

11. Coursey, J. S., & Kim, J., Nanofluid boiling: the effect of surface wettability. *International Journal of Heat and Fluid Flow*, 29 (2008) 1577-1585.

12. Kwark, S. M., Kumar, R., Moreno, G., Yoo, J., & You, S. M., Pool boiling characteristics of low concentration nanofluids. *International Journal of Heat and Mass Transfer*, 53 (2010) 972-981.

13. Ahmed, O., & Hamed, M. S., Experimental investigation of the effect of particle deposition on pool boiling of nanofluids. *International Journal of Heat and Mass Transfer*, 55 (2012) 3423-3436.

14. Ham, J., Kim, H., Shin, Y., & Cho, H., Experimental investigation of pool boiling characteristics in Al 2 O 3 nanofluid according to surface roughness and concentration. *International Journal of Thermal Sciences*, 114(2017) 86-97.

NANOFLUIDS AS WORKING FLUID IN THERMOSYPHON

A. Wlazlak[1], B. Zajaczkowski[1], S. Barison[2], F. Agresti[2], L.M. Wilde[3], M.H. Buschmann[3]*

[1]Wrocław University of Science and Technology,
St. Wyspiańskiego 27, 50-370 Wrocław, Poland

[2]CNR-ICMATE Institute of Condensed Matter Chemistry and Technologies for Energy,
Corso Stati Uniti, 4, 35127 Padova, Italy

[3]Institut für Luft- und Kältetechnik GmbH
Bertolt-Brecht-Allee 20, 01309 Dresden, Germany

*Corresponding author: Matthias.Buschmann@ilkdresden.de

Keywords: Thermosyphon, Nanofluids, Gold, Nanohorns, Silica

Introduction: Nanofluids are suspensions of particles with an average size of about 10-100 nm in various base fluids. The most common nanoparticles are metals or metal oxides dispersed in water. The addition of nanoparticles improves heat transfer processes which results in enhanced efficiency and miniaturization of energy transfer and storage systems. The motivation for studying on this topic comes from increasing global energy demands combined with the need for efficient and environmentally friendly solutions. Upward trends in excess heat that should be removed from electronic devices intensify research on such solutions. The usage of nanoparticles allows to omit clogging, sedimentation and abrasion - common problems occurring with larger particles [1, 2].

Aim of the study presented here is to investigate and compare thermal performance of thermosyphon (TS) employing different nanofluids. For that purpose, series of experiments in a test rig are conducted. Measurements employing water (baseline) , gold nanoparticles, single-walled carbon nanohorns stabilized with sodium dodecyl sulfate (SDS) and silica (SiO_2) stabilized with potassium hydroxide (KOH) are conducted. The differences between working fluids in terms of thermal performance are described and compared.

Test rig and employed nanofluids: The experiments are carried out employing the big ILK-thermosyphon, shown in Fig. 1. The device is made of a copper pipe with an inner diameter of 20 mm and a length of 1800 mm covered by an ARMAFLEX insulation (20 mm). Evaporator is heated and condenser cooled by coil heat exchangers ($d_i = 4$ mm, $l = 500$ mm) made of copper. Temperature of working fluid in evaporator is measured employing a special-designed probe consisting of six Pt 100 (Fig. 1 right). Temperature of inlet and outlet of cooling and heating water is determined employing Pt100 sensors. Volume fluxes of cooling and heating water are measured employing Krohne Optiflux 5000 flowmeters.

Internal pressure of TS is measured along the adiabatic section and in the condenser with the frequency of 1 kHz. Three transmitters each with a measurement range of 0…400 Pa are placed along the adiabatic section. In the condenser, data are taken by piezoresistive pressure transmitters with a measurement ranges of 0…104 Pa and 0…105 Pa.

Each measurement starts by adjusting inlet temperatures and volume fluxes of cooling and heating cycle. Inlet temperature of the heating medium is varied between 30°C and 85°C with an increment of 5 K. Inlet temperatures of condenser is 15°C. Volume fluxes in evaporator and condenser are kept constant at a value of 12 l/h. Testing time is one hour for each parameter combination.
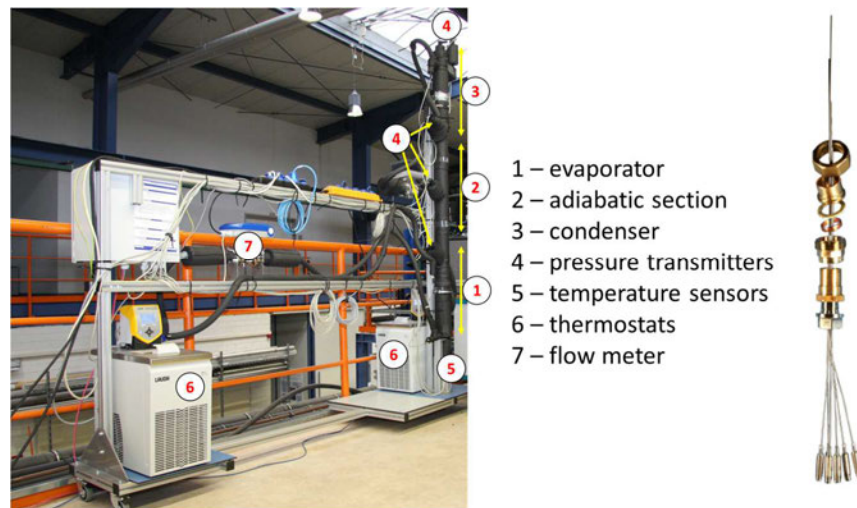
Fig.1. Test rig: thermosyphon with measurements system (left) and special-designed temperature probe (right).

Three kinds of nanofluids were tested and compared with water as reference data. Gold nanofluids were prepared by Particular GmbH (Germany). Nanoparticles with sizes varying between 50 and 70 nm were suspended in water with a concentration of 100 mg/L. Stabilization was carried out with KOH.

Single wall carbon nanohorns, commonly called nanohorns, are aggregates of graphene sheets. Thousands of them tend to associate with each other to form structures like dahlias or buds with high surface to volume ratio and large surface area [3]. A water based suspension of 0.1 g/L nanohorns (Carbonium Srl) stabilized with 0.01 g/L of SDS was prepared by high-pressure homogenization and is investigated in this study. The average hydrodynamic size of aggregates measured by dynamic light scattering (DLS) is between 100 and 150 nm.

The silica nanofluid is made of SIPERNAT©22S with a concentration of 2.0 vol. %. Stabilization is done with KOH so that a pH-value of 10.5 is achieved.

Discussion and Results: Results are exemplarily presented in Fig.2 to 4 for water, gold, nanohorn and silica nanofluids. Thermal resistance of the thermosyphon Rth (Fig. 2) is defined as the ratio of mean temperature difference between evaporator and condenser to transferred amount of heat. This parameter decreases with the increase of heat received at the condenser and reaches an almost constant value of about 0.078 W/mK for higher heat fluxes (approx. above 220 W). A significant difference in thermal resistance depending on the working fluid is found at low heat fluxes. The most noteworthy decrease in thermal resistance is caused by the silica nanofluid. Reductions up to 60 % compared to the baseline (water) are found. The presumed mechanism responsible for this effect is the nanoporous layer in the evaporation region formed by the silica nanoparticles. Boiling curves - heat taken out at the condenser versus overheating at evaporator wall - are presented with. Fig.3. Once again for high heat fluxes (inlet temperature of heating medium above 65°C) no big differences are seen between different working fluids. However, nanofluids change boiling regime significantly at low overheating. This finding points toward a change of bubble release behaviour due to a changed wall quality in the evaporator.
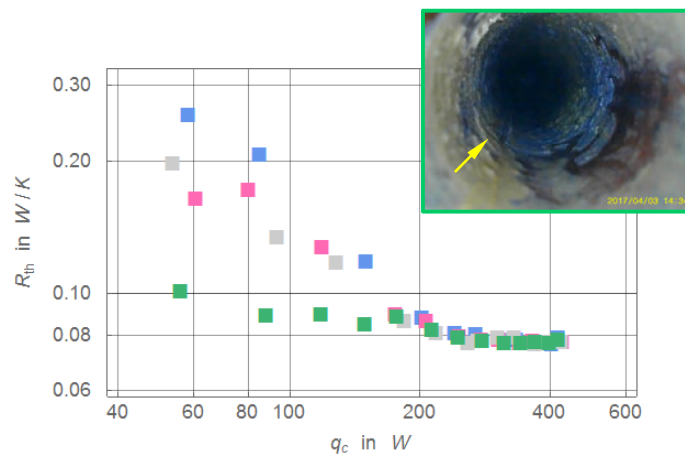
Fig. 2. Thermal resistance of different working fluids. Condenser inlet temperature was in all cases 15°C. Evaporator inlet temperature varied between 30°C and 85°C. Colours indicate water (blue), nanohorns nanofluid (grey), gold nanofluid (pink) and silica nanofluid (green). Insert shows interior of TS seen from the evaporator end after use of silica nanofluid. Yellow arrow indicates nanoporous layer formed by silica nanoparticles.
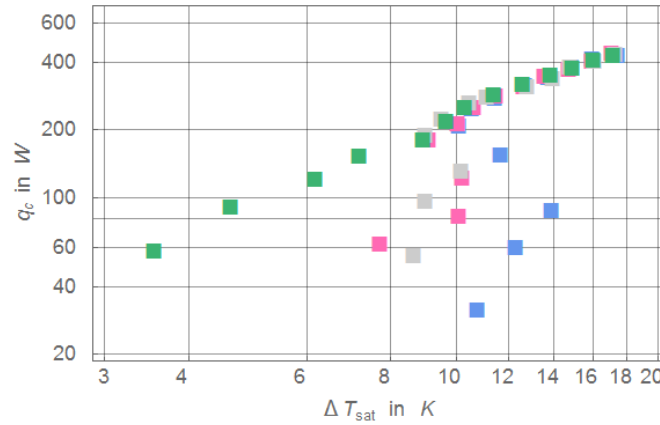
Fig. 3. Boiling curves for different working fluids. Conditions and symbols as in

Non-dimensional representation of data is shown in Fig.4. Here *Nu* denotes the Nusselt number according to eq. (1) and *D* is the non-dimensional averaged temperature of the TS.

$$Nu = \frac{q_c}{\bar{t}_e \cdot k \cdot d_i}; \qquad D = \frac{c_p}{\Delta h_p} \frac{t_{ei} + t_{eo} + t_{ci} + t_{co}}{4} \qquad (1)$$

Where $\bar{t}_e$ is the mean value between inlet and outlet of water in the evaporator, k is thermal conductivity of working fluid, d_i inner diameter of thermosyphon, c_p heat capacity of working fluid, Δh_p latent heat of working fluid and t_{ei}, t_{eo}, t_{ci}, t_{co} denote inlet and outlet temperatures of cooling and heating medium.
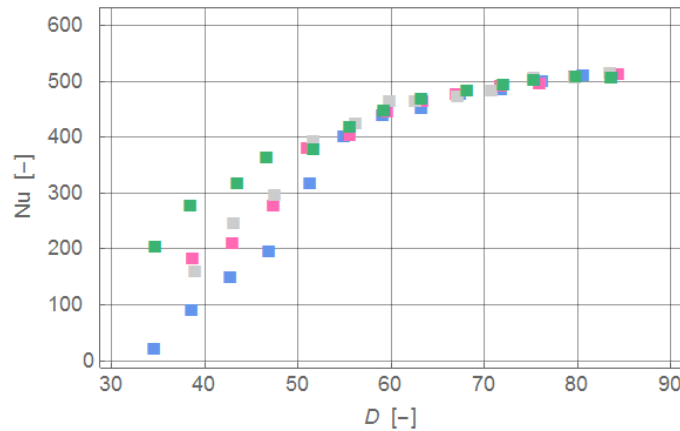
Fig.4. Normalised amount of transferred heat (Nusselt number correlation) in dependency of normalised mean temperature difference of thermosyphon. Conditions and symbols as in
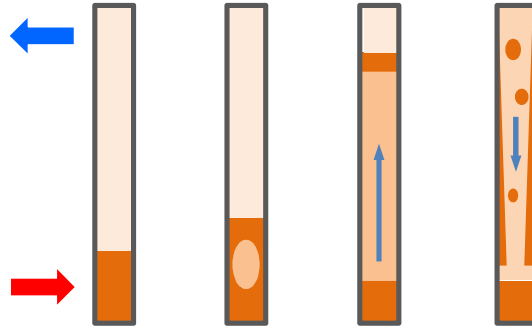
Fig. 5: Simplified sketch of geyser effect in thermosyphon. The sketches indicate from left to right: overheating of evaporator zone, forming of large bubble, expelling working fluid toward condenser and back falling working fluid.
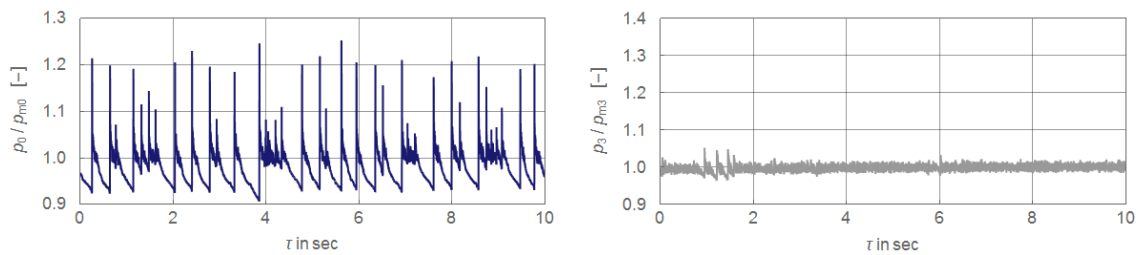
Fig. 6: Typical instantaneous pressure distribution for water (left) and nanohorn nanofluid under geysiring conditions. Inlet conditions at evaporator and condenser are identical in both cases (t_{ei} = 85 °C, tci = 25 °C)

Nusselt number increases monotonic with increasing normalized averaged temperature of TS. For low values of D, Nusselt number is significantly higher for nanofluid than for water. However, the increases depend strongly on the nanofluid. While the gold and the nanohorn nanofluid show nearly the same improvement the silica nanofluid gives significantly higher values. It is assumed, that the nanoporous layers are differently efficient formed. While for silica a massive layer is found (Fig.2) the coating found for the gold and the nanohorn nanofluid are mere loose nanoparticle deposits.

Besides the thermal performance the dynamical behaviour of the thermosyphon might be significantly affected by adding nanoparticles to the working fluid. This effect was especially seen with the nanohorn nanofluid.

Dynamical instabilities of a thermosyphon result from thermal instability mainly geysiring. Under geysiring the overheating of the working fluid followed by an eruption expelling larger parts of the working fluid into the condenser (Fig. 5). Such a behaviour is seen when the working fluid of our thermosyphon is pure water. A typical pressure distribution over time is

shown in Fig. 6 left plot. Changing the working fluid to the nanohorn nanofluid stabilized with SDS leads to a suppression of the instabilities observed with pure water.

Conclusions:

From the experiments carried out so fare the following conclusions are drawn.

- Nanofluids affect the thermal resistance of thermosyphons, in particular for low values of transported heat. The intensity of the effect depends on the nanofluid employed. Best results are obtained with a silica nanofluid with a concentration of 2 vol. %.
- Boiling behaviour is significantly influenced by nanoparticles forming nanoporous layers on the wall of the evaporator. For a given overheating of the evaporator wall a higher amount of heat can be transferred.
- As a side effect a substantial reduction of thermal instabilities – geysiring – is obtained when nanohorn nanofluid is employed as working fluid.

To summarize nanofluids offer a chance to improve the thermal performance of thermosyphons considerably. However, care has to be taken with respect to the nanofluid employed and the operation range of the device.

References:
1. M.H. Buschmann, Nanofluids in thermosyphons and heat pipes: Overview of recent experiments and modelling approaches, *Int. J. Therm. Sci.*, 72 (2014), 1–17.
2. V. Bianco, O. Manca, S. Nardini, and K. Vafai, *Heat Transfer Enhancement with Nanofluids*, CRC Press, 2015.
3. C. Pagura, S. Barison, C. Mortalo, N. Comisso, and M. Schiavon, Large scale and low cost production of pristine and oxidized single wall carbon nanohorns as material for hydrogen storage, *Nanosci. Nanotechnol. Letter*, vol. 4, 2(2012), 160–164.

NANOPARTICULATE DEPOSITION DURING CU-WATER NANOFLUID POOL BOILING ON ROUGHENED COPPER SURFACES

S. Mancin[1*], L. Doretti[2], T. P. Allred[3] and J. A. Weibel[3]

[1]Dept. of Management and Engineering, University of Padova, Str.lla S. Nicola 3, 36100, Vicenza, Italy

[2]Dept. of Civil, Architectural and Environmental Engineering, University of Padova, Via Venezia 1, 35131, Padova, Italy

[3]School of Mechanical Engineering, Purdue University, 585 Purdue Mall, 47907-2088, West Lafayette, IN, USA

*Corresponding author: simone.mancin@unipd.it

Keywords: Pool Boiling, Nanoparticulate Deposition, Wettability, Heat Transfer

Introduction: Boiling is widely relied upon in many different engineering systems: *e.g.*, chemical and nuclear reactors, refrigerating and air conditioning equipment, and thermal management of electronic devices. These applications have a shared constraint on the maximum heat flux that can be rejected by the cooling systems to ensure safe, reliable, and efficient operation.

The characterization of pool boiling has been a topic of worldwide research since Nukiyama [1] conducted experiments to measure a 'boiling curve' of the heat rejected from a surface submerged in stagnant liquid as a function of its temperature. It is well known that various surface treatment approaches can effectively enhance boiling heat transfer. In particular, microparticle coatings have been experimentally demonstrated to have promising capabilities for the enhancement of nucleate boiling heat transfer coefficients and critical heat flux (CHF) [2-3].

Recent work has led to new concepts for surface modification at the nanoscale. Nanostructured materials (*e.g.*, nanowire coatings, nanoporous layers, carbon nanotube arrays, etc.) have been also shown to enhance nucleate boiling (NB) and critical heat flux (CHF) [4-6]. A comprehensive review can be found in Ref. [7].

An alternative strategy to enhance boiling heat transfer is by seeding the fluid with a small concentration of nanoscale particles to produce a nanofluid. The boiling heat transfer behaviour of nanofluids has been extensively studied by many researchers who have observed some significant, though scattered, enhancements of the pool boiling CHF between 10% and 400% [8-12]. There are also contrasting reports of significant deterioration in boiling performance [13-16]. Results in the literature are inconsistent even for the same nanoparticle size/type under similar experimental conditions.

There are a few parameters that have been postulated to affect boiling heat transfer with nanofluids, which include morphological and thermophysical properties of nanoparticles and nanofluids, the long-term stability of the nanofluid suspension, the presence of surfactants and

ions, and the deposition and interaction of nanoparticles with the heating surface. As boiling heat transfer is very sensitive to surface topology and wettability, any change in the surface could alter the boiling behaviour. There is some general agreement on the fact that the enhancement or the deterioration observed during nanofluid boiling can be attributed to modification of the surface via nanoparticle deposition [17].

The present research activity aims to investigate nanofluid pool boiling to produce nanoparticulate-coated surfaces that can enhance the nucleated boiling heat transfer and critical heat flux. This paper presents preliminary nanoparticulate deposition results obtained during Cu-water (1.5 wt%) nanofluid pool boiling on a roughened copper surface.

The Cu-water nanofluid was obtained by seeding 25 nm copper nanoparticles into distilled pure water. Specifically, 25 g of copper nanoparticles were dispersed in 1.5 liters of distilled water, obtaining a 1.6 wt% Cu-water nanofluid, which was then stirred for 24 hr and sonicated for 6 hr to ensure uniform dispersion.

Discussion and Results: Tests are performed in experimental setups designed and built to study pool boiling of both pure water and nanofluids on smooth or enhanced surfaces. In order to avoid any contamination of the components by the nanoparticles contained in the nanofluid, two identical setups are used, one for the pure fluid tests and one for the nanofluid tests.

The test sample block is designed to have a characteristic heater size equal to the Rayleigh-Taylor wavelength, being 27.2 mm in the case of water at saturation condition at ambient pressure. Prior to each test, the test block is sealed into a polyether ether ketone (PEEK) (thermal conductivity, λ=0.28 W m^{-1} K^{-1}) base that exposes its top surface (smooth or enhanced) to the working fluid (water or nanofluid). The sample is then affixed into a pool boiling test apparatus that heats the surface in a controlled manner until CHF is reached.

In order to rigorously study the nanoparticulate deposition during nanofluid boiling, two copper samples were identically laser-etched to obtain a similar surface topography with uniform roughness. A microscope image and scanning electron microscope (SEM) image of one sample are reported in Figure 1; a profilometer analysis revealed that the values of the roughness, Ra were 359 ± 42 nm and 389 ± 41 nm for Sample A and Sample B, respectively. Furthermore, the static contact angle was measured on both samples and it was found to be 63. 2° ± 3.3° and 73.4° ± 3.7° for Sample A and Sample B, respectively.

(a)   (b)
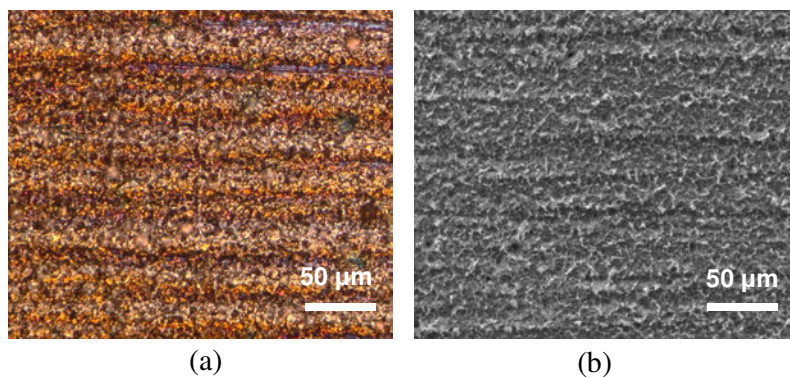
Figure 1: (a) Microscope image and (b) SEM image of the sample after laser-

roughening.

A benchmark reference boiling curve up to CHF was obtained for Sample A using pure water as the working fluid. Sample B was boiled in the Cu-water (1.6 %wt) nanofluid; the heat flux was increased continuously up to the CHF measured for Sample A, and then the sample was cooled down.
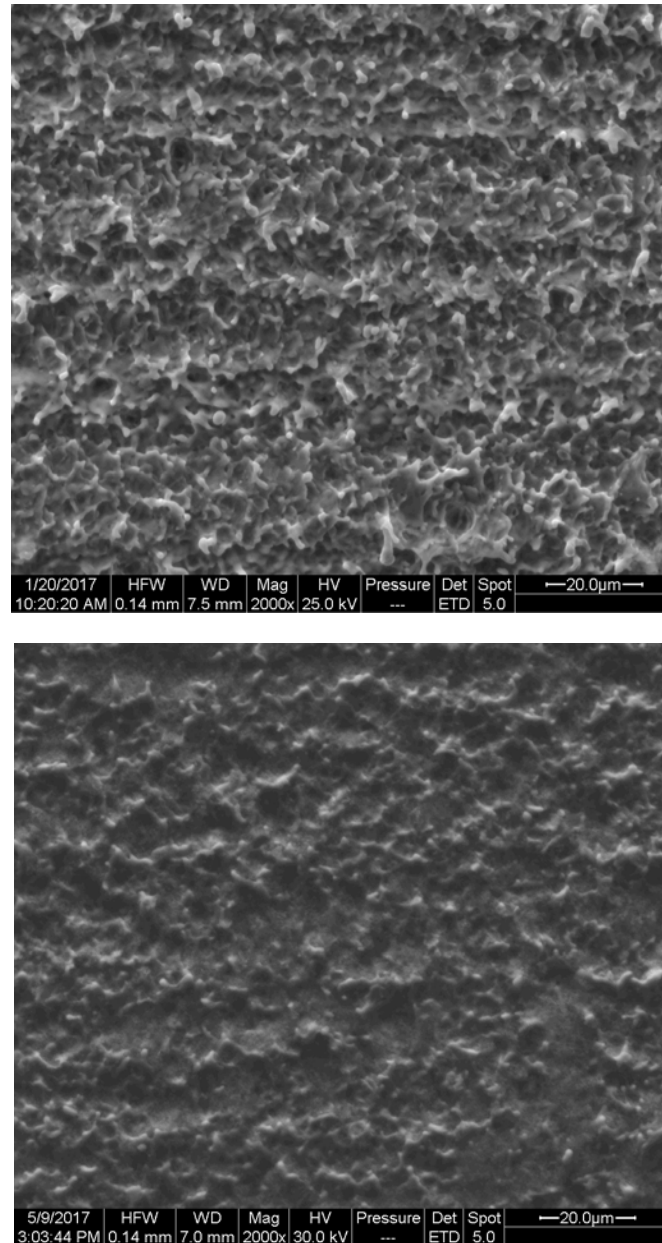
Figure 2: Uncoated (TOP) and coated (BOTTOM) surface of Sample B.

Figure 2 compares two SEM images taken before and after the nanofluid boiling on Sample B; a clear thin layer of nanoparticulate can be observed on the surface due to the deposition process occurred during the boiling process. The wettability of the surface remarkably changed; in fact, the contact angle varied from 73.4° ± 3.7° to 134.0° ± 3.4°.

As future work, the particulate deposition on the surface of Sample B, post nanofluid boiling, will be interrogated and evaluated as a permanent coating for nucleate boiling heat transfer and critical heat flux enhancement.

Conclusions: This work represents one of the first to investigate nanoparticulate deposition on a rough surface during nanofluid pool boiling. The preliminary results show that a thin layer of nanoparticles was deposited during the Cu-Water nanofluid pool boiling, which drastically modified the surface wettability and the pool boiling characteristics of the surface.

References:

1. S. Nukiyama, *J. of the Japan Society of Mech. Eng.,* 37 (206) (1934) 367-374
2. G.S. Hwang and M. Kaviany, *Int. J. Heat Mass Transf.* 49 (2006) 844-849
3. J.H. Kim, K.N. Rainey, S.M. You and J.Y. Pak, *J. Heat Transf.* 124 (2002) 500-506
4. Y.W. Lu and S. Kandlikar, *Heat Transf. Eng.* 32 (10) (2011) 827-842
5. S. Ujereh, T. Fisher and I. Mudawar, *Int. J. Heat Mass Transf.* 50 (2007) 4023-4038
6. S. Li, R. Furberg, M.S.Toprak, B. Palm and M. Muhammed, *Adv. Funct. Mater.* 18 (2008) 2215-2220
7. M.S. El-Genk and A.F. Ali, *Int. J. Multiphase Flow* 36 (2010) 780-792
8. M. Kedzierski, *J. Heat Transf.* 131 (2009) 043205
9. K-J. Park and D. Jung, *Int. J. Heat Mass Transf.* 50 (2007) 4499-4502
10. Z. Liu, J. Xiong and R. Bao, *Int. J. Multiphase Flow* 33 (2007) 1284-1295
11. K-J. Park, D. Jung and S.E. Shim, *Int. J. Multiphase Flow* 35 (2009) 525-534
12. R. Kathiravan, R. Kumar, A. Gupta, and R. Chandra, *J. Heat Transf.* 131 (2009) 081902
13. V. Trisaksri and S. Wongwises, *Int. J. Heat Mass Transf.* 52 (2009) 1582-1588
14. H.D. Kim and M.H. Kim, *App. Phys. Lett.* 91 (2007) 014104
15. I.C. Bang and S.H. Chan, *Int. J. Heat Mass Transf.* 48 (2005) 2407-2419
16. S.K. Das, N. Putra, W. Roetzel, *Int. J. Heat Mass Transf.* 46 (2003) 851-862
17. D. Wen, *Applied Therm. Eng*. 41 (2012) 2-9

MOLTEN SALT-BASED NANOFLUIDS WITH CERAMIC NANOPARTICLES FOR CONCENTRATED SOLAR POWER APPLICATION

A. Palacios[1], Z. Jiang[1], E. Mura[2], M.E Navarro[1], G.Qiao[2] and Y. Ding [1]

[1]BCES Birmingham Centre for Energy Storage, University of Birmingham, United Kingdom

[2]Global Energy Interconnection Research Institute Europe GmbH, Berlin, 10117, Germany

[*]Corresponding author: y.ding@bham.ac.uk

Keywords: Molten salts, Ceramic nanoparticle, Thermal energy storage, Heat transfer fluid

Introduction: For decades, nanofluids have been studied as heat transfer fluids (HTFs) in concentrated solar power (CSP) systems. Nanofluids present higher specific heat capacity and thermal conductivity than the pure fluid. The addition of a small concentration of nanoparticles can dramatically enhance the thermophysical properties of the base fluid (molten salt) [1].The heat transfer capacity is a key attribute in terms of storing the heat received from the sun and then transferring it when it is needed in a later use. Besides a high specific heat capacity to store energy, a high thermal conductivity is required. The thermal conductivity is a key parameter that can affect energy storage and cooling rate of the CSP system. The most reported nanoparticles used to enhance the thermal conductivity of molten salts are silicon dioxide, carbon nanotubes, carbon spheres, graphite flakes and titanium dioxide [2], [3]. In the present work, the effect of adding silicon dioxide to a ternary and quaternary molten salt is studied. The authors are intended to evaluate the effect of adding high thermal conductivity nanoparticles into HTFsto provide evidence of a heat transfer enhancement. Also the rheological behaviour of the heat transfer fluid during the charging/discharging proces was studied.

Materials and methodology: The molten salts listed in Table 1 were selected as the base fluid for this study. Silicon dioxide nanoparticles with 15-20nm diameter was used as ceramic high thermal conductivity nanoparticles. Nanofluids with different nanoparticles concentration (0.1, 0.5 and 1 wt%) were formulated. The procedure, see Figure 1, was conducted following Jo and Banerjee [4] three step method.
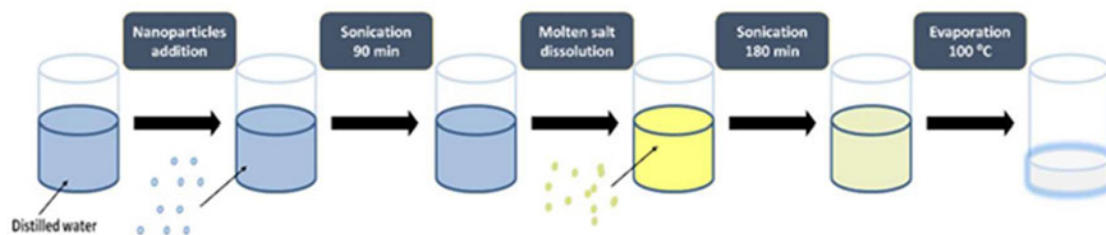
Figure 2: Three-step method nanofluid formulation

Table 1. Molten salts used as a base fluid in the present study.

Molten salt	Composition	Melting temperature (°C)
Ternary	$LiNO_3$-$NaNO_3$-KNO_3	120
Quaternary	$CaNO_3$-$LiNO_3$-$NaNO_3$-KNO_3	105

As it was mentioned before, the study is aimed to evidence the improvement of the heat transfer during the charging/discharging on LHTES technologies. A laser flash analyser (LFA427, Netzsch) and the three layer method were used with that purpose. TheThe measurements were conducted under nitrogen atmosphere and a temperature range from 50 to 400°C.

MCR 502 rheometer commercialised by Anton Paar was used to measure the viscosity of the nanofluid. The working temperature was varied from 250°C to 400°C with an interval of 50°C, the measurements were conducted with a share rate from 0.1 to 250 s^{-1} under air atmosphere.

Discussion and Results: The thermal diffusivity results for the ternary nanofluids are shown in Table 2. The thermal diffusivity of the nanofluids with 0.5% and 1% of silicon dioxide are higher than the pure ternary salt in the temperature range from 200 to 450ºC. At 450°C, the samples with 0.5 and 1% SiO_2 nanoparticles present a thermal diffusivity enhancement of 25% and 36%, respectively. The addition of SiO_2 nanoparticles (0.1%) does not lead to an enhancement of the thermal diffusivity.

The SiO_2 nanopaticles induce to a thermal diffusivity enhancement (10%) of the quaternary salt by means of adding a 1% in weight to the pure salt in the temperature range of 250 to 450°C (see Table 2). The thermal diffusivity increases with the silicon dioxide content, 0.5% and 1%, reaching an enhancement of 5% and 12%, respectively. Although the thermal diffusivity is increasing with the nanoparticle content, with 0.1 SiO_2 it presents lower values than the pure salt in the whole temperature range under study.

The viscosity of the ternary and quaternary molten salt formulations was also measured. The addition of silicon dioxide nanoparticles result on a substantially increase of the viscosity in both cases. In Figure 3 it can be seen the results for the ternary salt measurements with different amounts of nanoparticles. The viscosity is increasing with a higher nanoparticles content, when 0.5% and 1% of the nanoparticles were added, the overall viscosity was increased by about 47% and 60%, respectively. As expected, the viscosity of the formulations decrease with temperature.

Table 2. Thermal diffusivity of ternary and quaternary molten salt nanofluids.

Sample	Thermal diffusivity (mm^2/s)						
	200°C	250°C	300°C	350°C	400°C	450°C	Mean (200-450°C)
Ternary	0.118	0.123	0.125	0.128	0.130	0.108	**0.122**
Ternary + 0.1% SiO$_2$	0.108	0.113	0.117	0.108	0.081	0.107	**0.106**
Ternary + 0.5% SiO$_2$	0.111	0.115	0.118	0.122	0.126	0.143	**0.123**
Ternary + 1% SiO$_2$	0.112	0.120	0.128	0.135	0.144	0.170	**0.135**
Quaternary	0.126	0.135	0.146	0.152	0.163	0.184	**0.151**
Quaternary + 0.1% SiO$_2$	0.097	0.104	0.109	0.119	0.128	0.150	**0.118**
Quaternary + 0.5% SiO$_2$	0.118	0.122	0.126	0.131	0.139	0.194	**0.138**
Quaternary + 1% SiO$_2$	0.128	0.142	0.159	0.175	0.183	0.209	**0.166**

Regarding the quaternary based nanofluids, it can be seen (Figure 3) that the addition of silicon dioxide nanoparticles result on an increase of the viscosity up to 214% with a value close to 22 mPa·s at 250°C with 1% of SiO$_2$ nanoparticles. At higher temperatures (up to 400°C) the viscosity of the fluid decreases reaching values close to the quaternary pure salt, even lower in the case of 0.1 and 0.5% in wt. which the viscosity is reduced by 6%.
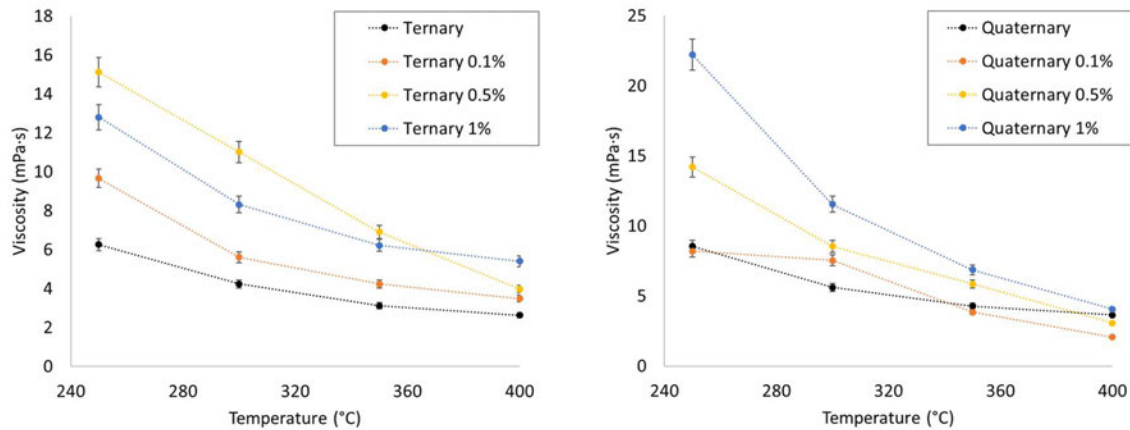
Figure 3. Viscosity of ternary (left) and quaternary (right) molten salt nanofluids with silicon dioxide.

Conclusions: In the present study, the experimental data of ternary and quaternary with different content of silicon dioxide nanoparticles are reported. The main outcomes from the experimental data analysed are shown as follows:

(1) The ternary molten salt presents a thermal diffusivity enhanced up to 25% and 36% by the addition of silicon oxide 0.5% and 1% in weight, respectively. At high temperatures (up to 400°C), the salt presents viscosity values close to 6% higher than the pure salt ones.

(2) The quaternary molten salt with 1% SiO_2 presents a thermal diffusivity 12% higher than the pure salt at 450°C. The addition of lower percentages of silicon dioxide does not lead to an enhancement. The rheological behavior of the nanofluid at 400°C shows a viscosity value close to the pure salt, within the tolerance of the equipment (±3%).

References:

[1] P. Kumar and D. Dey, A Recent Review on Thermo-Physical Properties of Nanofluid, *International Conference on Electrical, Electronics, and Optimization Techniques (ICEEOT)*, Chennai , India, Mar 03- 05, 2016.

[2] B. Jo and D. Banerjee, Enhanced Specific Heat Capacity of Molten Salt-Based Carbon Nanotubes Nanomaterial*s*, *Journal of Heat Transfer* 137 (2015) 91013.

[3] T. Bauer, N. Breidenbach, and M. Eck, Overview of Molten Salt Storage Systems and Material Development for Solar Thermal Power Plants, *The 2012 National Solar Conference for (SOLAR 2012),* Denver, Colorado, May 13-17, 2012.

[4] B. Jo and D. Banerjee, "Enhanced specific heat capacity of molten salt-based nanomaterials: Effects of nanoparticle dispersion and solvent material," *Acta Materialia* 75 (2014) 80–91.

MOUROMTSEFF NUMBER ANALYSIS ON NANOFLUID BASED SYSTEMS: FLAT PLATE SOLAR COLLECTORS

A. M. Genc[1], M. A. Ezan[2] and A. Turgut[2*]

[1]Dokuz Eylul University, The Graduate School of Natural and Applied Sciences, Mechanical Engineering Department, Tinaztepe Campus, Buca 35397, Izmir-Turkey

[2]Dokuz Eylul University, Engineering Faculty, Mechanical Engineering Department, Tinaztepe Campus, Buca 35397, Izmir-Turkey

* Corresponding author: alpaslan.turgut@deu.edu.tr

Keywords: Mouromtseff number, Al_2O_3-water nanofluids, flat plate solar collector

Introduction: In general, Nusselt number or heat transfer coefficient are used to determine the heat transfer capability of fluids. Alternatively, the Mouromtseff number, known as the figure of merit in the literature, is being used for comparison of the heat transfer capability for laminar or turbulent flows. It was presented by Mouromtseff (1942) [1] depending on the thermal properties of the fluid, such as density, heat capacity, dynamic viscosity and thermal conductivity [2]. For the fully developed flow inside a circular pipe [3], the Mouromtseff number (Mo) is defined as follows:

$$\text{Mo} = \frac{\rho^a k^b c_p{}^d}{\mu^e} \tag{1}$$

where the subscripts, *a, b, d,* and *e*, are determined by using an appropriate Nusselt number for the selected heat transfer application. Since the Mo number is an integrated non-dimensional parameter, it was commonly used to evaluate the thermal performance of a traditional heat transfer fluid, such as water or ethylene glycol, for either laminar or turbulent flow conditions. Recently, it has also been used to compare for nanofluids to compare the overall effectiveness of a candidate nanofluid with the traditional base fluid. It is well known that, in the case of the flow in a straight pipeline, either with constant wall temperature or heat flux, the Nusselt number converges to a constant value in the fully developed conditions. That is, for the fully developed conditions, the relative Mo number [4], which designates the ratio of the Mo numbers for nanofluid and base fluid, can be obtained as follows:

$$\text{FOM}_{\text{lam}} = \frac{\text{Mo}_{nf}}{\text{Mo}_{bf}} = \frac{h_{nf}}{h_{bf}} = \frac{k_{nf}}{k_{bf}} \tag{2}$$

FOM_{lam} is valid for only laminar and fully developed flow conditions inside pipes. For the fully developed turbulent flow conditions, on the other hand, the following figure of merit equation (FOM_{turb}) can be obtained by using the expression proposed by Vajjha and Das (2012) [5]:

$$FOM_{turb} = \frac{Mo_{nf}}{Mo_{bf}} = \frac{h_{nf}}{h_{bf}} = \left(\frac{\rho_{nf}}{\rho_{bf}}\right)^{0.8} \left(\frac{\left(k_{nf}\right)^{0.5}}{\left(k_{bf}\right)^{0.6}}\right) \left(\frac{\left(c_{pnf}\right)^{0.5}}{\left(c_{pbf}\right)^{0.4}}\right) \left(\frac{\left(\mu_{bf}\right)^{0.4}}{\left(\mu_{nf}\right)^{0.3}}\right) \tag{3}$$

Alternatively, FOM_{turb} can be obtained by using Dittus-Boelter correlation as follows:

$$Nu = 0.023\, Re^{0.8}\, Pr^{0.4} \tag{4}$$

$$FOM_{turb} = \frac{Mo_{nf}}{Mo_{bf}} = \frac{h_{nf}}{h_{bf}} = \left(\frac{\rho_{nf}}{\rho_{bf}}\right)^{0.8} \left(\frac{k_{nf}}{k_{bf}}\right)^{0.6} \left(\frac{c_{pnf}}{c_{pbf}}\right)^{0.4} \left(\frac{\mu_{bf}}{\mu_{nf}}\right)^{0.4} \tag{5}$$

In the current study, we have used Eq. (2) and Eq. (5) for the laminar and turbulent flow conditions, respectively. One can notice that the nanofluids are considered as more efficient than the base fluid if the FOM's are greater than unity. Recently, Minea and Moldovenau (2017) [6] investigated the effectiveness of TiO_2, Al_2O_3, and CuO nanofluids under laminar and turbulent flow conditions. They mentioned that the relative Mo number is an effective and straightforward way to find the effectiveness of nanofluids. In this study, the effectiveness of Al_2O_3-water nanofluids was investigated with using Mo number in laminar and turbulent flow conditions. The obtained results are compared with our previous numerical study [7] in which the effects of Al_2O_3-water nanofluids on the flat plate solar collectors (FPSCs) were investigated. Al_2O_3-water nanofluid is selected due to well-known thermophysical properties [8] and thermal performance [9, 10] based on our previous experimentations.

Discussion and Results: FOM's are calculated for fully developed laminar and turbulent flow conditions and the results are given in Figure 1. According to Eq. (2), FOM_{lam} depends on only the thermal conductivity of sample. Therefore, increasing the particle concentration improves the FOM_{lam} and it is greater than unity for all concentrations due to the higher thermal conductivity of nanofluids. Regarding the current non-dimensional performance metric nanofluids with higher concentrations have better performance in a thermal system.

However, in the case of turbulent flow the trend is in contrast with the laminar one. Although the thermal conductivity of the nanofluid samples increases with the concentration, Mo number in turbulent flow decreases due to the higher viscosity and lower specific heat capacity of nanofluids. So, the FOM_{turb} values are less than unity because the Mo number of water is higher

than the selected nanofluids. In this regards, it seems that investigated nanofluids are not favorable for the heat transfer applications under turbulent flow conditions. Moreover, the effectiveness of nanofluids decreases with increasing nanoparticle concentration. The current results are in contradiction with the previous works in the literature [5, 6] in which the turbulent flow conditions were investigated.
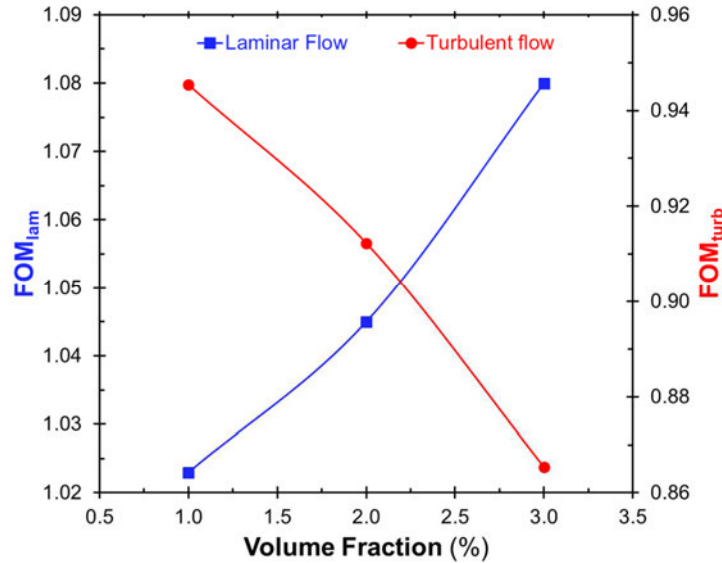
Figure 1 The FOM_{lam} for laminar conditions and the FOM_{turb} for turbulent conditions

In a recent work of the authors [7], a numerical model was developed to simulate the transient heat transfer of FPSCs. The influences of type of working fluids (either water or nanofluids), mass flow rate of the HTF and the climatic conditions were compared regarding the energetic and exergetic aspects. The mass flow rate of the heat transfer fluids is varied in a wide range, 0.004 to 0.06 kg/s, to introduce the effect of nanoparticle dispersion within water under laminar and turbulent flow conditions. Figure 2(a) shows the variations of the thermal efficiencies of the FPSC under various flow rates and particle concentrations in October. Here one can see that for the mass flow rates lower than 0.016 kg/s, the efficiency of the FPSC enhances as the particle concentration increases and the nanofluids are efficient than water. On the contrary, beyond 0.016 kg/s increasing the particle concentration has an adverse effect on the heat transfer and reduces the thermal efficiency of FPSC. It is also interesting to note that the thermal efficiencies of FPSCs with nanofluids are slightly lower than the ones with water at higher mass flow rates. In the current model, 0.016 kg/s is the critical mass flow rate for the transition to the turbulent flow condition. While at 0.016 kg/s only water shows turbulent behavior, beyond this value each of fluids is fully turbulent. One can realize that the inversion of the thermal efficiencies of FPSC at the verge of the turbulent is compatible with the relative Mo number variations for laminar and turbulent flow conditions that are given in Figure 1. Below 0.016 kg/s, in laminar flow zone, nanofluids are efficient since FOM_{lam} is higher at higher particle concentrations.

However, beyond 0.016 kg/s, in the turbulent flow zone, water becomes the efficient working fluid, and the particle concentration reduces the efficiency of the FPSC since the FOM_{turb} reduces with increasing concentration. Consequently, the FOMs are compatible with findings of the numerical model.
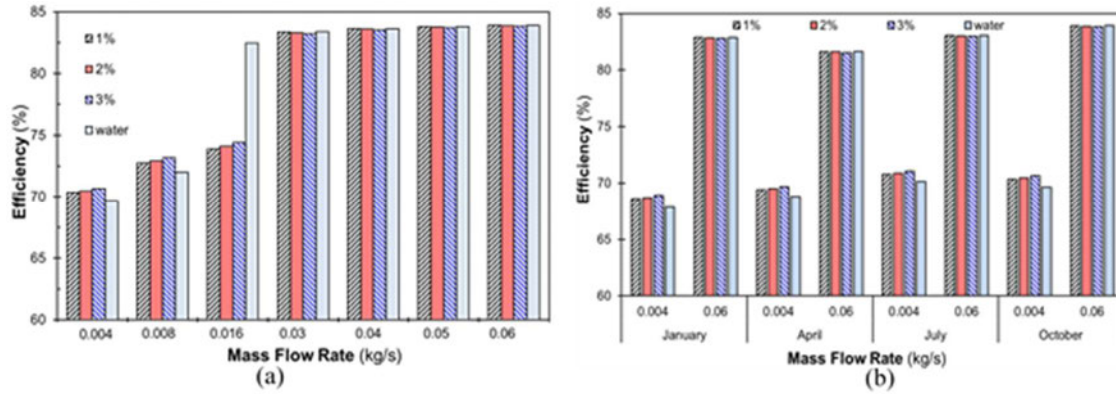
Figure 2 (a) Thermal efficiency of the FPSC for various mass flow rates in October (b) Thermal efficiency of the FPSC for various HTFs under different climatic conditions

In Figure 2(b), on the other hand, the thermal efficiencies are given at lower and higher mass flow rates for four different months. In each month, the efficiency of FPSC increases dramatically as the flow rate is increased from 0.004 g/s to 0.06 kg/s. Similar to the variations in Figure 2(a), there is an inversion point for the thermal efficiency of FPSC depending on the particle concentration. At lower flow rates (for *laminar flow*) the nanofluids are better than the water whereas at the higher flow rates (for *turbulent flow*) FPSCs with water as a working fluid have slightly higher efficiencies. That is, under both laminar and turbulent flow conditions, efficiency values are compatible with non-dimensional FOM_{lam} and FOM_{turb} values.

Conclusions: In this study, the effectiveness of Al_2O_3/water nanofluids are investigated with using relative Mo numbers for laminar and turbulent flow conditions. The results were compared with the numerical findings of the authors. Following conclusions can be listed:

- The effectiveness of selected nanofluids is higher than the base fluid under laminar flow conditions, and this effectiveness increases with increasing nanoparticle concentrations.
- For turbulent flow conditions, the Mo number of nanofluids are less than water, and the effectiveness of nanofluids decreases with increasing nanoparticle concentrations. For turbulent flow, nanofluids are not convenient for heat transfer applications.
- Non-dimensional FOM_{lam} and FOM_{turb} values are consistent with our previous numerical study for FPSC.

References:

1. Mouromtseff, I. E. (1942). Water and forced-air cooling of vacuum tubes nonelectronic problems in electronic tubes. Proceedings of the IRE, 30(4), 190-205.

2. Yu, W., France, D. M., Timofeeva, E. V., Singh, D., & Routbort, J. L. (2012). Comparative review of turbulent heat transfer of nanofluids. *International journal of heat and mass transfer*, *55*(21), 5380-5396.

3. Simons, R. E., Comparing Heat Transfer Rates of Liquid Coolants Using the Mouromtseff Number, Electronic Cooling, vol. 12,

http://electronicscooling.com/articles/2006/2006_may_cc.php, 2006.

4. Minea, A. A. (2013). Effect of microtube length on heat transfer enhancement of an water/Al 2 O 3 nanofluid at high Reynolds numbers. *International Journal of Heat and Mass Transfer*, *62*, 22-30.

5. Vajjha, R. S., & Das, D. K. (2012). A review and analysis on influence of temperature and concentration of nanofluids on thermophysical properties, heat transfer and pumping power. *International journal of heat and mass transfer*, *55*(15), 4063-4078.

6. Minea, A. A., & Moldoveanu, M. G. (2017). Studies on Al2O3, CuO, and TiO2 water-based nanofluids: A comparative approach in laminar and turbulent flow. *Journal of Engineering Thermophysics*, *26*(2), 291-301.

7. Genc, A. M., Ezan, M. A., & Turgut, A. Thermal performance of a nanofluid based flat plate solar collector: A transient numerical study. (Under Revision).

8. Turgut, A., Saglanmak, S., & Doganay, S. (2016). Experimental Investigation on Thermal Conductivity and Viscosity of Nanofluids: Particle Size Effect. Journal of The Faculty of Engineering and Architecture of Gazi University, 31(1), 95-103.

9. Turgut, A., & Doganay, S. (2014). Thermal performance of a single phase natural circulation mini loop working with nanofluid. High Temperatures--High Pressures, 43(4).

10. Doganay, S., & Turgut, A. (2015). Enhanced effectiveness of nanofluid based natural circulation mini loop. Applied Thermal Engineering, 75, 669-676.

NANOFLUIDS AS DIRECT SOLAR ENERGY ABSORBERS

A. Gimeno Furió[1*], J.E. Juliá[1], S Barison[2], F. Agresti[2], M.H. Buschmann[3] and C. Friebe[3]

[1]Mechanical Engineering and Construction Department

Universitat Jaume I, 12071 Castellón de la Plana, Spain

[2]CNR-ICMATE Institute of Condensed Matter Chemistry and Technologies for Energy, Corso Stati Uniti, 4, 35127 Padova, Italy

[3]Institut für Luft- und Kältetechnik GmbH

Bertolt-Brecht-Allee 20, 01309 Dresden, Germany

*Corresponding author: afurio@uji.es

Keywords: Solar nanofluid, Nanohorns, Silica, Absorption

Introduction:

Nanofluids are fluids (usually liquids) that contains nanoparticles between 1 and 100 nm suspended on it and they have been used to improve thermal conductivity and heat transfer of base fluid. The most common nanoparticles are metals or metal oxides dispersed in water. Nanoparticles are added because they improve heat transfer and absorption processes. It has been studied in different researches that thermal properties of nanofluids present differences regard to the conventional heat transfer fluids. On the other hand, solar nanofluids are defined as liquids that contain nanoparticles suspended that absorb solar radiation. These type of particles used to be metal (Au, Ag, Cu…) due to their resonance plasmon. These solar nanofluids were proposed as volumetric solar radiation receivers. Based water nanofluids may have advantages over water because the nanoparticles can directly absorb the solar radiation. Thus, it is possible to reach a high efficiency from solar radiation to thermal energy conversion process. Because of that, some research focuses on solar nanofluids as probable material used in future renewable energy technologies [1-3].

This work is based on the study of the energy absorbed for different water-based nanofluids.

Discussion and Results:

The experiments were carried out using an artificial sun which consists of ten lamps with a power of 2000 W each, shown in Fig. 1.

Figure 1 Lamps structure imitating an artificial sun lighting the samples

The inclination of the structure containing these ten lamps is 64±0.3° degrees in order to achieve the highest intensity in the experiment site.

It was also used a black plate (1 m x 1 m) with 5 glass tubes held on it. Tubes have an inner diameter of 25 mm and a length of 400 mm except for one which is a vacuum tube with an inner diameter of 20 mm and a length of 300 mm. All of them were closed with a rubber tap. In order to measure the working fluid temperature, five thermocouples Pt100 were introduced in each tube. Moreover, three more thermocouples were used to measure ambient temperatures. One of them was located behind the plate, another one at the front of the plate and last one, under the lamps. Before starting any test, thermocouples must be calibrated. A moisture meter was placed under the lamps and a light meter was placed at the top of the plate. There are also fans used to avoid reaching very high temperatures, one is located under the lamps to cold the light system; and the other fan is located in room´s wall to maintain an acceptable temperature in the chamber. It has to be mentioned, that all the experiments were carried out under controlled conditions.

Once the thermocouples were calibrated, the test starts by switching on the lamps and the fans. After that, the samples were heated during 4 hours and every second temperature value is registered. When this value remains constant, the artificial sun and the fans were switched off.

Four kinds of fluids were tested and compared with water as reference data. Silica nanofluid which is made of SIPERNAT©22S with a concentration of 0.01g/L and stabilized with KOH

reaching a pH value of 10.5. Two single wall carbon nanohorns suspensions (NH), were used. In one of them, 0.02 g/L nanohorns (Carbonium Srl) were stabilized with 0,005 g/L of sodiumdodecylsulphate (SDS), and the other one was stabilised adding 0,05 g/L of polyvinylpyrrolidone (PVP) and 0,005 g/L of SDS. Carbon nanohorns have been used because it has already test before that they play an important role improving solar radiation absorption [4-5]. Finally, a water solution of Chinese ink with a concentration of 0,2 g/L was used.

The whole set-up with the five different samples used is shown in Figure 2. In each plate, from left to right, tubes are named as A, B, S, C, D. A and S contains the highest concentration of the study fluid. Then, the working fluids were diluted to 1/10, 1/100 and 1/1000 which are in B, C and D tubes, respectively.

Figure 2 From left to right, from top to bottom: water, silica nanofluid, Chinese ink, carbon nanohorns + SDS and carbon nanohorns + SDS + PVP

This work is only focused on the study of temperature evolution for different fluids with respect to water, and then concentration comparisons do not fall within the scope of this paper.

The results obtained in heating-up the different fluids are presented in Figure 3. In order to study the solar energy absorbed by the fluids, temperature against time has been plotted for the samples studied.
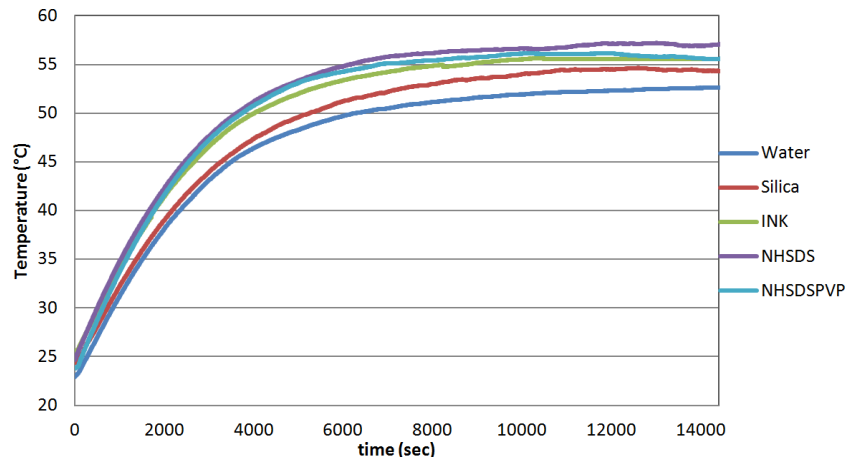
Figure 3 Temperature evolutions against time for different nanofluids in tube A

Representing these values, it is possible to observe that for darker fluids the temperature rises up faster than for white fluid or water. Moreover, black nanofluids reach a higher temperature than black ink solution, as expected, since nanofluids are suspensions with a fine dispersion of nanohorns that has a higher efficiency in absorption with respect to inks that typically contain micrometric particles.

Conclusions:

Silica nanofluid would not be effective for solar harvesting applications because there is not considerable improvement of energy absorption compared to water. In contrast, black fluids improve the absorption solar energy process. Water-based nanofluids present higher solar energy absorption than black Chinese ink due to the presence of nanoparticles whose specific surface area is large. Therefore, they would offer a chance to improve the efficiency of volumetric solar radiation receivers as direct absorbers.

Acknowledgement:

References:

1. B.A.J. Rose, H. Singh, N. Verma, S. Tassou, S. Suresh, N. Anantharaman, D. Mariotti, P. Maguire, *Investigations into nanofluids as direct solar radiation collectors*, Solar Energy, Volume 147, 2017, Pages 426-431, ISSN 0038-092X

2. S.H.A. Ahmad, R. Saidur, I.M. Mahbubul, F.A. Al-Sulaiman, *Optical properties of various nanofluids used in solar collector: A review, Renewable and Sustainable Energy Reviews*, Volume 73, 2017, Pages 1014-1030, ISSN 1364-0321

3. R.A. Taylor, P.E. Phelan, T.P. Otanicar, C.A. Walker, M. Nguyen, S. Trimble, R.S. Prasher *Applicability of nanofluids in high flux solar collectors.*   J. Renewable Sustainable Energy 3, 2011, 023104.

4. E. Sani, L. Mercatelli, S. Barison, C. Pagura, F. Agresto, L. Colla, P. Sansoni *Potential of carbon nanohorns-based suspensions for solar termal collectors.* Solar Energy Materials and Solar Cells, Volume 95, Issue 11, November 2011, 2994-3000

5. S. Barison, L. Fedele, F. Agresti, S. Rossi, S. Bobbo, C. Pagura *Carbon nanohorn-based nanofluids for solar thermal harvesting applications.* Journal of Nanoscience and Nanotechnology, Volume 15, Number 5, May 2015, 3488-3495

NANOFLUIDS WITH ENHANCED THERMAL PROPERTIES BASED ON METALLIC NANOPARTICLES FOR CONCENTRATING SOLAR POWER: A THEORETICAL AND EXPERIMENTAL PERSPECTIVE

J. Navas[1*], A. Sánchez-Coronilla[2*], R. Gómez-Villarejo[1], E. I. Martin[3], P. Martínez-Merino[1], T. Aguilar[1], J. J. Gallardo[1], R. Alcántara[1] and C. Fernández-Lorenzo[1]

[1]Departmento de Química Física, Universidad de Cádiz. Facultad de Ciencias, E-11510 Puerto Real (Cádiz) , Spain

[2]Departamento de Química Física, Universidad de Sevilla. Facultad de Farmacia, E-41012 Sevilla, Spain

[3]Departamento de Ingeniería Química, Universidad de Sevilla. Facultad de Química, E-41012 Sevilla, Spain

*Corresponding author: javier.navas@uca.es; antsancor@us.es

Keywords: Nanofluid, Concentrating Solar Power, Thermal Conductivity, Molecular Dynamics, Au and Pt nanoparticles

Introduction: One of the challenges facing society today is the need to meet the growing demand for energy while minimalizing the environmental impact on the planet [1]. Solar energy is a renewable source of energy that can be used to a large extent to this end. In this regard, the conversion of solar energy into electricity is of interest, and Concentrating Solar Power (CSP) systems play an important role as thermal energy converters to be used in electric power generation [2]. One line of research aimed at improving the efficiency of CSP plants involves improving the thermal properties of the Heat Transfer Fluid (HTF) used in these plants, which will lead to improvements in the heat transfer processes taking place. In this sense, the use of nanofluids seems to be an interesting alternative for improving the thermal properties of the base fluids [3,4], considering nanofluids as colloidal suspensions of nanometric systems in a base fluid. Suspending nanoparticles in an HTF has been shown to improve such properties as its thermal conductivity, heat transfer coefficient or isobaric specific heat [3-7].

Thus, the review of the literature reveals that CSP is one of the most interesting alternatives to conventional energy sources nowadays, and that there are advantages to be gained from the use nanofluids in CSP for high temperature applications. In this sense, the study of new nanofluids prepared with heat transfer fluids other than water or ethylene glycol is of great interest, particularly if these fluids are to have a future commercial use. The use of nanofluids within the heat transfer energy market is forecast to increase by over 2 billion dollars in the future, making it a promising field of study [8,9]. Thus, effective nanofluids that can optimise the use of a resources such as solar energy are candidates for consideration as value-added materials that produced a decreased impact on the environment [10,11].

Thus, taking into consideration that CSP could be a promising alternative to traditional sources of energy and that the thermal properties of nanofluids present clear advantages, the analysis from experimental and theoretical perspectives of nanofluids based on the base fluids that are used as HTFs in CSP plants is of interest. Therefore, this study involved the preparation of nanofluids based on the HTF used in CSP plants, which is the eutectic mixture of biphenyl ($C_{12}H_{10}$) and diphenyl oxide ($C_{12}H_{10}O$), and metallic nanoparticles.

Discussion and Results: The nanofluids are based on a commercial heat transfer fluid (HTF) used as a base fluid, being a eutectic mixture of biphenyl ($C_{12}H_{10}$, 26.5%) and diphenyl oxide ($C_{12}H_{10}O$, 73.5%). Also, we have prepared two kind on nanofluids based on nanoparticles of Au and Pt in order to analyse the thermal properties in function of the nature of the nanoparticles. The nanofluids were prepared using the one-step method, where the precursor of the metallic nanoparticles are transferred from aqueous phase to the base fluid, and after the reduction of the precursor is performed.

The nanofluids prepared were characterised in their basic properties, such as chemical and physical stability, density, viscosity, isobaric specific heat and thermal conductivity. The measurement of these properties leads to evaluate the improvement in the heat transfer coefficient of the nanofluids with respect to the base fluid. On the other hand, from Molecular Dynamics calculations, we have analysed the behaviour of the nanofluids. The isobaric specific heat and the thermal conductivity were estimated for the both systems analysed, based on Au and Pt nanoparticles. The arrangement of the base fluid and the phase transferring agent was analysed from the radial distribution function (RDF) and the spatial distribution function (SDF).
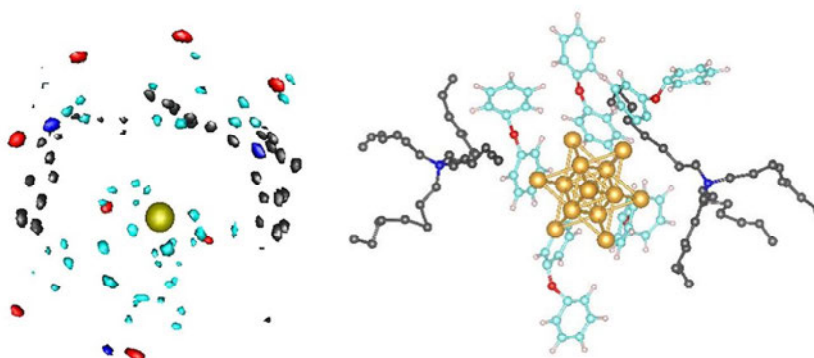
Figure 1. SDF for Au-nanofluid.

As results, particle size measurements, UV-vis spectroscopy ζ potential show a good stability for the nanofluids prepared. Also, an improvement of both isobaric specific heat (up to 10%) and thermal conductivity (up to 70%) is found for all the nanofluids prepared. These improvements lead to an enhancement in the efficiency of the nanofluids prepared with respect to the base fluid, analysed as the ratio between the heat transfer coefficient of the nanofluid and the base fluid. An increase up to 36% was observed in the heat transfer coefficient. From a

theoretical perspective, the isobaric specific heat and thermal conductivity values followed the same experimental trend. The analysis of the radial distribution functions (RDFs) and spatial distribution functions (SDFs) showed that the surfactant participates as an active component within the nanofluids, contributing to efficient heat transfer processes.

Conclusions: This work shows the preparation of the nanofluid based on a heat transfer fluid used typically in Concentrating Solar Power plants and Au and Pt nanoparticles synthesized in the base fluid used. An improvement of the thermal properties, such as isobaric specific heat, thermal conductivity and heat transfer coefficient has been found. Also, the effect of the interactions of the base fluid/surfactants/nanoparticles has been analysed in order to understand the behaviour of the nanofluids studied.

References:

1. J. Khan and M. H. Arsalan, Solar power technologies for sustainable electricity generation – A review, *Renewable and Sustainable Energy Review* 55 (2016) 414-425.
2. J. P. Bijarniya, K. Sudhakar and P. Baredar, Concentrated solar power technology in India: A review, *Renewable and Sustainable Energy Review* 63 (2016) 593-603.
3. J. Navas, A. Sánchez-Coronilla, E. I. Martín, M. Teruel, J. J. Gallardo, T. Aguilar, R. Gómez-Villarejo, R. Alcántara, C. Fernández-Lorenzo, J. C. Piñero, J. Martín-Calleja, On the enhancement of heat transfer fluid for concentrating solar power using Cu and Ni nanofluids: An experimental and molecular dynamics study, *Nano Energy* 27, (2016) 213-224.
4. R. Gómez-Villarejo, E. I. Martín, J. Navas, A. Sánchez-Coronilla, T. Aguilar, J. J. Gallardo, R. Alcántara, D. De los Santos, I. Carrillo-Berdugo, C. Fernández-Lorenzo, Ag-based nanofluidic system to enhance heat transfer fluids for concentrating solar power: Nano-level insights, *Applied Energy* 194 (2017) 19-29.
5. D. Singh, E. V. Timofeeva, M. R. Moravek, S. Cingarapu, W. H. Yu, T. Fischer, S. Mathur, Use of metallic nanoparticles to improve the thermophysical properties of organic heat transfer fluids used in concentrated solar power, *Solar Energy* 105 (2014) 468-478.
6. S. U. S. Choi, Nanofluids: from vision to reality through research, *Journal of Heat Transfer – ASME* 131 (2009) 033106.
7. D. H. Yoo, K. S. Hong, H. S. Yang, Study of thermal conductivity of nanofluids for the application of heat transfer fluids, *Thermochimica Acta* 455 (2007) 66-69.
8. D. S. Wen, G. P. Lin, S. Vafaei, and K. Zhang, Review of nanofluids for heat transfer applications, *Particuology* 7 (2009) 141-150.
9. CEA. Nanofluids for heat transfer applications. France: Marketing Study Unit, CEA; 2007.
10. S. K. Verma, and A. K. Tiwari, Progress of nanofluid application in solar collectors: a review, Energy Conversion and Management 100 (2015) 324-346.
11. H. A. Mohammed, A. A. Al-Aswadi, N. H. Shuaib, and R. Saidur, Convective heat transfer and fluid flow study over a step using nanofluids: a review, *Renewable and Sustainable Energy Review* 15 (2011) 2921-2939.

INFLUENCE OF HIGH TEMPERATURE EXPOSURE IN THERMAL AND OPTICAL PROPERTIES OF THERMAL OIL-BASED SOLAR NANOFLUID

A. Gimeno-Furio, N. Navarrete, R. Martínez-Cuenca, J.E. Julia* and L. Hernandez

Departamento de Ingeniería Mecánica y Construcción

Universitat Jaume I

12071 Castellón de la Plana, Spain

*Corresponding author: Enrique.julia@uji.es

Keywords: solar nanofluid, thermal oil, thermal cycling

Introduction: Solar nanofluids are transparent fluids in the visible and near infrared range with low loads of dispersed nanoparticles with high absorption for the solar radiation. These solar nanofluids were proposed as volumetric solar radiation receivers [1-2]. Additionally, if a thermal oil is used as the base fluid of the nanofluid, the nanoparticles directly absorbs the solar radiation, transferring the heat to the heat transfer fluid. In this way, high efficiency from solar radiation to thermal energy can be obtained, which makes these thermal oil-based solar nanofluid a promising material for future renewable energy technologies. However, industrial implementation of the solar nanofluids depend on several factors, including nanofluid stability, good thermal and optical response at temperatures as close as possible to that found in the applications and good response to high temperature exposure.

Discussion and Results: In this work, a solar nanofluid of Therminol 66 and tin (Sn) nanoparticles (80nm) is developed and characterized. The selection of Sn is based on their absorption spectrum in the visible range of solar radiation. In order to assure the solar nanofluid stability, different dispersants were evaluated and Diphenyl Sulphone (DS) was selected due to their good response under thermal cycling.

The solar nanofluid was kept up to 3 hours in an oven with a temperature up to 200ºC. Thermal and optical characterization of the solar nanofluid were perfomed before and after the high temperature exposure. These measurements include absorption spectrum, thermal conductivity, specific heat and particle size distribution of the sample. The measurements have been performed at room temperature and also at temperatures closer to those found in the industry.

The results obtained for the thermal oil- solar based nanofluid absorption spectrum at room temperature before the thermal cycling are shown in the next figure:
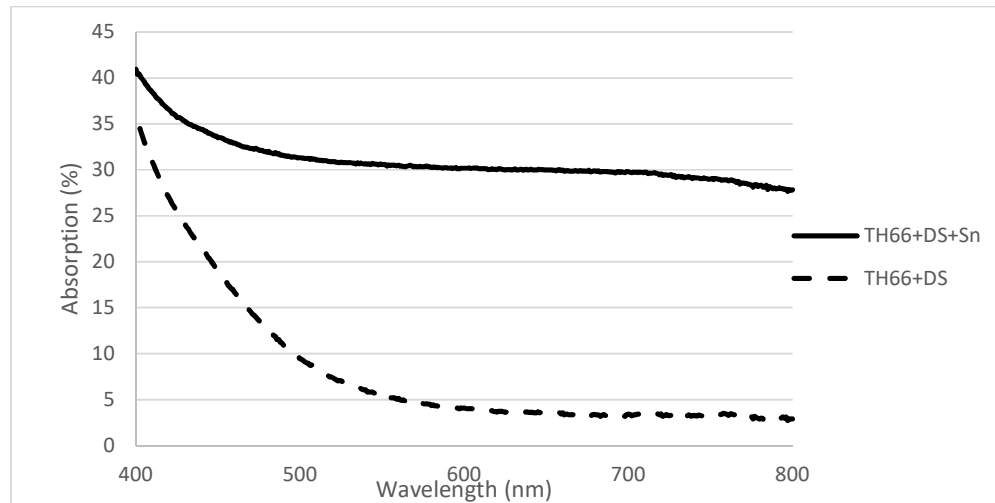
Fig 1. Absorption spectrum at room temperature of thermal oil-based nanofluid

Conclusions: Sn thermal oil-based nanofluids have been synthetized and thermal and optically characterized. This type of nanofluid can be used for solar harvesting applications since it has a constant absorption spectrum in the entire solar radiation wavelength. Thermal properties of Sn thermal oil-based nanofluids have been characterized at high temperature conditions showing expected results. The modification of the properties of the solar nanofluid after the high temperature exposure has been also evaluated.

References:

1. R.A. Taylor, P.E. Phelan, R.S. Prasher. *Experimental results for light-induced boiling in water-based graphite nanoparticle suspensions*, Proceedings of the ASME 2009 Summer Heat Transfer Conference 2009, pp. 1–9.
2. R.A. Taylor, P.E. Phelan, T.P. Otanicar, C.A. Walker, M. Nguyen, S. Trimble, R.S. Prasher *Applicability of nanofluids in high flux solar collectors.* J. Renewable Sustainable Energy 3, 2011, 023104. http://dx.doi.org/10.1063/1.3571565

SYNTHESIS OF TIN/ETHYLENE GLYCOL SOLAR NANOFLUID BY A FEMTOSECOND LASER-ASSISTED TECHNIQUE

R. Torres Mendieta[1], R. Mondragón[2], V. Puerto Belda[1*], O. Mendoza Yero[1], J. Lancis[1], G. Mínguez Vega[1] and J. E. Juliá[2]

Departamento de Química, CICECO, Universidade de Aveiro, 3810-193 Aveiro, Portugal

*Corresponding author: vpuerto@uji.es

Keywords: Nanotechnology, nanoparticles, laser ablation, femtosecond laser, absorption, optical properties

Introduction: Nowadays, solar energy extends over wide geographical areas and is becoming an essential means to keep up to the ever-increasing worldwide energy demand with minimal environmental impact. Traditionally, in conventional solar–thermal systems a heat transfer fluid is surrounded by a black surface absorber that convert the majority of the incoming solar radiation into heat that is subsequently transferred to the fluid. However, as the heat generation at the absorber is separated from the fluid, this causes radiative losses and the consequent lower in the efficiency. In 2009, solar nanofluids, an innovative type of nanofluids that are able to direct harvest solar radiation, were proposed for renewable solar thermal power applications [1]. The basic idea of a solar nanofluid is to use heat transfer fluids, which usually have low absorption in the visible and near infrared range in combination with nanoparticles. In this way, a volumetric absorption within the solar fluid itself is promoted, which increases the photothermal efficiency by at least 10% [2].

Discussion and Results: In this work, tin/ethylene glycol nanofluid samples were prepared by using pulsed laser ablation in liquids (PLAL) [3] techniques and the standard two-step method. The synthesis of PLAL's solar nanofluid was carried out using a Ti:Sapphire laser (Femtopower Compact Pro, Femtolasers), that emits pulses of 30 fs intensity full width at half maximum (FWHM) with a central wavelength of 800 nm and 1 kHz repetition rate. The thickness of the ethylene glycol (EG) layer above the tin was about 1 mm. The laser beam with a size of 6 mm diameter was focused by a lens of 75 mm with a mean power of 180 mW while moving the target perpendicular to the beam propagation axis at a constant velocity of 0.45 mm/s. The interaction of the pulsed laser radiation with the solid tin immersed in the ethylene glycol promotes the extraction of material from its surface in the form of an ablation plume. Tin nanoparticles (NPs) are formed from the ejected material and they are collected in the ethylene glycol as colloids creating the solar nanofluid.

For comparison, we also made a solar nanofluid with commercial tin nanoparticles by carefully mixing the nanoparticles with ethylene glycol at the same concentration. Commercial tin NPs were purchased from US Research Nanomaterials, Inc. NPs have a primary particle size of 60–80 nm and a density of 7310 kg/m^3 according to the manufacturer. Nanofluids were prepared by

dispersing the corresponding amount of solid in ethylene glycol (EG; reagent grade, Scharlab S.L.). To break the agglomerates in the powder, the dispersion process was carried out by ultrasonic treatment with an ultrasonic probe UP400s (Hielscher Ultrasonics Gmbh, Germany). The nanofluid was sonicated for 15 min immersed in an ice bath until the highest degree of dispersion was achieved.

To assure a good behaviour of the nanofluid through the time, it is important to characterize its stability for prolonged periods of time. A visual inspection of as-produced nanofluids over time was carried out. Figure 1 shows an image of PLAL nanofluid (top) and nanofluid synthesized by using the two-step method with commercial NPs (bottom) after 1, 4 and 10 days from its production. It was observed that a sedimentation of the heavier NPs at the base of the cuvette occurred. However, the stability of the nanofluid produced by PLAL was higher.
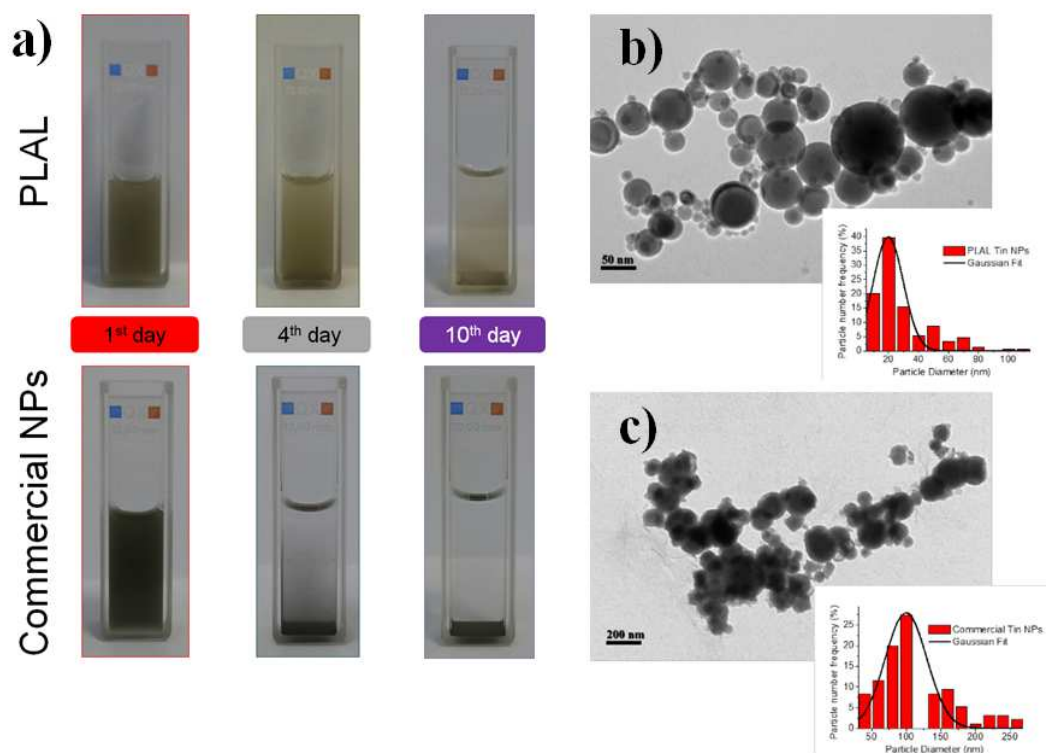

Figure 1. a) Picture of the solar nanofluids at the 1st, 4th and 10th day showing nanoparticle sedimentation over the time. Transmission electronic microscopy micrographs of b) nanofluid prepared by PLAL, c) nanofluid prepared by using commercial tin NPs. The inset of both micrographs represents a histogram showing the statistical size distribution of NPs contained in both nanofluids.

Micrographs of the NPs are shown in Figure 1. Nanoparticles produced by PLAL (Fig. 1 b)) show a higher sphericity and less aggregation than those synthesized by a chemical methods (Fig. 1 c)).

To evaluate the sunlight absorption capability of the nanofluid, which is directly related to the nanofluid efficiency, the transmission solar spectral irradiance through 1 cm of the nanofluid was calculated. For this purpose, the reference solar spectral irradiance, $I(\lambda)$, ASTM G-173 for a mass air of 1.5 (see Figure 2) was considered. The transmission solar spectral irradiance through the nanofluid is obtained by multiplication of the reference solar spectral irradiance by the transmittance spectra in 1 cm of nanofluid. In this way, we can qualitatively identify the transmission of our nanofluid related to the solar spectrum. Figure 2 shows the results for a) the PLAL nanofluid and b) the two-step nanofluid developed with commercial tin NPs. It is observed that for the first and second days both samples have a similar transmission behaviour. However, after the fourth day, the transmission of the PLAL sample is clearly lower. This can be attributed to its enhanced stability and is corroborated by visual inspection in Figure 1 a).
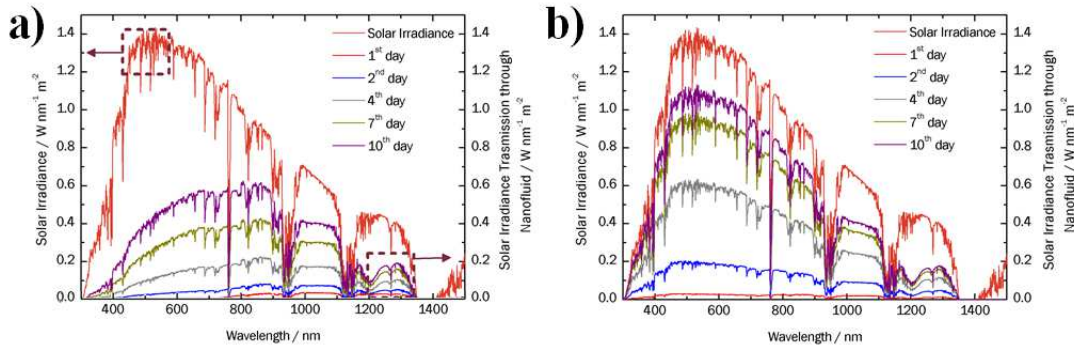
Figure 2. Reference solar spectral irradiance ASTM G-173 and the transmission of solar spectral irradiance through 1 cm of the nanofluid several days after formation: a) PLAL and b) commercial nanofluid.

In a first order approximation, calculations of the fraction of the incident power absorbed in the nanofluid after a path length of 1 cm have been done at the fourth, seventh and tenth days in order to study the temporal evolution of nanofluid performance. A detailed mathematical description of the methodology used can be found in Ref. [4]. In short, the experimental extinction coefficient of NPs decoupled from the base fluid contribution can be extracted from the transmission spectra. Then, the Rayleigh theory is used to calculate the scattering albedo which is required to calculate the spectral absorption coefficient, $\mu_{abs}(\lambda)$. Finally, to evaluate the sunlight absorption capability of nanofluid, the fraction F of the incident power absorbed in the fluid after a path length l within it is calculated from Equation [1]:

$$F(l) = 1 - \frac{\int_{\lambda_{min}}^{\lambda_{max}} I(\lambda) \cdot e^{-\mu_{abs}(\lambda) \cdot l} d\lambda}{\int_{\lambda_{min}}^{\lambda_{max}} I(\lambda) d\lambda} \qquad [1]$$

where λ represents the wavelength, λ_{max} represents the maximum wavelength considered, λ_{min} the minimum wavelength considered, $\mu_{abs}(\lambda)$ the spectral absorption coefficient, and $I(\lambda)$ represents the solar spectra irradiance. In our calculations the sunlight absorption was calculated for the spectrum between 400–1500 nm and path length l=1 cm. This calculation considers ethylene glycol as base fluid and tin as the NPs. Under this circumstances, the simulation predicts that the absorbed sunlight fraction of the nanofluid synthesized by PLAL is at least the double than the commercial one as show in Table 1 [5].

Table 1. Absorbed sunlight fraction of the nanofluid for different days.

Day	PLAL nanofluid	Commercial nanofluid
4th	67%	29%
7th	57%	19%
10th	48%	18%

Conclusions:

In this contribution, it was demonstrated that PLAL can be used to produce direct volumetric absorbers with remarkable thermal properties composed by tin and ethylene glycol for its exploitation in the harvesting of solar radiation field. By means of visual observation, DLS, the measurement of the thermal conductivity, and transmission spectra of the samples through the time, we show that the nanofluid produced by PLAL traps the electromagnetic radiation in a more convenient manner than nanofluids produced through conventional synthesis methods. Additionally, it shows a better stability against sedimentation.

References:

1. T. P. Otanicar, P. E. Phelan, and J. S. Golden, Optical properties of liquids for direct absorption solar thermal energy systems, *Sol. Energy* 83 (2009) 969-977.
2. A. Lenert and E. N. Wang, Optimization of nanofluid volumetric receivers for solar thermal energy conversion, *Sol. Energy* 86 (2012) 253-265.
3. V. Amendola and M. Meneghetti, Whats controls the composition and the structure of nanomaterials generated by laser ablation in liquids solutions, *Phys. Chem. Chem. Phys.* 15 (2013) 3027-3046.
4. R. Mondragón, R. Torres-Mendieta, M. Meucci, G. Mínguez Vega, E. Juliá, and E. Sani, Synthesis and characterization of gold/water nanofluids suitable for thermal applications produced by Femtosecond Laser Radiation, *J. Photonics Energy* 6 (2016) 034001.
5. R. Torres Mendieta, R. Mondragón, V. Puerto Belda, O. Mendoza Yero, J. Lancis, G. Mínguez Vega, and J. E. Juliá, Characterization of tin/ethylene glycol solar nanofluids synthesized by femtosecond laser radiation, *ChemPhysChem* 18 (2017) 1055-1060.

NANOROUND – A PROPOSAL FOR A NUMERICAL ROUND ROBIN TEST FOR SIMULATION OF NANOFLUIDS

A. A. Minea[1], A. Huminic[2], G. Huminic[2], J. Tibaut[3] and J. Ravnik[3],*

[1]Faculty of Materials Science and Engineering, Technical University "Gheorghe Asachi" from Iasi, Iasi, Romania

[2]Transilvania University of Brasov, Brasov, Romania

[3]Faculty of Mechanical Engineering, University of Maribor, Slovenia

*Corresponding author: jure.ravnik@um.si

Keywords: Round robin test, Nanofluid models, Laminar flow in a pipe

Introduction: Heat transfer in straight tubes and channels was the subject of numerous researches for the last century [1, 2]. The development of new applications stimulated a great interest to study flow and heat transfer in micro-channels [3, 4]. A number of theoretical and experimental investigations devoted to this problem were performed during last years [5–8] and data on heat transfer in laminar and turbulent flows in micro/macro channels with different geometry were obtained. Several special problems related to heat transfer in channels were extensively discussed in the literature: effect of axial conduction in the wall, viscous dissipation effect [8-14] and comprehensive surveys may be found in [13-16].

Nanofluids (i.e. suspensions nanometre-sized particles in a base liquid) have been a subject of tremendous efforts during last years. Researchers have been focusing on the production procedures, on measuring nanofluid properties as well as on numerical modelling of nanofluids. Several models and numerical approaches as well have been proposed [17]. The models differ in terms of the used limitations and assumptions, which were taken into account as well as in terms of the description of the nanofluid. Single-phase approaches with effective properties have been used as well as two phase Euler – Lagrange and other approaches were considered. Researchers have proposed the use of an additional convection-diffusion equation for nanoparticle concentration and have been determining nanofluid properties based on the spatially and temporarily varying concentration [17]. A vast amount of literature on the subject exists, where different models have been proposed and tested on different flow and heat transfer configurations to a varying degree of success against other numerical or experimental test cases. However, the models and computational approaches have not been tested on an equal footing in order to establish the optimal modelling approach. Thus, based on the available literature, it is still not clear, which is the best way of modelling nanofluids in numerical simulations in order to provide as accurate as possible results and facilitate engineers in the design process of devices, which use nanofluid as a working fluid. Thus, we propose to start the *NANOROUND* project – a numerical round robin test aimed at comparing numerical nanofluid models.

Round robin test: With this paper, we intent to set a base to invite research groups to participate in a numerical round robin test for simulation of nanofluids. Commercial, open-source or in-house computational fluid dynamics codes may be used based on any numerical method. The groups are invited to use their preferred nanofluid model and simulate the one of the two test cases described below. Each group should make their own grid sensitivity and time step analyses. A document describing the boundary conditions in detail will be made available on the *NANOROUND* project website.

Test cases: Test cases were selected based on the existing literature and also by checking the details inserted by each groups. Finally, for preliminary readings we have chosen two experimental studies [18, 19] with a simple geometry and well defined initial and boundary conditions. Both have considered laminar flow of nanofluids in a pipe with constantly heated walls. They both have considered water based nanofluids with different particle concentrations as well as pure water for comparison. When a nanofluid enters the heated test section, it is heated up and the temperature at the wall was measured in several locations along the pipe.

The boundary and initial conditions of the two test cases can be summarized as follows: a constant temperature nanofluid enters the test section. At the inlet, the flow is laminar (Reynolds number is around 1000), fully developed and steady. As it travels through the pipe it is heated by a prescribed heat flux on the walls. The pipe is straight and at the outlet an outlet boundary condition may be prescribed. At the walls a no-slip boundary condition may be applied.

By this time, the authors of this paper worked most on test case A that is explained further on. Test case A is based on Colla et al. [19]. In Figure 1 a scheme of the experiment is shown. Results of measurement for test case A are given in Table 1, were placement of temperature sensors is shown and all measurements are in mm. Pipe length is 2m and the pipe diameter is d = 8mm.
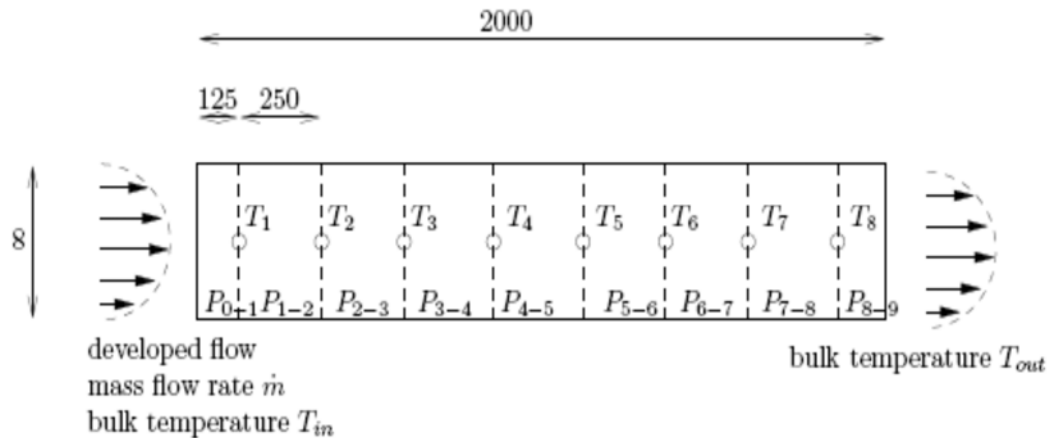
Figure 1: A sketch of the test case.

Table 1: Experimental values for test case A [19].

inlet							
mass flux, $\dot{m} = 0.0061151\,kg/s$							
bulk temperature at inlet, $T_{ie} = 19.57^\circ C$							
water properties at inlet: $\rho = 998.295\,kg/m^3$, $k = 0.597685\,W/mK$,							
$c_p = 4184.36\,J/kgK$, $\mu = 1.012429 \cdot 10^{-3}\,Pas$							
Reynolds number at inlet, $Re = \frac{4\dot{m}}{\pi d \mu} = 961.4$							

outlet							
bulk temperature at outlet, Tout = 27.38∘C							

wall temperature [$^\circ C$]							
T_1	T_2	T_3	$T4$	$T5$	$T6$	T_7	T_8
25.6	28.0	28.7	29.5	30.2	30.9	31.8	32.7

power [W]								
$P0{-}1$	$P1{-}2$	$P2{-}3$	$P3{-}4$	$P4{-}5$	$P5{-}6$	$P6{-}7$	$P7{-}8$	$P8{-}9$
12.6	25.2	25.2	25.2	25.0	24.9	24.9	24.8	12.4

Based on Colla et al. [19] experimental conditions we fixed the initial and boundary conditions as seen in Table 1.

Temperature dependent water properties to be taken into account for simulation are in Table 2. All expressions should be used with temperature expressed in $^\circ C$.

Table 2. Water properties

Density:
$\rho(T)\ [kg/m^3] = 1.31839028583 \cdot 10^{-9} \cdot T^5 - 4.1415691320879 \cdot 10^{-7} \cdot T^4$
$+0.0000627465524729587 \cdot T^3 - 0.00812457260548172 \cdot T^2$
$+0.0554068116720146 \cdot T + 999.90837195736$
Thermal conductivity:
$k(T)\ [W/mK] = -0.0000000000074354379 \cdot T^5$

$+2.43717635743 \cdot 10^{-9} \cdot T^4 - 0.0000002889967610567 \cdot T^3$

$+5.15309471096903 \cdot 10^{-6} \cdot T^2 + 0.00185267131276284 \cdot T + 0.561293060017584$

Specific heat at constant pressure:

$c_p(T) \ [J/kgK] = -4.088550653591 \cdot 10^{-8} \cdot T^5$

$+0.0000117146192195605 \cdot T^4 - 0.00137712095636289 \cdot T^3$

$+0.0902711920148249 \cdot T^2 - 2.99500832260219 \cdot T + 4217.11488982432$

Viscosity:

$\mu(T) \ [Pas] = 2.414 \cdot 10^{-5} \times 10^{247.8/(T+133.15)}$

Using the above mentioned properties, preliminary results were obtained in Ansys Fluent and CFX [20] solvers using different settings (studying also the influence of gravity), profiles for inlet velocity and also considering conduction in the copper tube. Some of the preliminary results are summarized in Figure 2.
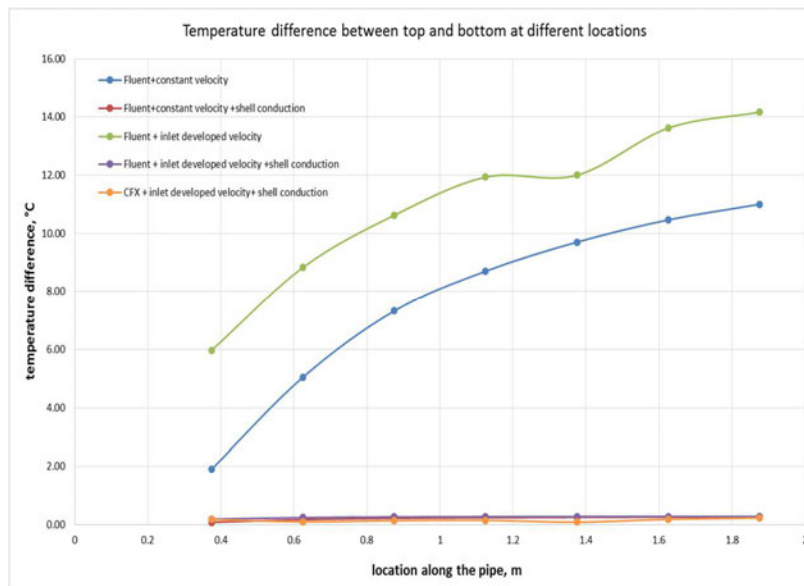
a.
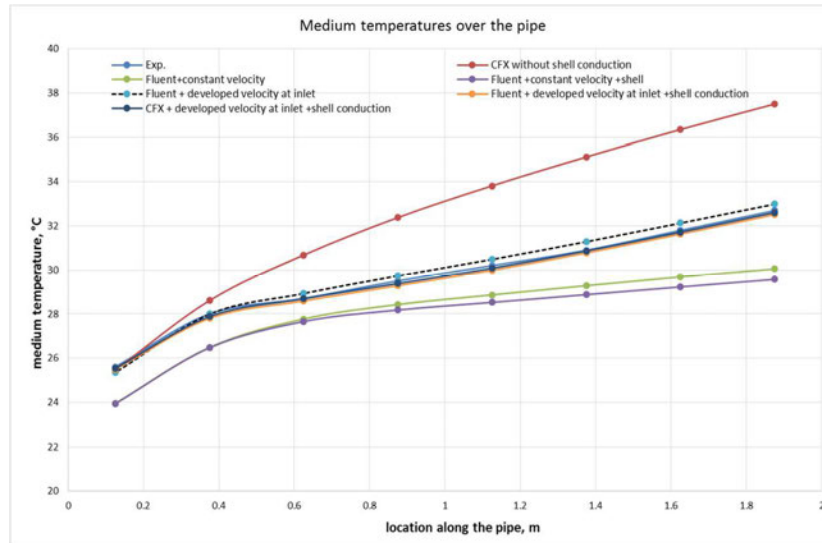
b.

Figure 2. Preliminary results: a. difference in temperature between top and bottom of the pipe at different locations along the pipe; b. medium temperature at a certain point.

Also, by performing our calculus both in Fluent and CFX we noticed strong influence of gravity, which change the classical (Hagen-Poiseuille) velocity profile and generate also a rotational flow, which clearly influence the heat transfer.

The aim of the *NANOROUND* numerical simulations will be to predict measured wall temperatures as well as to export results in a prescribed and organized manner to facilitate comparison between different groups, nanofluid models and computational approaches.

Summary: Efforts were done to validate the experimental results obtained by Colla et al [18] since the performed experiment was very detailed and we worked on every point validation and not on an overall one in order to attain extremely accurate results and to establish a very well defined base for the numerical study. A lot of possible scenarios were considered as one can see from preliminary results inserted. This technique was not applied until now, as far as the authors are aware.

In conclusion, we propose to start the *NANOROUND* project – a numerical round robin test aimed at establishing the advantages and disadvantages of nanofluid models. Research groups with expertise in computational fluid dynamics and nanofluid modelling are welcome to participate. The project dissemination activities will include a website to publish the results and findings as well as a scientific paper reporting on the results. Presentation at the next European Symposium on Nanofluids is also planned.

References:

1. Petukhov B.S. (1967) Heat transfer and drag of laminar flow of liquid in pipes. Energy, Moscow.
2. Kays W.M., Crawford M.E. (1993) Convective Heat and Mass Transfer, McGraw-Hill, New York.
3. Ho, C.M. Tai, Y.-C. (1998) Micro-electronic mechanic systems (MEMS) and fluid flows, Ann. Rev. Fluid Mech. 30, pp 5–33.
4. Gad-el-Hak, M. (1999) The fluid mechanics of micro-devices. The Freeman Scholar Lecture, J. Fluid Eng. 12, pp1 5–33.
5. Reynaud S., Debray F., Frans J.-P., Maitre, T. (2005) Hydrodynamics and heat transfer in two-dimensional mini-channels, Int. J. Heat Mass Transfer 48 3197–3211.
6. Wang B.X., Peng, X.F. (1994) Experimental investigation on liquid forced- convection heat transfer through microchannels, Int. J. Heat Mass Transfer 37 (1) 73– 82.
7. Peng X.F., Peterson G.P. (1995) The effect of thermofluid and geometric parameters on convection of liquid through rectangular micro-channels, Int. J. Heat Mass Transfer 38, 755–758.
8. Peng X.F., Peterson, G.P. (1996) Convective heat transfer and flow friction for water flow in micro-channel structures, Int. J. Heat Mass Transfer 39, 2599–2608.
9. Maranzana G., Perry, I. Maillet D. (2004) Mini- and microchannels: influence of axial conduction in the walls, Int. J. Heat Mass Transfer 47 3993–4004.
10. Tunc, G. Bayazitoglu, Y. (2001) Heat transfer in micro-tubes with viscous dissipation, Int. J. Heat Mass Transfer 44, 2395–2403.
11. Koo J., Kleinstreuer, C. (2004) Viscous dissipation effects in micro-tubes and micro-channels, Int. J. Heat Mass Transfer 47, 3159–3169.
12. Sobhan, C.B., Garimella, S.V. (2001) A comparative analysis of studies on heat transfer and fluid flow in micro-channels, Microscale Thermophys. Eng. 5, 293–311.
13. Hassan, I.. Phuttavong P,. Abdelgawad, M (2004) Micro-channel heat sinks: an overview of the state of the art, Microscale Thermophys. Eng. 8, 183–204.
14. Morini, G.L. (2004) Single-phase convective heat transfer in micro-channels: overview of experimental results, Int. J. Thermal Sci. 43, 631–651.
15. Garimella S.V., Sobhan, C.B. (2003) Transport in micro-channels- a critical review, Ann. Rev. Heat Transfer 13, 1– 50.
16. Minea, AA. (2017) Advances in New Heat Transfer Fluids: From Numerical to Experimental Techniques, CRC Press.
17. Wen, D. & Ding, Y. Experimental investigation into convective heat transfer of nanofluids at the entrance region under laminar flow conditions, International Journal of Heat and Mass Transfer, 47 pp. 5181–5188, 2004.
18. Colla, L., Fedele, L., & Buschmann, M. H. (2015). Laminar mixed convection of TiO2-water nanofluid in horizontal uniformly heated pipe flow. International Journal of Thermal Sciences, 97, 26–40.
19. Ansys commercial code

DEVELOPMENT OF THE BOUNDARY ELEMENT METHOD FOR SIMULATION OF NANOFLUIDS

J. Ravnik* and J. Taibaut

Faculty of Mechanical Engineering, University of Maribor, Slovenia

*Corresponding author: jure.ravnik@um.si

Keywords: Boundary element method, Variable material properties, Nanofluids

Introduction: Many natural phenomena involve energy transfer, which is governed by the diffusion and convection transport processes. In nature and for most engineering purposes, heat transfer occurs in environments, where the velocity of the fluid changes within the domain in question. Fluid properties, such as density, specific heat and heat conductivity are usually considered as constant. However, there are examples, where changes in fluid material properties must be considered. One example is a case, where large temperature differences are present in the simulation domain. Since material properties are temperature dependent, these must be considered. Another example are nanofluids [1]. These are suspensions of nanometre-sized particles in a base liquid. The properties of the suspension (when modelled as a single phase liquid with modified properties) depend on the concentration of the particles, which in turn depends on the flow field.

Transport phenomena, such as momentum, mass and heat transferred are governed by the diffusion-convection partial differential equations. Numerical solution of these is a challenging task. Many numerical algorithms have been proposed. In this paper, we develop the boundary element method for simulation of nanofluids with variable material properties.

Numerical method: Fluid flow and heat transfer are governed by systems of nonlinear partial differential equations. When nanofluids are considered in a single-phase Eulerian framework the fluid material properties also vary with location and time due to the changes in temperature and nanoparticle distribution. We developed a boundary element based method for simulation of such systems. The method is based on the use of the fundamental solution of the underlying partial differential equation to write an integral representation of the governing equations. We implemented it on the velocity-vorticity formulation of Navier-Stokes equations and solved it by a domain decomposition approach. Treatment of variable material properties has implemented by a careful derivation of the integral formulation of the governing equations to give a field gradient free representation. The employed domain decomposition approach leads to sparse over-determined systems of linear equations, which are solved in a least-squares manner.

Validation: The developed fluid flow and heat transfer solver has been validated using several benchmark test cases. The standard lid driven cavity and natural convection in a cavity cases were used to establish the validity of the method and assess the solution convergence properties on different mesh designs. We found that the developed method is second order accurate and is,

due to the used of the fundamental solution of the governing PDE, able to capture the physics of flows using relatively coarse meshes.

Discussion and Results: The developed numerical method was used to simulate enhancement of free convection in several configurations, [2-4]. In Figure 1 geometry and boundary conditions of the simulation cases are presented. An example of results is shown in Figure 2. The main conclusion drawn from the analysis was that the use of a nanofluid as compared to base fluid enhances heat transfer the most when conduction is the dominant heat transfer mechanism. In convection-dominated flows, the enhancement achieved by nanofluid is lower.
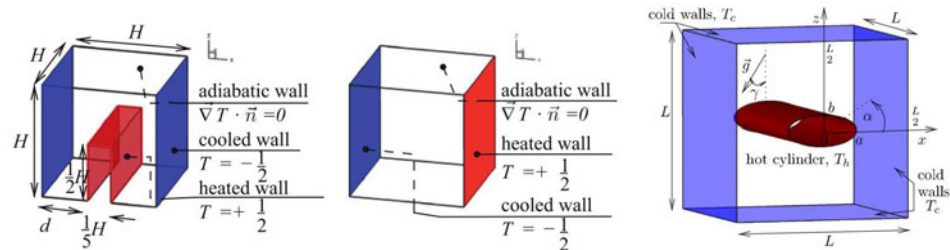
Figure 1: Geometry and boundary conditions of the simulation cases.
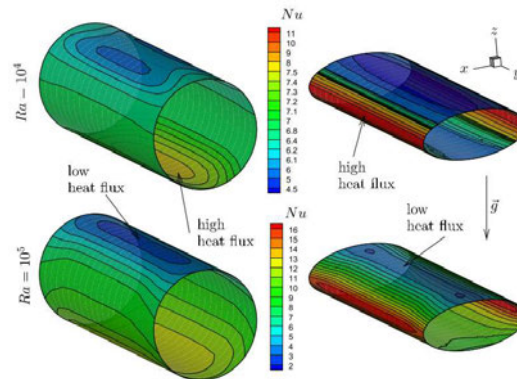
Figure 2: Example analysis of heat flux distribution for one of the simulation cases.

Summary: We developed a boundary element based numerical technique, which is able to simulate flow and heat transfer of fluid with variable material properties. The developed technique was validated and tested by simulating free convection of a nanofluid.

References:

1. Choi, S. U. S. Enhancing thermal conductivity of fluids with nanoparticles. *Develop. Appl. Non Newtonian Flows*, 66 (1995) 99–106

2. Ravnik, J., Skerget, L., and Hribersek, M. Analysis of three-dimensional natural convection of nanofluids by BEM. *Engineering Analysis with Boundary Elements*, 34 (2010), 1018–1030.

3. Ravnik, J., & Škerget, L. A numerical study of nanofluid natural convection in a cubic enclosure with a circular and an ellipsoidal cylinder. *International Journal of Heat and Mass Transfer*, 89 (2015) 596–605.

4. Kramer Stajnko, J., Jecl, R., and Ravnik, J. Numerical simulation of convective flow in a non-Darcy porous cavity filled with nanofluid. *International Journal of Computational Methods and Experimental Measurements*, 4 (2016) 454–463.

NANOFLUID THERMAL BOUNDARY LAYER

J.T.C. Liu*, D. Hopper, D. Jaganathan, J.L. Orr, J. Shi, F. Simeski and M. Yin

School of Engineering EN2760 and the Centre for Fluid Mechanics, Brown University, Providence, Rhode Island 02912, USA

*Corresponding author: joseph_liu@brown.edu

Keywords: Nanofluids, Convective Heat Transfer, Heat Transfer Enhancement, Adiabatic temperature

Introduction: Application of nanofluids in heat transfer enhancement involves flowing nanofluids in, for instance, forced convective heat transfer situation, as in the experiments of Wen and Ding [1] and of Jung, et al. [2] in microchannels. They showed that the leading edge region of the microchannels gave significant heat transfer enhancement as function of increasing nanofluid volume fraction. In this case, it is of theoretical importance to understand the convective thermal boundary layer behaviour that resembles the channel leading edge over a large streamwise distance before the boundary layers merge, whereas the downstream fully developed region has much less spectacular heat transfer behaviour.

The continuum description [3] of the nanofluid boundary layer is in general in compressible form, even though the base fluid is incompressible. This is because of the dependence of the nanofluid thermophysical properties on the nanoparticle concentration, which in turn, is subjected to nanoparticle diffusion through possible Brownian diffusion and thermal diffusion effects. On the basis that nanofluid heat transfer experiments are carried out at very dilute nanofluid volume fractions, a series of papers [4-6] devised a perturbation scheme for small volume concentrations. This reduced the problem into perturbation about the base fluid; the nanofluid effect becomes linear and separable nanofluid momentum, diffusion and thermal boundary layer equations.

The Basic Equations for Nanofluid Boundary Layer Flow: Because of the dependence of the nanofluid thermophysical properties on the concentration of nanoparticle volume fraction, the fundamental equations are necessarily in the form for a compressible fluid, even though the individual constituents, such as the base fluid and the dispersed nanoparticles, are individually incompressible. The continuum description is synthesized by Buongiorno [3]. Use is made of the two-dimensional flat plate as an approximation for the leading edge of a semi-infinite micro channel in the developing region prior to the merging influence of the upper and lower walls. The two-dimensional boundary later continuity and momentum equations for steady flow are given in [5,6]; we state the energy equation that is augmented from that used in [5,6] to include the effect of viscous dissipation. It is presented first in dimensional form for discussion purposes

Thermal energy:
$$\rho\left(u\frac{\partial h}{\partial x}+\upsilon\frac{\partial h}{\partial y}\right)=-\frac{\partial q}{\partial y}+\mu\left(\frac{\partial u}{\partial y}\right)^2$$

where the nanofluid static enthalpy is $h=\int c\,dT,\ c=dh/dT$ is the nanofluid heat capacity and T is the absolute temperature, The work done by the pressure gradients is not present for the zero streamwise and normal pressure gradients in this case. The normal component of the heat flux vector is q and includes the mechanisms of conduction and thermal energy transport owing to nanoparticle concentration diffusion

$$q=-\left(k\frac{\partial T}{\partial y}\right)-\left(\rho_p D\frac{\partial\phi}{\partial y}h_p\right)$$

where k is the nanofluid thermal conductivity, ρ_p is the nanoparticle density, D is the Brownian diffusion coefficient [7], ϕ is the nanoparticle phase volume fraction, $h_p=c_pT$ is the static enthalpy of the nanoparticle phase, c_p is it's heat capacity. Thermal equilibrium is assumed between the base fluid and the nanoparticle phase [3]. The rate of viscous dissipation is the last term in the thermal energy equation, to include this effect, it will be shown that it is convenient to let the nanofluid temperature remain dimensional. Thu the nanofluid energy equation in boundary layer form becomes

$$\rho*c*\left(u*\frac{\partial T}{\partial x*}+\upsilon*\frac{\partial T}{\partial y*}\right)=\frac{1}{\mathrm{Re\,Pr}_f}\frac{\partial}{\partial y*}\left(k*\frac{\partial T}{\partial y*}\right)+\frac{\phi_\infty}{\mathrm{Re}\,Sc_f}\frac{\partial}{\partial y*}\left((\rho c)*D*\frac{\partial\Phi}{\partial y*}T\right)+\frac{U^2/c_f}{\mathrm{Re}}\mu*\left(\frac{\partial u*}{\partial y*}\right)^2$$

subscript ∞ denote conditions in the free stream, the Prandtl number is $\mathrm{Pr}_f=\nu_f/\kappa_f$, where the subscript f pertains to the base fluid, the kinematic viscosity and thermal diffusivity are $\nu_f=\mu_f/\rho_f,\ \kappa_f=k_f/\rho_fc_f$, respectively. The Schmidt number is $Sc_f=\nu_f/D_{ref}$, the dimensionless nanoparticle density heat capacity product is $(\rho_pc_p)*=\rho_pc_p/\rho_fc_f$, $D*=D/D_{ref},\ D_{ref}=k_BT_{ave}/6\pi\mu_fr_d$. The Brownian diffusion coefficient is evaluated at the average temperature T_{ave}, so that $D*=1$, k_B is the Boltzmann constant, r_d is the average nanoparticle radius.   While the heat transfer problem in absence of viscous dissipation is thoroughly discussed in [5,6], the present work discusses the adiabatic wall problem, which completes the overall study of the nanofluid thermal boundary layer. The dependency of the nanofluid density, heat capacity, thermal conductivity and viscosity upon the nanofluid concentration necessitates the computation of the volume concentration according to the diffusion equation for $\Phi=\phi/\phi_\infty$, it is derivable from continuity equation for the nanoparticle species in terms of its mass fraction and then related to the volume fraction for dilute concentration [5,6]. Thermal diffusion is neglected.

Thermophysical Properties: The continuum description [7] requires input from separate considerations of the thermophysical properties, and are represented in terms of the volume fraction. To first order in the volume fraction, in dimensionless form normalized by the corresponding quantity of the base fluid,

$$\rho^* = 1 + \phi_\infty (\rho^*)'_{\phi=0} \Phi + \vartheta(\phi_\infty^2)$$

$$\rho^* c^* = 1 + \phi_\infty (\rho^* c^*)'_{\phi=0} + \vartheta(\phi_\infty^2)$$

$$\mu^* = 1 + \phi_\infty (\mu^*)'_{\phi=0} \Phi + \vartheta(\phi_\infty^2)$$

$$k^* = 1 + \phi_\infty (k^*)'_{\phi=0} \Phi + \vartheta(\phi_\infty^2)$$

where $(\chi^*)'_{\phi=0}$ is the slope of $\chi^*(\phi)$ at the origin. The representations are in "general form" in that they could be obtained from various separate considerations discussed in [5,6] and will not be elaborated here. The preference is to use properties recently obtained from molecular dynamics simulations [9-11], although this is performed only for gold-water nanofluids. Denoting by subscript MD for molecular dynamics, the properties extracted from [9-11] by [5] are $(\rho^*)'_{\phi=0,MD} \cong 18.7$, $(\rho^* c^*)'_{\phi=0,MD} \cong -2.37$, whereas results for viscosity and thermal conductivity are only available in [9] and subject to interpretation [5], are $(\mu^*)'_{\phi=0,MD} \cong 10$, $(k^*)'_{\phi=0,MD} \cong 20$. **Dilute**

Nanoparticle Concentration-Perturbation for $\phi_\infty \ll 1$: In general, nanofluid heat transfer experiments (e.g., [1,2]) are performed for dilute nanoparticle concentration. In this case, simplifications result from a perturbation analysis for $\phi_\infty \ll 1$. The perturbation expansion is first applied to the partial differential equations, incorporating the thermophsical properties (which are already in perturbation form), the results are subjected to the similarity transformation of the Blasius-Pohlhausen type [12] for both perturbation orders: $\eta = y^*/\sqrt{x^*/\mathrm{Re}}$ with streamfunction $\psi^* = \psi/UL = f(\eta)\sqrt{x^*/\mathrm{Re}}$ and transformed velocity components $u^* = f'(\eta)$, $v^* = (\eta f' - f)/2\sqrt{x^*/\mathrm{Re}}$, where primes denote differential with respect to η. The small volume fraction perturbation reduces the boundary layer equation to an incompressible form, in which only the zeroth order momentum equation is nonlinear. The momentum and diffusion problems remain unchanged for the present problem and we refer to [5,6] for details of the similar solutions. The perturbation for the thermal boundary layer is stated more explicitly $\theta_H = \theta_{H,0} + \phi_\infty \theta_{H,1} + \vartheta(\phi_\infty^2)$ and $\theta_P = \theta_{P,0} + \phi_\infty \theta_{P,1} + \vartheta(\phi_\infty^2)$. The zeroth order ($\theta_{H,0}$) and first order ($\theta_{H,1}$) heat transfer problems are identical to that discussed in [5,6]. The viscous dissipation effect enters through the particular solutions $\theta_{P,0}$ for the base fluid for an insulated wall [12], the the first order nanofluid thermal boundary layer equation obtained is

$$\theta''_{P,1} + (\mathrm{Pr}_f/2)(f_0\theta'_{P,1} + f_1\theta'_{P,0}) = -[(k*)'_{\phi=0} - (\rho*c*)'_{\phi=0}]\Phi\theta''_{P,0} - (k*)'_{\phi=0}\Phi'\theta'_{P,0} - \mathrm{Pr}_f[(\rho_p c_p)*/Sc_f](\Phi'\theta_{P,0})'$$

$$-2\mathrm{Pr}_f[(\mu*)'_{\phi=0}\Phi(f''_0)^2 + 2f''_0 f''_1]$$

$$\theta'_{P,1}(0) = 0, \quad \theta_{P,0}(\infty) = 0$$

The numerical integration results for gold-water nanofluid using molecular dynamics properties is shown in Figure 1. The diffusion layer for $\Phi(\eta)$ is much thinner than that of the thermal boundary layer owing to the large Schmidt number for which $Sc_f = 2\times10^4$ (for nanoparticle radius of $10nm$) and $\mathrm{Pr}_f = 7$. Referring to Figure 1, the $\Phi_W = 1$ case is equivalent to a solid wall for which there is no nanoparticle flux at the wall, $\Phi'(0) = 0$. The $\Phi_W = 0$ case is one in which the wall is porous and nanoparticles are removed by a magnitude equal to the free stream concentration ϕ_∞, resulting in a lowered adiabatic wall temperature. The $\Phi_W = 2$ case is one in which nanoparticles are injected at the wall by a magnitude equal to the free stream concentration ϕ_∞, resulting in increased adiabatic wall temperature. The effect is mainly due to the dependence of transport properties dependent on the volume concentration near the wall. The bulge of the temperature profiles $\theta_{P,1}(\eta)$ is due to the maximum of the viscous dissipation in the interior of the boundary layer.
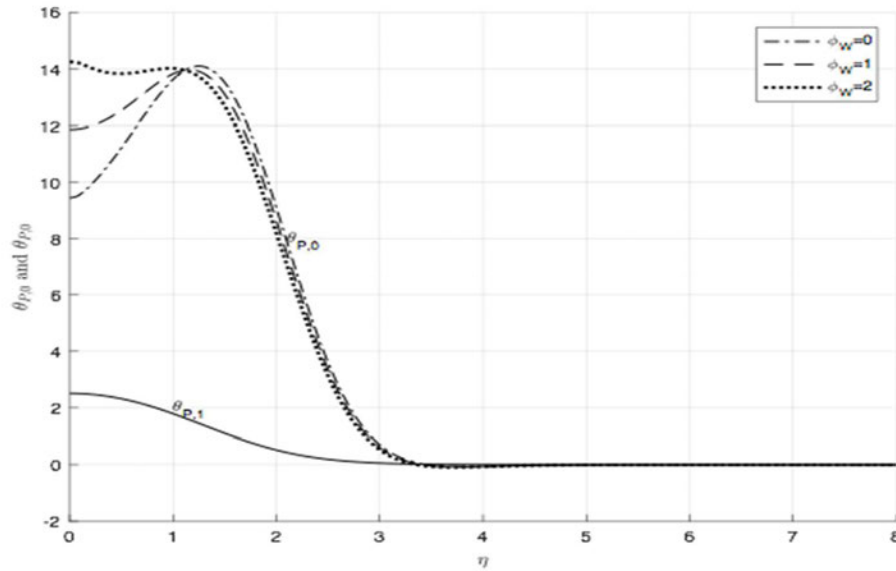

Figure 1. Dimensionless temperature profiles $\theta_{P,0}$ (solid line) and $\theta_{P,1}$ (dashed lines) vs. η. Adiabatic wall temperatures $\theta_{P,1}(0;\Phi_W)$: $\theta_{P,1}(0;0) = 9.46, \ \theta_{P,1}(0;1) = 11.87, \theta_{P,1}(0;2) = 14.86$.

Concluding Remarks: The present particular solution $\theta_{P,1}(\eta)$ can always be combined with the heat transfer solution θ_H obtained in [6] to form the general solution for the heat transfer with viscous dissipation. The possibilities of applying the continuum framework to estimate heat transfer capabilities, relative to skin friction rise, depends on the availability of nanofluid properties. This could be obtained through further applications of molecular dynamics to other combination of nanoparticles and base fluids, or, via experimentally obtained properties.

References:

1. D. Wen and Y. Ding, Experimental investigation of nanofluids of the entrance region under laminar flow conditions, *International Journal of Heat and Mass Transfer* 47 (2004) 5181-5188.
2. J.-Y. Jung, H.-S. Oh, H.-Y. Kwak, Forced convective heat transfer of nanofluids in micro channels, *International Journal of Heat and Mass Transfer* 52 (2009) 466-472.
3. J. Buongiorno, Convective transport in nanofluids, *ASME Journal of Heat Transfer* 128 (2006) 240-250.
4. J.T.C. Liu, On the anomalous laminar heat transfer intensification in developing region of nanofluid flow in channels or tubes, *Proc. of the Royal Society* A 408 (2012) 2383-2398.
5. J.T.C. Liu, M.E. Fuller, K.L. Wu, A. Czulak, A.G. Kithes and C.J. Felten, Nanofluid flow and heat transfer in boundary layers at small nanoparticle volume fraction: zero nanoparticle flux at solid wall, Archives of Mechanics 69 (Warszawa 2017) 75-100.
6. C.J.B. de Castilho, M.E. Fuller, A. Same and J.T.C. Liu, Nanofluid flow and heat transfer in boundary layers: the influence of concentration diffusion on heat transfer enhancement, *Journal of Heat Transfer Engineering* (accepted for publication, 2017).
7. P.A. Lagerstrom, *Laminar Flow Theory,* Princeton University Press, Princeton, N.J., 1996.
8. A. Einstein, On the motion of small particles suspended in liquids at rest required by the molecular-kinetic theory of heat, *Annalen der Physik* 17 (1905) 549-560.
9. G. Puliti, *Properties of Gold-Water Nanofluids Using Molecular Dynamics,* Ph.D. Thesis, Univ. Notre Dame, 2012.
10. G. Puliti, S. Paolucci and M. Sen, Thermodynamics of gold-water nanofuids using molecular dynamics, *J. Nanoparticle Research* 14 (2012), article no. 1296.
11. S. Paolucci and G. Piliti, Properties of nanofluids, in *Heat Transfer Enhancement with Nanofluids,* Eds., Bianco, V., Manca, O., Nardini, S. and Vafai, K., pp.1-44, CRC Press, New York, 2015.
12. H. Schlichting, *Boundary Layer Theory, 7th edition* (Translated by J. Kestin), McGraw-Hill, New York, 1979.

TAILORING THE PROPERTIES OF NANOPARTICLES BY ALD NANOCOATINGS

D. Valdesueiro*, A. Goulas and B. van Limpt

Delft IMP B.V., Molengraaffsingel 10, 2629 JD, Delft, The Netherlands

*Corresponding author: d.valdesueiro@delft-imp.nl

Keywords: Atomic layer deposition, nanoencapsulation, nanoparticles, nanocoatings

Introduction: In this paper we present a gas-phase coating technology, atomic layer deposition (ALD),that allows the deposition of nanometer-thin conformal coatings on a wide variety of particles. The versatility of ALD covers both the nature and size of the particles, as well as to the chemistry of the coating. For example, particles ranging from nanoparticles to particles of several hundreds of micrometers can be coated with this technique. Additionally, the nature of the substrate can be ceramic (e.g. Al_2O_3, TiO_2, SiO_2), metallic (Ti), and polymeric (powder coating paints), amongst many others. The nature of the coating can be also selected from metal oxides (Al_2O_3) or nitrides (e.g. AlN), pure metals (e.g. Pt), organic coatings and even inorganic-organic hybrid coatings [1]. These thin films can be also used for nanofluid applications, achieving an encapsulation of the nanoparticles comprising the nanofluids without interfering with their intrinsic heat properties.

ALD is a coating process that relies on a layer-by-layer growth mechanism in which the coating chemistry is split into two half-reactions. Each of these reactions is self-limiting, such that at most a monolayer of a compound can be deposited per cycle (Figure 1). In this way, we have full control over the coating thickness: the number of times that the alternating feed of the two precursors is repeated determines the thickness of the achieved coating [2].
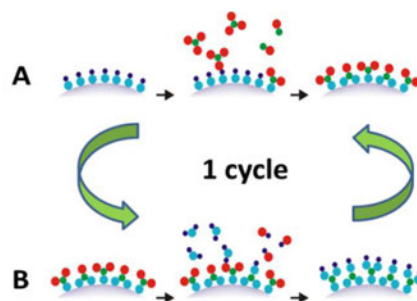
Figure 1. Reaction mechanism of one cycle of atomic layer deposition.

In recent years, atomic layer deposition (ALD) has become a standard tool to apply ultrathin and conformal coatings on substrates of complex geometries, mostly driven by an interest from semiconductor industry applications. The intrinsic advantages of controlling the structure growth at the (sub)nanometer level, while coating complex surfaces – either for providing

protection to the substrate or boosting its activity – are also relevant for other industrial applications related to particle technology, such as nanofluids.

In a nutshell, in this presentation we will also show two examples of the influence of nanometer-thin aluminium oxide films on two different applications that can be relevant in the development of nanofluids. One example shows the encapsulation of a polymer-based powder with nanometer-thin films, which confined the softened core material without altering the thermal properties. That can be of use with nanofluids based on phase change materials. The second example consisted of using an alumina layer to improve the affinity between an inert core and a radioactive isotope, to be used as tracer in hydrodynamic studies of concentrated solar plants. This application can be interesting in order to investigate the coating performance at elevated temperatures. A more detailed description is given below, aiming at incorporate this coating process as a potential technique to boost the industrial application of nanofluids.

Discussion and Results: The first example is the tuning of the surface finish of a standard polyester-based powder coating paint, from gloss to matt (Figure 2, left), by depositing ultrathin films of Al_2O_3 on the powder coating particles [3]. The coating experiments were performed in a fluidized bed reactor at 1 bar and 27 °C, using an alternating exposure of the particles to the two precursors (trimethylaluminium and water). By varying the number of coating cycles from 1 to 9, we deposited alumina films ranging from 1 to 30 nm. When the average alumina shell was thicker than 6 nm, the shell prevented the flow of the core particles, even though the powder particles did soften above their glass transition temperature. With the particles morphology intact, this resulted in a rough and matte surface finish of the coating after curing. Additionally, the alumina coating acted as a barrier able to encapsulate the softened powder coating above the glass transition temperature, without altering other thermal properties as such as the glass transition temperature (Figure 2, right). This type of application can be extended to the encapsulation of phase change materials with thin alumina films, that would contain a molten core without modifying the thermal properties, which is of crucial importance in the development of efficient nanofluids.
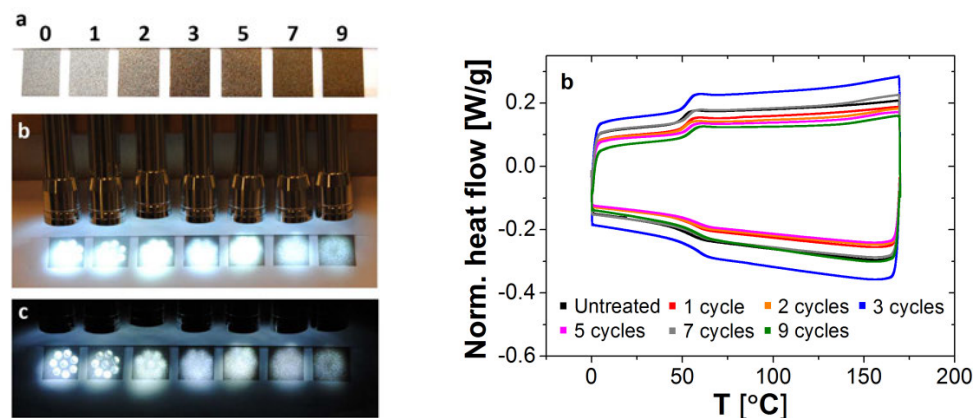

Figure 2. (left) Tuning of the surface finish of the paint from gloss to matte depending

on the thickness of the deposited aluminium oxide film. (right) Differential scanning calorimetry profiles of the uncoated and coated powder coating samples.

The other example that we will show in the presentation is the enhanced radio-activation efficiency of SiC (silicon carbide) particles to be employed as tracers in studies using PEPT (Positron Emission Particle Tracking) for the development of concentrated solar plants [4].

SiC particles have by nature a poor affinity towards ^{18}F ions, normally used as radio-active ion. To overcome that, γ-Al$_2$O$_3$ particles are used as tracers due to their good activation efficiency. However, using a different particle as tracer might induce a change in the hydrodynamic behaviour of the tracer due to mismatches in geometry, density or particle size with the particles used as heat transfer fluid. To overcome that, we coated SiC particles with aluminium oxide. The resulting SiC-Al$_2$O$_3$ core-shell structure shows a good labelling efficiency, comparable to γ-Al$_2$O$_3$ tracer particles (Figure 3, left).

The thickness of the alumina films, which ranged from 5 to 500 nm, was measured by elemental analysis and confirmed with FIB-TEM (focus ion beam – transmission electron microscope), obtaining consistent results from both techniques. By depositing such a thin film of alumina, properties that influence the hydrodynamic behaviour of the SiC particles, such as size, shape and density, are hardly altered, ensuring that the tracer particle shows the same flow behaviour as the other particles (Figure 3, right). The thin alumina coatings applied to study a heat transfer fluid used in concentrated solar plants can be also used within a similar context in nanofluids that have to resist elevated temperatures. This example of a coated SiC opens the possibility to investigate how these materials can perform at more demanding temperatures.
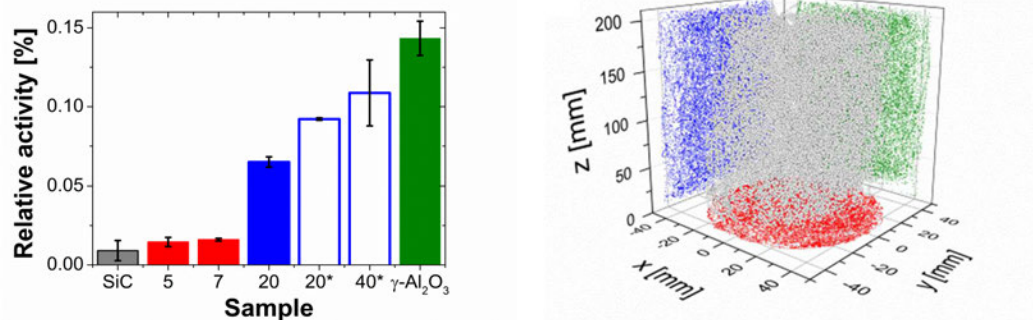
Figure 3. (left) Activation efficiency of the uncoated and alumina-coated SiC particles, and γ-Al$_2$O$_3$ particles, normally used as tracers. (right) Trajectory of the alumina coated-SiC tracer during a PEPT experiment.

Conclusions: In this presentation we will show the process of depositing ultrathin films on particles with the coating technique atomic layer deposition, and will present two examples on how the performance of a material can be tuned without altering other physical properties such

as density, heat capacity, shape or size. Additionally, we will explain how the coating process works, and what can be further done with this versatile technique, aiming at a scaled up process able to produce coated particles at industrially relevant volumes. Finally, we will discuss how this technique could contribute to the development of new nanofluids. This technique can be interesting for this emerging application, since from other fields is has been proven that ultrathin films can enhanced the performance of other materials, perhaps applications for nanofluids being the next one.

References.

1. Miikkulainen, V., et al., Crystallinity of inorganic films grown by atomic layer deposition: Overview and general trends. Journal of Applied Physics, 2013. 113(2): p. 1-101.
2. George, S.M., Atomic layer deposition: An overview. Chemical Reviews, 2010. 110(1): p. 111-131.
3. Valdesueiro, D.H., H, et al., Tuning roughness and gloss of powder coating paint by encapsulating the coating particles with thin Al_2O_3 films. Submitted for publication, 2017.
4. Valdesueiro, D., et al., Enhancing the activation of silicon carbide tracer particles for PEPT applications using gas-phase deposition of alumina at room temperature and atmospheric pressure. Nuclear Instruments and Methods in Physics Research, Section A: Accelerators, Spectrometers, Detectors and Associated Equipment, 2016. 807: p. 108-113.

ENVIRONMENTAL ASSESSMENT OF ADVANCED HEAT MANAGEMENT SOLUTIONS

J. Krupanek[1*], B. Michaliszyn[1], Ł. Lelek[2] and J. Kulczycka[2]

[1]Instytut Ekologii Terenów Uprzemysłowionych, Kossutha 6 st., 40-844 Katowice, Poland

[2]Instytut Gospodarki Surowcami Mineralnymi i Energią PAN, ul. Wybickiego 7A, 31-261 Kraków, Poland

[*]Corresponding author: j.krupanek@ietu.pl

Keywords: Life Cycle Perspective, environmental assessment, heat evacuation, Metal Matrix Composites, carbon materials

Introduction:

For heat management there are used many solutions in the electronic and automotive industries, based on metal materials including copper and aluminium. To improve the performance a wide range of solutions based on nanomaterials is researched including Metal Matrix Composites and Nanofluids.

It is expected that improved thermal management can give new technological opportunities and environmental benefits. Higher utilization of advanced materials can improve performance without increasing the costs. At the same time consumption of raw materials and energy can decrease and waste generation during processing, manufacturing and/or dismantling phases can be reduced. To explore a full potential of the novelty solutions they should be developed with respect to Life Cycle environmental performance of their final applications taking into consideration their environmental efficiency, impacts, risks and waste management issues.

Approaches of integrating various aspects of environmental assessment of innovative heat management solutions are being advanced in relevant research projects [1,2]. As an example an integrative approach to environmental assessment was applied in the project Smart Thermal conductive Al MMCs by casting – THERMACO funded by the European Union 7th Framework Program which aim was to develop Metal Matrix Composites based on metal structures (aluminium) and carbon crystalline forms (Thermal Pyrolytic Graphite, Graphene, diamonds) characterised with high heat conductivity.

Discussion and Results:

Life Cycle Assessment - LCA was the key method used in the study accompanied by Environmental Impact Assessment including assessment of health risk and analysis of waste management requirements. LCA is a tool quantifying impact on the environment in a holistic an established procedure [3], standardised according to PN-EN ISO 14040:2009 LCA [4].

Purpose of the LCA study in the Thermaco project was to assess the environmental performance of the new Al-MMC materials with respect to current heat evacuation solutions based on copper and to analyse various production paths to find those having the lowest environmental impact. It took into consideration all the aspects, direct and indirect, that could potentially affect the environment and are associated with the innovative heat management options.

The analysis of innovative solutions in the Life Cycle Perspective was performed in a tiered approach:

- Screening of predefined composite material combinations in Life Cycle perspective including assessment of the production processes of basic (aluminium, copper) and carbon materials. It was accompanied with assessment of environmental impact and health risks related to releases to the environment of the carbon materials during their life cycle,
- Comparative assessment in Life Cycle perspective of the designed functional materials and component demonstrators taking into account real data from the technical experiments carried out in the project and considering technologies of their production. It was accompanied with assessment of environmental impacts generated in the production of the MMC materials and components with identification and quantification of emissions to the environment, analysis of abatement measures, wastes generation and their appropriate utylisation and analysis of occupational health hazards,
- Comparative assessment of the designed demonstrators of functional components intended for energy and automotive industries and prospected basic scenarios of their application in final products. They were assessed in the full Life Cycle perspective with identification and evaluation of potential environmental benefits such as: reduced weight of the components, reduced waste generation or energy savings. It included evaluation of their potential environmental performance during consumption phase. Moreover an extensive prognosis of the waste management requirements in post-consumption phase with analysis of utylisation options was performed and the results were integrated in the LCA assessment.

A data set of inputs and outputs LCI (Life Cycle Inventory) was prepared with preparation of the balance sheet, identification and calculation for functional units representing the analysed system, the elements coming out from the environment and the elements going out of the system to environment (e.g. CO_2 emissions to air, emissions to water etc.) [5]. It was done basing on technical expert knowledge, literature data, analyses and simplified modelling of the technological processes, and using of EcoInvent 2.2 database. Life Cycle perspective of the functional components is presented in figure 1.
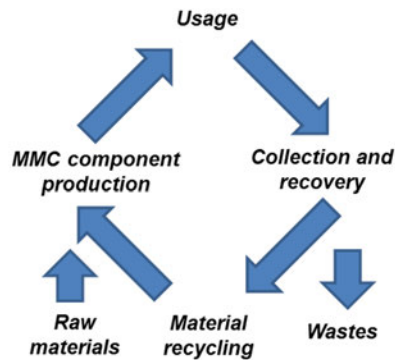
Figure 1. Life Cycle Perspective of Al-MMC materials

In the final stage of the LCA, the impact categories and characterizing models were defined. The aggregate potential impact on the environment was estimated and quantified taking into account the impact on all components of the environment (i.e. output: emissions to water, air, waste, etc.) and also the consumption of resources (i.e. inputs: materials and energy) throughout the life cycle. The environmental performance of the innovative solutions was compared based on cumulated eco-indicator (Figure 2). It referred to the results of current state or a fixed level (benchmarking) resulting from the currently used criteria of assessing the efficiency of environmental performance.
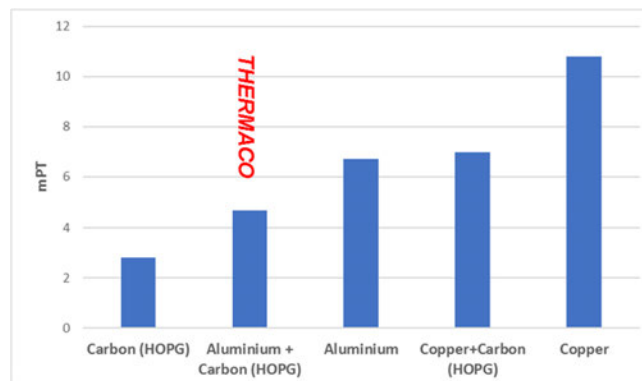
Figure 2. Examples of Life Cycle environmental impact of heat management materials

Summary:

Results of the overall Environmental Assessment of the materials and functional components studied in the project were used as the base for the decision process in field of development and application of new technology solution or modernization of existing products.

It was found out that environmental impacts are related predominantly to production of basic materials (especially carbon materials) used in manufacturing of Thermaco composites. Thus, it is very important to well account for environmental benefits during the use phase of the materials

which can outbalance environmental costs of manufacturing processes: less material used for production, lighter vehicles.

The main achievements of the study in the scope of assessing environmental aspects of the innovative heat management solutions were:

- New knowledge and competences developed by research and industrial partners,
- Recommendations for design of the materials and their applications in products
- Tailoring and optimisation of production processes,
- Recommendations for raising benefits in consumption phase,
- Defining requirements for dismantling of products and processing of waste material in post-consumption phase.
- Directions of future research regarding heat evacuation solutions.

References:

1. A. Jovanovic, M. Cordella, *Life cycle assessment (LCA)&Risk Analysis in nanomaterials related NMP projects*, Information booklet, Specialist Brainstroming and Coordination Meeting March 2, Brussels (Belgium), 2011
2. G. Barbiero, S. Scalbi, P. Buttol, P. Masoni, S. Righi, *Combining life cycle assessment and qualitative risk assessment: The case study of alumina nanofluid production*, Science of The Total Environment, Vol. 496, 2014 pp 122-131.
3. Z. Kowalski, J. Kulczycka, M. Góralczyk, *Ekologiczna ocena cyklu życia procesów wytwórczych*, PWN, Warszawa 2007.
4. JB Guinée, M. Gorrée, R. Heijungs, G. Huppes, R. Kleijn, L. van Oers, A. Wegener Sleeswijk, S. Suh, U. de Haes, H. de Bruijn, R. van Duin and MAJ. Huijbregts *Life Cycle Assessment: An Operational Guide to the ISO Standards*. Kluwer Academic Publishers, Dordrecht, The Netherlands, 2002.
5. O. Jolliet, A. Brent, M. Goedkoop, N. Itsubo, R. Mueller-Wenk, C. Peña, R. Schenk, M. Stewart, B. Weidema: *LCIA Definition* Study of the SETAC-UNEP Life Cycle Initiative. UNEP, 2003.

GRAPHENE NANOFLUIDS – NEW AND INTERESTING RESULTS IN A SOLAR THERMAL COLLECTOR

F.E.B. Bioucas, S. Vieira, M.J.V. Lourenço*, F.J.V. Santos and C.A. Nieto de Castro

Centro de Química Estrutural, Faculdade de Ciências da Universidade de Lisboa
Campo Grande, 1749-016 Lisboa, Portugal
*Corresponding author: mjlourenco@ciencias.ulisboa.pt

Keywords: Nanofluid, Heat Transfer Fluid, Solar Thermal Collector, Graphene

Introduction: A solar thermal collector can be optimized in different aspects, such as the use of a better insulation material to reduce the heat losses, a better absorber with a better specific coating (2), or a better heat transfer fluid. Heat transfer fluids based on water and ethyleneglicol are widely known and used in typical solar collectors. Our intention is to improve the heat transfer efficiency of a heat transfer fluid composed of water and ethyleneglicol with graphene, creating a pumpable nanofluid which could be used industrially. A second purpose is to achieve equilibrium between cost/efficiency without retrofitting.

Experimental/Theoretical Study:

Solar collector: The solar collector was bought from PHYWE company, but several modifications were made. In Figure 1 the schematic of our solar. In this work, we measured the temperature at four different points: cold current entering the collector (A), hot outlet current leaving the collector (B), the temperature of the water bath (C) and the ambient temperature. We also used a gear pump, a magnetic flow meter to measure the flow velocity, and a flow regulator value to adjust the flow.
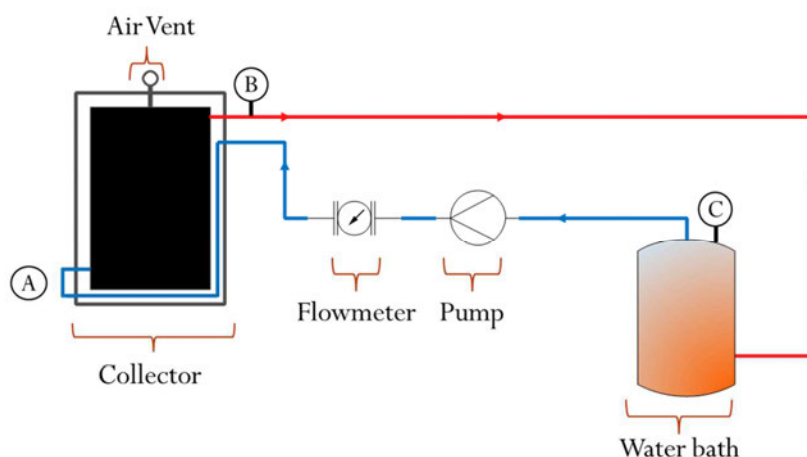

Figure 1: Schematic of the solar collector unit.

Heat transfer fluid: The nanofluids were prepared in a two-step process: first the base fluid was prepared and then the graphene was added to the base fluid and sonicated with Hielscher UP200HT with a probe S26d40 at amplitude of 50%, a pulse cycle of 50% and a frequency of 25±1Hz for three minutes.

The graphene used in this experiment was obtained from Skyspring Nanopowder and Nanoparticles (US), the graphene has a thickness of 6 – 8 nm and an average particle diameter of 15 μm.

Tests: In this work two different tests were performed and the parameters of each tests are present in table I. In Test I, the base fluid and the three nanofluids were tested inside our laboratory using a halogen lamp with 1000 W of power to simulate the sun radiation. This test was performed in order to have the same exact conditions for each fluid, and in fact we were able the have the same ambient temperature, we didn't have the influence of the atmospheric conditions (wind, clouds, variation of the ambient temperature) and we were also able to start all the experiments at the same temperature. The projector was only turned on when the difference between the inlet and outlet temperature was below 0.2 ∘C.

In the second test, Test II, we used the heat transfer fluid that showed the best and worst performance and tested them in a real situation: outside with the solar radiation and the influence of the atmospheric conditions. Two tests were performed for each HTF at similar atmospheric conditions; the results present in this paper are the average of these values. The solar collector was covered with an insulation blanket, when the difference between the temperature of the inlet and outlet were below 1.0°C the blanket was removed.

Table 1: Experimental paramenters of Test I and Test II.

	Test I - Halogen Lamp	**Test II – Solar radiation**
Radiation Source	Halogen lamp (1000 W)	Sun (800 – 950 W)
Distance to light source	0.65 m	-
Tilt	90 °	30 °
Flow velocity	100±10 ml/min	
Water heater volume	1,8 l	
Test duration	200 min	120 min
Influence of atmospheric conditions	None	Wind, Clouds and $\Delta T_{exterior}$

Discussion and Results:

Test I: From figure 2, which shows the outlet temperature of the heat transfer fluid, it is possible to conclude that with the higher concentration of graphene one can achieve a higher temperature than the base fluid (with a difference of 1.8°C). Identical results were observed for the inlet current (3.0°C), and for the water bath (1.2°C).
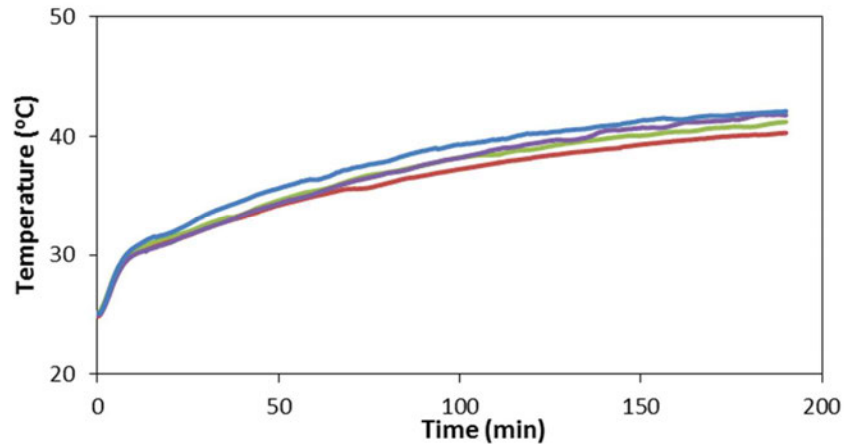
Figure 2: Temperature of the outlet current in function of time, ▬ base fluid, ▬ base fluid with 0.05 wt% graphene, ▬ base fluid which 0.08 wt% of graphene and ▬ base fluid with 0,10 wt% of graphene.

Test II: The second test was performed outside and thus all the measurements were influenced by the atmospheric conditions such wind, clouds and the variation of the ambient temperature, oscillating between 30 and 38 °C. The base fluid and the base fluid with 0.10 wt% of graphene were tested, two tests were performed for each heat transfer fluid in similar atmospheric conditions. In figure 3 the efficiency of the two fluids is presented. It is possible to see that there is an oscillation in the data, which derive from the influence of the atmospheric conditions. From the figure 3 it is also visible that the base fluid with 0.10 wt% of graphene has a higher efficiency than the base fluid, as the base fluid has average efficiency of 54.66% and the nanofluid has an efficiency of 60,56%.
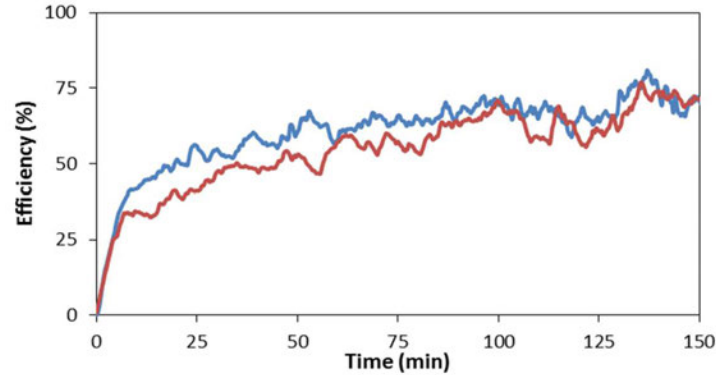
Figure 3: Efficiency of the solar collector, ▬ base fluid and ▬ base fluid with 0.10 wt% of graphene.

Conclusions: The current work shows that graphene can be used on a solar collector in order to improve the efficiency. In a controlled environment, the heat transfer fluid with graphene achieved a higher temperature in the outlet and inlet currents as well as in the water bath. An increase of 5.9% in efficiency is achieved in comparison with the base fluid.. Although these results show a possible use of graphene in a commercial solar thermal collector further studies are necessary. In this paper the experiment was performed in short periods of time (maximum of 3h), in the future these periods should be increased to a week in order to understand the full behavior of this system. Furthermore, we intend to integrate a dynamic light scattering technique in order to know the real concentration of the graphene in the heat transfer fluid, since it becomes attached to the wall, lowering the initial concentration flowing in the solar collector.

References:

1. S.M.S. Murshed and C.A. Nieto de Castro, Conduction and convection heat transfer characteristics of ethylene glycol based nanofluids – A reviews, *Applied Energy* 184(2016) 681–695.
2. S. Vieira, *PhD Thesis*, Universidade de Lisboa (2015).

Magnetic nanofluids for electric power engineering applications

M. Rajnak[1,3], **M. Timko**[1*], **P. Kopcansky**[1], **T. Tobias**[1], **K. Paulovicova**[1], **J. Kuchta**[2], M. **Franko**[2], **J. Kurimsky**[3], **B. Dolnik**[3], **R. Cimbala**[3]

[1]Institute of Experimental Physics SAS, Watsonova 47, 04001 Košice, Slovakia

[2]Electrotechnical research and projecting company, Trenčianska 19
018 51 Nová Dubnica, Slovakia

[3]Faculty of Electrical Engineering and Informatics, Technical University of Košice, Letná 9,
04200 Košice, Slovakia

[*]Corresponding author: timko@saske.sk

Keywords: transformer oil, iron oxide nanoparticles, transformer, cooling.

Introduction/Background: The increasing global electric power consumption and related demands on reliability and performance of insulating and cooling materials have stimulated intensive research on novel cooling and insulating media in power systems. In the process of electric power transmission and distribution, the transformers play a key role. On the other hand, these electrical devices have been statistically found as the most critical part of an electric power network [1]. The regions of intense temperature between the transformer's core and windings and between the windings cause degradation of the winding insulation as well as the conductive components of the transformer. One of the important materials providing the proper function, reliability and protection of the transformers is transformer oil which is often based on mineral oil [2]. The primary function of the transformer oil is to insulate and cool a transformer. It must therefore have high dielectric strength, thermal conductivity, and chemical stability. However, to cope with the increasing demand of future high voltage networks and small size of transformers, the development of more effective cooling and insulating liquid medium is extensively required. In the last years, the transformer oil based nanofluids have been produced to meet the necessary attributes [1].

One of the dielectric and cooling nanofluids intensively investigated as a potential replacement of the transformer oil is the magnetic nanofluid (ferrofluid) based on transformer oil [3–5]. Besides the increased thermal conductivity, the cooling by magnetic nanofluid relies on thermomagnetic convection [6]. This refers to a convective heat transfer that makes use of the spatial gradient in the magnetic susceptibility of the nanofluid that is produced in the presence of a temperature gradient. When a magnetic fluid is exposed to a non-uniform magnetic field in the presence of a temperature field, besides convectional gravitational body force, the varying susceptibilities result in a non-uniform magnetic body force. In other words, as the heat load increases, the magnetization of the magnetic nanofluid decreases, leading to the increase in the nanofluid flow velocity and consequently, faster heat transfer from the heat

source [7]. The thermomagnetic convection in various magnetic nanofluids and under different conditions was reported in numerous papers [8–10].

Surprisingly, the presence of magnetic nanoparticles in transformer oils can enhance not only the thermal transport properties of the oil, but have a positive impact on the dielectric breakdown field strength of the oil. This peculiar finding was reported for the first time in [4]. Moreover, it was also highlighted that the propagation velocity of the streamer is reduced due to the presence of the nanoparticles. Theoretical modeling demonstrated that this velocity reduction is a crucial phenomenon leading to the understanding of the higher breakdown field strength of the magnetic nanofluid [11]. However, complete comprehension of the breakdown mechanism requires further experimental and theoretical study.

In this paper, we report on the experimentally tested cooling effectiveness of a magnetic nanofluid applied in a specially designed transformer. The localized temperatures in various regions in the transformer are compared for two cases, when the cooling medium is the transformer oil and the magnetic nanofluid.

Discussion and Results: For the purpose of our investigation, we have designed a small model transformer T1N-5-400/230. When designing the transformer, the attention was paid to providing good conditions for the expected thermomagnetic convection in the magnetic nanofluid. Thus, in order to increase the stray magnetic field and create more space for the convection, the transformer with a gap between the primary and secondary winding and between the winding and the core was constructed. The model of the transformer is depicted in Fig. 1.
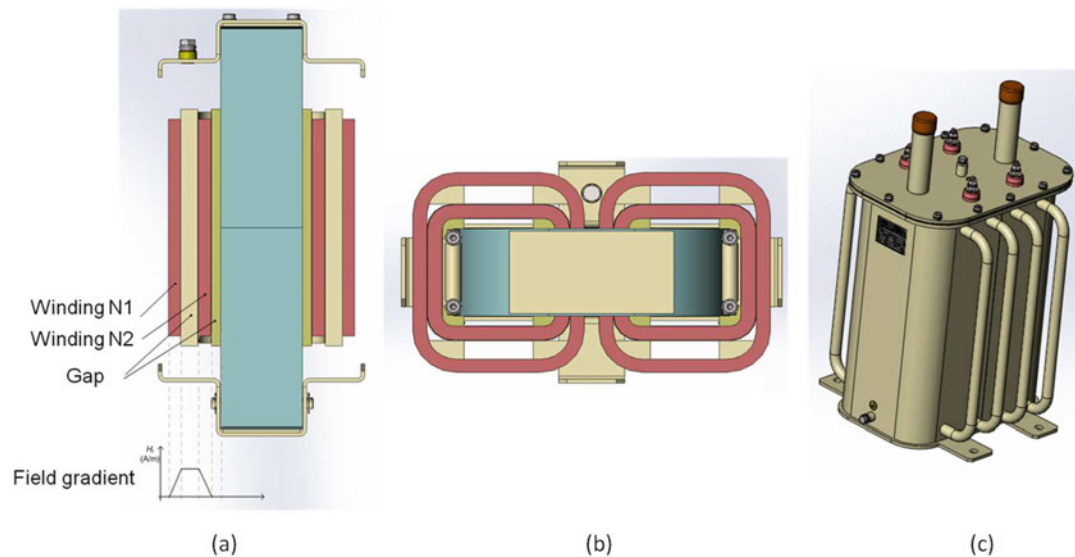

Fig. 1 The scheme of the model transformer used to test the cooling effectiveness of the magnetic nanofluid. (a) front view cross-section, (b) top view cross-section, (c) transformer tank.

The transformer was filled firstly with a commercial transformer oil Mogul Trafo CZ-A, and then with a magnetic nanofluid based on this oil and iron oxide nanoparticles. The basic physical parameters of the oil are as follows: the pour point of the oil is -42 °C, the flash point is greater than 150 °C, the relative density is 870 kg/m^3, and the viscosity at 40 °C is 11 mm^2/s, as provided by the manufacturer. The magnetic nanoparticles for the nanofluid were synthesized by the well-known chemical co-precipitaion method [14] from aqueous solution of Fe^{2+} and Fe^{3+} ions in the presence of NH$_4$OH at 80-82 °C. The synthesized magnetite nanoparticles were covered with a single surfactant layer (vegetal oleic acid, C$_{18}$H$_{34}$O$_2$, 65-88%, Merk). The chemisorption was followed by the washing with distilled water with magnetic decantation to remove residual unreacted salts, followed by flocculation (acetone) to remove free surfactant. The purified magnetite nanoparticles were dispersed in the transformer oil. Finally, 6 litters of magnetic nanofluid were prepared for the experiment. The magnetic mass fraction (particle concentration) in the nanofluid was 2.85 %, as determined from magnetic measurements.

In order to compare the cooling ability of the transformer oil and the magnetic nanofluid, we performed the heating tests of the loaded transformer with an apparent power of 4.3 kVA. The temperature sensors monitoring the temperature evolution were located at various places within the transformer. In Table 1, the saturated temperature values are presented for the transformer filled with the pure oil and the nanofluid. The values were taken at the time when the transformer was 10 hours under the load.

	Lower shell	Upper shell	Core down	Core up	Winding down	Winding up	Coolant down	Coolant up
Pure oil, T (°C)	70.2	71.58	53.12	56.07	56.35	34.71	48.6	68.15
Nanofluid T (°C)	69.06	71.02	52.71	55.75	56.03	34.15	43.82	67.39
ΔT (°C)	1.14	0.56	0.41	0.32	0.32	0.57	4.78	0.78

Table 1 Comparison of the cooling effect of the transformer oil and the magnetic nanofluid in the model transformer T1N-5-400/230.

As one can see from Table 1, the temperature of the loaded transformer at various locations is lower when the transformer is filled with the magnetic nanofluid. The greatest temperature difference was found when measuring the coolant temperature at the bottom of the transformer shell. The average transformer temperature difference is 1.05 °C in favour of the magnetic nanofluid. This cooling enhancement is associated with the increased thermal conductivity of the

transformer oil due to the presence of the nanoprticles. It is known that the large surface area of the nanoparticles allows for more heat transfer. Besides the effective thermal interaction of the nanoparticles, the high mobility of the nanoparticles, attributable to the nanosize, leads to the enhanced thermal transport properties too. The particle movement may bring about micro-convection of the magnetic nanofluid and hence increase the heat transfer. Moreover, owing to the created gaps between the windings and the core, the stray magnetic field and temperature gradients give rise to the thermomagnetic convection of the nanofluid, intensifying so the heat transfer. It is worth to notice that according to the laws of insulation aging it is clear that the lower the temperature, the slower the insulation deterioration. Thus, lowering the operating temperature of the transformer by using the magnetic nanofluid can result in the higher loadability and longer service life of the transformer.

Summary/Conclusions: In this study we have tested the cooling effect of a magnetic nanofluid based on transformer oil and iron oxide nanoparticles. The tests were carried out in a model transformer with the apparent power of 4.3 kVA. It was found that the transformer temperature is lower in the case when filled with the magnetic nanofluid instead of the transformer oil. The average temperature difference is 1.05 °C. This effect stems from the enhanced thermal transport properties of the transformer oil due to the presence of magnetic nanoparticles and induced thermomagnetic convection in the gap between the transformer windings and the core.

References:

[1]   M. Rafiq, Y. Lv, C. Li, M. Rafiq, Y. Lv, and C. Li, "A Review on Properties, Opportunities, and Challenges of Transformer Oil-Based Nanofluids, A Review on Properties, Opportunities, and Challenges of Transformer Oil-Based Nanofluids," *J. Nanomater. J. Nanomater.*, vol. 2016, 2016, p. e8371560, Jul. 2016.

[2] R. Bartnikas, *Electrical Insulating Liquids*. Philadelphia, PA: Astm Intl, 1994.

[3]   J.-C. Lee, H.-S. Seo, and Y.-J. Kim, "The increased dielectric breakdown voltage of transformer oil-based nanofluids by an external magnetic field," *Int. J. Therm. Sci.*, vol. 62, pp. 29–33, Dec. 2012.

[4]   V. Segal, A. Hjortsberg, A. Rabinovich, D. Nattrass, and K. Raj, "AC (60 Hz) and impulse breakdown strength of a colloidal fluid based on transformer oil and magnetite nanoparticles," in *Conference Record of the 1998 IEEE International Symposium on Electrical Insulation, 1998*, 1998, vol. 2, pp. 619–622 vol.2.

[5]   K. Raj and R. Moskowitz, "Ferrofluid-cooled electromagnetic device and improved cooling method," US5462685 A, 31-Oct-1995.

[6]   I. Nkurikiyimfura, Y. Wang, and Z. Pan, "Heat transfer enhancement by magnetic nanofluids—A review," *Renew. Sustain. Energy Rev.*, vol. 21, pp. 548–561, May 2013.

[7]   V. Chaudhary, Z. Wang, A. Ray, I. Sridhar, and R. V. Ramanujan, "Self pumping magnetic cooling," *J. Phys. Appl. Phys.*, vol. 50, no. 3, p. 03LT03, 2017.

[8]   A. Lange, "Thermomagnetic convection of magnetic fluids in a cylindrical geometry," *Phys. Fluids*, vol. 14, no. 7, pp. 2059–2064, May 2002.

[9]   H. Rahman and S. A. Suslov, "Thermomagnetic convection in a layer of ferrofluid placed in a uniform oblique external magnetic field," *J. Fluid Mech.*, vol. 764, pp. 316–348, Feb. 2015.

[10]   A. Lange and S. Odenbach, "Patterns of thermomagnetic convection in magnetic fluids subjected to spatially modulated magnetic fields," *Phys. Rev. E*, vol. 83, no. 6, p. 066305, Jun. 2011.

[11]   J. G. Hwang, M. Zahn, F. M. O'Sullivan, L. A. A. Pettersson, O. Hjortstam, and R. Liu, "Effects of nanoparticle charging on streamer development in transformer oil-based nanofluids," *J. Appl. Phys.*, vol. 107, no. 1, p. 014310, Jan. 2010.

[12]   L. Vékás, M. V. Avdeev, and D. Bica, "Magnetic Nanofluids: Synthesis and Structure," in *NanoScience in Biomedicine*, D. Shi, Ed. Berlin, Heidelberg: Springer Berlin Heidelberg, 2009, pp. 650–728.

Characterization Of Nano-Encapsulated Metal Alloy Phase Change Materials For A Molten Salt-Based Nanofluid

Nuria Navarrete[1,*], Rosa Mondragón[1], Dongsheng Wen[2], Maria E. Navarro[3], Yulong Ding[3], J. Enrique Julia[1]

[1] Dpto. de Ingeniería Mecánica y Construcción, Universitat Jaume I, 12071 Castellón, Spain.

[2] Institute of Particle Science and Engineering, University of Leeds, LS3 PJT, Leeds, UK.

[3] Birmingham Centre of Energy Storage, University of Birmingham, B15 2TT, Birmingham, UK.

*nnavarre@uji.es

Keywords: Thermal storage, Solar energy, Nanofluids, Molten salts, Phase-change materials

INTRODUCTION: A nanofluid is a Heat Transfer Fluid (HTF) or Thermal Energy Storage (TES) material with enhanced heat transfer properties by the addition of nanoparticles [1]. Their use usually implies an increment in the thermal conductivity of the fluid, but additional enhancements in the heat capacity of molten salts and ionic liquids have been registered [2].

Heat capacity of fluids can also be increased by using nanoencapsulated Phase Change Materials (nePCM). These nanoparticles are composed of a PCM core and a covering shell with high melting temperature. Thus, an increase in the heat capacity of the nanofluid compared to the base fluid can be obtained due to the latent heat of the cores [3]. The main drawbacks of nePCM are the complexity in the synthetization process of the shell and the high supercooling they sometimes present (the difference between the core melting and crystallization temperatures, due to homogeneous crystallization)[4].

The present work proposes a nanofluid composed of a mixture of molten nitrates widely used in Concentrated Solar Power plants, and nePCM consisting of an Al/Cu nucleus encapsulated by the metallic oxide formed when exposed to oxygen. NePCM and nanofluids with different concentrations have been characterized regarding their physical and thermal properties, and the suitability of the encapsulation has been proven for high temperature working conditions.

METHODS: Nanoparticles of an Aluminium-Copper alloy in an 80%Al-20%Cu percentage were obtained from Advanced Powder Technologies LLC. The base fluid used was the mixture of sodium and potassium nitrates known as solar salt (60% and 40% wt. respectively. Labkem, analytical grade ACS). Nanofluids consisting of solar salt and Al/Cu nanoparticles with mass concentrations of 0.5%, 1%, 1.5%, 5% and 10% were synthesized adding the nanoparticles to the previously mixed nitrates and mechanically blending.

range from 25 to 85ºC and concentration between 0.1 and 1 g/l. Both devices rely on Dynamic Light Scattering (DLS) method which is commonly used to characterize the size of nanoparticles dispersed in liquids.

RESULTS AND CONCLUSIONS:

The properties of graphene oxide (GO) and water-based nanofluids were determined in respect to concentration, temperature range (25-85ºC) and the amount of added sodium dodecyl sulfate (SDS). The main findings are:

- The mean hydrodynamic diameter of graphene-oxide flakes increases with decreasing concentration of graphene nanoparticles. Literature data on this dependency are ambiguous.
- The size of nanoparticles decreases with increasing temperature. Nanofluids are water-based and thus bad quality results for temperatures higher than 75ºC may occur due to intensive evaporation and possibility of bubble formation. The research on the GO size dependency on the temperature is not available in the literature and there is no possibility to compare the results.
- Added surfactant did not affect the particle size distribution with a recognizable trend.

The results require further analysis. Although, DLS is said to be reliable for spherical particles, the rough estimation of sizes and trends depending on conditions is also possible for non-spherical objects as well. Care should be taken with respect to the working conditions.

ACKNOWLEDGEMENT:

REFERENCES:

[1] A. Wlazlak, B. Zajaczkowski, M. Woluntarski, and M. H. Buschmann, "Thermosyphon performance in dependence of carbon-based nanofluids," in *Proceedings of 3rd Thermal and Fluids Engineering Conference*, 2018.

[2] A. Wlazlak, B. Zajaczkowski, S. Barison, F. Agresti, L. M. Wilde, and M. H. Buschmann, "Nanofluids as working fluid in thermosyphon," in *1st European Symposium on Nanofluids, Abstract Collection*, 2017, pp. 172–177.

[3] A. Wlazlak, B. Zajaczkowski, L. M. Wilde, and M. H. Buschmann, "Effect of various nanofluids on thermal performane of the thermosyphon," in *Proceedings of 16th International Heat Transfer Conference*, 2018.

A Proposal for Thermal Conductivity Measurements of Magnetic Nanofluids Under the Influence of External Magnetic Field

Serkan Doğanay [1], Levent Çetin[2,*], Alpaslan Turgut [3]

1 Dokuz Eylül University, The Graduate School of Natural and Applied Sciences, 35390, İzmir, Turkey

2 İzmir Kâtip Çelebi University, Department of Mechatronics Engineering, 35620, İzmir, Turkey

3 Dokuz Eylül University, Department of Mechanical Engineering, 35390, İzmir, Turkey

*Corresponding e-mail: levent.cetin@ikc.edu.tr

Keywords: magnetic nanofluid, magnetic field, thermal conductivity, MEMS, Fe_3O_4

INTRODUCTION: Magnetic nanofluids or ferrofluids are colloids which comprise of nano-sized magnetic particles suspended in a non-magnetic carrier liquid. The magnetic particles typically can be magnetite (Fe_3O_4), maghemite (γ-Fe_2O_3), cobalt etc. with their excellent magnetization properties where the non-magnetic carrier liquids can be water, ethylene-glycol, oil, kerosene. They have the potential to be utilized in many different applications such as lubrication, sealing, ink jet printers, dampers, clutches, optical filters, optical sensors, biosensors, biomedical, drug delivery, refrigeration, cooling devices [1]. The ability of being manipulated by an external magnetic makes magnetic nanofluids attractive for especially micro-electromechanical systems (MEMS). Among these micro-sized systems, microfluidics become prominent for heat transfer applications. So that, it is important to investigate the thermal properties such as thermal conductivity of the magnetic nanofluids in the absence and presence of the external magnetic field before employing them in microfluids or other smart cooling devices. In this study, the thermal conductivity of Fe_3O_4-water magnetic nanofluid has been measured under the effect of external magnetic field and the methodology of the magnetic field dependent measurements has been discussed.

METHODS: Fe_3O_4 water magnetic nanofluid with 20% wt. concentration has been supplied commercially from US Research Nanomaterials. The average particle diameter of the sample is 15-20 nm. In order to generate magnetic field, permanent magnets are used. A simple magnet holder design was used for applying magnetic field to the magnetic nanofluid sample. The magnetic field strength was controlled by altering the distance between magnets. The generated magnetic field was measured by a gaussmeter. The magnetic flux density in the air gap between two magnets was simulated. The simulation results were also validated the experimental data obtained by gaussmeter. The thermal conductivity of the magnetic nanofluid was measured by 3-omega method.

RESULTS AND CONCLUSIONS: Experiments were carried out with two different orientation of the external magnetic field. First, perpendicular and then parallel orientations were applied. That means, the magnetic field lines are parallel or perpendicular to the temperature gradient caused by measurement probe. Figure 1 indicates that the thermal conductivity increases with the application of the external magnetic field. The possible reason behind this phenomenon can be explained by the chain aggregation formation of the magnetic nanoparticles under the influence of the external magnetic field [2].
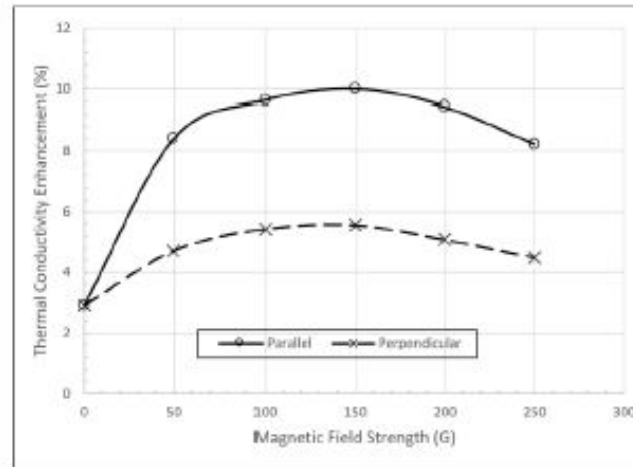
Figure 1 Thermal conductivity enhancement in respect to the external magnetic field strength for both parallel and perpendicular orientation.

Figure 1 also reveals that the thermal conductivity enhancement decreases after 150 G. That can be related with the non-uniformity of the external magnetic field after that point. In the non-uniform magnetic field, there will be a force acting on the magnetic nanoparticles [3]. This causes to the breaking of the chainlike structure and therefore the decrement of the thermal conductivity. Moreover, the thermal conductivity is higher when the applied external magnetic field is parallel to the temperature gradient.

REFERENCES

[1] L.J. Felicia, S. Vinod, J. Philip, Recent Advances in Magnetorheology of Ferrofluids (Magnetic Nanofluids)-A Critical Review. Journal of Nanofluids 5 (2016) 1-22.

[2] J. Philip, P.D. Shima, B. Raj, Enhancement of thermal conductivity in magnetite based nanofluid due to chainlike structures. Applied Physics Letters 91 (2007).

[3] N. Pamme, Magnetism and microfluidics. Lab Chip 6 (2006) 24-38.

Wettability Behaviour of Nanofluids

Nur Çobanoğlu[1], Ziya Haktan Karadeniz[2,*], Alpaslan Turgut[3]

[1] Department of Mechanical Engineering, Graduate School of Natural and Applied Science, İzmir Katip Çelebi University, 35620, İzmir, Turkey

[2] Department of Mechanical Engineering, İzmir Katip Çelebi University, 35620, İzmir, Turkey

[3] Department of Mechanical Engineering, Dokuz Eylül University, 35397, İzmir, Turkey

*Corresponding e-mail: zhaktan.karadeniz@ikc.edu.tr

Keywords: Nanofluids, Surface Tension, Contact Angle, Wettability

INTRODUCTION:

This study presents the discussion of the surface tension (ST) and contact angle (CA) measurements of nanofluids which were done in Izmir Katip Celebi University within the scope of Nanotension Project which is a part of NANOUPTAKE COST Action, and comparison of the results with the available data in the literature.

METHODS:
Measurements were performed with graphene oxide+distilled water (GO+DIW) (length of flakes=800-1000 nm, 0.1 g/l), alumina+distilled water (Al_2O_3+DIW) (averaged size 122-125 nm, 0.1 vol.%) and gold+distilled water (Au+DIW) (size < 10 nm, 10 mg/l) nanofluids. ST of nanofluids were measured by using pendant drop method (Biolin Scientific Attension Theta - Optical Tensiometer) and Du Noüy ring method (Biolin Scientific Attension Sigma 701 - Force Tensiometer). CA of samples on V2A 1.4301 stainless-steel substrate was measured by using sessile drop method (Biolin Scientific Attension Theta - Optical Tensiometer). During experiments temperature ranged between 21.5°C and 23.7°C.

RESULTS AND CONCLUSIONS:

Figure 1 shows the comparison of ST results with the available data in the literature (temperature range between 20°C and 30±2°C, size of nanoparticles between 5-nm to 200-nm) [6-16]. A reduction in ST with reference to base fluid has been observed for all nanofluids and for both devices in the present study. Results for water are comparable with the results in literature except simulation result reported by Sinha and Singh [1]. For Al_2O_3+DIW nanofluid,

both a decrement and an increment were observed. Although, [2] and [3] used same methods with us, they found increasing ST compared with the base fluid. There is a lack of studies about ST of Au+DIW and GO+DIW nanofluids. For Au+DIW nanofluid, ST results by sessile drop method [4] were lower than our results but in the simulations of Au-DIW nanofluid [1], ST was found more than the base fluid and our results. Zheng [5] found the ST of GO+DIW nanofluid greater than the base fluid, which is contrary to our results. Sinha and Singh [1] have reported an increase in the ST with increasing hydrophilicity and a decrease with increasing hydrophobicity as a result of simulations for Au-DIW nanofluids. In the concentration range between 1.72 and 14.78 vol.%, ST increases from 64.02 to 79.84 mN/m for hydrophilic nanoparticles whereas it decreases from 63.03 to 48.77 mN/m for hydrophilic nanoparticles. Considering the hydrophilic or hydrophobic behaviour of the fluid, the main reason of decrease in ST of nanofluids may be the hydrophobic nature of nanoparticles. Hydrophobic nanoparticles are gathered on the free surface of the fluid. The repulsive force between particles and fluid molecules increases the interfacial spacing at the interface and reduces the attractive forces between fluid molecules in bulk fluid, thus causes to reduction in surface tension [12-15]. The maximum reduction has been obtained in gold-DIW nanofluid and it might be the result of using stabilizer, which is already mentioned in the literature [16]. Decrement in CA can be the reasoned by considering the improvement of surface wettability via hydrophilic behavior of the stainless steel. Figure 2 reports the CA values. Comparing the data with literature is difficult due to the custom-made surface samples.
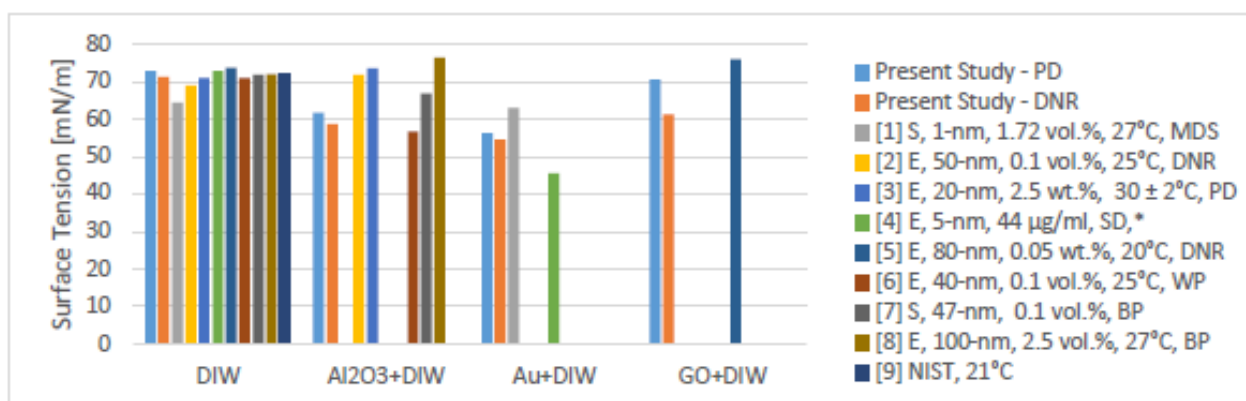

Figure 1. Surface tension of nanofluids. (E: Experimental, S: Simulation; PD: Pendant Drop, SD: Sessile Drop, WP: Wilhelmy Plate, BP: Bubble Pressure, DNR: Du Noüy Ring, MDS: Molecular Dynamic Simulation; *:The nanoparticles were functionalized with a proprietary carboxylic acid and the solution could contain <0.1% of residual hydroxides.)

Figure 2. Contact angle of nanofluids (E: experimental, S: Simulation; SD: Sessile Drop; SS: Stainless steel, R: Roughness)

REFERENCES:

[1]   N. Sinha and J. K. Singh, "Effect of nanoparticles on vapour-liquid surface tension of water: A molecular dynamics study," *J. Mol. Liq.*, vol. 246, pp. 244–250, 2017.

[2]   M. H. U. Bhuiyan, R. Saidur, M. A. Amalina, R. M. Mostafizur, and A. Islam, "Effect of nanoparticles concentration and their sizes on surface tension of nanofluids," *Procedia Eng.*, vol. 105, pp. 431–437, 2015

[3]   A. R. Harikrishnan, P. Dhar, P. K. Agnihotri, S. Gedupudi, and S. K. Das, "Effects of interplay of nanoparticles, surfactants and base fluid on the surface tension of nanocolloids," *Eur. Phys. J. E*, vol. 40, no. 5, p. 53, 2017.

[4]   S. Vafaei, K. Chinnathambi, and T. Borca-Tasciuc, "Liquid–gas surface tension voltage dependence during electrowetting on dielectric testing of water and 5–90 nm gold nanofluids," *J. Colloid Interface Sci.*, vol. 490, pp. 797–801, 2017.

[5]   Z. Z. Zheng, "Experimental investigation on surface tension of water-based graphene oxide nanofluids," in Advanced Materials Research, 2015, vol. 1082, pp. 297–301.

[6]   D. D. Li, W. L. Zhao, J. K. Li, Y. X. Guan, and Z. M. Liu, "Thermophysical Performances of Al2O3-Water Nanofluids and Its Heat Transfer Enhancement in Heat Pipe," in *Materials Science Forum*, 2011, vol. 688, pp. 339–343.

[7]   R. Hadidimasouleh, M. S. Yaghmaee, R. Riahifar, and B. Raissi, "Modeling Of The Surface Tension Of Colloidal Suspensions," *Surf. Rev. Lett.*, vol. 24, no. 4, p. 1750050, 2017.

[8]   Z. Zhou, Q. Di, B. Liu, X. Ma, and B. Cai, "Experimental Study on the Surface Tension of Al2O3-H2O Nanofluid.," in Materials Science Forum, 2016, vol. 852.

[9]   P. J. Linstrom and W. G. Mallard, "NIST chemistry webbook." National Institute of Standards and Technology Gaithersburg, MD, 2001.

[10]   J. T. Cieśliński and K. A. Krygier, "Sessile droplet contact angle of water–Al2O3, water–TiO2 and water–Cu nanofluids," Exp. Therm. Fluid Sci., vol. 59, pp. 258–263, 2014.

[11]   D. H. Prajitno, V. Trisnawan, and D. G. Syarif, "Effect of Spreading Time on Contact Angle of Nanofluid on the Surface of Stainless Steel AISI 316 and Zircalloy 4," in *IOP Conference Series: Materials Science and Engineering*, 2017, vol. 196, no. 1, p. 12028.

[12]   G. Lu, Y.-Y. Duan, and X.-D. Wang, "Surface tension, viscosity, and rheology of water-based nanofluids: a microscopic interpretation on the molecular level," *J. nanoparticle Res.*, vol. 16, no. 9, p. 2564, 2014.

[13]   S. Zhang, X. Han, Y. Tan, and K. Liang, "Effects of hydrophilicity/lipophilicity of nano-TiO2 on surface tension of TiO2-water nanofluids," *Chem. Phys. Lett.*, vol. 691, pp. 135–140,

2018.

[14]   M. Radiom, C. Yang, and W. K. Chan, "Characterization of surface tension and contact angle of nanofluids," in *Fourth International Conference on Experimental Mechanics*, 2010, vol. 7522, p. 75221D.

[15]   S. M. S. Murshed, S.-H. Tan, and N.-T. Nguyen, "Temperature dependence of interfacial properties and viscosity of nanofluids for droplet-based microfluidics," *J. Phys. D. Appl. Phys.*, vol. 41, no. 8, p. 85502, 2008.

[16]   S. S. Khaleduzzaman, I. M. Mahbubul, I. M. Shahrul, and R. Saidur, "Effect of particle concentration, temperature and surfactant on surface tension of nanofluids," *Int. Commun. Heat Mass Transf.*, vol. 49, pp. 110–114, 2013.

THE EFFECT OF OXIDIZED CARBON NANOHORN NANOFLUID POOL BOILING ON AN ALUMINUM SURFACE

Alexandra Gimeno-Furio[1], Leonor Hernandez[1], Simona Barison[2], Filippo Agresti[2], Luca Doretti[3] and Simone Mancin[4]

[1] Department of Mechanical Engineering and Construction, Universitat Jaume I, 12071, Castelló, Spain
[2] CNR-ICMATE Institute of Condensed Matter Chemistry and Technologies for Energy, 35127 Padova, Italy
[3] Department of Management and Engineering, University of Padova, 36100, Vicenza, Italy
[4] Department of Civil, Architectural and Environmental Engineering, University of Padova, 35131, Padova, Italy

*Corresponding e-mail: simone.mancin@unipd.it

Keywords: pool boiling, nanofluids, critical heat flux, contact angle, coating

INTRODUCTION:

Boiling is known as one of the most effective mechanisms of heat transfer and it is used in many engineering applications that require high heat flux dissipation. It has been demonstrated that the use of nanofluids can enhance the heat transfer efficiency. Several factors as type, size and concentration of nanoparticles, characteristics and geometry of the surface heater, presence of surfactants and pressure have an influence on boiling behaviour [1-4]. The objective of the present study was to investigate the difference in pool boiling between based-water nanofluid and water. The nanofluid used for the pool boiling was based on water using oxidized carbon nanohorns (oxCNH) at 0.1% weight concentration on an aluminium (Al) surface. Before and after the boiling test, scanning electron microscopy (SEM) and contact angle (CA) measurements were performed to characterize and evaluate the resulting coated surface. Also the boiling curves of both fluids were measured.

METHODS:

Pool boiling tests were carried out in an experimental setup that consists of an Al surface, which was exposed to the working fluid and heated by electrical cartridge heaters. All the pool boiling experiments took place inside a confined chamber in order to avoid contamination. On the top, there is a condenser, which is directly fed with the vapour formed.

On the other hand, CA measurements were obtained by image processing. Finally, to study the effect of the pool boiling on the surface and evaluate if deposition of nanoparticles has

taken place, SEM images were performed with a SIGMA Zeiss instrument (Carl Zeiss SMT Ltd., UK).

RESULTS AND CONCLUSIONS:

SEM images of the Al surface before and after the boiling are presented in Fig. 1. Nanoparticles deposition was observed after the pool boiling.

a)   b)
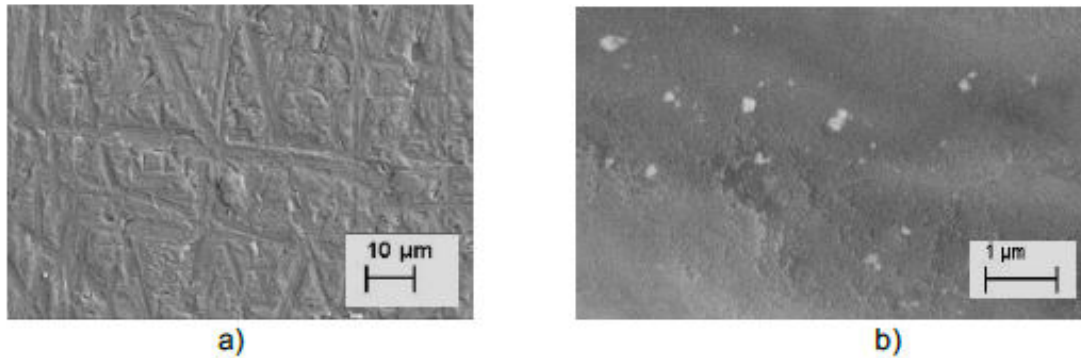
Fig. 1 SEM images of Al surface (a) before and (b) after the pool boiling.

The values obtained for the CA measurements are for water 74° and oxCNH 76.3° on Al surface before the boiling and then, 70.6° and 69° for water and oxCNH, respectively, on the Al surface after the pool boiling. The boiling curves for water as reference and oxCNH nanofluid are given in Fig. 2, showing that nanofluid wall superheat values are higher than those for water. In fact, there is not any noticeable effects of the nanoparticles deposited layer on the contact angle measurements.
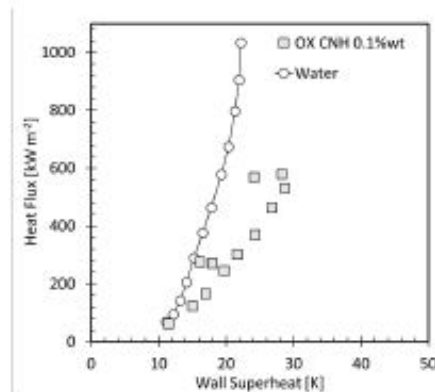
Fig. 2 Boiling curves of water as reference and oxCNH 0.1% wt in water.

REFERENCES:

[1] H.S. Ahn, M.H. Kim, A review on critical heat flux enhancement with nanofluids and surface modification, J. Heat Transf. 134 (2) (2011) 784-790.

[2] R. Shanthi, Sh. Sundaram, V. Ramalingam, Heat transfer enhancement using nanofluids-an overview, Therm. Sci. 16 (2012) 423-444.

[3] J. Barber, D. Brutin, L. Tadrist, A review on boiling heat transfer enhancement with nanofluids, Nanoscale Res. Lett. 6 (2011) 280.

[4] F. Rostamian, N. Etesami, Pool boiling characteristics of silica/water nanofluid and variation of heater surface roughness in domain of time, Int. Comm. In Heat and Mass Transf. 95 (2018) 98-105.

Numerical simulation of a nanofluid in a pipe flow

Jan Tibaut [1], Tilen Tibaut [1], Jure Ravnik[1,*],
[1] Affiliation 1 Faculty of mechanical engineering, University of Maribor, 2000 Maribor, Smetanova 17

*Corresponding e-mail: jan.tibaut@um.si

Keywords: Nanofluids, single-phase model, mixture model, water, pipe flow

INTRODUCTION:

In the framework of the NANOROUND project, started within NANOUPTAKE to compare and validate different nanofluid modelling approaches, we present preliminary results of simulations of laminar nanofluid flow in a heated pipe. We present two models that can solve the flow of a nanofluid. In order to validate our models, we have first, performed water flow simulations in a pipe. Thus, we could compare the numerical simulated flow of water with the numerically simulated flow of nanofluid and look at the differences.

Nanofluids are a mixture of a base fluid and nano particles. The base fluid is usually water. Two approaches can be considered in order to simulate flow of a suspension of particles. The Euler-Euler method or the Euler-Lagrange method. In this study, we used the first method. In this procedure, the fluid and the particles are considered as a continuous fluid. We present the single phase model and the mixture model. An investigation using the single phase model was presented by Ravnik et. al [1]. In this model, the properties of the fluid are obtained from empirical correlations. The mixture model is more complex. The model requires an additional equation in order to solve the dispersion of nano particles in the fluid. Khalili et. al [2] presented the model in order to simulate the flow of nanofluid in a circular enclosure. An experimental investigation into the problem, which we have simulated, was done by Colla et. al [3].

We performed a number of numerical simulations of the nanofluid flow using the same setup. The mass flow rate, heat flux and particle volume fraction were changed.

METHODS: We tested two numerical models in order to simulate the flow of a nanofluid in a heated pipe. The same test case was implemented as it was presented in the experimental test case by Colla et. al [4].

Four conservation laws were implemented in order to solve the fluid flow. Let us consider the vector $\vec{v}$ as velocity vector field. Firstly, the continuity equation for incompressible fluid flow is employed:

$$\vec{\nabla} \cdot \vec{v} = 0. \tag{1}$$

Secondly, the momentum conservation equation with the Boussinesque approximation of the lift force was implemented:

$$\rho \cdot \vec{v}\vec{\nabla}\vec{v} = -\vec{\nabla}p + \eta\Delta\vec{v} - \rho\beta\vec{g}(T - T_0),$$ (2)

where ρ is the fluid density, η is the dynamic viscosity and β is the thermal expansion. After the velocity field is solved, the temperature field is determined with the energy equation:

$$\vec{\nabla} \cdot (\rho\vec{v}h) = \vec{\nabla} \cdot (\lambda\vec{\nabla}T),$$ (3)

where T is the temperature, h is the enthalpy and λ is the thermal diffusivity. The last conservation law is the concentration conservation:

$$(\vec{v} \cdot \vec{\nabla})\varphi = -\vec{\nabla}(\vec{j}_B + \vec{j}_T),$$ (4)

φ is the particle volume fraction, $\vec{j}_B$ is the Brownian motion and $\vec{j}_T$ is the thermophoresis [5]. The water simulation was performed with equations (1), (2) and (3). In addition, the single phase model was also solved with this three equations. In this model: ρ, η and λ are the properties of the nanofluid. The nanofluid properties were solved from empirical expression, where the properties of the base fluid and nano particles are considered [1]. The second model is the mixture model. In this model equation (4) is employed [2]. This additional equation solves the particle volume in the domain.

REFERENCES:

[1] J. Ravnik and L. Škerget, 'A numerical study of nanofluid natural convection in a cubic enclosure with a circular and an ellipsoidal cylinder', *Int. J. Heat Mass Transf.*, vol. 89, pp. 596–605, 2015.

[2] E. Khalili, A. Saboonchi, and M. Saghafian, 'Natural Convection of Al₂ O3 Nanofluid Between Two Horizontal Cylinders Inside a Circular Enclosure Natural Convection of Al₂ O₃ Nanofluid Between Two Horizontal Cylinders Inside', *Heat Transf. Eng.*, vol. 38, no. 2, pp. 177–189, 2017.

[3] L. Colla, L. Fedele, and M. H. Buschmann, 'Laminar mixed convection of TiO₂-water nanofluid in horizontal uniformly heated pipe flow', *Int. J. Therm. Sci.*, vol. 97, pp. 26–40, 2015.

[4] L. Colla, L. Fedele, and M. H. Buschmann, 'Nanofluids suppress secondary flow in laminar pipe flow', in *International Conference on Heat Transfer and Fluid Flow*, 2015, pp. 1–4.

[5] A. N. Morozov and A. V Skripkin, 'Spherical particle Brownian motion in viscous medium as non-Markovian random process', *Phys. Lett. A*, vol. 375, no. 46, pp. 4113–4115, 2011.

CFD modelling of volumetric vapour generation and its applications to the receiver design

Raúl Martínez-Cuenca, Alexandra Gimeno-Furió, Nuria Navarrete, Salvador Torró, Sergio Chiva, Leonor Hernández

[1] Department of Mechanical Engineering and Construction, Universitat Jaume I, 12071, Castelló, Spain

Corresponding e-mail: raul.martinez@uji.es

Keywords: Computer Fluid Dynamics, Multiphase Flow, Radiation, Boiling

INTRODUCTION:

Classic solar-thermal receivers base their performance on the heating of the containers surface. This leads to both high surface temperatures and high radiative losses. Also, accident scenarios may lead to critical heat flux conditions thus degrading the surface material. These drawbacks are tackled when the whole volume of the receiver is used as an absorber. In particular, direct volumetric vapour generation has been proposed to further improve the efficiency of solar receivers [1]. The fluid mechanics of these systems is quite complex given that: (1) the nanofluid absorbs the light field to generate the secondary phase; (2) the two fluid phases exchange mass, momentum and energy; (3) the members of the secondary phase interact between (coalescence and break-up); (4) the secondary phase scatters the light field. Therefore, simple design tools are not able to provide a proper description of their performance. In this contribution we propose the use of Computer Fluid Dynamics to account for these effects. A simple proof-of-concept design example is given.

METHODS:

The simulation relies on the so-called two-fluid model [2]. Here, the nanofluid is modelled as a single phase with constant density and viscosity, and vapour bubbles are modelled as a Eulerian dispersed phase with a given diameter distribution.

The source term for the vapour is modelled as $f \, N \, V_b$, being f the nucleation frequency of a site, N the nucleation site volumetric density, and V_b the mean volume of the generated bubbles. To include the bubble scattering, a simple experiment was carried out (see Figure 1). A LED panel was used as light source, and a diffuser served to generate air plumes with different gas-hold up conditions. Image processing permitted to propose a correlation for the scattering coefficient in terms of the volumetric gas concentration.
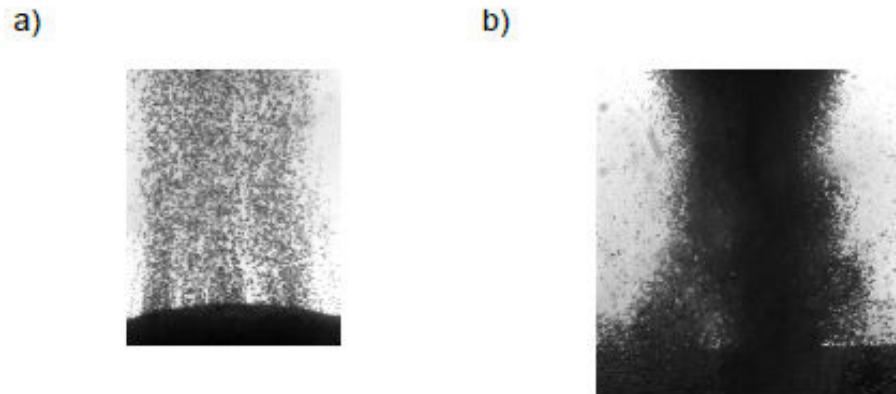
a)   b)

Figure 1: Sample images for low (a) and high (b) gas hold-up conditions.

RESULTS AND CONCLUSIONS:

Figure 2 shows the results for a cylindrical receiver on three scenarios. In case a), a high nanoparticle concentration limits the gas generation to the regions near the surface. This is an undesirable configuration, as most part of the receiver is not acting as expected. In order to avoid it, the nanoparticle concentration can be reduced to produce a most uniform gas distribution, as shown in case b). Alternatively, at high nanoparticle concentrations in a) may be preserved if the receiver diameter is reduced as in c).
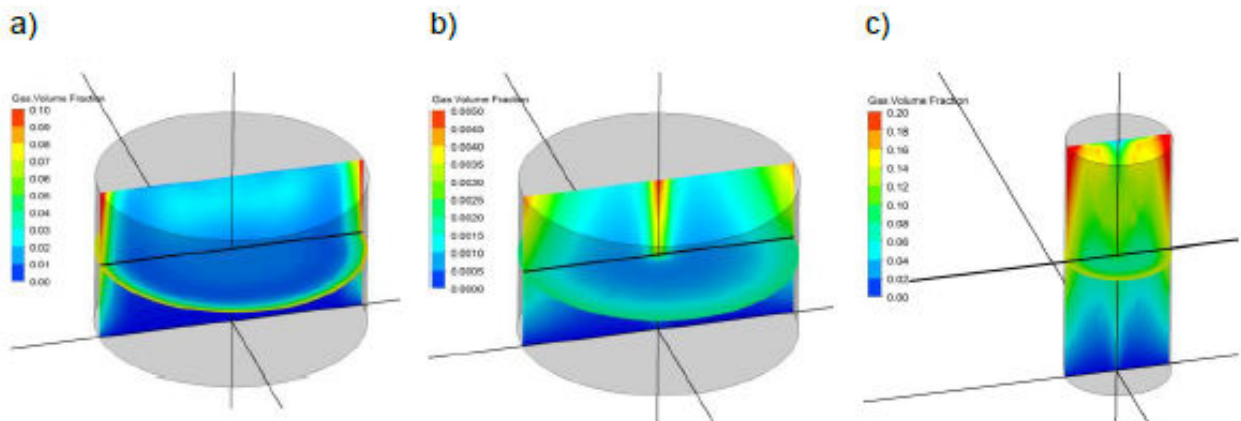
a)   b)   c)

Figure 2: Gas distribution for the three scenarios considered.

REFERENCES:

[1] G. Ni, N. Miljkovic, et al. Nano Energy 17, 290-301 (2015).
[2] S. Yamoah, R. Martínez-Cuenca, et al. Chemical Engineering Research & Design 98, 17-35 (2015).

Plasmonic Nanofluids for Solar Cells Applications

S. Kassavetis, C. Kapnopoulos, P. Patsalas, and S. Logothetidis

Nanotechnology Lab LTFN, Aristotle University of Thessaloniki, GR-54124
Thessaloniki, Greece

*Corresponding e-mail: skasa@physics.auth.gr

Keywords: plasmonics, laser ablation, electrospray, silver, transition metal nitrides

INTRODUCTION: Nanomaterials and especially the nanoparticles paves novel interdisciplinary ways in a wide-range of applications, from electronics to medicine (biosensors) to energy harvesting (solar cells) and buildings (self-cleaning). This work focus on fabrication and the properties of plasmonic nanomaterials and specially plasmonic nanofluids for solar energy harvesting applications. [1, 2]

METHODS: The plasmonic nanofluids were fabricated using a combination of Laser Ablation processes in aquatic and isopropanol solutions. The 532 nm beam of a picosecond (ps) Nd:YAG laser is used to ablate a silver target and to form silver NPs in the solutions. Secondly, the 532 nm and 355 nm beams of a nanosecond (ps) Nd:YAG laser was employed to refine the silver NPs size distribution and in this way to tune the localized surface plasmon resonance (LSPR) of the plasmonic nanofluid.

The optical properties of the plasmonic nanofluids were evaluated by optical transmittance measurements in the Visible-UV spectral range, while the NPs size distribution and their concentration in the liquid were evaluated after analysis of the transmission spectra and by dynamic light scattering (DLS).

Electrospraying was used to spray to incorporate/add the metal NPs in the structure of an organic solar cell. Thus, the plasmonic solution was sprayed on top of the hole transport layer and in this way a plasmonic layer was introduced at the interface between the hole transport layer (PEDOT:PSS) and the active (P3HT:PCBM) layer.

RESULTS AND CONCLUSIONS: Silver was used as the target material for the fabrication of plasmonic nanofluids. The 532 nm beam from the ps laser resulted to the fabrication of silver nanofluids that showed a broad, not so intense plasmonic peak at the ~ 400 nm, due to the large variation in the size distribution of the Ag NPs. The size of the Ag NPs in the aquatic solution was refined by irradiating the nanofluid with an out-of-focus 532 nm and 355 nm beams from the ns laser. The plasmonic peak in the absorbance spectra appeared more intense (the absorption increases from 0.3 to 0.9) and the analysis showed the absorption peak is less broad, thus the Ag NPs size distribution is narrower, and the under the curve

area is double as a result of the Ag NPs population increase due to the successful fragmentation of the pristine Ag NPs.

The Ag plasmonic nanofluids were electrospayed into the organic solar cells layers. Specifically they were mixed with PEDOT:PSS and developed on top of the P3HT:PCBM photoactive blend, in order to take advantage of the plasmonic effects.

The devices were tested under AM1.5G at 1000 W/m^2 of illumination, which showed the fabrication of efficient plasmonic solution processed solar cells with improved V_{oc}, FF and J_{sc} values and slightly higher power conversion efficiency compared to this of the non-plasmonic/reference ones.

Finally, the case of the fabrication and the properties of the transition metal nitride nanofluids as well as their possible applications is discussed. [3]

REFERENCES:
1. Kassavetis, S, Kaziannis S, Pliatsikas N, Avgeropoulos A, Karantzalis A, Kosmidis C, Lidorikis E, Patsalas P., "Formation of plasmonic colloidal silver for flexible and printed electronics using laser ablation", Applied Surface Science 336 (2015) 262-266.

2. H.A. Atwater, A. Polman, "Plasmonics for improved photovoltaic devices", Nat. Mater. 9 (2010) 205–213.

3. P Patsalas, N Kalfagiannis, S Kassavetis, G Abadias, DV Bellas, Ch Lekka, E Lidorikis, "Conductive nitrides: Growth principles, optical and electronic properties, and their perspectives in photonics and plasmonics", Materials Science and Engineering: R: Reports 12 (2018) 1- 55.

Performance evaluation of a solar cooling system with nanofluids

Furio Cascetta[1], Bernardo Buonomo[1,2], Luca Cirillo[1], Sergio Nardini[1,2*]

[1] Dipartimento di Ingegneria, Università degli Studi della Campania "L. Vanvitelli", Real Casa dell'Annunziata, Via Roma 29, Aversa, Italy

[2] Sun Energy Europe S.r.l., Academic Spin-Off, Via B. De Capua 26, 81043 Capua (CE), Italy

*Corresponding e-mail: sergio.nardini@unicampania.it

Keywords: Solar Cooling, Nanofluids, Transient simulation, Renewable Energy, Energy Management.

INTRODUCTION: An interesting solution for air conditioning in summer time is a solar cooling system. The use of nanofluids is a possibility to enhance thermal performance of solar components. A review on the applications of nanofluids in solar energy field is developed by Khanafer and Vafai [1]. The objective of our investigation is to model and simulate a complete solar cooling system made up of ETCs (evacuated thermal solar collectors), thermal storage tank and LiBr-H_2O based single effect absorption chiller. As working fluids nanofluids with three particale volume concentration are considered: pure water, Al_2O_3-water based with two different volumetric concentrations 3% and 6%.

METHODS: The solar system, based on a single effect absorption chiller (15 kW of power), is fully modelled in TRNSYS with weather data of Naples as the reference climate data. The ETSCs, a storage tank, a hydraulic pump and a controller are considered for the hot loop. Physical properties of the Al_2O_3 nanoparticles and water such as thermal conductivity, specific heat capacity, density and dynamic viscosity are evaluated from literature. Thermal efficiency solar collector equations are given in Ghaderian and Sidik [2].

RESULTS AND CONCLUSIONS: Simulations are performed for the whole summer season, i.e. from June to September. The nanofluid flows into the collectors and reaches a hot storage tank at temperature $T_{coll,o}$ by means of a pump. In the tank nanofluid heats water at temperature $T_{st,o}$, which is lower than 90°C. Hence, the ETSC$_s$ work isolated from the chiller and the loop of the first part of the system continues until the water inside the storage tank reaches the required working temperature. The TRNSYS simulation was run with 1-hour time step. The selected system successfully maintained the room temperature below the set point value of 26 °C, even when the ambient temperature was more than 32 °C during peak summer season, Figure 1.
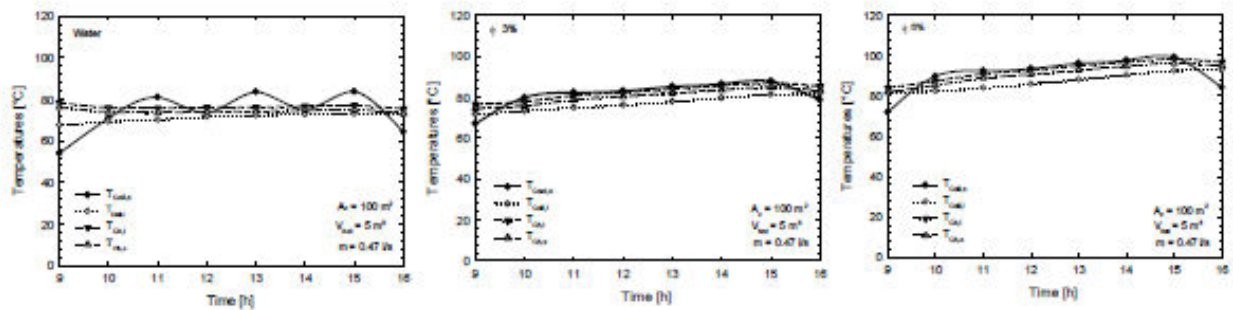
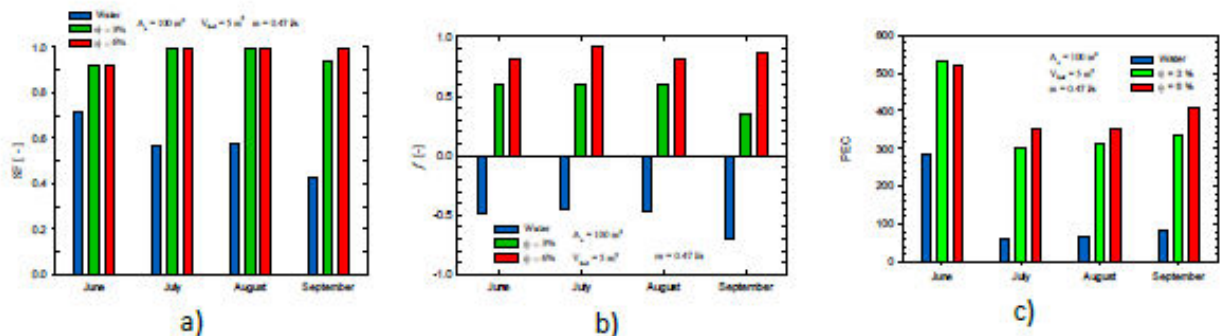Figure 1. Temperatures profile in a typical summer day (30 July)

Figure 2. Performance results vs month: a) solar fraction; b) primary energy savings; c) PEC

In terms of SF (Solar Fraction), Figure 2a, configuration with nanoparticles is better for whole cooling season, obtaining SF=1 in July, August, September and July and August for ϕ=6% and 3%, respectively. Considering the fractional energy savings, f, configuration with ϕ=6% offers greater savings than pure water. Finally, the configuration with particle concentration of ϕ=3% presents higher pumping energy consumption than the other two. Compared with pure water, the pumping energy consumption is higher because the viscosity of the fluid is higher. Compared with nanofluid with ϕ=6%, the pumping energy consumption for lower concentration is higher because the effect of outlet hot water temperature from absorption chiller on temperature of the storage tank is greater, thus the pump remains on for longer. However, the difference is minimum in terms of energy cost so PEC for collectors which use nanofluids with ϕ=6% is higher in summer season.

REFERENCES

[1] K. Khanafer and K. Vafai. (2018). A review on the applications of nanofluids in solar energy field. Ren. Energy. 123, pp. 398-406.

[2] J. Ghaderian and N.A.C. Sidik. (2017). An experimental investigation on the effect of Al2O3/distilled water nanofluid on the energy efficiency of evacuated tube solar collector. Int. J. of Heat and Mass Transf. 108, pp. 972-87.

Towards highly stable nanofluids for Concentrating Solar Power

Javier Navas[1,*], Teresa Aguilar[1], Paloma Martínez-Merino[1], Ivan Carrillo-Berdugo[1], Antonio Sánchez-Coronilla[2], Elisa I. Martín[3], Roberto Gómez-Villarejo[1], Juan Jesús Gallardo[1], Rodrigo Alcántara[1], Concha Fernández-Lorenzo[1]

[1] Physical Chemistry Department, University of Cádiz, E-11510, Puerto Real (Cádiz), Spain

[2] Physical Chemistry Department, University of Seville, E-41012, Seville, Spain

[3] Chemical Engineering Department, University of Seville, E-41012, Seville, Spain

*Corresponding e-mail: javier.navas@uca.es

Keywords: Nanofluid, Stability, Concentrating Solar Power.

INTRODUCTION: The colloidal suspension of a nanomaterial in a base fluid, typically called nano-colloids or nanofluid, is an emerging system that can be used as heat transfer fluid (HTF) due to the enhanced thermophysical properties with respect to the conventional fluids, such as air, water, ethylene glycol, or synthetic oils [1-4]. That is why nanofluids are considered as potential HTFs which will improve the efficiency of the exchangers involved in renewable power generation [5]. But stabilization of nanofluids is one of the main requirements for this kind of systems, since high stability leads to good and sustainable thermal properties [6]. Therefore, the use of 2D nanomaterials could be a major advance in these systems since these nanomaterials present good physical stability, which is reflected in low sedimentation levels when they are in colloidal suspension due to the higher planar surface. Furthermore, these 2D structures usually show high intrinsic thermal conductivity values. But really, to our knowledge, there is not a systematic methodology for preparing nanofluids with high stability.

METHODS: This study involved the preparation of nanofluids based on the eutectic mixture of diphenyl oxide and biphenyl as the base fluid, this being a typical HTF used in Concentrating Solar Power (CSP) plants that use parabolic trough technology (PTC). MoS_2 nanostructures were used to prepare the nanofluids. But the most important contribution in this work is the introduction for the first time of a systematic methodology to prepare stable and improved nanofluids. A rationalized procedure is presented for defining beforehand the composition of a stable nanofluid; the method determines the appropriate amounts of surfactant and nanomaterial and makes it possible to control the morphology of the nanostructures.

Also, stability of the nanofluids were determined from UV-vis spectroscopy for evaluating the sedimentation process, and from particle size measurements using the Dynamic Light Scattering technique. Moreover, thermal properties were evaluated. Isobaric specific heat was measured using the Temperature-Modulated Differential Scanning Calorimetry (TMDSC) technique. Also, thermal conductivity was obtaining from diffusivity measurements using light flash technique.

RESULTS AND CONCLUSIONS: Different nanostructures were obtained in function of the surfactant used. But, nanofluids prepared were stable after few days. Particle size were about 500 nm. Also, an increase of isobaric specific heat up to 7.5% was obtained. Also, an increase of thermal conductivity up to 57% was found for nanofluids based on 2D nanostructures.

REFERENCES:

[1] A. Mwesigye, Z. J. Huan and J. P. Meyer, *Appl Energ*, 2015, **156**, 398-412.

[2] S. Lee, S. U. S. Choi, S. Li and J. A. Eastman, *J Heat Trans-T Asme*, 1999, **121**, 280-289.

[3] K. S. Suganthi, V. L. Vinodhan and K. S. Rajan, *Appl Energ*, 2014, **135**, 548-559.

[4] M. J. Chen, Y. R. He, J. Q. Zhu and D. S. Wen, *Appl Energ*, 2016, **181**, 65-74.

[5] J. Navas, A. Sánchez-Coronilla, E. I. Martín, M. Teruel, J. J. Gallardo, T. Aguilar, R. Gómez-Villarejo, R. Alcántara, C. Fernández-Lorenzo, J. C. Piñero and J. Martín-Calleja, *Nano Energy*, 2016, **27**, 213-224.

[6] S. Chakraborty, I. Sarkar, K. Haldar, S. K. Pal and S. Chakraborty, *Appl Clay Sci*, 2015, **107**, 98-108

NANOTENSION
Round robin test for surface tension and contact angle of nanofluids

Matthias H. Buschmann[1]

[1] Institut fuer Luft- und Kaeltetechnik Dresden,
Bertolt Brecht Alle 22, 01309 Dresden (Germany)

*Corresponding e-mail: Matthias.Buschmann@ilkdresden.de

Keywords: nanofluids, surface tension, contact angle, round robin test

NENOTENSION joins ten European institutions in a round robin test for measuring surface tension and contact angle of nanofluids. So far four different nanofluids – all water based – are experimentally investigated. The talk will present first results and data analysis.

GEOAIR
H2020 proposal – First experiences

Matthias H. Buschmann[1]

[1] Institut fuer Luft- und Kaeltetechnik Dresden,
Bertolt Brecht Alle 22, 01309 Dresden (Germany)

*Corresponding e-mail: Matthias.Buschmann@ilkdresden.de

Keywords: nanofluids, surface tension, contact angle, round robin test

The main objective of GEOAIR is to develop passive long-distance heat transfer systems to employ geothermal heat for the air-conditioning of multi-family residential buildings. The project incorporates an approach to increase the power output of the photovoltaic system of such a building. GEOAIR combines these two renewables with local heat storage to achieve an enhanced decarbonisation.

The proposal was launched January 2018 by a group of five NANOUPTAKE collaborators and three additional partners. Nanofluids are proposed to be used as working fluids in novel types of thermosyphons.

Experiment Investigation of Nanoparticle-assisted Enhanced Oil Recovery and Oil Reservoir Characterization

Zhonlgiang Hu [1], Dongsheng Wen [1,2,*], Hui Gao[1], Ehsan Nourafkan[1]

[1] School of Chemical and Process Engineering, University of Leeds, LS2 9JT, Leeds, UK

[2] School of Aeronautic Science and Engineering, Beihang University, 100191, Beijing, China

*Corresponding e-mail: d.wen@leeds.ac.uk

Keywords: nanoparticle, enhanced oil recovery, subsurface sensor, nanoparticle transport

INTRODUCTION: Predictions have shown that our demand for oil and gas will continue to grow in the next decade, and future supply will become more reliant on tertiary recovery and from nonconventional resources. However, current reservoir characterization methodologies, such as well logs, cross-well electromagnetic imaging and seismic methods, have their individual limitations on detection range and resolution[1, 2]. Here we propose a pioneering way to use carbon quantum dots (CQDs) as nanoparticle tracers, which could not only transport through a reservoir functioning as conventional tracers, but also act as sensors to obtain useful information inside beyond tracers. These hydrothermally produced CQDs from Xylose possess excellent stability in high ionic strength solutions, durable absorbance and fluorescence ability due to multi high-polarity functional group on their surfaces. Our core-flooding results reveal that CQDs can transport easily through packed columns and reservoir core samples, showing tracer-like migration capability regardless of particle concentration and ionic strength, as detected by both UV-Vis (On-line) and CLSM (off-line) measurements. We also demonstrate that quantitative oil saturation detection in unknown core samples can be achieved by such CQDs based on its breakthrough properties influenced by the presence of oil phase.

METHODS: CQDs were facilely prepared by one-step hydrothermal carbonization of D-(+)-Xylose, an abundant and renewable precursor available in most biomass and agricultural waste materials, as shown in Fig. 1a. The obtained CQDs were first characterized by UV/Vis spectrometer and fluorescence spectroscopy to check their absorbance spectra over various light wavelengths together with their luminescent properties. Other characterization includes morphology and size by TEM, concentration derived from the fluorescent intensity, Raman spectra and FTIR. The transport properties of CQDs are checked both in column packed with glass beads, and sandstone core. The temperature are varied from ambient condition to 80

°C, while the salinity was fixed at the level of API brine. Oil saturation was detected by the breakthrough curves (BTCs) of CQDs.

RESULTS AND CONCLUSIONS: The results show that the CQDs have a good mobility at elevated salinity and temperature (Fig.1 a&b). Based on the time (expressed in PV) when the CQDs breakthrough achieves 40%, 50% and 60%, the calibration curves (S_{or} against breakthrough time) are generated in Fig. 1d. The five-pointed star in Fig. 5d shows that by using calibration curve for 60% breakthrough, the calculated oil saturation is 24.0%, close to the real oil saturation of 25.1%.
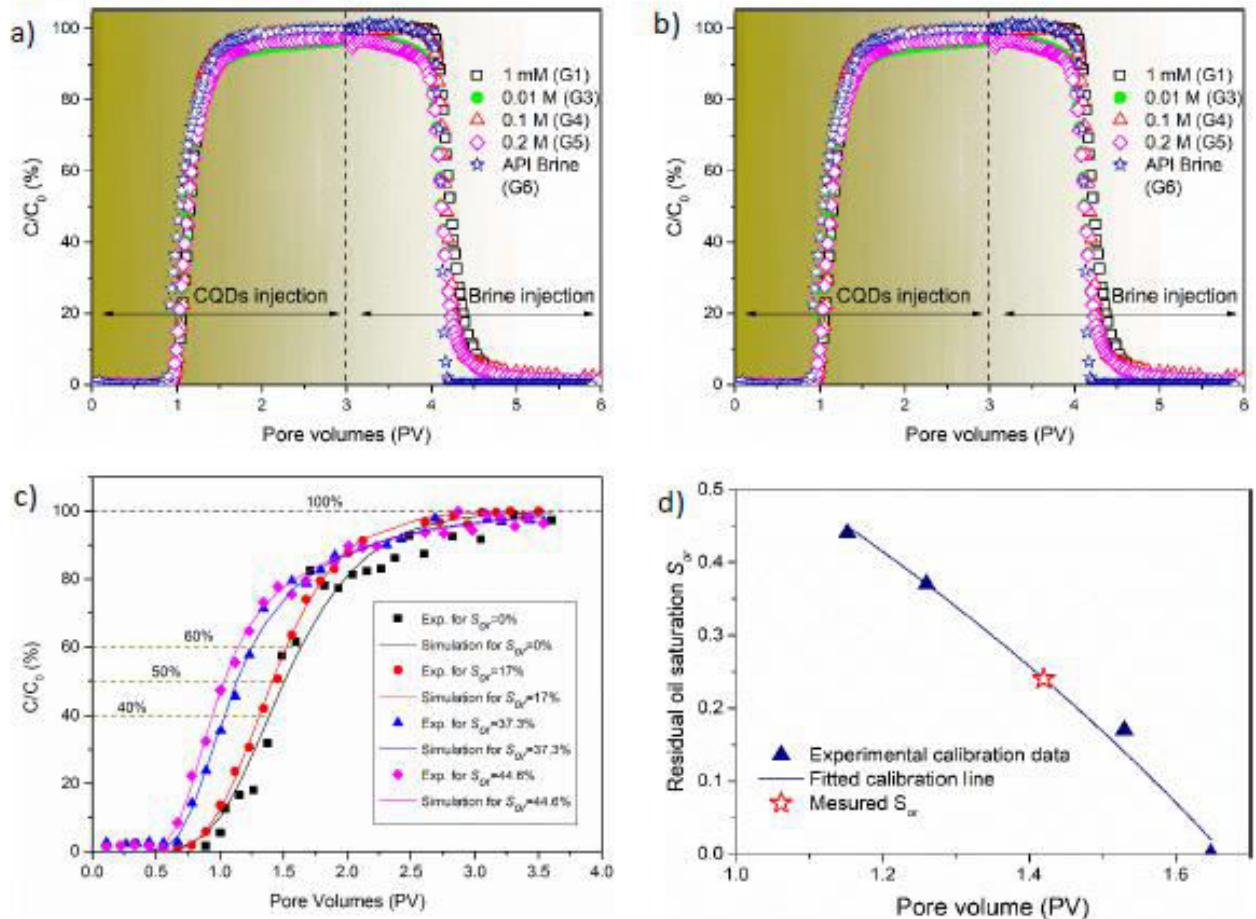

Figure 1. a) BTCs for CQDs (~10 ppm) at room temperature, with varying ionic strengths of the base electrolyte. b) BTCs for CQDs dispersed in API brine, and in glass bead column at elevated temperatures (25, 60 and 80 °C). c) BTCs as a function of injection time for samples containing different water fractions at S_{or}, when injecting CQD suspension at 0.5 mL/min into sandstone core. d) using the calibration curve to determine the oil saturation.

REFERENCES: [1]. H. Yu, Doctor of Philosophy, The University of Texas at Austin, 2012.
[2]. G. R. Dickens, C. K. Paull and P. Wallace, Nature, 1997, 385, 426-428.

7. Conclusions

7. Conclusions

WG1: Heating

A total of 19 contributions have been presented by the Nanouptake participants in the three workshops of this WG1, Heating Working Group: 7 in the first workshop and 6 in each of the following workshops.

Two main research areas can be identified in the contributions: a) nanofluids preparation and evaluation of thermophysical properties (including new nanofluids mixtures) and b) evaluation of thermal and fluid dynamic behaviours in convective heat transfer and fluid flow.

The presented abstracts highlight that different heat transfer applications using nanofluids can be identified, and also that a good combination between the experimental and the modelling field (analytical, numerical, CFD, etc) can be of interest for the advance of nanofluids in heating applications.

Some identified possible improvements in the field can be the definition of standards for the nanofluids preparation (sonication time, stability, etc) and also for the correct measurement of heat transfer properties (conductivity, etc) and heat transfer coefficients.

New directions of this area are the combination of nanoparticles in hybrid mixtures and the use of magnetic nanoparticles to improve the heat transfer.

Two fundamental results have been obtained in the activity. The first is related to is related to the experimental evaluation of convective heat transfer coefficient by different teams and for different duct geometries for the heating in laminar and turbulent regimes. The second the comparison among numerical models in convective heat transfer in circular tubes in laminar regime.

WG2: Cooling

A total of 18 contributions have been presented by the Nanouptake participants in the three workshops of this WG2, Cooling Working Group: 6 in the first workshop, 11 in the second and 7 in the third workshop.

Three different types of research contributions are presented in this Working Group: those focusing on measuring thermal properties of developed nanofluids that could be used in cooling applications, another testing their heat transfer behaviour in flow channels directly related to their cooling performance in real application, and other more focused on modelling and simulation these thermal properties and features.

A wide variation of base fluids and nanoparticles were used to obtain the resulting nanofluids with application in the cooling field, also including magnetic and hybrid nanofluids. Also different industrial applications of nanofluids have been presented in the cooling field: heat exchangers, automotive cooling, wind turbine refrigeration, power transformers, spray cooling, etc.

From the presented contributions and also as a result of the debate and discussion after the presentations, the main identified challenges are mainly related with the long-term stability and the high viscosity of the nanofluids, cooling feature measurement anomalies as well as with the inconsistency of the thermophysical properties measured by different research groups. With the objective of enabling round robin test among the Nanouptake network (which could help to obtain consisted measured data required by any possible nanofluid industrial application), a database of developed nanofluids and available measuring equipment's in the different Nanouptake members was developed in the last part of the COST Action. The database is available with private access for the Nanouptake participants in the website of the COST Action: http://www.nanouptake.eu/database/.

WG3: Storage

A total of 20 contributions have been presented by the Nanouptake participants in the three workshops of this WG3, Storage Working Group: 7 in the first workshop, 4 in the second and 9 in the third workshop.

Two main types of contributions in the field of thermal storage and nanoparticles, those related with latent heat storage and evaluating phase change materials, and those related with sensible heat storage and mainly focusing in the enhancement of heat capacity of molten salts (solar salt, nitrate salts, HITEC, etc) when adding different types of nanoparticles. An interesting possibility is also present where thermal storage of a heat transfer fluid or a molten salt can be increased by using nanoencapsulated materials, increasing both specific heat capacity and latent heat provided by the phase change of the core of the nanoparticle.

Some of the industrial applications for the nanofluids in these storage contributions lie within different fields: mainly are related to concentrated solar power (CSP), but also to geothermal heat exchangers, heating, ventilating and air conditioning (HVAC) systems, etc

In this Working Group, most part of the contributions present experimental work, but there are also some including modelling.

As in the previous working group conclusions, in this case is also valid the idea that there is a need to perform round robin tests in this field, as a starting point to standardized the nanofluids synthesis and also to avoid the experimental scatter in the nanofluids thermophysical results.

WG4: Boiling, Solar Application, Modelling and Others

A total of 38 contributions have been presented by the Nanouptake participants in the three workshops of this WG4 Working Group: 10 in the first workshop, 17 in the second and 11 in the third workshop. This working group includes more than three different fields with a quite active research, which explains the larger number of contributions in the section compared with the previous ones. When splitting into the different research areas in this Working Group, a total of 10 boiling contributions were presented, 16 of solar, 10 of modelling and 3 of other areas.

Within the boiling contributions, interesting results regarding the enhancement of heat transfer with phase change when using nanofluids can be observed. Some of the industrial applications presented in these contributions are heat pipes, thermosyphons, surface coating, etc.

A wide variety of solar applications with nanofluids have been presented in the different contributions in this field: solar thermal collectors, solar cells, solar cooling systems, concentrated solar power, direct absorption solar systems (DASC), etc.

Different modelling techniques have been presented in these sections. It is important also to highlight that some of the contributions from this area have been also allocated in the previous Working Group, as were also related to those specific energy areas.

The need of round robin tests in all the working group, has crystalized in here in two specific joint works:

- Nanoround, about the most suitable CFD approach when dealing with nanofluid flow, which is a field of great importance for large area of applications. The round robin test was lead by A.A. Minea, from the Technical University "Gheorghe Asachi" from Iasi (Romania), and involved six international research groups. The results were published in open access in a joint article "NanoRound: A benchmark study on the numerical approach in nanofluids' simulation" with 18 authors from 7 organizations https://doi.org/10.1016/j.icheatmasstransfer.2019.104292
- Nanotension, about measuring contact angle in three different nanofluids. This thermophysical property is relevant for heat transfer with phase change. The round robin test was lead by M.H. Buschmann, from ILK Dresden (Germany), and involved measurements from nine international groups within the Nanouptake network. The results were published in a joint article "The contact angle of nanofluids as thermophysical property" with 23 authors from 16 organizations: https://doi.org/10.1016/j.jcis.2019.04.007